P-340

CR-180869

National Aeronautics and
Space Administration

# FULL SCALE TECHNOLOGY DEMONSTRATION OF A MODERN COUNTERROTATING UNDUCTED FAN ENGINE CONCEPT

## ENGINE TEST

December 1987


by
**GE Aircraft Engines**
**GE36 Project Department**
**Cincinnati, Ohio 45215**


**Prepared for**

**National Aeronautics and Space Administration**


(NASA-CR-180869) FULL SCALE TECHNOLOGY DEMONSTRATION OF A MODERN COUNTERROTATING UNDUCTED FAN ENGINE CONCEPT. ENGINE TEST (GE) 340 p CSCL 21E

N90-10049

Unclas
G3/07 0237153





**NASA-Lewis Research Center**
**Contract NAS3-24210**

CR-180869

National Aeronautics and
Space Administration

# FULL SCALE TECHNOLOGY DEMONSTRATION OF A MODERN COUNTERROTATING UNDUCTED FAN ENGINE CONCEPT

## ENGINE TEST

## FOREWORD

This report presents the results of engine tests and a discussion thereof, as conducted by GE Aircraft Engines, Cincinnati, Ohio. These engine tests were performed on behalf of the NASA Lewis Research Center, Cleveland, Ohio, under Contract NAS3-24210. The program was carried out under the technical cognizance of Mr. R.D. Hager of the Advanced Turboprop Project Office. The contract effort was conducted at the Evendale Plant of GE Aircraft Engines by the GE36 Project Department.

# TABLE OF CONTENTS

## TABLE OF CONTENTS (Continued)

TABLE OF CONTENTS (Concluded)

# LIST OF ILLUSTRATIONS

## LIST OF ILLUSTRATIONS (Continued)

## LIST OF ILLUSTRATIONS (Continued)

## LIST OF ILLUSTRATIONS (Continued)

## LIST OF ILLUSTRATIONS (Continued)

## LIST OF ILLUSTRATIONS (Concluded)

# LIST OF TABLES

## 1.0 ENGINE TEST SUMMARY

This Engine Test Report covers the UDF™ (unducted fan) Engine 082-001 ground testing at the GE Aircraft Engines Peebles Test Facility and includes Builds 1 through 3 of Engine 082-001. Note: A new build number indicates a significant change in engine hardware.

The UDF™ engine successfully completed a ground-test program exceeding 100-hours duration. The basic concepts of the engine have been successfully demonstrated. Some of the accomplishments are as follows:

- Full thrust (25,000 pounds corrected) demonstrated
- Full propulsor rotor speed demonstrated (1393+ rpm)
- Specific fuel consumption (sfc) was better than predicted; sfc of < 0.24 lb/hr/lb was demonstrated
- Flawless operation of the F404 gas generator
- Counterrotation of structures, turbines, and fan blades
- Actuation system operation successfully demonstrated
- Control system operation successfully demonstrated
- New fan blade design successfully demonstrated
- Reverse thrust successfully demonstrated.

The UDF™ was ground tested at Peebles for a total run time of 100:51 hours. This was split between Builds 1 through 3 as follows.

| Build | Run Time per Build | Total Run Time |
|---|---|---|
| 1 | 5:24 | 5:24 |
| 2 | 29:20 | 43:44 |
| 3 | 66:07 | 100:51 |

In Figures 1-1 through 1-4, the engine run time is a function of Stage 1 propulsor fan speed (XN48), Stage 2 propulsor fan speed (XN49), exhaust gas temperature (T46), and thrust, respectively. Thrust data were available for Build 3 only. Note that on the plots of run time as a function of propulsor

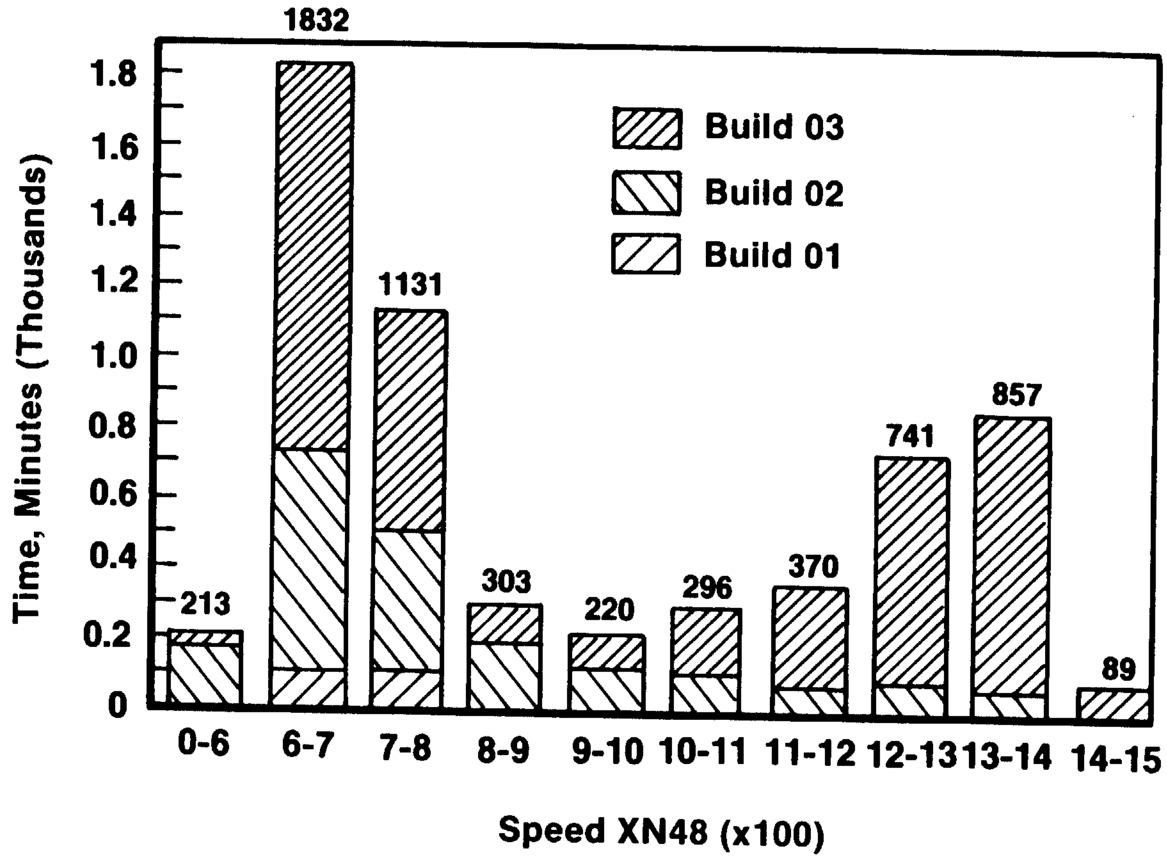


Figure 1-1. Total Run Time at Various XN48, Times as of July 8, 1986.

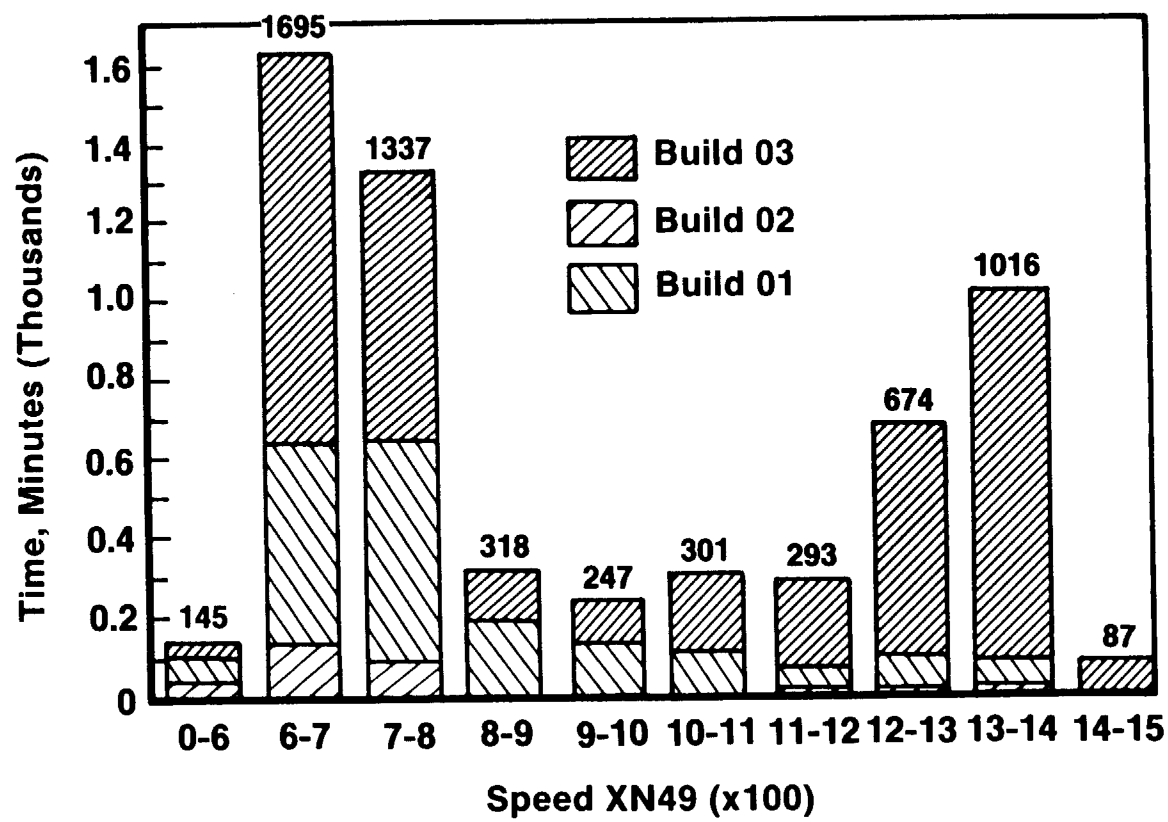


Figure 1-2. Total Run Times at Various XN49, Times as of July 8, 1986.

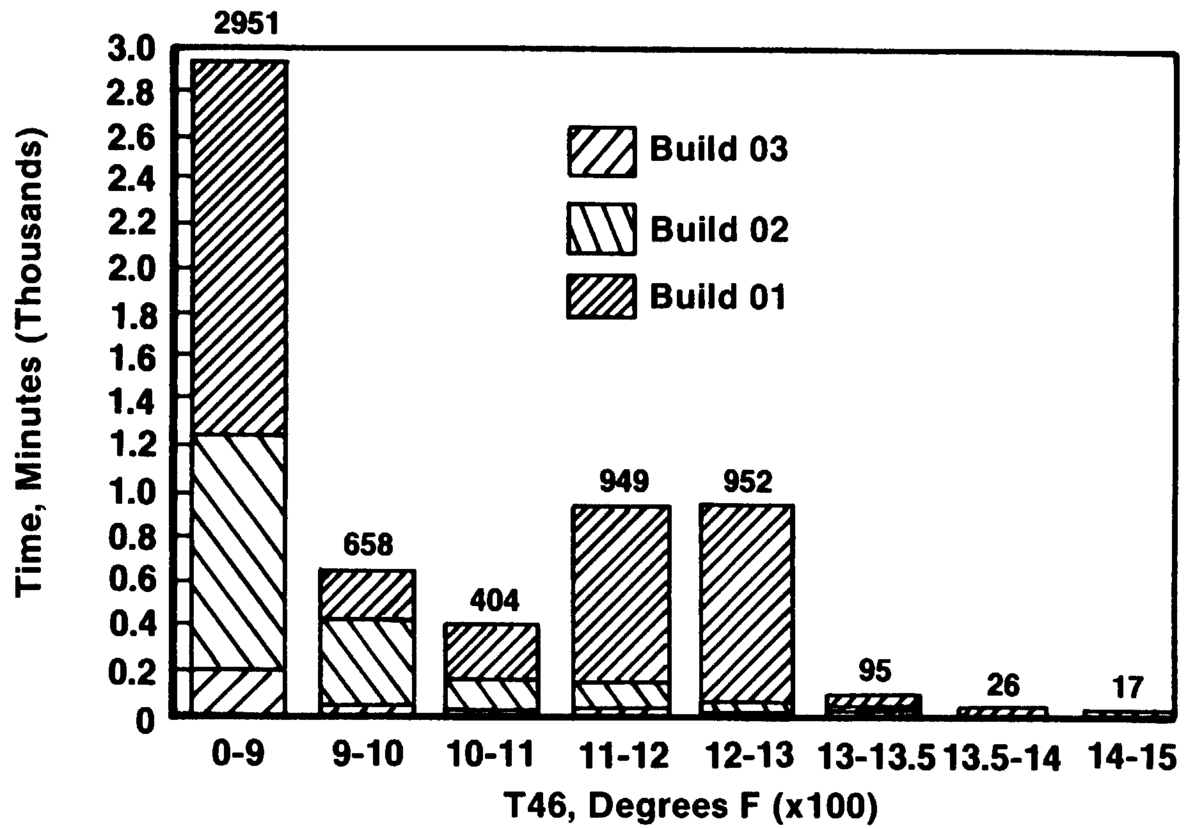


Figure 1-3. Total Run Time at Various T46, Time as of July 8, 1986.

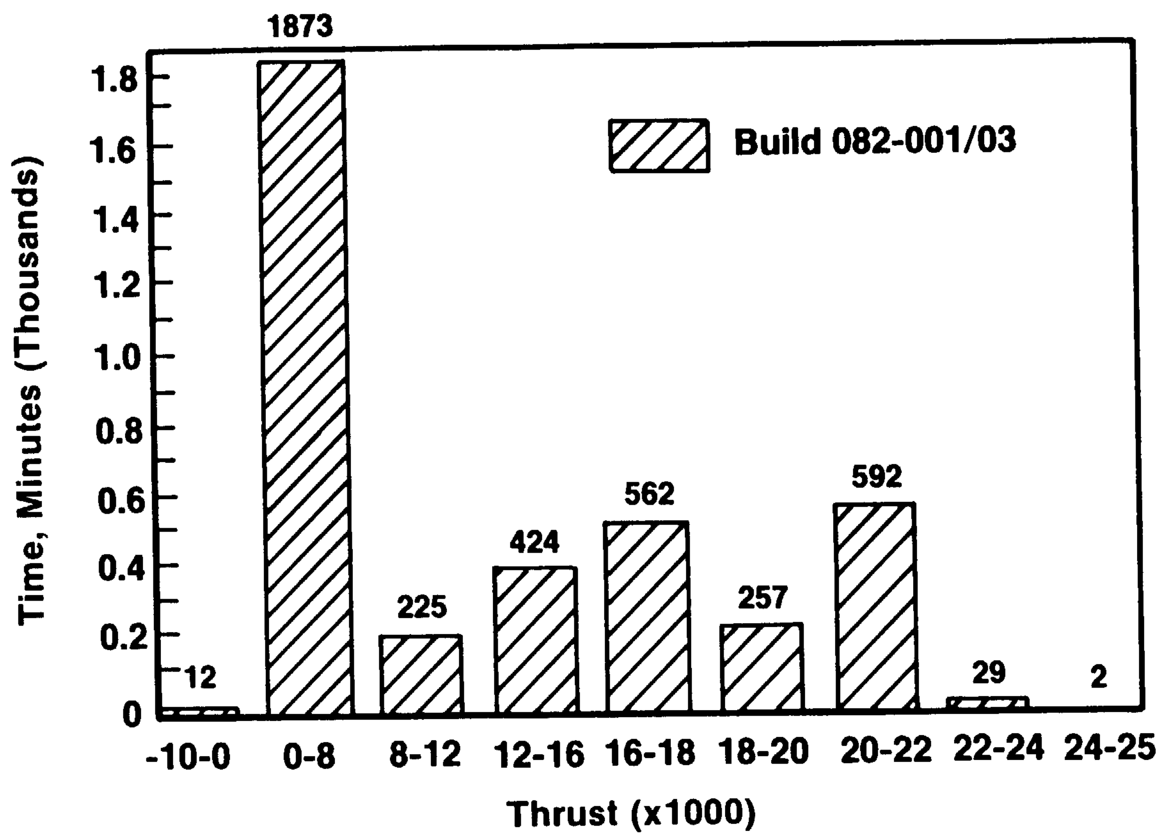


Figure 1-4. Run Time at Various Thrust Levels, Build 082-001/03 Only.

speed, there is a large amount of time spent in the ranges of 600 to 700 rpm and 700 to 800 rpm. Most of this time was spent in the immediate vicinity of 700 rpm, which is idle for this engine. Also note that the vast majority of time spent in the 1400 to 1500 rpm range was actually spent near 1400 rpm.

## 1.1 SIGNIFICANT HARDWARE CHANGES AND MODIFICATIONS

Significant hardware changes and modifications which occurred during the UDF™ ground test are listed below. A more detailed discussion is provided in the sections enumerated.

| | Section |
|---|---|
| **Build 1 to 1A** | |
| Forward stationary carbon seal and 2R bearing replaced | 3.1 |
| **Build 1A** | |
| Forward telemetry system antenna modified | 3.2 |
| Added pipe-elbow air scoops to exhaust nozzle to aid aft telemetry system cooling | 3.3 |
| **Build 1A to Build 2** | |
| All propulsor turbine blades replaced (Stages 1-4 and 6-11) | 3.4 |
| Propulsor turbine blade tip clearances increased | 3.4 |
| Damper pins added between all propulsor turbine blades | 3.4, 3.5 |
| Spool distress repaired | 3.4 |
| Pipe-elbow scoops were replaced with aerodynamic air scoops | 3.3 |
| Leading edge plugs were installed in propulsor fan blades | 3.11 |
| Installed redesigned stationary exhaust nozzle (centerbody) | 3.7, 7.3 |
| Installed hardware to solve subidle oil leak problem | 3.6 |
| **Build 2** | |
| Propulsor Stage 2, No. 7 fan blade replaced after blade-out | 3.10 |
| Added additional holes to telemetry system air scoops | 3.3 |
| Installed compressor discharge pressure (PS3) accumulator system | 6.0 |
| Installed redesigned fan bypass bleed valve diffuser | 3.9 |

| | Section |
|---|---|
| Build 2 to Build 3 | |
| Installed redesigned propulsor Stages 1 and 2 fan blades | 3.11 |
| Installed improved PS3 accumulator system | 6.0 |
| Build 3 | |
| No significant changes | |
| Postbuild 3 | |
| Replaced all propulsor Stage 1 turbine blades | 3.17 |
| Replaced three propulsor Stage 11 turbine blades | 3.17 |
| Added positive mechanical retention feature to 1R bearing nut | 3.17 |
| Replaced 1R and 2R bearings | 3.17 |
| Repaired IGV (inlet guide vane) - lip replaced with honeycomb | 3.17 |
| Drilled oil drain holes in propulsor | 3.17 |
| Borescope ports added to mixer frame to gain better access to Stage 1 turbine blades | 3.17 |
| Replaced actuator control rods | 3.17 |
| Installed additional air scoops for cooling aft telemetry system | 3.3 |

## 1.2 OVERALL HISTORY OF UDF™ ENGINE TESTING

Tables 1-1 through 1-3 present an overall history of UDF™ testing.

Table 1-1. GE36 Test History - Engine 082-001, Build 1/1A.

| Date (1985) | | TRT |
|---|---|---|
| Aug. 29 | First Run to Idle; Broken Carbon Seal Caused Internal Oil Leak Resulting in a Rotor Unbalance; Caused a Turbine Rub Which Cracked Some Stage 11 Turbine Blades | 0:02 |
| Aug. 30-Sept. 11 | Engine Removed from Site; Carbon Seal and 2R Bearing Replaced | |
| | Build 1A | |
| Sept. 14 | Engine Returned to Test; Idle Achieved | 0:11 |
| Sept. 15-17 | Worked Instrumentation Faults | |
| Sept. 18 | Mechanical Check-Out | 0:14 |
| Sept. 19 | Mechanical Check-Out<br>Reached Full Propulsor Speed | 1:10 |
| Sept. 20-26 | Modified Forward Telemetry Antenna | |
| Sept. 27 | Reached 22,000 lbf; Shutdown Due to High Aft Telemetry Temperatures | 3:43 |
| Sept. 28-Oct. 1 | Added Air Scoops to Exhaust Nozzle to Cool Aft Telemetry System | |
| Oct. 2 | Reached 24,000 lbf; Engine S/D Following Stall (Stage 1 Turbine Blade Failure) | 5:24 |
| Oct. 3 | Engine Removed for Repair | |

Table 1-2. GE36 Test History - Engine 082-001, Build 2.

| Date (1986) | | Build 2 Run Time | TRT |
|---|---|---|---|
| Jan. 30-31 | Resumed Testing; Mechanical Check-Out; Reached 22,000 Thrust | 3:38 | 9:02 |
| Feb. 2-3 | Testing With Facility Fans On; Fan Bypass Bleed Valve Calibration; Bleed Valve Diffuser Can Failure; Engine Trim Balance (20,000 Maximum Thrust) | 9:49 | 15:13 |
| Feb. 5-8 | Repaired Instrumentation and Aft Telemetry System | 13:28 | 18:52 |
| Feb. 9 | Telemetry System Check-Out (to 1200 rpm Fan Speed); Started Down Power Calibration Ran Twice to 24,000 Thrust; on 2nd 24,000 Pt. Lost Stage 2, No. 7 Fan Blade Shell | 15:16 | 20:40 |
| Feb. 17-18 | Engine Health Check - With New Blade Reached 1200 rpm Fan Speed; 16,000 Thrust; Tested with Vortex Destroyer | 16:30 | 21:54 |
| Feb. 28 | Turbine Frame Stress Investigation; 1000 rpm Maximum Fan Speed | 20:36 | 26:00 |
| March 5 | Stress Survey; 1029 rpm Maximum Fan Speed | 22:55 | 28:19 |
| March 6-30 | Moved Engine from Site 4A to 3D | | |
| April 1-2 | Stress Survey; 1150 rpm Maximum Fan Speed | 25:44 | 30:68 |
| April 3-7 | Added Additional Holes to Aft Telemetry System Cooling Scoops | | |
| April 8 | Reverse Testing/Cooling Scoop Testing | 26:22 | 31:46 |
| April 18 | Control Verification; Control Fault Caused Stage 2 Overspeed; Engine Shutdown | 28:30 | 33:54 |
| April 19-23 | Installed PS3 Accumulator to Slow Propulsor Accel Rate | | |
| April 24 | Engine Test With PS3 Accumulator; 1150 rpm Maximum Fan Speed | 29:20 | 34:44 |

Table 1-3. GE36 Test History - Engine 082-001, Build 3.

| Date (1986) | | Build 3 Run Time | TRT |
|---|---|---|---|
| June 20 | Returned to Test; Achieved Idle | 0:16 | 35:02 |
| June 23 | Reverse Testing; | 0:45 | 35:29 |
| | Mechanical Check-Out; 1270 rpm Maximum Fan Speed | 2:07 | 36:51 |
| June 24 | Mechanical Check-Out/Trim Balance Reached 24,000 Maximum Thrust | 4:33 | 39:17 |
| June 25 | Trim Balance/Bleed Valve Calibration Reached 18,000 Thrust | 8:18 | 43:02 |
| June 26 | Bleed Valve Calibration/Trim Balance Reached 23,000 Thrust | 10:00 | 44:44 |
| June 29 | Bleed Valve Calibration; Reached 19,000 Thrust | 12:17 | 47:01 |
| June 30 | Down Power Calibration; Shutdown from 19,000 Thrust Due to Fuel Leak; Aft Propulsor Rotor Locked up Until Engine Cooled | 12:51 | 47:35 |
| July 1 | Down Power Calibration; Reached 24,000 Thrust; | 17:36 | 52:20 |
| | Performance Optimization Testing | 20:18 | 55:02 |
| July 3 | Performance Optimization/Vibration Survey/Trim Balance; Reached 21,000 | 25:38 | 60:22 |
| | Thrust Control Tests; Reached 24,000 lbf | 29:53 | 64:37 |
| July 4 | Reverse Testing (to 850 rpm Fan Speed) | 30:34 | 65:28 |
| July 4-7 | LCF Cycles (100) | 59:45 | 94:29 |
| July 8 | Bodes; Reached 21,000 Thrust; Trim Balance; Reached 22,000 Thrust; | 62:31 | 97:15 |
| | Propulsor Rotors Locked Together after a Normal Shutdown | 66:07 | 100:51 |
| | End of Ground Testing at Peebles | | |

# 2.0 INTRODUCTION

## 2.1 ENGINE DESCRIPTION

The UDF™ engine is a new aircraft engine concept that is based on an ungeared, counterrotating, unducted ultra-high-bypass turbofan configuration. This engine is being developed by General Electric to provide a high thrust-to-weight ratio power plant with exceptional fuel efficiency for subsonic aircraft application.

The engine encompasses the operational flexibility and fuel efficiency of a two-spool core gas generator with the propulsive efficiency of a propeller (moderate diameter and tip speed). The engine is based on an aft-mounted, counterrotating power turbine that aerodynamically couples with a basic gas generator engine and provides for direct conversion of the gas generator engine power into propulsive thrust without requiring a gearbox or additional shafting. The concept of counterrotating fan blades is being utilized to capitalize on the full propulsive efficiency of this configuration; that is, the exit swirl from the first blade row is recovered by the second row and converted into propulsive thrust. The turbine transmits its power through two counterrotating power turbine frames which, in turn, transmit power to the UDF™ blades through the polygonal support rings which act as the primary-load carrying support structure for the fan blades. This isolates the turbine flowpath from out-of-round distortions from the fan blade loads.

The counterrotating turbine rotors, power turbine frames, fan blades, and static structures are components which comprise the "propulsor" for the UDF™ engine. Mounted in front of the propulsor is a gas generator engine which provides the required gas horsepower. The gas generator is a modified production F404 turbofan engine.

Figure 2-1 shows a cross-sectional view of the UDF™ engine. An enlarged cross section of the propulsor is presented in Figure 2-2. Figures 2-3 and 2-4 are UDF™ photos at Peebles Test Site 4A, and Figure 2-5 depicts a UDF™ at Test Site 3D.

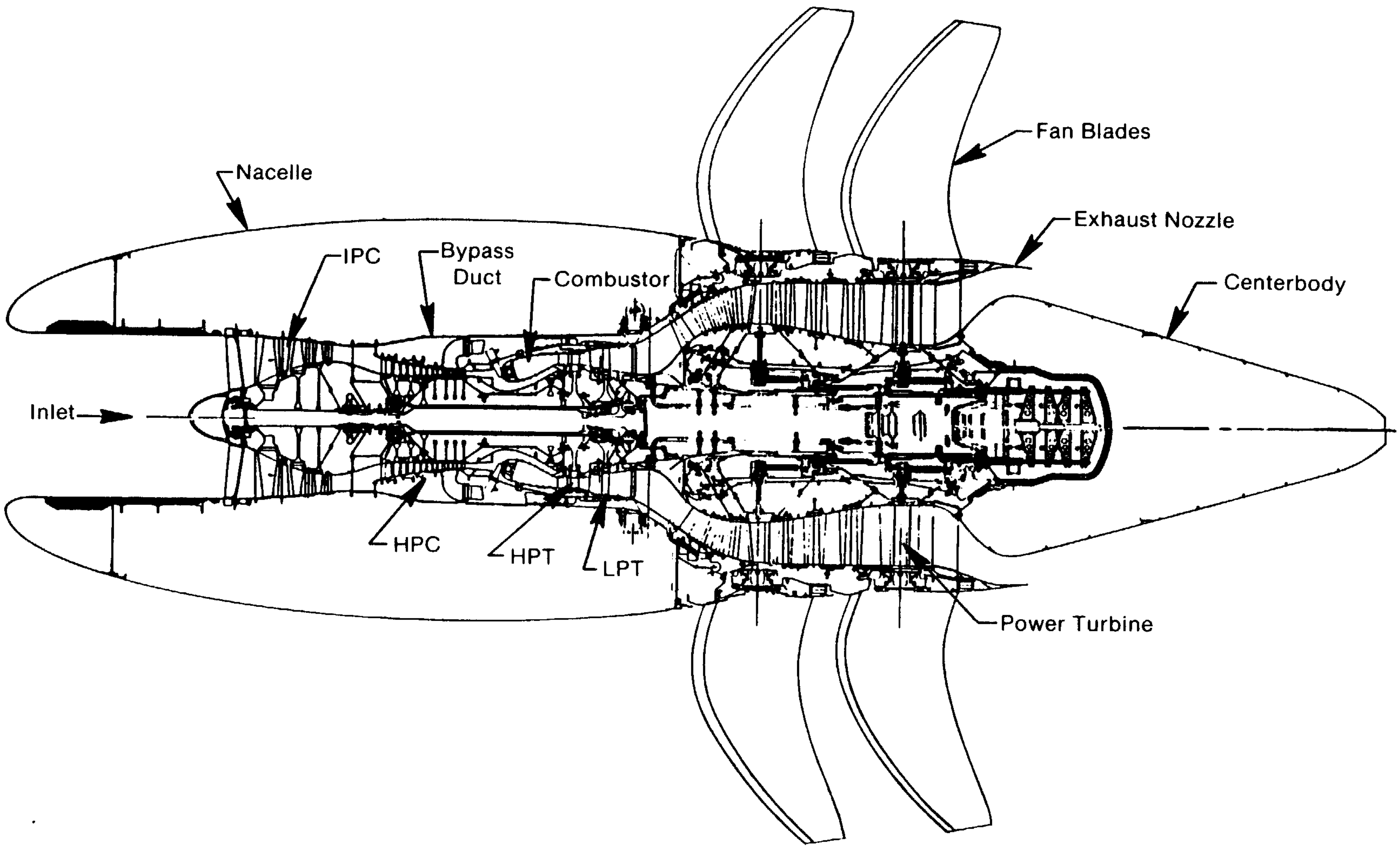


Figure 2-1. Cross Section of Unducted Fan Engine.

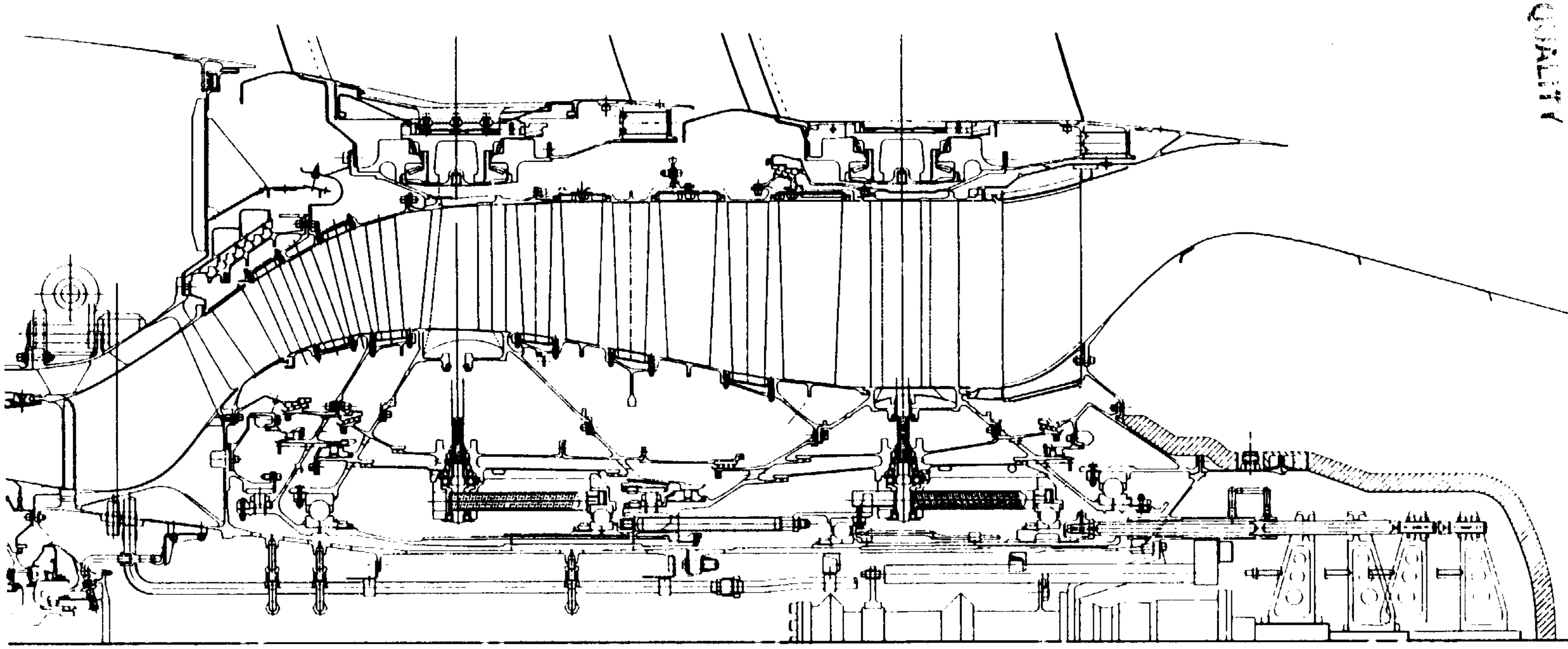

Figure 2-2. Cross Section of UDF™ Engine (Enlarged View).

~~ORIGINAL PAGE~~ IS
~~OF POOR QUALITY~~


Figure 2-3. UDF™ Engine at Peebles Test Site 4A.



ORIGINAL PAGE
BLACK AND WHITE PHOTOGRAPH

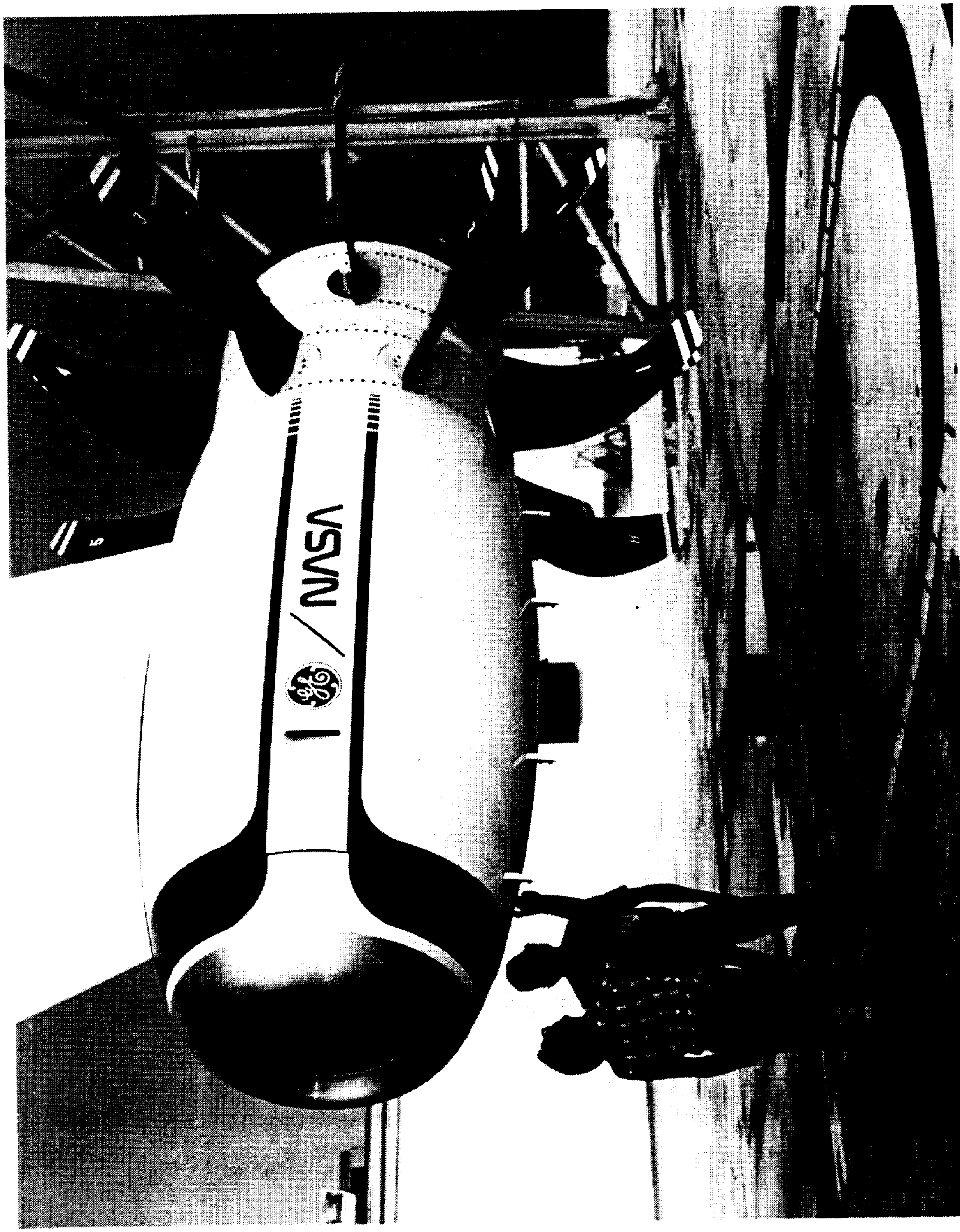


Figure 2-4. UDF™ Engine at Peebles Test Site 4A.

ORIGINAL PAGE
BLACK AND WHITE PHOTOGRAPH

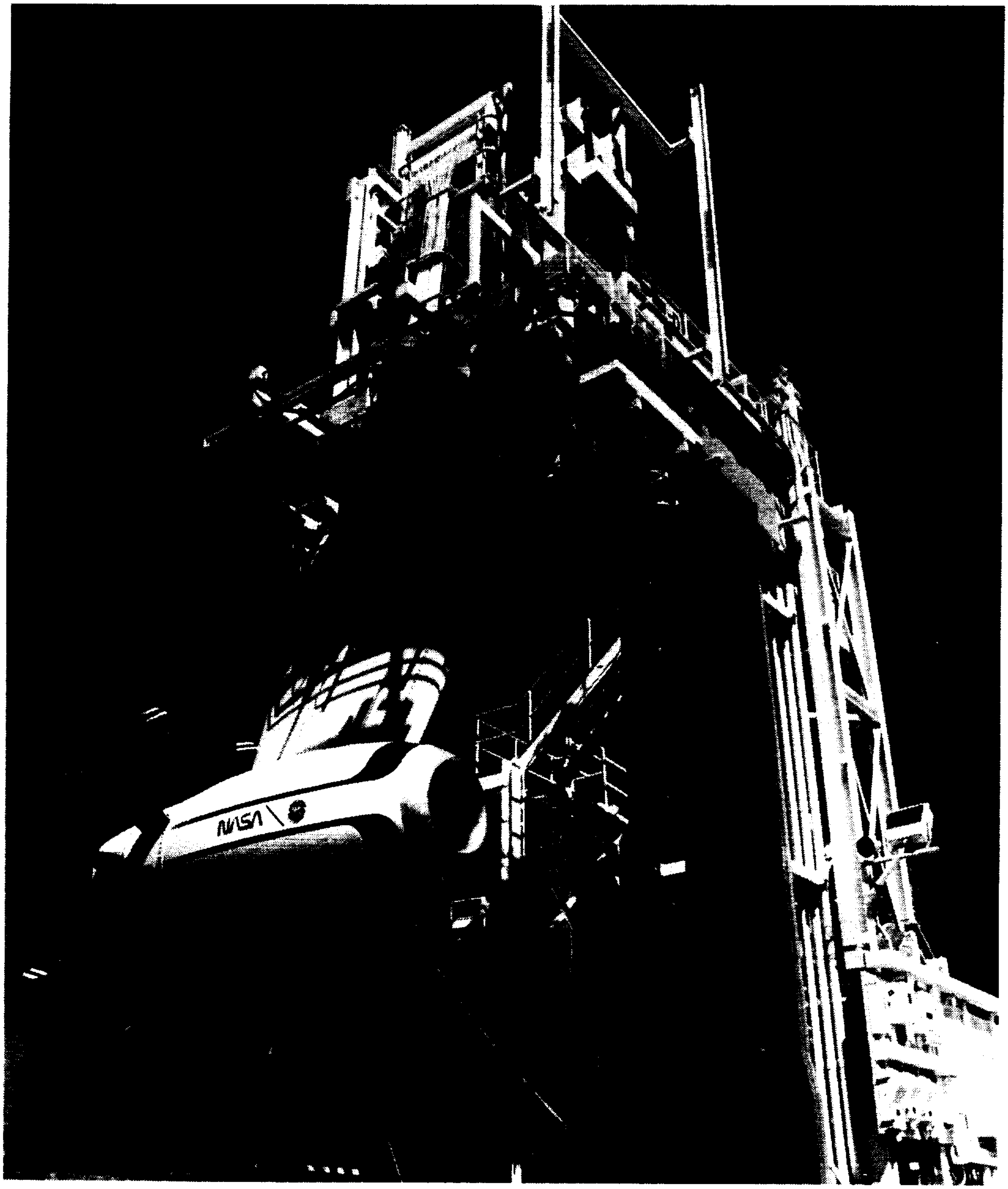


Figure 2-5. UDF™ Engine at Peebles Test Site 3D.



ORIGINAL PAGE IS
OF POOR QUALITY

The major design characteristics of the UDF™ engine are as follows:

Gas Generator

| | |
|---|---|
| Model | F404-GE-400 |
| Type | Low bypass turbofan |
| Fan | 3-stage axial flow |
| Compressor | 7-stage axial flow |
| Turbines | |
| Low pressure | One stage |
| High pressure | One stage |
| Rotor speeds | |
| Fan | 13,270 rpm (100%) |
| Compressor | 16,810 rpm (100%) |
| Maximum airflow | Approximately 140 lbm/s |
| Thrust | 16,000 lbf class |
| Thrust-to-weight ratio | 8:1 class |
| Overall compression ratio (maximum climb) | 26:1 |

UDF™ Engine Propulsor

| | |
|---|---|
| Maximum nacelle diameter | 76.4 inches |
| Fan blade tip diameter | 11.67 feet |
| Fan design point tip speed, physical (maximum cruise; 35,000 ft; 0.80 Mach; ISA) | 780 feet/second |
| Fan rotor speed | 1393 rpm (100%) |
| Fan disk loading, class SHP/A (maximum cruise; 35,000 ft; 0.80 Mach; ISA) | 87 HP/ft$^2$ |
| Fan blade radius ratio | 0.415 |
| Power turbine inlet temperature (SL, T/O, ISA +27° F). | 1310° F |

The gas generator/propulsor combination produces an engine with a net thrust of 25,000 pounds. Other significant design features which have been incorporated into this engine are:

- Advanced unducted fan aerodynamics that incorporate custom-tailored composite fan blades over an inner titanium spar that serves as the attachment mechanism to the engine for the fan blades.

- Fully developed and available gas generator to provide the necessary power for the engine.
- DEC (digital electronic control) that provides overall engine control by monitoring gas generator power and speed and propulsor speeds and pitch angles. The engine uses the existing gas generator control and a separate propulsor control to minimize development costs without sacrificing control flexibility.
- Hydraulic/mechanical actuation system enabling setting the fan blade pitch angle of the two fan blade rotors either together or differentially; this system is driven by the control system.
- Modular assembly of the gas generator and propulsor.
- Individually replaceable propulsor fan blades with the engine installed on the aircraft or test stand.

## 2.2 INSTRUMENTATION

The UDF™ instrumentation consists both of static and rotating instrumentation, with the rotating instrumentation being read out by telemetry on the rotors. Static instrumentation includes temperature, pressure, kulite, strain gage, and accelerometer instrumentation on the engine, pylon, and nacelle. Rotating instrumentation includes temperature, pressure, and strain gage instrumentation on the counterrotating rotors. Detailed information on UDF™ instrumentation is contained in the Instrumentation Plan (Statement of Work Paragraph 4.2 of Contract No. NAS-24210). Included in this is Drawing No. 4013341-034, which shows the engine cross section with the location of engine instrumentation and the corresponding parameter names. Reference GE36 Second Ground Test TPS No. MA-0004 for a detailed description of the instrumentation system and for a list and description of all parameters.

# 3.0 REVIEW OF UDF™ TESTING

The following significant events, data points, and problem areas from UDF™ testing will be expanded upon in the indicated sections:

| | Builds Involved | Section |
|---|---|---|
| Forward stationary carbon seal failure | 1 | 3.1 |
| Forward telemetry antenna repair | 1 | 3.2 |
| Telemetry system temperature problem (includes reverse thrust test data) | 1,2,3 | 3.3 |
| Stage 1 turbine blade failure and stall event | 1 | 3.4 |
| Turbine blade damper effectiveness | 1,2,3 | 3.5 |
| Subidle oil leak problem | 1,2 | 3.6 |
| Stationary exhaust nozzle (centerbody) replacement | 1,2 | 3.7,7.3 |
| Fan bypass bleed valve calibration | 2,3 | 3.8 |
| Fan bypass bleed valve diffuser failure/replacement | 2 | 3.9 |
| Propulsor fan-blade-loss event | 2 | 3.10 |
| Propulsor fan blade history and test data | 1,2,3 | 3.11 |
| Power turbine frame stress investigation | 2 | 3.12 |
| Effect of "vortex destroyer" on stress | 2,3 | 3.13 |
| Effect of test site change on stress | 2,3 | 3.14 |
| Rotor lockup after shutdown resulting from fuel leak | 3 | 3.15 |
| LCF/HCF (low cycle fatigue/high cycle fatigue) testing | 1,2,3 | 3.16 |
| Rotor-to-rotor lockup/propulsor disassembly and rebuild | 3 | 3.17 |
| Miscellaneous hardware: stress data | 1,2,3 | 3.18 |
| Oil leak/oil gulping problem | 2,3 | 3.19 |
| Heat transfer and secondary flow system | 1,2,3 | 4.0 |
| Engine systems dynamics | 1,2,3 | 5.0 |
| Bearings and seals | 1,2,3 | 6.0 |
| Performance | 1,2,3 | 7.0 |
| Engine operability | 1,2,3 | 8.0 |
| Engine control | 1,2,3 | 9.0 |
| Nacelle structures | 1,2,3 | 10.0 |

## 3.1 FORWARD STATIONARY CARBON SEAL FAILURE

After the first engine start, the engine was shut down due to a low oil level warning. Carbon seal pieces were found in the propulsor scavenge screens. The engine was removed from the test site, and the propulsor was separated from the gas generator. After separation, it was found that the forward stationary carbon seal was damaged. It was determined that the seal was damaged during assembly. The 2R bearing was also found damaged, this due to carbon seal debris. New hardware was added to the engine to help guide the propulsor rotors together to avoid any damage to the seal (Figure 3-1), which was completely replaced with new hardware, along with the 2R bearing. The propulsor was remated with the gas generator with no problems, and the engine was put back on test. There were no oil leaks when the engine tests resumed.

While running the engine with the damaged carbon seal, the resulting internal oil leak caused an unbalance in the rotors. This unbalance caused the Stages 7, 9, and 11 propulsor turbine blades to rub hard against the inner 6-11 spool. Twenty-two Stage 11 blades were found to have cracks in the root. It was decided to not replace these blades but to closely monitor their stress levels.

## 3.2 FORWARD TELEMETRY ANTENNA REPAIR

Operational problems with the forward telemetry system were caused by insufficient clearance between the static and rotating forward telemetry antenna components. These components were modified to increase the cold running clearance from 0.135 to 0.250 inch, as diagrammed in Figure 3-2.

## 3.3 TELEMETRY SYSTEM TEMPERATURE PROBLEMS

Problems with the telemetry system, due to high temperatures, resulted in design changes to increase cooling. Cooling scoops were added to the rotating exhaust nozzle to bring in additional ambient air to cool the telemetry system (especially that of Stage 2). Prior to the addition of cooling scoops, there were flush vent holes in the exhaust nozzle. The following summarizes the design changes:

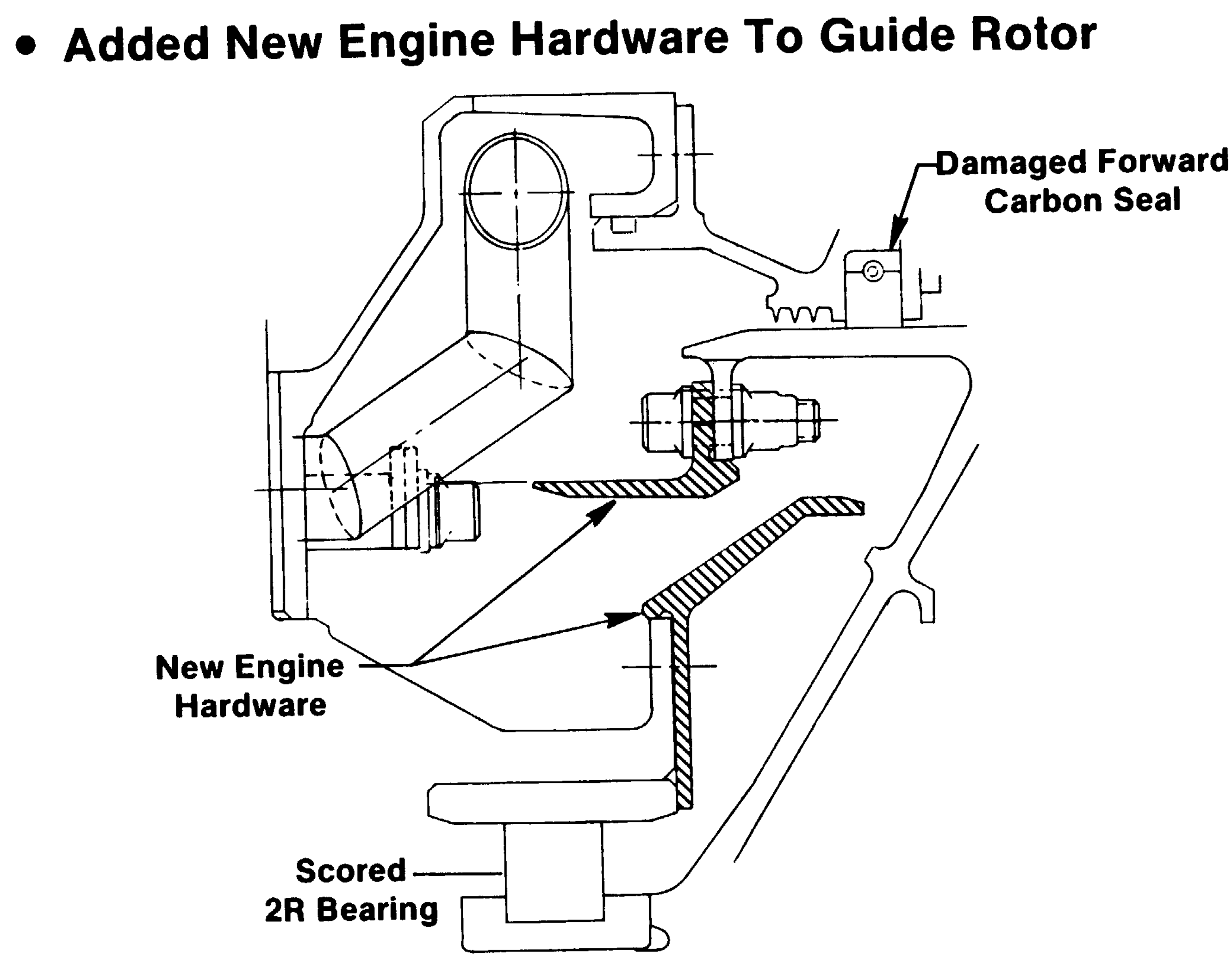


Figure 3-1. Carbon Seal Assembly Fix.

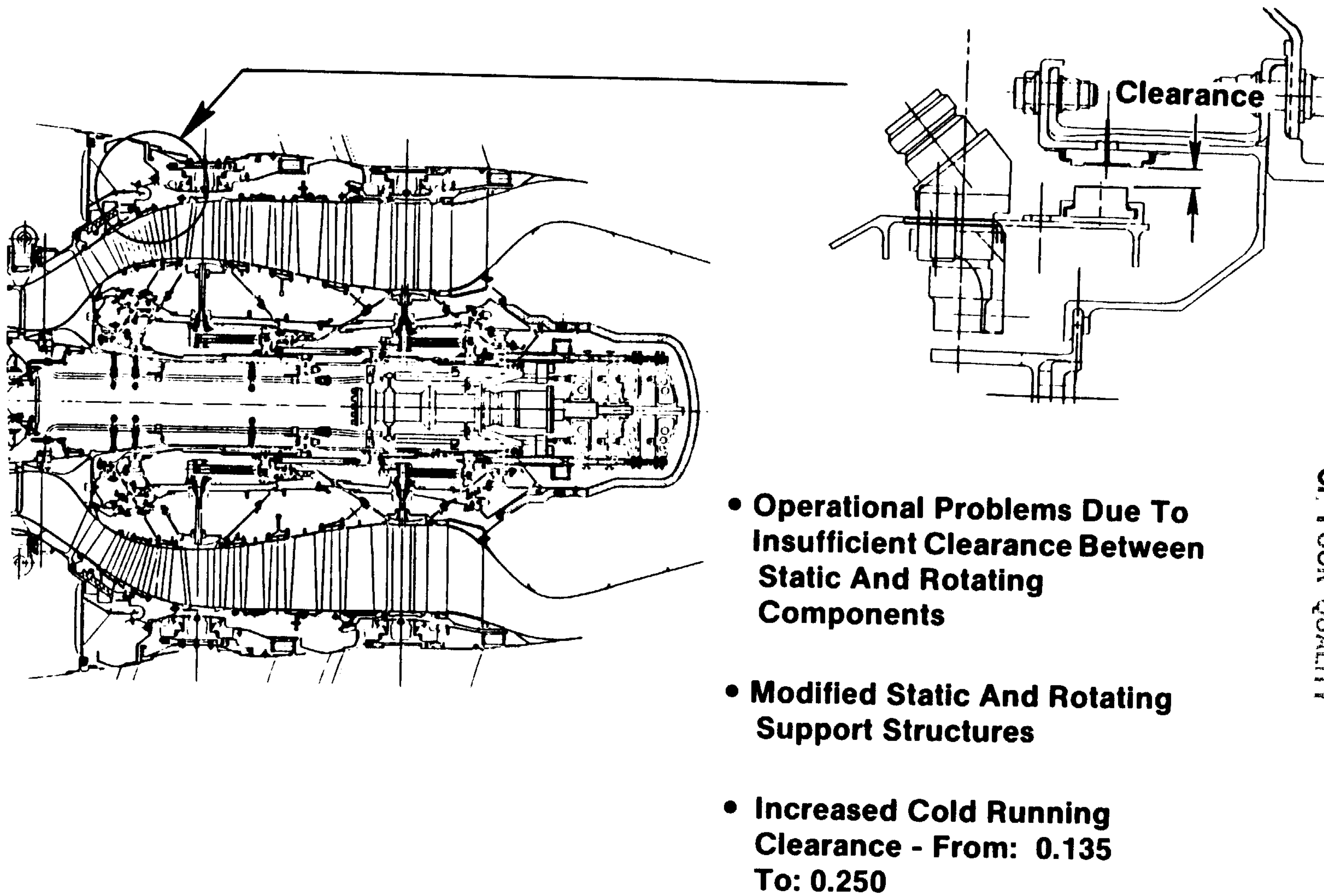


Figure 3-2. Forward Telemetry System Support.

| Configuration | Run Time With Configuration |
|---|---|
| No Scoops - flush holes (0.468-inch diameter) in exhaust nozzle, 60 total. Build 1; August 29 to September 27, 1985<br>Data Symbol: None | 3:43 hr |
| Pipe Elbow Scoops - with 0.375-inch diameter openings, 30 total. Build 1; October 2, 1985<br>Data Symbol: Pipe | 1:41 hr |
| Aerodynamic Scoops - with 0.500-inch diameter openings, 30 total. Build 2; January 30 to April 2, 1986<br>Data Symbol: Aero | 25:44 hr |
| Modified Aerodynamic Scoops - four 0.188-inch diameter holes added to side of scoops, 30 total. Build 2; April 8 to 24, 1986. Build 3; June 20 to July 8, 1986<br>Data Symbol: Mod Aero | 69:43 hr |

The addition of four holes to the side of the scoops were an attempt to increase flow to the telemetry system during static ground testing. Sixty of the modified aerodynamic scoops will be used for flight test. Figures 3-3 and 3-4 illustrate the telemetry system and cooling scoop designs.

Figures 3-5 through 3-8 show both raw telemetry temperature data and data normalized with the ambient temperature ($T_{AMB}$). The data was normalized due to the large variation in ambient temperature which has a direct effect on the telemetry temperatures. Note that temperatures recorded during Configuration 3 were cooler than those of Configuration 4. This shows the effect of ambient temperature on the telemetry temperatures. Also during Configuration 4, there was more test time and more time at power which would tend to increase temperatures. Also note that there is no data for the first two configurations for Stage 1; the thermocouple was not reading at those times. The telemetry temperature limit set during ground testing, after the first configuration, was 300° F.

During reverse thrust testing, Stage 2 telemetry temperatures increased throughout the time the engine was in reverse. Figures 3-9 and 3-10 show the telemetry temperatures during a reverse thrust cycle. This was the fifth of a series of consecutively run reverse cycles.

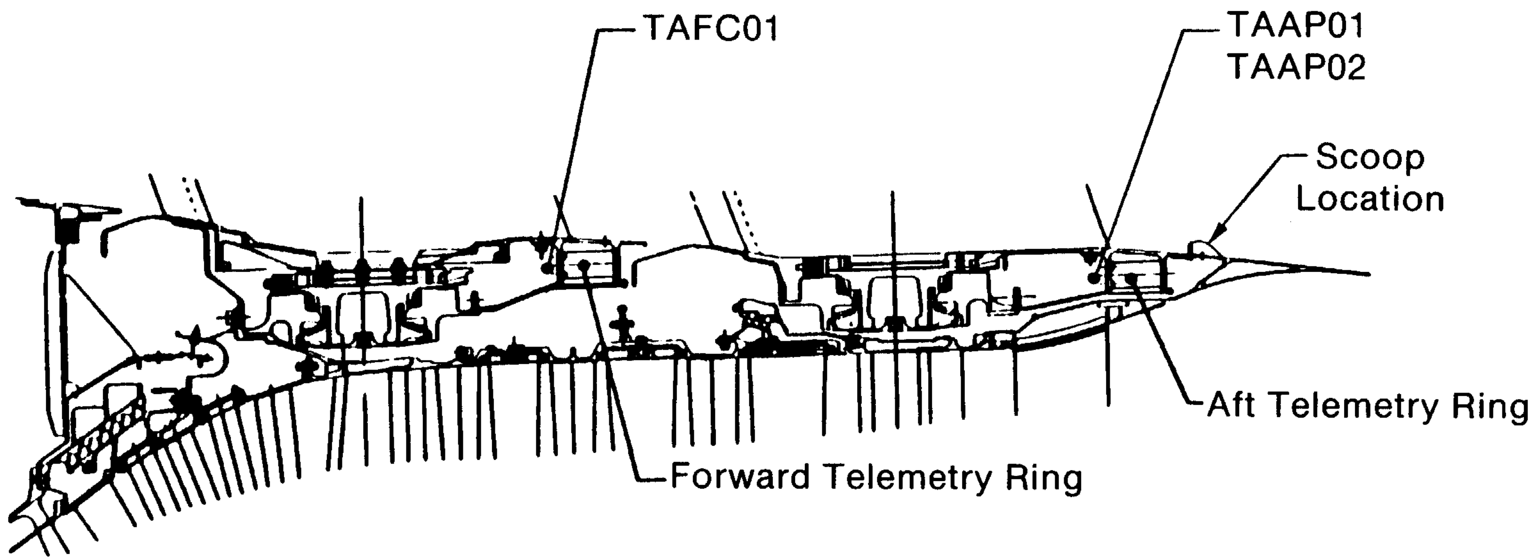


Figure 3-3.  GE36 Telemetry System.

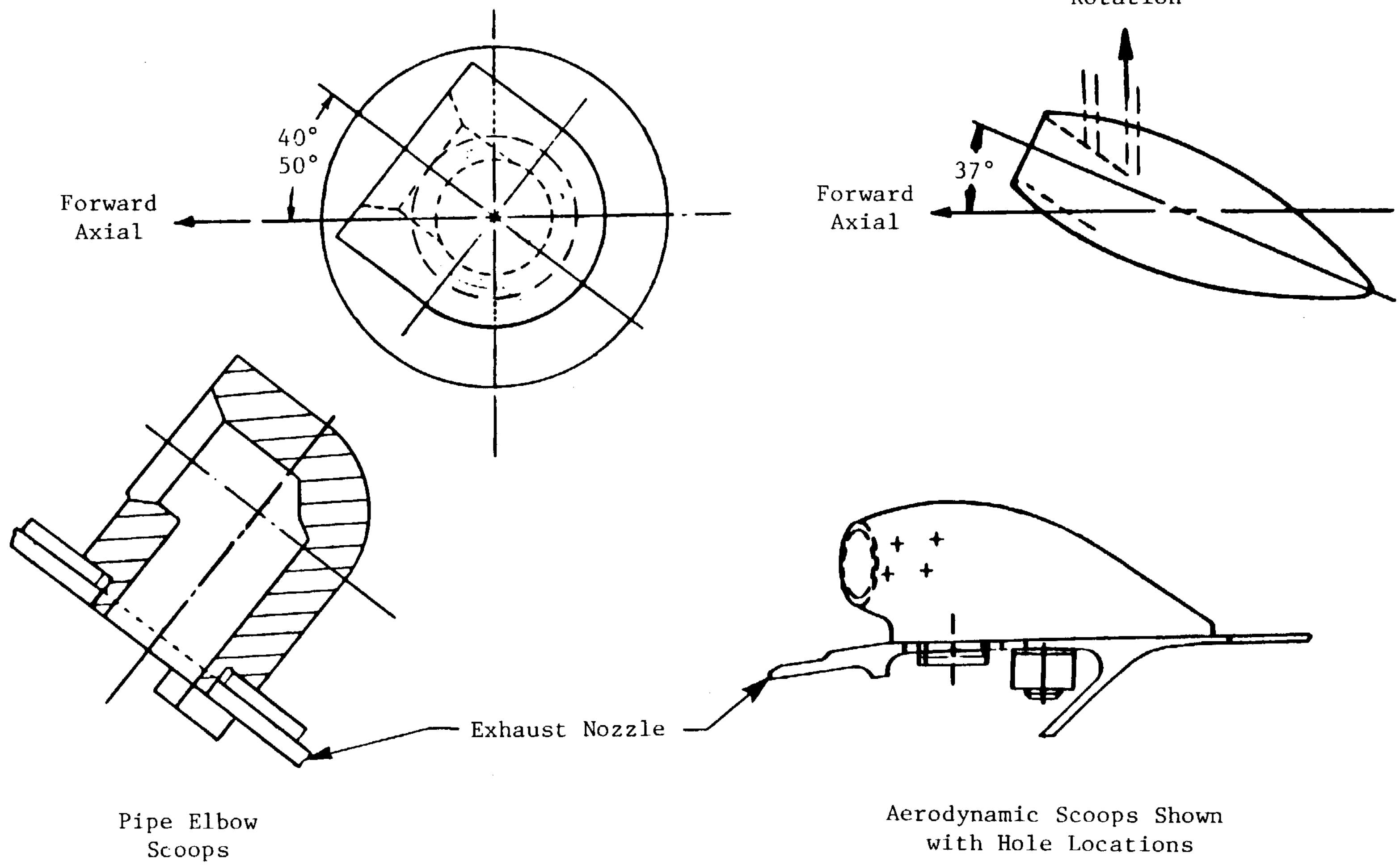


Figure 3-4. Telemetry System Scoop Designs.

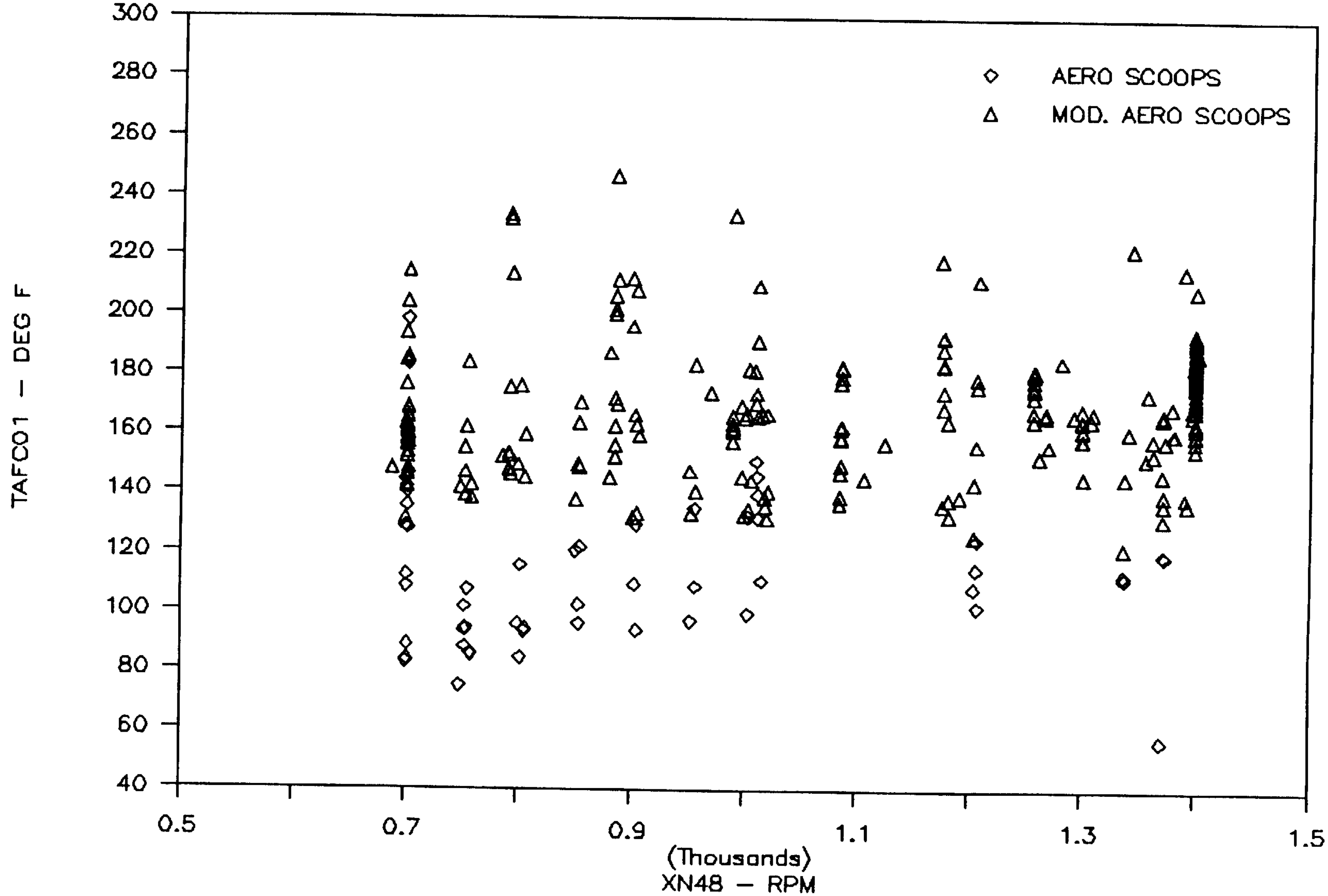


Figure 3-5. Forward Telemetry Temperatures - Raw Data.

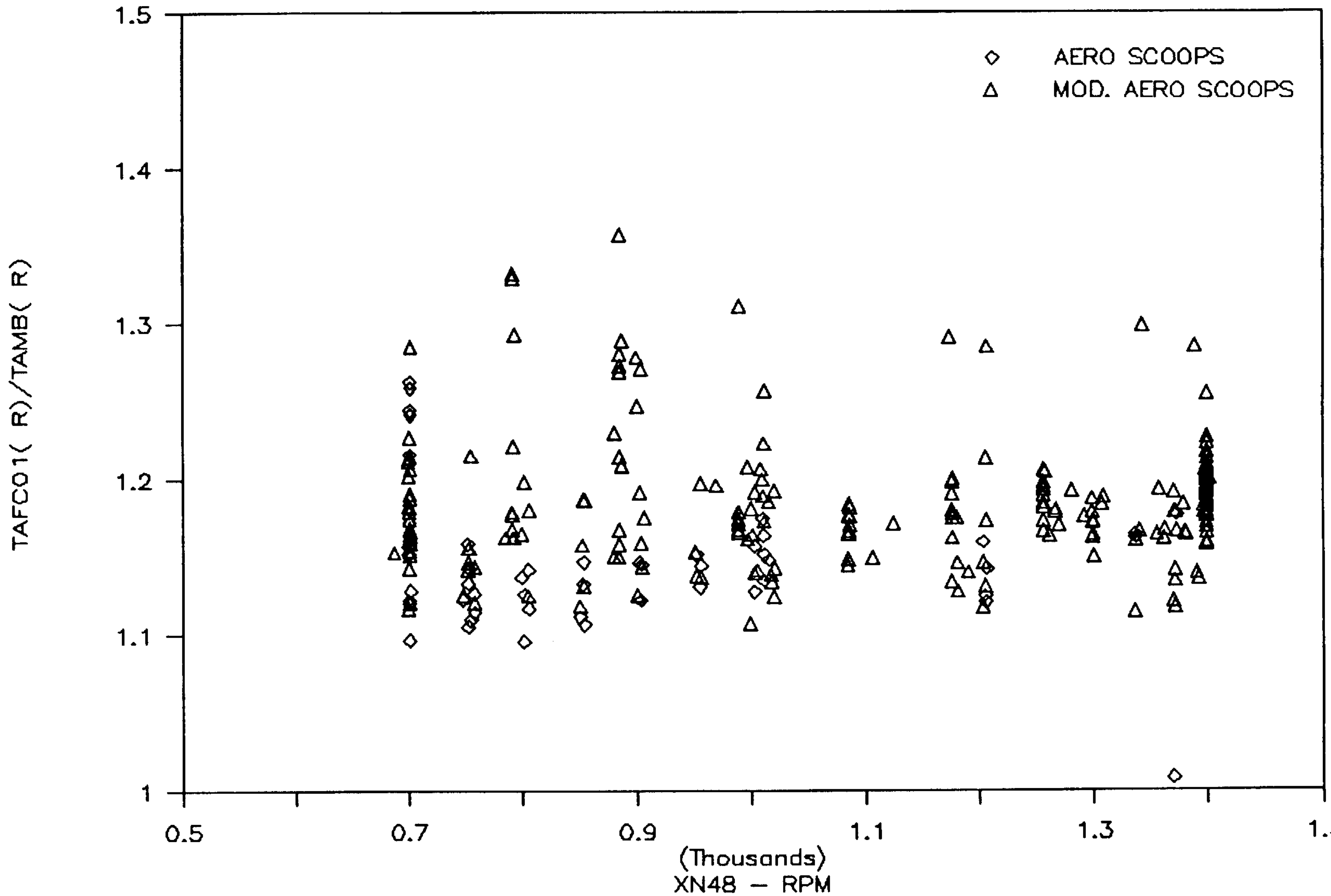


Figure 3-6. Forward Telemetry Temperatures - Normalized with $T_{AMB}$.

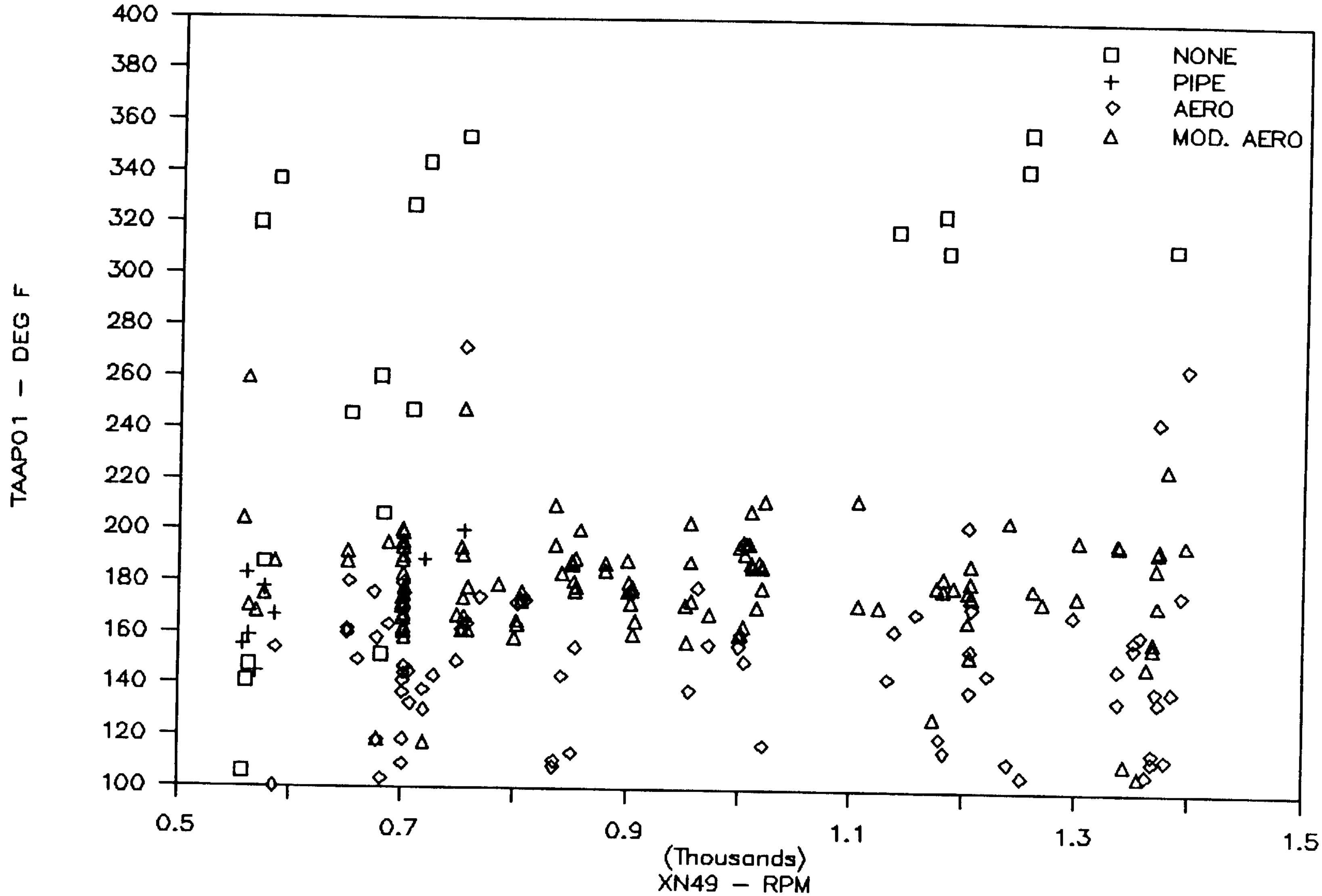


Figure 3-7. Aft Telemetry Temperatures - Raw Data.

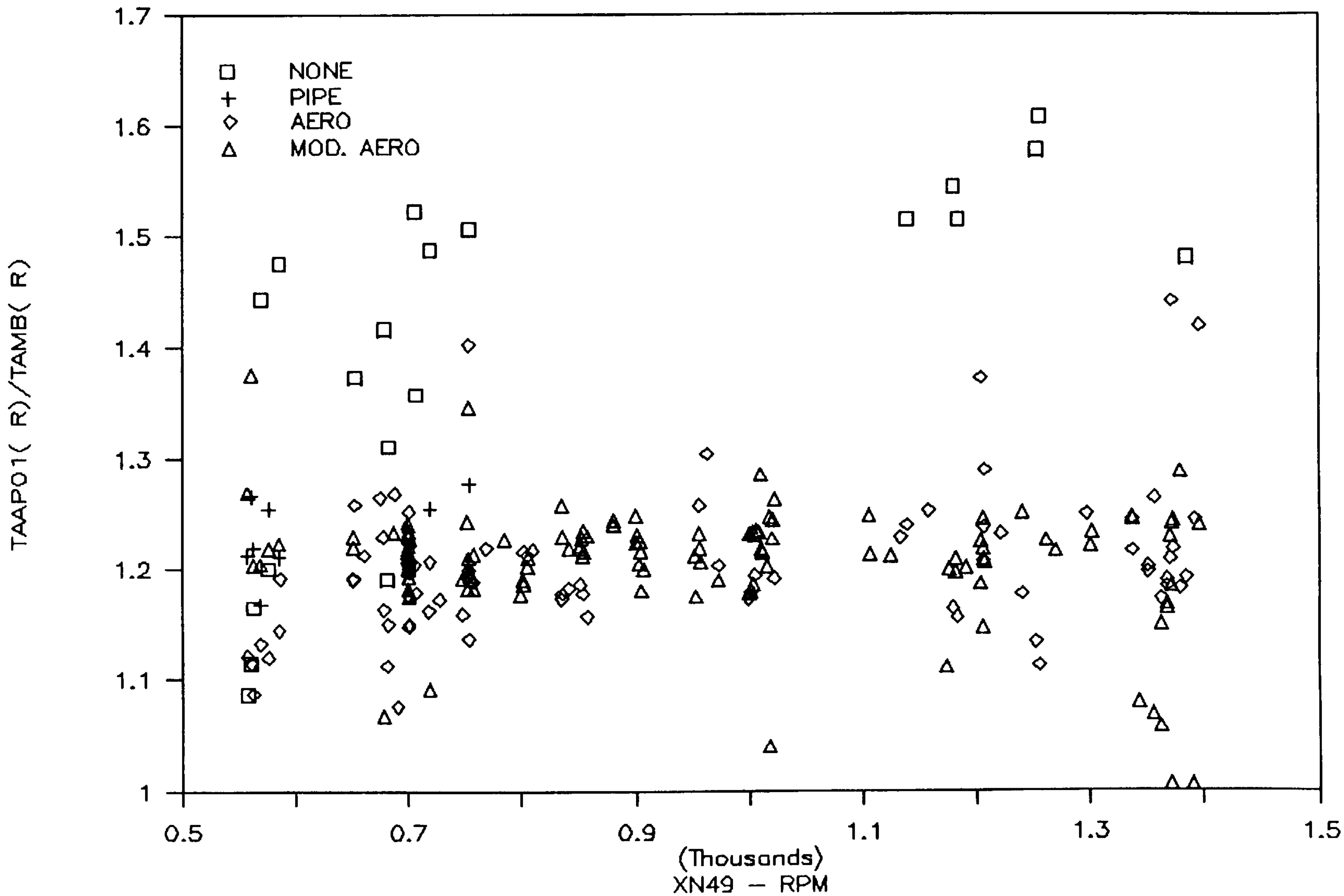


Figure 3-8. Aft Telemetry Temperatures - Normalized with $T_{AMB}$.

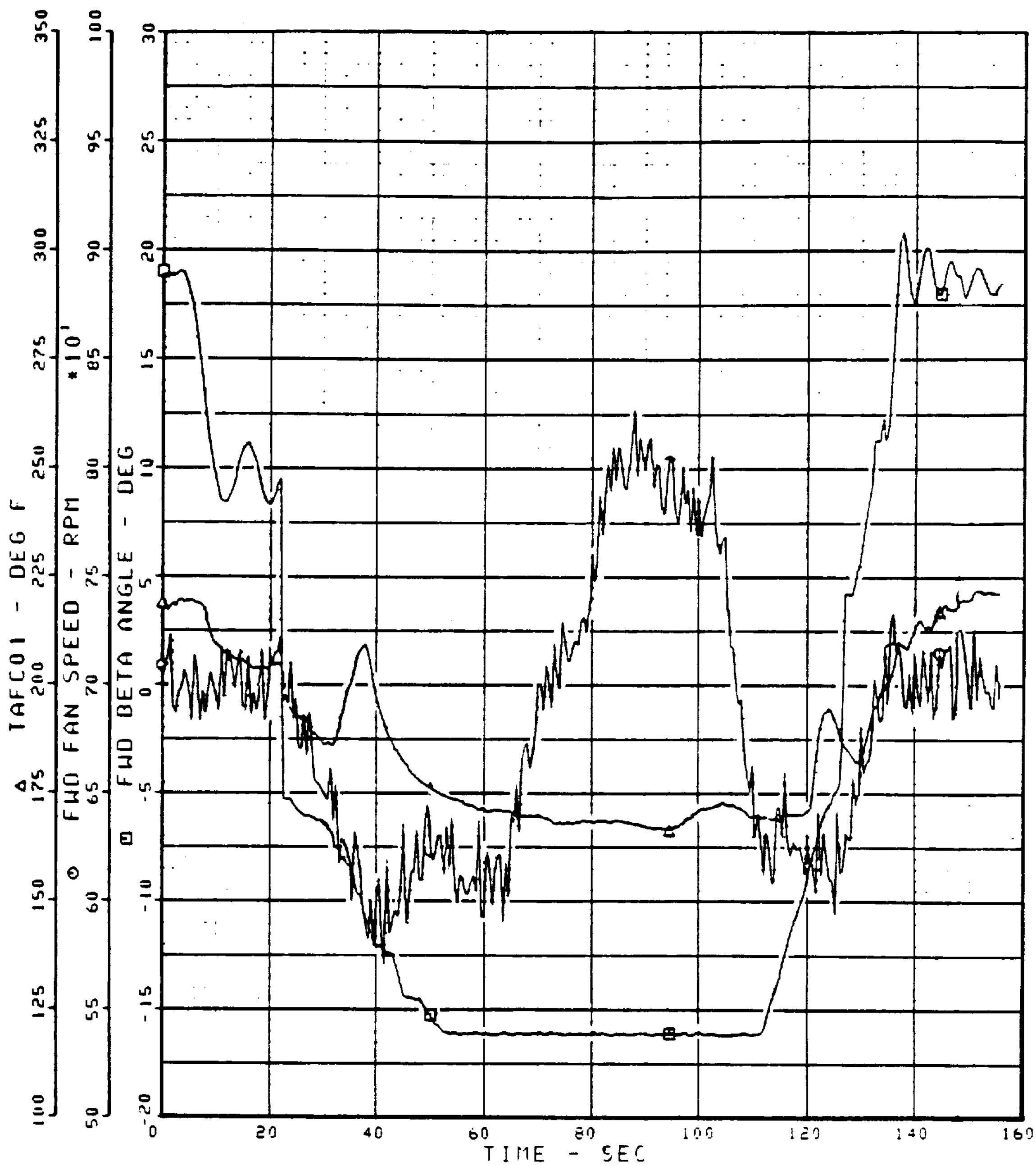


Figure 3-9. Forward Telemetry Temperatures - Reverse Testing.

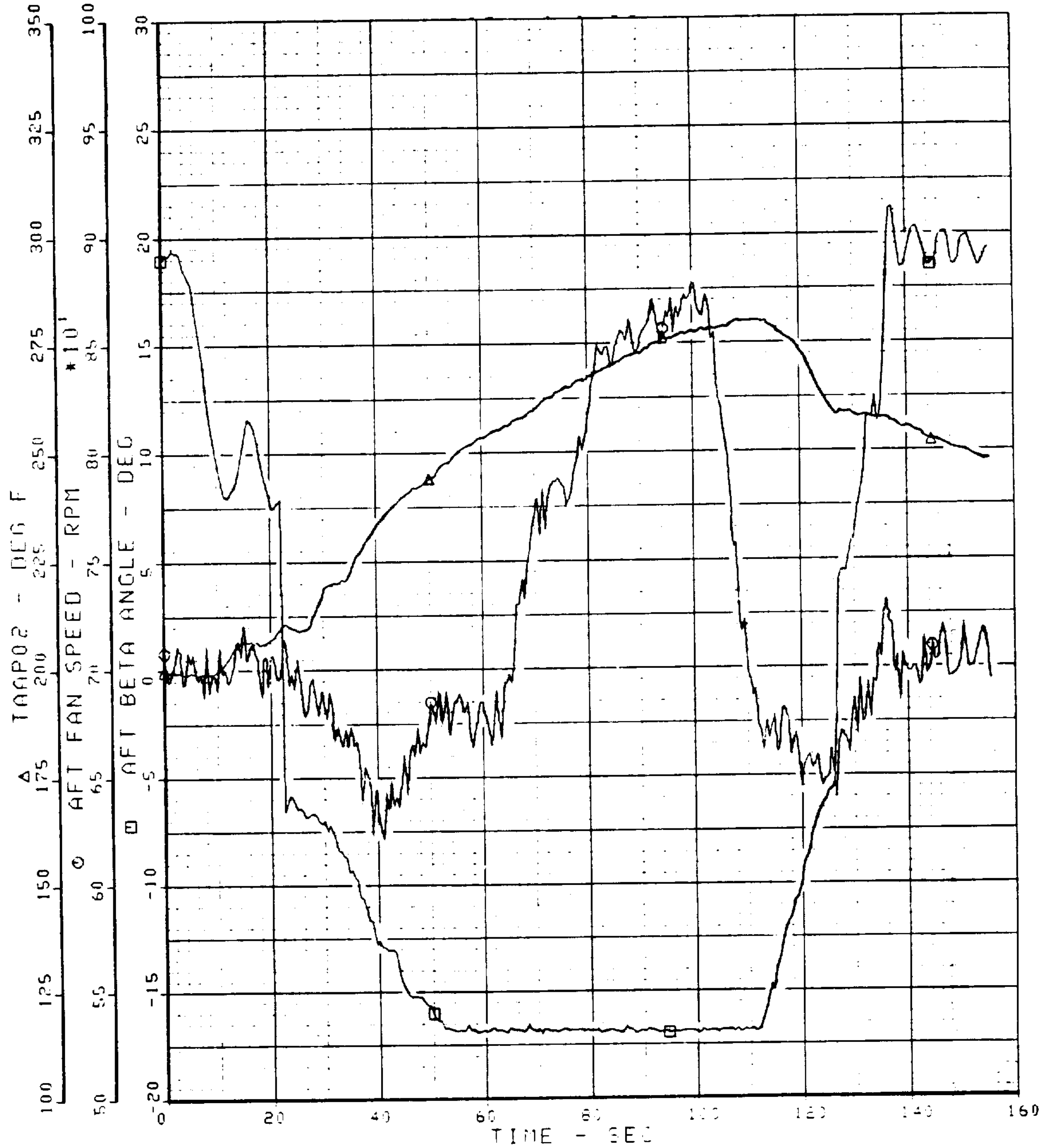


Figure 3-10. Aft Telemetry Temperatures - Reverse Testing.

## 3.4 STAGE 1 TURBINE BLADE FAILURE AND STALL EVENT

### Sequence of Events

- Engine operating on point at takeoff power (24,000 lbf), 1,350 rpm propulsor fan speed for 4 minutes
- Stage 1 turbine blade failure: high cycle fatigue (first flex) cracking at blade root resulting in aft lean of blades
- Contact of Stage 1 blades with Stage 2
- Reduction of Stages 1 and 2 flow area
- IPC stall
- Engine stopcocked about 1.5 seconds after stall initiation
- Rotor axial excursion
- Secondary damage to remaining stages resulting from failure of Stage 1
- Additional rubs experienced by Stages 7, 9, and 11
- Fast coast-down
- Rotor-to-rotor lockup.

Figure 3-11 shows a diagram summarizing the hardware damage.

### Results

During testing, prior to the stall, significant first flexural vibratory response had been observed on all stages of power turbine blading (Figures 3-12 and 3-13). Teardown revealed significant damage to Stage 1. Several blades had large leading edge root cracks and were leaning aft toward Stage 2. One local segment of blades was buckled aft into Stage 2. All Stage 2 leading and trailing edges, as well as all Stage 3 leading edges, were bent circumferentially and severely rubbed. Stages 1, 7, 9, and 11 exhibited severe tip rub. While Stages 7, 9, and 11 had rubbed previously during Build No. 1 due to oil leakage past a broken carbon seal, the poststall rubs were more severe. Stage 4 had very light tip rub only at the trailing edge. Stages 2, 3, 6, and 8 exhibited no tip rub. Stage 10 rubbed only one blade, which was bent at the platform. Stages 7, 9, and 11 had several bent airfoils. The rotor inner

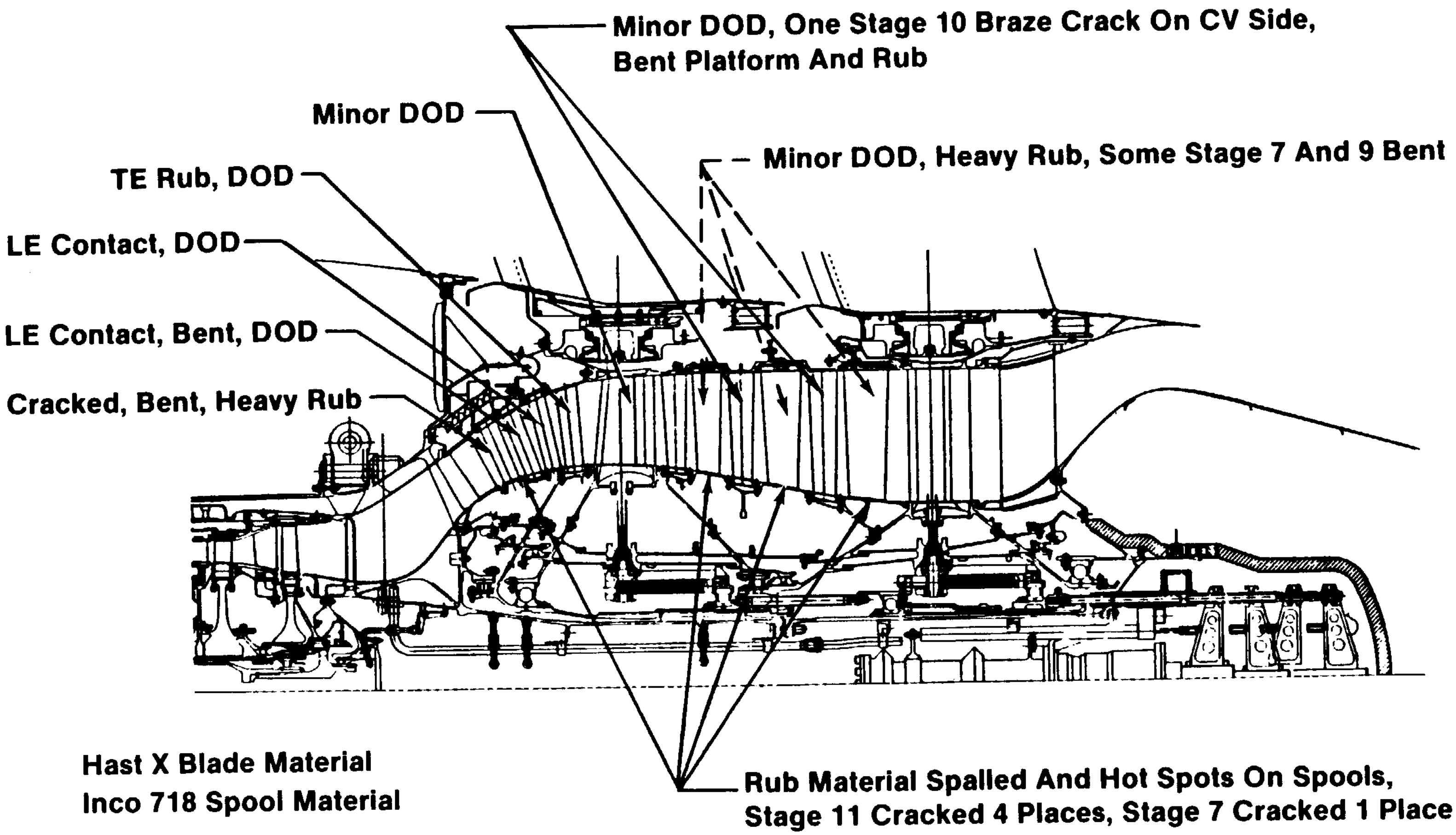


Figure 3-11. Summary of Hardware Damage.

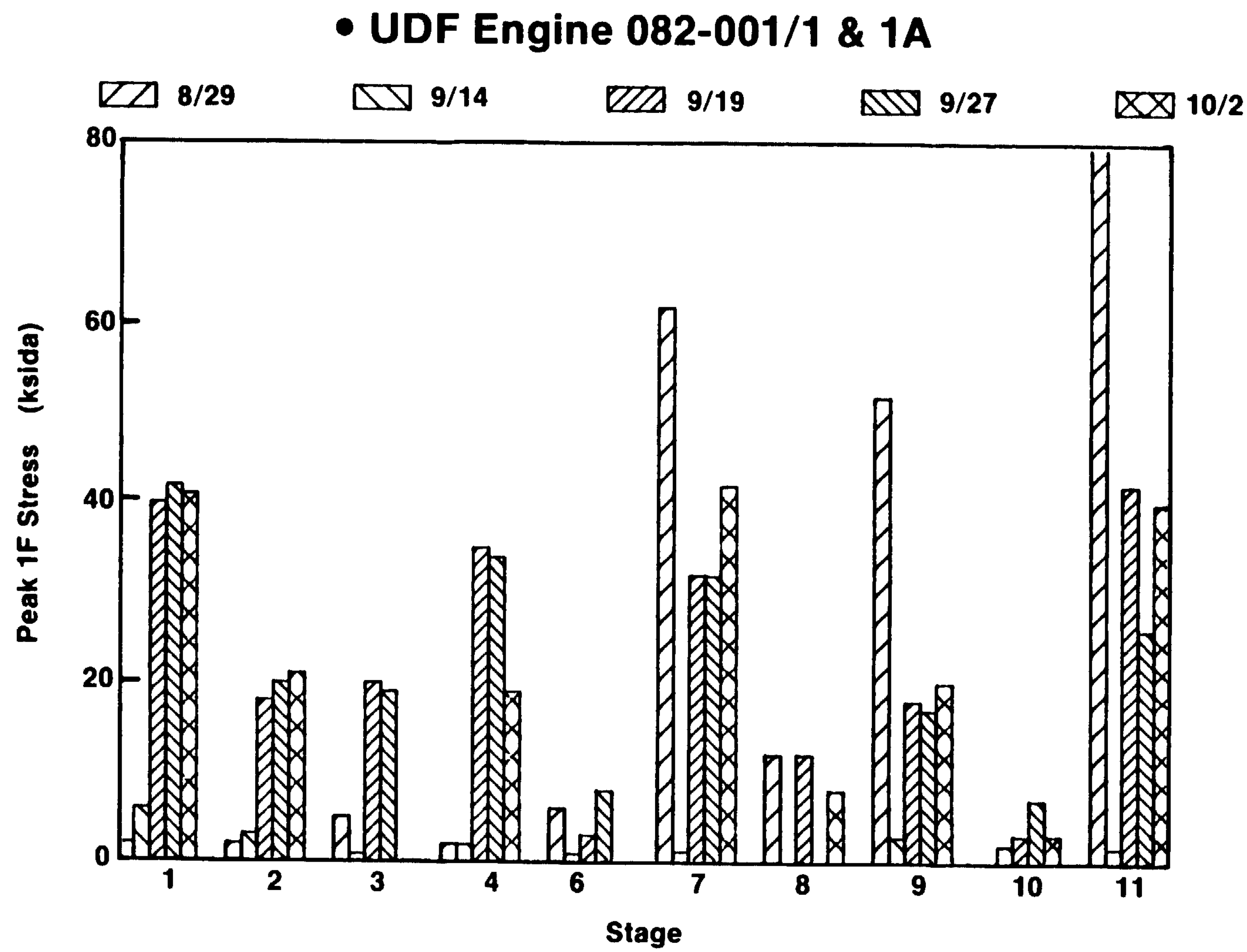


Figure 3-12. Turbine Blade 1F Stress Trend.

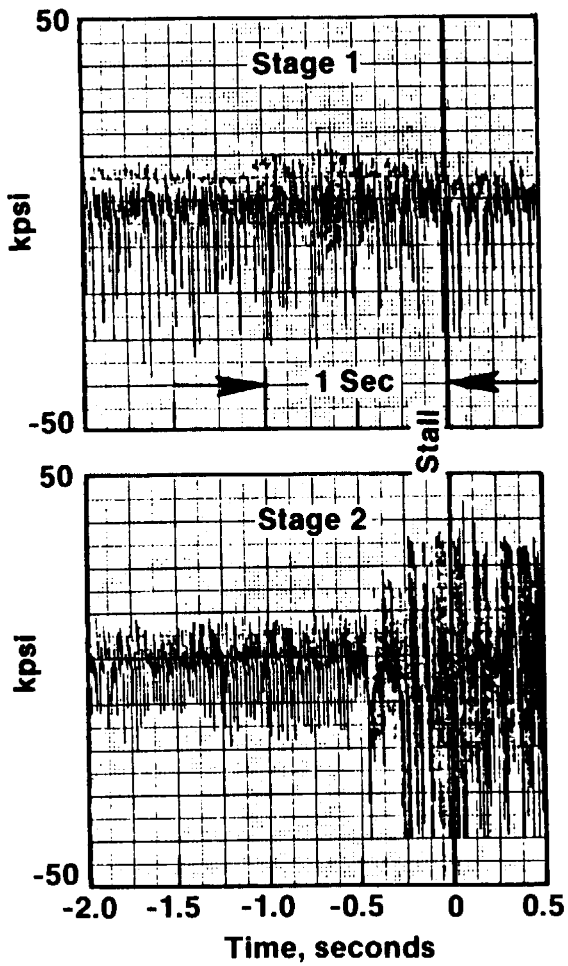


- Morning Run Similar To 9-19-85 And 9-27-85 Runs
- Accel To 1200 - Back Off For Stage 1 20 Per Rev/1F
- Accel To 1300 - Back Off For Stage 7 8 Per Rev/1F
- Accel To Thrust - Back Off For T46
- Accel To Thrust And Stabilize
- Stress Stable Until 0.5 - 1 Second Before Stall

Figure 3-13. History of Turbine Blade Response, Run to Thrust and Stall.

ORIGINAL PAGE IS
OF POOR QUALITY

spools exhibited local burn spots at Stages 1, 7, 9, and 11 rub locations, with cracking evident at Stages 7 and 11. Domestic object debris damage was confined to the power turbine flowpath. Nicks and dents were significant only on the forward turbine blade stages. The power frame and OGV (outlet guide vanes) airfoils exhibited only minor debris damage.

Metallurgical evaluation of the Stage 1 blades found root leading edge cracks on 117 of 124 airfoils. However, none of the airfoils were completely separated. Crack lengths varied from approximately 0.02 to 1.2 inch. SEM (scanning electron microscopy) revealed evidence of high cycle fatigue along the entire fracture surface. Evidence of root fatigue cracking was also found on Stages 2, 4, 6, and 11. Stages 7 and 9, and the one bent Stage 10 blade, were found to have tensile cracks at the root braze joints and tensile tears in some of the platform braze joints. Local burn spots on the spools showed evidence of severe overtemperature of the Inco 718 substrate. Four locations at Stage 11 and one at Stage 7 were confirmed cracked.

Posttest review of recorded data indicated stable engine operation while sitting on point until approximately 0.5 to 1 second prior to the stall. At that time, propulsor speed started dropping slowly while the control increased fuel flow to compensate, and vibratory response on the forward turbine blade stages showed a sudden increase.

### Conclusions

Based on the responsiveness of all stages of power turbine blading at first flexural frequency, it is concluded that the blade and spool design configuration did not provide effective dovetail Coulomb damping as anticipated. Hardware condition indicates that the Stage 1 blades were cracked to varying degrees prior to stall and that these cracks propagated in high cycle fatigue while sitting on point on October 2, 1985. As the cracks grew, the blades leaned further aft until one or more contacted Stage 2, causing the slow drop-off in propulsor rotor speed prior to the stall. Contact with Stage 2 rolled the leading edge, resulting in a sudden reduction in power turbine flow function. The reduction in flow function caused the F404 gas generator to stall. The remainder of the damage was secondary during the rapid shutdown.

### Corrective Action

All power turbine blades were replaced for Build 2. Spanning across adjacent blades, coulomb dampers (in the form of René 41 pins) were designed for all stages of blading as illustrated in Figure 3-14. Effectiveness of the damper design has been substantiated by component rig spin ("whirligig") and bench wear tests. Although no evidence of fatigue was indicated for the power frames, dampers were also added to Stage 12 as a precaution due to a predicted first flexural response with the outlet guide vane passing frequency. Strain gages have also been added to the Stages 5 and 12 power frame airfoils for Build 2.

Low cycle fatigue and crack growth analyses of the spools indicate that they have sufficient life capability for the remainder of planned testing. The spools have been weld repaired and the rub coats stripped and reapplied to provide additional margin.

Because of the severity of rub during Build 1 when oil leaked past the forward intershaft carbon seal and during the Build 1A stall, power turbine blade tip clearances have been increased an additional 0.050-inch on the outer attached blades and 0.030-inch on the inner attached blades, and all tips have been tapered to 0.005 to 0.015-inch thickness as a precautionary measure.

## 3.5 TURBINE BLADE DAMPER EFFECTIVENESS

Coulomb damper pins were added to all turbine blade stages (1-4, 6-11) and to Stage 12 power turbine frame airfoils (Section 3.4 and Figure 3-14). Figure 3-15 demonstrates the Stage 1 turbine blade vibratory-stress reduction resulting from the addition of the damper pins. Figure 3-16 shows the Stage 1 vibratory stress in relation to the scope limits before and after addition of the dampers. Figures 3-17 through 3-26 illustrate the vibratory stress for all turbine blade stages after installation of the dampers. Data are from an accel to 25,000 lbf, except for Stage 11 blades data (bad telemetry signal) which is from an accel to 22,000 lbf. Section 3.11 contains stress data for the turbine frame blades.

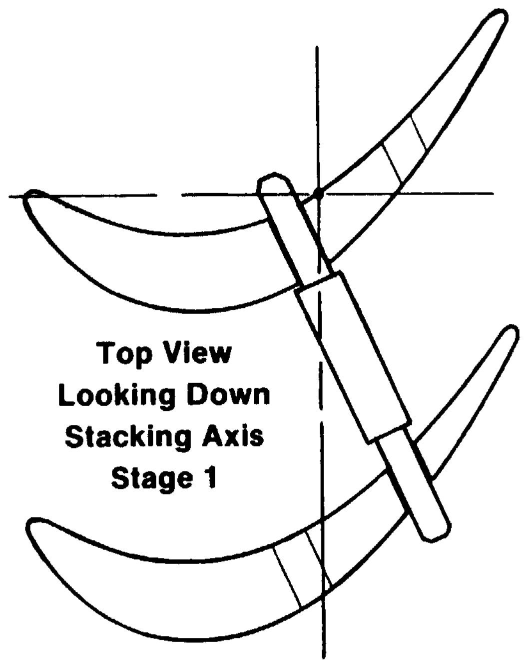


- Blade-To-Blade Damper Pins
- Increased Tip Clearance
  + 0.050 Inch Stages 1, 3, 7, 9, 11
  + 0.030 Inch Stages 2, 4, 6, 8, 10
- Reduced Tip Thickness
  (0.030 → 0.015)

Figure 3-14. Turbine Blade Fix.

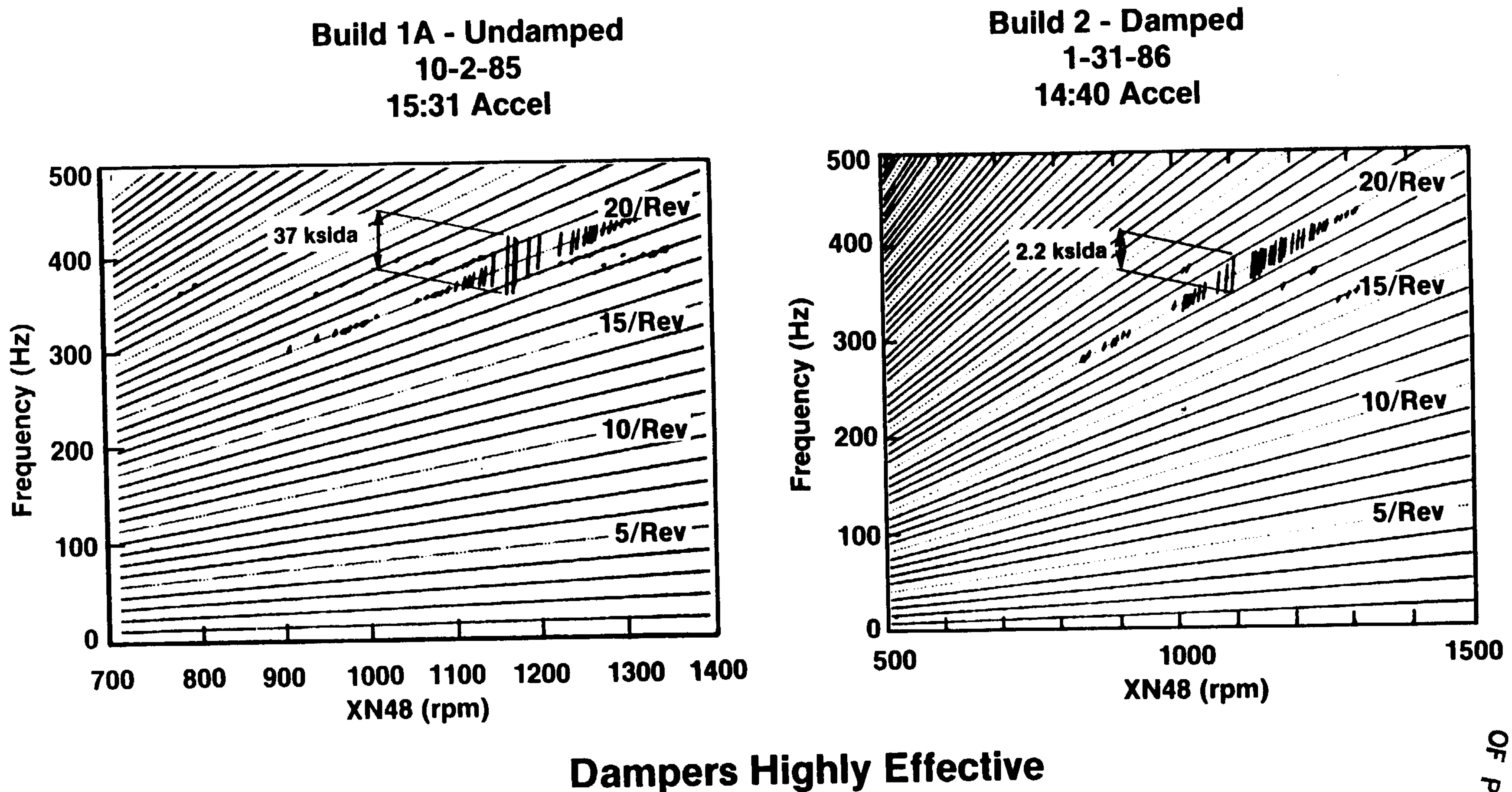


Figure 3-15. Power Turbine Blade Vibratory Response, Damper Effectiveness - Stage 1.

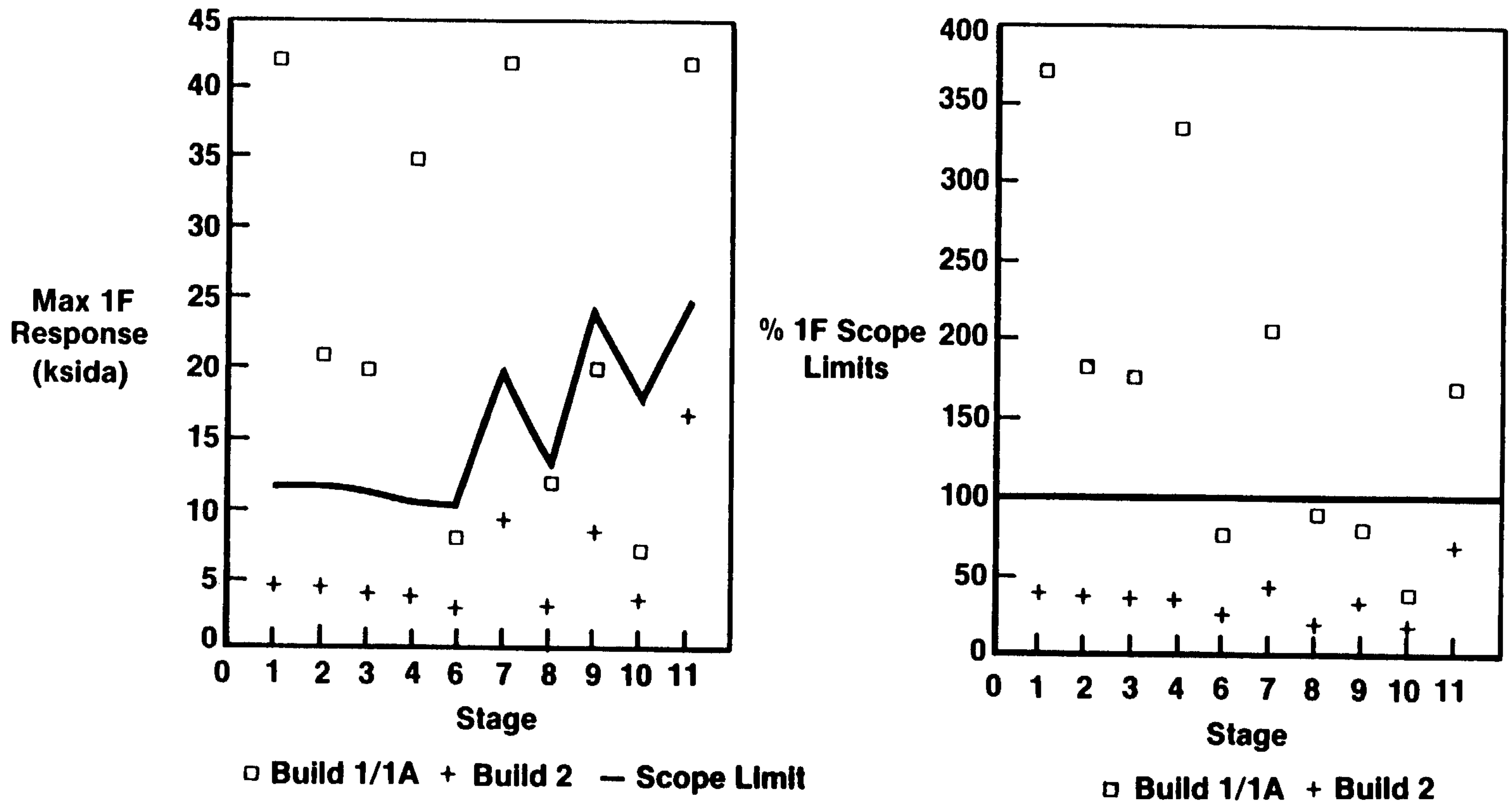


Figure 3-16. Power Turbine Blade Vibratory Response, Build 1 (Undamped) versus Build 2 (Damped).

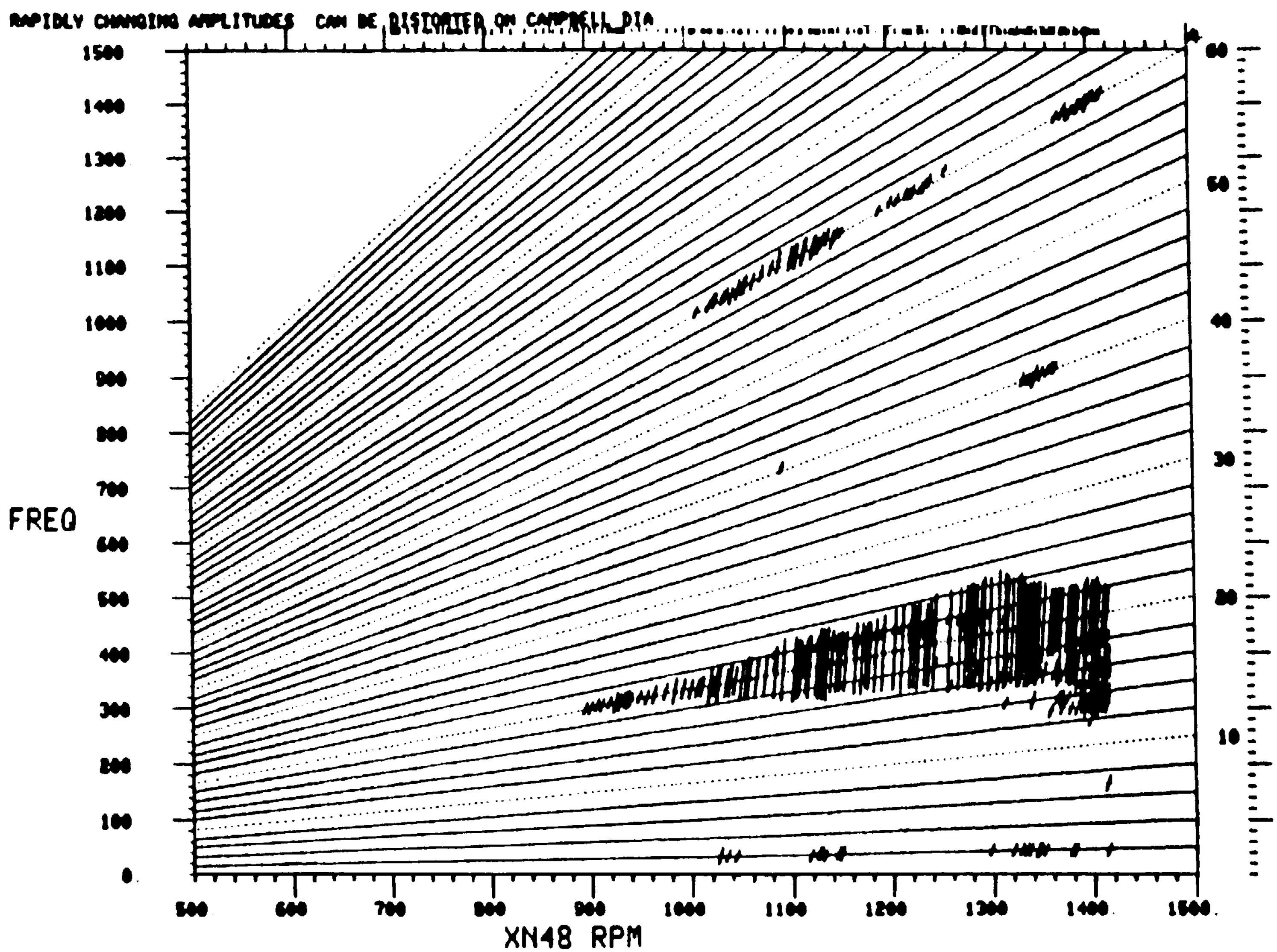


Figure 3-17. Stage 1 Turbine Blade Response, Accel to 25,000 lbf Thrust: February 4, 1986.

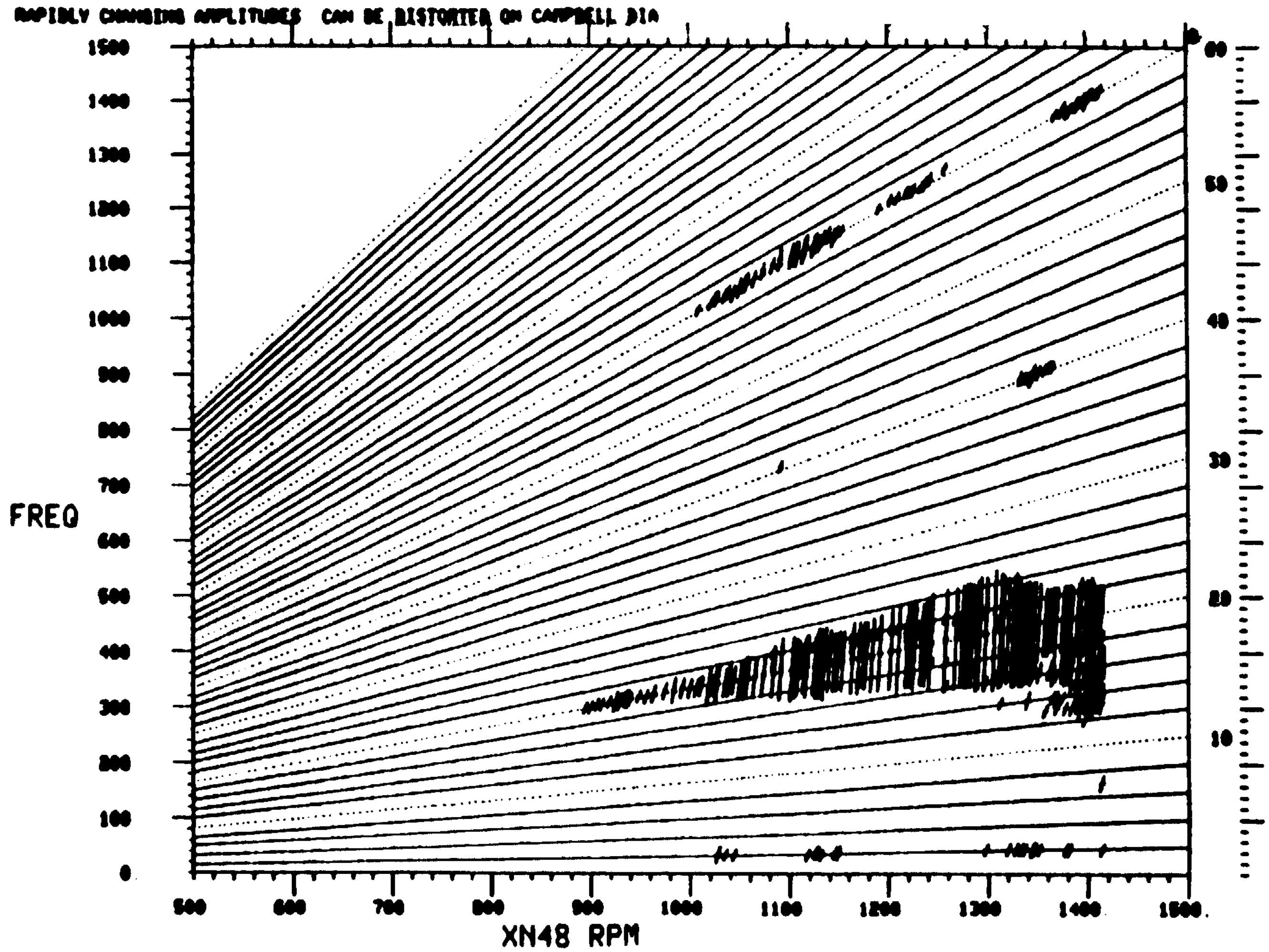


Figure 3-18. Stage 2 Turbine Blade Response, Accel to 25,000 lbf Thrust: February 4, 1986.

ORIGINAL PAGE IS
OF POOR QUALITY

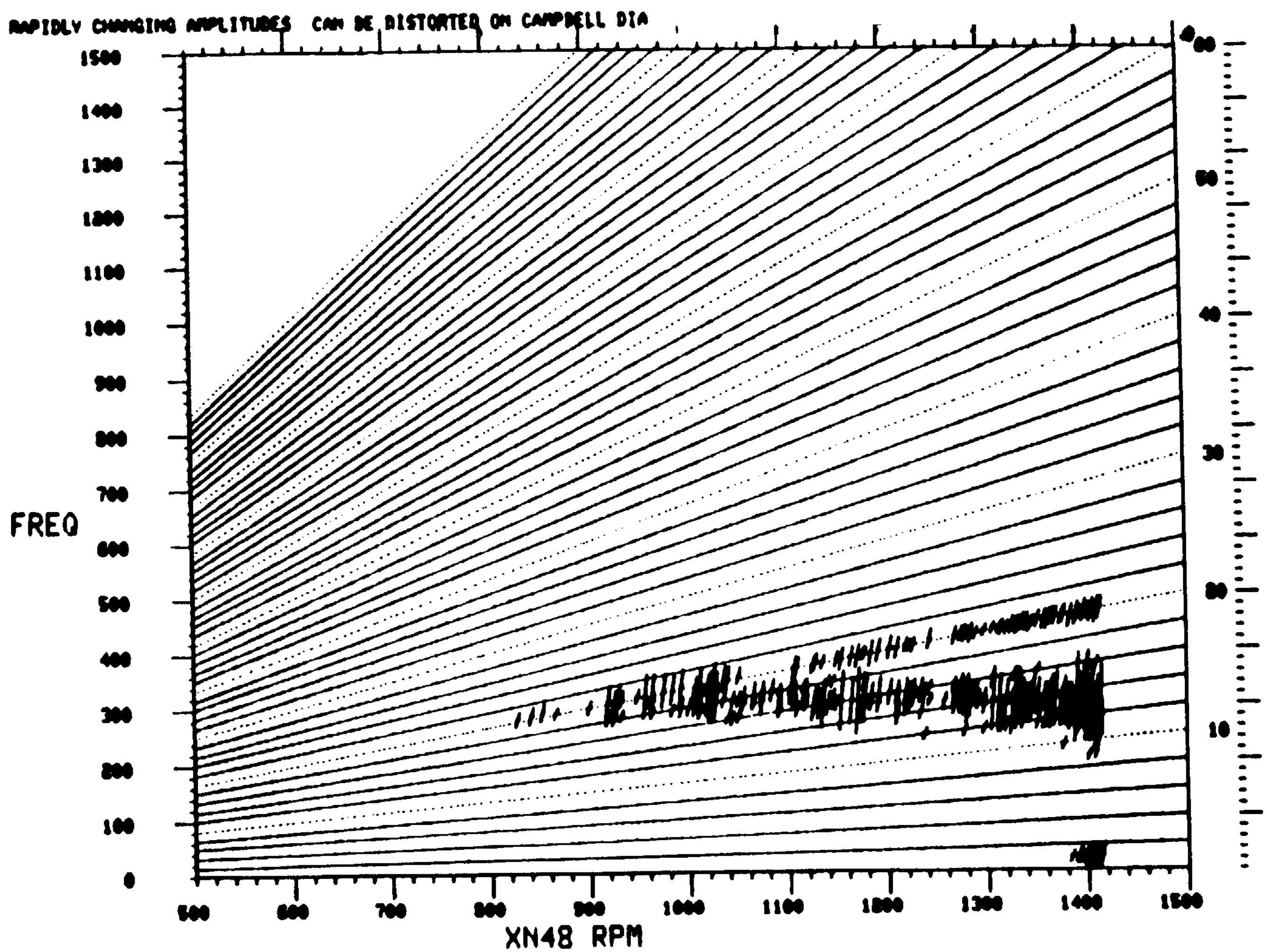


Figure 3-19. Stage 3 Turbine Blade Response, Accel to 25,000 lbf Thrust: February 4, 1986.

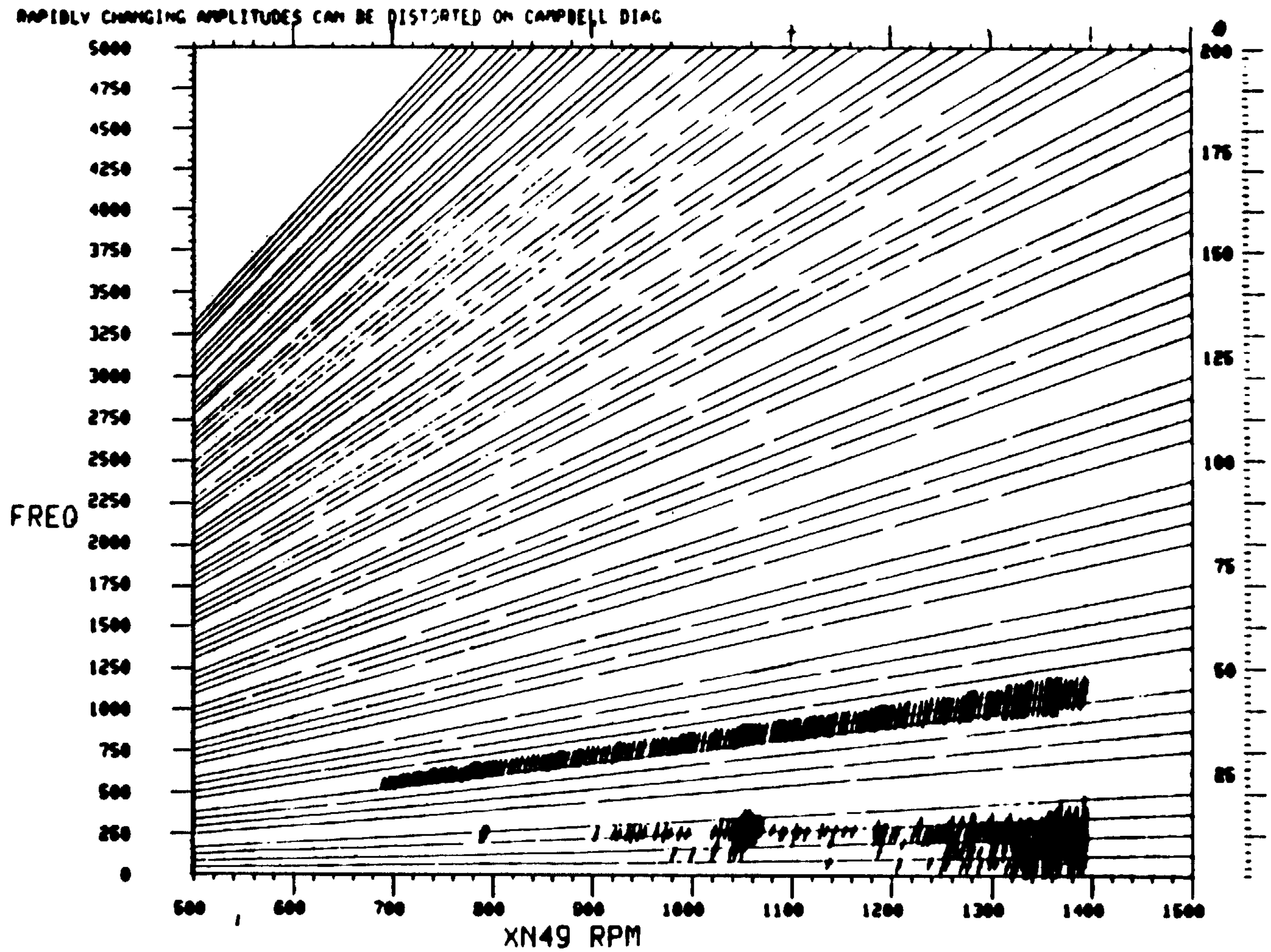


Figure 3-20. Stage 4 Turbine Blade Response, Accel to 25,000 lbf Thrust: February 4, 1986.

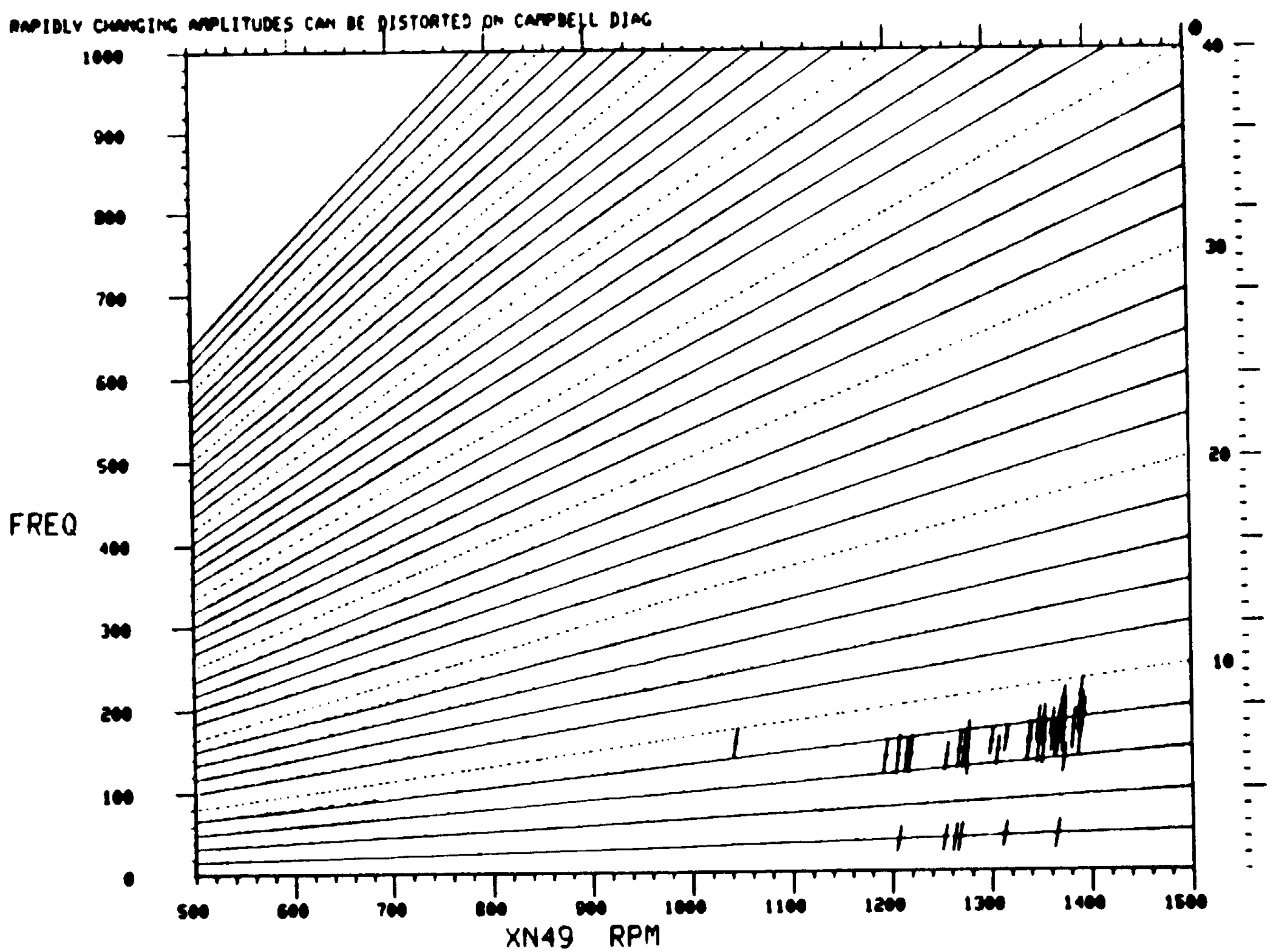


Figure 3-21. Stage 6 Turbine Blade Response, Accel to 25,000 lbf Thrust: February 4, 1986.

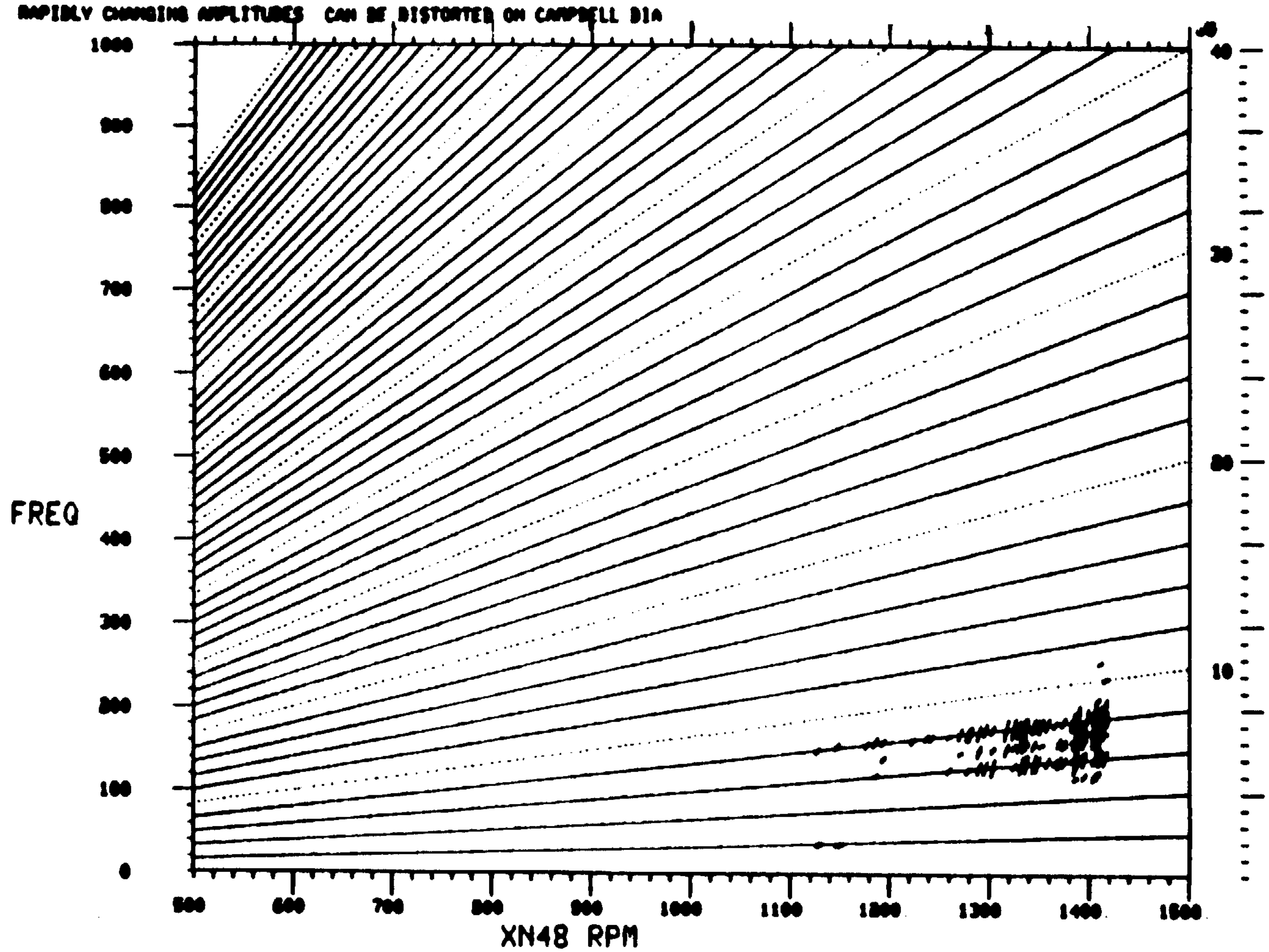


Figure 3-22. Stage 7 Turbine Blade Response, Accel to 25,000 lbf Thrust: February 4, 1986.

ORIGINAL PAGE IS
OF POOR QUALITY

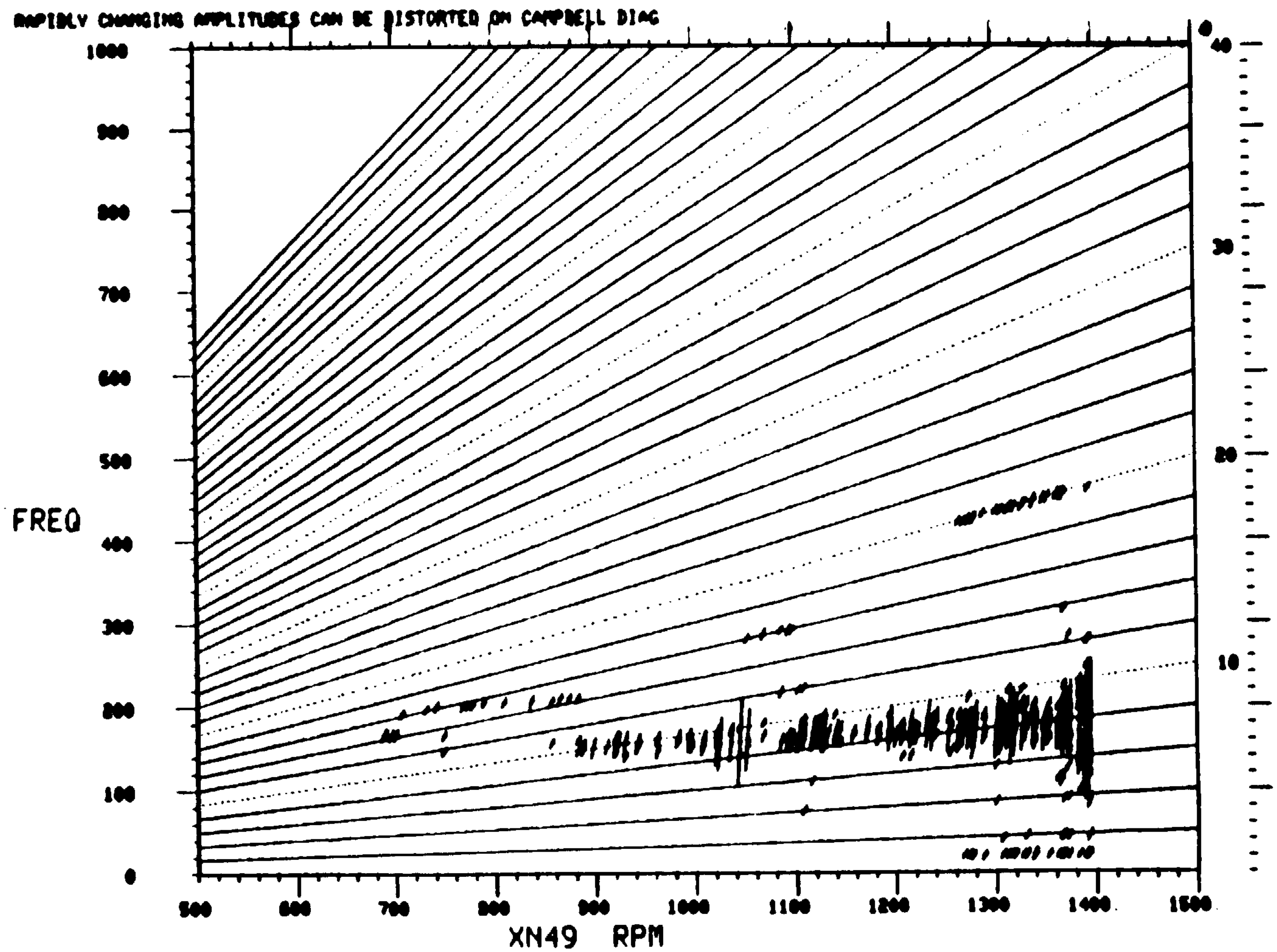


Figure 3-23. Stage 8 Turbine Blade Response, Accel to 25,000 lbf Thrust: February 4, 1986.

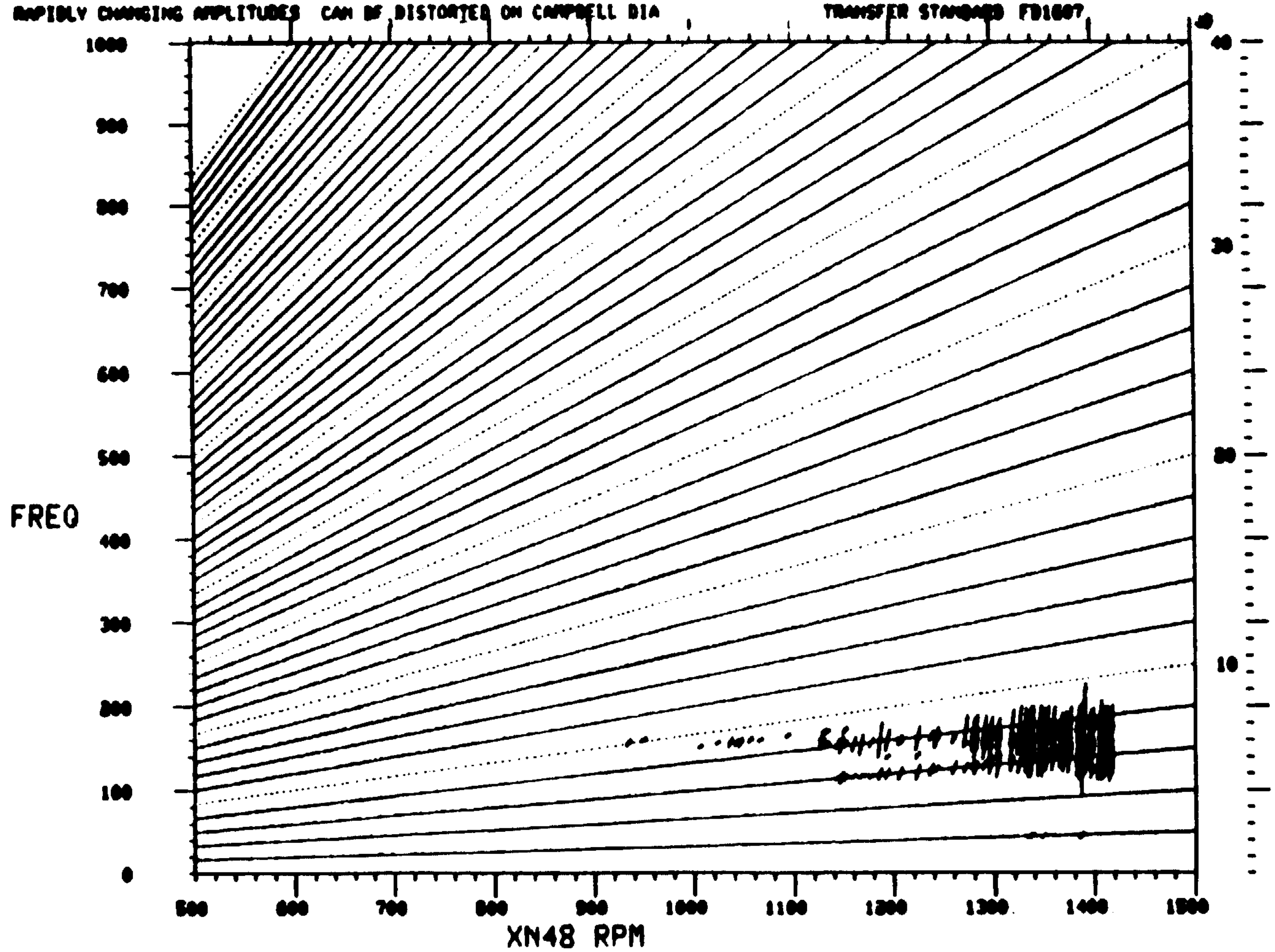


Figure 3-24. Stage 9 Turbine Blade Response, Accel to 25,000 lbf Thrust: February 4, 1986.

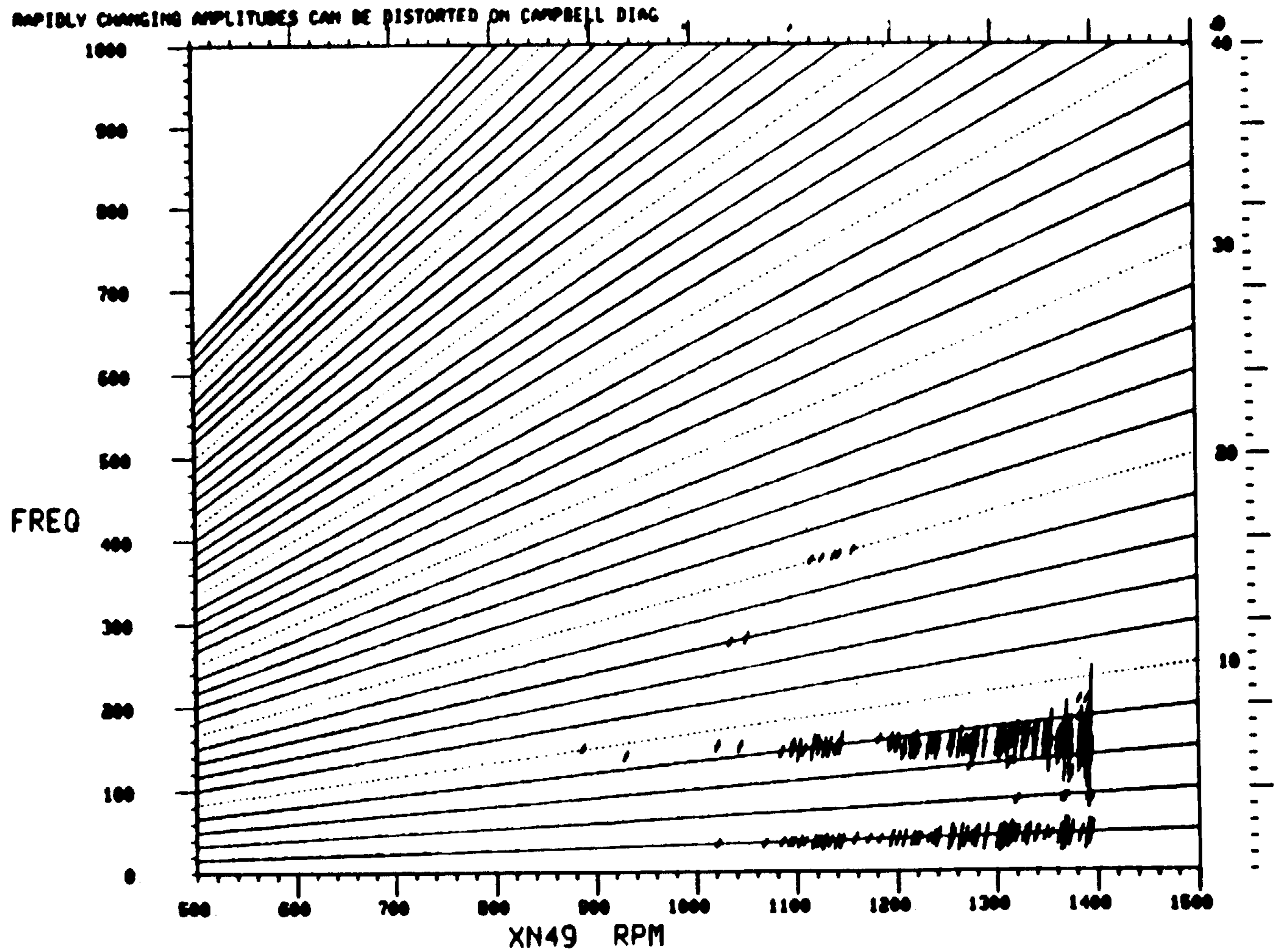


Figure 3-25. Stage 10 Turbine Blade Response, Accel to 25,000 lbf Thrust: February 4, 1986.

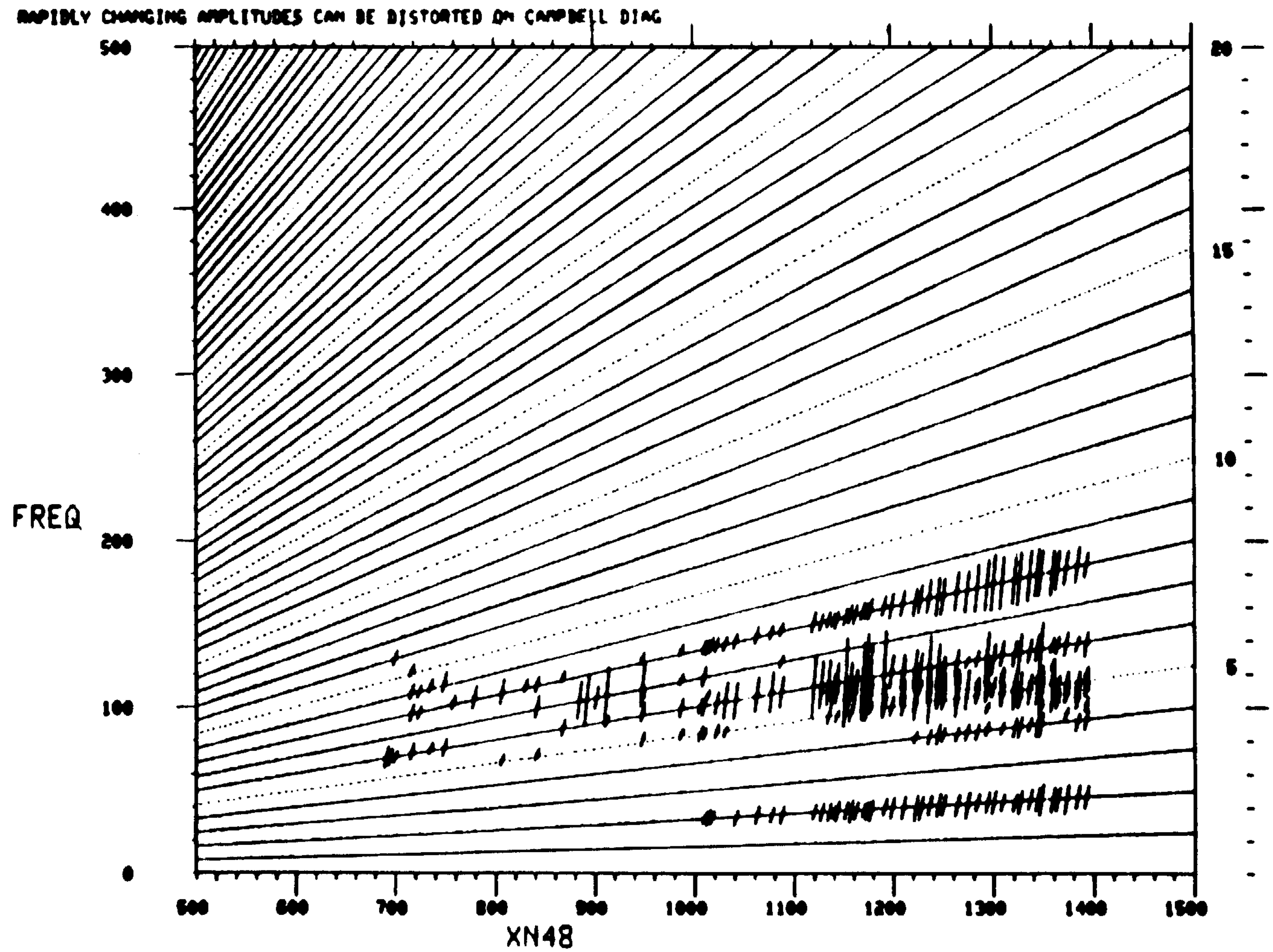


Figure 3-26. Stage 11 Turbine Blade Response, Accel to 22,000 lbf Thrust: January 11, 1986.

ORIGINAL PAGE IS OF POOR QUALITY

## 3.6 SUBIDLE OIL LEAK PROBLEM

After the carbon seal failure from assembly damage was repaired, the propulsor still leaked oil into the rotors, flowpath, and nacelles. Oil loss was visible, both during operation and on shutdown, in the form of smoke and oil drips. The oil was leaking through the carbon seals during low speed operation. Although the amount of oil lost was not large, it was decided that it was desirable to reduce the amount of smoke after shutdown.

During early operation, much of the engine testing was at subidle speeds and below, as control and starting problems were worked out. The design idle speed was 650 rpm. Initial testing proved that idle speed had to be increased to 700 rpm for several reasons: the 650-rpm idle speed was too close to the subidle rotor critical; the vibration level was unacceptable; the telemetry cooling system was not effective at the lower speed; and propulsor stresses were lower at the higher idle speed.

Test data showed that the pressure drop on the aft carbon seal approached zero using the 650-rpm idle speed. The carbon seal leaked without a positive pressure drop. At 700 rpm, the seal pressure drop is increased enough to limit the oil loss out of the aft carbon seal. At higher power settings, the pressure drop across the seal is well above that which is required for oil sealing.

At low speeds (subidle), for very short runs, and during starts until the elevated idle speed is reached, the propulsor sump is not scavenged properly. At low speeds, the oil is not pumped to the ends of the rotating sumps where it can be scavenged. Due to the frame design, scavenge lines at each end of the sump run uphill initially; this forms a trap that requires some small sump pressure to overcome prior to flowing to the scavenge element. The scavenge pump used (from a CF6-50 engine) has a reputation as one that is difficult to get primed and establish full scavenge flow. For these reasons, a subidle lube bypass valve was designed and installed on the propulsor lube system.

The initial bypass system was a facility design - air actuated and controlled by the engine stopcock. In order to preclude complete loss of oil to the engine in a control or valve failure, the system was designed to divert most, but not all, of the supply oil to the propulsor. At subidle, supply oil was diverted to the scavenge circuit just at the exit of the air oil cooler. Hoses and hardware used were made on site and were not flight quality. The system, combined with the new higher idle speed, reduced or eliminated the low speed leak/smoke problem.

For flight-test, the system had to be replaced with a digital electronic-controlled solenoid valve. The facility system as configured above did not function as desired on engine shutdown. The scavenge pressure decay lagged the supply pressure decay, so that the propulsor supply was actually diverted to a higher pressure circuit, and briefly, oil flow was increased to the propulsor. This condition was somewhat alleviated by removing the air oil cooler from the scavenge circuit (which was not required) and by lowering line losses in the bypass circuit with flight quality hardware. These changes ended the leak and smoke problems.

## 3.7 STATIONARY EXHAUST NOZZLE (CENTERBODY) REPLACEMENT

Between Builds 1 and 2, a redesigned centerbody was installed on the engine. This redesign was necessary, because analysis and wind tunnel testing indicated that at some flight conditions there would be an undesirable flow separation from the centerbody. The predicted flow separation data for both centerbodies is shown in Figure 3-27. No flow separation was detected or predicted for ground testing. Figure 3-28 compares the two centerbody designs. Further information is provided in Section 7.3, Performance.

## 3.8 FAN BYPASS BLEED VALVE CALIBRATION

During Builds 1 and 2, tests were performed to calibrate the fan bypass air (from the gas generator) bleed valve. This was done to provide necessary information about the amount of fan bleed air required to maintain stall margin in the UDF™. These data are extrapolated for use in finding the amount of bleed air required in flight.

## 3.9 FAN BYPASS BLEED VALVE DIFFUSER FAILURE/REPLACEMENT

During Build 2, the fan bypass bleed valve diffuser failed in high cycle fatigue (Figure 3-29). Until a redesigned diffuser (Figure 3-30) could be

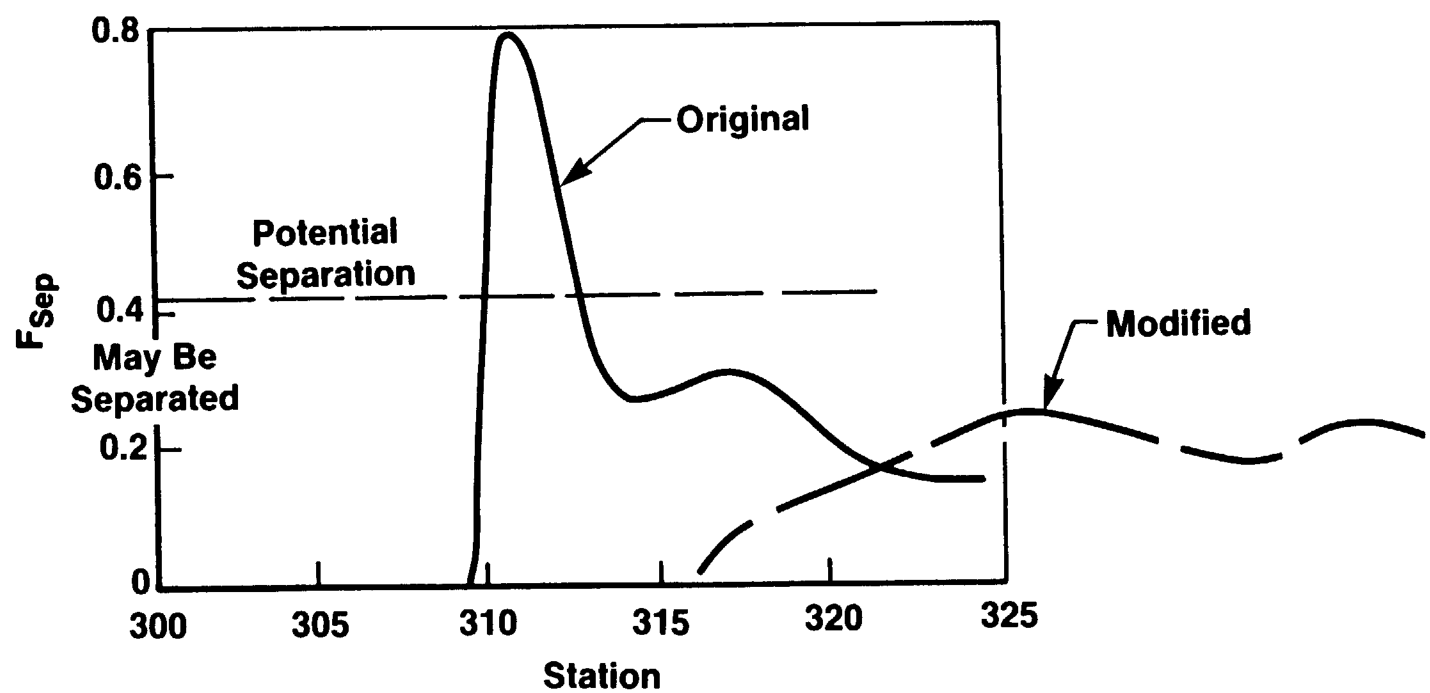


Figure 3-27. UDF™ Engine Centerbody Separation Parameter, Cruise Condition M = 0.72; 35,000; $PT8/P_0$ = 1.4.

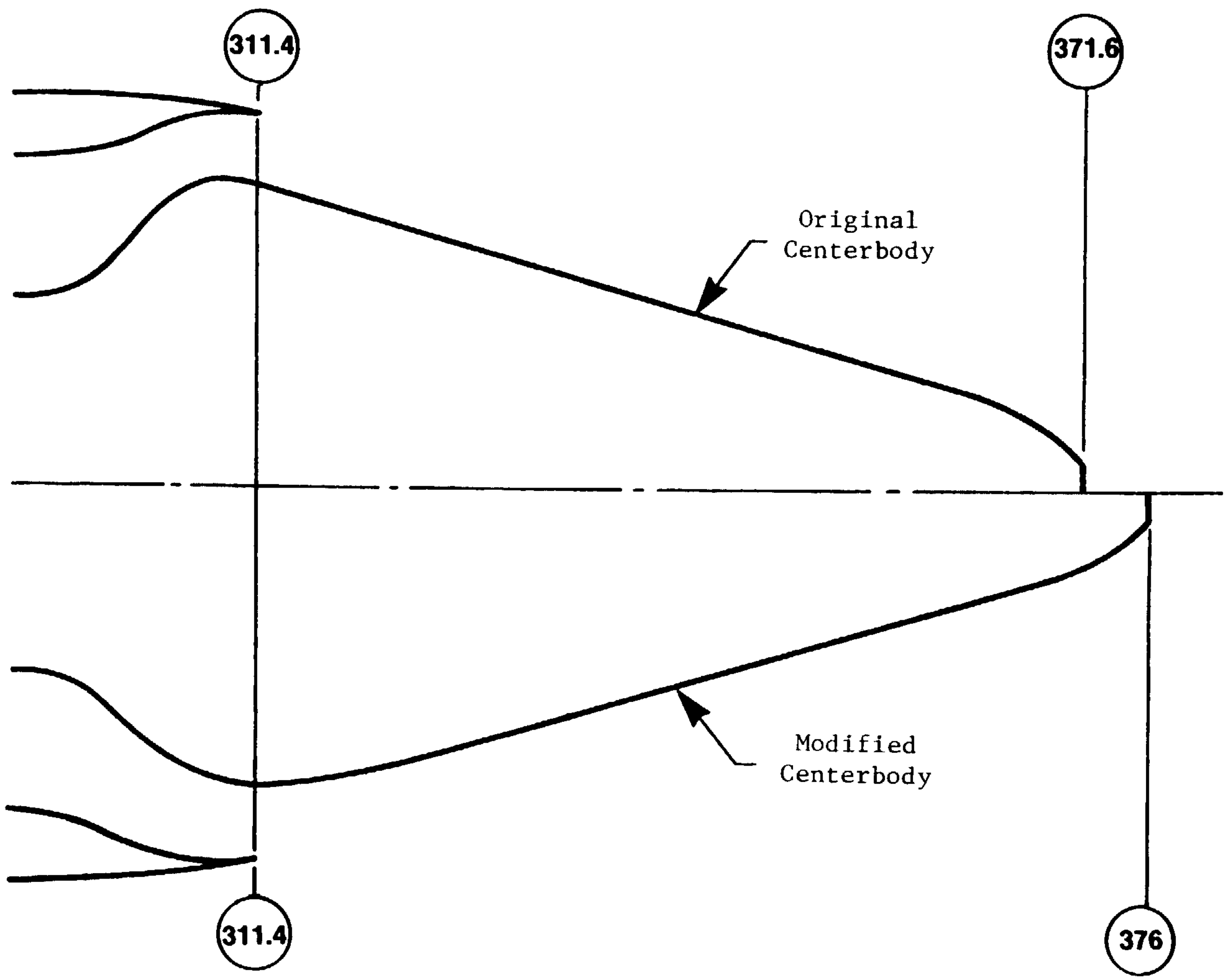


Figure 3-28. UDF™ Engine - Redesigned Centerbody.

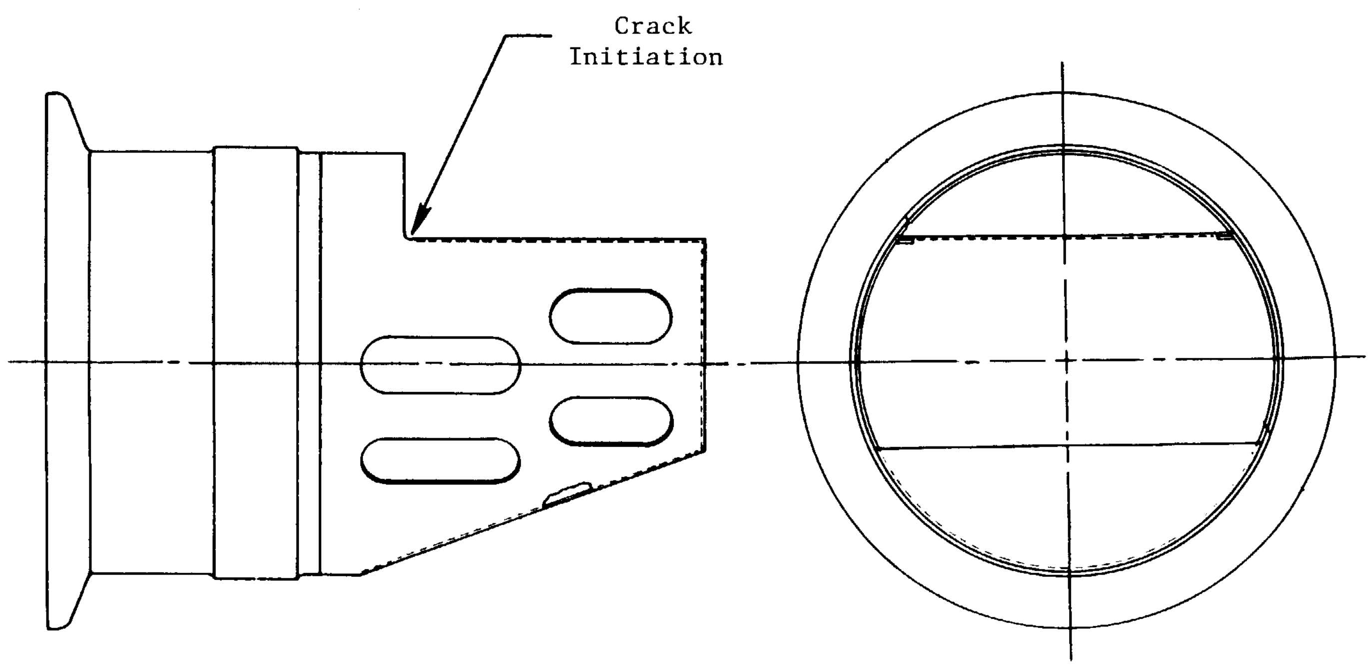


Figure 3-29. Bypass Bleed Valve Diffuser.

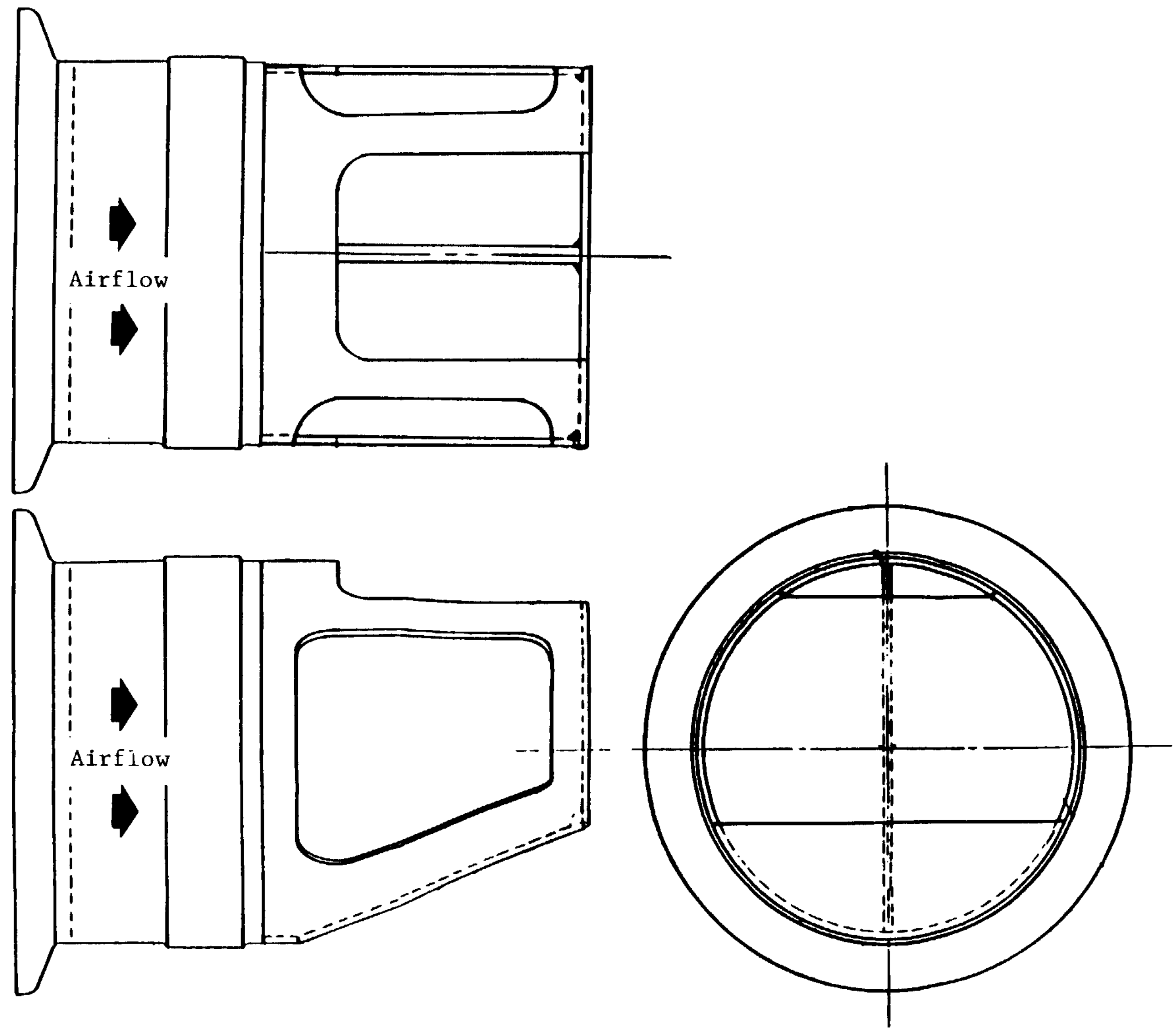


Figure 3-30. Redesigned Bypass Bleed Valve Diffuser.

designed and manufactured, the damaged portion of the diffuser was cut off and used "as is." When the redesigned diffuser was available, it was installed on the engine.

## 3.10 PROPULSOR FAN-BLADE-LOSS EVENT

### Summary of Event

- The engine reached test point: 24,000 lbf, 1371 rpm propulsor fan speed.
- Stage 2, No. 7 composite fan blade shell separated from titanium spar and was released; however, the spar remained attached to the trunnion.
- No high fan stress or other anomalies prior to blade loss.
- Shutdown initiated at blade loss - 1 second chop to idle and stopcock within 9 seconds.
- No gas generator stall.
- Propulsor spool-down was normal.
- Due to a large imbalance (approximately 260,000 gm/inch) caused by the missing composite, a noticeable amount of engine vibration was experienced.
- Control/actuation system functioned normally after blade loss.

### Spar Damage

Inspection of the spar following shutdown indicated the titanium had cracked at the EB (electron beam) weld line the entire width of the spar. The EB weld crack was clearly visible over the midspan of the blade (Figure 3-31).

### Secondary Damage

Blade No. 6, which was next to the released blade, had a slight nick in the polyurethane coating where the composite material from Blade 7 hit Blade 6 before striking the ground. The nick was an indication that only light contact occurred.

The isolators contain an absorption material which is intended to yield under high unbalance conditions such as blade loss. Deformation of the aft

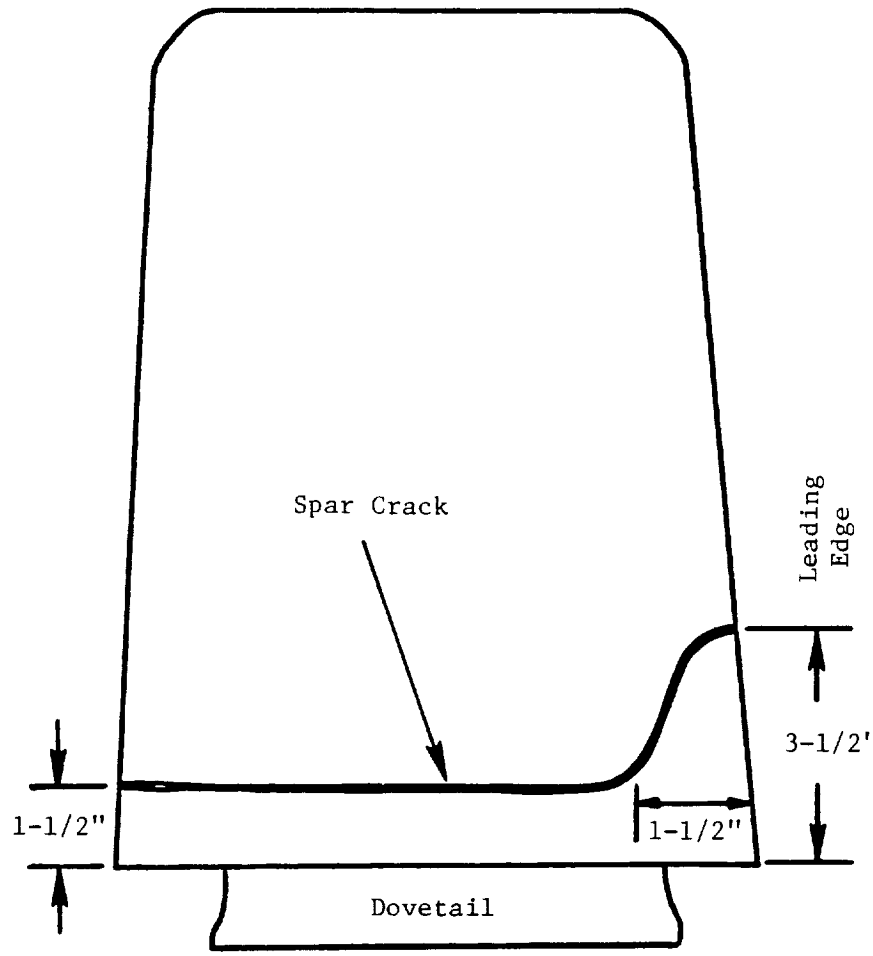


Figure 3-31. Spar Schematic.

isolator pads was observed, and the isolators were returned to the vendor for inspection. The aft isolators had their original values of spring rate and damping coefficient. Since there was deformation of the aft isolator pads, they were refurbished as a precautionary measure and returned to engine test. No damage to the forward isolator was observed.

There was also concern that the transfer gearbox attached to released blade trunnion No. 7 may have suffered some damage. The gearbox was torn down and both the MPI (magnetic particle inspection) and FPI (fluorescent penetrant inspection) of the gears and pinnions indicated no abnormal wear.

Bolts attaching the Stage 12 power frame to the rotating exhaust nozzle showed interference with the OGV assembly, with the heaviest wear at blade Location 7. The OGV assembly is designed to clear the bolt circle by 0.100 to 0.160 inch. The OGV assembly showed light wear all the way around, with a 1-inch section indicating a harder rub. No repair was required. The OGV assembly had no other distress.

The Stage 11 turbine blades rubbed the inner spool at some time during the event, leaving a 4-inch x 3/8-inch rub mark on the inner rotor. The rub coincided with Stage 2 fan blade Location 4. The indication was a surface discoloration with no measurable depth. The Stage 11 blade trailing edge tip did not have any discoloration or tip curl that would suggest a heavy rub.

Both Stages 1 and 2 fan blades were returned to Evendale for inspection. No debonding was found in the Stage 1 set, but one Stage 2 blade was found to have a section of composite separating from the spar.

### Fan Blade Corrective Action

Corrective action included the addition of a portable ultrasonic scan of all fan blades following each hour of engine run time. Ultrasonic scanning at Evendale proved to give accurate results when trying to determine if debonding has occurred. The ultrasonic scan used when the blades were returned to Evendale indicated a Stage 2 blade had started to debond. Portable scan equipment also verified debonding of the composite. Because the previous test method, ping checking, indicated the debonded blade was acceptable, the ping test was discarded as a debonding check.

### Test History of Failed Fan Blade

The blade that failed had been run 20:40 hours prior to the failure. A breakdown of run time versus propulsor fan speed is provided in Figure 3-32.

## 3.11 PROPULSOR FAN BLADE HISTORY AND TEST DATA

### 3.11.1 Fan Blade Test History

None of the original design Stage 1 fan blades had to be replaced due to failure or debonding. After Build 2, the blades were replaced with redesigned blades with mechanical retention features. Figures 3-33 and 3-34 compare the original and redesigned fan blades. All of the redesigned Stage 1 fan blades ran through Build 3 without problems.

Some of the original design Stage 2 fan blades failed inspection during Builds 1 and 2 due to debonding. These were replaced once any discrepancy was found. Figure 3-35 depicts the history of the Stage 2 blades during Builds 1 and 2. Investigation into the two debonded blades found after Build 1 determined that the probable cause of debonding was from propagation from cracks in the foam inside the blades. This foam filled the cavity between the composite shell and the titanium spar. Cracks in the foam during manufacturing propagated into the shell/spar bond. A design change was made (Figure 3-36) to try to prevent this from happening.

Section 3.10 discusses the Stage 2 fan blade failure in Build 2. After this fan blade failure, the engine was limited to 1000-rpm fan speed until the redesigned fan blades were available (Build 3 testing).

### 3.11.2 Fan Blade Test Data

Figure 3-37 summarizes fan blade vibratory stresses for Builds 1, 2, and 3. Figures 3-38 through 3-42 present specific examples of stress data. Note there are differences in fan blade stress levels with seemingly equivalent test points. This difference is caused to a large degree by differing wind conditions (that is, wind direction, velocity, gusting). Figure 3-43 depicts the strain gage locations. Location No. 4, which gives the highest first flex vibratory stress, is the strain gage used for the given data.

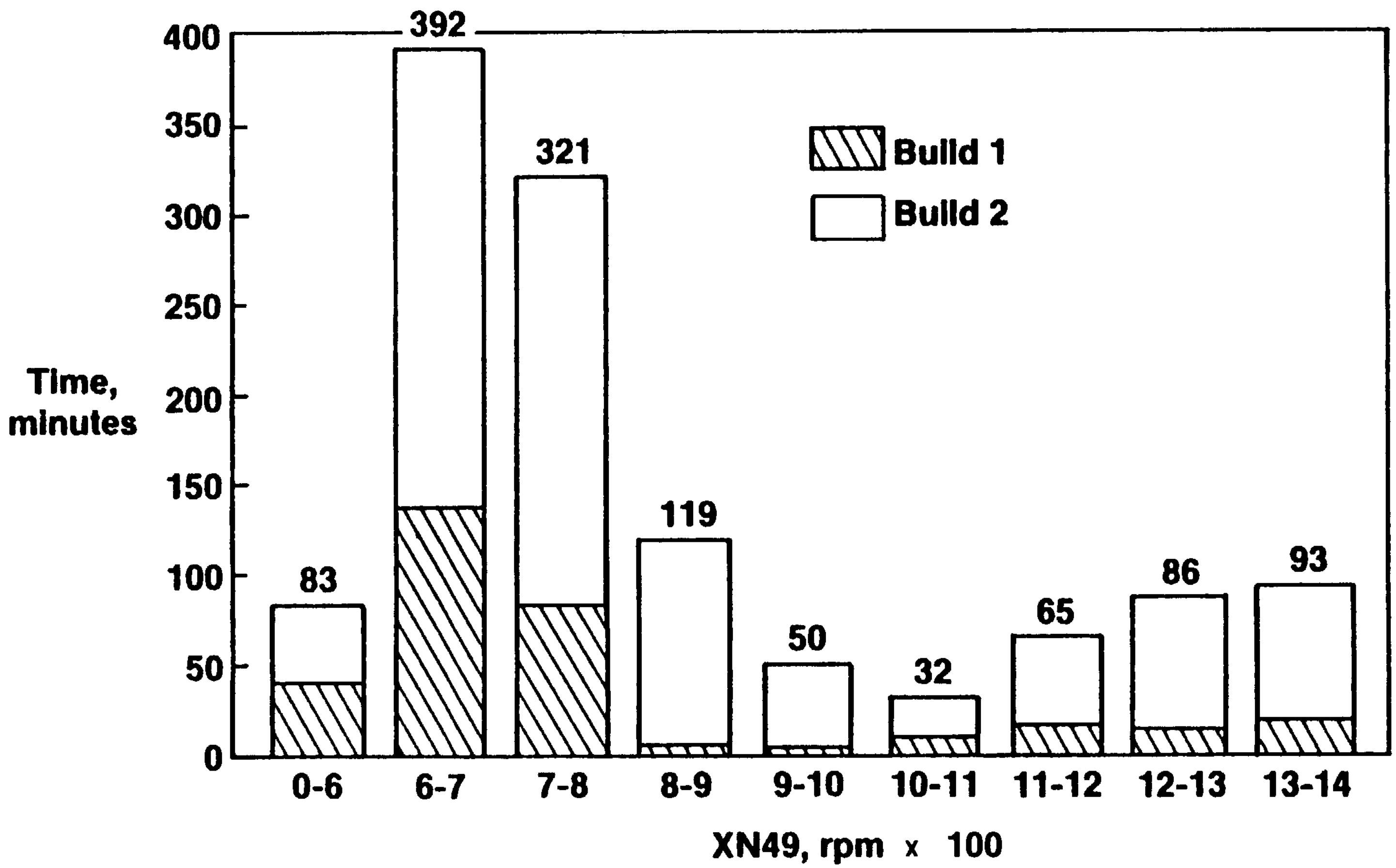


Figure 3-32. Total Run Until Fan Failure.

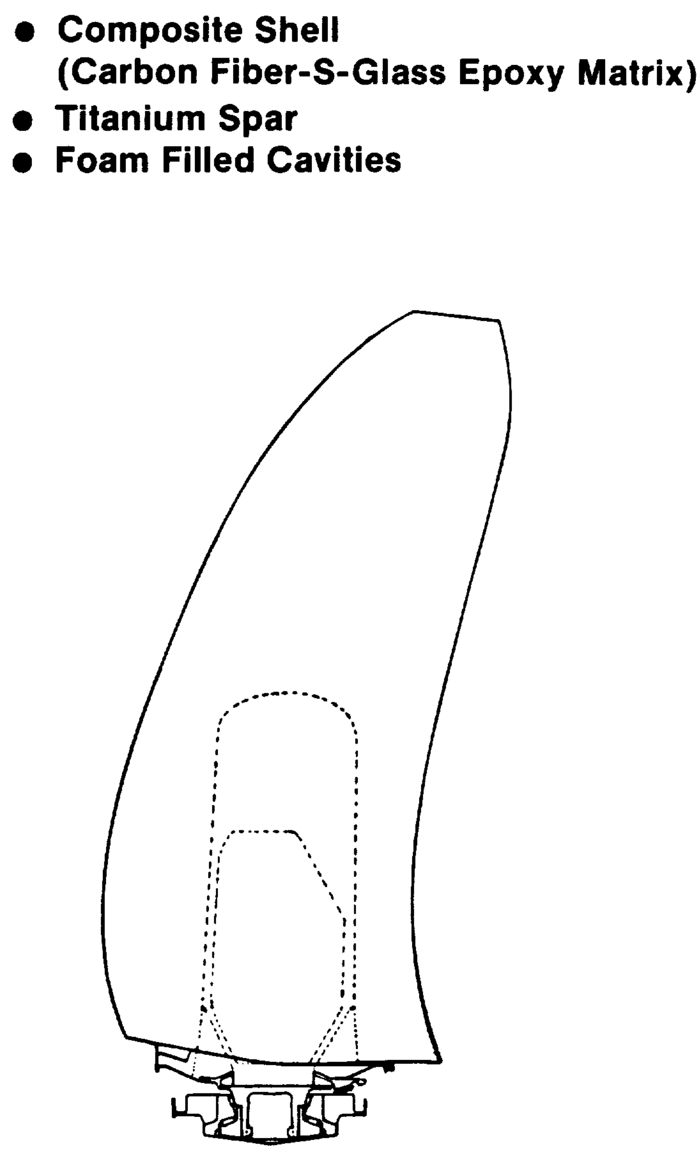


Figure 3-33. Original Fan Blade Airfoil Mechanical Design.

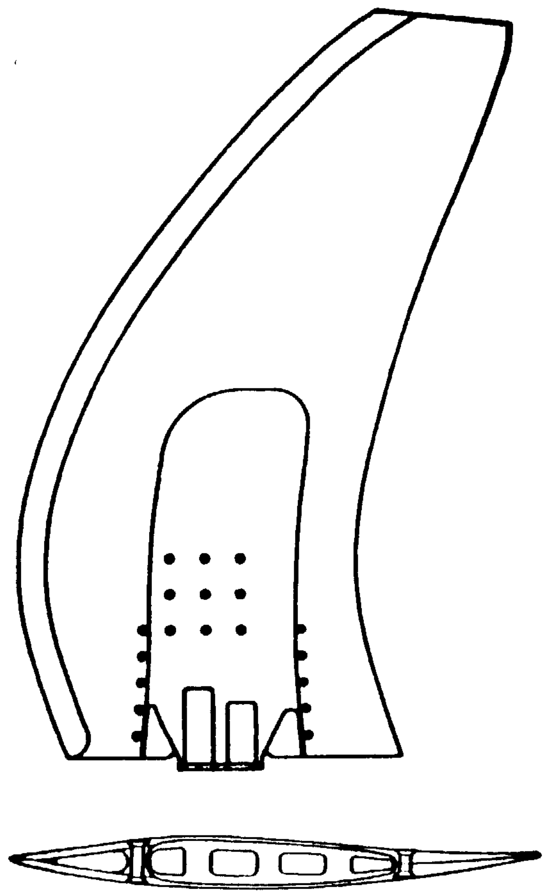

- Solid Spar with EDM Pockets (2 Plugs)
- Same Ply Lay-Up Pattern
- Add One 0.005" Adhesive Layer on Spar Surface
- Positive Shell Retention
- New Foam Material, Rohacell, Replaces Syntactic Foam
- Composite Channel Sections at Spar LE to Reinforce Spar/Shell Bond Joints
- Composite Close Out at Airfoil Base
- Wider LE Lap Joints
- Solid Composite in TE Cavity
- Improved Shell Taper Pattern at Root
  - Full Ply Length on the Spar Surface

Figure 3-34. Improved Fan Blade Mechanical Design.

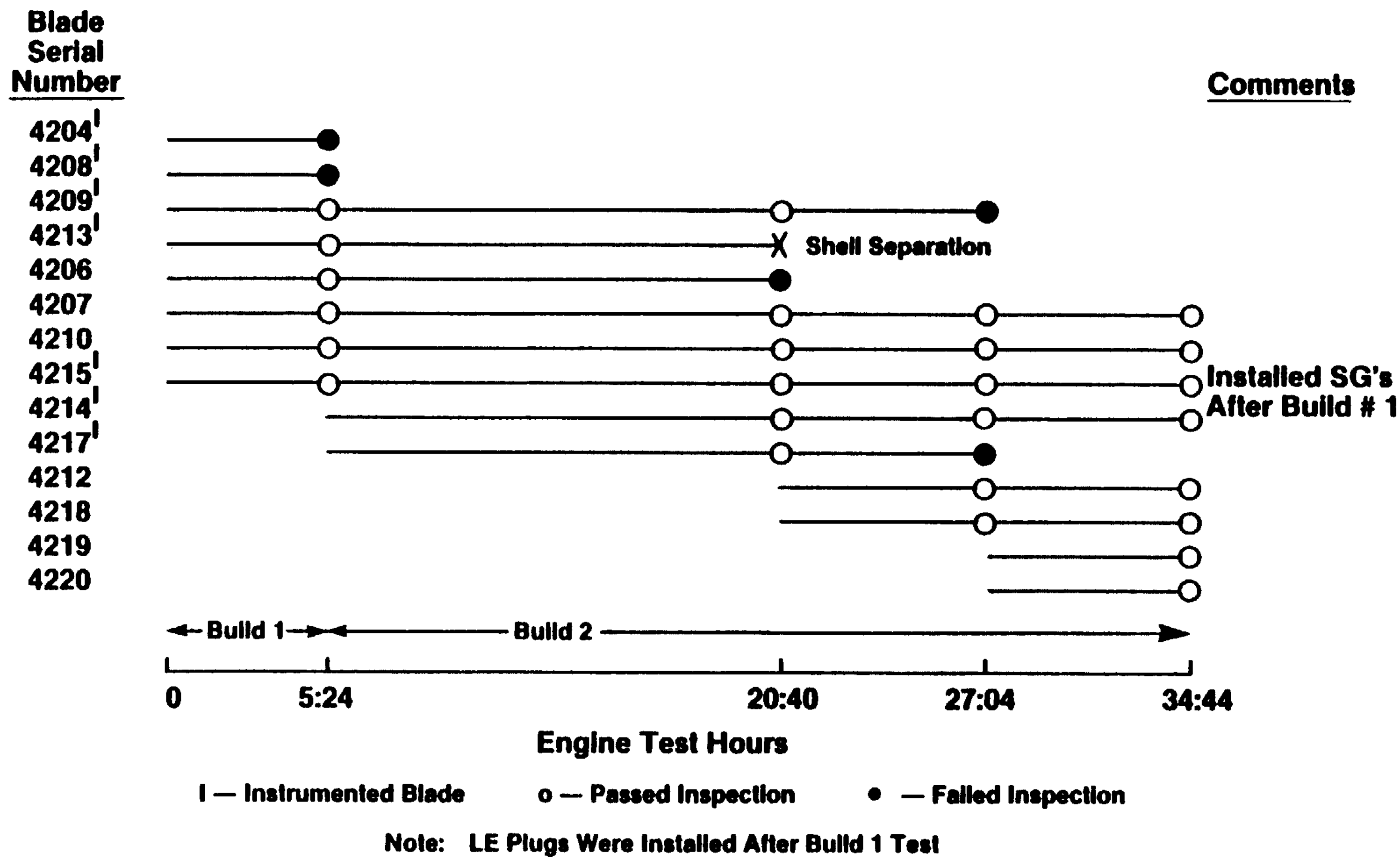


Figure 3-35. Stage 2 Fan Blades Engine Test History.

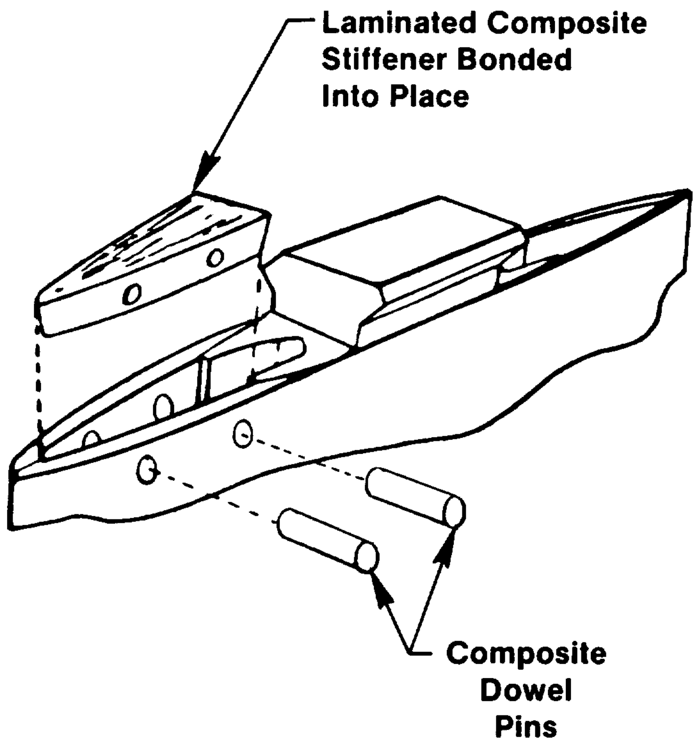


- **Plug Retrofit Creates Stiff 'Closed-Box' To Preclude Crack Propagation And Increase Tolerance To Thermal Cycling**

Figure 3-36. Fan Blade Structural Improvement.

| | Stage 1 | | Stage 2 | |
|---|---|---|---|---|
| | 1/Rev | 2/Rev | 1/Rev | 2/Rev |
| ● Build 1 | | | | |
| - Part Power | 0 | 6-8 | 0 | 4-6 |
| - 24K Run | 1.0 | 7-8 | 1.0 | 5-6 |
| ● Build 2 | | | | |
| - Mechanical Check | 1.0 | 6-8 | 1.0 | 10-12 |
| - Mismatched Speed | 1.0 | 3-5 | 1.0 | 7-10 |
| - 25K Run | 1.0 | 4-6 | 1.0 | 8-10 |
| - Health Verification Run | 1.0 | 3-4 | 1.0 | 7-8 |
| ● Build 3 | | | | |
| - Mech. Checkout - 24K | 1.5 | 5.1 | 1.5 | 8.7 |
| - LCF Cycles | 0.8 | 1.3 | 1.0 | 4.6 |

Figure 3-37. Fan Blade Response Summary - ksi pp.

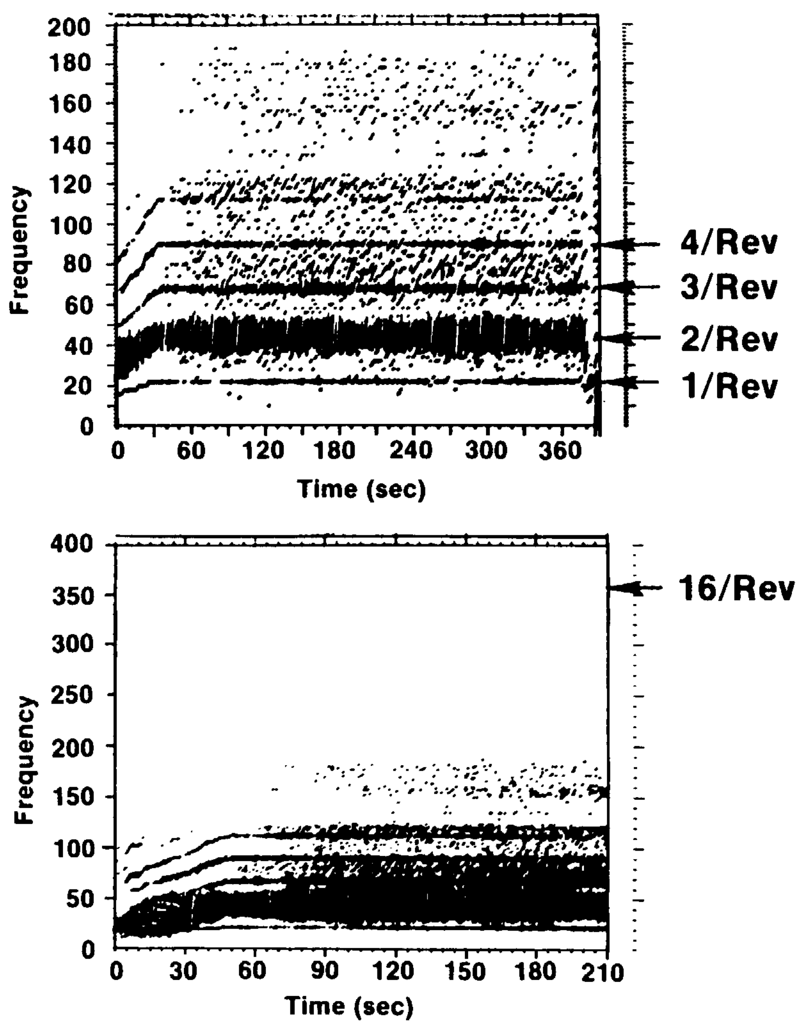


- **Blade Stable**
- **No Flow Separation Induced Vibration**
- **Low/Rev Responses**
  - **- Less Than 35% Scope Limit**
    - **10 ksi Overall**
    - **8 ksi at 2/Rev**
    - **2 ksi at 3/Rev**
    - **1 ksi at 4/Rev**
    - **Nondiscernable at 16/Rev**

**24,000 lbf Thrust Run: October 2, 1986**
**5 ksida =**

Figure 3-38. Stage 1 Fan Blade Response Summary.

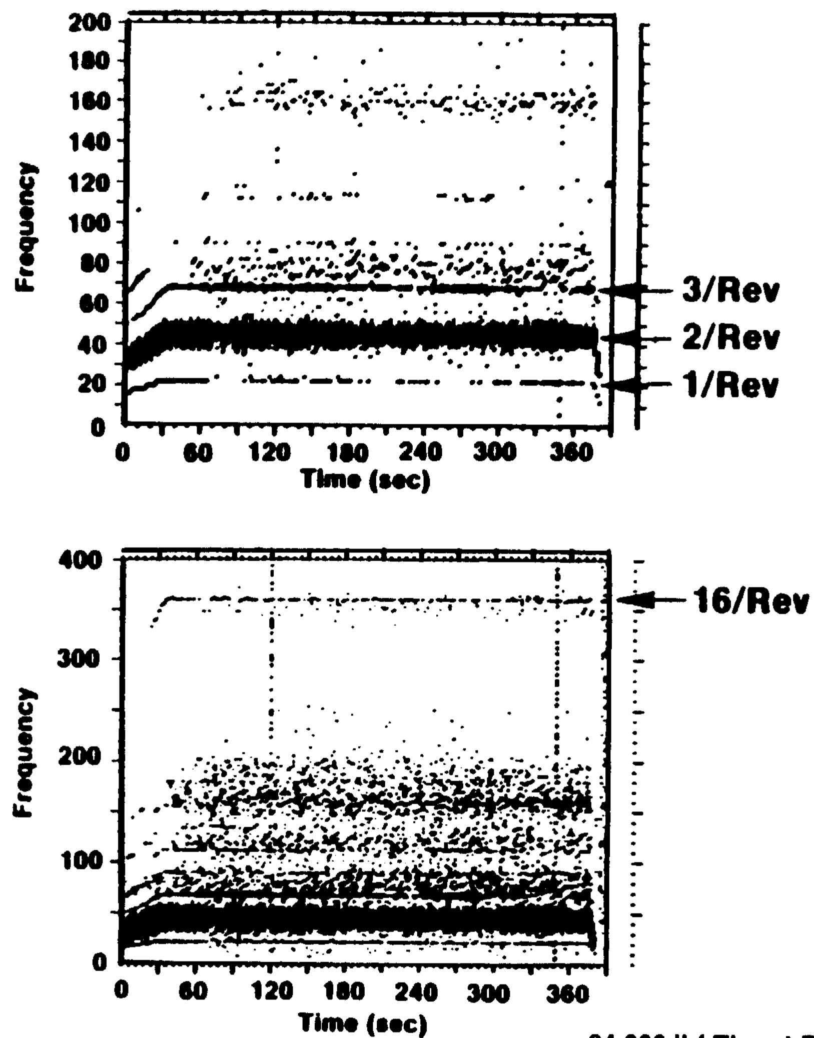


- **Blade Stable**
- **No Flow Separation Induced Vibration**
- **Low/Rev Responses**
  - **- Less Than 35% Scope Limit**
    - **8 ksi overall**
    - **7 ksi at 2/Rev**
    - **1 ksi at 3/Rev**
    - **Nondiscernable at 16/Rev**

24,000 lbf Thrust Run: October 2, 1986
5 ksipp = /

Figure 3-39. Stage 2 Fan Blade Response Summary.

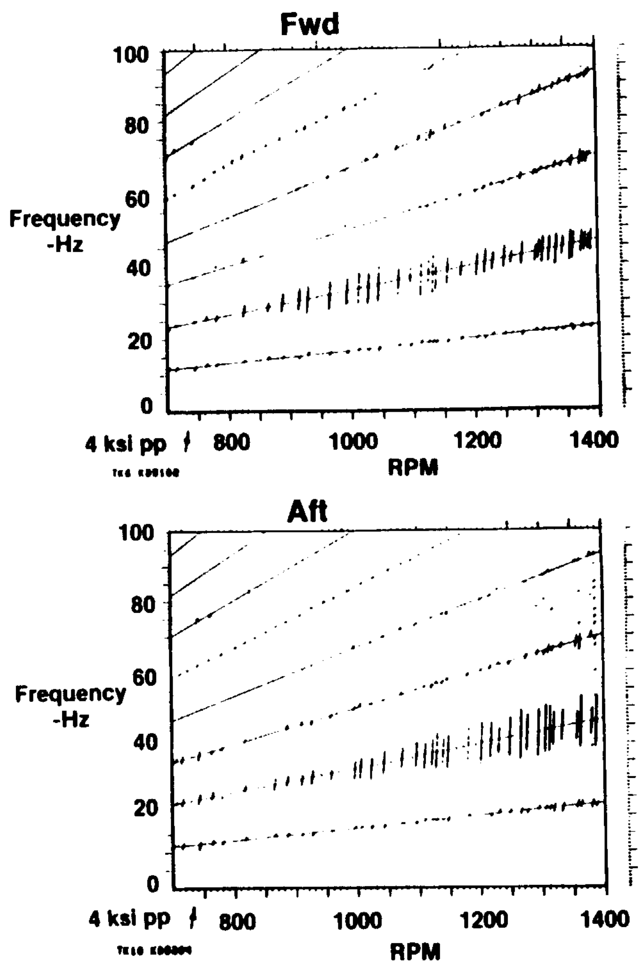


- No Flutter
- No Separated Flow Vibration
- Per Rev Responses — ksi pp

| | 1/Rev | 2/Rev | 3/Rev |
|---|---|---|---|
| Stage 1 | (0.5/1.0)* | 4.0/8.0 | 3.0/5.0 |
| Stage 2 | 1.0/2.0 | 9.0/15.0 | 1.5/3.0 |

* (Steady/Peak**)
** Due to 6-18 mph Unsteady Crosswind

Figure 3-40. Fan Blade Response Summary - February 4, 1986 Maximum Power Run (25,000 lbf Corrected Thrust).

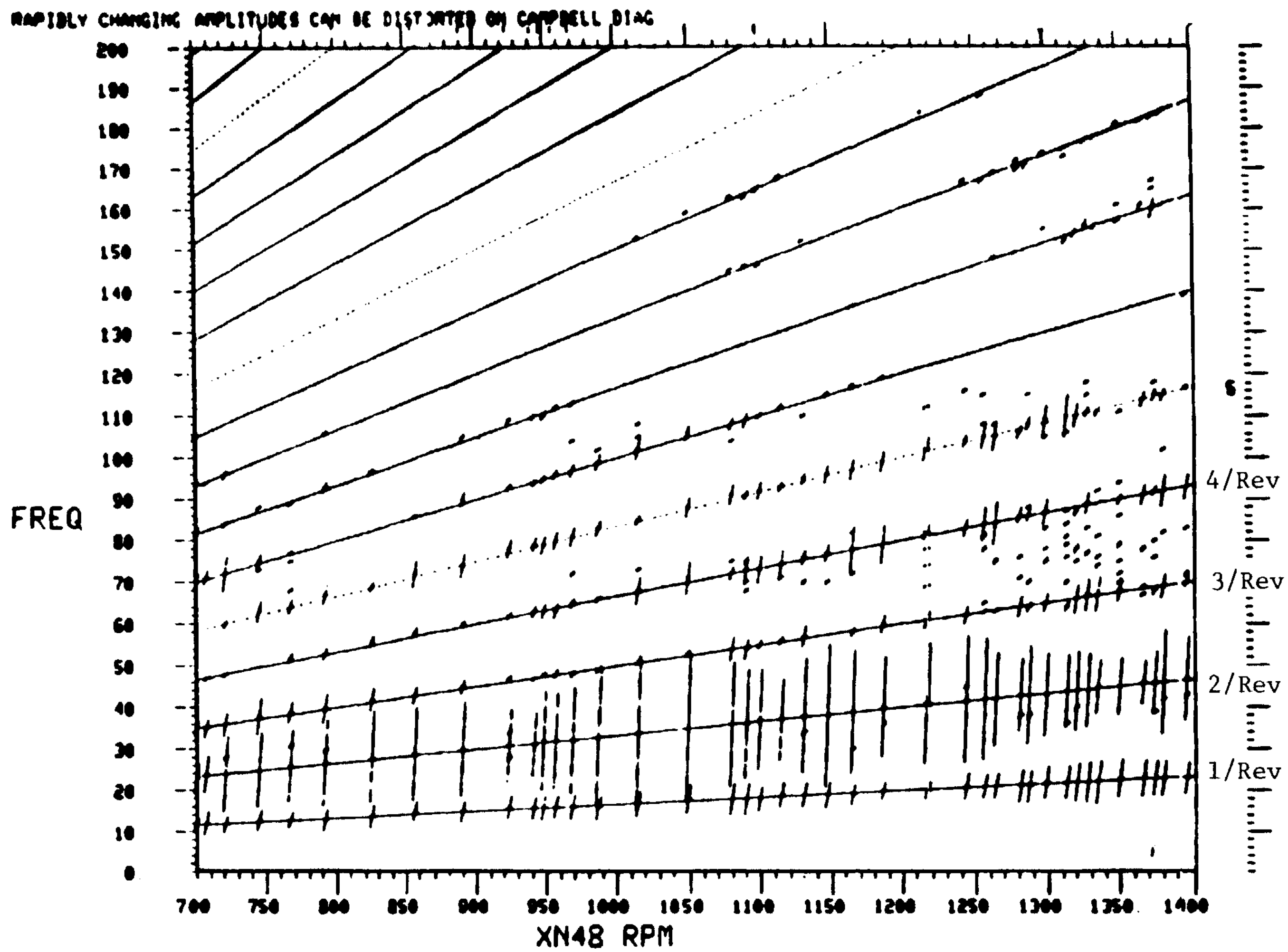


Figure 3-41. Stage 1 Fan Blade Response, Accel to 24,000 lbf: June 24, 1986.

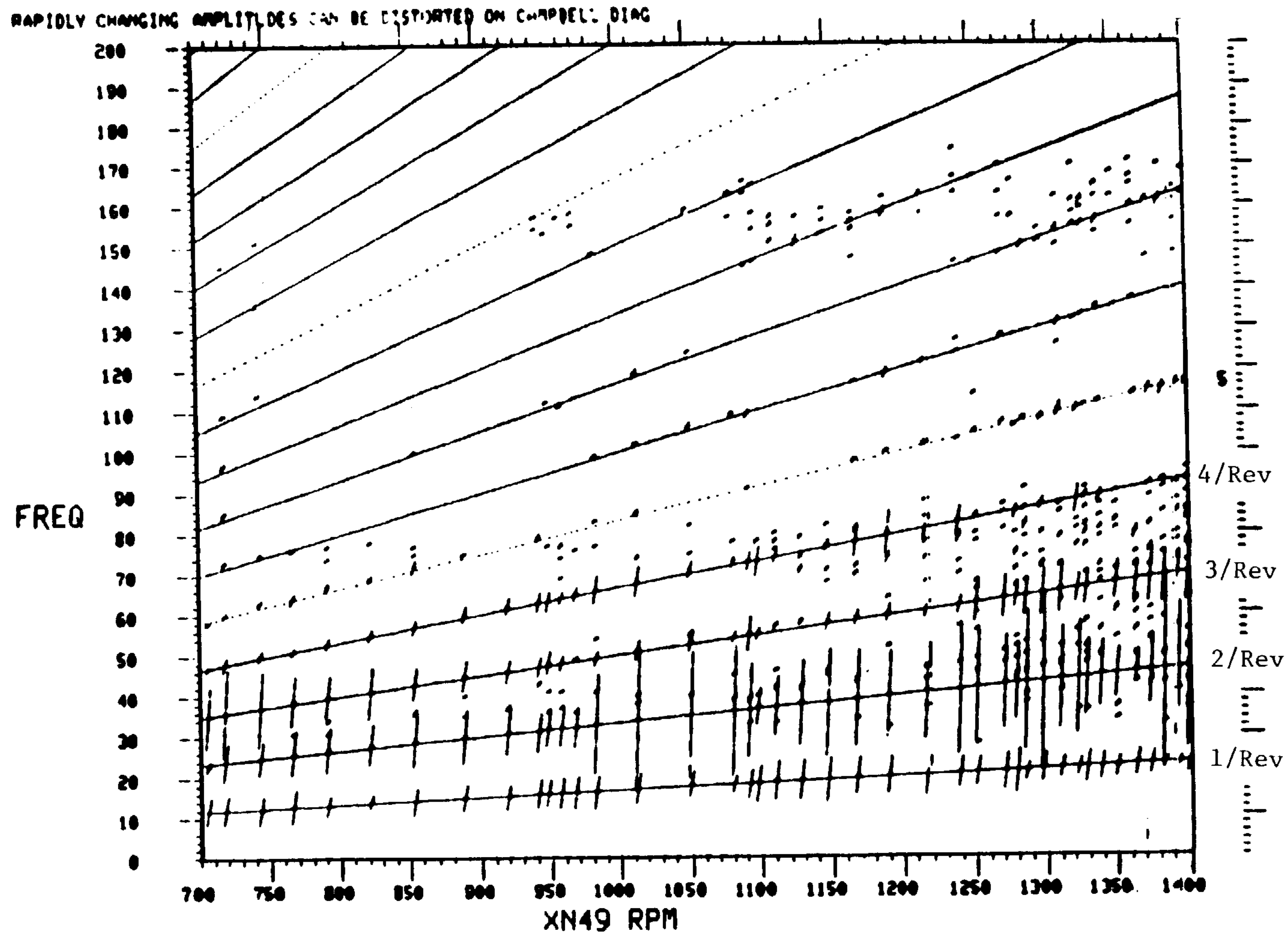


Figure 3-42. Stage 2 Fan Blade Response, Accel to 24,000 lbf: June 24, 1986.

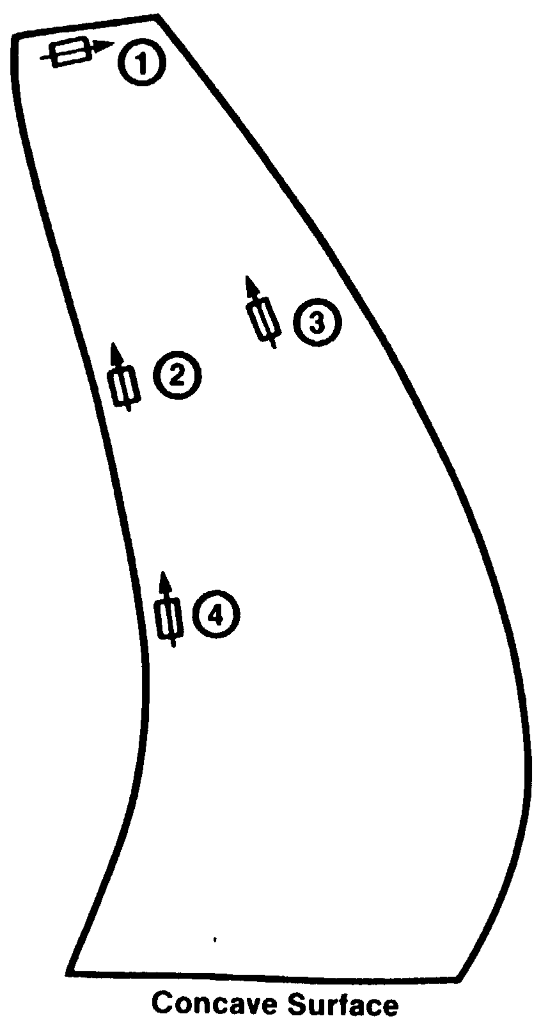


- **Total Of 16 Gages Per Stage**
  **4 Gages/Blade And 4 Blades/Stage**

**1 - Gage - Sensitive To 1 Torsion And High Order Modes**

**2 - Gage - Sensitive To 2 Flex And I/P Forced Response**

**3 - Gage - Sensitive To Axial Mode And High Order Flex Modes**

**4 - Gage - Location of Highest SS Stress And 1 Flex Vibratory Stress**

Figure 3-43. Fan Blade Strain Gage Locations.

### Fan Blade Response with Facility Fans

At the first test site (4A) a set of 12 facility fans were arranged in front of the UDF™ inlet. Figure 3-44 shows a schematic of the facility fan configuration. These fans attempt to simulate forward velocity of an engine and try to smooth out airflow through and around the engine. It was desired to see if some combination of these fans would lower fan blade stress. The results can be seen in Figure 3-44; the first data point (no fans on) gave a lower vibratory stress level than with any number of fans on. Stress levels varied widely, depending on the number of fans that were on, but all levels were higher than those without any fans. Since the engine centerline and the facility fan centerline were not in line, it was believed that the fans created additional disturbances in the flow field instead of smoothing the airflow.

## 3.12 POWER TURBINE FRAME STRESS

During Build 2, power turbine frame vibratory stresses were higher than predicted. The stresses were found to be predominantly 2/rev forced response. This was caused from the fan Rotor 2 nodal, first flex mode (note that the turbine frame and the fan blade rotor are mechanically linked). This causes the frame stress to track the fan blade stress. Figure 3-45 provides a stress comparison.

A detailed investigation into the frame stress allowed the vibratory stress limits to be increased for the forced response mode (Figure 3-46). A summary of this investigation and its results is in Table 3-1; supporting data is shown in Figures 3-47 and 3-48. Build 3 data is presented in Figure 3-49.

## 3.13 EFFECT OF VORTEX DESTROYER ON STRESS

Vortices were seen between the ground and the fan blades at the bottom of the engine. Visualization of these vortices was aided by having moisture on the ground or by releasing smoke bombs. To see if the placement of a vortex destroyer (a large metal grating) under the fan blades would reduce the fan blade and power turbine frame vibratory stress levels, a vortex destroyer was placed under the fan blades approximately 6 inches off the ground. Fan blade

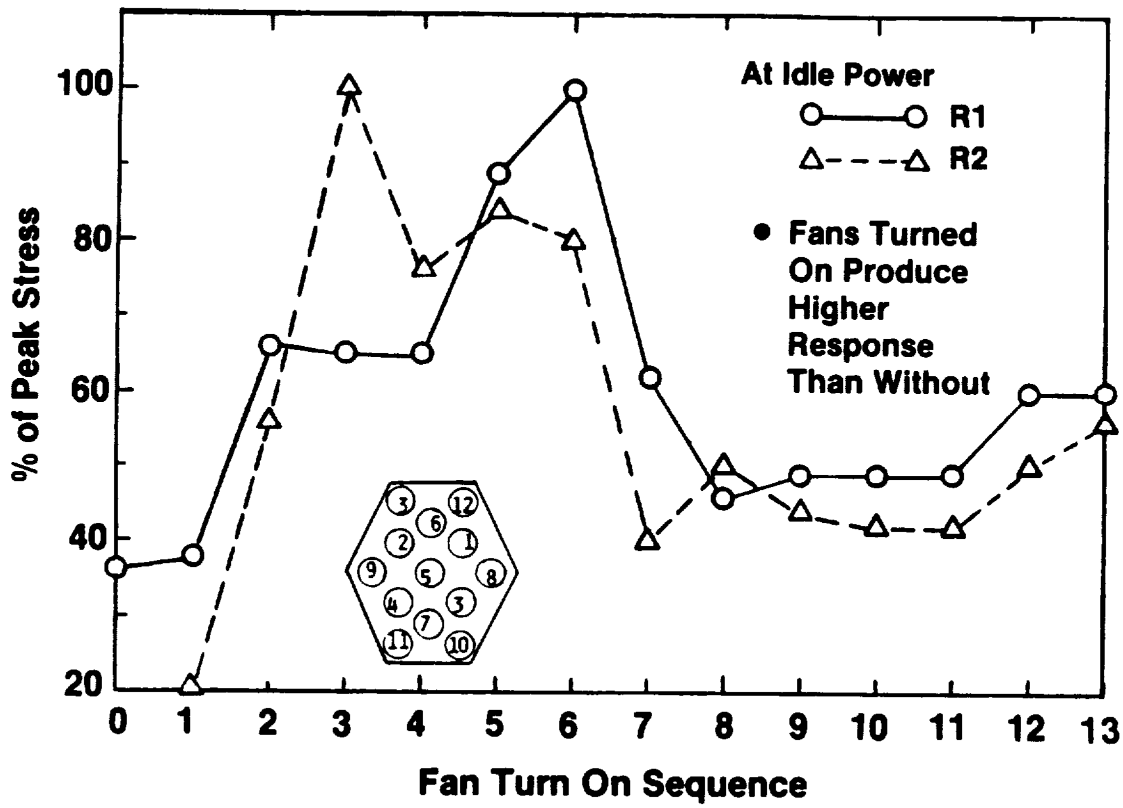


Figure 3-44. Fan Blade Response with Facility Fans Turned On.

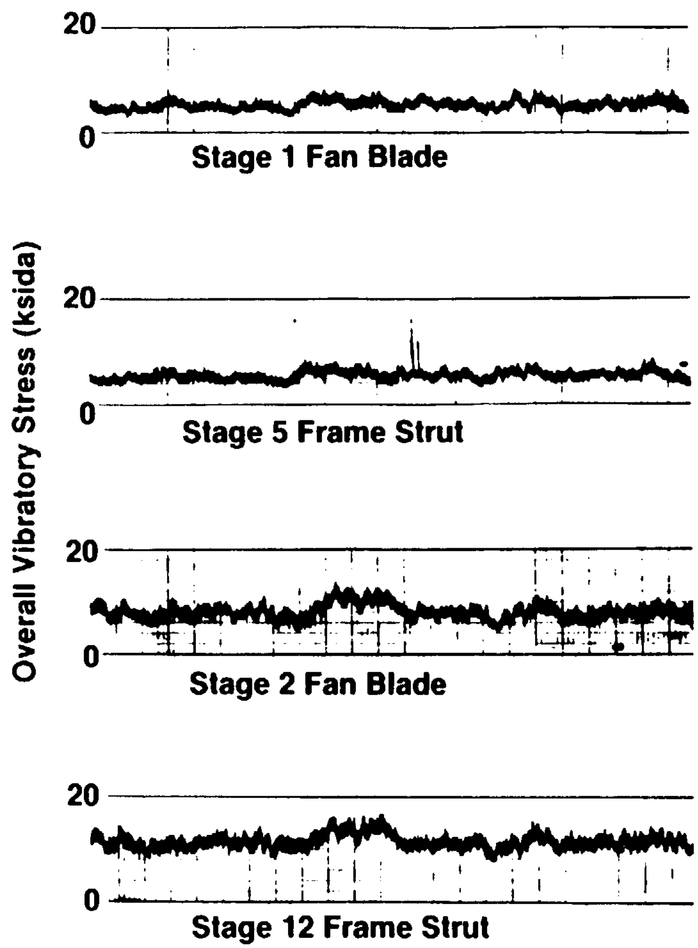


- **Build 2 Observations**
  - **Higher Than Expected Vibratory Stress**
  - **Predominantly 2/Rev Forced Response**
  - **Frames Track Fan Blades**
- **Diagnosis**
  - **Fan Rotor 2 Nodal — 1st Flexible System Mode**
  - **Limits Not Well Defined for This Mode**

Figure 3-45. Power Turbine Frames Vibratory Response Summary.

# Results:

- **Updated Scope Limits Versus Site 4A Response**
- **HCF Testing**

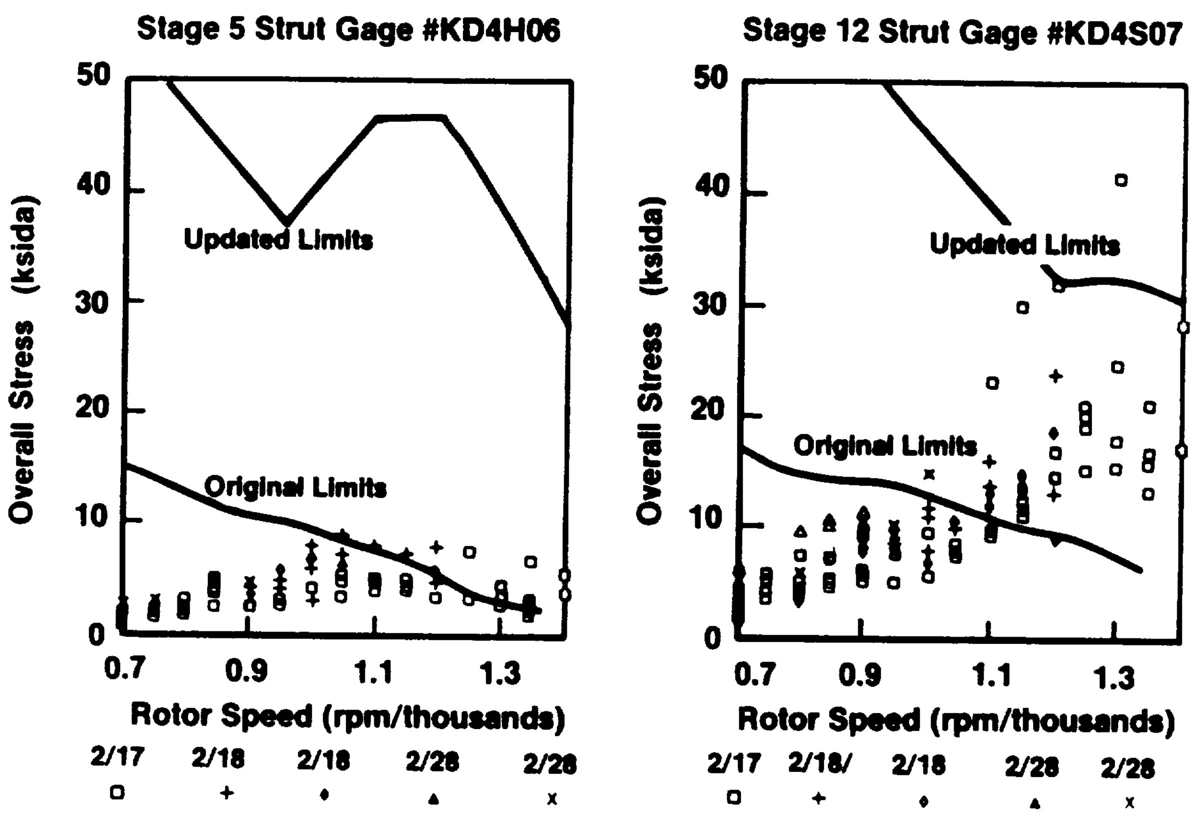


Figure 3-46. Power Turbine Frames Vibratory Response, Updated Scope Limits Versus Site 4A Response.

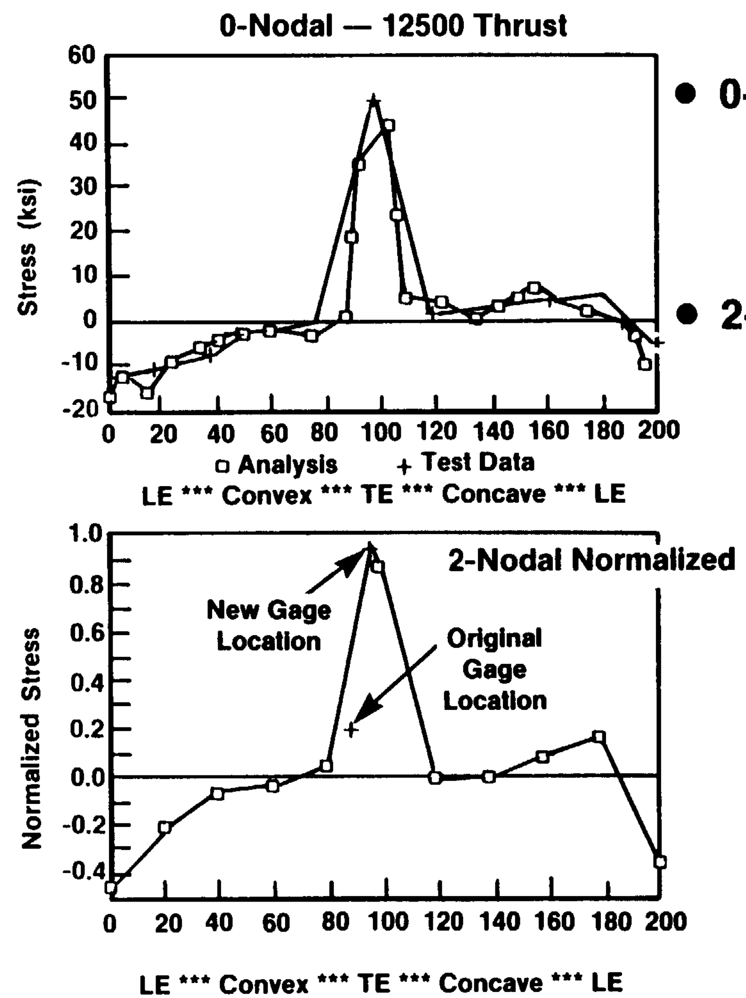


- **0-Nodal Load**
  - Mean Stress Analysis Correlated
  - High Local Root TE Stress Confirmed
- **2-Nodal Load**
  - High Local Stress/Deflection Controlled Loading Confirmed
  - Original Gage Location
    - Selected for Airfoil Modes
    - Poor for 2N Mode
  - New Gages Applied
    - Higher Response Location
    - Used to Correlate Original Gages

Figure 3-47. Power Turbine Frames Vibratory Response, Stage 12 Component Strain Distribution Test Results.

- **Frame Properties Better Than Material Handbook Average**

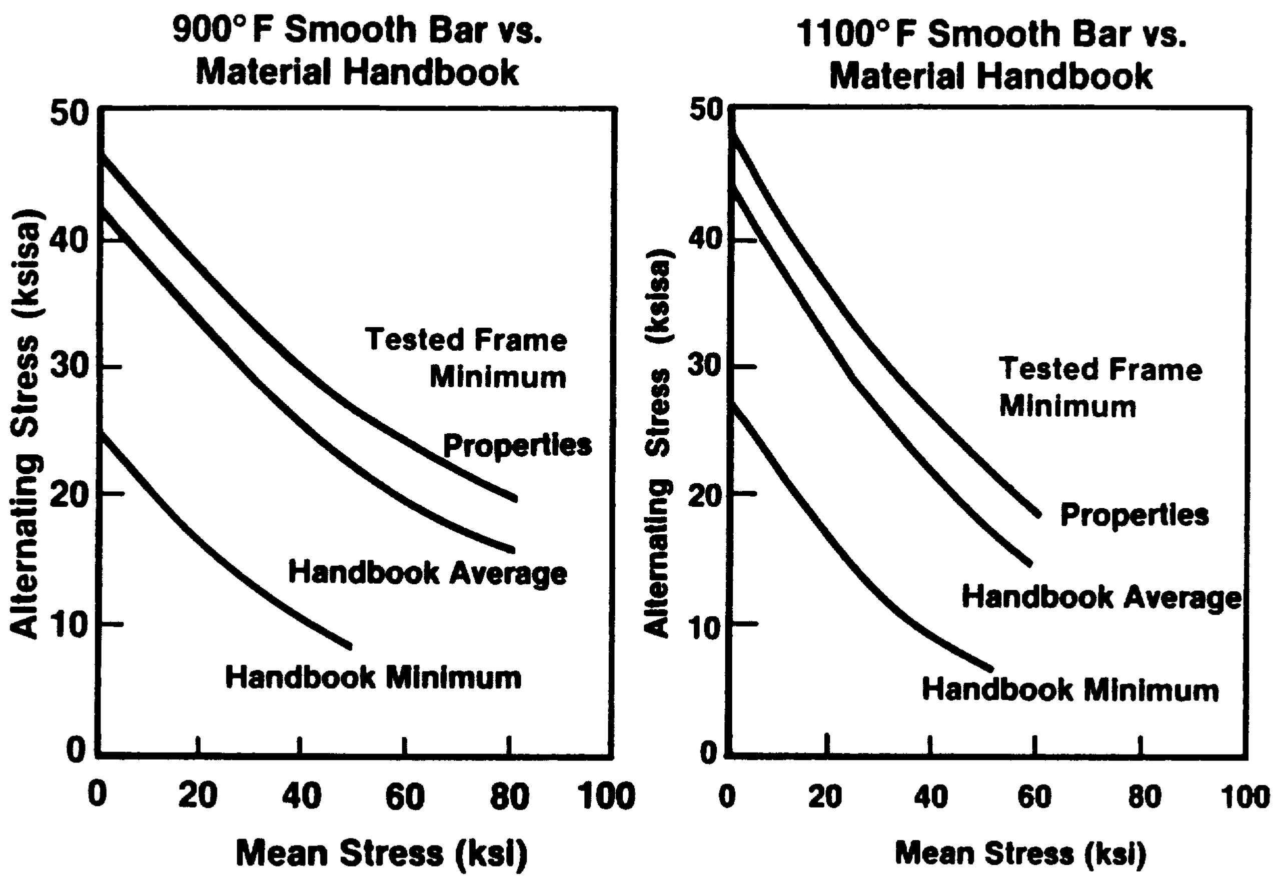


Figure 3-48. Power Turbine Frames Vibratory Response, Material HCF Test Results.

- **Peak Levels**
  - **Consistent with Build 2**
  - **Below Scope Limits**

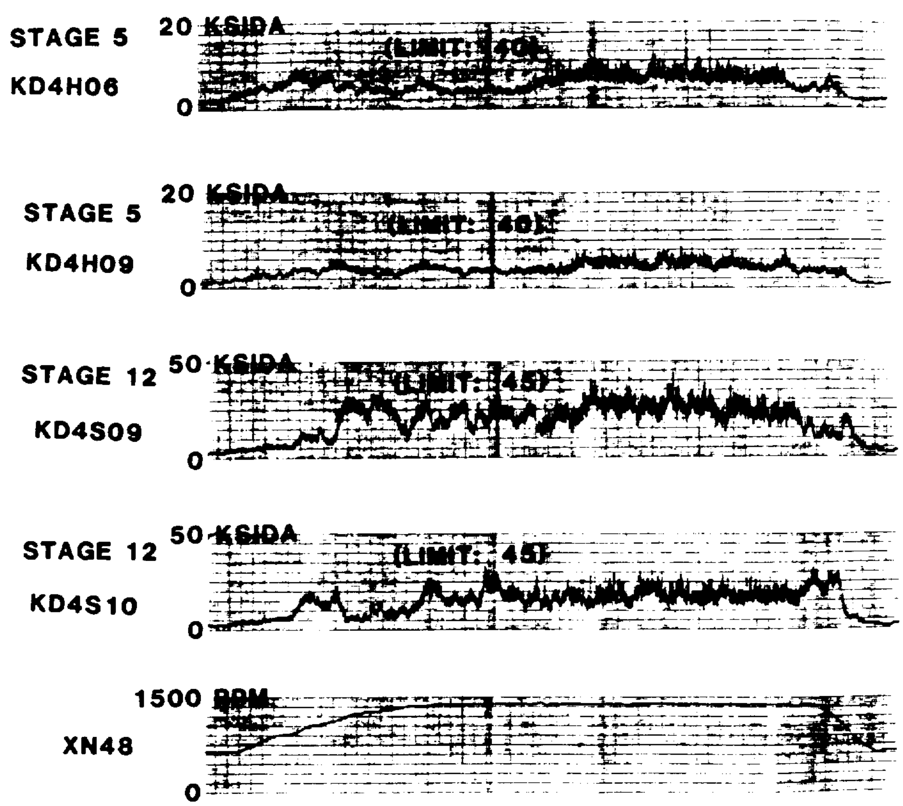


Figure 3-49. Power Frame Vibratory Response, Build 3.

stress data both with and without the vortex destroyer is contained in Figure 3-50. The same type of data are shown for the turbine frames in Figure 3-51. Since this testing was performed after the Stage 2 fan blade loss, and before installation of the redesigned fan blades, the engine was limited to 1000-rpm fan speed, thus limiting available analytical data for comparison. The vortex destroyer seemed to have a small positive or negligible effect on stresses; however, it was decided to complete all remaining engine testing with the destroyer in place. Wind conditions and the limited data (due to the 1000-rpm fan speed limit) did make comparisons difficult.

Table 3-1. Power Turbine Vibratory Response Resolution.

| | |
|---|---|
| Vortex Destroyer | No Significant Effect (Section 3.13) |
| Change Test Sites | Slight Improvement (Section 3.14) |
| Component Strain Distribution Test | Mean Stress Analysis Verified |
| | Stage 12 Engine Gage Poorly Located for 2N Mode |
| | New Stage 12 Gage Applied Which Read Maximum Stress |
| Material HCF Testing | Significant Property Improvement Over Handbook Average |
| Updated Scope Limits | Stage 5 Frame Okay |
| | Stage 12 Frame Marginally Okay |

## 3.14 EFFECT OF TEST SITE CHANGE ON STRESS

To try to reduce vibratory stress levels in the fan blades and the forced vibration of the power turbine frames, the engine was moved from Site 4A to 3D. The site change increased the clearance between the ground and fan blades from 28 inches to 64 inches as well as eliminated the frontal blockage area at Site 4A caused by the permanent facility fan system that was in front of the UDF™ inlet. Stress data are shown from both sites for the fan blades (Figure 3-52) and the turbine frames (Figure 3-53). There was no significant decrease in either fan blade or turbine frame stresses. Fan blade stress data, after the site change, was prior to the installation of the redesigned fan blades

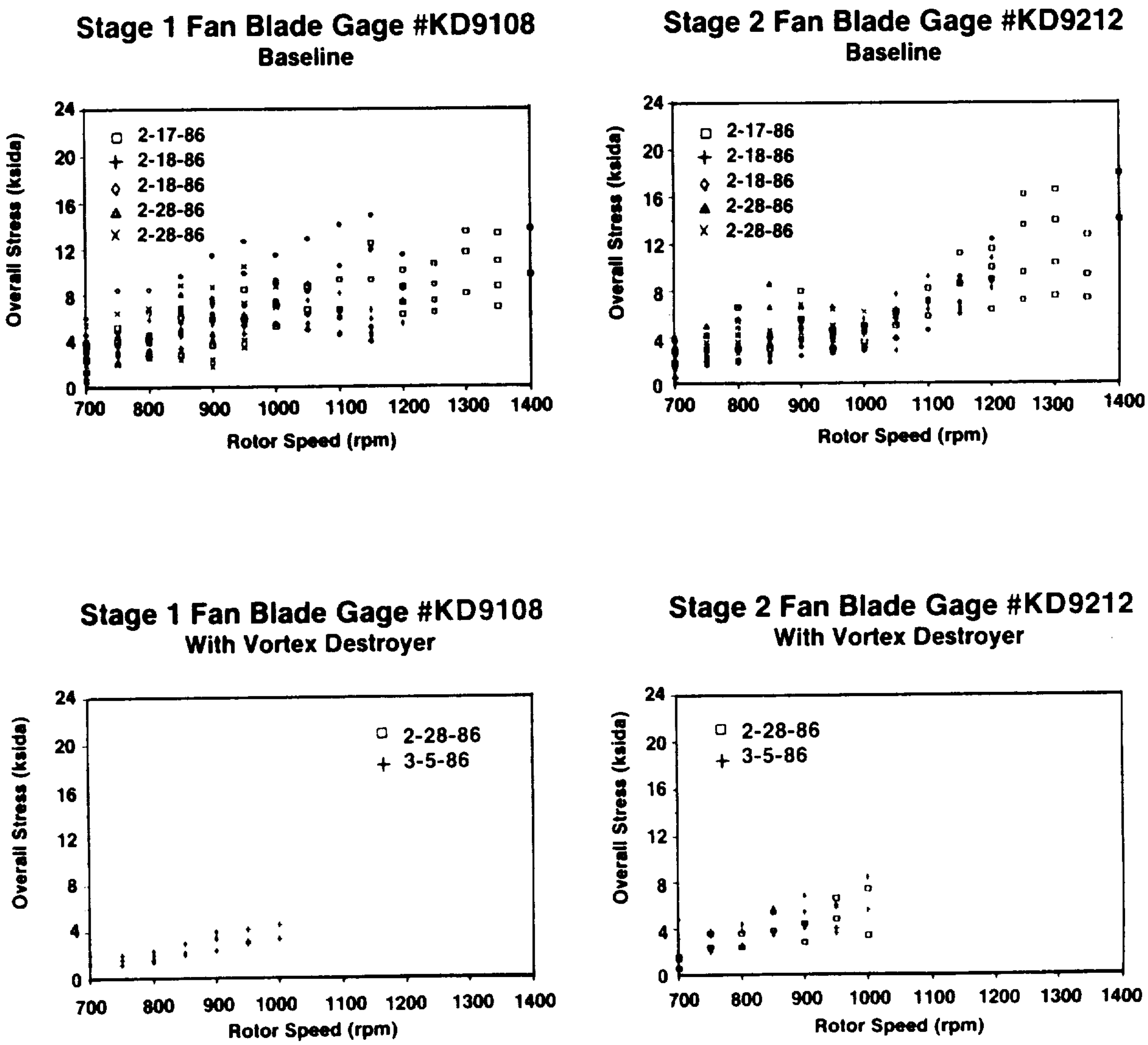


Figure 3-50. Fan Blades Vibratory Response, Effect of Vortex Destroyer.

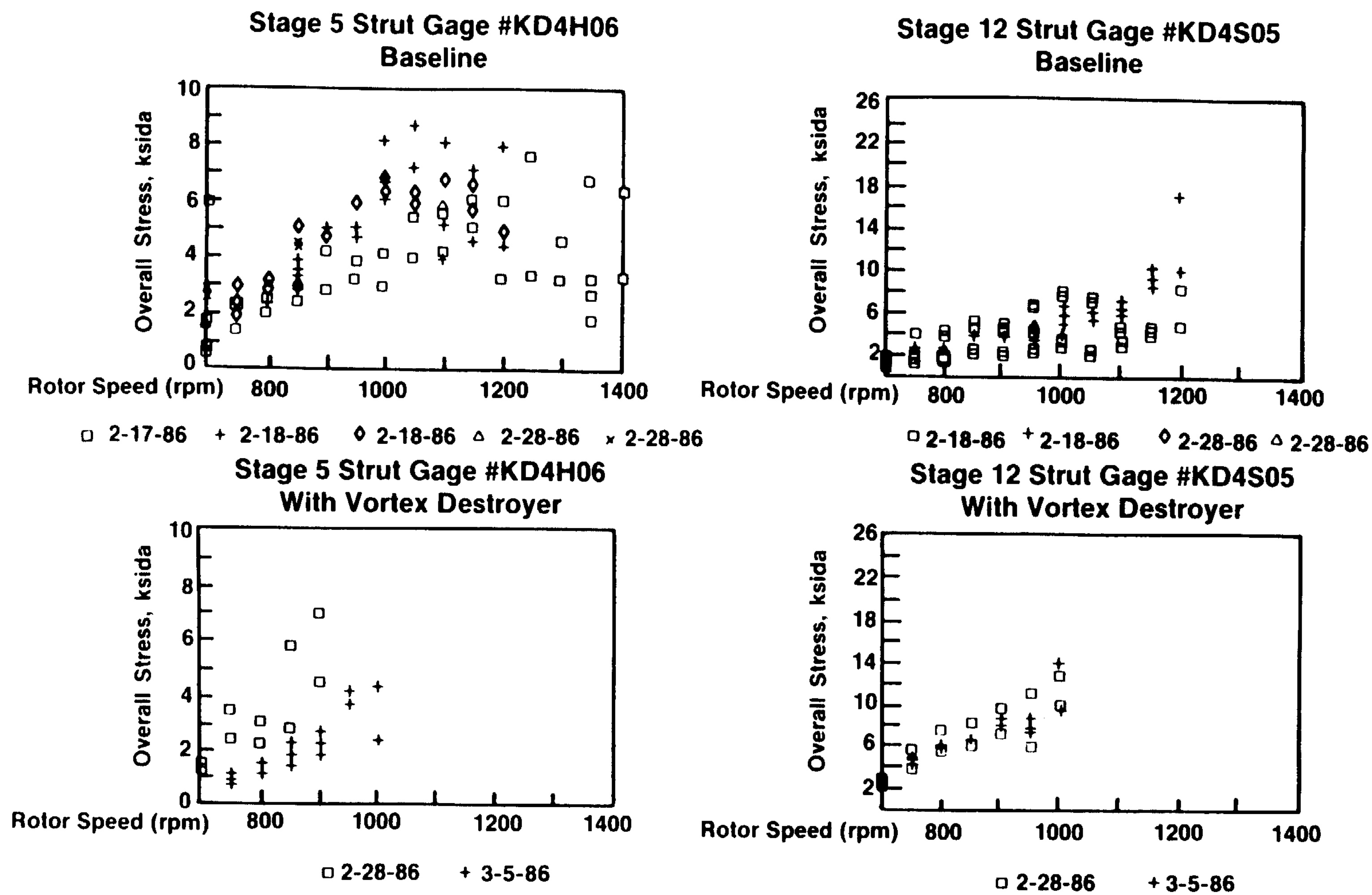


Figure 3-51. Power Turbine Frames Vibratory Response, Effect of Vortex Destroyer.

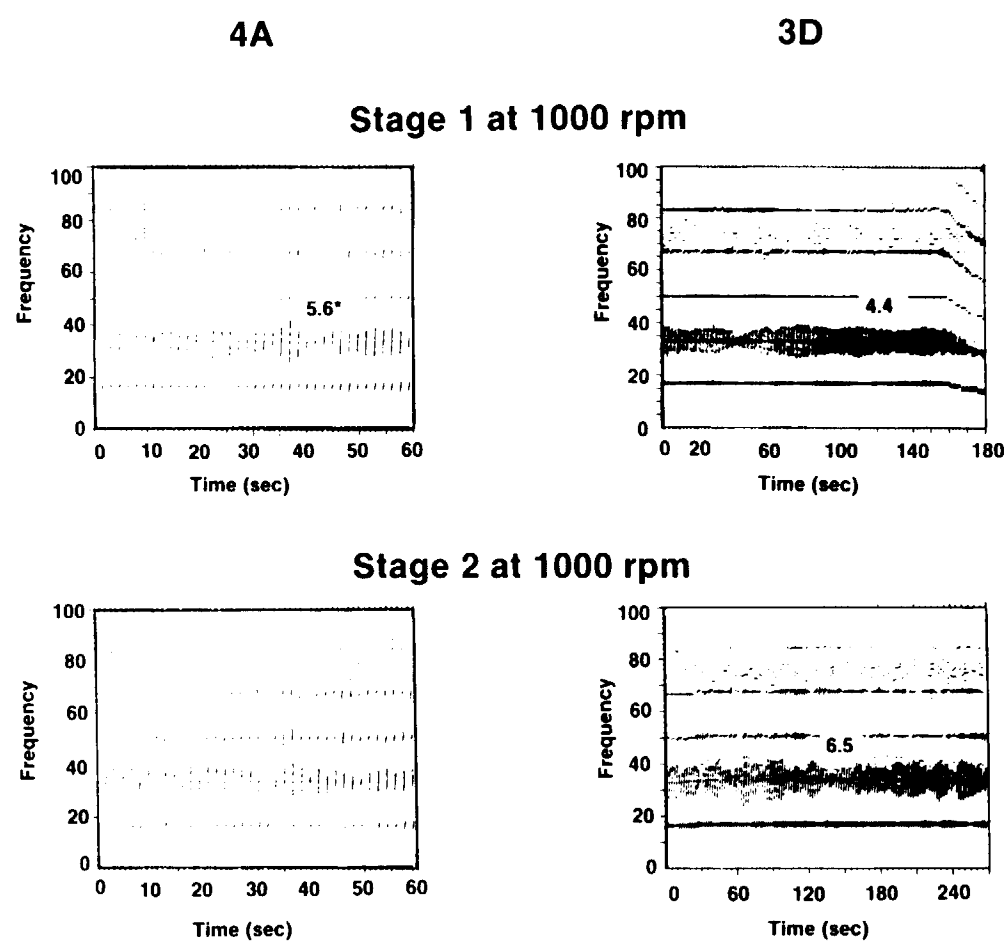


- Site Differences
  - Ground Clearance Increased from 28” on 4A to 64” on 3D
  - Reduced Frontal Blockage at 3D
- Results
  - No Apparent Differences in Low Speed Response Level or Content
  - Maximum Steady State Speed Obtained on 3D is 1000 rpm, No Maximum Power Runs
  - Low Ambient Winds During 3D Testing

*Peak Stress in KSIDA

Figure 3-52. Fan Blade Response Comparison, Site 3D Versus Site 4A.

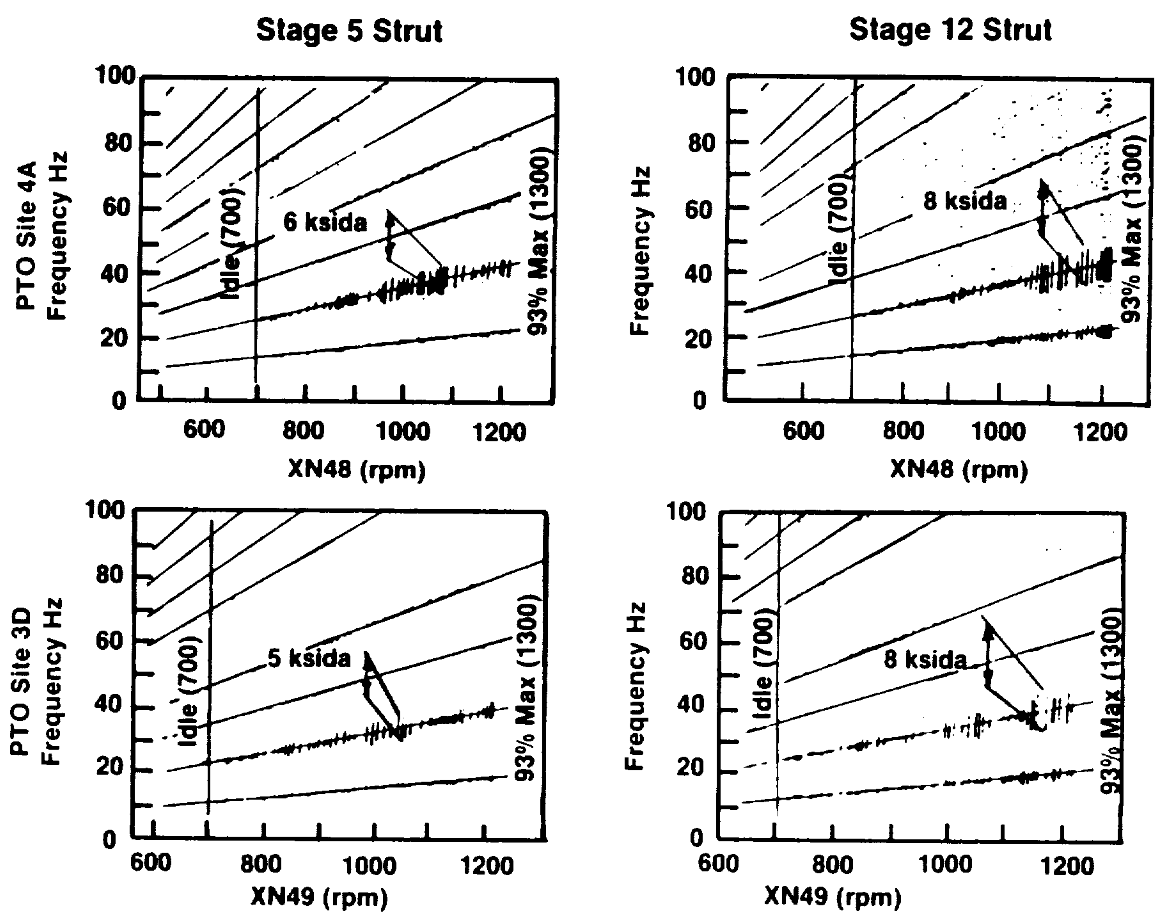


Figure 3-53. Power Turbine Frames Vibratory Response, Effect of Site Change.



C-2

so that a direct comparison of fan blade stress could be made. Fan speed was limited to 1000 rpm until the redesigned fan blades were installed. Turbine frame stress data, after the site change, is from Build 3 (after installation of the redesigned fan blades).

## 3.15 ROTOR LOCKUP AFTER SHUTDOWN RESULTING FROM FUEL LEAK

While running a power-down calibration at 19,000 lbf on June 30, 1986, a fuel leak was observed, and the engine was quickly shut down. After propulsor spool down, the Stage 2 rotor would not rotate until the engine had cooled for several hours. At that time, the exact cause was not known; however, based on a later teardown, it is believed that the IGV lip seal had deflected thermally and bound to the 1-4 inner spool. When the engine had cooled sufficiently, the IGV and the spool separated enough to allow rotation of the Stage 2 rotor. From looking at strain gage data for Stages 1 and 2 turbine blades, it appears (Figure 3-54) that the IGV and spool had started to rub as early as June 24. Heat generated from this interference eventually closed the Stage 1 turbine blade clearance causing severe turbine blade tip rubs; Section 3.17 discusses this further.

## 3.16 LOW/HIGH CYCLE FATIGUE TESTING

During Build 3, 100 low cycle fatigue cycles were run for endurance testing. The cycle that was run is shown in Figure 3-55.

No dedicated high cycle fatigue testing was necessary because cycles in excess of $1 \times 10^6$ were accumulated through the course of normal testing. The number of cycles accumulated on each component was calculated using the component first flex natural frequency and the engine run time versus propulsor rpm relationship.

Table 3-2 shows the number of high- and low-cycle fatigue cycles that the turbine blades, fan blades, and power frame airfoils experienced.

## 3.17 ROTOR-TO-ROTOR LOCKUP/PROPULSOR DISASSEMBLY AND REBUILD

During an attempt to make a normal start, it was noticed that the forward and aft rotors although locked together could be turned with force. During

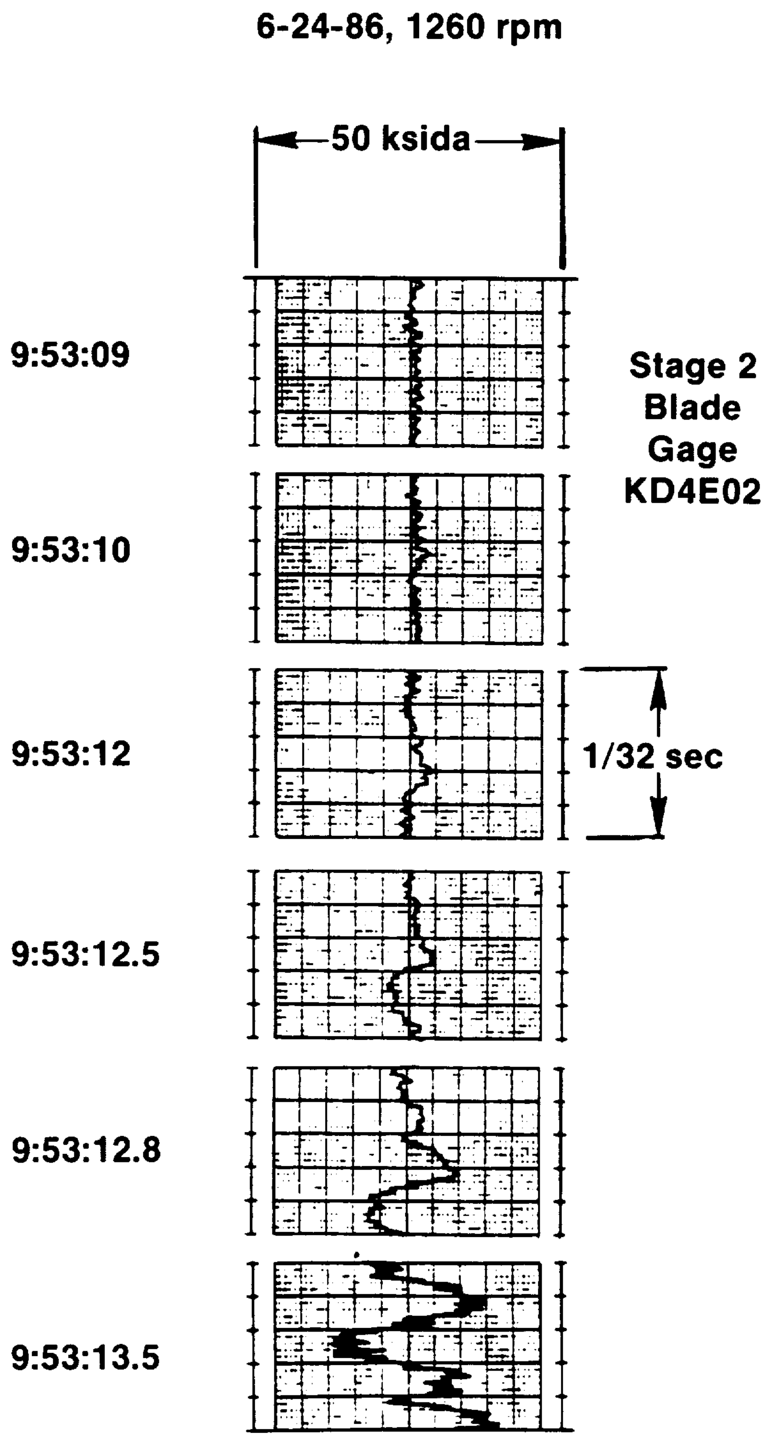


Figure 3-54. Suspected IGV/Spool Rub.

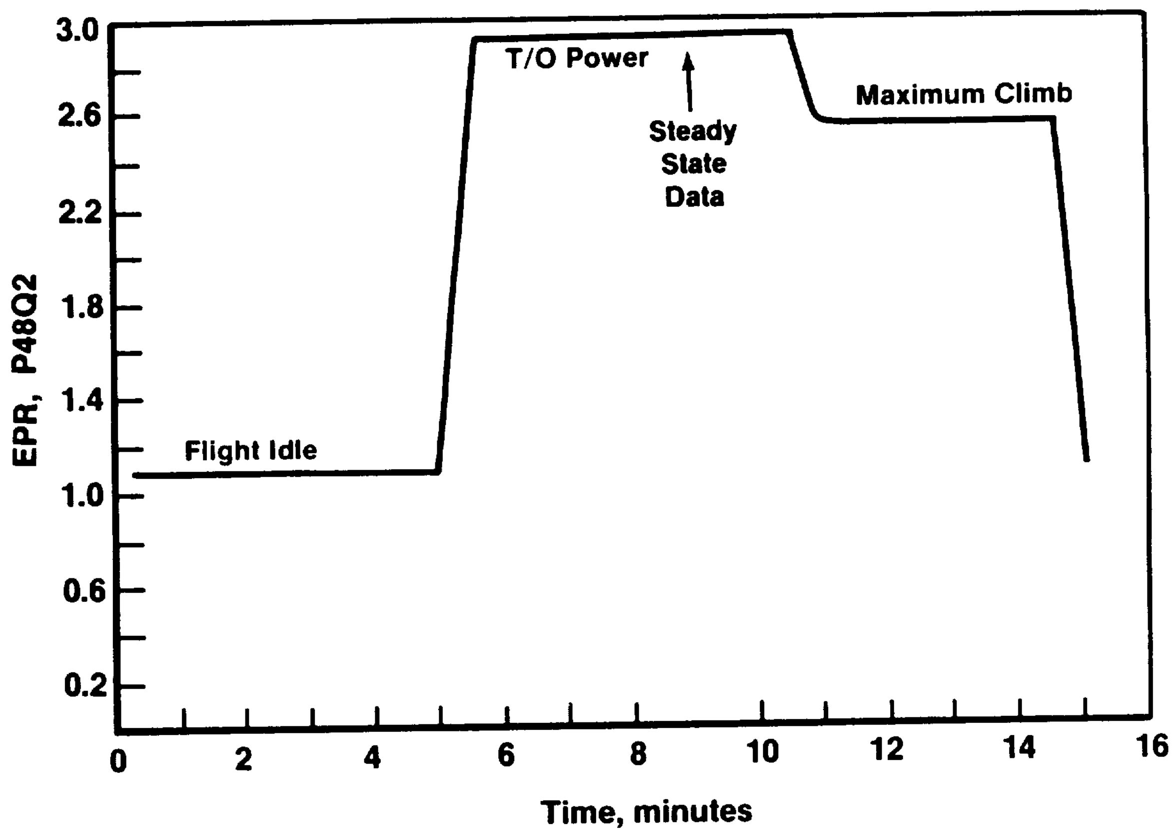


Figure 3-55. Low Cycle Fatigue Cycle.

trim balancing, previously, the engine had run up to 22,000 lbf. No problems occurred before the rotors locked. The force required to turn the rotors increased when the blade actuation system was commanded to full reverse. It was found that the forward actuator would not move to full reverse (-20°), but only went to -12°. The rotors did not free up as the engine cooled, and the decision was made to remove it from the test site to investigate the problem.

Table 3-2. GE36 HCF Cycle Count.

| Turbine Blades | HCF Cycles | LCF Cycles | Remarks |
|---|---|---|---|
| Stage 1 | $6.23 \times 10^6$ | 100 | 53 Cracked Blades |
| Stage 2 | $4.09 \times 10^6$ | 100 | No Discrepancies |
| Stage 3 | $5.00 \times 10^6$ | 100 | No Discrepancies |
| Stage 4 | $18.18 \times 10^6$ | 100 | No Discrepancies |
| Stage 6 | $14.10 \times 10^6$ | 100 | No Discrepancies |
| Stage 7 | $7.5 \times 10^6$ | 100 | No Discrepancies |
| Stage 8 | $15.15 \times 10^6$ | 100 | No Discrepancies |
| Stage 9 | $1.2 \times 10^6$ | 100 | No Discrepancies |
| Stage 10 | $2.5 \times 10^6$ | 100 | No Discrepancies |
| Stage 11 | $1.3 \times 10^6$ | 100 | 3 Cracked Blade |
| Fan Blades<br>Stages 1/2 | $3.69 \times 10^6$/<br>$3.78 \times 10^6$ | 100<br>100 | No Discrepancies |
| Power Frames<br>Stage 5/12 | $4.04 \times 10^6$/<br>$4.2 \times 10^6$ | 100<br>100 | No Discrepancies |

When the engine was returned to the vertical build stand, it was noted that the rotors rotated freely. The actuation system was exercised and found that the forward system still would not travel to the full reverse extension. With the actuation system in the stopped reverse position, the rotors became bound in the same manner as seen on the test stand. A scale was utilized to measure the force required to rotate the forward rotor holding the aft rotor stationary. With the engine vertical and the actuator fully forward (feather or 90°), the force to turn the Stage 1 rotor was 4 lb. When the actuator was driven fully aft (full reverse or -20°), the rotors bound, and the force which was required to turn the forward rotor increased to 40 lb.

| | Full Forward | Full Reverse |
|---|---|---|
| Forward Rotor | 4 pounds | 40 pounds |
| Aft Rotor | 5 pounds | 10 pounds |

The above tabulation provides a comparison of the forces required to turn the rotors independently, with the other held stationary. It was also found that the lack of full travel in the actuator could easily be seen when watching the actuator. The forward system lacked 0.5 inch of its full travel. As the pressure in the hydraulic system was increased (actuator in reverse), the force required to turn the forward rotor increased to 40 lb at 600 psi. The decision was made to pull the propulsor from the gas generator and begin the teardown to investigate the rotor binding.

Removal of the propulsor revealed problems unrelated to the rotor binding. Inlet guide vanes to the propulsor had cracks at the trailing edge ID (inner diameter) braze. The ID was very irregular, and evidence of contact with the Stage 1-4 inner spool was noted. The area between the IGV and the inner seal was black from oil coking, and the Stage 1-4 inner spool was discolored from varnishing. Figure 3-56 diagrams the IGV seal area as-designed, and after test. Figure 3-57 shows the ALF (aft looking forward) view of the tear/crack.

The IGV had worn a 0.010-inch groove in the Stage 1-4 inner spool around the entire circumference. The heat generated by the continual interference between the IGV and spool resulted in a spool growth that closed the Stage 1 blade tip clearance. The spool had heavy rub indications where the Stage 1 blade tips rubbed. The Stage 1 blade rub appears to have begun as early as June 24, after 3 hours of Build 3 testing (Figure 3-58). Examination of the strain gage data for Stages 1 and 2 of the power turbine indicates the IGV-to-inner spool rub occurred prior to the Stage 1 blade rub (Section 3.15).

The Stage 1 blades were found to have HCF cracks that initiated at the leading edge root. The blades with the most visible cracks are illustrated in Figure 3-59. There is a total of 124 Stage 1 blades; of these, 19 blades had

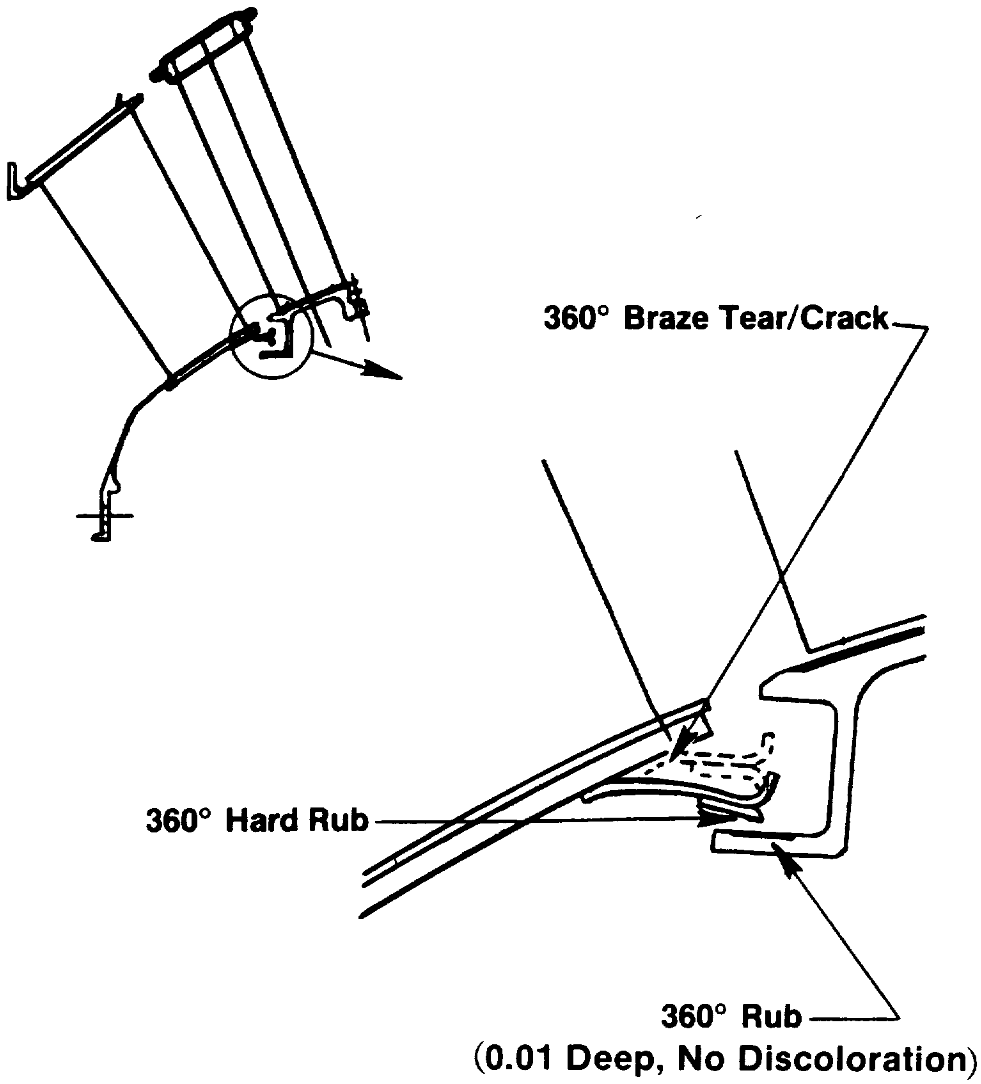


Figure 3-56. IGV and 1-4 Inner Spool.

Figure 3-57. IGV Crack/Tear at Braze Joint (ALF).

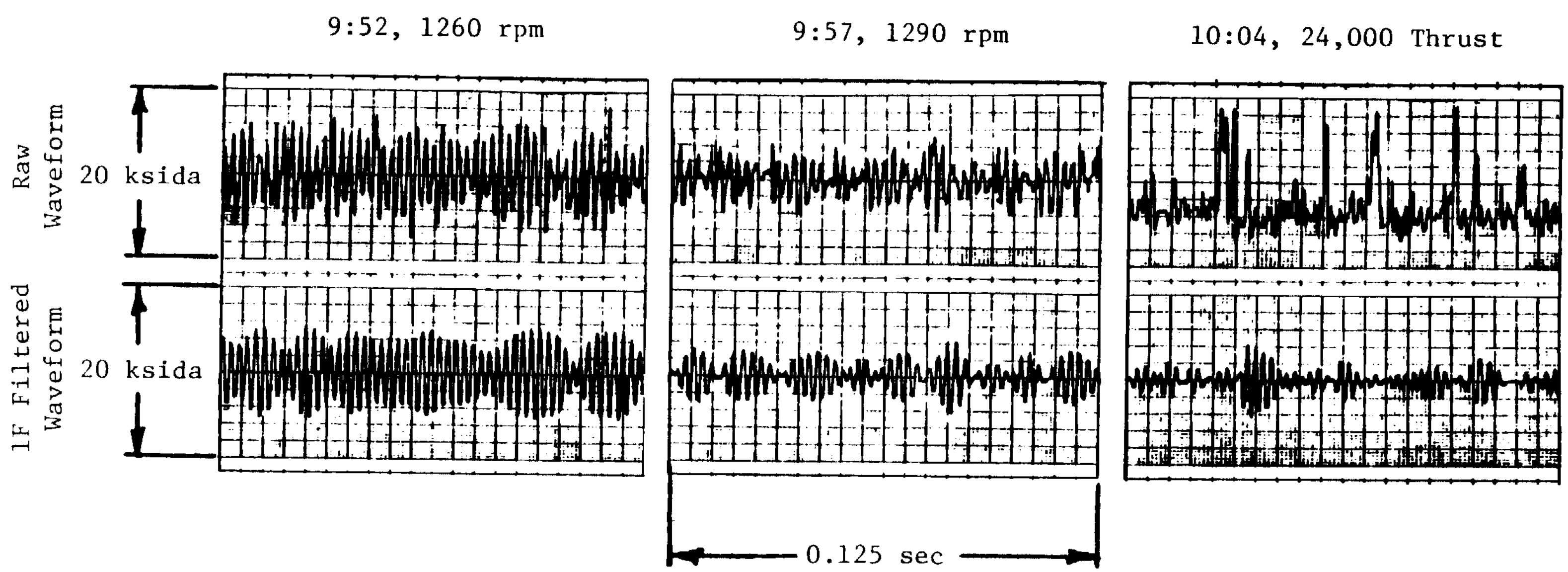


Figure 3-58. Suspected Stage 1 Rub.

~~ORIGINAL PAGE IS~~
OF POOR QUALITY

Figure 3-59. Stage One Blade Cracks at Leading Edge Root.

cracks visible to the naked eye, and an additional 34 were found cracked when examined at 40×. The entire set was removed, and new blades were installed. Tip clearance was increased an additional 0.037 inch at the blade leading edge and 0.016 inch at the trailing edge for the new set of blades.

The Stage 2 polygonal ring was removed, followed by the outer seal. The seal teeth had no damage, and coating wear was normal for the engine run time. A cross-sectional view of the seal is shown in Figure 3-60.

Following removal of the Stage 1 polygonal ring, the aft stationary hardware was removed. The eight actuator control rods which penetrate the No. 2 bearing static housing were all observed to have varying degrees of wear. The heaviest wear was on the rods at 12 and 6 o'clock. The aft support had heavy scoring on the forward OD (outer diameter) where the aft actuator travels over it. Wear marks were in the same position as the sting tube support brackets. Blocks providing support were reduced to lightweight springs during rebuild. The scored area was cleaned and covered with a Teflon coating (Emralon 333) to reduce friction between the actuator and support. The coating when scratched will not flake but will lubricate to protect the material below.

The aft actuation subassembly was lifted out followed by a borescope of the forward sumps. Entering the sump through the mid-driveshaft actuator rod cutouts revealed the source of the binding rotors. The No. 1 roller bearing (1R) outer race nut had come completely off (Reference Figures 6-2 and 6-3, Section 1.1). The actuator could not travel the full distance because the nut was interfering with the last 0.5 inch of actuator travel.

The 6-12 assembly, less the midshaft, was removed for further inspection and set in the teardown tooling.

Upon removal of the forward actuator, the 1R bearing housing was removed so that access to the 1R bearing could be made. The outer race nut was laying inside the actuator assembly, and the outer race was found almost completely off. The rollers were pushed inward and the two shafts were easily separated. The rollers sustained disassembly damage, making the bearing not serviceable but repairable. The outer race had no visible grooves. The outer race nut backed off as a result of Stage 1-5 rotor aft shaft growth caused by thermal expansion.

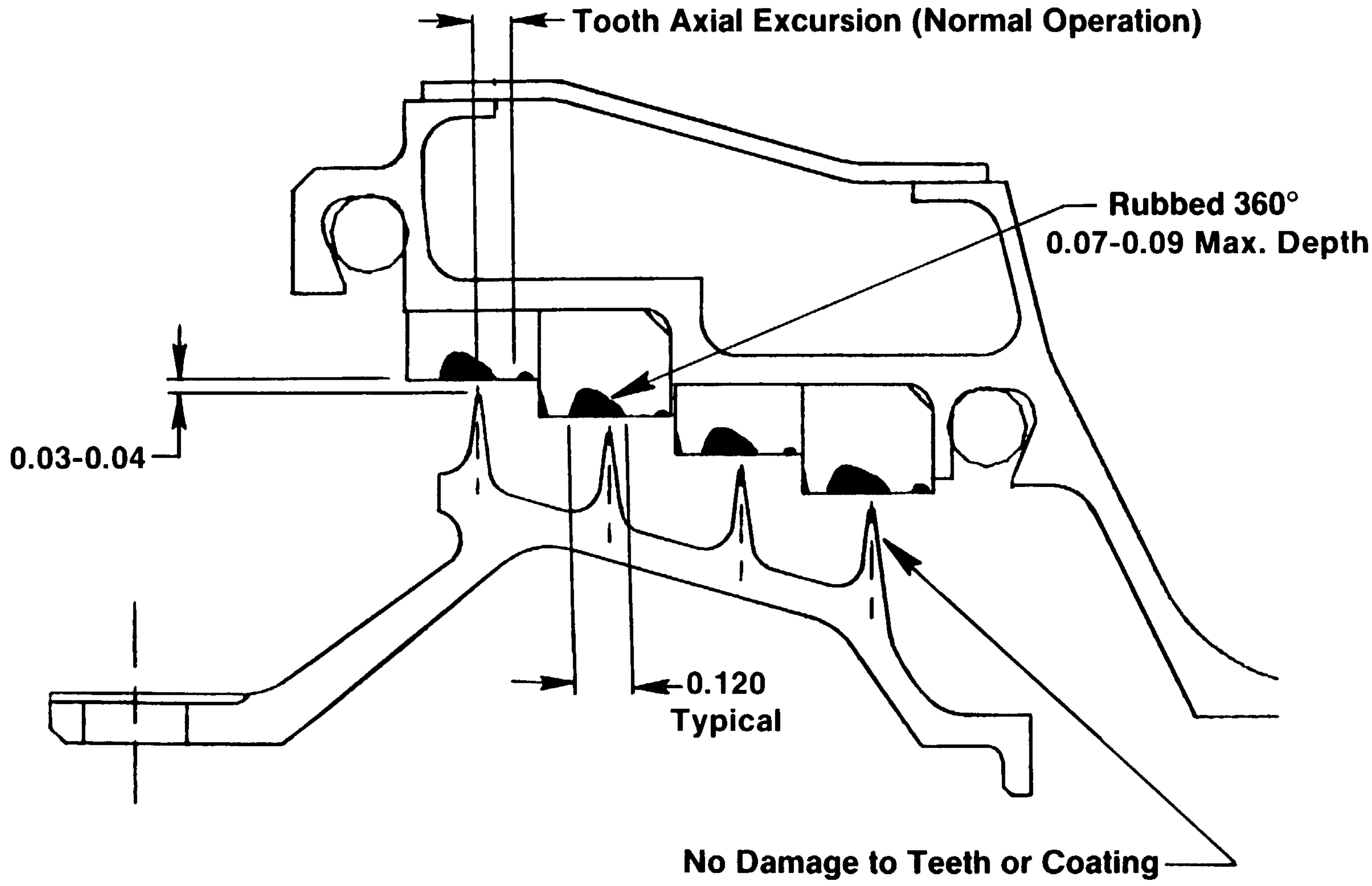


Figure 3-60. Aft Outer Flowpath Seals.

Because the carbon seal aft of the 1R bearing, sealing the cavity, was in remarkably good condition and repairable, the seal was removed for inspection, the carbon segments were replaced, and the seal assembly installed. The mid-sump seal aft of the carbon seal had rubbed grooves about 0.14-inch long × 0.04-inch deep in the honeycomb. As shown in Figure 3-61, the honeycomb and seal teeth were all serviceable and reused.

All Stage 11 blades were heavily rubbed, and Stage 10 was lightly rubbed (Figure 3-62); 3 Stage 11 blades were discovered with cracks in the leading edge root, and the inner spool had evidence of a hard rub. The outer spool (odd rotor) aft stages are cantilevered from the Stage 5 power frame. If the 1R bearing were not providing adequate radial support, it would account for a rub at the aft stages of the outer spool. The 3 cracked Stage 11 blades were replaced prior to rebuild. Table 3-3 summarizes the results of the turbine blade inspection.

Table 3-3. Turbine Blade Inspection Summary.

| Stage | 1 | 2 | 3 | 4 | 6 | 7 | 8 | 9 | 10 | 11 |
|---|---|---|---|---|---|---|---|---|---|---|
| No. of Blades | 124 | 118 | 120 | 94 | 90 | 72 | 84 | 54 | 82 | 56 |
| No. Cracked (1× Visual) | 19 | 0 | 0 | 0 | 0 | - | - | - | - | 0 |
| Additional No. Cracked (Borescope) | 0 | 0 | 0 | 0 | - | 0* | 0* | 0* | 0 | 3 |
| Additional No. Cracked (10× Visual) | 0 | 0 | - | - | - | - | - | - | - | - |
| Additional No. Cracked (40× Visual) | 34 | - | - | - | - | - | - | - | - | - |
| Total Cracked | 53 (42.7%) | 0 | 0 | 0 | 0 | 0 | 0 | 0 | 0 | 3 (5.4%) |

* Approximately 25% Sample; Others Inspected 100%

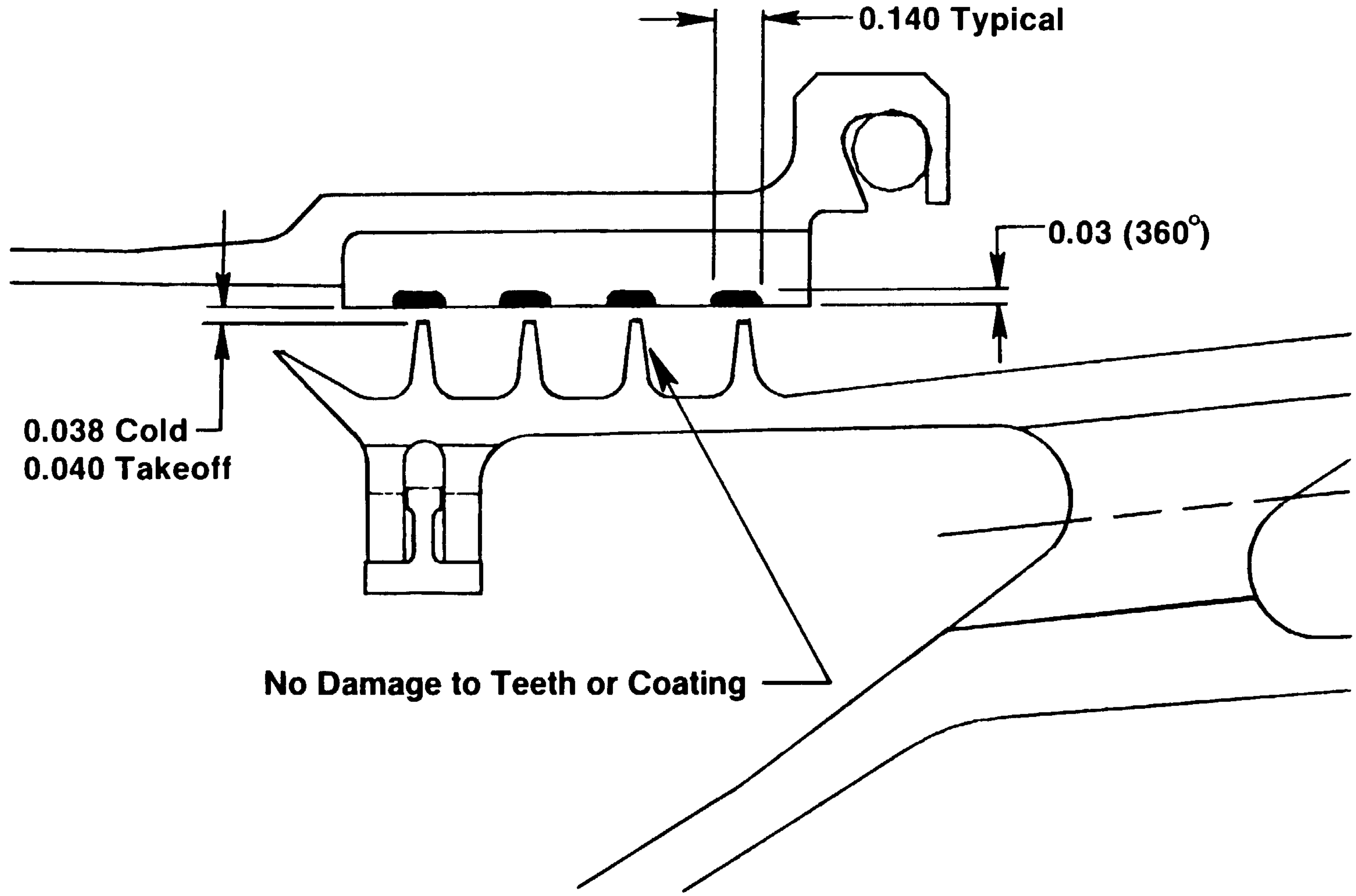


Figure 3-61. Midsump Seals.

7-8-86, 10:45, 22,300 Thrust

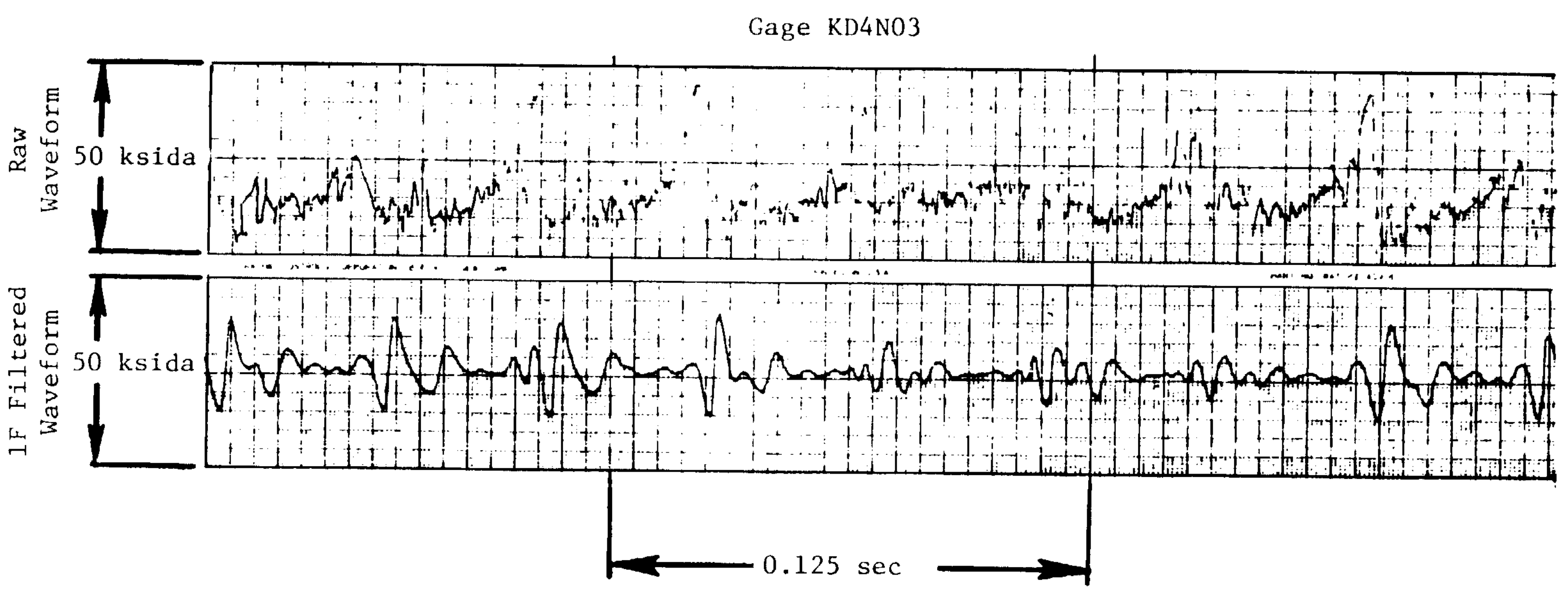


Figure 3-62. Suspected Stage 11 Rub.

The 2R bearing was removed for a detailed examination at Evendale. One roller had a rounded micro dent which would not affect the design intent of the part. The 2R bearing was serviceable and was stored for later use, if required.

Corrective action for the binding rotors included an improved locking feature for the 1R outer race nut and other spanner nuts in the propulsor assembly. Upon installation of a new No. 1 roller bearing, the spanner nut was installed with a small amount of Loctite applied axially in four places across the threads of the nut. Both threaded surfaces were cleaned and dried prior to nut installation. An additional locking feature was added with two pins installed between the shaft and nut, which were also tack welded in place (Reference Figure 6-4). The inner race nut was installed only with Loctite. A new carbon seal was also installed to replace the one damaged from the 1R bearing problem. In addition, the 1B inner race nut had Loctite applied; all others were untouched and remained as they were.

The IGV was repaired and modified to include a honeycomb seal to prevent spool damage if a reoccurrence of the rub persists in later engine operation. Figure 3-63 is a view of the IGV/spool seal area. During assembly of the propulsor to the gas generator, the gap between the IGV and spool was checked and measured at 0.125 to 0.188 inch, with a minimum of 0.125 inch per the drawing.

Oil drain holes were drilled into the 1-4 inner, 1-2 outer, and 3-4 outer turbine spools to drain any accumulated oil.

Borescope ports were added through the mixer frame flange for better visibility to the IGV and Stage 1 blades. The inspection interval was set at 10 hours to keep better records of Stage 1 blade activity and IGV spool gap.

## 3.18 MISCELLANEOUS HARDWARE STRESS DATA

This section presents data on hardware that had no indication of high stress (vibratory stress was always under limits) during testing and has not been previously presented in other sections.

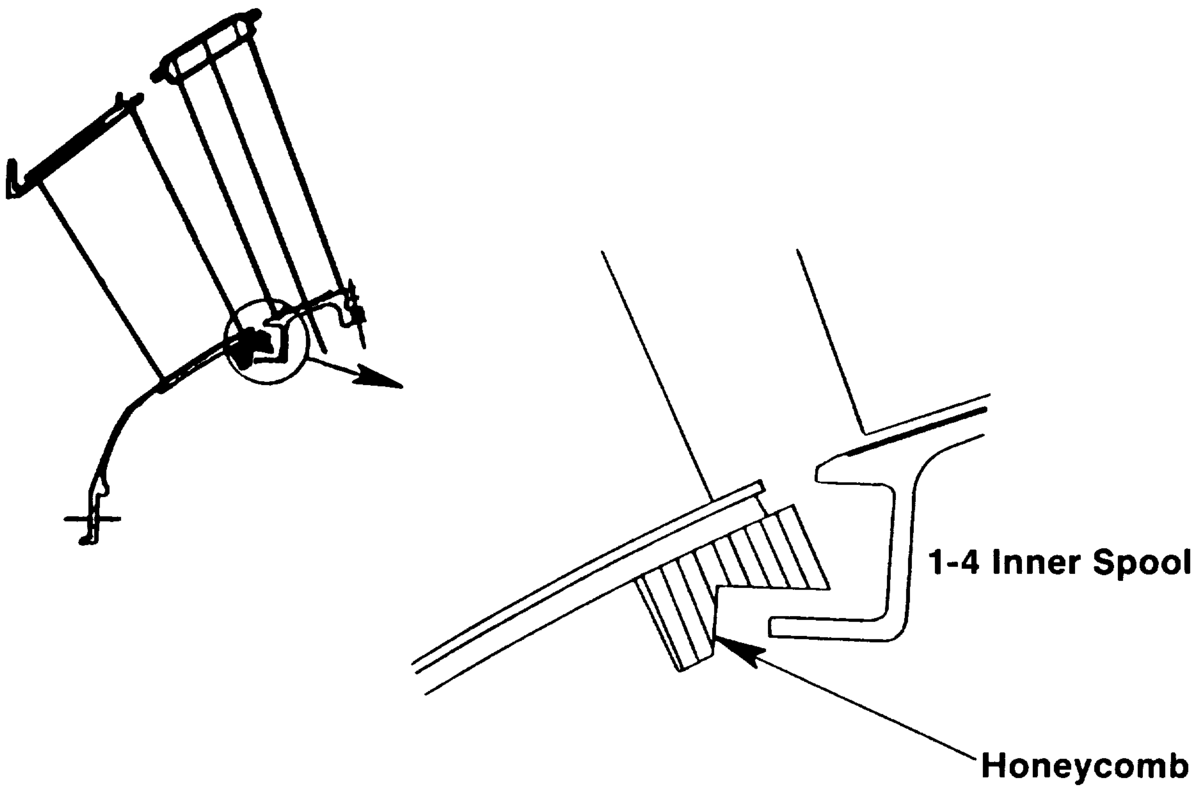


Figure 3-63. IGV and 1-4 Inner Spool.

| Nomenclature | Limits (ksida) | Figure |
|---|---|---|
| Outer Guide Vanes (OGV) | 20.0 | 3-64 |
| Inner Guide Vanes (IGV) | 3.4 | 3-65 |
| Forward Outer Rotating Seal | 74.0 (2/rev)<br>11.0 (3,4/rev)<br>8.0 (5/rev) | 3-66 |
| Aft Outer Rotating Seal | 15.0 | 3-67 |
| Turbine Spools | 30.0* | |
| 1-4 Outer | | 3-68 |
| 7-11 Outer | | 3-69 |
| 6-11 Inner | | 3-70 |

* 10.0 for Turbine Blade Rubs

## 3.19 OIL LEAK/GULPING PROBLEM

During the latter portion of Build 2 and, more markedly, during Build 3, the propulsor oil consumption limited the UDF™ test time (oil consumption increased from 0.35 to 1.58 quarts/hour from Build 2 to Build 3). The engine was limited to about 2.5 hours of testing to allow for reservicing of the propulsor oil tank. By this stage of testing, the test site facility remote oil fill system had been removed since it would not be available for flight-test.

Two major leaks contributed to the high oil consumption. The carbon seal in the starter gearbox was leaking into the core nacelle and then back into the fan, and oil leaked through worn actuation rods and seals in the aft sump wall into the sting tube area in the center of the propulsor (aft stationary support). Oil lost into the sting tube could be pumped out after engine shutdown. A total of 39 quarts was recovered during Build 3 testing (66 hours). The fan nacelle and propulsor rotors remained dry, indicating the oil loss was not through the main propulsor carbon seals. Oil was also found leaking from an instrumentation fitting in the aft sump wall. The propulsor lube oil leak limited the engine test time in two ways.

First, as previously stated, the low lube level inside the sting tube required careful monitoring to ensure that enough oil did not collect to flow out of the mixer frame. The cavity was pumped approximately every 2.5 hours, and about 2.5 quarts were removed each time (toward the end of Build 3).

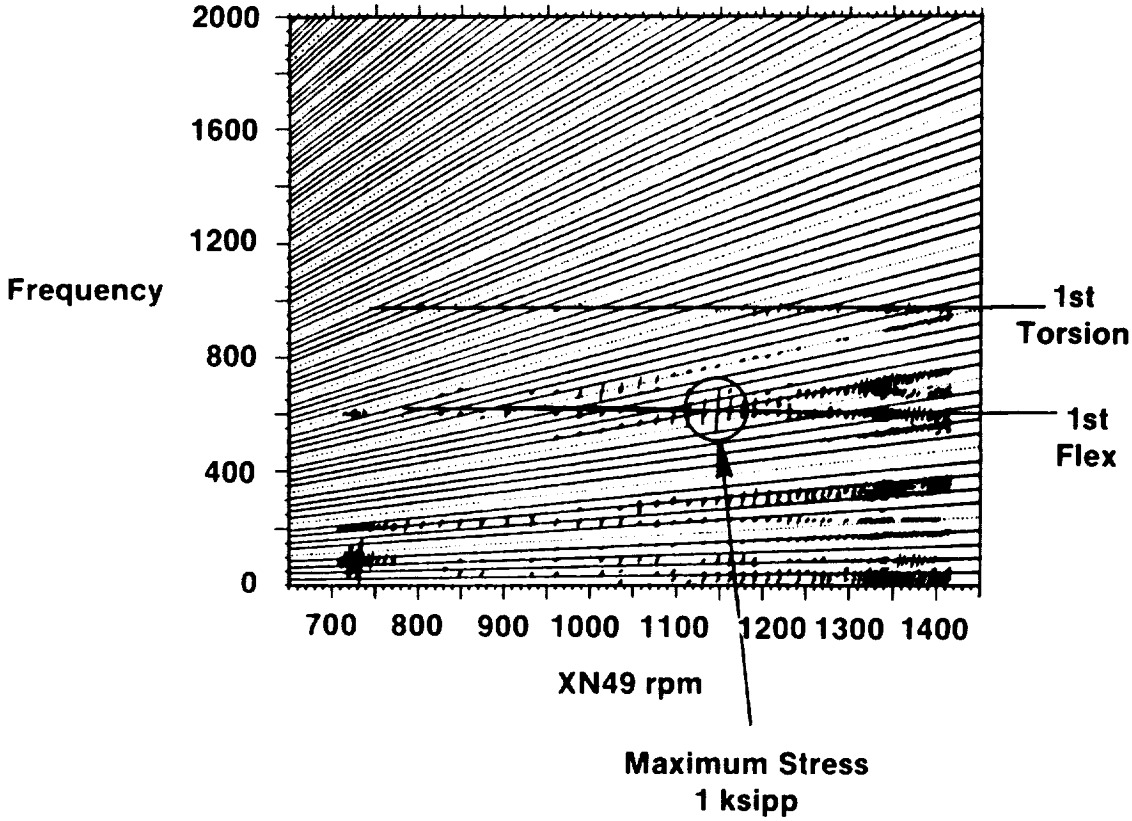


- 1F And 1T Responses
- Low Amplitude
- Maximum Allowable 20 ksipp
- Predicted Values
  - 1F 600 Hz
  - 1T 970 Hz
- Data Typical For Engine Testing To Date

Figure 3-64. Power Turbine OGV - Engine Test Data.

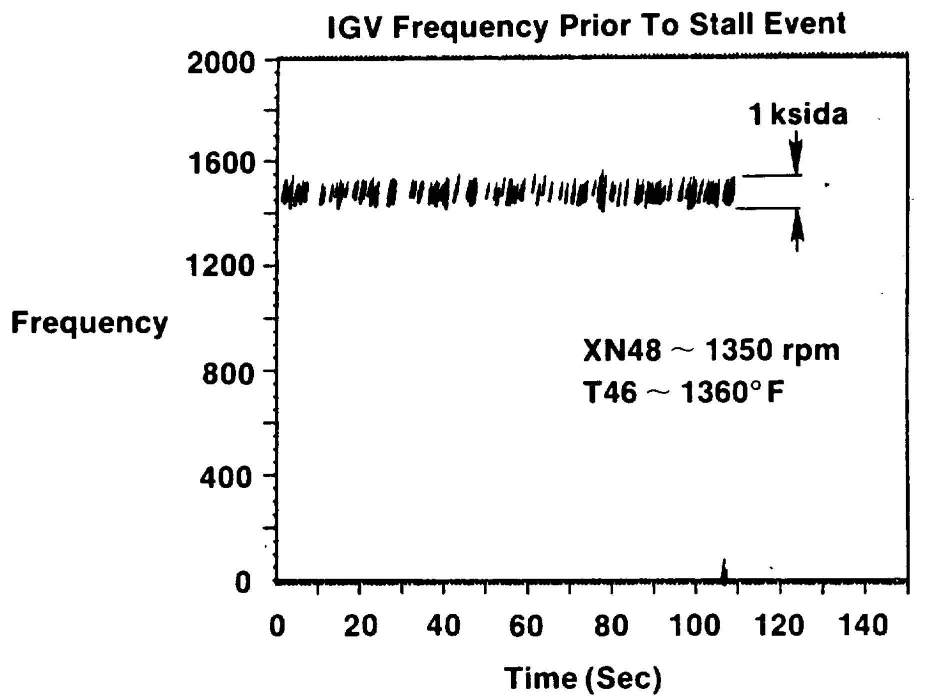


- Engine Test Dynamic Strain Gage Frequency = 1475 Hz (1 Flex)

- Predicted 1st Flex Frequency Is 1425 Hz

- Allowable Stress Level Is 3.4 ksida

- Trace Is Typical Of Vane Data Seen During Engine Test

Figure 3-65. Power Turbine IGV - Engine Test Data.

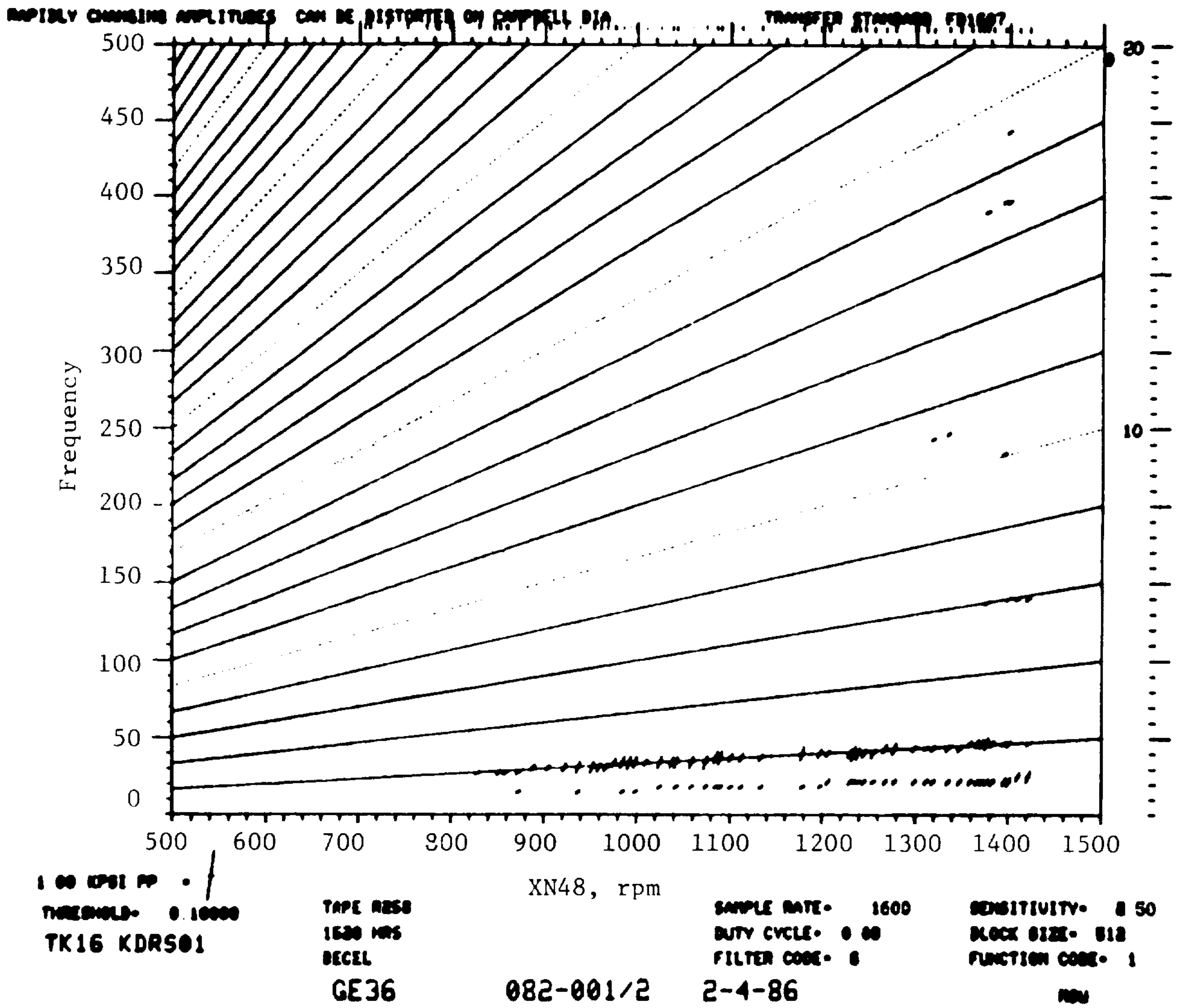


Figure 3-66. Forward Outer Rotating Seal Response, Decel from 25,000 lbf Thrust: February 4, 1986.

ORIGINAL PAGE IS
OF POOR QUALITY

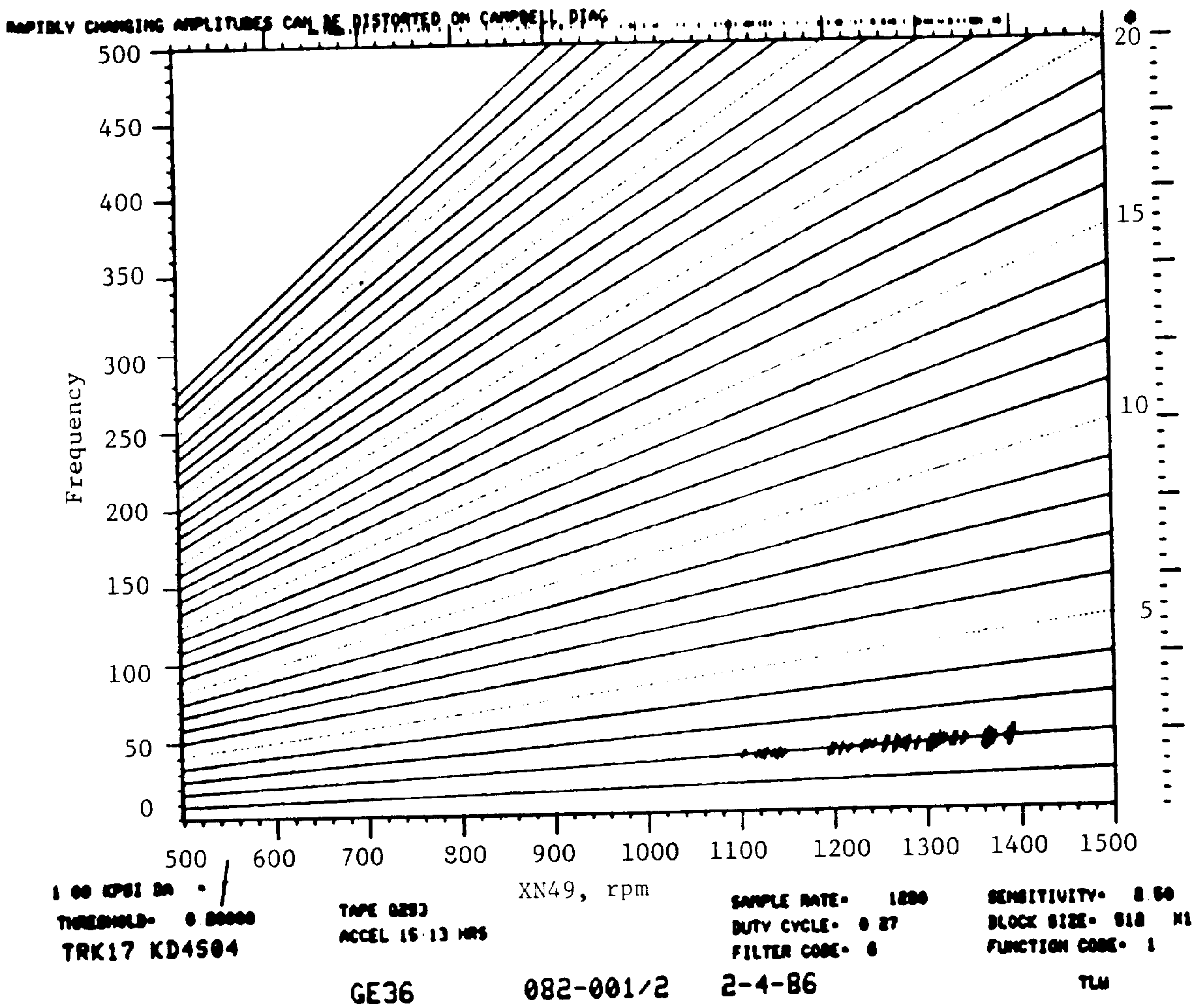


Figure 3-67. Aft Outer Rotating Seal Response, Accel to 25,000 lbf Thrust: February 4, 1986.

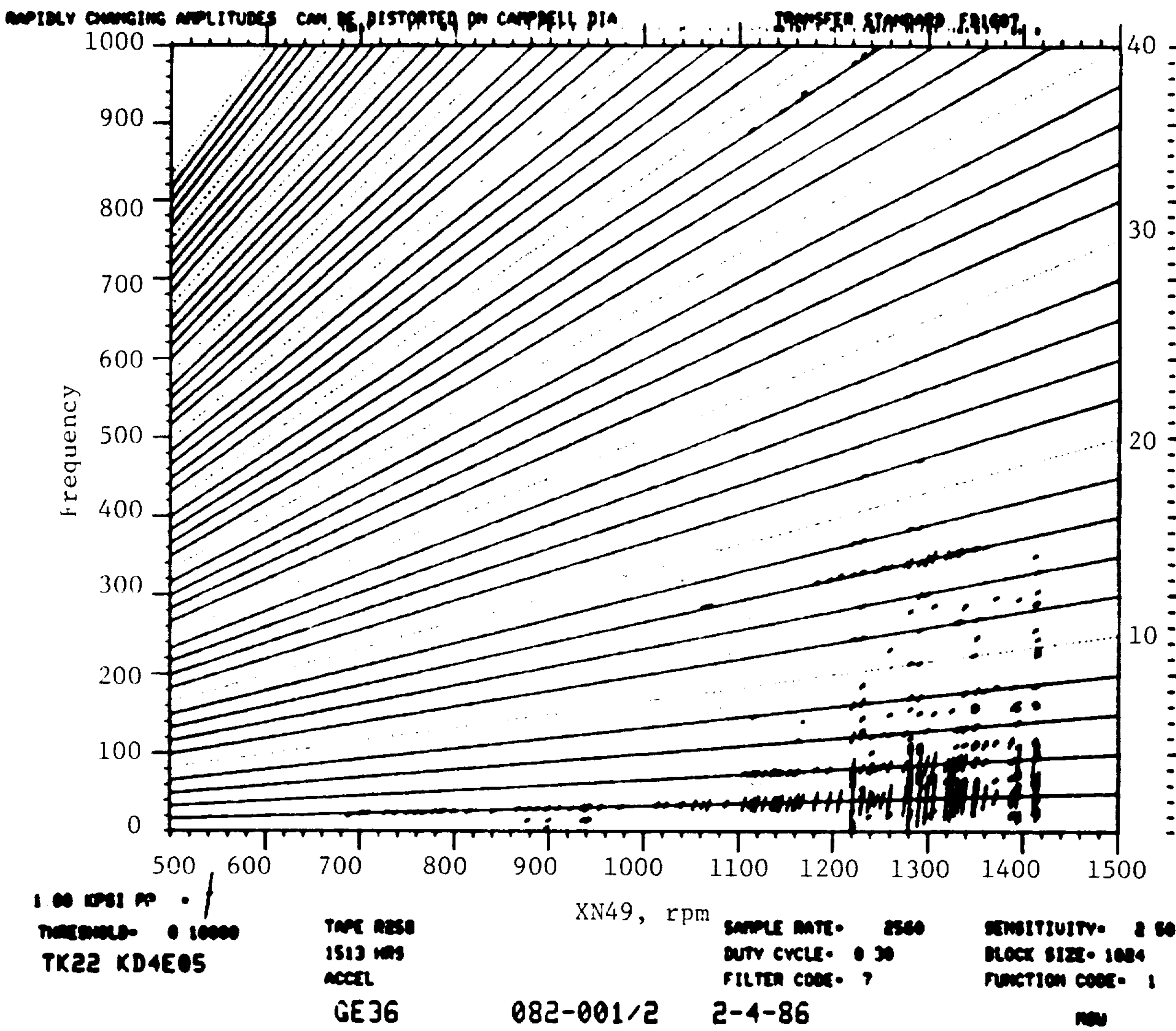


Figure 3-68. Outer Turbine Spool Response (1-4), Accel to 25,000 lbf Thrust: February 4, 1986.

ORIGINAL PAGE IS
OF POOR QUALITY

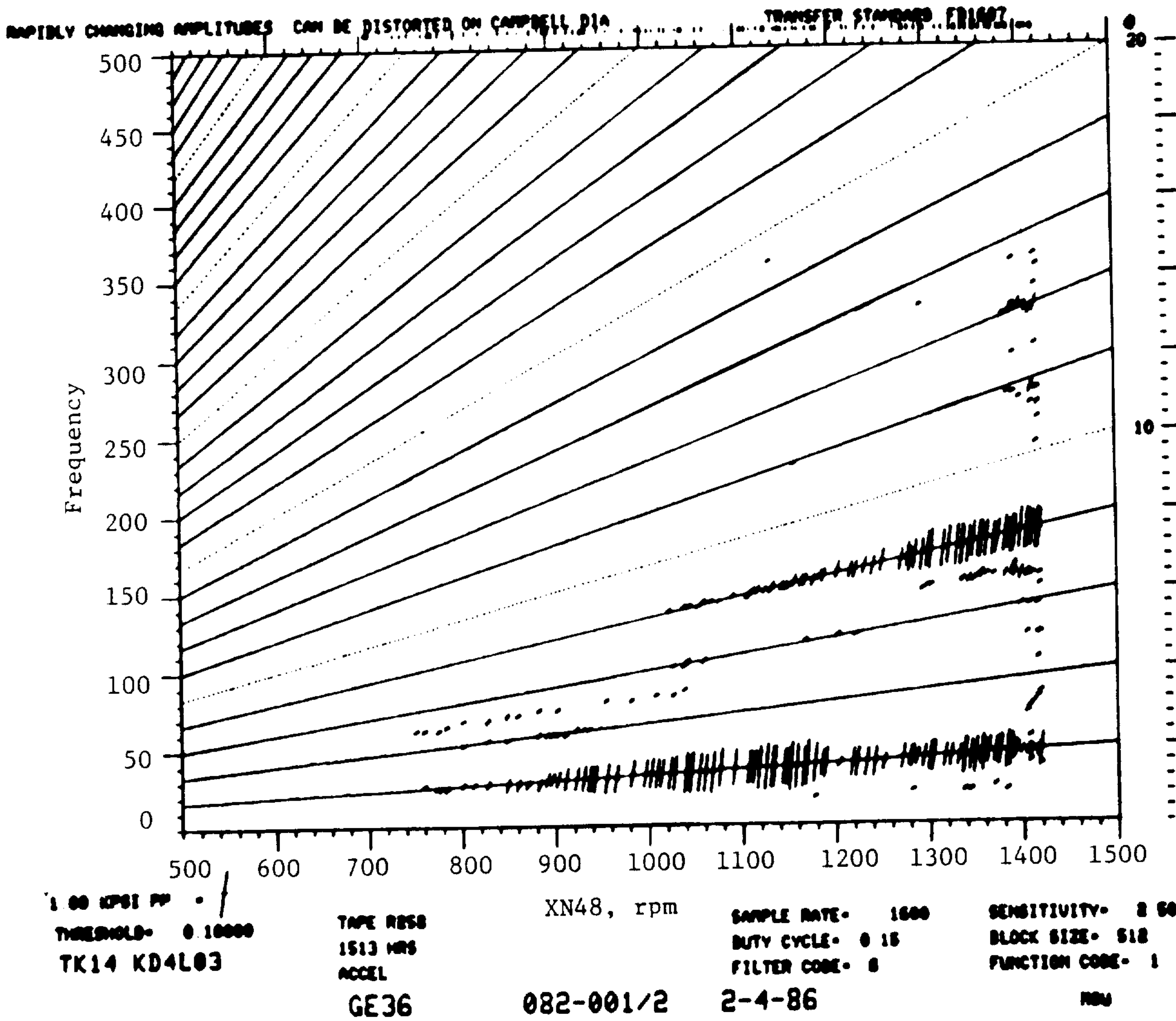


Figure 3-69. Outer Turbine Spool Response (7-11), Acceleration to 35,000 lbf Thrust: February 4, 1986.

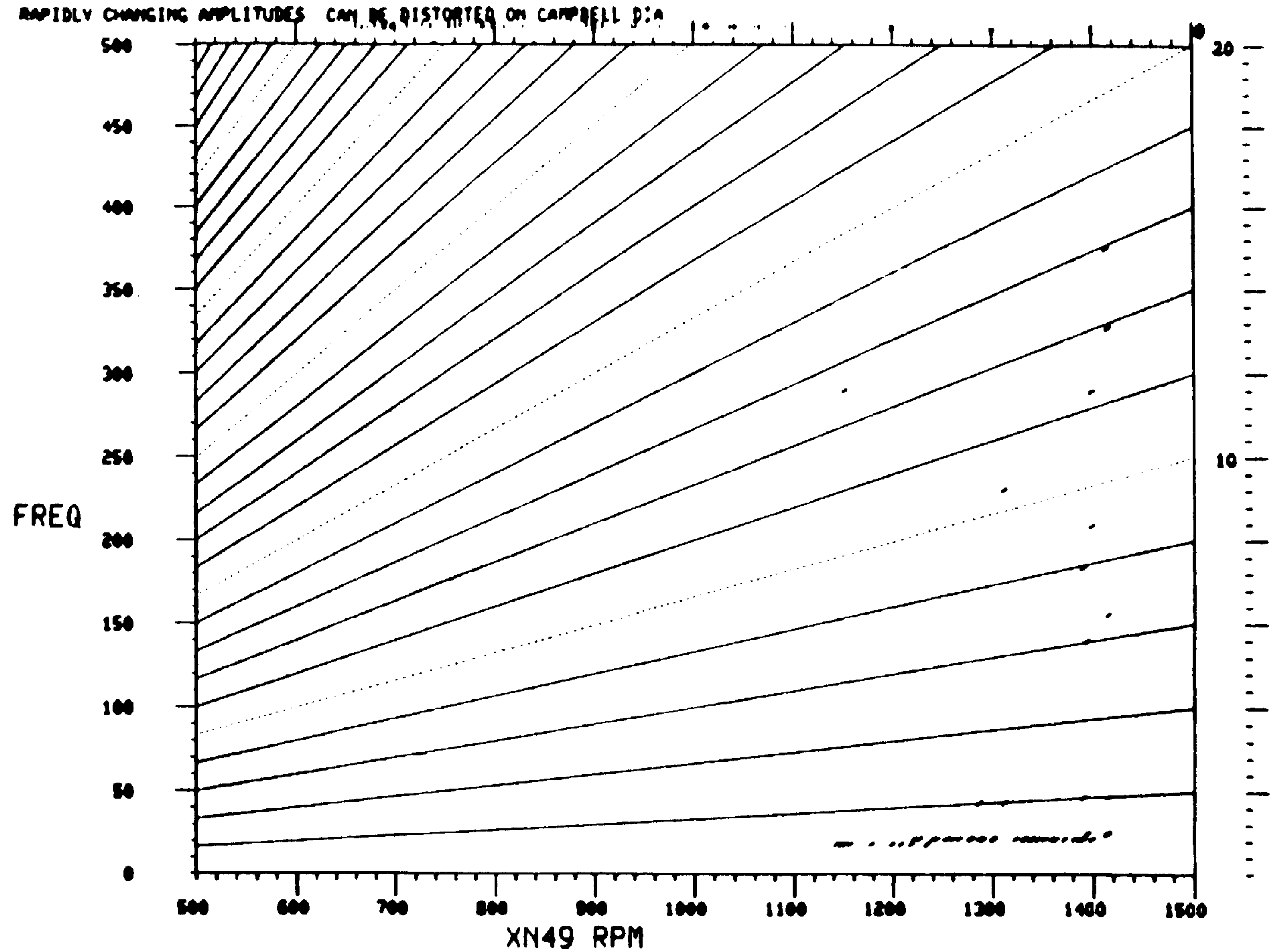


Figure 3-70. Inner Turbine Spool (6-11) Response, Accel to 25,000 lbf Thrust: February 4, 1986.

Second, combined with the excessive leakage, the gulp limited testing duration. The propulsor gulps about 2.5 quarts of oil with increasing power from idle to maximum. This is consistent over all engine testing. As speed is reduced, the oil level will return. That is, it will return if the propulsor is not losing oil from leaks in the sump wall or gearbox carbon seal. With a normal oil consumption rate, oil gulping is not a problem with the 11 quart tank.

Following Build 3, the leaks were fixed; new actuation rods and seals were installed in the actuation system, a new starter adapter gearbox was installed, and the instrumentation fittings were replaced. A larger scavenge port was installed in the new starter adapter gearbox to improve scavenging and to keep oil away from the aft carbon seal that leaked on Build 3. A new flight-type static vent air demister was installed, and oil drain holes were added to the turbine spools.

# 4.0 HEAT TRANSFER AND SECONDARY FLOW SYSTEM

## 4.1 MIXER FRAME HEAT TRANSFER

The mixer frame flow circuit is shown in Figure 4-1. At takeoff power, film-hole flow is 15% less than predicted, outer flowpath secondary flow is 10% less than predicted, and total sump flow is 6% higher than predicted. The outer flowpath flow and sump flow are determined through use of pressure tap readings, and film-hole flow is determined by subtracting these flows from the total fan bypass flow.

Figure 4-2 provides a comparison of mixer frame predicted and measured internal pressures at takeoff power; whereas, a comparison of predicted and measured flowpath static pressures at takeoff power is depicted in Figure 4-3. Although very few pressure readings are available, test data indicates that the pressure drop across the film holes is close to that predicted. The low film-hole flow appears, therefore, to be due to undersized film flow area.

The total pressure drop available to the frame film holes is very low, making BFM (backflow margin) a concern. The regions of minimum BFM are the inner flowpath fairing upstream of the strut leading edge and strut leading edge cavity at the root. A comparison of predicted and measured pressures for engine Build 1 is shown in Figure 4-4. While the BFM across the inner flowpath fairing film holes is slightly less than predicted, the BFM across the strut leading edge cavity film holes is much higher than predicted.

Installation of power turbine blade dampers for engine Build 2 resulted in a lower level BFM. The inner flowpath fairing pressures for engine Build 2 are shown in Figure 4-5 for takeoff and maximum cruise, the minimum backflow condition. Takeoff pressures are taken from test data, and the maximum cruise pressures are predictions based on test results. The 0.79% BFM at maximum cruise condition is low, but it is in a very localized region. The BFM in all other regions is significantly higher.

Figure 4-6 illustrates mixer frame metal temperatures, both predicted and actual, for hot day takeoff power. All thermocouple data have been scaled up to hot day conditions by multiplying the raw data by the ratio of the hot day

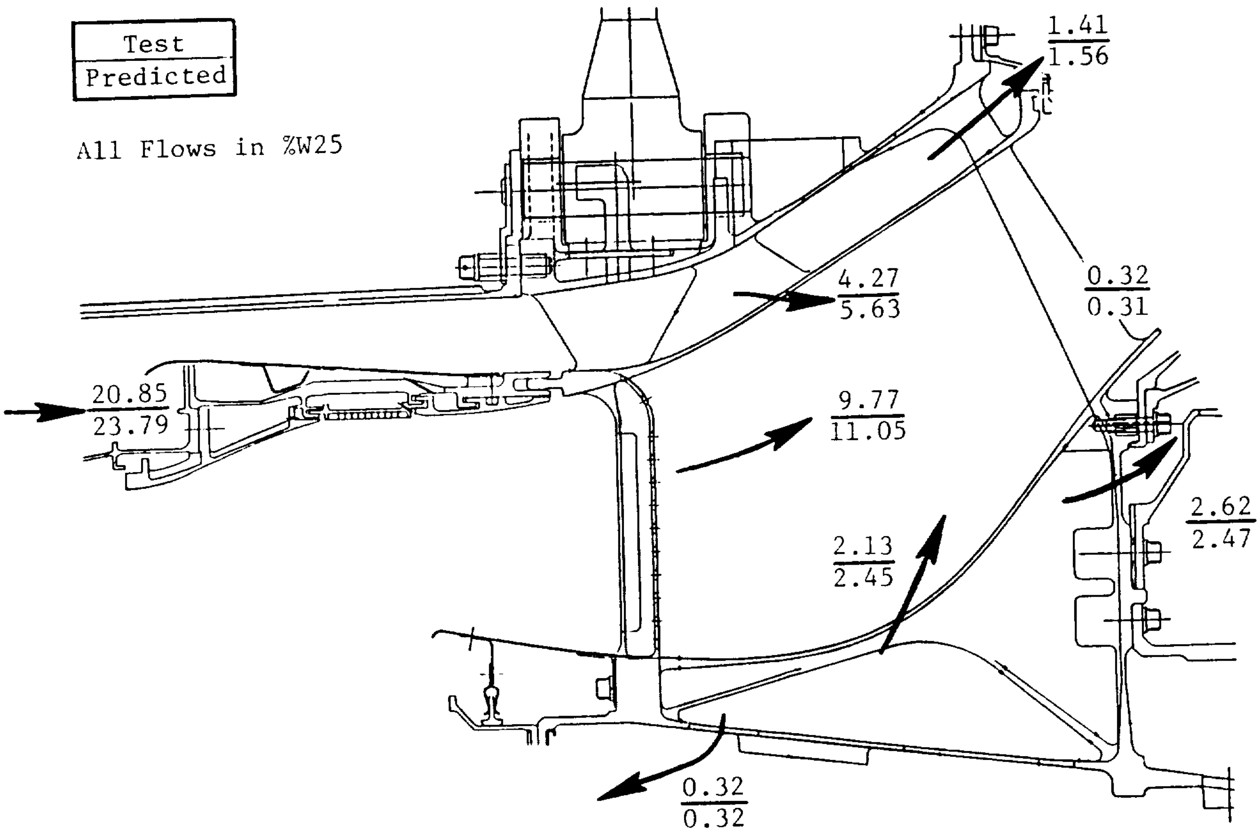


Figure 4-1. Mixer Frame Flows at Takeoff Power, Test Versus Predicted.

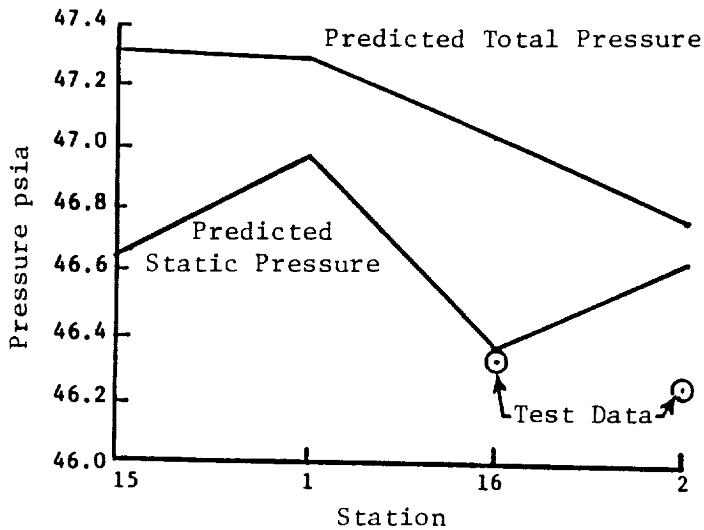


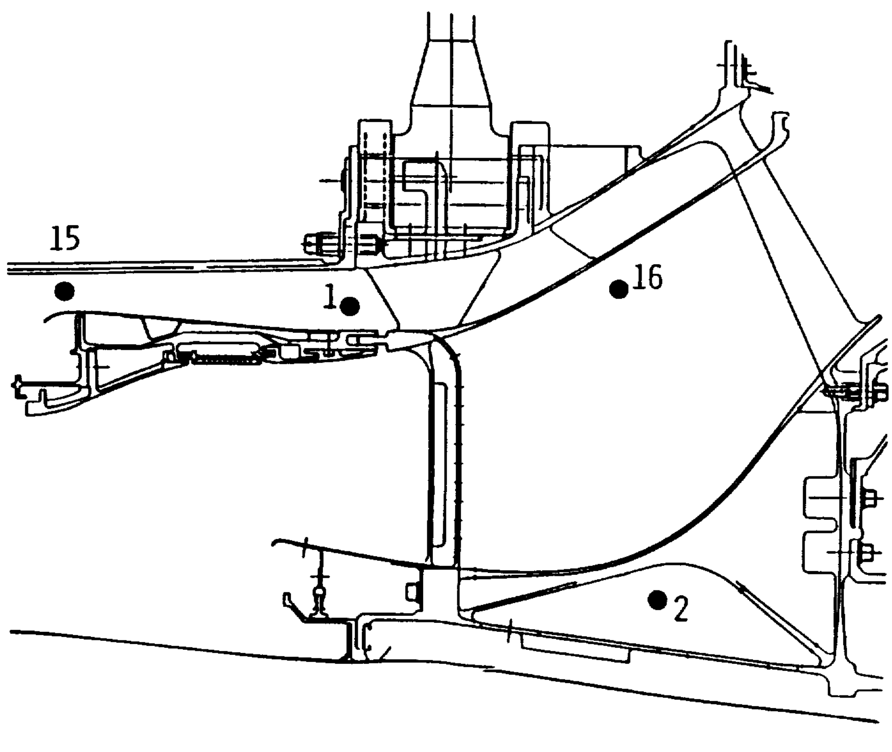


Figure 4-2. Mixer Frame Pressure Losses Comparison of Measured and Predicted Pressures.

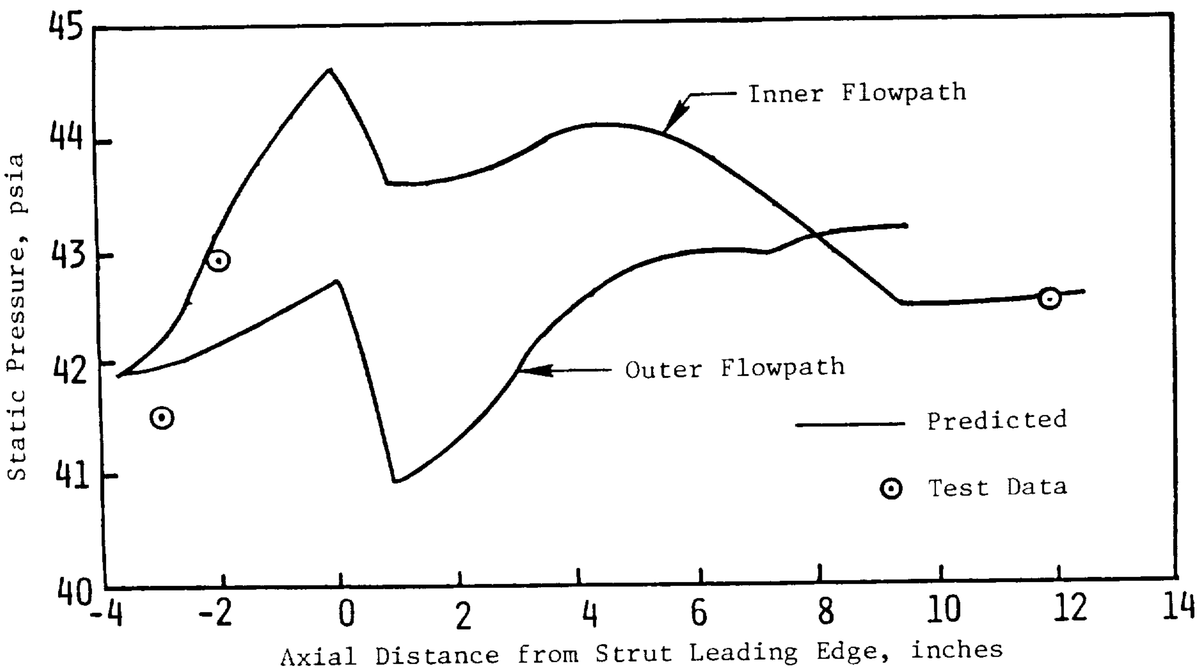


Figure 4-3. Mixer Frame Flowpath Static Pressure Distribution Takeoff Power.

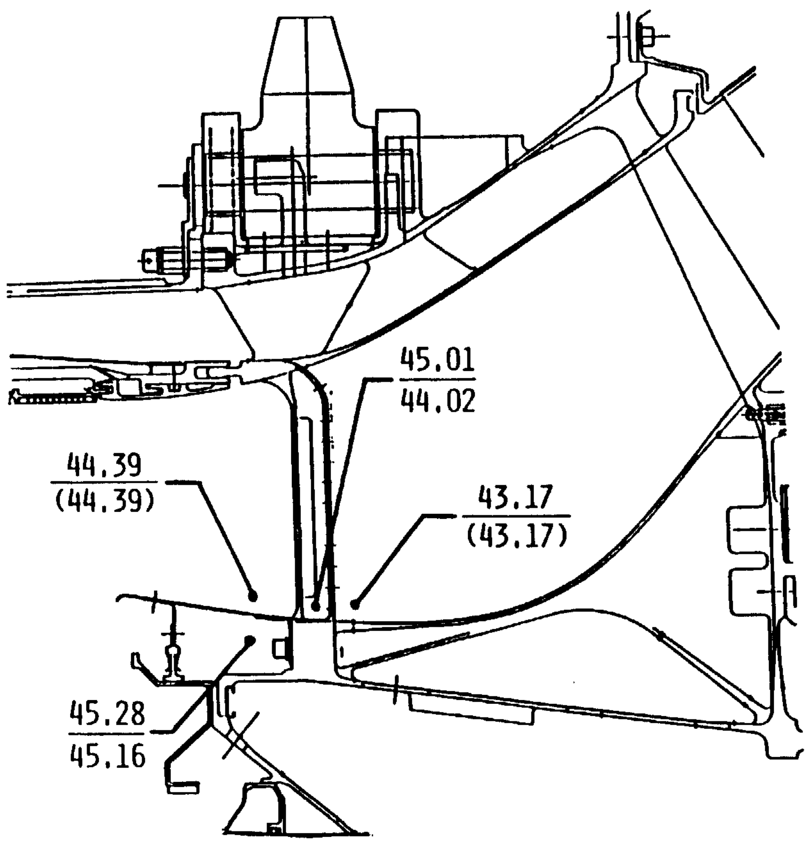


TEST DATA / PREDICTED : TEST DATA / (INPUT)

- INNER BAND BACKFLOW MARGIN IS 2.0% VS 1.7% PREDICTED.
- STRUT LEADING EDGE BACKFLOW MARGIN IS 4.3% VS 2.0% PREDICTED.
- BACKFLOW MARGIN IS HIGHER IN ALL OTHER REGIONS.
- MIXER FRAME ANALYTICAL FLOW MODEL HAS BEEN MODIFIED TO REFLECT TEST RESULTS.

Figure 4-4. Mixer Frame Backflow Margin - Build 01 Engine.

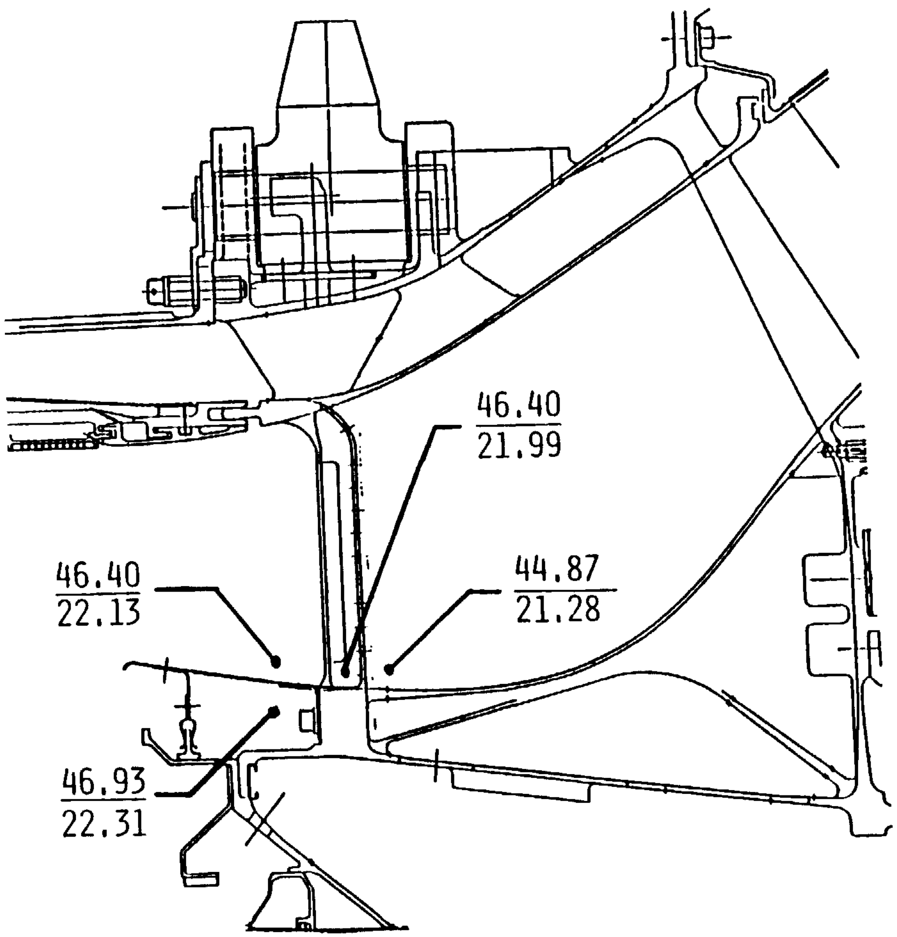


$\frac{\text{TAKEOFF}}{\text{MAX CRUISE}}$

- BFM = 1.1% AT TAKEOFF.
- BFM = .79% AT MAXIMUM CRUISE CONDITION.
- LOWER BUILD 02 BACKFLOW MARGIN IS RESULT OF LOWER POWER TURBINE FLOW FUNCTION.
  - INSTALLATION OF POWER TURBINE BLADE DAMPERS.

Figure 4-5. Mixer Frame Backflow Margin - Build 02 Engine.

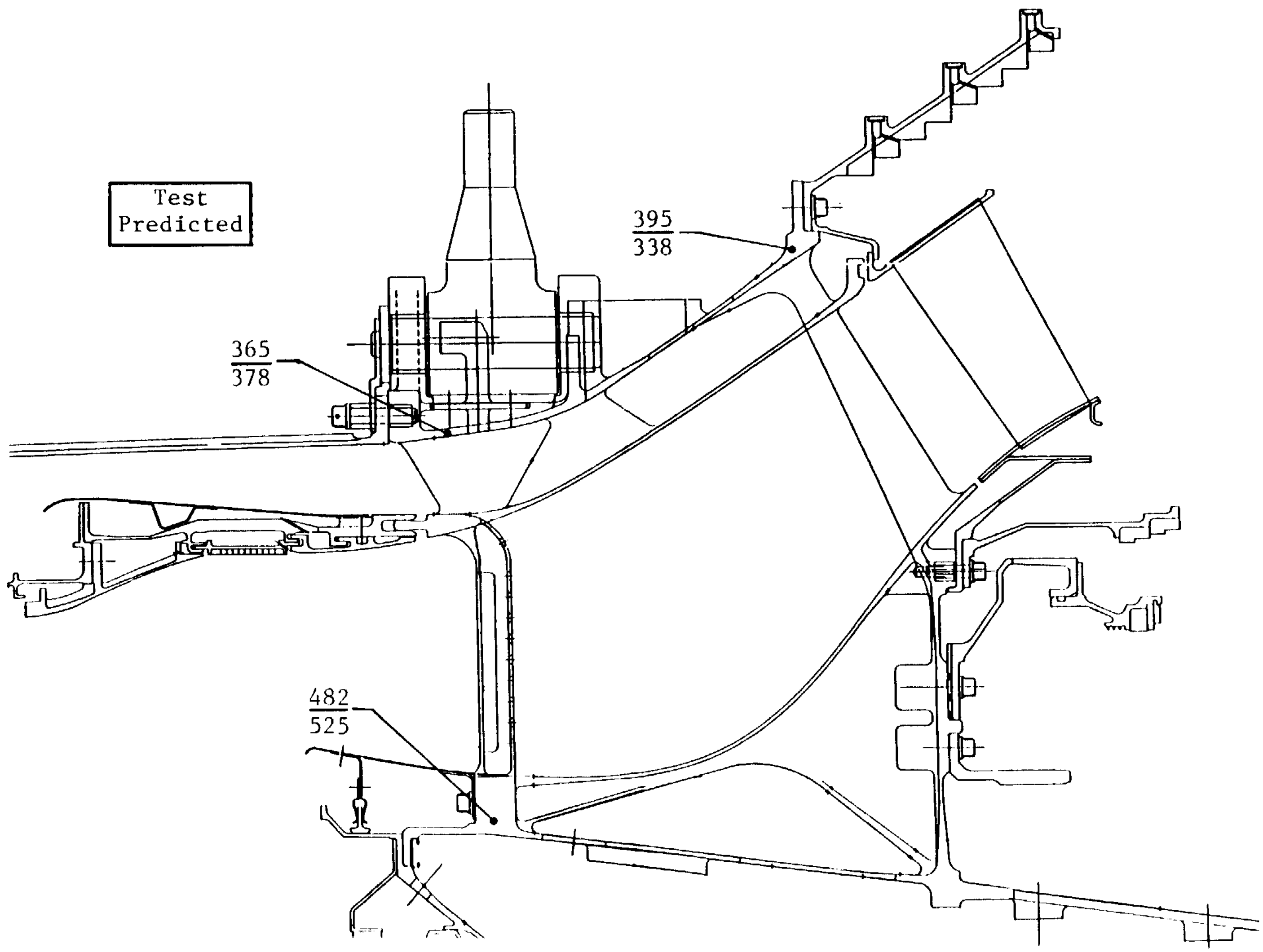


Figure 4-6. Mixer Frame Temperatures.

ambient temperature over the test day ambient temperature. No thermocouples are available along flowpath portions of the frame, but the existing thermocouple readings indicate that the frame is adequately cooled. Also, there are no visible signs of overtemperature.

## 4.2 POWER TURBINE SECONDARY FLOW SYSTEM

Figure 4-7 illustrates the power turbine secondary flow system. The flow rates, predicted and actual, are tabulated in Table 4-1. Although the total secondary flow for engine Build 1 neared prediction, the Stage 1 inner flowpath purge flow was significantly lower than predicted. This redistribution of flow is a result of a mixer frame supply hole flow coefficient that is lower than predicted and shafting hole flow coefficients that are greater than predicted. The increased pressure drop across the mixer frame supply holes, combined with reduced pressure drop through the shafting annular holes, serves to lower the supply pressure to the forward seal. Also, the sump vent flow was higher than predicted due to large carbon seal leakage areas. This additional vent flow results in a further decrease in Stage 1 purge flow.

During Build 1 testing, Stage 1 cavity temperature was 830° F at takeoff power, as compared to 795° F predicted. Although there was no evidence of gas ingestion, it was observed that the forward seal $\Delta P$ decreases with increase in power setting. Figure 4-8 plots $\Delta P$ versus P46Q2.

Extrapolation of the test data indicates that for Build 1 testing, backflow could occur at maximum power. To maintain positive flow in all cases, the mixer frame supply hole area was increased from 5.4 $in^2$ to 5.84 $in^2$. The resulting increase in forward seal $\Delta P$ from Build 1 testing to Build 2 testing is significant (Figure 4-8); however, the impact of this area increase on the remaining purge flows is negligible. The aft labyrinth seal flow increased significantly from Build 1 to Build 2 testing, presumably due to an increased seal clearance, indicated by a reduction in pressure drop across the seal.

During Build 3 engine testing, rubs occurred on two middle inner flowpath seals (G and H). There is an increase in the flows of these two seals, but because the system is metered for the most part by the supply hole and the shafting holes, the total secondary flow increases only slightly (Figure 4-7).

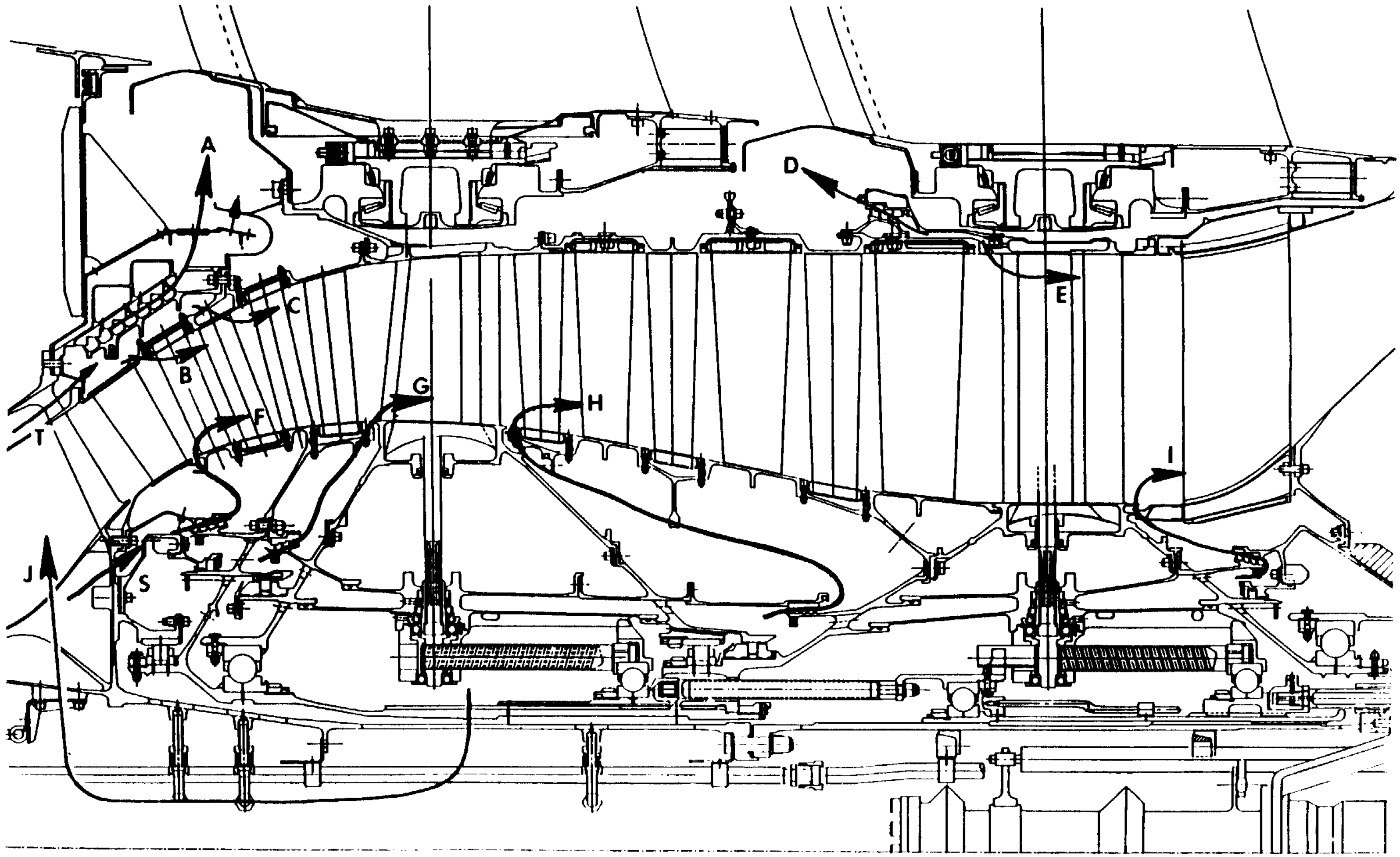


Figure 4-7. Power Turbine Secondary Flow Circuit.

Table 4-1. Power Turbine Secondary Flow (%W25), Takeoff Power.

| | Flowpath Seals | | | | | | | | | | | |
|---|---|---|---|---|---|---|---|---|---|---|---|---|
| | A | B | C | T | D | E | F | G | H | I | J | S |
| Predicted | 0.573 | 0.868 | 0.122 | 1.563 | 0.296 | 0.682 | 0.382 | 0.444 | 0.340 | 0.373 | 0.025 | 2.543 |
| Build 1 | 0.638 | 0.659 | 0.107 | 1.404 | 0.297 | 0.719 | 0.114 | 0.444 | 0.385 | 0.385 | 0.303 | 2.621 |
| Build 2 | 0.568 | 0.702 | 0.100 | 1.370 | 0.293 | 0.687 | 0.231 | 0.411 | 0.375 | 0.516 | 0.185 | 2.697 |
| Build 3 | 0.568 | 0.702 | 0.100 | 1.370 | 0.292 | 0.634 | 0.186 | 0.458 | 0.486 | 0.492 | 0.182 | 2.729 |

- PROBLEM: EXTRAPOLATION OF TEST DATA INDICATES THAT FORWARD SEAL COULD BACKFLOW AT MAX POWER.
- CAUSE: UNDERSIZED SUPPLY HOLE AND OVERSIZED ANNULUS HOLES REDUCE THE SEAL SUPPLY PRESSURE.
- SOLUTION: INCREASE SUPPLY HOLE AREA.

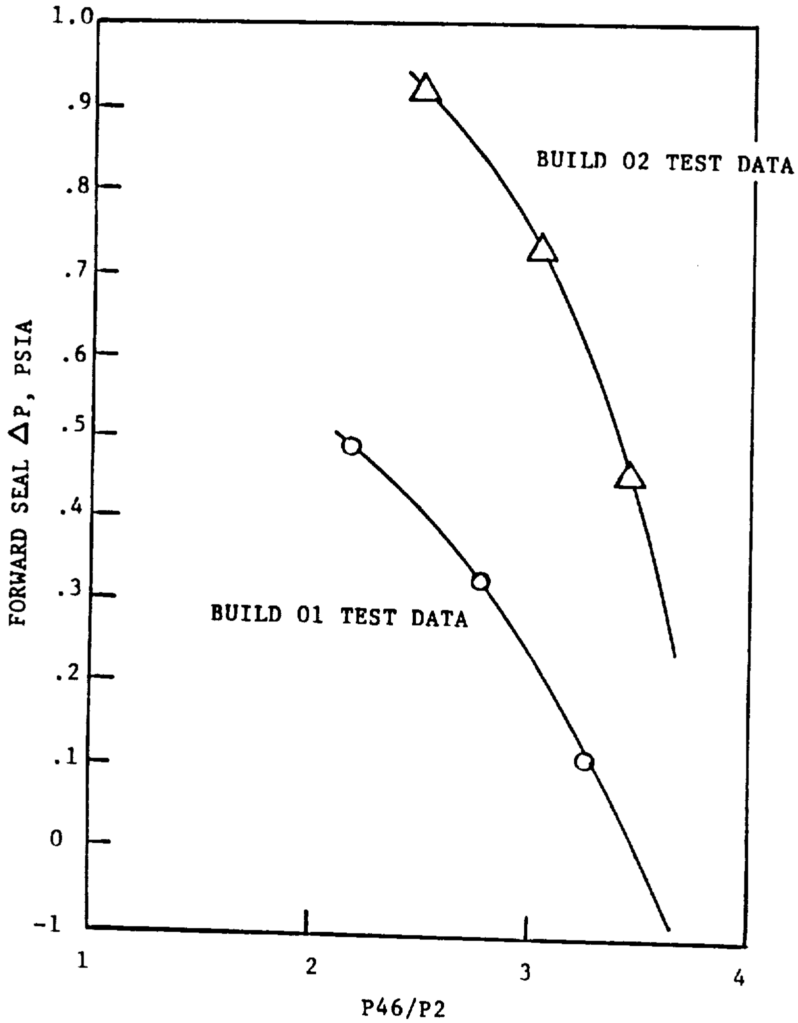


Figure 4-8. Potential Forward Seal Problem.

It should be noted that the very limited amount of instrumentation makes direct measurement of most of the individual flows impossible. The available pressure and temperature readings were used to rebalance the analytical flow network model which yields the best estimate of the flow distribution. The two flows leaving the mixer frame (S and T) are directly measured.

According to thermocouple data, all cavities are adequately purged. A comparison of predicted and actual temperatures is presented in Figure 4-9.

## 4.3 POWER TURBINE HEAT TRANSFER

The power turbine spool and frame temperatures, predicted and actual, are shown on Figures 4-10 and 4-11 for hot day takeoff power. The original predictions (Figure 4-10) were determined using a finite difference heat transfer program. The actual temperatures (Figure 4-11) have been scaled up to hot day conditions, as described in the mixer frame section. Because the fan bypass air temperature is lower than predicted, most of the cavity temperatures are also lower. The cavity temperatures have a direct impact on the inner spool temperatures. Unfortunately, there was too little instrumentation to be able to draw any firm conclusions about inner spool temperatures, as compared to predictions.

## 4.4 NACELLE VENTILATION

The nacelle ventilation system is depicted on Figure 4-12, with component temperatures at takeoff condition. All thermocouple data have been scaled up to hot day conditions, as described in the mixer frame section. Although some components are higher in temperature than predicted, all of the hardware is adequately cooled.

During initial engine Build 1 testing, ambient air was to be brought in to the nacelle cavity aft of the Stage 2 telemetry through radial holes in the cowling. However, poor ventilation in that region led to an overheating of the aft telemetry, probably due to a low level of static pressure at the inner flowpath. A total of 30 air scoops were then mounted to the holes. The additional ventilation air resulted in the temperatures presented in Figure 4-13.

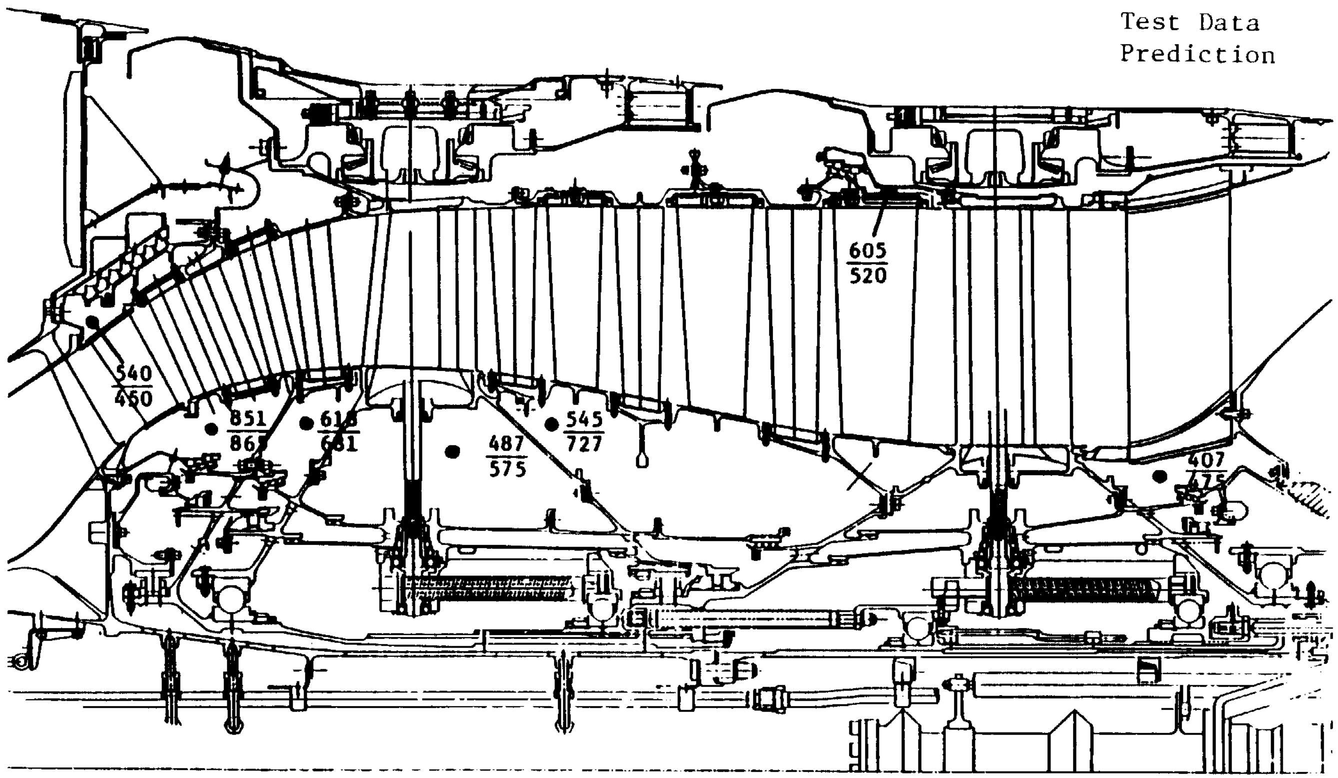


- Test Data Corrected to Hot Day Takeoff
- Inner Cavity Temperatures Are Below Prediction
- Outer Flowpath Seal Packing Air Temperature Is Above Predicted
- No Evidence of Gas Ingestion.

Figure 4-9. Rotor Cavity Temperatures at Takeoff Power.

ORIGINAL PAGE IS
OF POOR QUALITY

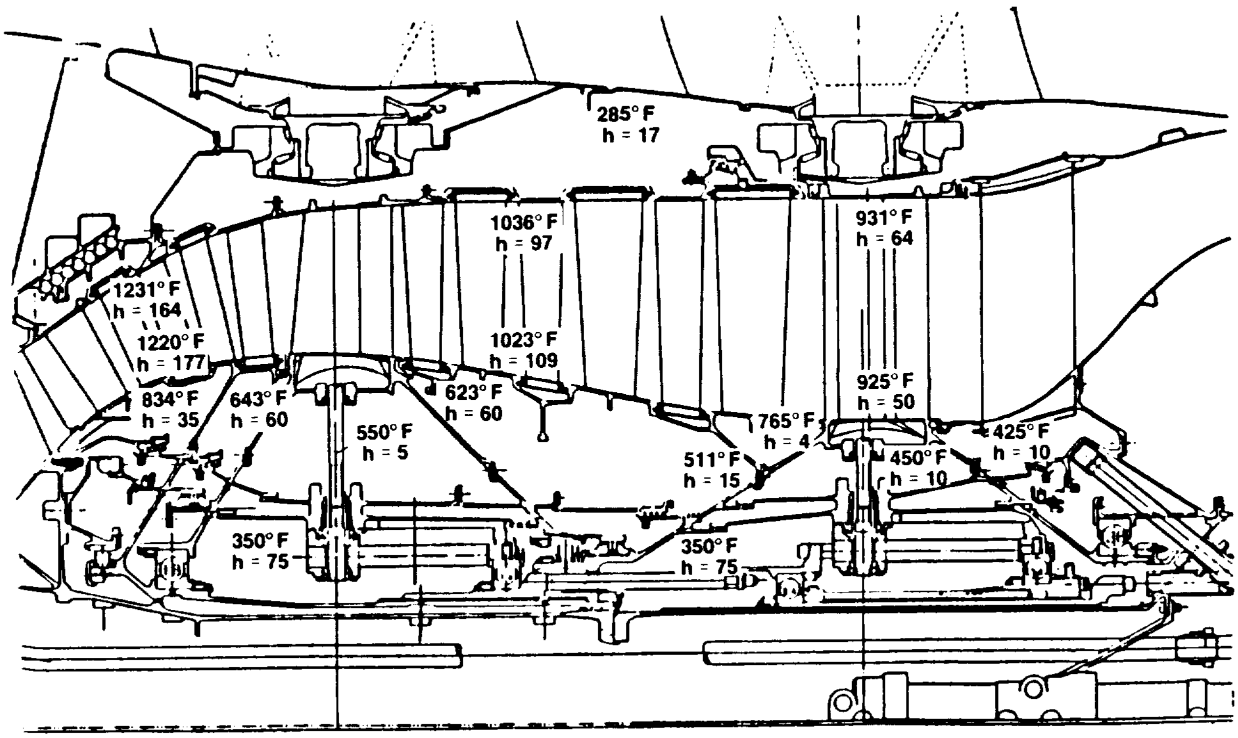


**Hot Day (+27° F) Rated Take-Off**
**Steady-State Conditions**
**h = [BTU/hr. ft.$^2$ °F]**

Figure 4-10. Power Turbine Temperatures Based on Analysis.

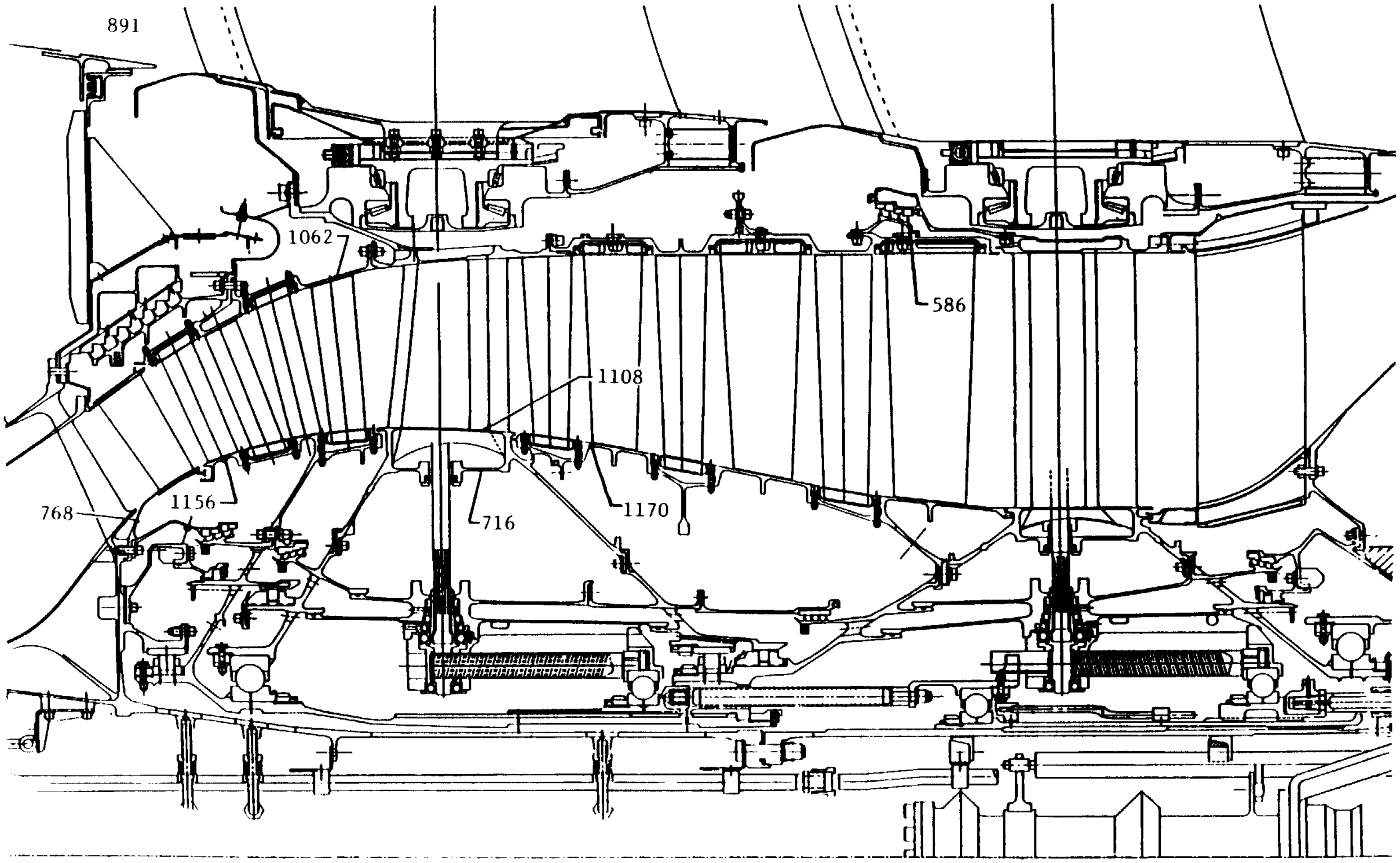


Figure 4-11. Spool Temperatures, Hot Day Takeoff.

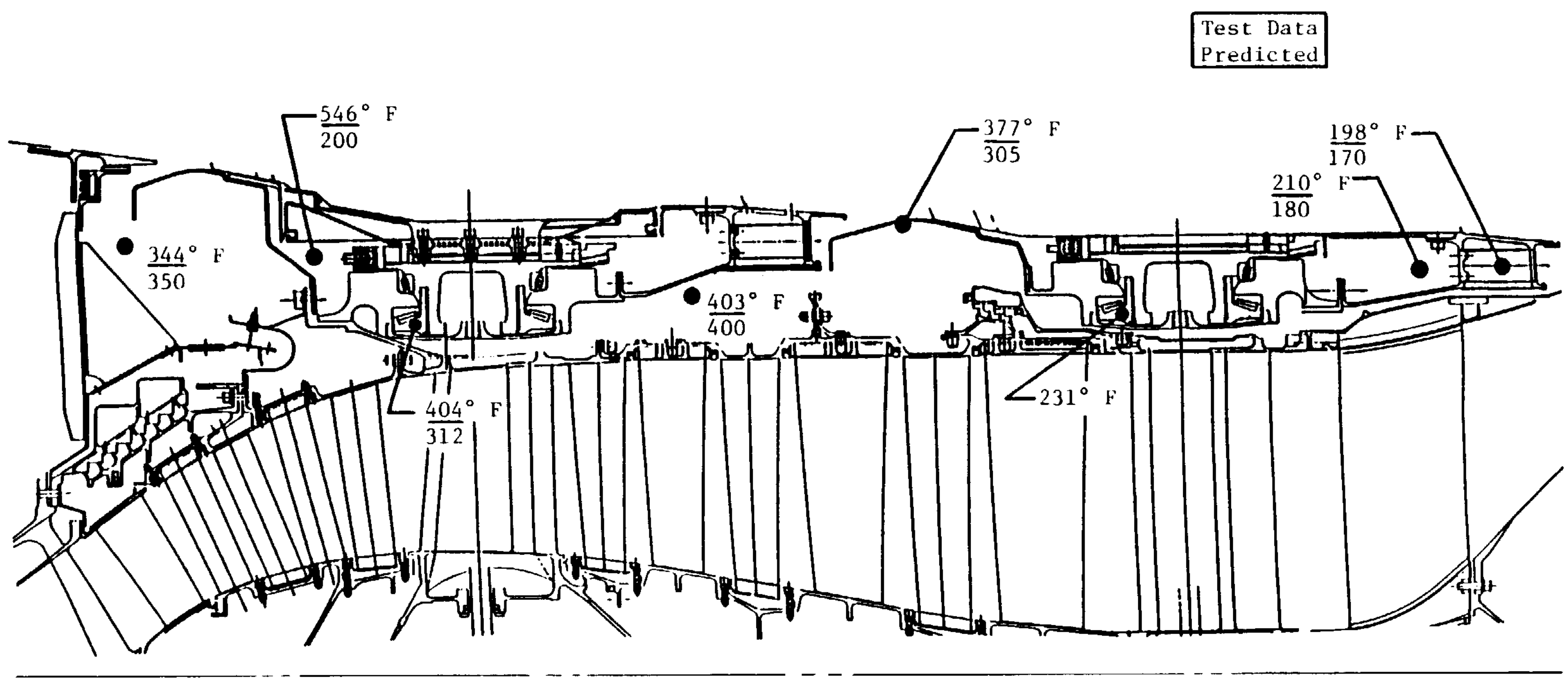


Figure 4-12. Nacelle Temperatures Based on Test Data at Takeoff Power.

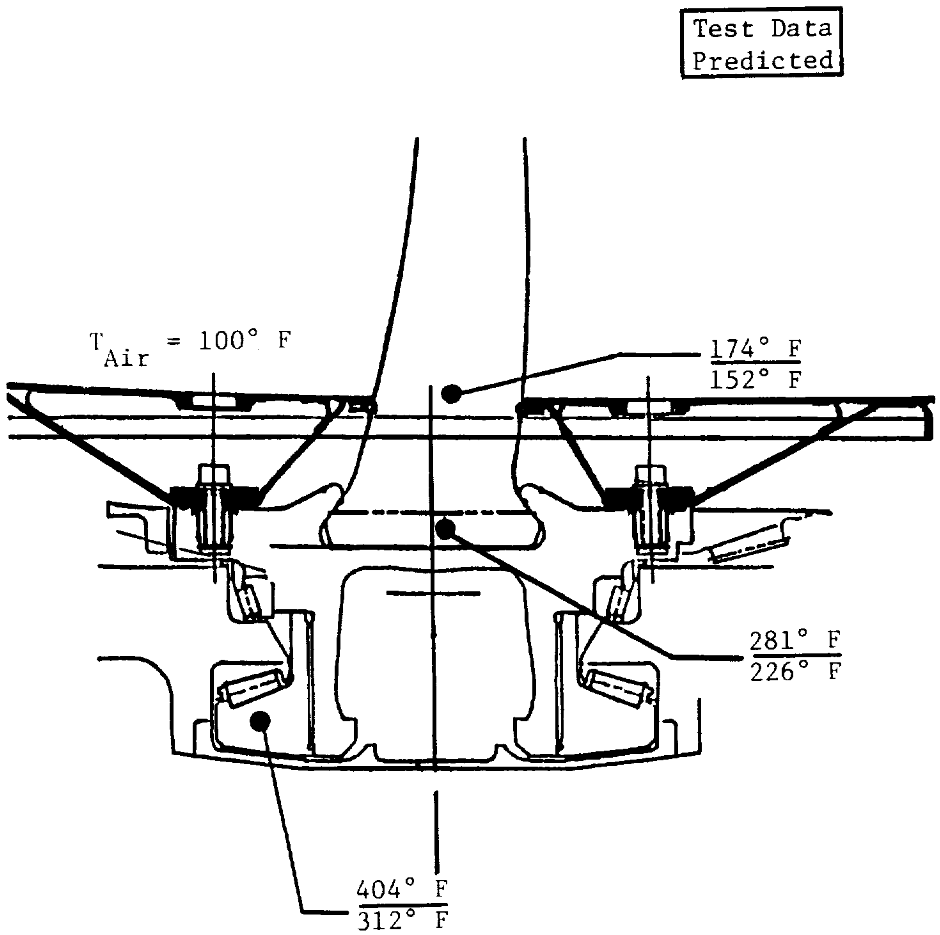


Figure 4-13. Forward Fan Blade Hub Temperatures; Hot Day Takeoff, Mach = 0.0, Full Thrust.

It was determined during initial Build 1 testing that, although the aft telemetry modules were adequately cooled, the solder which fixes the thermocouple leads to the aft telemetry circuit board, was overtemperatured. Even though the solder temperature is not measured directly, it was found that the solder melts when the nearby air thermocouple reaches a temperature of just over 300° F.

The solder, although adequately cooled during high power, is marginally cool at idle conditions. Set to match the prop flow at takeoff, the scoop direction is misaligned with the flow direction at idle. For +27 DTAMB conditions, the solder temperature is 219° F at takeoff, 235° F at flight idle, and 283° F at ground idle.

Figure 4-13 gives a breakdown of the forward fan blade hub temperatures for hot day takeoff. The 404° F trunnion temperature is taken from thermocouple data. All other temperatures are determined by rebalancing the heat transfer model on the basis of the trunnion temperature. All temperatures are higher than predicted, but are still within allowable limits.

## 4.5 CENTER CAVITY VENTILATION

The center cavity is portrayed (Figure 4-14) with temperatures at takeoff power; normal operating temperatures are as listed. The actuator axial position sensor (LVDT) temperature of 312° F is well below the normal operating temperature of 360° F (the maximum temperature limit is 400° F). The speed sensor temperature was not measured directly, but it is probably less than the LVDT temperature since it sees less radiation from the cavity wall than does the LVDT. In addition, the sump oil may provide a sink to the speed sensor. There is no indication of speed sensor or LVDT overtemperature problems.

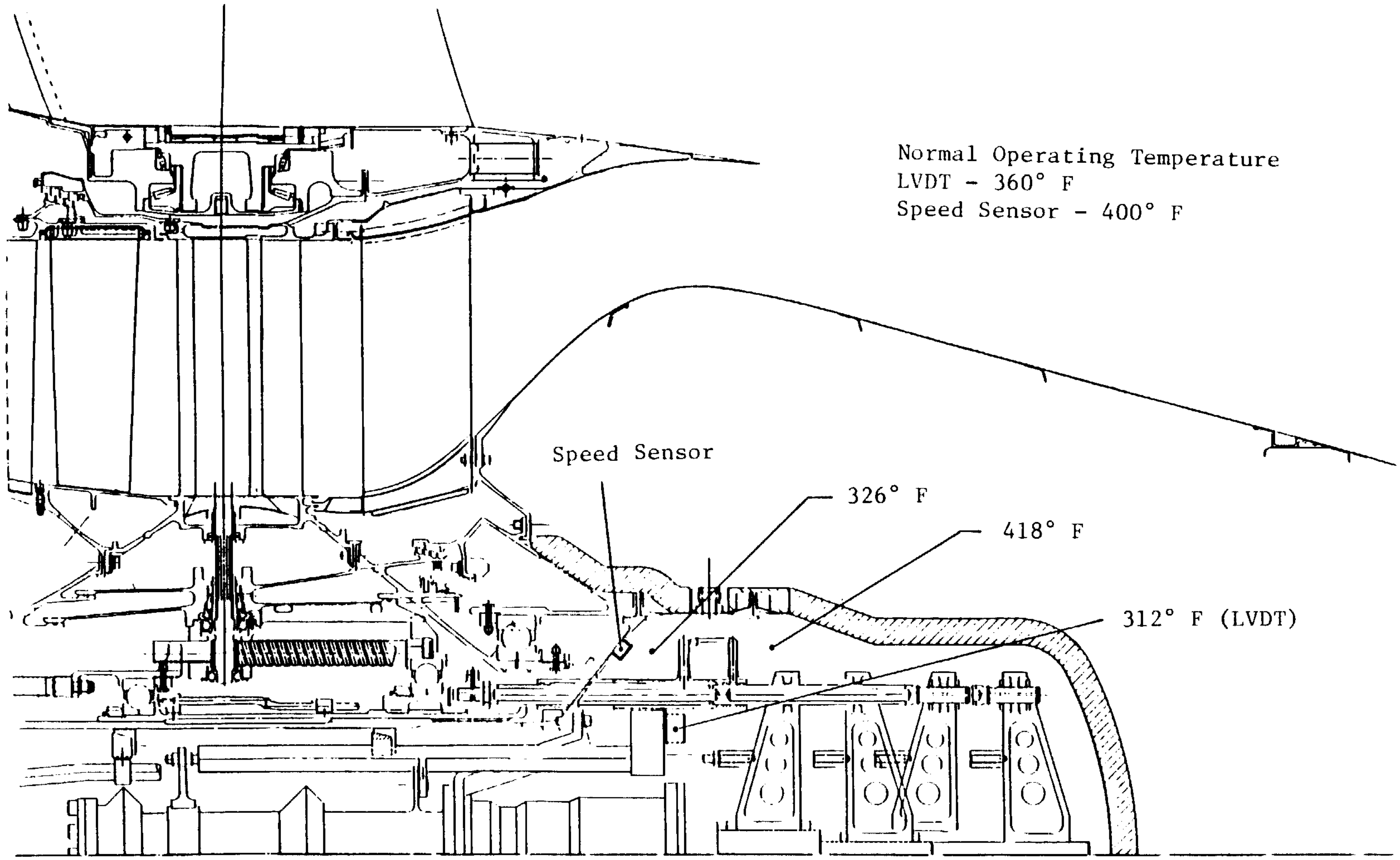


Figure 4-14. Center Cavity Ventilation at Takeoff Power.

## 5.0 ENGINE SYSTEM DYNAMICS

Valuable engine dynamics experience was obtained during ground testing of the UDF™ Demonstrator Engine (GE36 S/N 082-001). This ground testing, along with a series of mechanical impedance tests conducted on the support system and Peebles test facility, was used to modify and verify the analytical model of the engine. Topics that are discussed in a later section regarding this subject include such gas generator vibration signatures as: synchronous 1/rev IPC and HPC responses, linear subidle UDF™ 1/rev signature and its dependency on support structure/test facility stiffness, linear UDF™ 1/rev response recorded in the operational speed range, and nonlinear UDF™ 1/rev response observed during the Stage 2 propulsor airfoil separation event.

The UDF™, with its counterrotating propulsion system, also demonstrated that more sophisticated methods and hardware are required beyond turbofan engine experience with regards to propulsor trim balancing and vibration measuring techniques.

### Gas Generator Vibration Signature

The gas generator used to power the GE36 Demonstrator is an F404 engine. Its rear frame is replaced by the mixer frame, and the gas generator is mated to the UDF™. Gas generator synchronous IPC (intermediate pressure compressor) and HPC (high pressure compressor) vibration levels were well within the prescribed F404 limits throughout ground testing. Both the maximum IPC and HPC 1/rev levels observed in the operational speed range during testing occurred at the F404 fan case vertical location. The maximum IPC 1/rev response was 0.24-inch/second (average velocity) at 11,700 rpm and was observed during Build 3 testing.

Figure 5-1 presents IPC signatures for Builds 1A, 2, and 3, demonstrating that the IPC 1/rev levels remained similar and low throughout ground testing. The maximum HPC 1/rev response was 0.28-inch/second at 13,700 rpm as observed on Build 2. Figure 5-2 compares HPC 1/rev vibration signatures for Builds 1A, 2, and 3 (F404 fan case vertical location). Like the IPC vibration signature, the HPC synchronous response remained similar and low throughout testing.

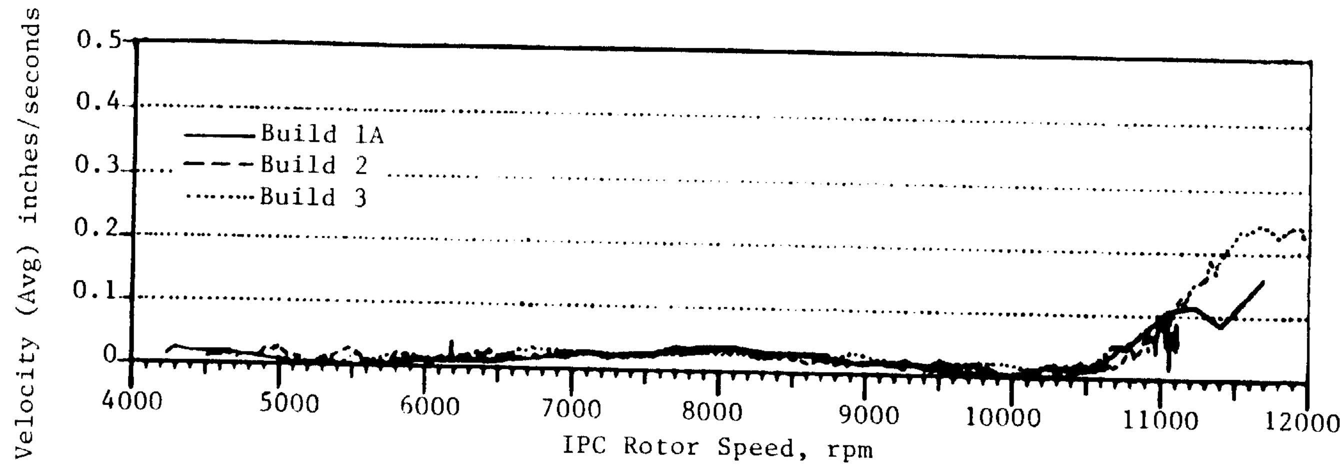


Figure 5-1. IPC One-Per-Rev Signature Comparison.

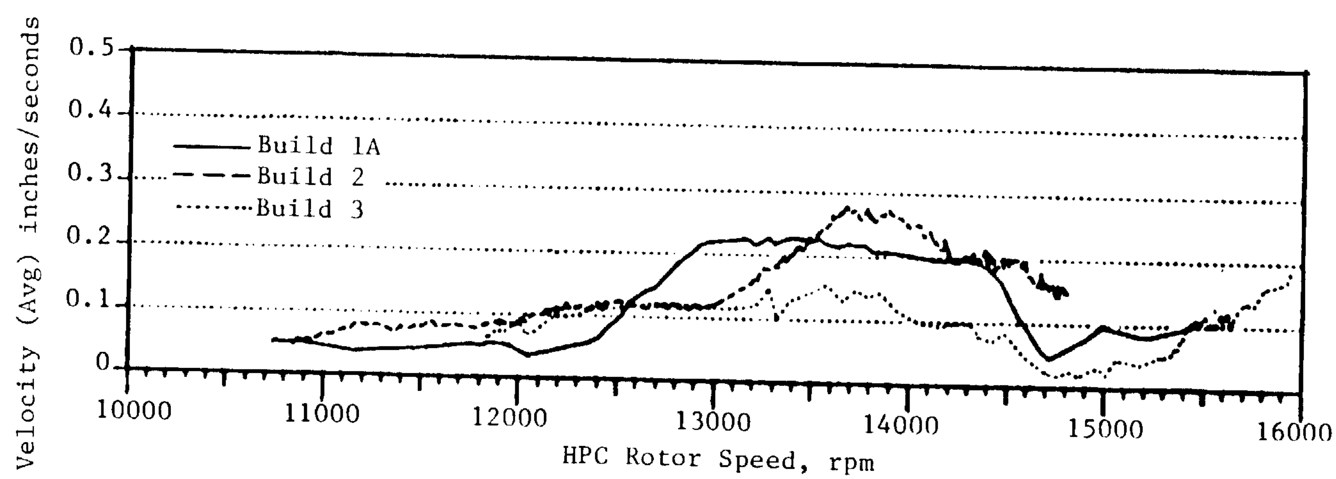


Figure 5-2. HPC One-Per-Rev Signature Comparison.

The F404 predicted engine dynamics show little change between the turbofan engine and the GE36 gas generator application. These predictions were verified by comparing the vibration data from the check-out (at GE-Lynn) of the turbofan configuration with the results observed during the GE36 ground test. Demonstrating little change between both configurations, the results are shown in Figures 5-3 and 5-4; readings were taken at the F404 midframe horizontal location (only common accelerometer location between the two configurations) for the IPC and HPC 1/rev vibration signatures, respectively.

### UDF™ Vibration Signature

The test facility and aircraft structure play a major role in the overall support structure stiffness of the engine and resulting rigid body mode definition of the entire system. Mechanical impedance tests were conducted during January 1986 (between Builds 1A and 2) to obtain the support structure stiffness. The pylon/isolators system was tested with the pylon attached to ground to obtain pylon and isolator stiffnesses and also mounted at Peebles Site 4A facility to obtain the entire support system stiffness. These results were incorporated in both updated linear and nonlinear (propulsor blade-out) analytical dynamic models and will be referenced in subsequent discussion of UDF™ vibration results.

The rigid-body modes occur primarily in the subidle speed range. Since the demo engine was tested at both Sites 4A and 3D, subidle resonances were subject to change due to the differences in facility stiffness properties. To demonstrate these differences, a comparison of Build 2 UDF™ 1/rev vibration signature obtained during engine starts at both sites are shown in Figures 5-5 and 5-6. Figure 5-5 compares the subidle vibration signatures at the F404 fan case vertical location (vertical direction for Peebles test is in line with the strut). The signatures indicate that the overall support system stiffness was softer at Site 3D in this direction. Figure 5-6 compares the two subidle signatures at the same location in the horizontal (normal-to-strut) direction. Overall system stiffness effects at Site 3D acted to decouple the predominant rigid-body modes observed at Site 4A.

The UDF™ 1/rev operational speed range vibration signature at the No. 2 ball bearing housing location is illustrated in Figure 5-7 for the vertical

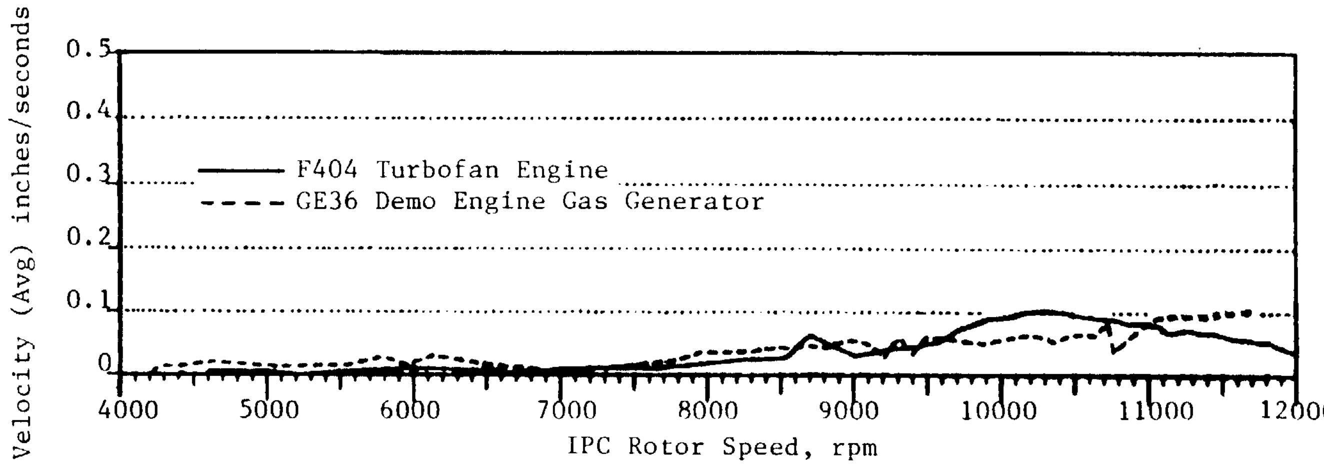


Figure 5-3. IPC One-Per-Rev Signature Comparison.

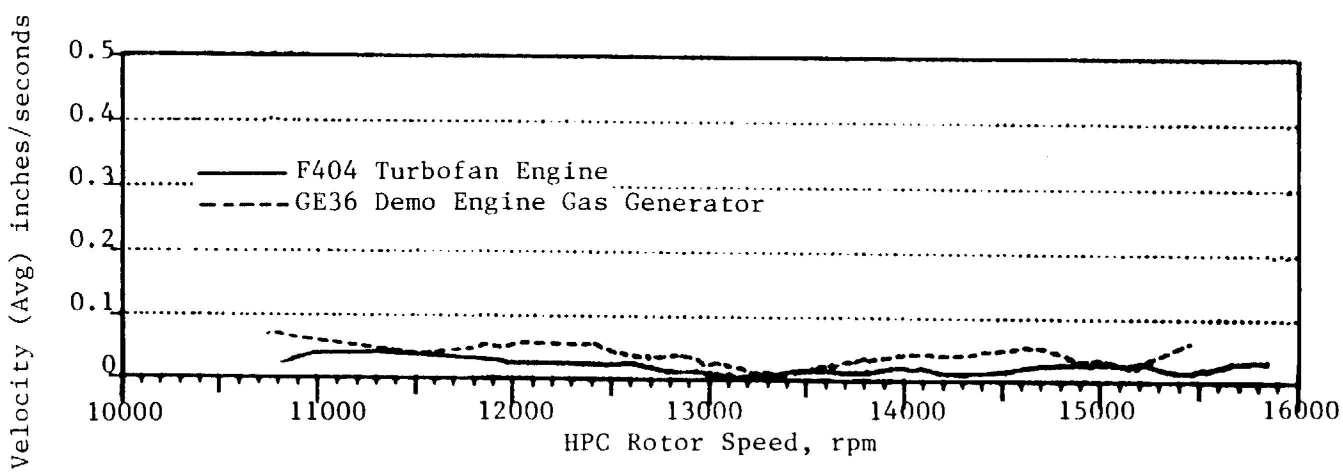


Figure 5-4. HPC One-Per-Rev Signature Comparison.

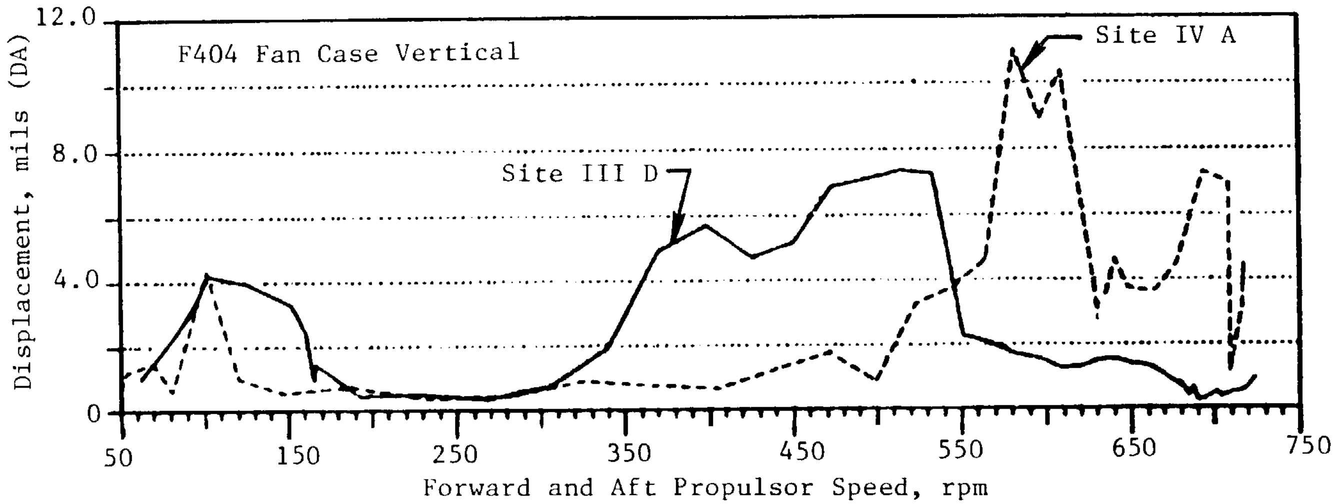


Figure 5-5. Subidle UDF$^{TM}$ One-Per-Rev Vibration Signature Comparison.

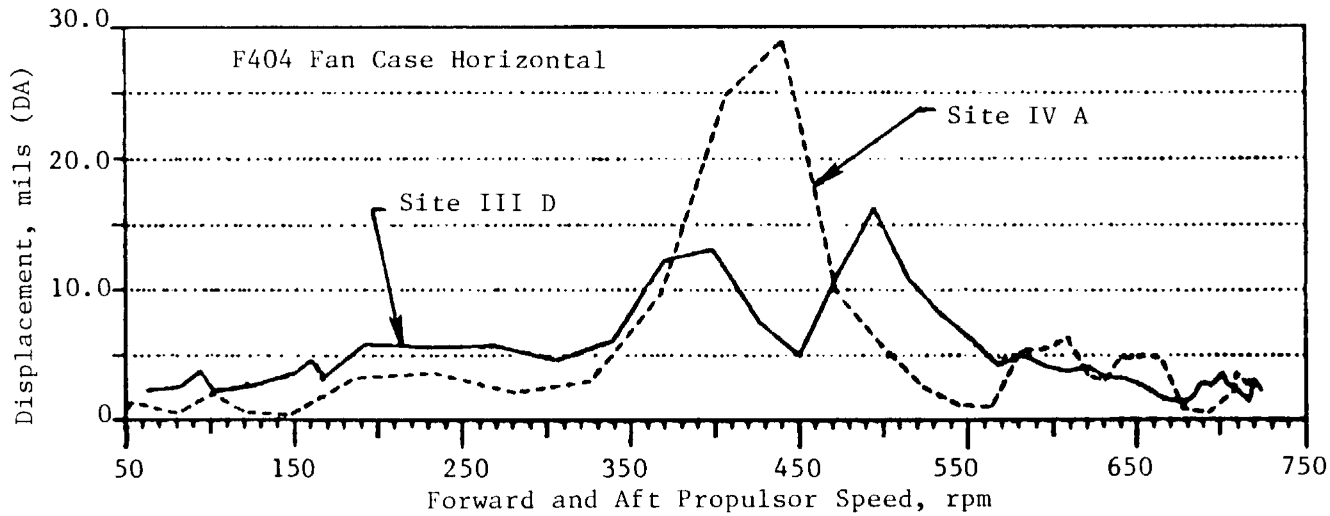


Figure 5-6. Subidle UDF$^{TM}$ One-Per-Rev Vibration Signature Comparison.

direction and in Figure 5-8 for the horizontal direction; each indicates the deflection in mils (DA) as a function of propulsor speed for accels conducted to 24,000 lbf at Sites 4A (Build 2) and 3D (Build 3). Although the signatures are similar, differences in levels were noted; the differences in levels are accounted for by two explanations. The first is that the propulsor blades were modified, and a nominal correction weight was added to the Stage 2 rotor between runs. The second explanation deals with the repeatability of vibration on a closely synchronized counterrotating propulsion system; this subject will be discussed in a later section.

### Stage 2 Airfoil Separation Event

The Stage 2 propulsor airfoil separation event that occurred on Build 2 (Site 4A) led to an opportunity to modify and verify the nonlinear dynamic model predictions (by mechanical impedance test results) for this event and, subsequently, to apply this knowledge to the blade-out design criteria of the aircraft application. The dynamics, both actual and predicted, were presented during the May 13, 1986 Quarterly Review at the Nasa-Lewis Research Center in Cleveland, Ohio. A major benefit resulting from this event was proof that the pylon isolators function as designed. This was demonstrated by a significant reduction of motion through the isolators, and the fact that the isolators soften with the increased loading and, thus, lower the system resonant speed.

### Trim Balance Experience

The initial efforts to trim balance the propulsors during Build 2 were hampered by the hardware used. The basic trim balance test sequence was to separate propulsor speeds by 100 rpm (1.67 Hz) and take amplitude and phase readings from the existing SD119C Trim Balance Analyzer unit at predetermined steady-state speed conditions. Making the initial trim balance unsuccessful, the built-in 3 Hz (%1.5 Hz) bandwidth tracking filter of the SD119C unit did not adequately separate the vibration response of the two rotors and, thus, did not give correct amplitude and phase information.

A modified SD119C unit was purchased with a 1.0 Hz (%0.5 Hz) bandwidth tracking filter and was evaluated during Build 3 testing. Improvements were achieved in the balance of each rotor utilizing this new unit and applying

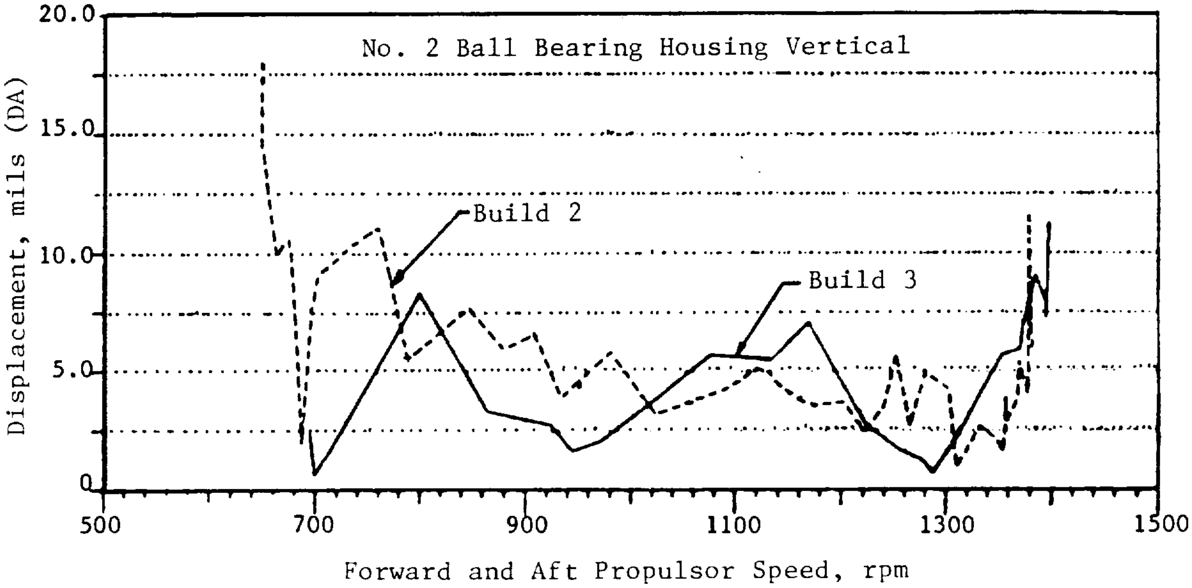


Figure 5-7. UDF™ One-Per-Rev Vibration Signature on 2 Minute Accel to 24,000 lb Thrust, Housing Vertical.

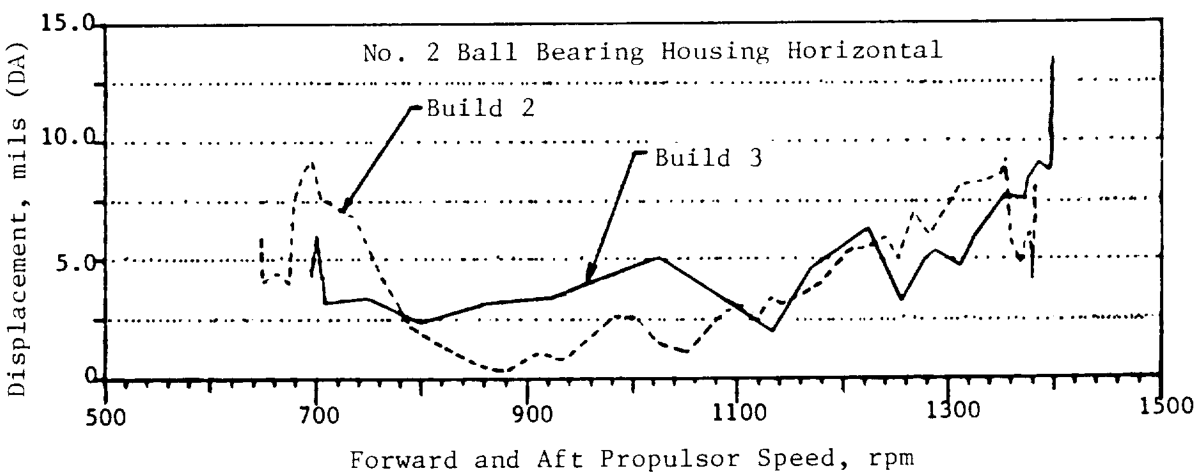


Figure 5-8. UDF™ One-Per-Rev Vibration Signature on 2 Minute Accel to 24,000 lb Thrust, Housing Horizontal.

force correction weights. The sensitivity to the force unbalance was determined to be 325 gram-inches/mil which is 2 to 3 times less sensitive than fan unbalance in a large bypass turbofan engine. But even with the improvements noted above, the vibration response observed during power hooks (constant rpm thrust excursions) was still considered undesirable. The test on this build ended before a good set of high thrust data could be obtained during the power hook excursions.

The amount of data accumulated in these balance exercises did, however, indicate that one or more excitation sources, other than a pure force unbalance, was contributing significantly to the UDF™ vibration signature of the engine. Efforts are currently underway to evaluate each of the following possible sources:

- Changes in either force or mechanical moment unbalance due to the blade actuation system (from low- to high-power condition)

- Aerodynamic moment unbalance being introduced by any propulsor-blade tracking problem.

### Measuring Techniques

For a simple one degree of freedom system, the maximum sensed deflection would lag the forcing function (rotor unbalance) by 90° at its first natural frequency. The deflection level is a function of the unbalance force magnitude, the damping, and the mode shape at this given frequency. For a single rotor application, such as a high bypass turbofan engine, the maximum static deflection at any circumferential location, even though not necessarily equal, would occur in one revolution of the rotor and would be repeatable from one revolution to another, provided the unbalance or rpm were unchanged. Using this simple one degree of freedom system and assuming that the mode shapes in the vertical and horizontal directions are identical, Figure 5-9 demonstrates this point.

The UDF™ engine, on the other hand, may not sense the maximum deflection at a given circumferential location during a revolution of its counterrotating propulsor rotors. For example, assume that both the forward and aft rotors are exactly synchronized, that the forcing functions are equal at each rotor, and the mode shapes are identical in both the vertical and horizontal planes.

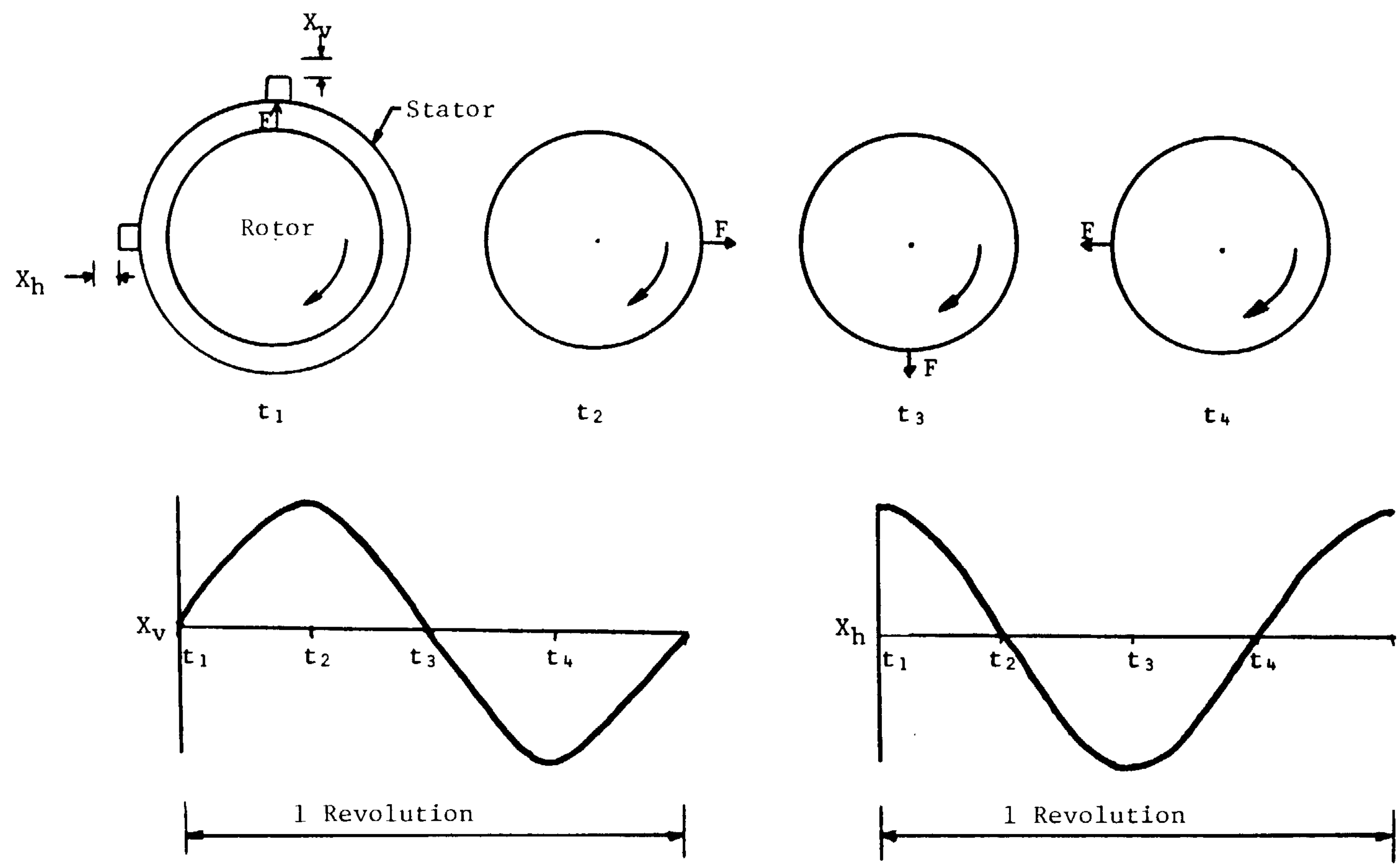


Figure 5-9. Maximum Static Deflection.

Now, using the single rotor example above, we have two cases (Figures 5-10 and 5-11) which show either the vertical or the horizontal deflection at a maximum level, and the other plane at a minimum.

This example indicates that for a given revolution, if the vertical location is at the maximum level, the horizontal response is zero, and vice versa. This example also shows that the maximum deflections in each plane are equal, and that the minimum deflections are not only equal but are, in fact, zero. Expanding this example into real-world application, we find that the maximum response in a given plane will always result in the minimum response occurring in its orthogonal plane.

First, let the force unbalance of each rotor be different. In this case, maximum deflection for both the vertical and horizontal planes will still be equal, as will the minimum levels, but these minimum values will no longer be zero. Second, let the mode shape definition and force unbalance be different. At this point, neither maximum nor minimum deflections between the two planes would be expected to be equal. The final step in approaching the real world is to leave the one degree of freedom system and enter the actual multidegree freedom system situation. This step does nothing more than to vary the phase-angle lag between the lined up forces, and the resultant maximum deflection circumferential location, as a function of the engine dynamics.

Test data is provided in Figure 5-12 demonstrating the above discussion and illustrating the UDF™ 1/rev response at ground idle power for the approximately orthogonally mounted accelerometers at the No. 2 ball bearing housing location. Also shown is the phase-angle lag between the forward and aft propulsor 1/rev indicators. The phase data indicates that the rotors are close but not totally synchronized. The vibration data shows the 1/rev levels are modulating at the same frequency as the propulsor rotors difference frequency. These data demonstrate, as earlier stated in the discussion, that the maximum response in one plane occurs at the minimum response of the other plane, and vice versa. The two rotors unbalance line up at a phase-angle lag of 240° to yield the maximum vertical response and at a phase-angle lag of 60° to yield the maximum horizontal response.

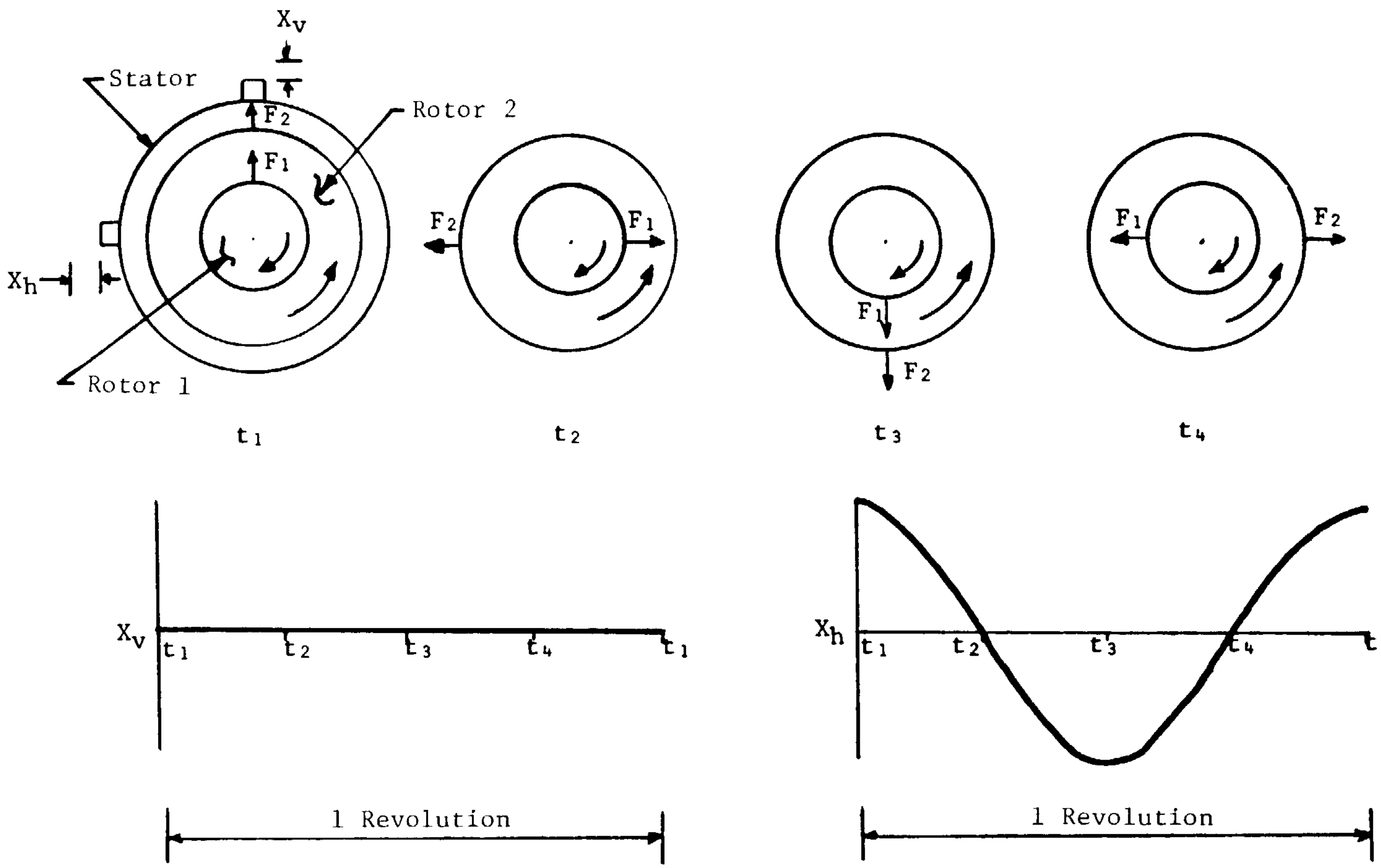


Figure 5-10. Unbalance Forces Lineup in Vertical Plane.

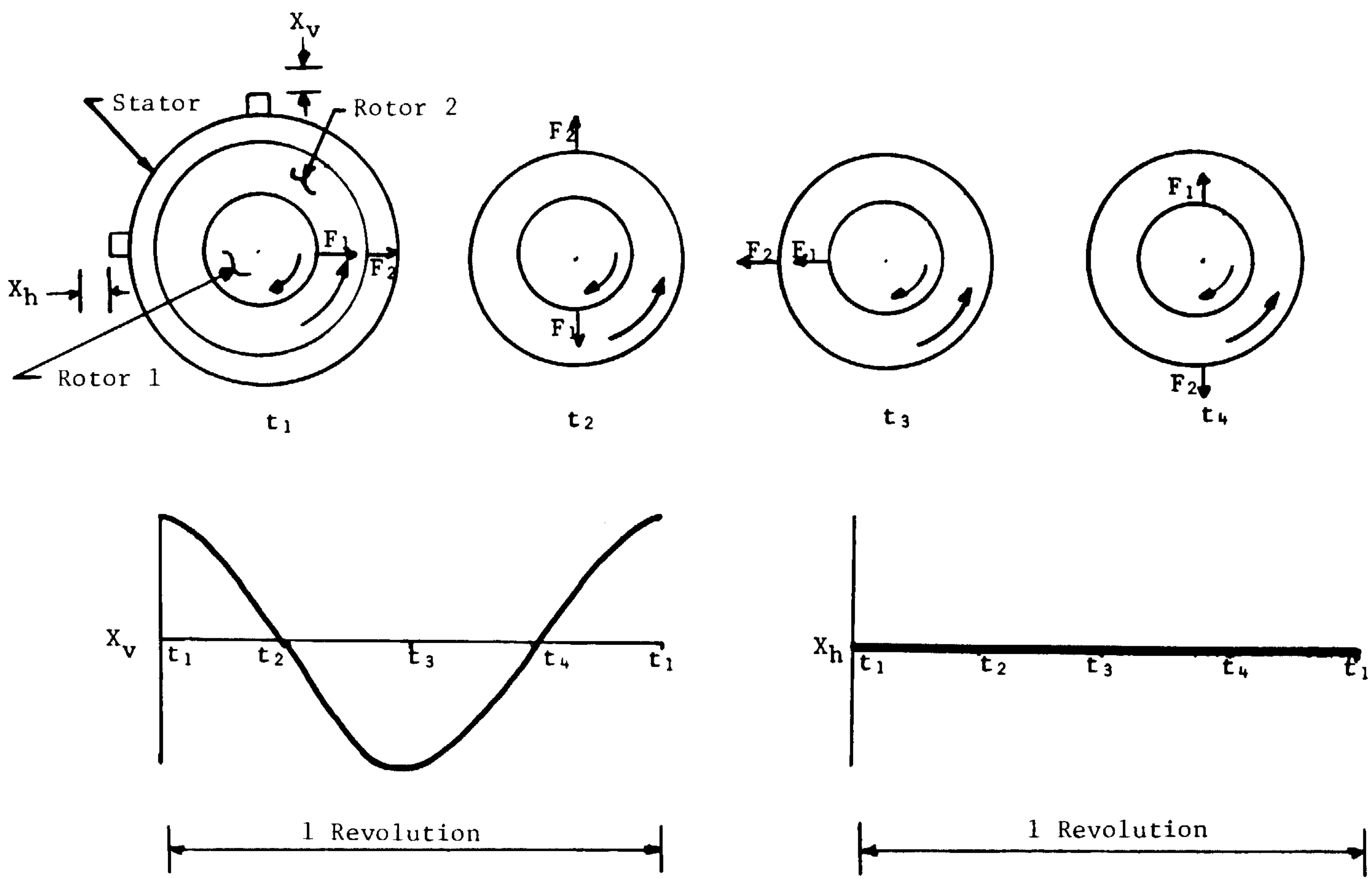


Figure 5-11. Unbalance Forces Lineup in Horizontal Plane.

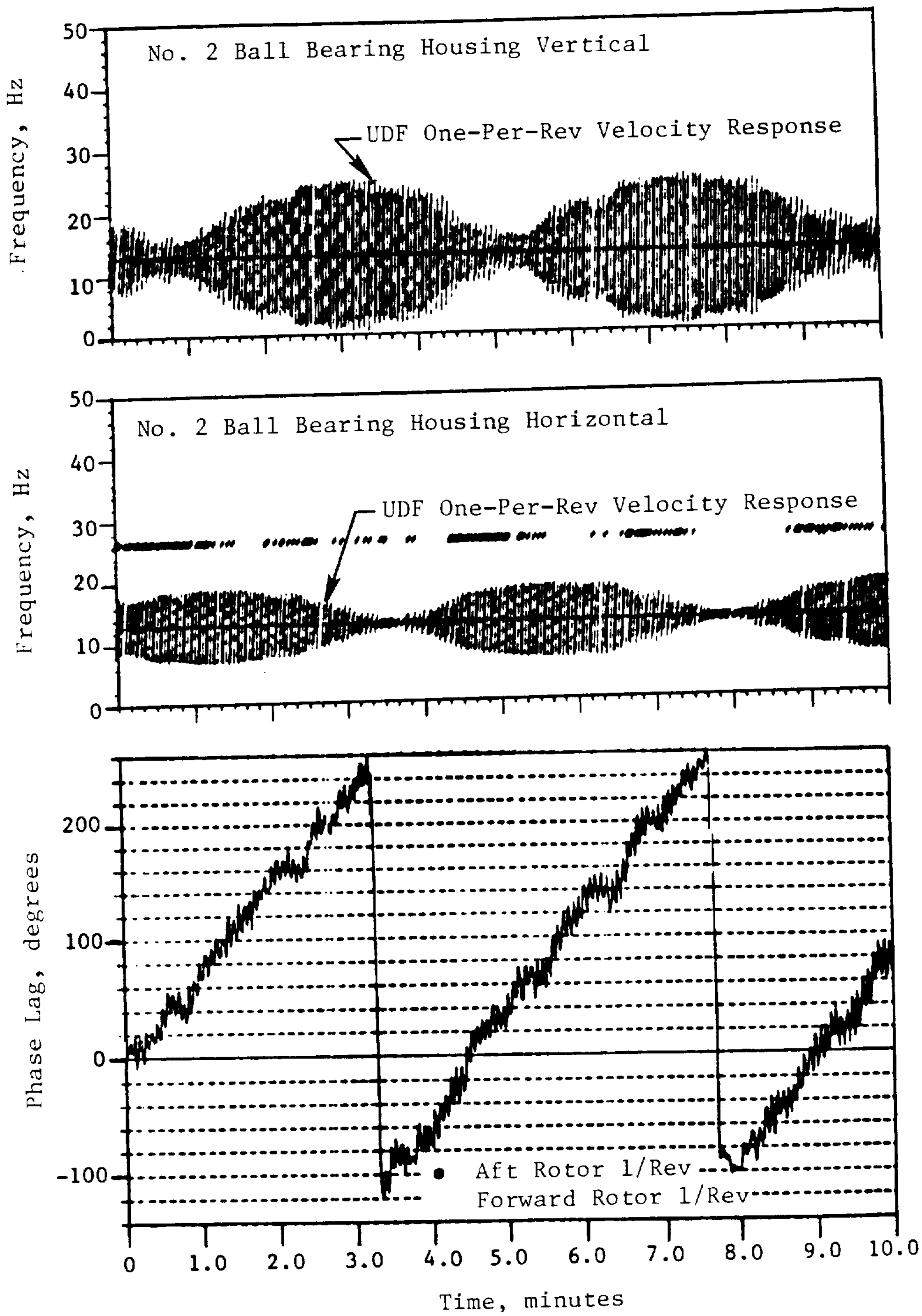


Figure 5-12. GE36 Demonstrator Engine 082-001/3 T/D 7-1-86 Time History Plots at Ground Idle Power.

This discussion explains why variation in vibration would be expected in the UDF™ 1/rev levels shown in Figures 5-7 and 5-8. Although the rotors are not precisely synchronized during the throttle advances, they are close, and therefore, the response at any given speed is dependent upon the orientation of the unbalances to each other and to the sensing device.

Realizing that this characteristic existed prior to initiation of ground testing, GE Aircraft Engines developed a system to optimize the chance of capturing the maximum vibration level each revolution. The automatic vibration engine shutdown/aircraft monitoring system has two sets of orthogonal accelerometers mounted on the engine. Each signal of the orthogonal accelerometer goes through a software package that takes the square root of the sums of the responses squared. This method vastly increases the probability of capturing the maximum vibration response each revolution and is, by far, a more accurate measuring tool for synchronized counterrotating rotors than the conventional method utilized to measure high bypass turbofan engine vibration.

# 6.0 BEARINGS AND SEALS

This section covers the main propulsor bearings and all actuation system support bearings. All of the bearings performed well during ground testing, from a design standpoint. Some problems arose as a result of debris produced during manufacture of other engine parts; however, engine operability was not compromised. Seals in the fan blade retention system performed well during testing except for a few torn fan blade thrust bearing seals resulting from insufficient lubrication.

## 6.1 HARDWARE CONDITION

### 6.1.1 Rotor Support Main Bearings

#### Debris Ingestion

The main bearings operated well, which was to be expected, as they had ample capacity.

The two roller bearings were replaced twice during ground testing when they were exposed at disassembly. They were replaced because debris damage had scored some of the rollers. The debris was comprised almost exclusively of 0.007-inch-diameter steel shot particles, with some other manufacturing and wear debris present in very small quantities. Prior to engine teardown, oil sample analysis had identified the possibility of a debris problem.

A blind cavity in the forward intershaft carbon seal land, designed to prevent possible thermal coning, had trapped a quantity of steel shot during the peening process. The shot did not wash out during manufacture but was sluiced out by the hot lube oil during engine running.

Causing extensive scoring of the rollers, the shot became imbedded in the soft silver plate of the rolling element retainer of the bearing. This would cause both a breakdown of the hydrodynamic lube film because of the high loads and low rotational speeds and a diminished fatigue life. However, no surface distress due to rubbing was observed.

Bearings were returned to the manufacturer for refurbishment, although only inner rings and cages were usable. The rings were rehoned and the cages stripped and replated. The design of the roller retention features permitted roller removal without damage to the cage.

To prevent further debris damage, the blind cavity was ultrasonically cleaned and sealed closed with a nichrome strip (Figure 6-1). This was fairly successful, although one or two pieces of shot were still found in subsequent oil samples.

### Retention Nut Loosening

The outer ring retention nut of the 1R intershaft bearing came loose and completely disengaged during the final stage of ground testing; this permitted axial movement of the outer ring.

The nut is believed to have jammed the actuation system preventing blade-angle adjustment. On teardown, forward and aft rotors could not be separated in the normal disassembly sequence. This was caused by the rollers no longer being in contact with the outer raceway. Borescope inspection prior to disassembly had shown the rollers still engaged, so running in this disengaged condition had not occurred. When the rotors were separated, the bearing was found to be in remarkably good condition, except for the damage to the roller corners caused when the rollers dropped into the region of the outer shaft, from which the ring had moved, and hung up on the shaft shoulder (Figures 6-2 and 6-3).

Examination of the spanner nut indicated no obvious thread damage, and the Vespel insert retention feature appeared undamaged. The appearance of the raceway did not indicate any running off the normal roller path; however, some coning was indicated. The shaft coning was in the direction to move the shaft radially away from the nut, and the wedge effect would exert an axial force on the nut in the direction to promote untorquing. There was no damage from ring spinning on either the outer ring OD or the shaft bore.

For subsequent engine testing, a hole was line-drilled axially in the thread, and a roll-pin was mechanically locked in the thread to prevent the nut becoming untorqued (Figure 6-4).

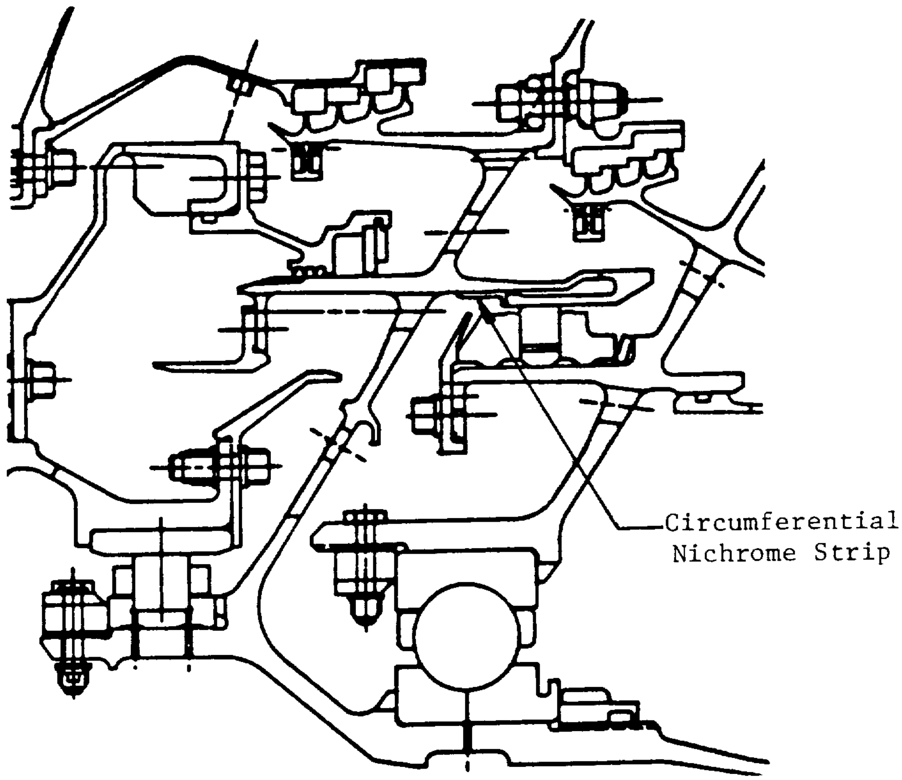


Figure 6-1. Seal Cavity Closure.

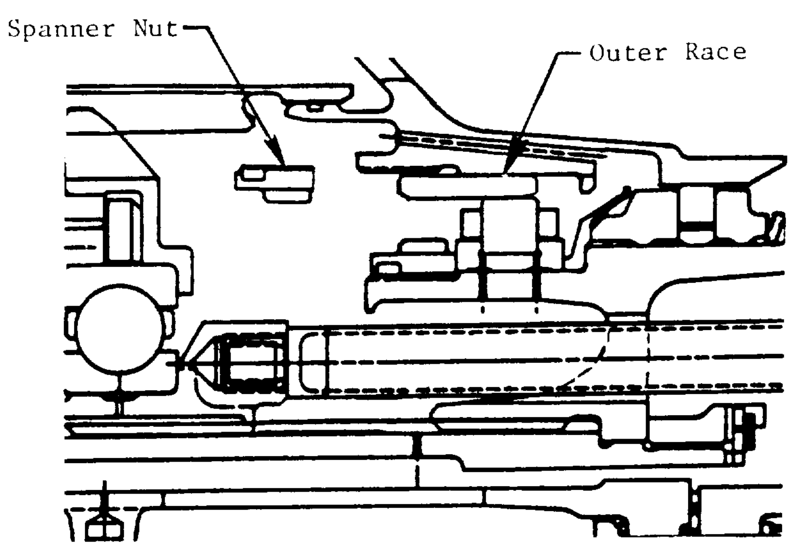


Figure 6-2. Possible Running Condition with 1R Spanner Nut Loose.

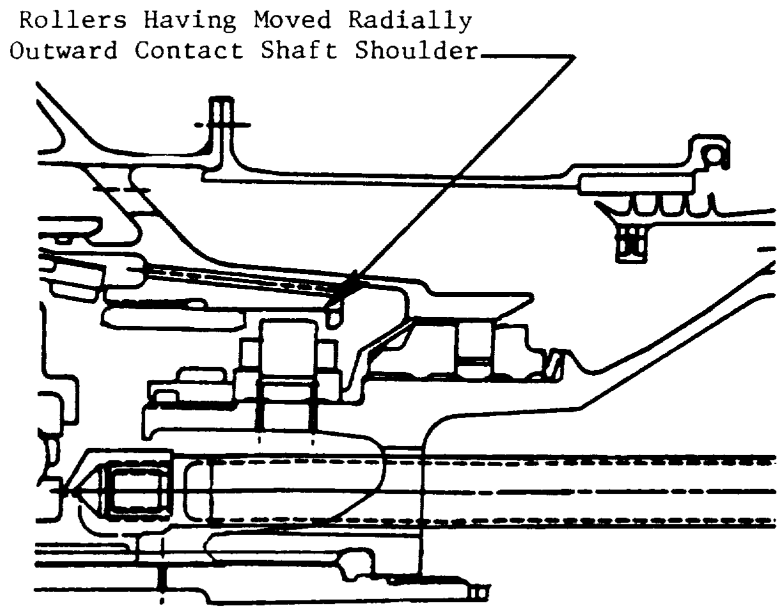


Figure 6-3. Disassembly Problem and Roller Corner Damage.

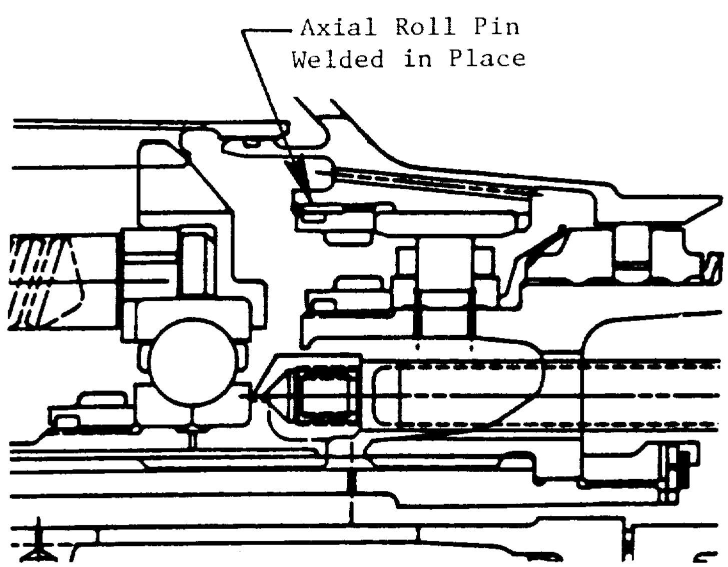


Figure 6-4. Problem Solution - Positive Nut Locking.

### 6.1.2 Inner Actuation Bearings

#### Actuation Ball Bearings

No problems were encountered with the large mainshaft actuation ball bearings. These bearings were examined at the last teardown for any evidence of irregular wear or cage impact that might occur due to the calculated axial distortion of the outer ring from the four gear rack loads, but no indication of abnormalities was seen.

#### Radial Quill Shaft Gearbox Bearings

The inner bearings supporting the radial shafts could not be seen without teardown of the gearboxes; however, since no problem existed and they operated flawlessly, no teardown was performed.

The outer gearboxes were examined because of the loosening of the outer housing nut. The nut butts against and clamps the outer ball bearing, which locates the pinion gear. The cause of the loosening was found to be a stackup problem incurred by a change in a washer thickness (Figure 6-5), and the problem was corrected. Although the bearings are grease lubricated, most of the grease had been expelled, and some bearings showed wear.

### 6.1.3 Actuation Tapered Roller Bearings

The tapered roller bearings supporting the counterbalance torque tubes and bevel gears were examined and showed no deleterious effect except for some slight corrosion. This problem was manifest because the grease lubricating these bearings is centrifuged outwards, and the bearings are not adequately protected from the high humidity experienced during testing, some of which occurred during moderate rain.

### 6.1.4 Fan Retention Bearings and Seals

#### Setup Bearing

The setup bearing is incorporated to react the blade overturning moment and carry most of that load. However, at speed, the centrifugal load is sufficiently high that a very large moment would be required to unseat the main

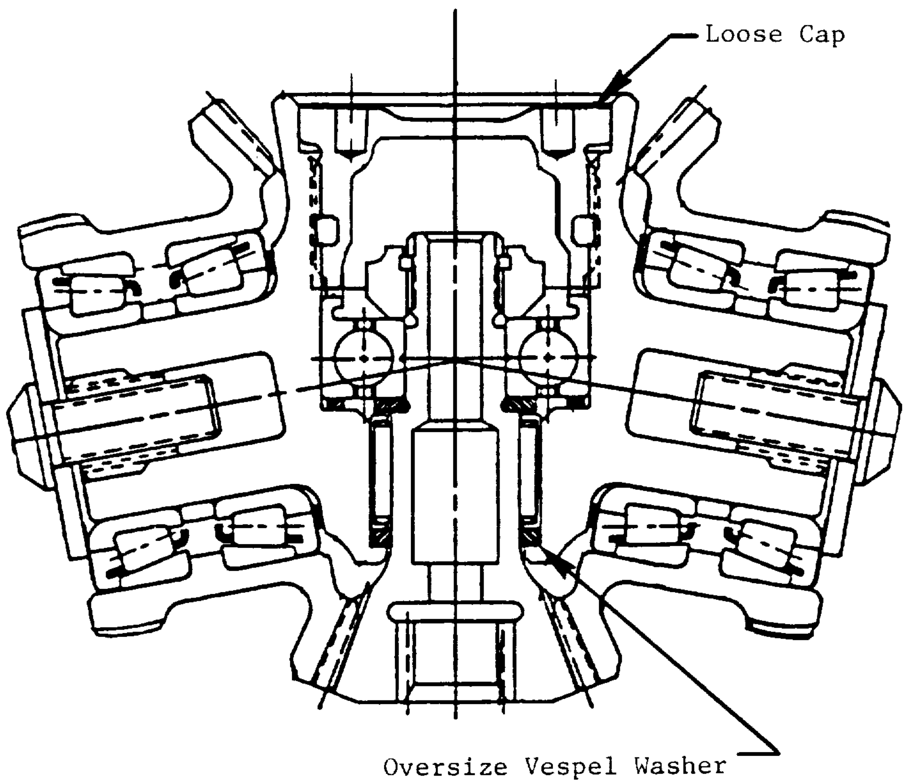


Figure 6-5. Gearbox Stackup Problem Causing Incorrect Loading of Ball Bearing and Cap Looseness.

thrust bearing. Therefore, the setup bearing has a relatively easy life. The only problem associated with these bearings was, again, corrosion. Although protected by a silicone seal and lubricated by grease, because the grease is permeable, some corrosion was seen, but not severe and none on the active surfaces of the bearing.

### Fan Thrust Bearing

Bearing Condition and Seal Condition - The main fan thrust bearing reacts the considerable centrifugal load of the blade and is subjected to dither from blade vibrations and actuation system load fluctuations. Therefore, false brinelling and fretting were the major concerns.

Most noticeable about the condition of the bearings was the disparity in appearance between forward and aft rotor parts. The front rotor was in a much hotter environment, sometimes as much as 100° F hotter. Bearings from this rotor were slightly blued, but the aft rotor bearings were not discolored. Some fretting corrosion was present on both rotor bearings; however, this had not progressed to the point were the bearings were unserviceable.

The lubricant in the forward rotor was dry and discolored; whereas, the aft rotor grease looked like new. Grease seals in some of the forward rotor parts had been torn due to lack of lubrication.

The roller wear paths on the raceway of the cup and cone showed evidence of bearing distortion due to the unsymmetrical loads caused by the housings deflecting, as was predicted by finite element analysis. The bearing cone had been made more flexible to compensate; however, even the cone bending was not enough to provide an even loading. Deflection analysis was performed using a lighter blade weight than we currently have (Figures 6-6 and 6-7).

Thread Clamp Condition - During ground check-out for flight, play in the trunnion support bearings was discovered which caused blade tip movement. The clamp load was measured using a unique eddy-current technique for determining the stretch in the trunnion threads. The technique had been calibrated during ground testing at Peebles to substantiate the torques used at assembly. The results revealed a loss of clamp load, and the rings were returned to Evendale for retorquing the trunnions. This gave us the opportunity to examine all the

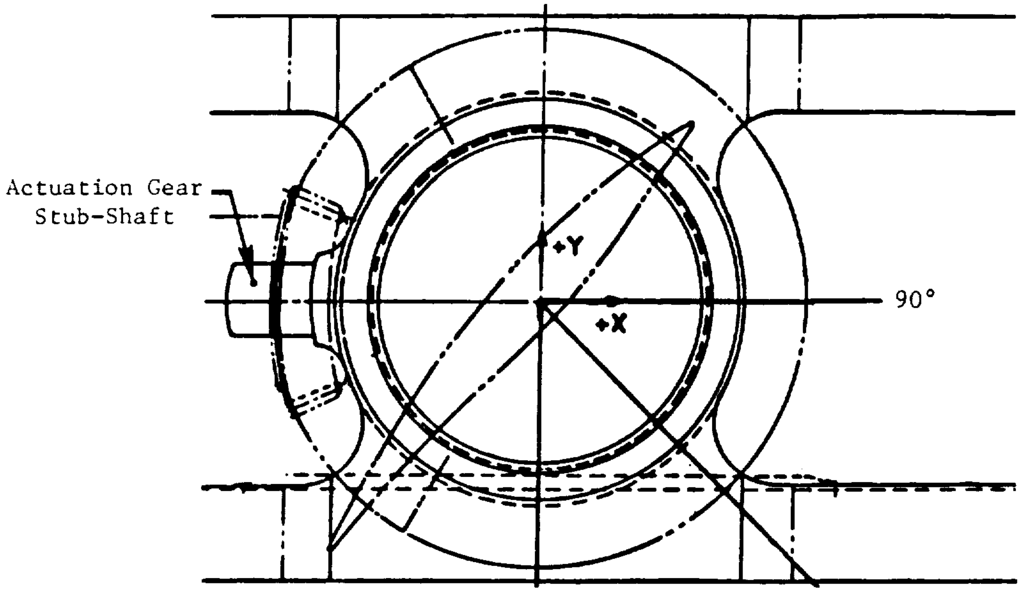


Figure 6-6. Bearing Housing Deflection.

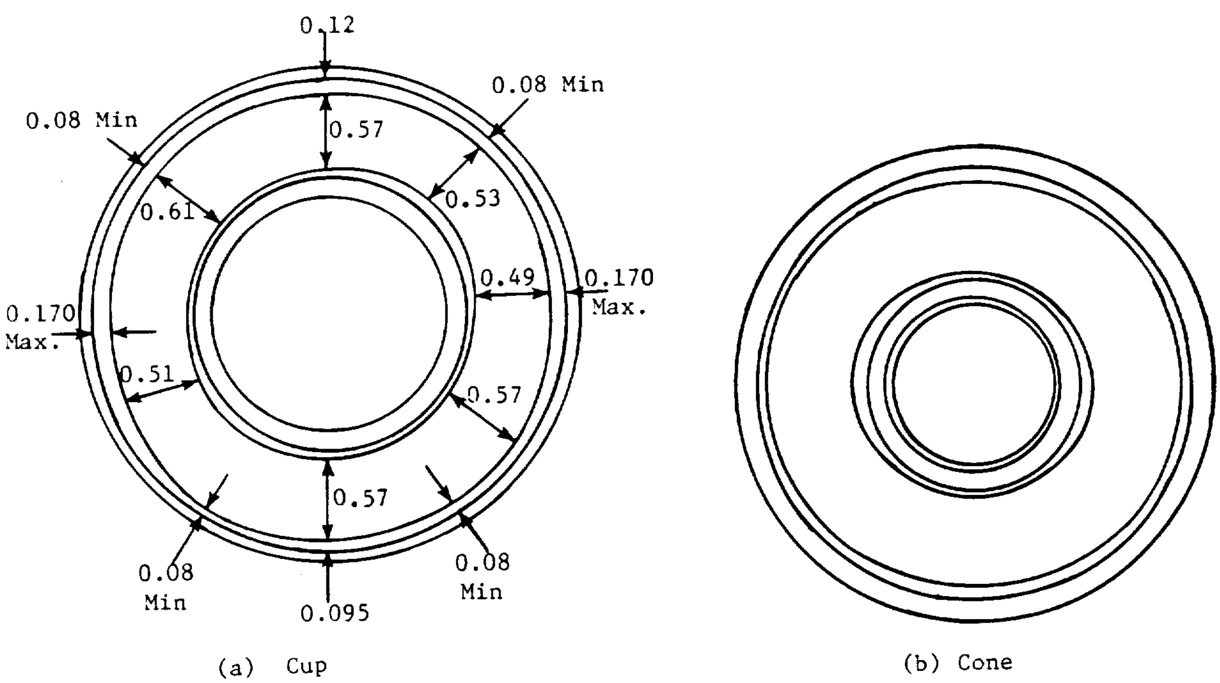


Figure 6-7. Irregular Wear Pattern of Roller "Path".

trunnion bearings. Thus, the condition of all of the retention bearings was known. Due to minor surface distress, coupled with increased trunnion/bearing thread torque, two bearings were replaced; however, all other bearings were acceptable for flight testing as is. The consumable parts (seals, shims, and grease) were also replaced where necessary.

## 6.2 MEASURED TEMPERATURES

### 6.2.1 Rotor Support Main Bearings

The main bearings were instrumented initially with three thermocouples at each bearing location. The thermocouples were at 120° circumferential locations; however, loss of signal and lack of available recording channels left only one gage at each position providing good data.

#### Steady-State Temperatures

The bearing temperatures were influenced by environment (oil, metal, and cavity temperatures) and by engine speed. The intershaft bearings ran hotter than the Stage 2 rotor supports, as would be expected due to the higher relative speed (Figure 6-8).

The Stage 1 rotor bearing temperatures increased from 240° F at 700 rpm (idle) to 340° F at 1393 rpm (maximum thrust). The Stage 2 rotor bearing temperatures were lower, with that of the 2B bearing rising 50° F, to 250° F at maximum thrust. Oil supply temperature rose 100° F over the same ranges.

#### Transient Temperatures

The bearings did not pick up temperature very rapidly during fast accels. A 40° F rise in intershaft bearing temperatures is attributable to increased centrifugal loads. The Stage 2 rotor support bearings changed little during a 2-minute accel to full power. However, a 4-minute accel/decel demonstrated a similar 40° to 50° F rise in all bearings (Figures 6-9 and 6-10).

### 6.2.2 Fan Retention Thrust Bearings

The fan retention tapered roller bearings were not instrumented; however, thermocouples were placed inside the trunnion adjacent to the bearing. Since

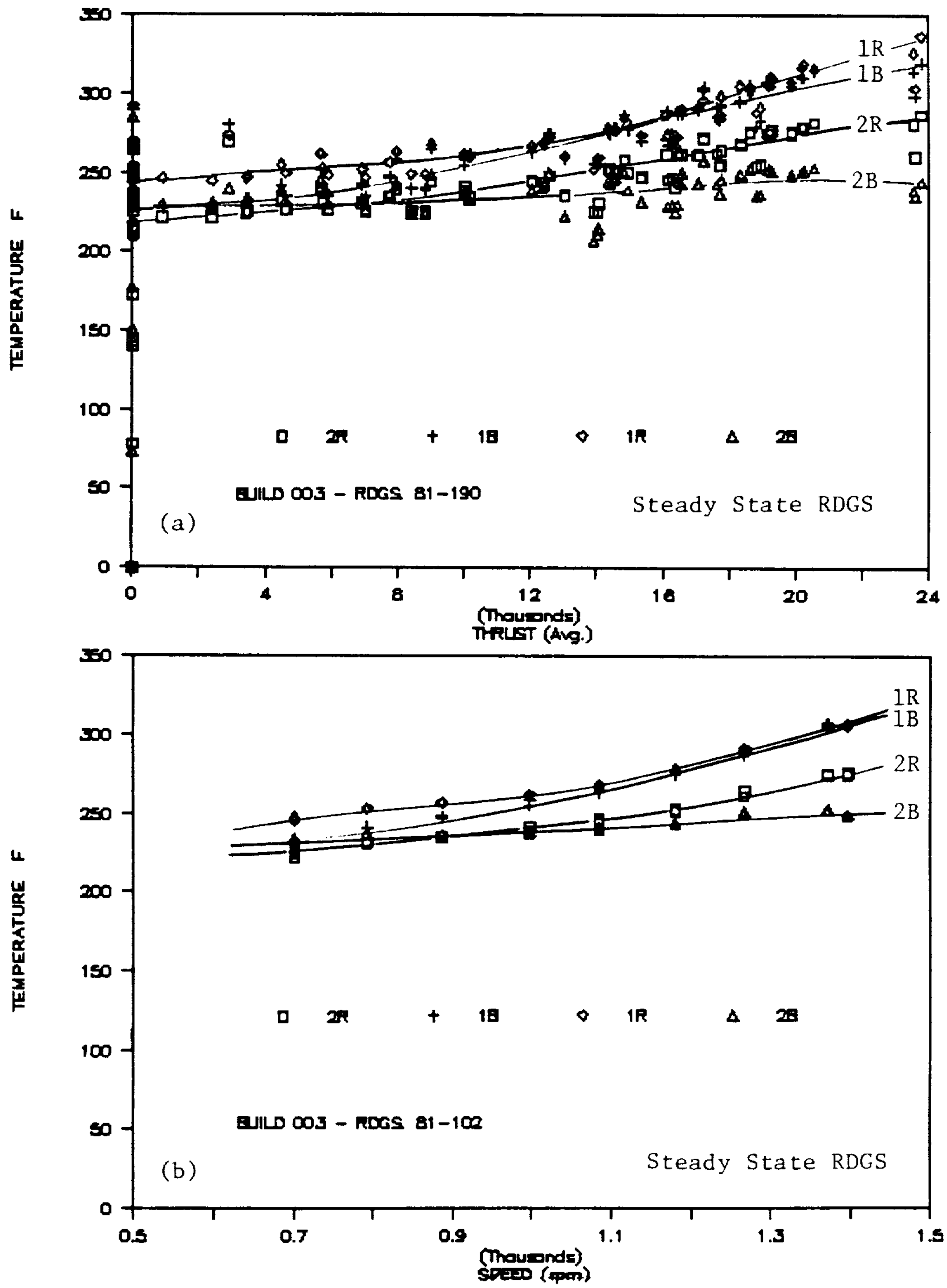


Figure 6-8. Main Propulsor Bearings.

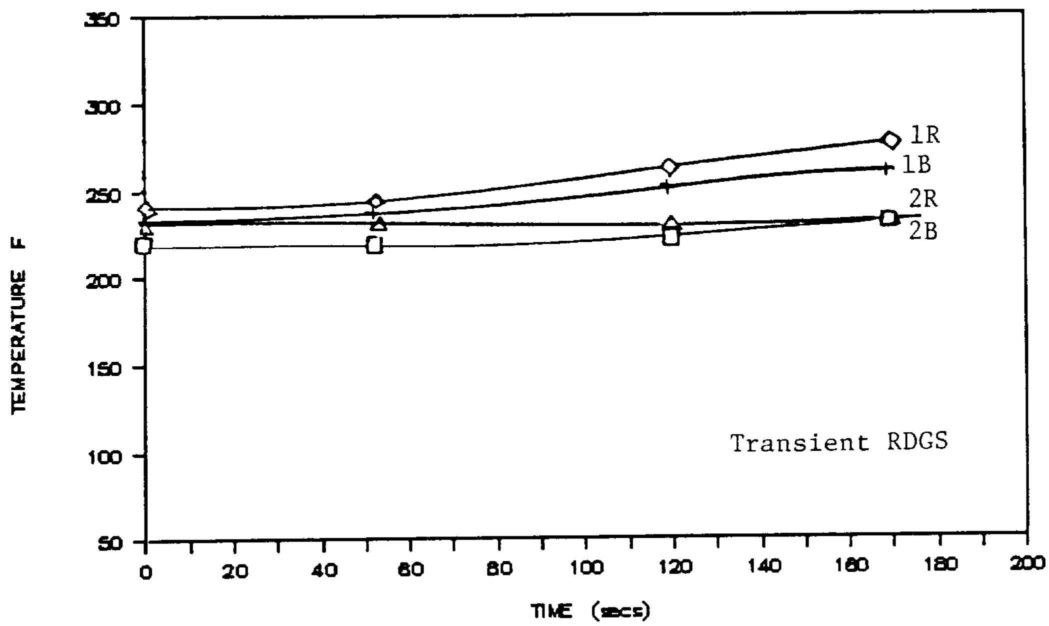


Figure 6-9. Main Propulsor Bearings, 2 Minute Accel to 24,000 lbs Thrust.

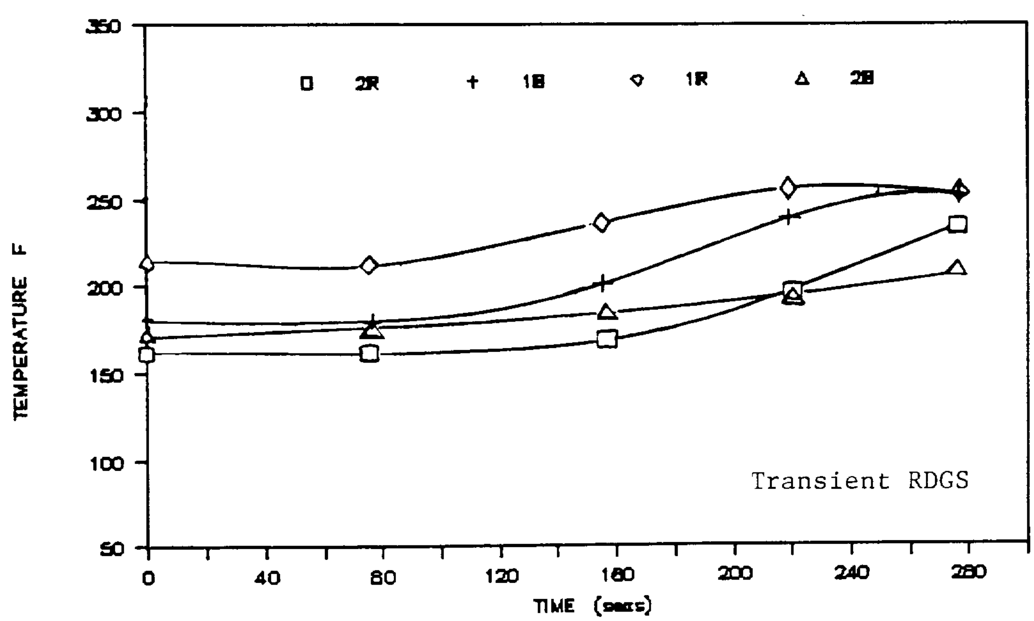


Figure 6-10. Main Propulsor Bearings, 4 Minute Accel/Decel to 1200 rpm.

this is a closed cavity, the temperature would not be too far from that of the bearing.

### Steady-State Temperatures

The forward hub temperatures rose from approximately 340° F at 700 rpm to about 390° F at 1393 rpm. The aft hub went from 190° to 250° F in the same range (Figure 6-11).

### Transient Temperatures

There was little difference between a 2-minute accel and a 4-minute decel, in that the temperatures of both forward and aft hubs rose about 20° to 40° F. This is due to the fact that the thermocouples were in a closed cavity and, although influenced by turbine air gas temperatures, they are shielded from the immediate effect by the fan ring bulkhead plate (Figure 6-12).

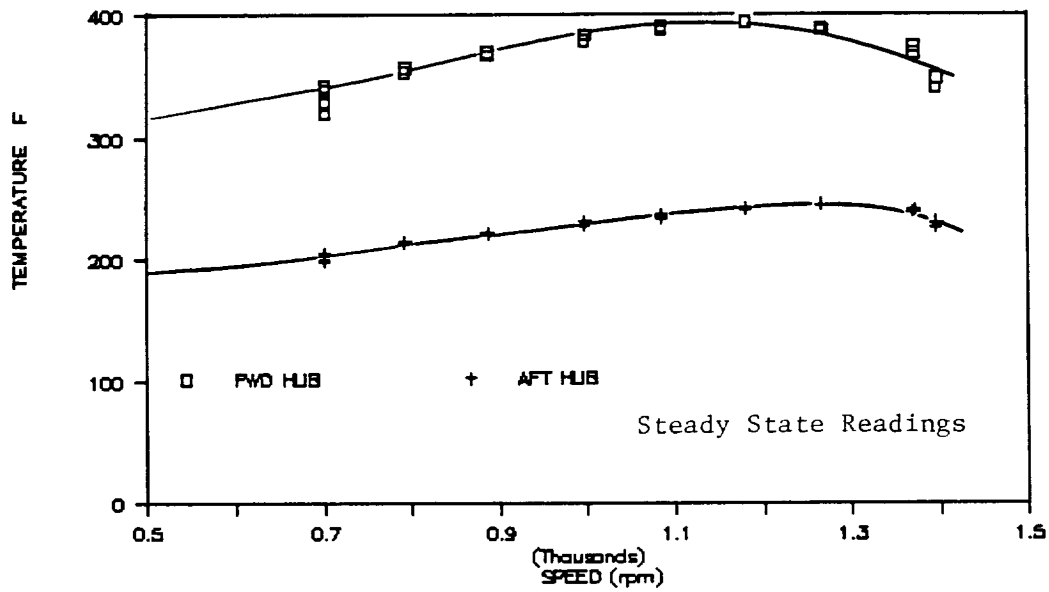


Figure 6-11. Forward and Aft Fan Hub Temperatures.

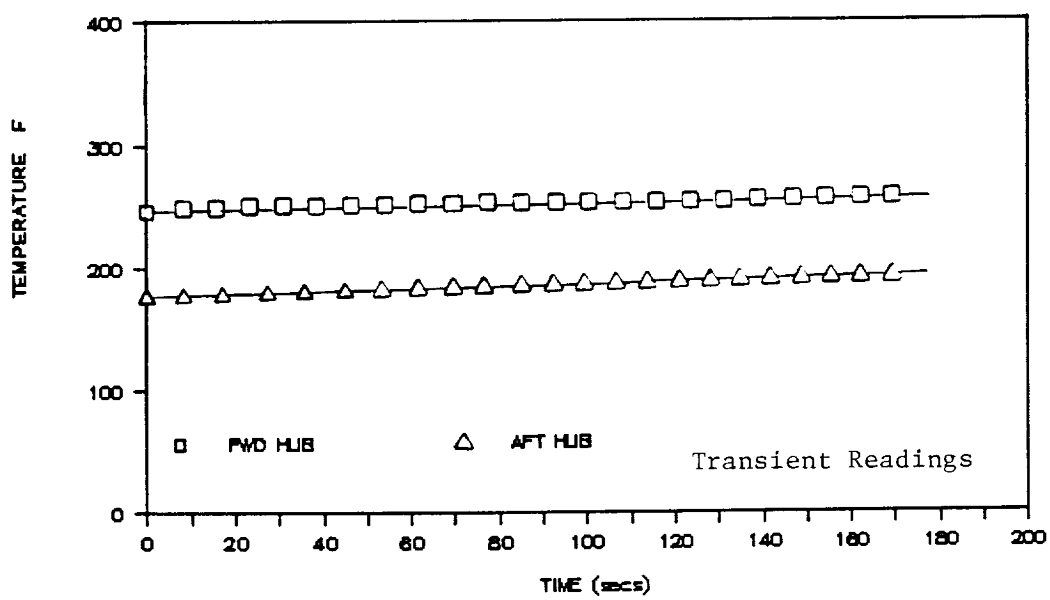


Figure 6-12. Forward and Aft Fan Hub Temperatures, Accel to Full Power.

# 7.0 PERFORMANCE

This section describes the steady-state data acquired during Build 3 testing at Peebles Site 3D and the various analyses employed to support the test effort. The major items covered are as follows:

- Data summary
- Data reduction methodology
- Comparison between pretest predictions and reduced test data
- LCF cyclic testing and resultant deterioration
- Comparison between ground and flight pretest cycles and reduced test data
- Overall summary
- Key results
- Conclusions.

## 7.1 DATA SUMMARY

During Build 1 testing at Site 4A, a total of 46 steady-state DMS (data management system readings were taken, none of which were usable for performance analysis since all the points were recorded mainly for mechanical checkout and were not stable.

During Build 2 testing, 104 steady-state DMS readings were taken at Site 4A, and an additional 31 at Site 3D. Some of the data points were usable for analysis.

Table 7-1 shows the breakdown of steady-state DMS readings for Build 3. Note that of the total of 358 data points recorded, 27 readings were expressly taken to define the baseline performance, with an additional 48 data points recorded to map the UDF™ performance at off-schedule conditions. Table 7-2 shows the chronology of the acquired data.

Appendix A presents a listing of the Build 3 steady-state data points.

## 7.2 DATA REDUCTION METHODOLOGY

Figure 7-1 shows the schematic of the engine and the positioning of the performance-related instrumentation.

Table 7-1. Data Summary.

| Breakdown of Steady-State DMS Readings for Build -03. | |
|---|---|
| | Points |
| Zero Readings | 86 |
| Ground Idle Readings | 2 |
| Flight Idle Readings | 16 |
| Trim Balance Data Readings | 36 |
| Bleed Evaluation Readings | 28 |
| EPR Power Hooks | 48 |
| Down Power Calibration | 27 |
| LCF Cycles | 102 |
| Miscellaneous Data Points | 15 |
| Total | 358 |

Table 7-2. Chronology of the Acquired Data.

| Breakdown of Steady-State DMS Readings for Build -03 | | |
|---|---|---|
| Readings | Date | Points |
| 1 to 5 | 6/20/86 | 5 |
| 6 to 15 | 6/23/86 | 10 |
| 16 to 31 | 6/24/86 | 16 |
| 32 to 47 | 6/25/86 | 16 |
| 48 to 56 | 6/26/86 | 9 |
| 57 to 70 | 6/29/86 | 14 |
| 71 to 77 | 6/30/86 | 7 |
| 78 to 149 | 7/1/86 | 72 |
| 150 to 197 | 7/3/86 | 48 |
| 198 to 209 | 7/4/86 | 12 |
| 210 to 251 | 7/5/86 | 42 |
| 252 to 304 | 7/6/86 | 53 |
| 305 to 330 | 7/7/86 | 26 |
| 331 to 358 | 7/8/86 | 28 |
| Total | | 358 |

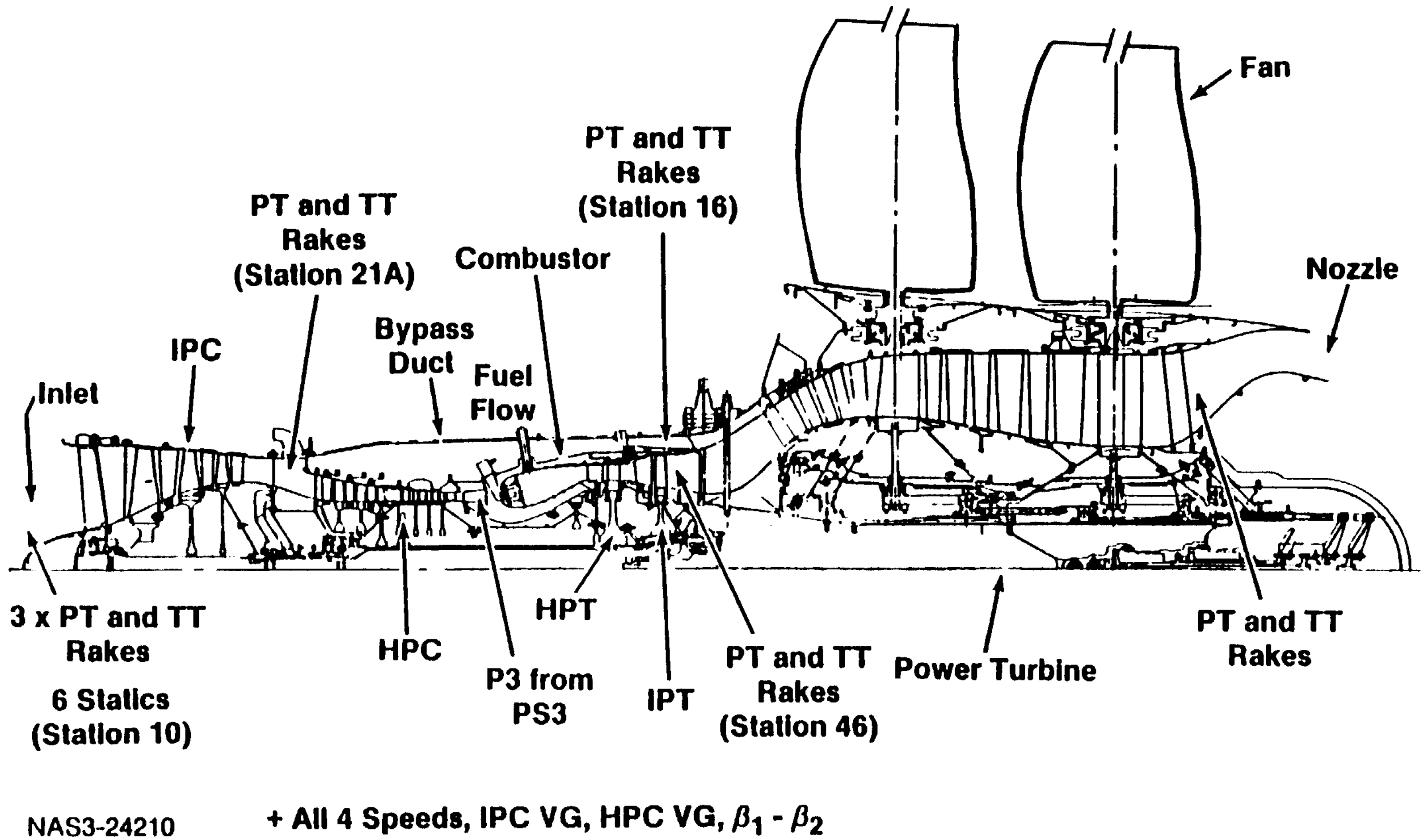


Figure 7-1. Instrumentation for UDF™/F404 Demo.

IPC

| | |
|---|---|
| Inlet flow | - From inlet total rakes, circumferential pressure statics, physical area, flow coefficient |
| Pressure ratio | - From inlet and exit total pressure rakes |
| Efficiency | - From inlet and exit total pressure and temperature rakes. |

HPC

| | |
|---|---|
| Flow | - From HPT flow function (iteration) |
| Pressure ratio | - From IPC exit conditions and stratification logic to define inlet pressure, PS3 correlation to define P3 |
| Efficiency | - From matching core overall performance. |

Bypass Duct

| | |
|---|---|
| Flow | - From IPC exit conditions and stratification logic |
| Pressure drops | - Measurements at IPC exit and duct exit |
| Temperatures | - Measurements at IPC exit and duct exit. |

Combustor

| | |
|---|---|
| Efficiency | - Assumed (map value) |
| Pressure drops | - Assumed (map value) |
| Fuel flow | - Measured (including all parameters for corrections). |

HPT

All parameters assumed (map).

IPT

| | |
|---|---|
| Efficiency | - Energy balance with IPC |
| Exit from IPT | - (T46) - From fuel flow and inlet airflow, together with assumed secondary flows |
| | - (P46) - Measured. |

Mixer Frame

Assumed losses, mixing characteristics.

Secondary Flows

Assumed level and distribution (based on model test and some measurements).

Power Turbine

| | |
|---|---|
| Inlet | - Mixer frame exit conditions, secondary flows |
| Exit | - From total pressure and temperature rakes |

| | |
|---|---|
| Power | - From airflow, delta temperature |
| Efficiency | - From delta temperature and delta pressure. |

Core Nozzle

| | |
|---|---|
| Inlet | - PT (power turbine) exit conditions |
| Exit | - Ambient conditions. |

Thrust

| | |
|---|---|
| Installed | - Measured |
| Core component | - From PT exit conditions, nozzle coefficients |
| Uninstalled | - From installed thrust, assumed drags |
| UDF™ component | - From uninstalled thrust and core thrust. |

## 7.3 COMPARISON OF PRETEST PREDICTIONS AND REDUCED TEST DATA

The steady-state data points used for the performance evaluation were restricted to the down power calibration and maximum power points recorded on July 1 and July 3, 1986. Data points taken for UDF™ mapping EPR (engine pressure ratio) power hooks were recorded on July 1, 1986. The pretest prediction used to compare the test data is the Status D5C cycle. The Status D5C cycle was expressly defined for Build 3, and it includes the following major items:

- PT derates on efficiency due to open clearances and the blade damper pins
- PT flow function adjustments for open clearances and the blade damper pins
- Revised exhaust nozzle characteristics as a result of new nozzle hardware.

Core Performance - Figure 7-2 shows the overall core (F404) temperature ratio versus pressure ratio. Note that the core performance is approximately as predicted at takeoff power conditions and is better than predicted at lower powers (70% takeoff and below). Figure 7-3 presents IPC stall margin versus corrected flow, illustrating that the IPC operating line was approximately as predicted.

Power Turbine Performance - Figure 7-4 shows the PT flow function versus the PT energy function. The PT flow function was within 0.5% of the predicted value at higher powers (80% takeoff and above). Figure 7-5 illustrates the PT

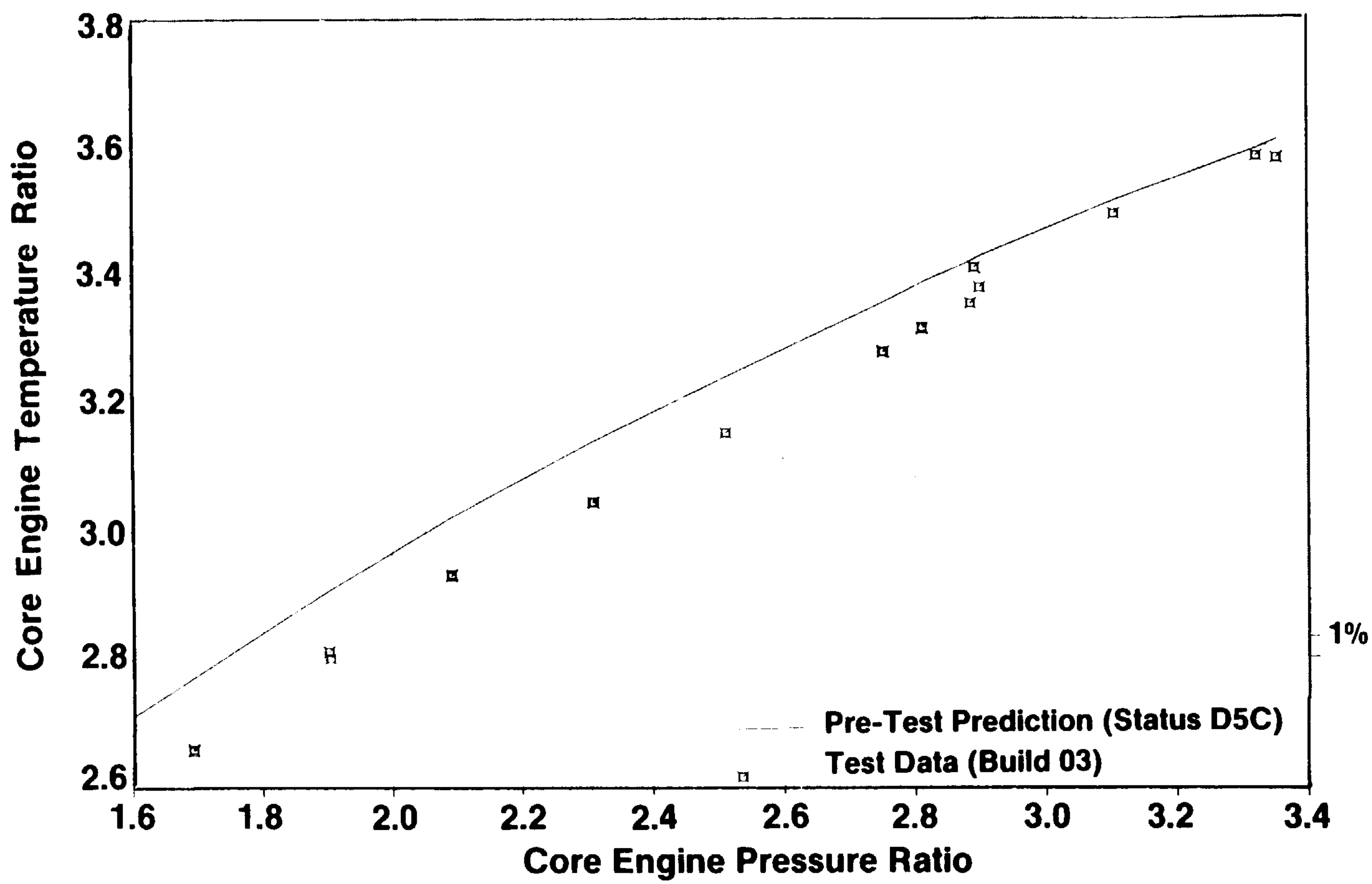


Figure 7-2. Core Engine Temperature Ratio Versus Pressure Ratio.

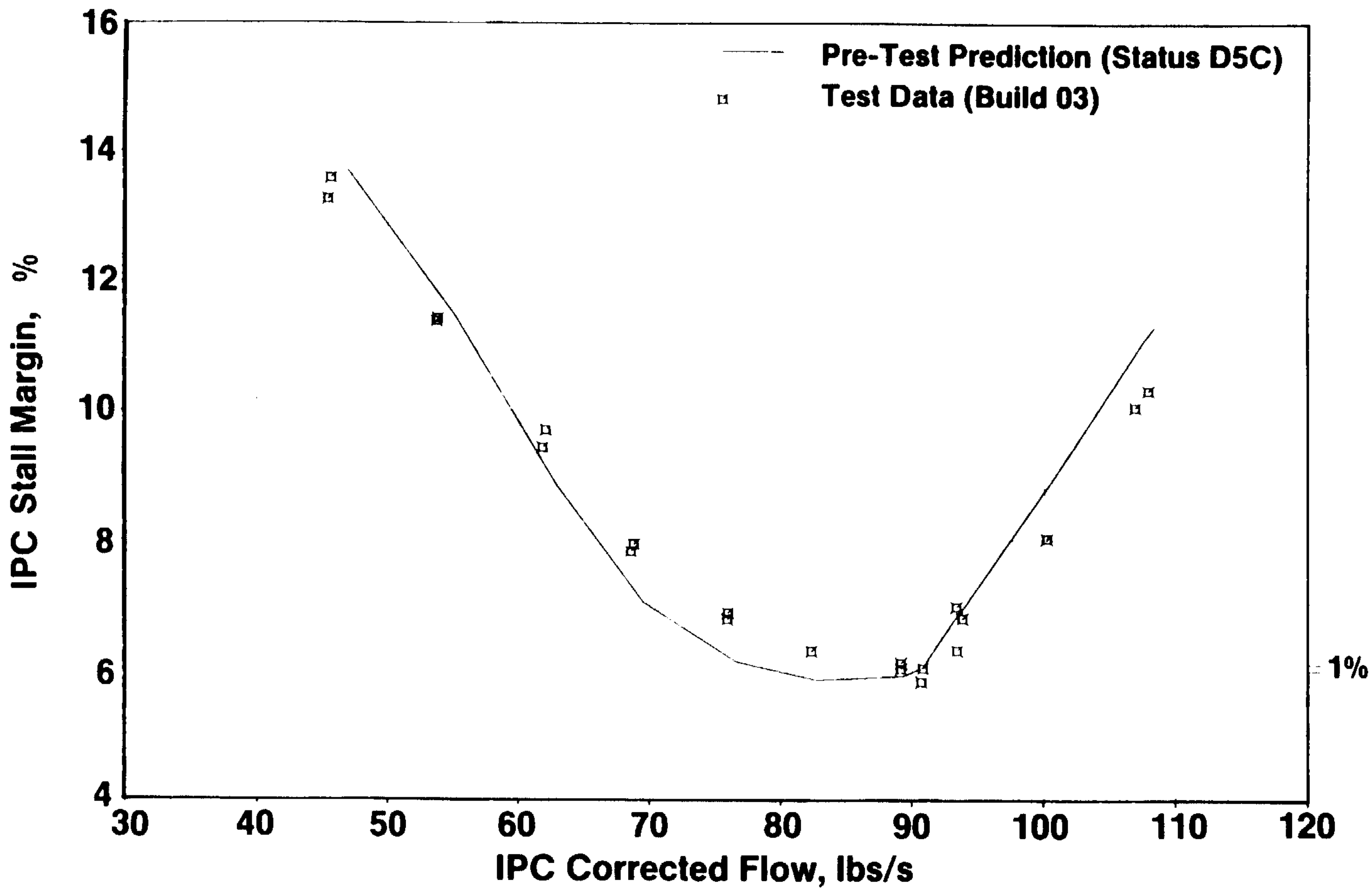


Figure 7-3. IPC Stall Margin Versus IPC Corrected Flow.

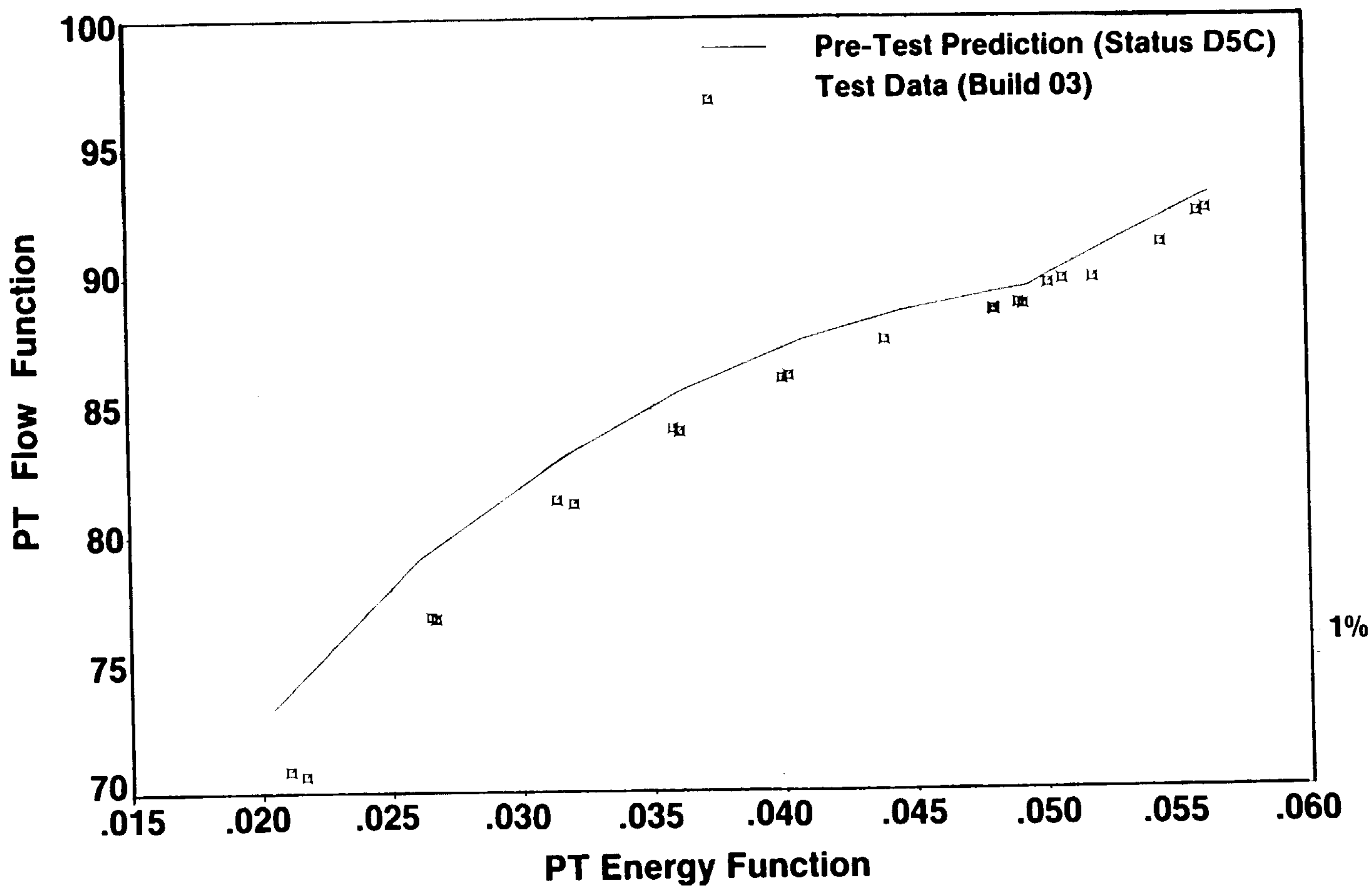


Figure 7-4. Power Turbine Flow Function Versus Energy Function.

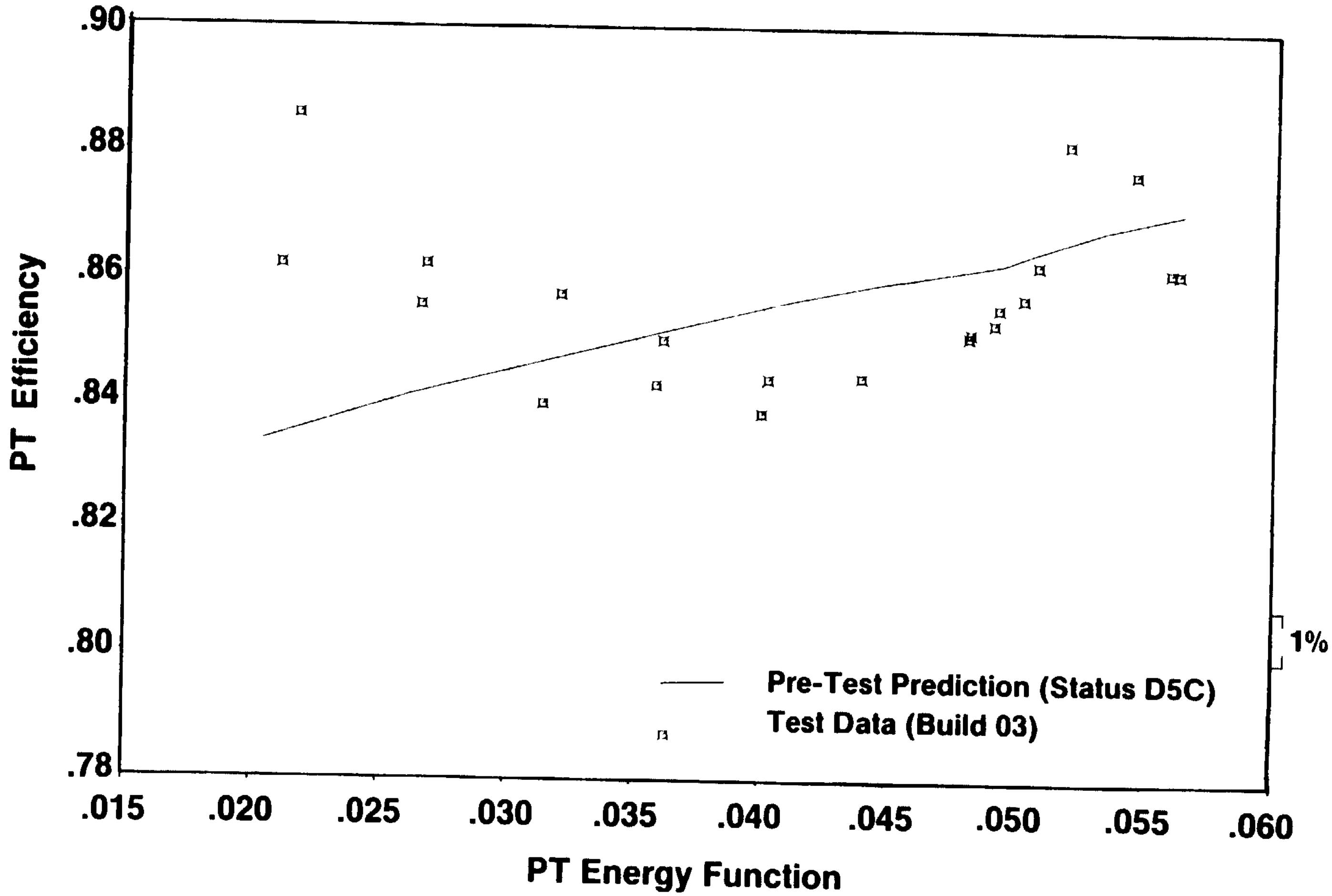


Figure 7-5. Power Turbine Efficiency Versus Energy Function.

efficiency versus PT energy function. The efficiency was within +1.5% of the predicted value and within the scatter range observed in LP turbines of large turbofan engines.

UDF™ Performance - Figure 7-6 depicts the UDF™ thrust coefficient versus power coefficient. Note that the test data describe a shallower slope than predicted. Thrust coefficient is approximately 4% worse than predicted at a power coefficient of 1.95 (takeoff condition), nearly as predicted at power coefficient of 1.70 (92% takeoff), and approximately 4% better than predicted at power coefficient of around 1.32, which covers a range of power from 30% to 80% takeoff thrust. Figures 7-7 and 7-8 compare predicted versus actual UDF™ rotor blade pitch angles for front and rear rotors, respectively.

Overall Performance - Figure 7-9 shows corrected installed specific fuel consumption (SFCI1R) versus corrected installed thrust (FNI1QA). The SFCI1R can be seen to be approximately 4% poorer than predicted at takeoff power. At 92% takeoff thrust the SFCI1R is about as predicted; whereas, at 80% takeoff thrust and below, SFCI1R is 4% to 6% better than predicted. Most of the discrepancy between actual and predicted performance is due to the characteristic exhibited by the UDF™, as discussed above under "UDF™ Performance." Magnitude of overall improvement in excess of that expected from the UDF™ performance at 70% takeoff thrust and below is due to the core engine performance being better than predicted, as discussed in "Core Performance."

Nozzle Performance - Between Builds 1 and 2, a redesigned stationary exhaust nozzle (centerbody) was installed on the engine. The original plug was analytically predicted to have flow separation at cruise conditions. The plug was redesigned so that no flow separation would occur at any flight condition. Figure 7-10 compares the original and redesigned plug lines. Scale models were made of both the original and redesigned plugs, and then tested. Figure 7-11 makes a comparison of the separation parameter ($F_{sep}$) for the two plugs at cruise conditions, illustrating that the new plug lines would keep $F_{sep}$ below potential separation conditions. Figure 7-12 shows a comparison between predicted and actual engine test data for both plugs to demonstrate good match between prediction and data. Figure 7-13 presents a comparison between predicted and engine test nozzle flow coefficient versus core engine pressure ratio (P46Q2). Note that at P46Q2 of 2.9 and below (approximately

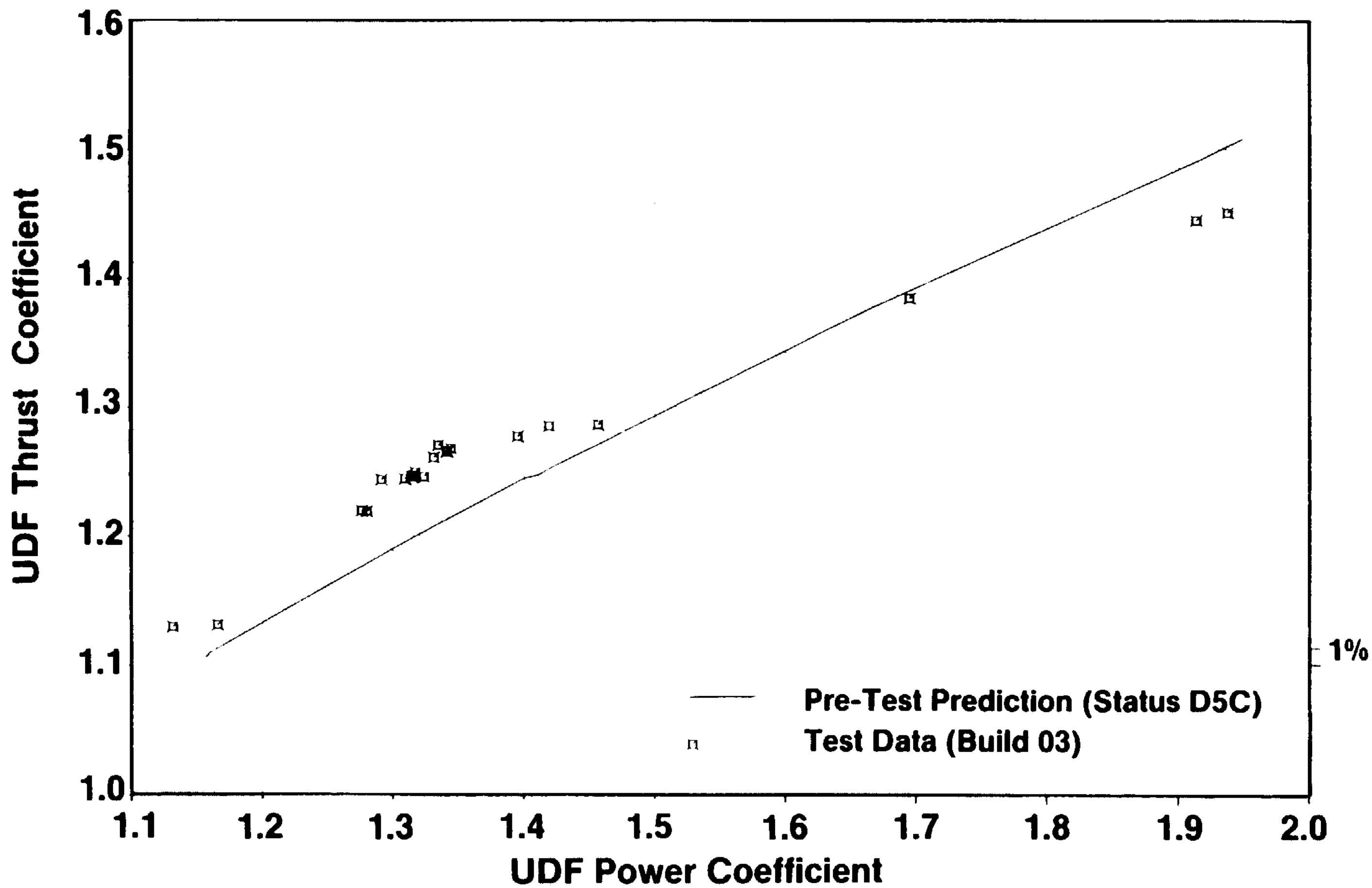


Figure 7-6. UDF™ Thrust Coefficient Versus Power Coefficient.

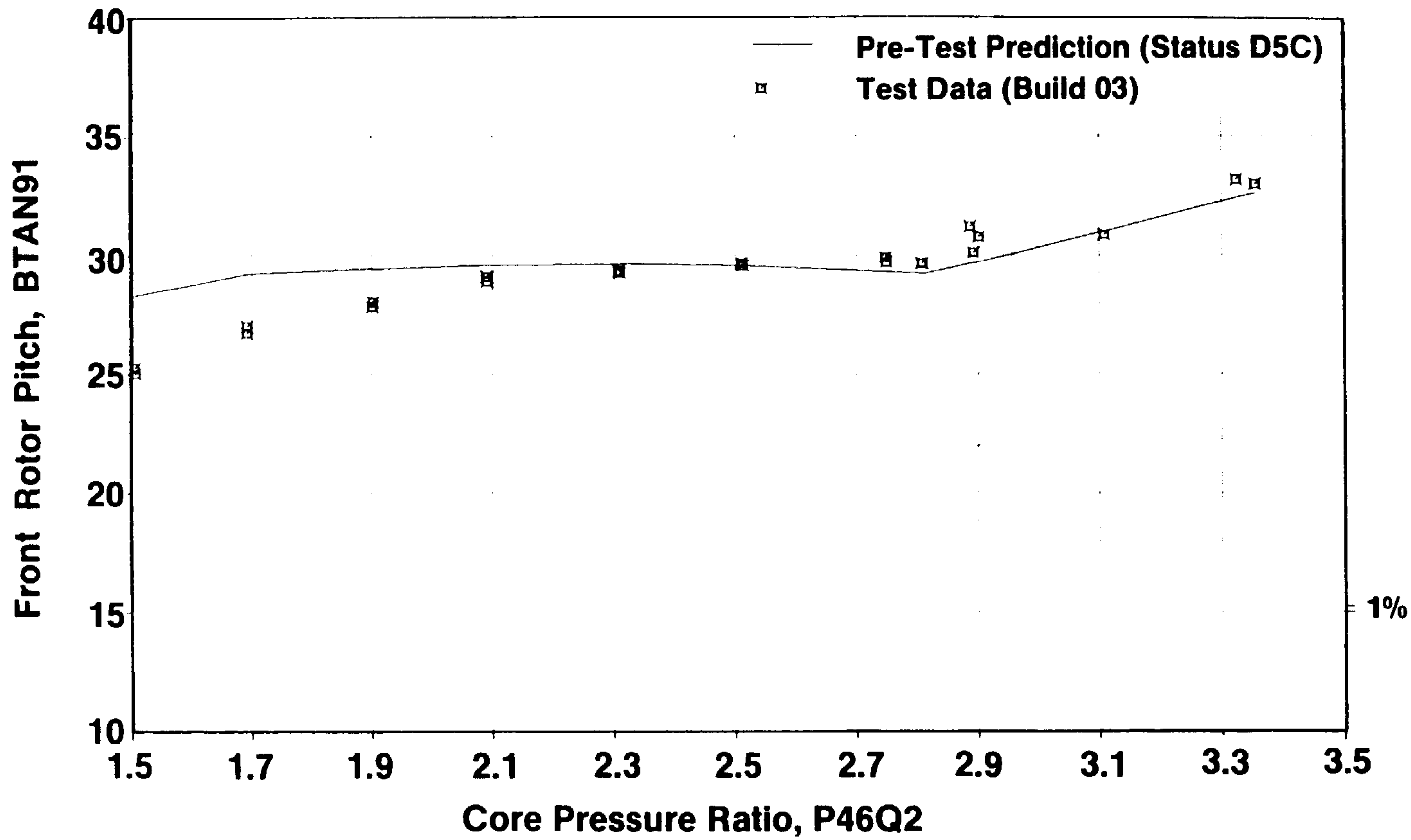


Figure 7-7. Front Rotor Blade Angle Versus Core Engine Pressure Ratio.

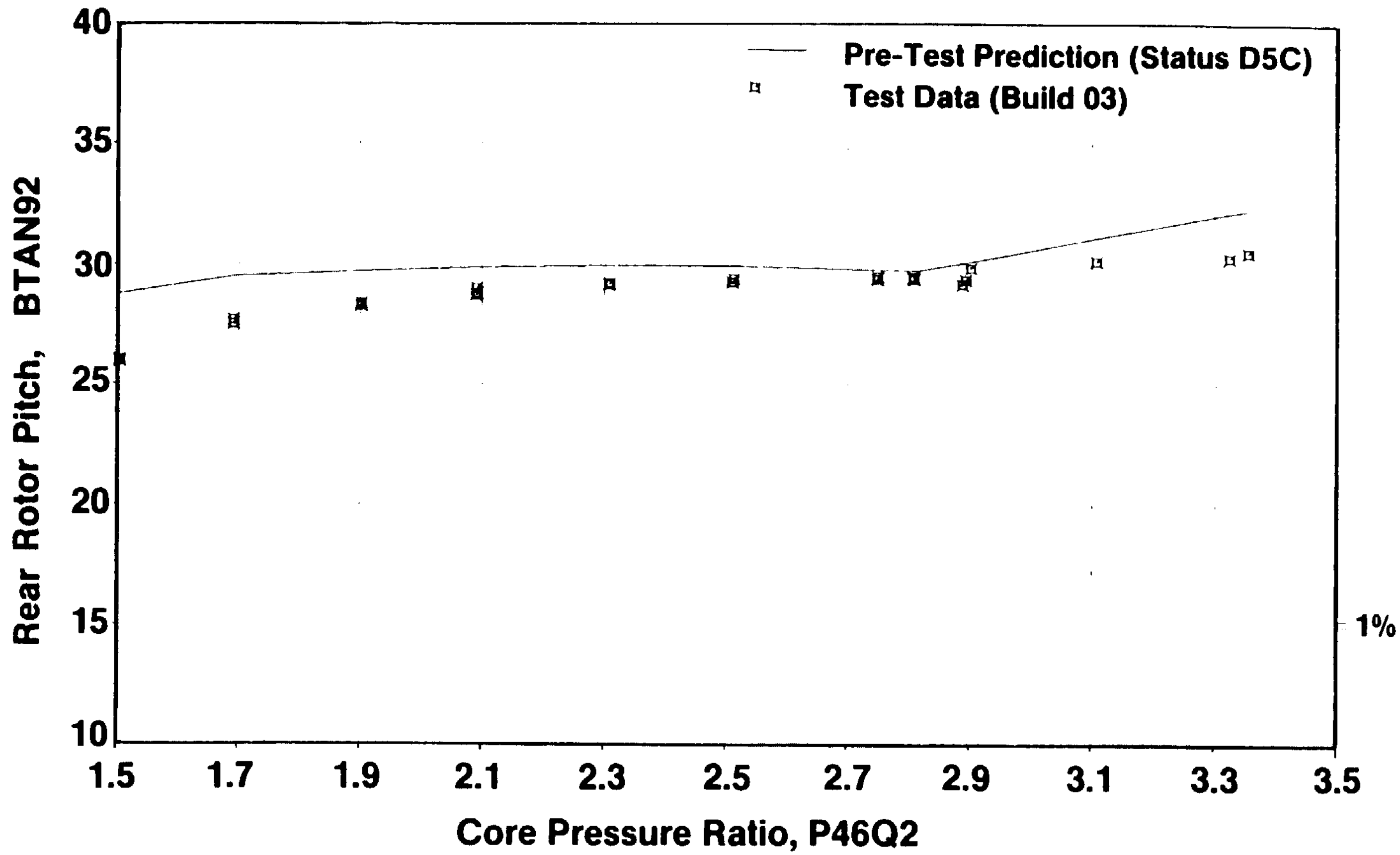


Figure 7-8. Rear Rotor Blade Angle Versus Core Engine Pressure Ratio.

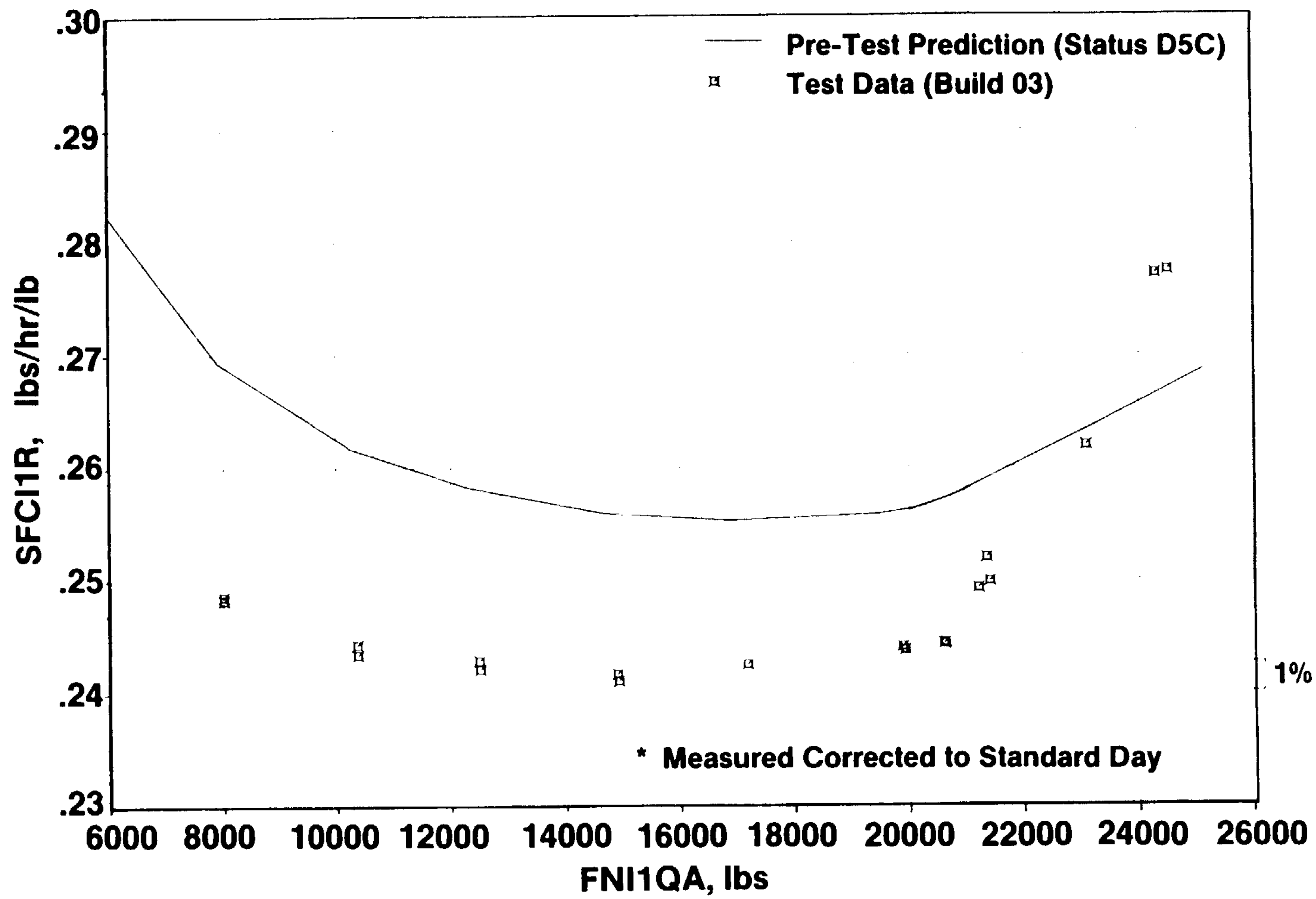


Figure 7-9. Corrected SFC Versus Corrected Thrust.

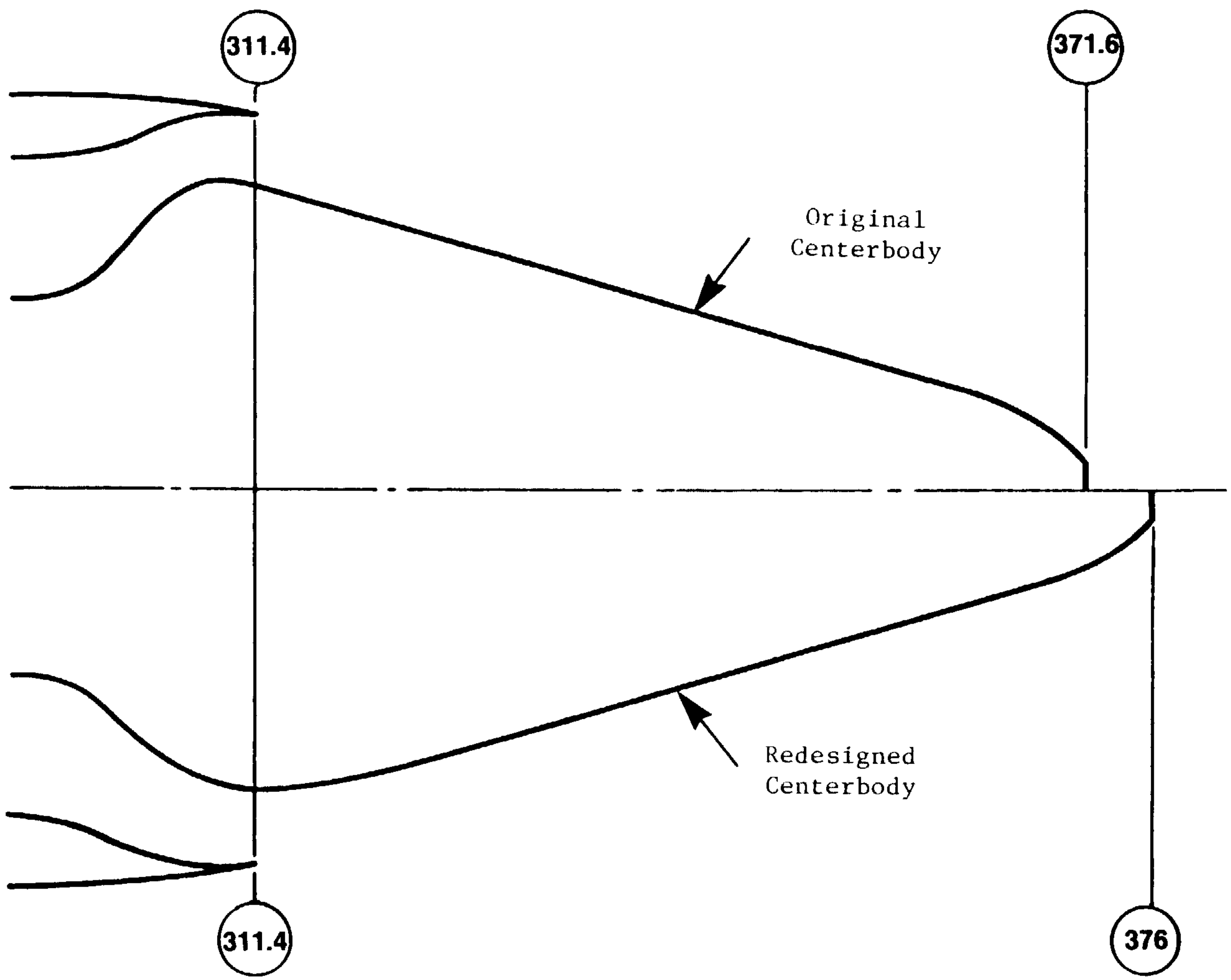


Figure 7-10. UDF™ Engine - Redesigned Centerbody.

Cruise Condition $M = .72$, 35K, $PT8/P_0 = 1.4$

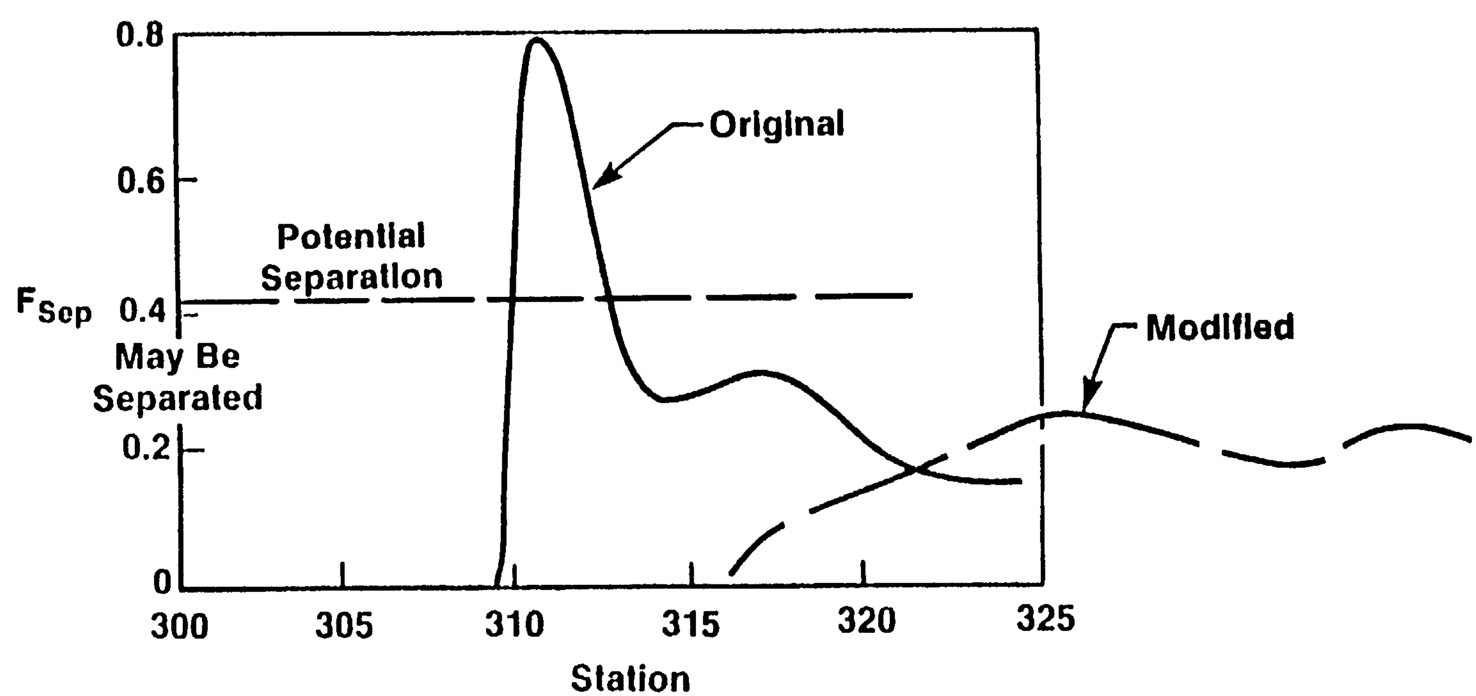


Figure 7-11. UDF™ Engine Centerbody Separation Parameter.

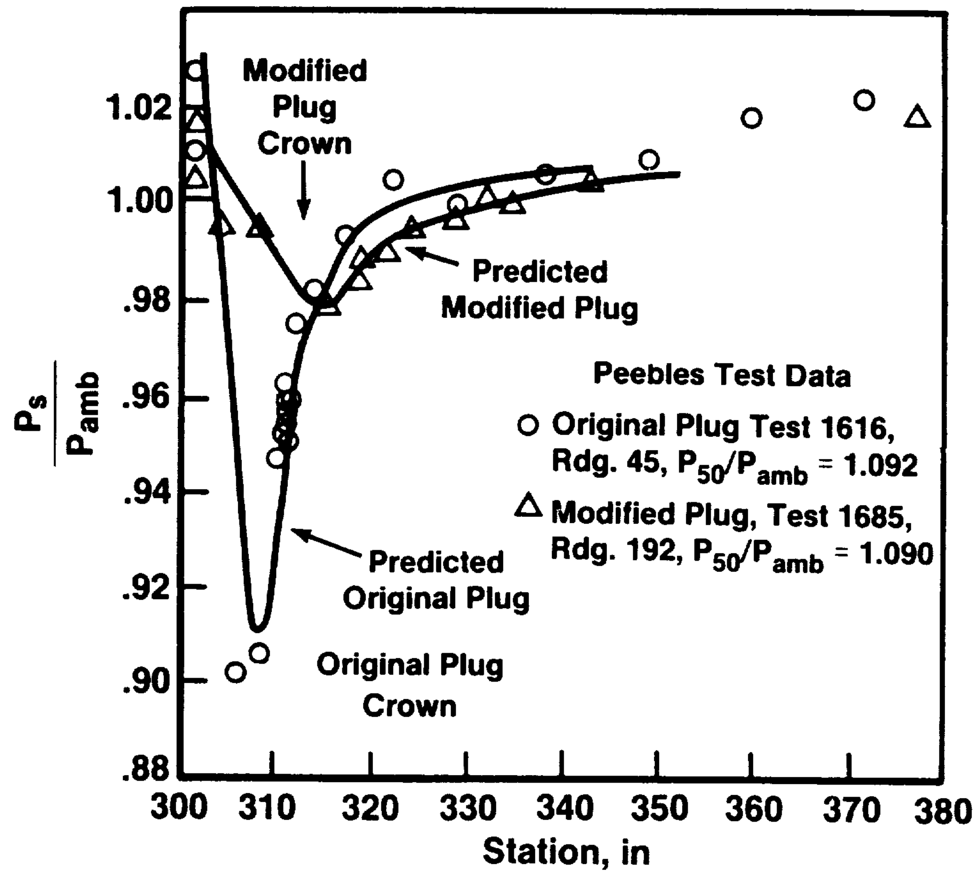


Figure 7-12. UDF™ Engine - Core Plug Static Pressures.

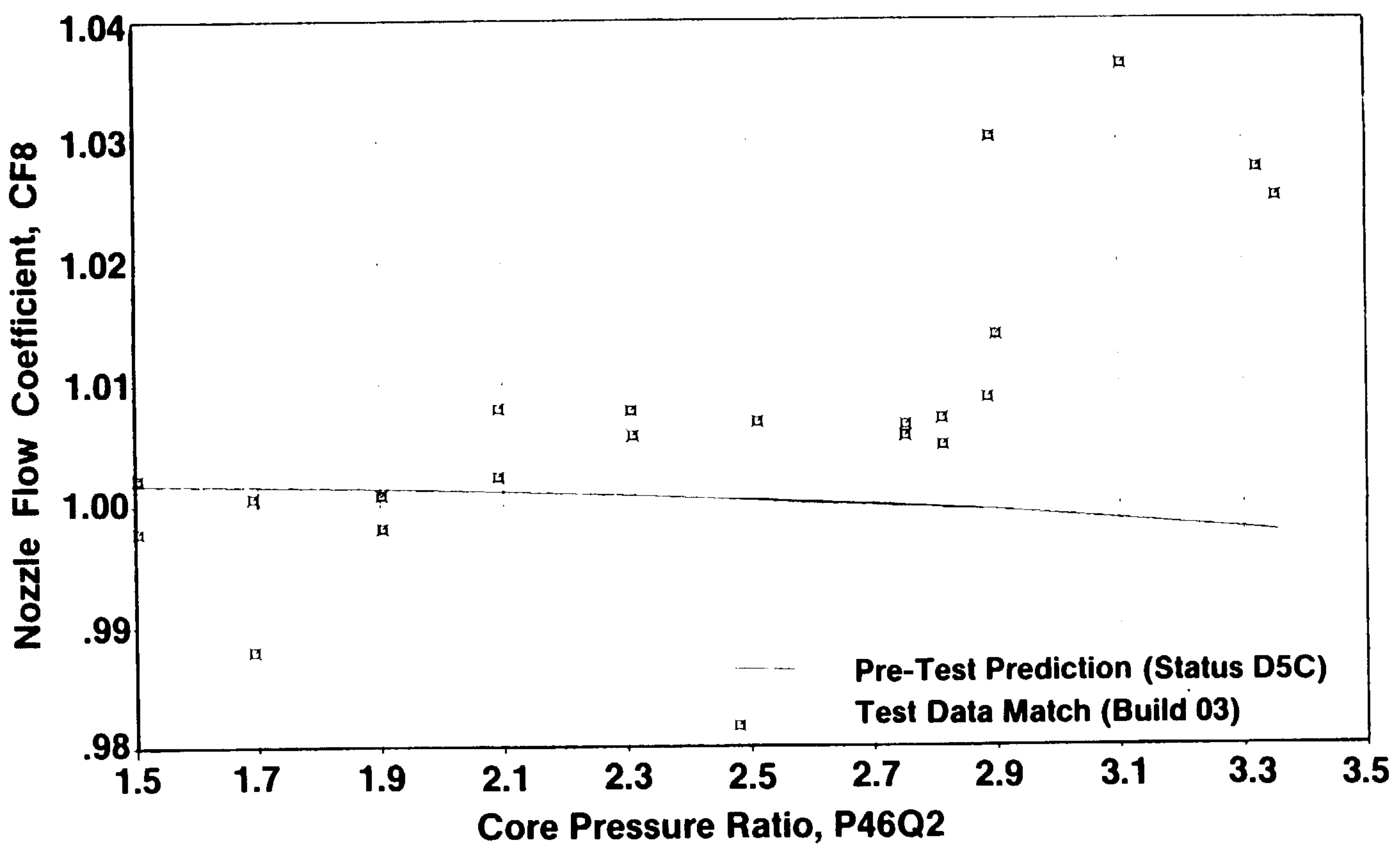


Figure 7-13. Nozzle Flow Coefficient Versus Core Engine Pressure Ratio.

80% takeoff thrust and below) the calculated flow coefficient is within +1% of the prediction. However, at takeoff power there is a discrepancy of about 3%. This is probably due to the fact that the flow coefficient is sensitive to the UDF™ exit pressure which was not a measured parameter, but rather, the value being assumed from the performance maps. This discrepancy is not a concern, since 3% change in flow coefficient changes sfc at thrust by only 0.005%.

EPR Hooks - These test points were run to map UDF™ performance at off-schedule speeds. The test was conducted at six different propulsor rotational speeds where the propulsor speed would be held constant, and core power level would be varied by demanding various EPR levels; hence, EPR hooks.

Figure 7-14 shows installed corrected specific fuel consumption (SFCI1R) versus installed corrected thrust (FNI1QA) for on-speed schedule and constant propulsor speed pretest prediction, with Figure 7-15 showing the equivalent reduced test data. Note that the on-speed schedule lines on both figures are the same as those found in Figure 7-9. The test further proved that the UDF™ characteristics were different than predicted, with significantly higher speed sensitivity than prediction.

## 7.4 LCF CYCLIC TESTING AND RESULTANT DETERIORATION

The LCF testing involved running the engine through a power cycle as is illustrated in Figure 3-54; a total of 100 complete cycles were run. In the following comparisons, a sample of early data is compared with a sample of late data in order to quantify the magnitude of scatter as well as the magnitude and source of deterioration. Figure 7-16 shows that the wind conditions were relatively consistent, and all data points, except one, were within the prescribed performance testing wind envelope.

Figure 7-17 shows that at corrected installed thrust, corrected installed specific fuel consumption deteriorated by approximately 0.040%.

Figure 7-18 demonstrates that at EPR, corrected installed thrust followed the predicted trends and showed no signs of degradation. This indicates that the power extraction at EPR by the LP turbine and the thrust produced by the UDF™ for LP turbine power remained unchanged during the tests. Figure 7-19

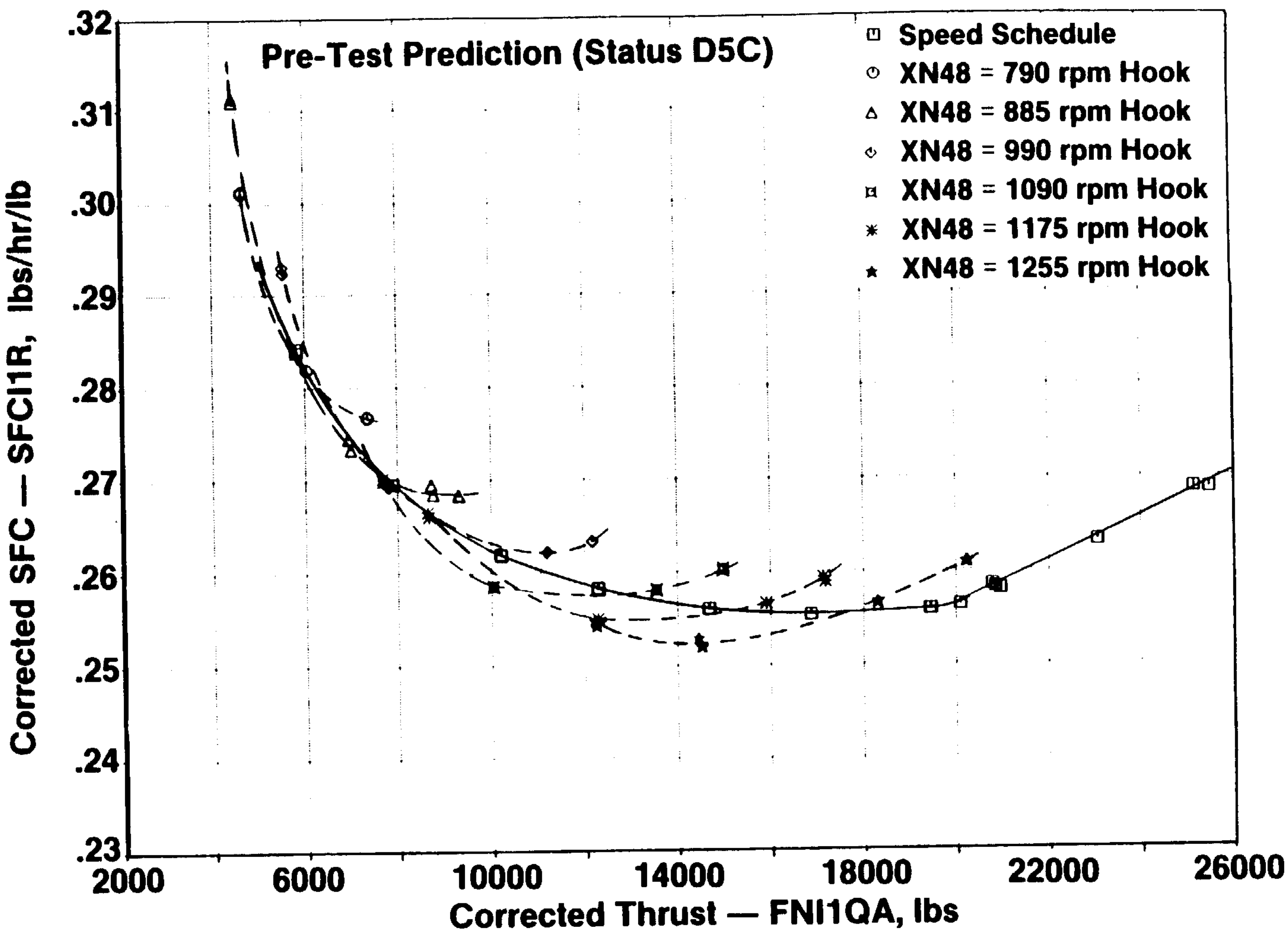


Figure 7-14. Corrected SFC Versus Corrected EPR Power Hook Evaluation.

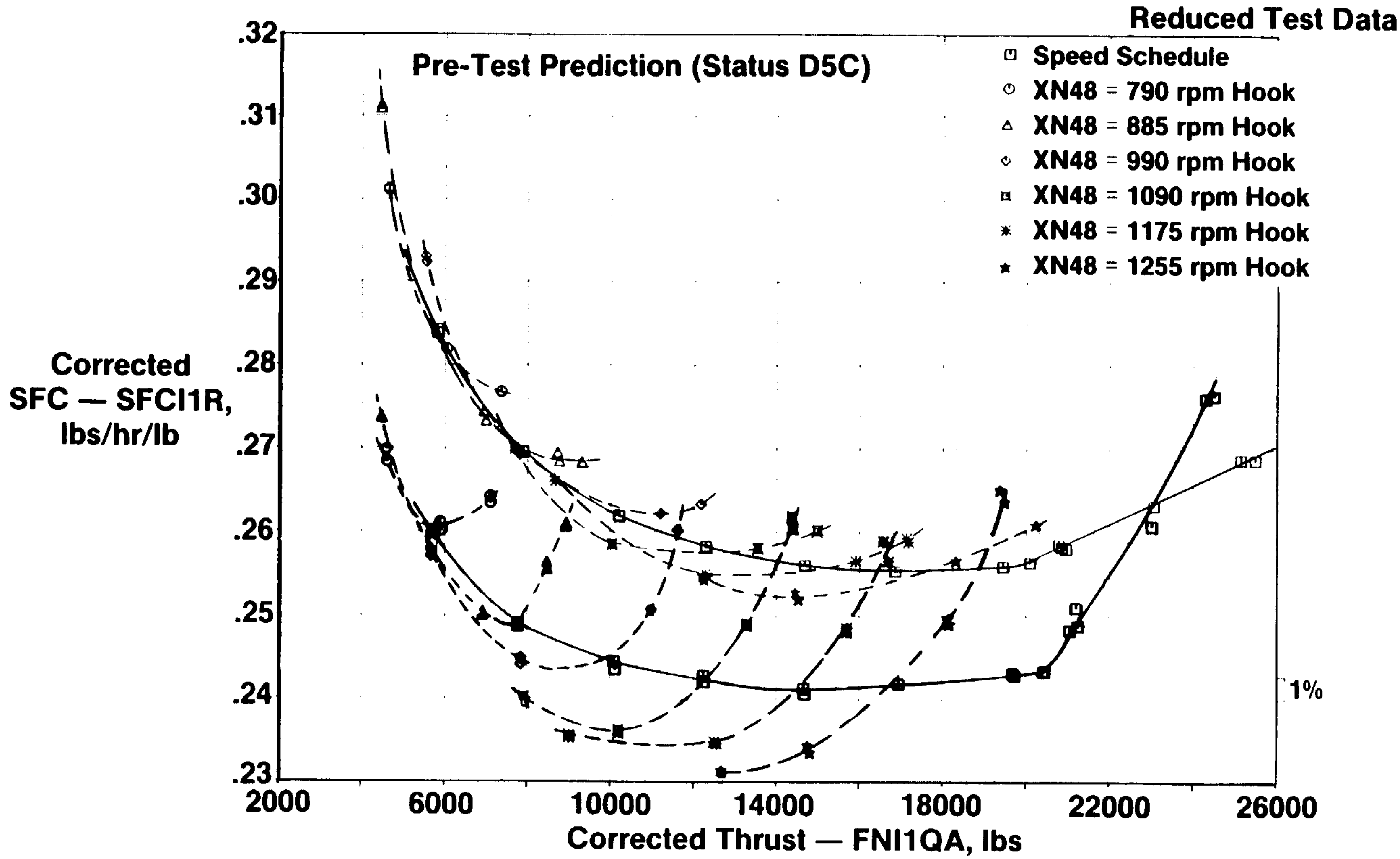


Figure 7-15. Corrected SFC Versus Corrected EPR Power Hook Evaluation.

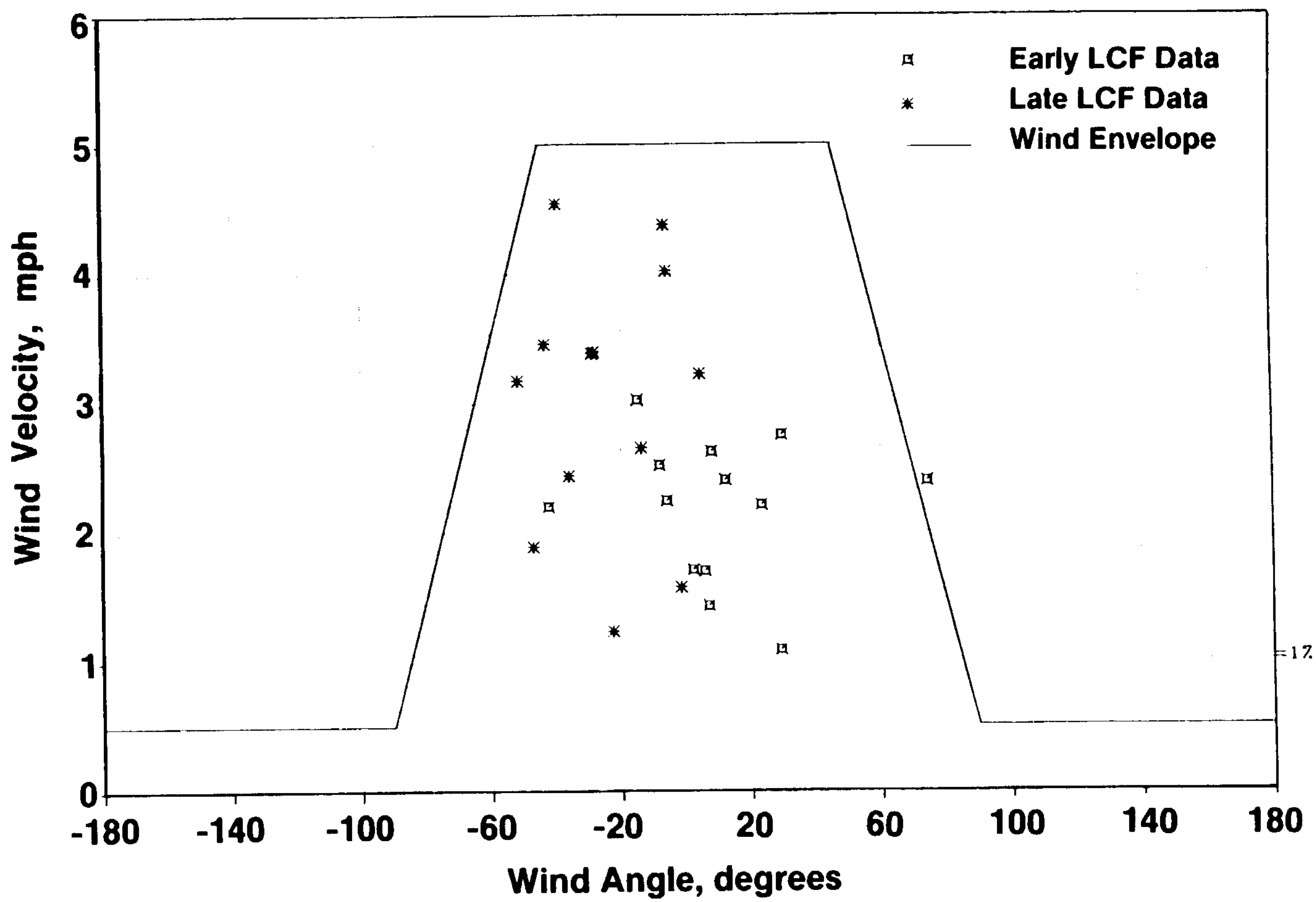


Figure 7-16. Wind Velocity Versus Wind Angle.

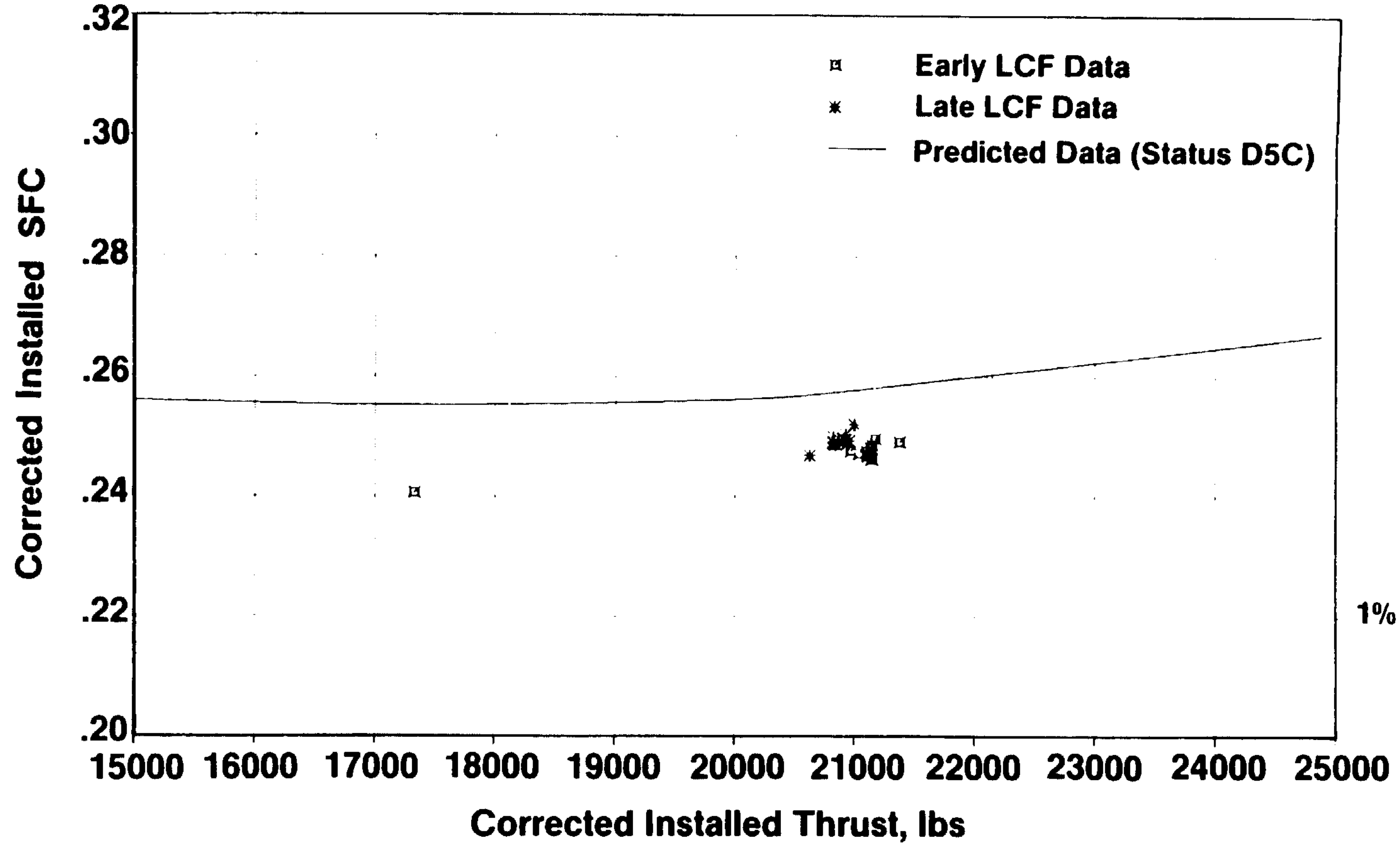


Figure 7-17. Corrected SFC Versus Corrected Thrust.

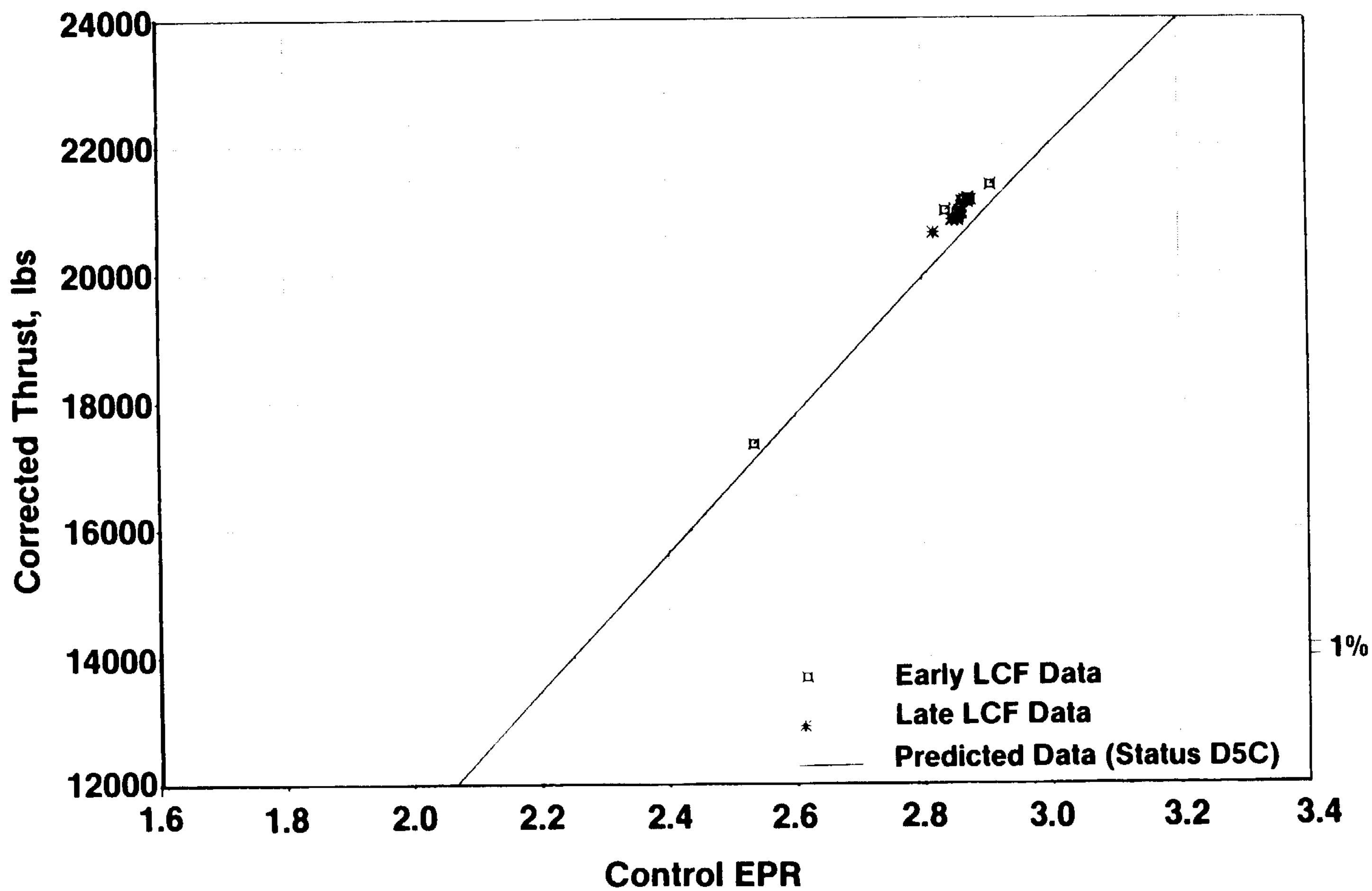


Figure 7-18. Corrected Thrust Versus Corrected Pressure Ratio.

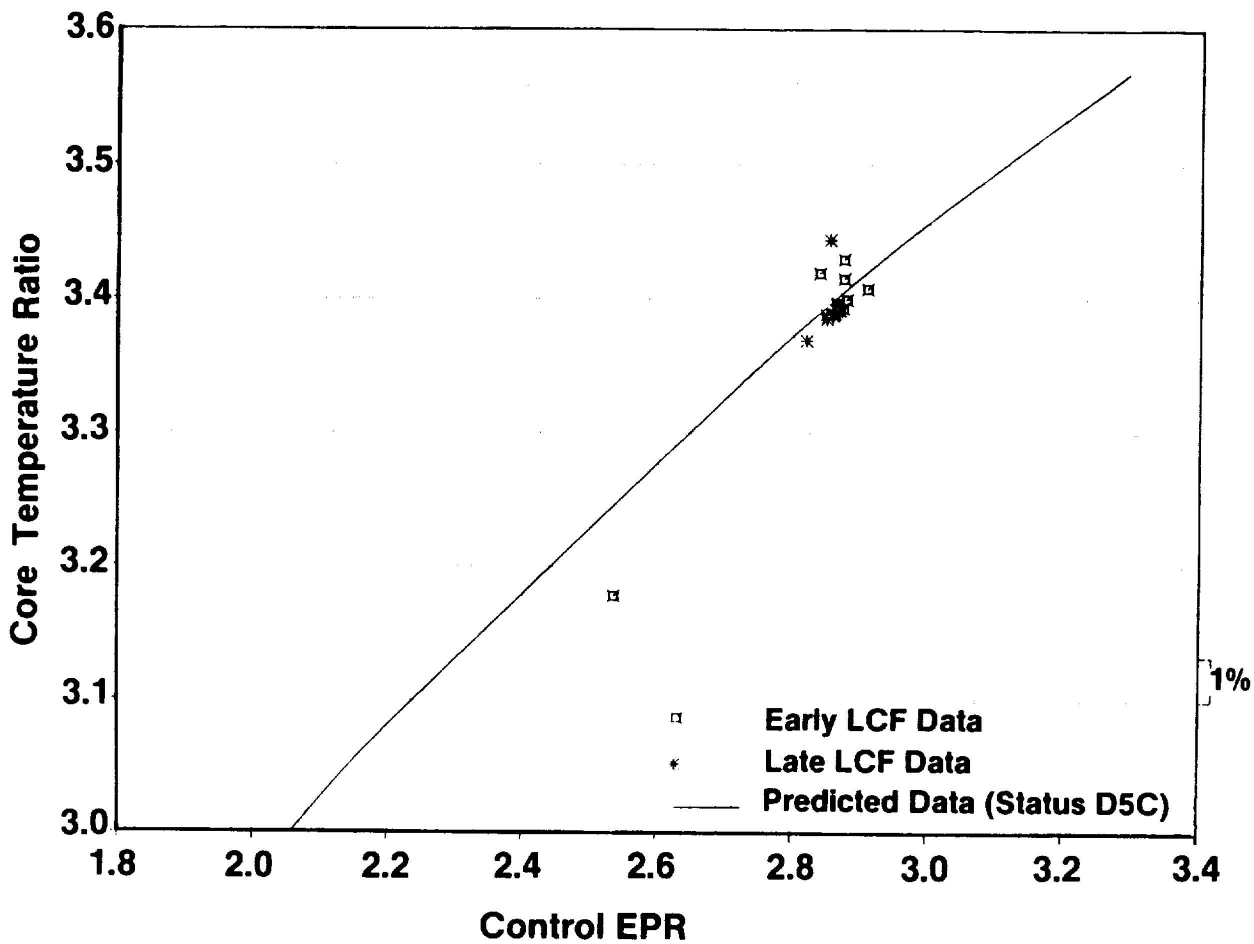


Figure 7-19. Core Temperature Ratio Versus Control Pressure Ratio.

reveals that at EPR, core engine temperature ratio was essentially unchanged, and the core showed little or no signs of deterioration.

Figure 7-20 illustrates that at EPR, intermediate power compressor (IPC) efficiency was down 0.60 points during the latter part of the test compared to the early part of the test. However, Figure 7-21 shows that at EPR, IPC flow follows the predicted trends, confirming that inlet flow and core engine power output remained consistent. This implies a dirty IPC, which is further substantiated by Figure 7-22 indicating that the flow versus speed characteristic of the IPC deteriorated, with approximately 0.50% drop in corrected IPC flow at corrected IPC speed.

In general, there was no evidence of mechanical deterioration, with performance degradation due mainly to a dirty intermediate power compressor.

## 7.5 DEFINITION OF PREFLIGHT TEST CYCLE

The base cycle used for Build 3 pretest predictions was the Status D5C cycle. Listed below are the changes made to the Status D5C cycle to define the preflight test cycle; this being the Status D8B cycle:

- Modify IPC flow-speed characteristics
- Modify IPC efficiency characteristics
- Modify HPC flow-speed characteristics
- Modify HPC efficiency characteristics
- Revise bypass duct losses and effective area
- Scale IPT efficiency
- Modify LPT efficiency characteristics
- Modify LPT flow function characteristics
- Modify UDF™ thrust coefficient characteristics at Mach No. = 0.00, no change at Mach No. ≧ 0.20
- Use NASA MPS test-derived UDF™ maps for Mach number ≧ 0.67
- Extra cooling air scoops for telemetry system modeled.

## 7.6 COMPARISON BETWEEN GROUND PRETEST CYCLES AND REDUCED TEST DATA

The following comparisons between the ground pretest cycle (Status D5C), flight pretest cycle (Status D8B), and reduced test data are made to compare



C-3

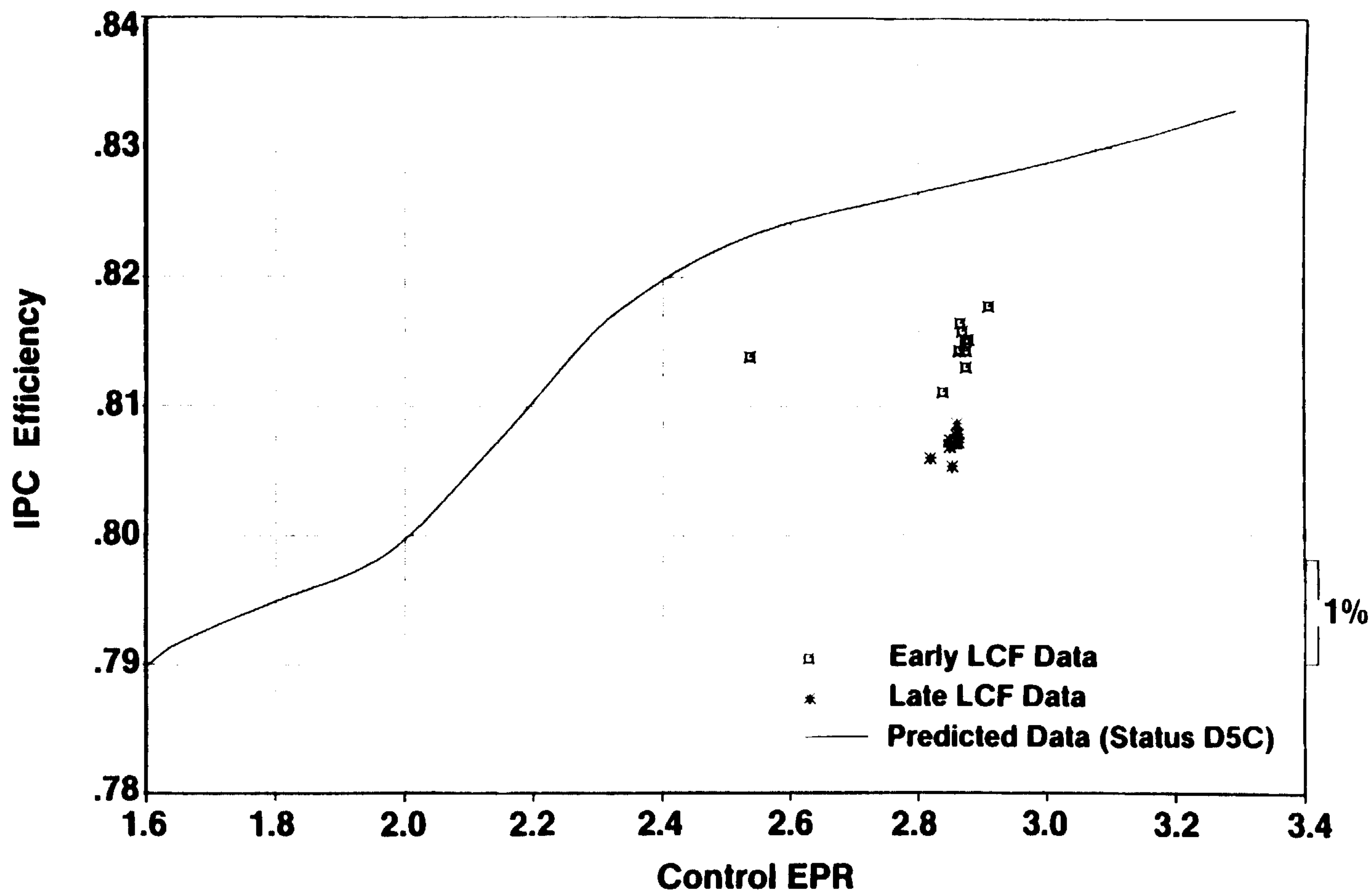


Figure 7-20. IPC Efficiency Versus Control Pressure Ratio.

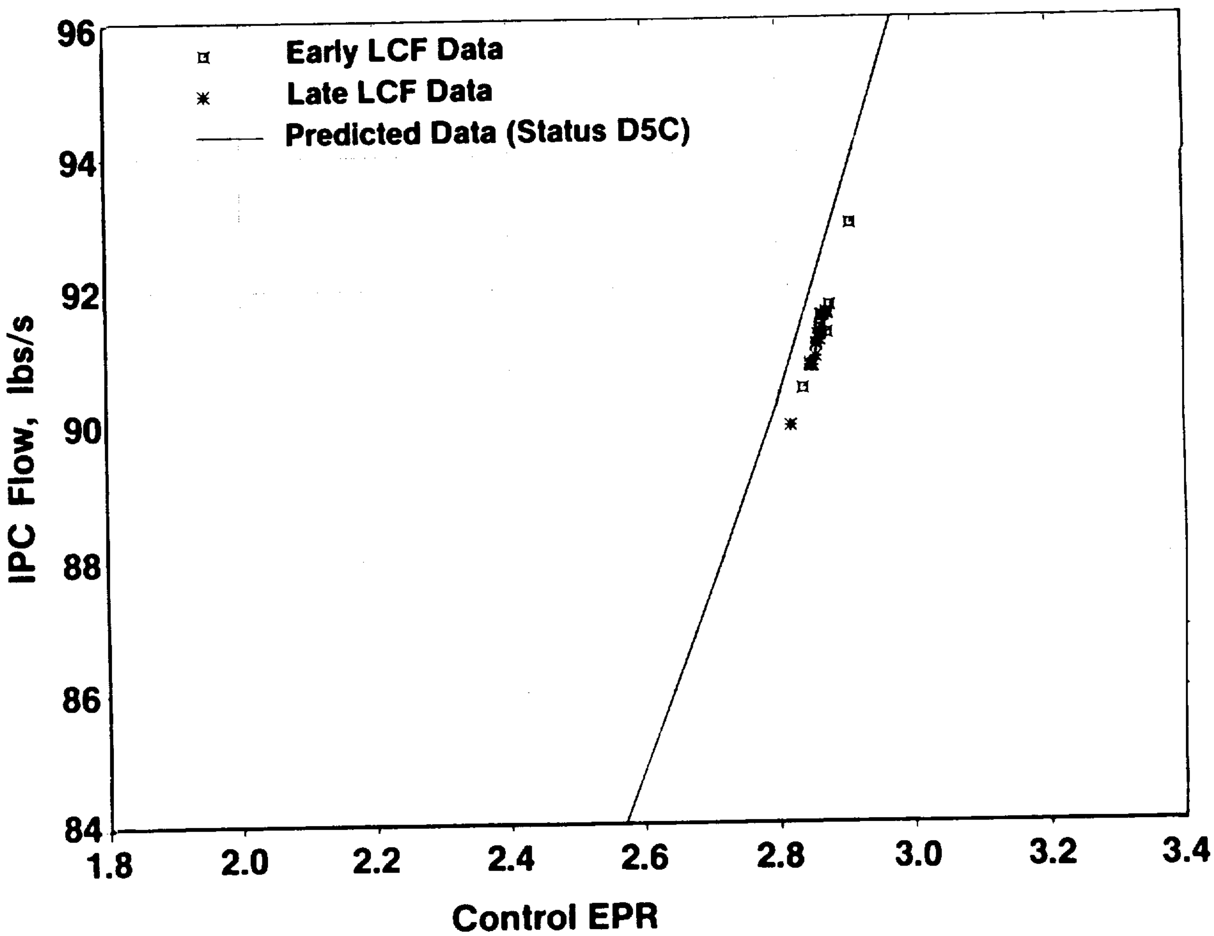


Figure 7-21. IPC Flow Versus Control Pressure Ratio.

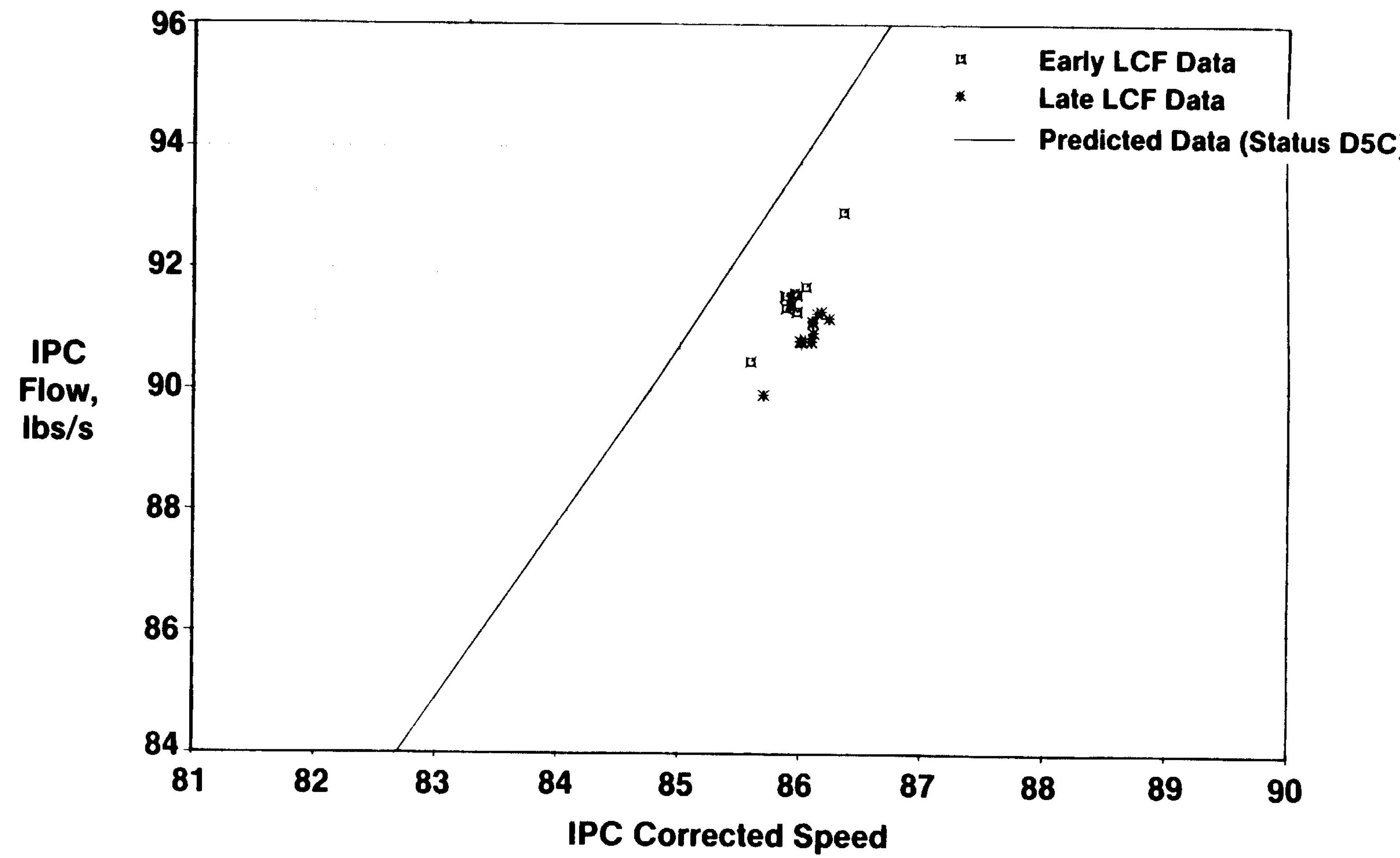


Figure 7-22. IPC Flow Versus IPC Corrected Speed.

the starting status, ending status, and data used to define the ending status against each other.

Figure 7-23 shows the core temperature ratio versus core pressure ratio. Figure 7-24 illustrates LPT flow function versus LPT energy function. Figure 7-25 demonstrates IPC stall margin versus IPC corrected flow. Figure 7-26 is a comparison of UDF™ thrust coefficient versus UDF™ power coefficient. Figure 7-27 depicts the overall performance, corrected installed sfc versus corrected installed thrust. Note that in all of the above comparisons, the Status D8B cycle more closely matches the test data than did the Status D5C cycle.

## 7.7 PERFORMANCE SUMMARY

In the testing of the UDF™ engine at Peebles, the following performance and capabilities were demonstrated:

Performance

- 25,000 lbf installed corrected thrust
- 0.232 lb/hr/lbf installed corrected specific fuel consumption
- 15,000+ physical total shaft horsepower.

Capabilities

- Running at full power statically
- Data was repeatable statically
- Prediction of low speed, low pressure, counterrotating turbine performance with an accuracy comparable to that of high speed, conventional, low pressure turbines.

Comparing data recorded early and late in the LCF testing, performance deterioration was confined to a dirty IPC; there was no evidence of mechanical deterioration.

## 7.8 KEY RESULTS

The F404 gas generator provided repeatable and predictable performance and was better than predicted at lower powers (below 70% takeoff power).

UDF™ blade performance sensitivity to rotational speed was much greater than predicted.

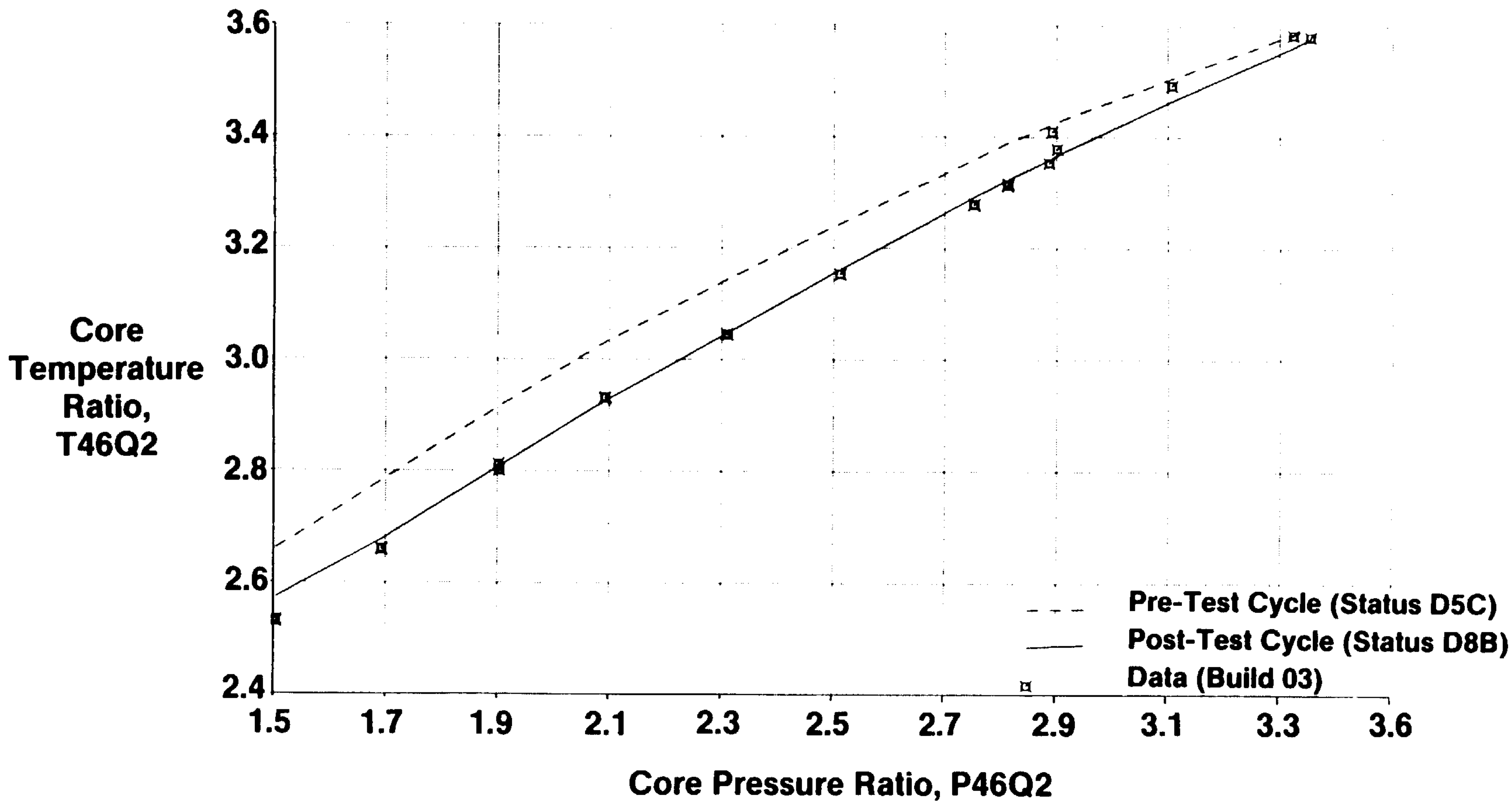


Figure 7-23. Compare Pretest Cycle Versus Posttest Cycle Versus Test Data.

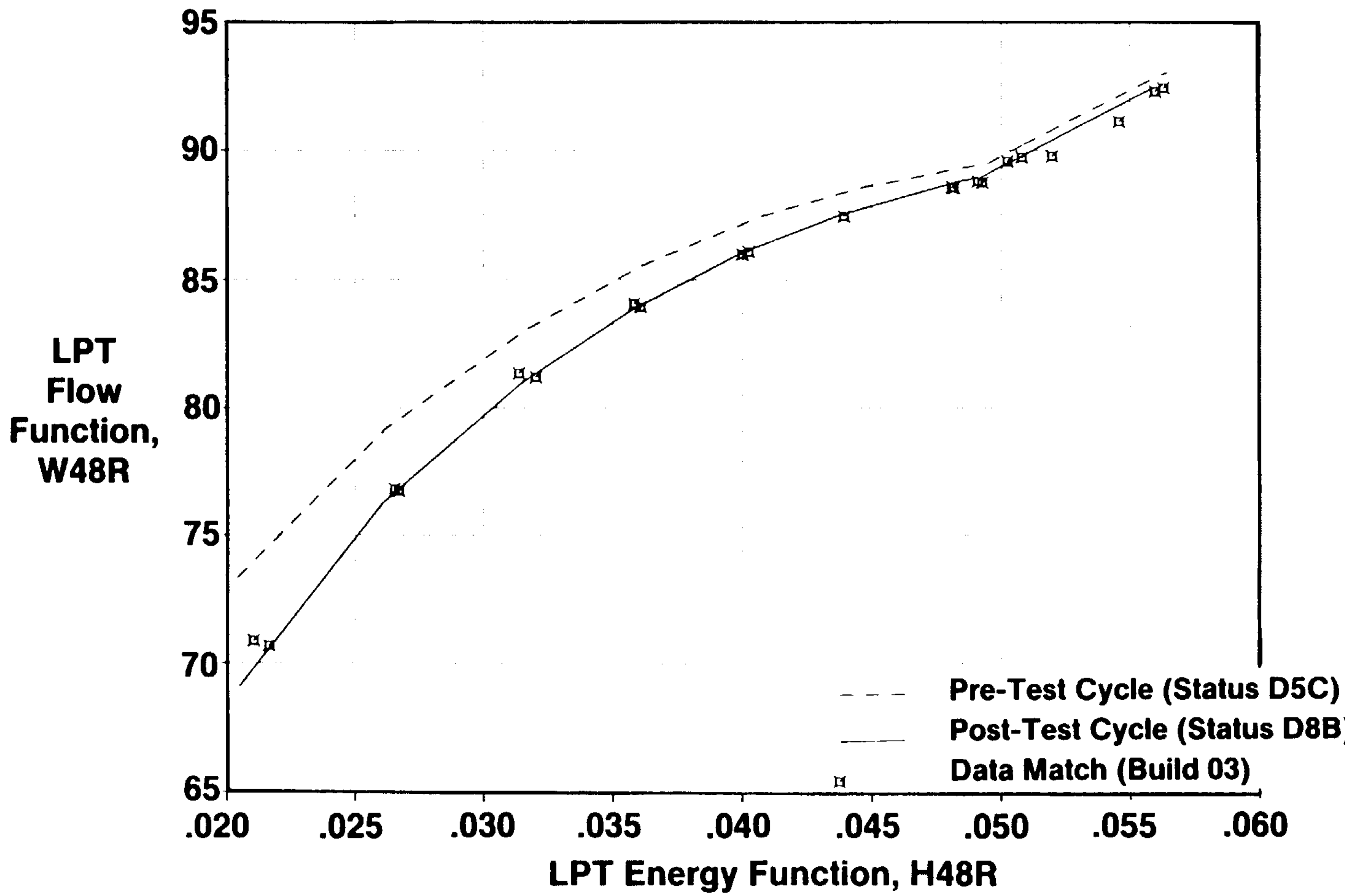


Figure 7-24. Compare Pretest Cycle Versus Posttest Cycle Versus Test Data.

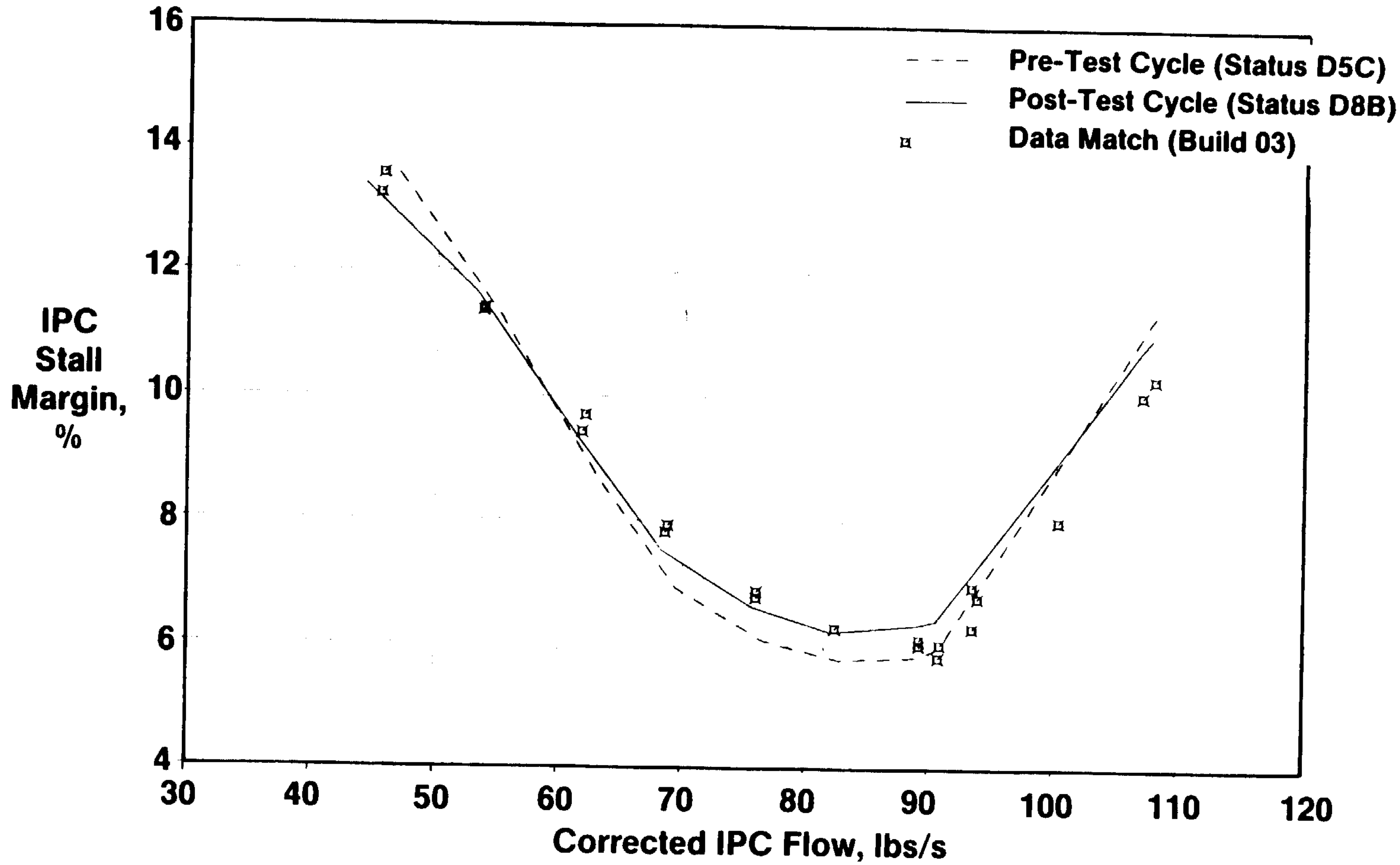


Figure 7-25. Compare Pretest Cycle Versus Posttest Cycle Versus Test Data.

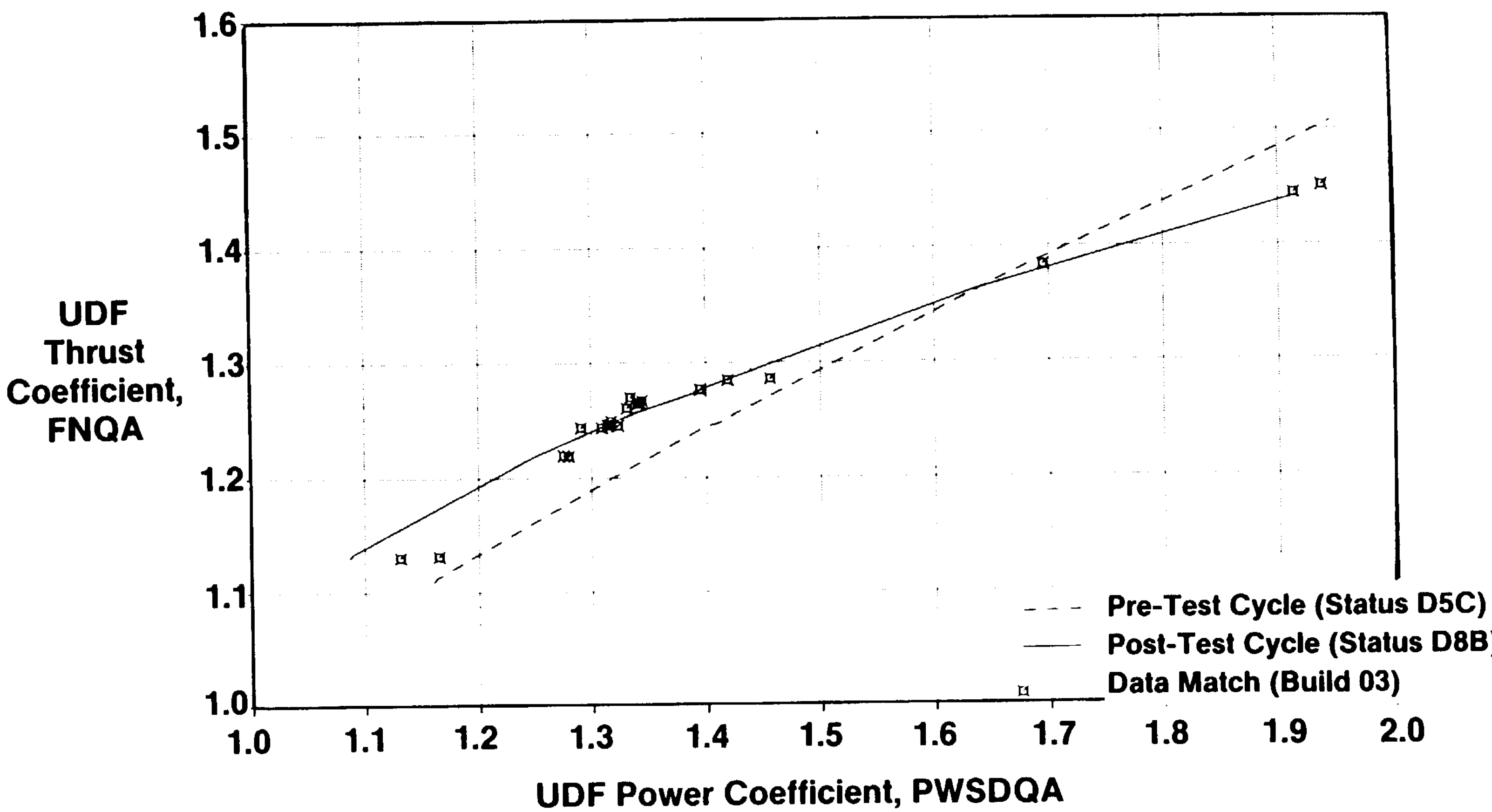


Figure 7-26. Compare Pretest Cycle Versus Posttest Cycle Versus Test Data.

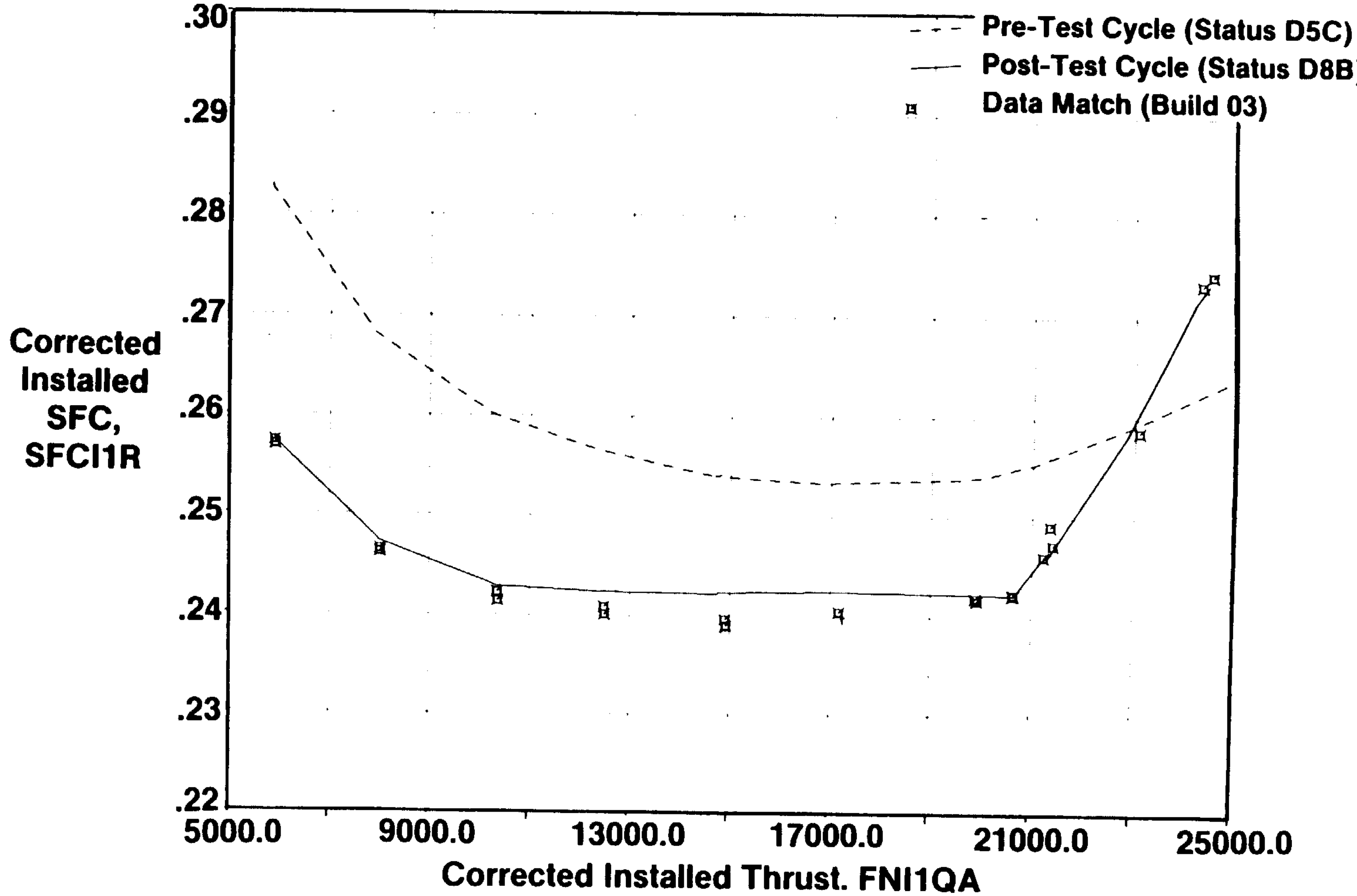


Figure 7-27. Compare Pretest Cycle Versus Posttest Cycle Versus Test Data.

At power coefficient = 1.32, thrust coefficient was 4% better than predicted (approximately 60% takeoff power). At power coefficient = 1.95, thrust coefficient was 4% worse than predicted (approximately 100% takeoff power).

Power turbine efficiency was approximately as predicted, being within +1.5 points over the major portion of the operating range. The flow function was within +0.5% of prediction at high powers (above 80% takeoff thrust).

Overall performance was better than predicted up to 92% takeoff power (23,000 lbf corrected installed thrust), but was poorer than predicted beyond 92% takeoff power (23,000 lbf corrected installed thrust) due to UDF™ speed sensitivity as noted above.

At 60% takeoff thrust (15,000 lbf), sfc was approximately 5.50% better than predicted. At 92% takeoff thrust (23,000 lbf), sfc was approximately as predicted. At 100% takeoff thrust (25,000 lbf), sfc was approximately 4.00% worse than predicted.

# 8.0 ENGINE OPERABILITY

The most important operability concern with the GE36 proof-of-concept engine is the stability of the IPC (F404 compressor). Replacing the F404 variable area exhaust nozzle with the GE36 UDF™ propulsor assembly reduced the Station 48 (F404 nozzle/UDF™ power turbine inlet) flow function by about 15%. This raises the IPC operating line (Figure 8-1) and reduces the stall margin. To help increase IPC stall margin and ensure stall-free operation of the IPC, two design modifications were incorporated:

- Variable Stator 1 and more closed IGV schedule (raises the IPC stall line)
- IPC bleed system (lowers the IPC operating line).

The GE36 proof-of-concept HPC has an adequate stability margin since the stall and operating lines are similar to those for the F404. Due to the more limited operating range and flight envelope encountered during GE36 ground and flight test, the stall margin requirements are lower.

## 8.1 IPC STALL MARGIN

Steady-state IPC operating lines at 2,750 ft/0Mn/+31° F and at 38,000 ft/0.80Mn/ISA, as predicted by the Status D6C cycle model, are shown in Figures 8-2 and 8-3. Also shown is the nominal IPC stall line and the, statistically, worst-case IPC stall line which includes analytical estimate of effects due to deterioration, inlet pressure distortion, and IPC tracking error. The nominal stall line shown in these figures is from the F404 green run results with the GE36 variable geometry schedule (Figures 8-1 and 8-4).

Transient cycle model predictions of IPC operating line migration during decel transients from maximum power with no IPC bleed and with maximum IPC bleed are included in Figures 8-2 and 8-3. These predictions demonstrate the need for, and potential of, the IPC bleed system to prevent IPC stalls during rapid decel transients.

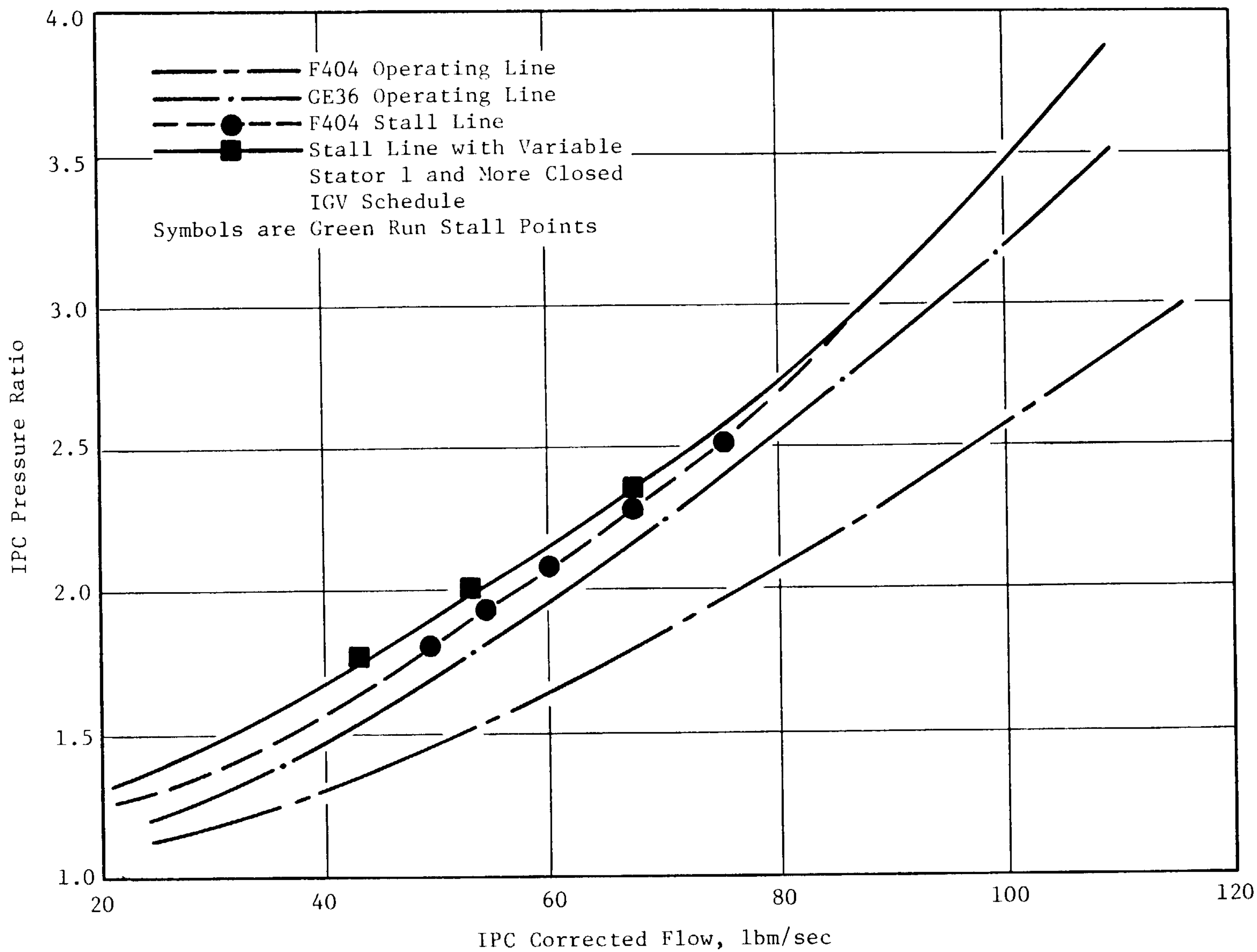


Figure 8-1. IPC Operating and Stall Line Sea Level Static.

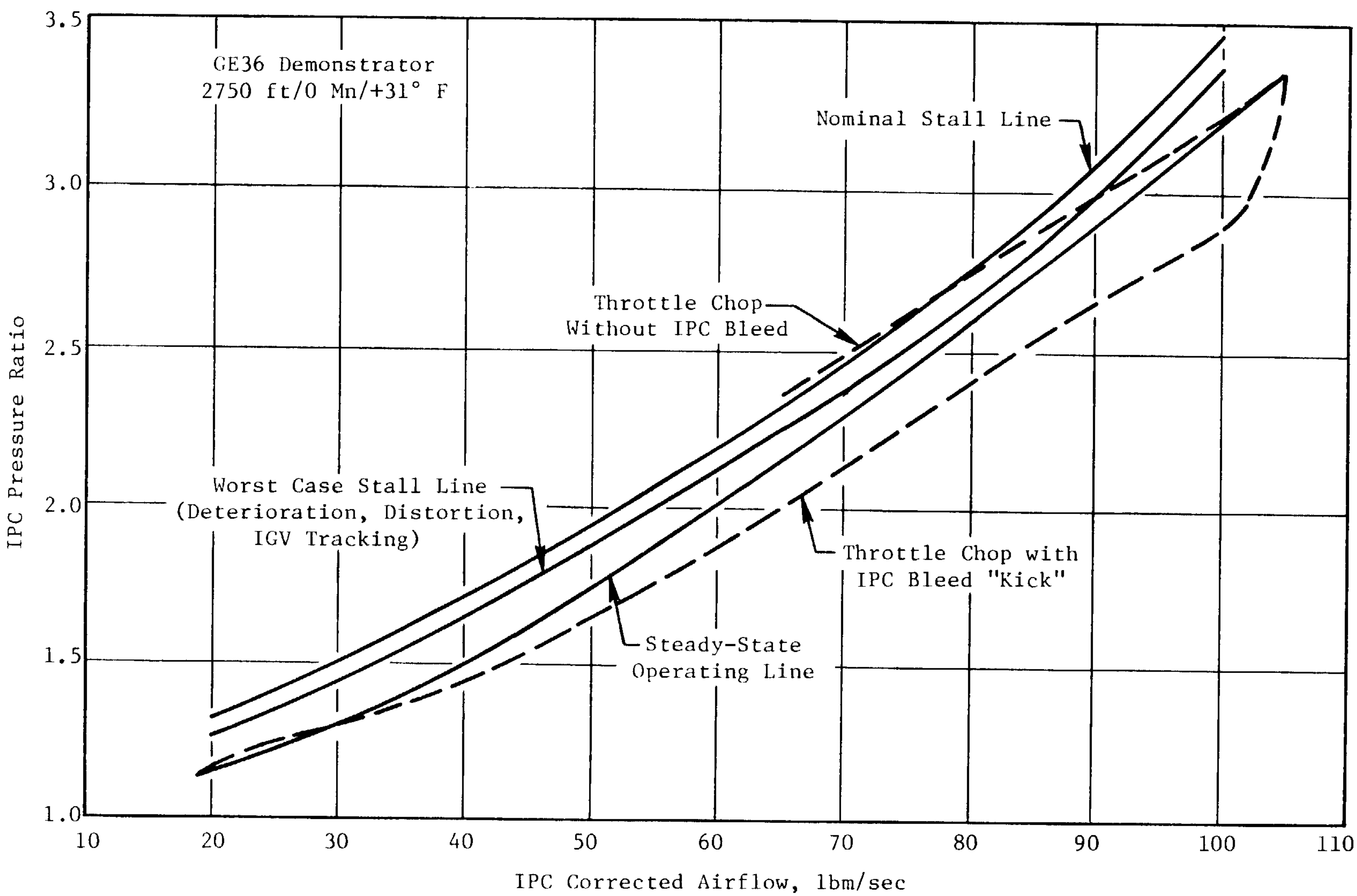


Figure 8-2. Steady-State IPC Operating Lines; 2750 ft.

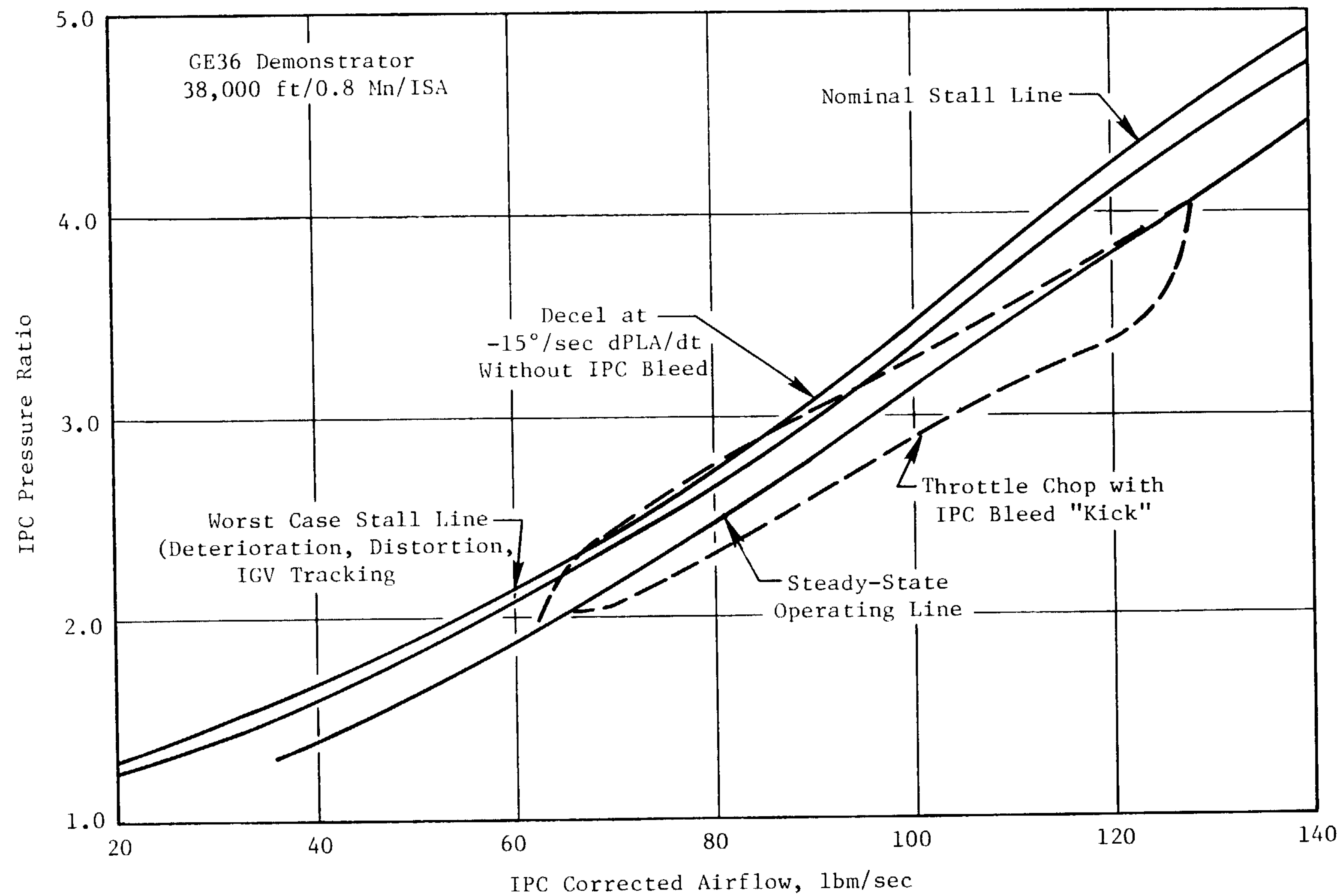


Figure 8-3. Steady-State IPC Operating Lines; 38,000 ft.

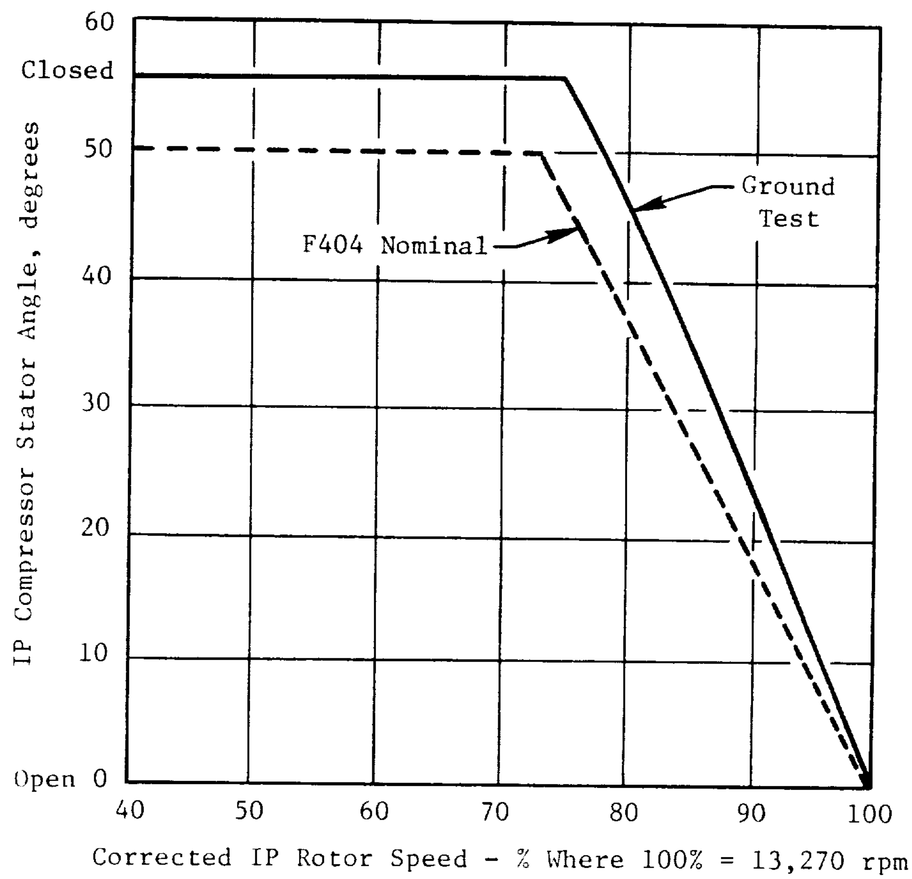


Figure 8-4. IPC Stator Schedule.

### 8.1.1 IPC Bleed Control System

The IPC bleed valve position is controlled by the DEC. The control logic opens the bleed valve in response to any one of the following inputs:

a. d(PLA)/dt - throttle retard rate > threshold

b. PLA - throttle step > threshold

c. d(P)/dt - IPC exit pressure decay rate > threshold

d. IPC P/P - scheduled maximum allowable P/P (f[XN2R]).

Thresholds "a" and "b" indicate a decel transient condition to the control, in which case additional IPC stall margin could be required. Threshold "c" would be exceeded in the event of engine surge. Schedule "d" is designed to maintain a minimum level of IPC stall margin under all normal operating conditions.

If thresholds a, b, or c are exceeded, the control logic is designed to "kick" the valve full open, hold for 5 seconds after the last demand for full open, and then ramp close in 5 seconds. The slow closing will avoid transient pressure pulses. In addition, for Input c, the control downtrims fuel flow to maximum authority, further decreasing engine system pressures. If scheduled Value d is exceeded, the control modulates the bleed valve to maintain the scheduled maximum allowable IPC pressure ratio. In the event multiple inputs are received, the valve kicking logic takes precedent.

### 8.1.2 Control Threshold for Throttle Retard Rate

Figures 8-2 and 8-3 show the PRS usage (stall pressure ratio normalized to stall line), as predicted by the transient cycle model, during decel transients from maximum power without IPC bleed. Shown are decels at various PLA rates at 2,750 ft/0Mn/+31° F and at 38,000 ft/0.8Mn/ISA. Also indicated in these figures is the current status available PRS and the minimum available PRS as a worst-case estimate. Figure 8-5 shows that with the current level of available margin at SLS (sea level static) conditions, an IPC stall would be predicted during a throttle chop from maximum power without IPC bleed, yet a decel transient at -10°/second d(PLA)/dt would not consume all of the current available margin. A decel transient from high power at -10°/second d(PLA)/dt, without IPC bleed, was successfully accomplished without stall during ground

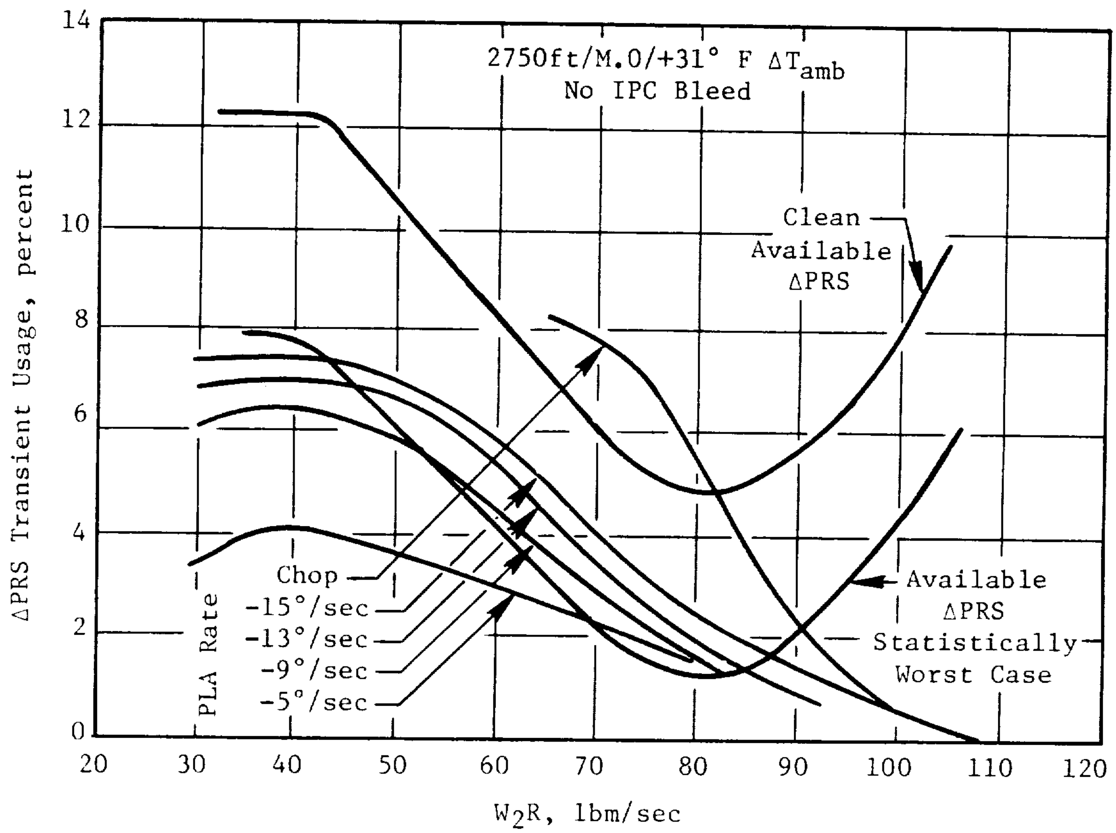


Figure 8-5. Predicted IPC ΔPRS Usage During Throttle Decels; 2750 ft.

testing; thus, confirming the analytical prediction. At altitude, however, the operating line migration during a decel exceeding -9°/second d(PLA)/dt is expected to consume all of the available margin, even at the current quality of the engine (Figure 8-6).

Considering the statistically worst-case IPC stability condition, Figures 8-5 and 8-6 show that even an IPC bleed kick threshold of -5°/second d(PLA)/dt is not sufficient to assure stall-free operation. This illustrates the necessity of the maximum allowable P/P schedule (bleed valve modulation).

### 8.1.3 Maximum Allowable IPC Pressure Ratio Schedule

The maximum allowable IPC pressure ratio (P15/P2 versus XN2R) was set at approximately 1% above the engine ground test operating level (Figure 8-7). This was accomplished at the end of ground testing, after analysis of control measurement data. The effect of the expected control measurement variation on this maximum allowable P/P schedule was determined to be equivalent to approximately +0.015 PRS (pressure ratio schedule).

This bleed modulation function will be effective during steady-state operation if the IPC operating line migrates upward due to the altitude/Mach effects (not predicted) or deterioration effects. It will also be effective during decel transients which do not exceed IPC bleed kick threshold levels.

### 8.1.4 Final IPC Bleed Control Status

During the engine ground testing, the IPC bleed system was successfully demonstrated; proper mechanical function and pressure relief capability were verified. Each of the control inputs (a through d) were individually checked and verified. By the end of the ground test, threshold levels were adjusted to appropriate levels, as follows:

a. d(PLA)/dt (throttle rate threshold = -5°/second)
b. PLA (throttle step threshold = -2°/0.25 second)
c. d(P15)/dt (IPC exit pressure decay rate threshold = -20%/second
d. P15/P2 versus XN2R (scheduled maximum allowable IPC pressure ratio set at approximately 1% above engine ground test operating level).

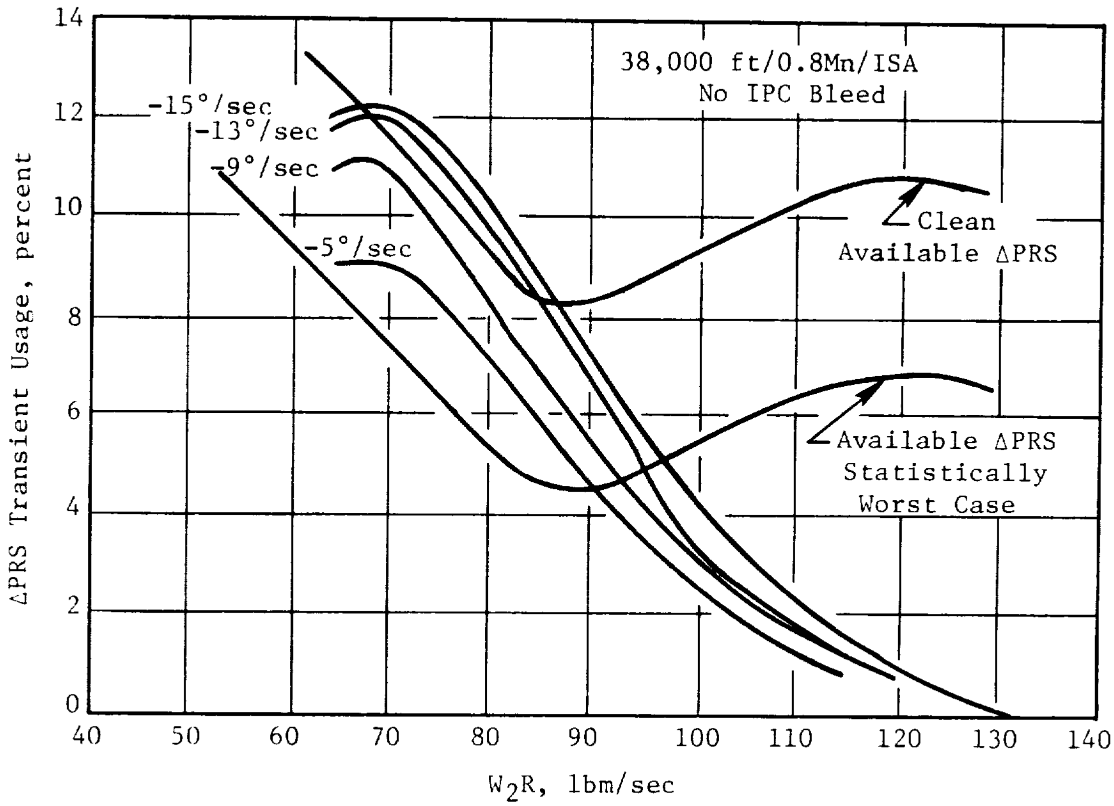


Figure 8-6. Predicted IPC ΔPRS Usage During Throttle Decels; 38,000 ft.

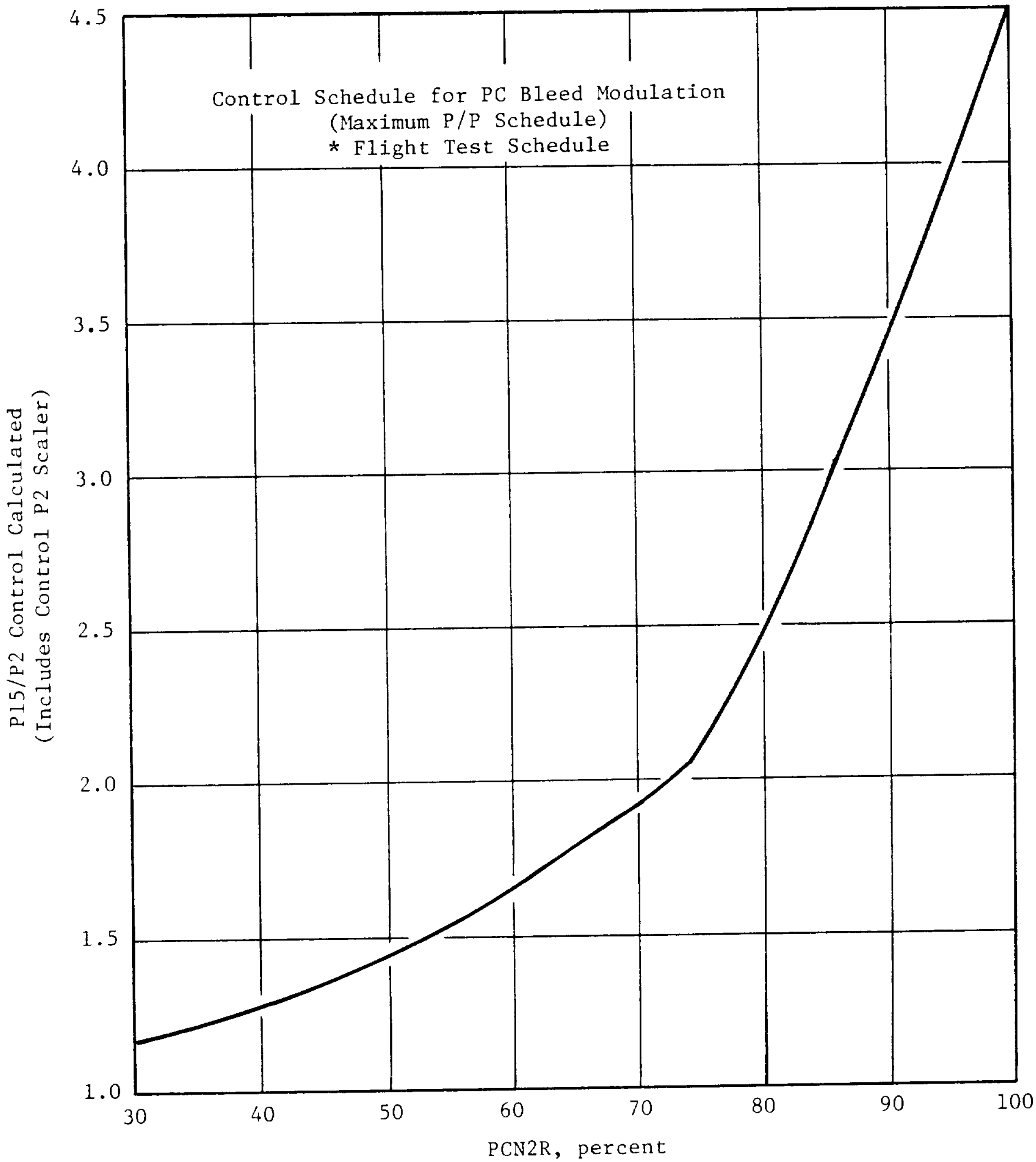


Figure 8-7. Maximum Allowable IPC Pressure Ratio.

Figures 8-8 and 8-9 show the predicted PRS usage during decel transients at 2,750 ft/0Mn/+31°F and at 38,000 ft/0.8Mn/ISA, with bleed system control thresholds set as defined previously. For decel transients which exceed -5°/second d(PLA)/dt, the kick function is effective, and the PRS transient usage is zero. This was demonstrated during a throttle chop from high power in which the bleed valve kicked open, and the transient data indicated that the IPC operating line during decel was lower than the steady-state level. For decel transients which do not exceed -5°/second d(PLA)/dt, the bleed modulation function is effective. If the operating line migrates above the steady-state ground test level, the control will modulate the bleed to maintain the maximum allowable P/P during the decel.

Figures 8-8 and 8-9 show that the IPC bleed control system should prevent the IPC operating line from migrating to even the worst-case stall line, thus, assuring stall-free operation.

## 8.2 TRANSIENT TESTING EXPERIENCE

Table 8-1 summarizes the significant transient tests conducted. Small PLA accels and decels were conducted to verify control functions and to adjust control gains to appropriate levels to ensure control stability; control fault trips were checked, resulting in throttle chops and stopcocks.

Several unintentional decel transients were encountered, both operator and control initiated, due to instrumentation faults and operating limits. For cycle operability evaluation, large PLA accels, decels, and bodes were conducted. All transient testing of the demonstrator engine during ground testing was accomplished without adverse results.

## 8.3 ENGINE TRANSIENT PERFORMANCE ANALYSIS AND PREDICTIONS

The transient cycle model is used to predict the operating line migration of the compression components during engine transients. In order to foresee any stall or operational problems prior to transient testing, good agreement between the cycle model predictions and test data is necessary. Two engine transients conducted during the ground test were simulated by the transient cycle model with good results; a throttle chop from 97% thrust and a throttle

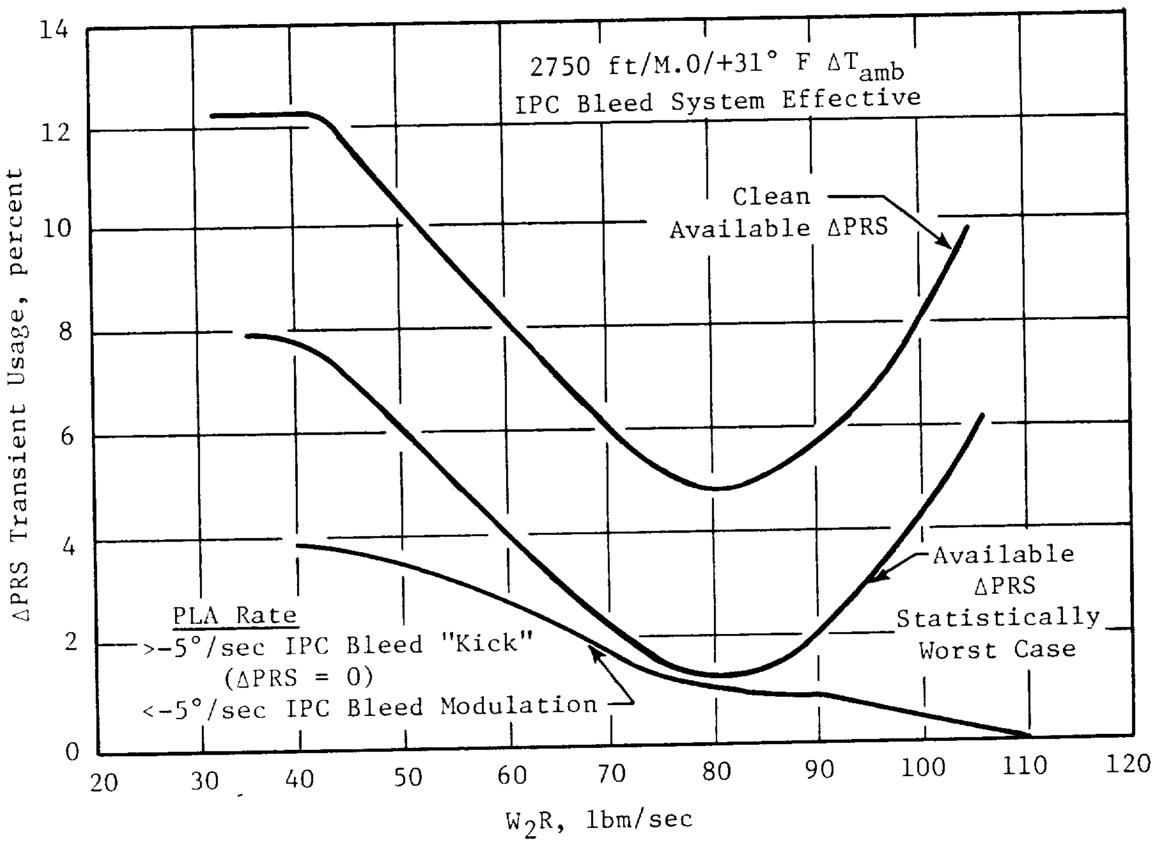


Figure 8-8. Predicted IPC ΔPRS Usage During Throttle Decels; 2750 ft.

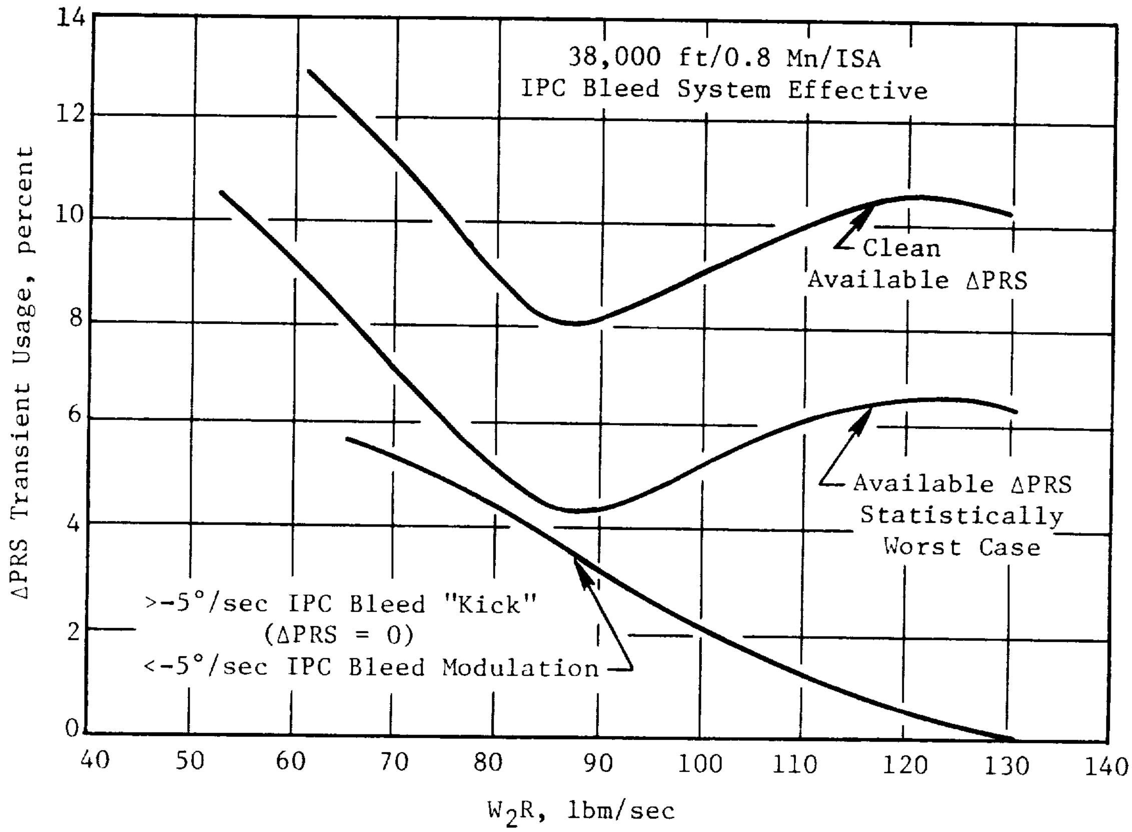


Figure 8-9. Predicted IPC ΔPRS Usage During Throttle Decels; 38,000 ft.

burst to 20,000 thrust. Figures 8-10 and 8-11 show the transient cycle model simulations, as compared to the test data, for selected parameters.

The results of these comparisons provide confidence in transient cycle model predictions of IPC operating line migration during decel transients which were used in designing and optimizing the IPC bleed control system.

Table 8-1. Significant Transients - GE36 Proof-of-Concept.

| Date | Maneuver | Reason |
|---|---|---|
| 2-09-86 | Throttle Chop from 24,000 Fn | No. 7 Aft Blade Debonded |
| 4-18-86 | Stopcock at 11,000 Fn | XN49 O/S Trip |
| 7-8-86 | 10 Throttle Bursts to 18,000 Fn | Planned |
| 7-8-86 | 2 Throttle Bursts to 20,000 Fn | Planned |
| 7-8-86 | Throttle Burst to 21,000 Fn, Chop to Idle | Planned/Overspeed |
| 7-8-86 | 2 Bodes (Chop from 20,000 Fn to Idle, Burst to 20,000 Fn) | Planned |

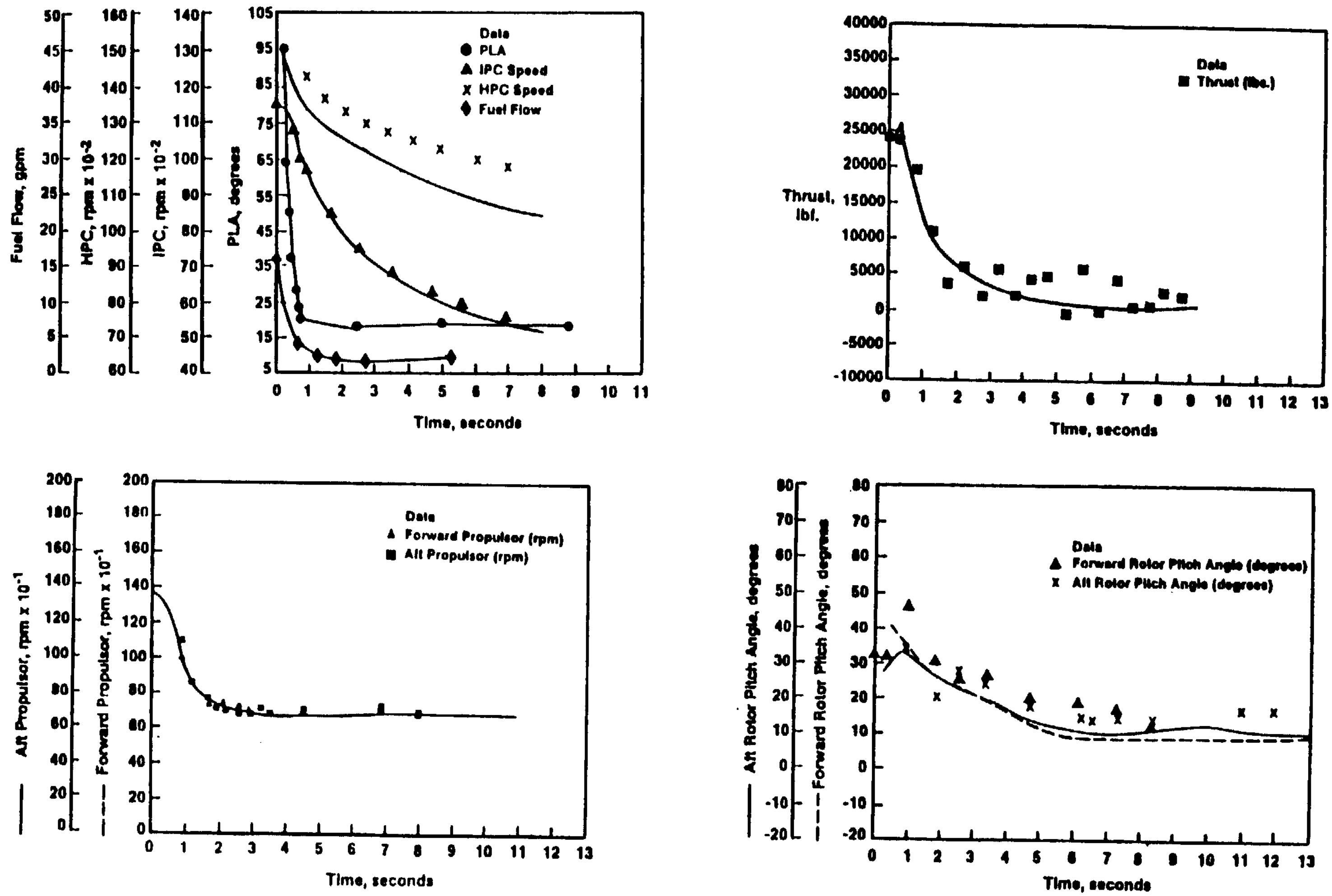


Figure 8-10. Transient Testing Analytical Comparison with Updated Transient Cycle Deck T/C from 97% Takeoff Thrust.

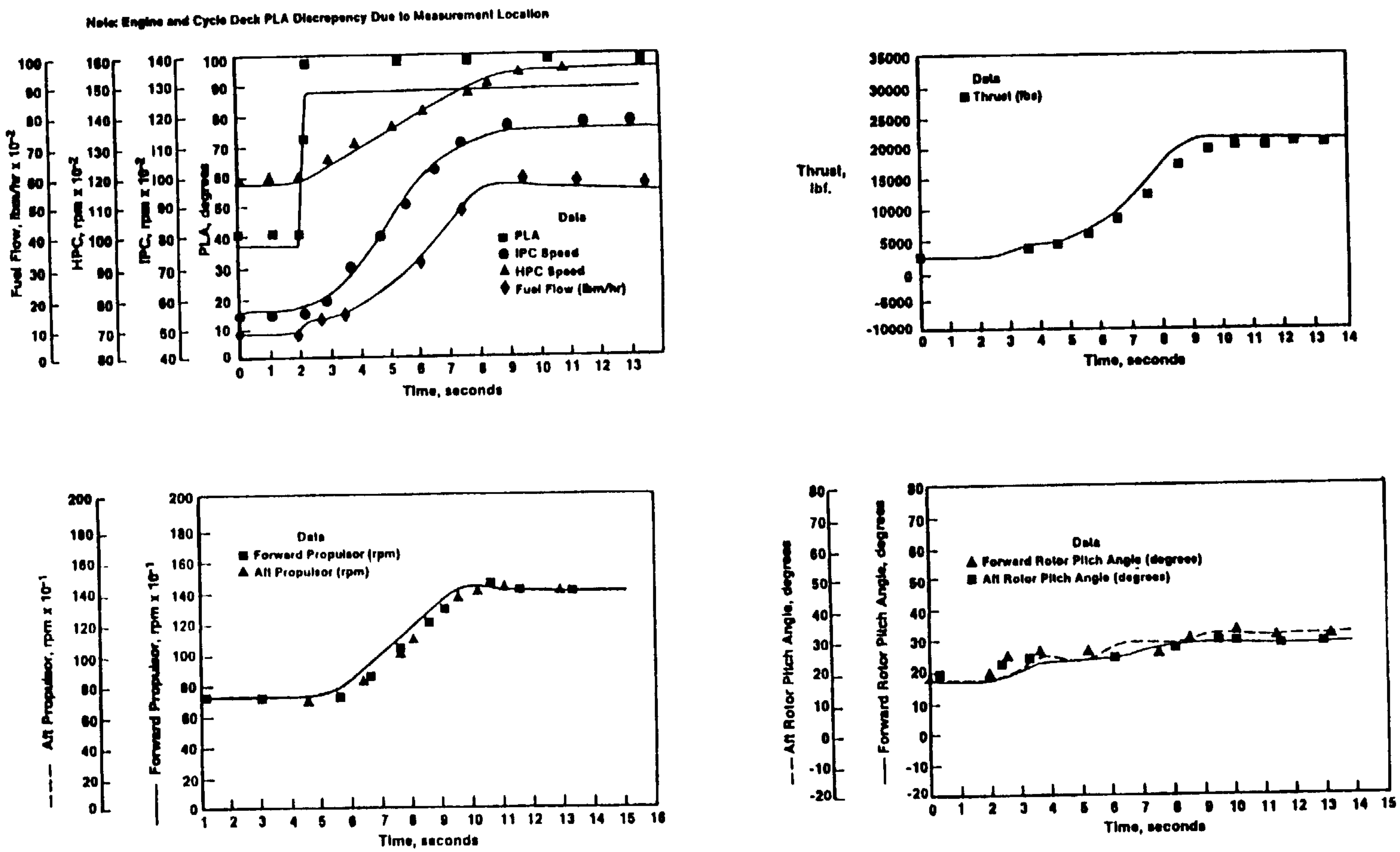


Figure 8-11. Transient Testing Analytical Comparison with Updated Transient Cycle Deck Burst to 20,000 lb Thrust.

# 9.0 ENGINE CONTROL

This section provides a summary of the GE36 control system performance during the ground test program performed at GE's engine test facility near Peebles, Ohio. This summary is divided into three parts; each portion covers the milestones associated with each of the three engine builds.

## 9.1 BUILD 1 - ENGINE CONTROL TESTING

The control system performance for Build 1 was successful. A limited amount of testing was performed due to the propulsor turbine failure.

### 9.1.1 Speed Sensing Anomaly

During Build 1 testing, it was discovered that the speed being sensed by the control for the forward propulsor rotor (XN48) was incorrect. A further study as to the cause showed that the gaps in the target wheel, which was divided into eight segments, were inducing a superfluous signal onto the magnetic speed-sensing pickups (Figure 9-1). This caused a higher sensed speed, up to two times actual. The situation was initially corrected by a change in speed signal processing. A more elegant solution was identified for implementation on Build 2. This solution consisted of locating the teeth on the target wheel directly at the segment gaps (Figure 9-2).

### 9.1.2 Pitch Control

For Build 1, the engine was controlled to pitch angle, rather than to propulsor speed.

### 9.1.3 Gas Generator Control

The gas generator control performed as expected. The EPR (engine pressure ratio), HP (high pressure) and IP (intermediate pressure) stator control, and the control of the duct bleed system all exhibited stable operation during this engine build testing. A new control strategy for stall avoidance and recovery for the duct bleed system was identified during this build and was incorporated into the control system during Build 2.

- Original Design
- **8 Segments Total**
- **1 Tooth Centered In Each Segment**

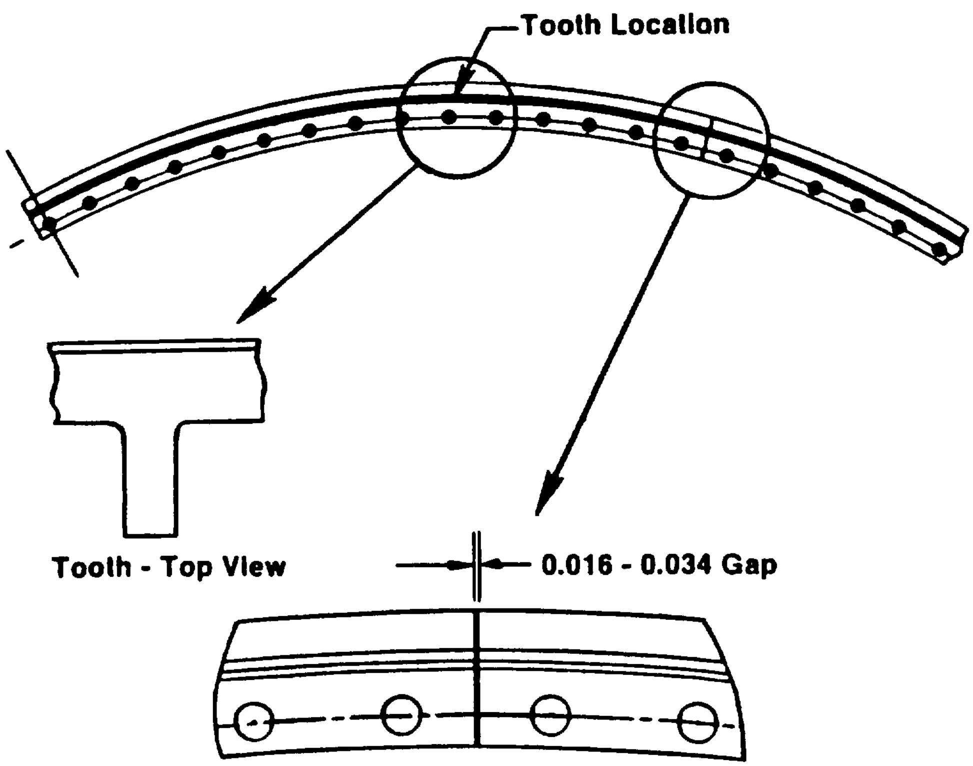


Figure 9-1. Fan Speed Sensor Segments.

- Redesign

- **8 Interlocking Segments**
- **1 Tooth Per Segment**
- **Tooth Positioned On End**
- **Gap Width Reduced**

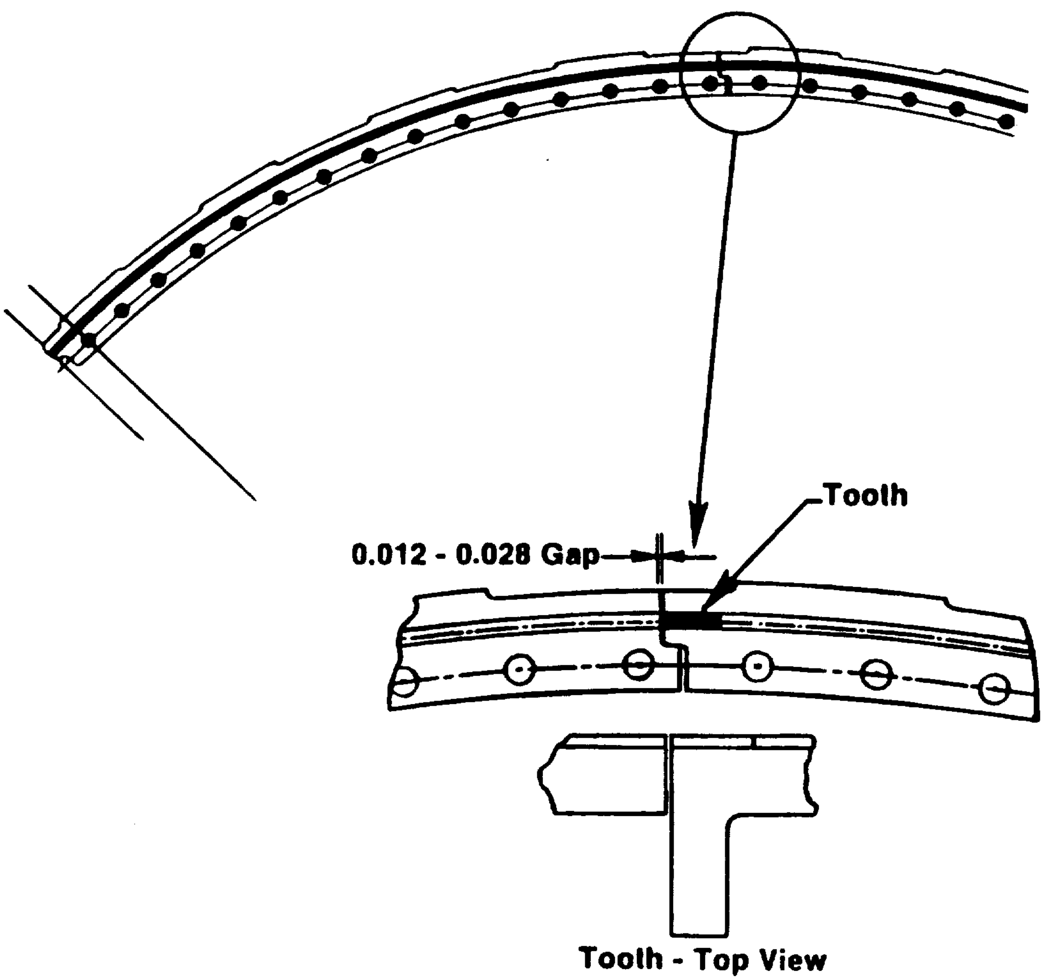


Figure 9-2. Fan Speed Sensor Segments.

### 9.1.4 Throttle System

The throttle system was redesigned to minimize hysteresis. The resolver was relocated to the HMU (hydromechanical unit) fuel lever to provide a more accurate indication of fuel lever angle. A rotary potentiometer was added to the system at the throttle converter to provide an input for PLA which would provide for a reverse indication and redundancy for the resolver.

### 9.1.5 Engine Starting

Starting tests during this build achieved expected results. The engine was first dry motored to check instrumentation and control signals. After successful dry motoring, the engine was wet motored (engine motoring with fuel on), also without incident. After wet motoring, the engine was fired to idle power. The control performed as expected, successfully controlling HP rotor speed to the HP rotor starting speed schedule. Due to the aforementioned speed sensing anomaly, limited propulsor speed control testing was performed.

### 9.1.6 Off-Engine Harnesses

Crosstalk was observed on multiconductor off-engine cables during testing as well as inaccuracies on alternating current type sensors. This situation was corrected by placing twisted pairs for each circuit inside the same shield and removing unused pairs.

### 9.1.7 Lube Oil Bypass

Scavenge capability of the propulsor lube oil system was marginal during Build 1 testing. A solution was identified for use on Build 2. This solution involved installing in the propulsor lube system a bypass valve which allowed lube oil into the propulsor only after a light-off had been detected by the control. This prevented excess lube oil from entering the propulsor during start operations, thus minimizing the effects.

## 9.2 BUILD 2 - ENGINE CONTROL TESTING

Due to lessons learned during Build 1 testing, Build 2 testing involved further testing of the engine in the realms of transient testing, verification of control schedules, and modifications to the control. This testing further demonstrated the stability of the control system. Full control was maintained under a blade-out condition.

### 9.2.1 Speed Control

Closed-loop speed control (modulation of fan pitch to maintain scheduled fan speed) was used by the control successfully for all power settings, with the exception of reverse and windmill testing. The propulsor speed was demonstrated to be stable from 550 rpm to 1400 rpm and from idle to 25,000 lbs, corrected thrust. This modulation of pitch to control fan speed also was demonstrated for Mach numbers up to 0.1 using facility fans.

### 9.2.2 Duct Bleed

Modifications to the duct (fan bypass) bleed control logic were verified for P15Q2, PLA chop, and simulated stall. A throttle chop from 97% takeoff thrust was performed without IPC stall; also, unrestricted throttle chops from all power settings were performed. Figure 9-3 is a schematic of the engine bleed system.

### 9.2.3 Transient Testing

A limited number of small, part, and full power throttle chops and small part power accelerations were performed. During a throttle burst from idle to 1150 rpm, an overspeed incident occurred. It was determined to have been caused by the fan pitch actuator becoming force-limited due to a too rapid response time of the gas generator. A fix was identified to slow down the accel rate of the core by putting an accumulator on the CDP (compressor discharge pressure) sensing line to the HMU. A preliminary fix was installed on the engine which adequately slowed the core accel rate. A more polished design was used on Build 3.

As a result of the blade-out incident, the engine was chopped from 24,000 corrected thrust to idle, then stopcocked approximately 10 seconds later. As illustrated in Figures 9-4 through 9-8, the control system maintained complete control during the blade-out, chop to idle, and subsequent stopcock.

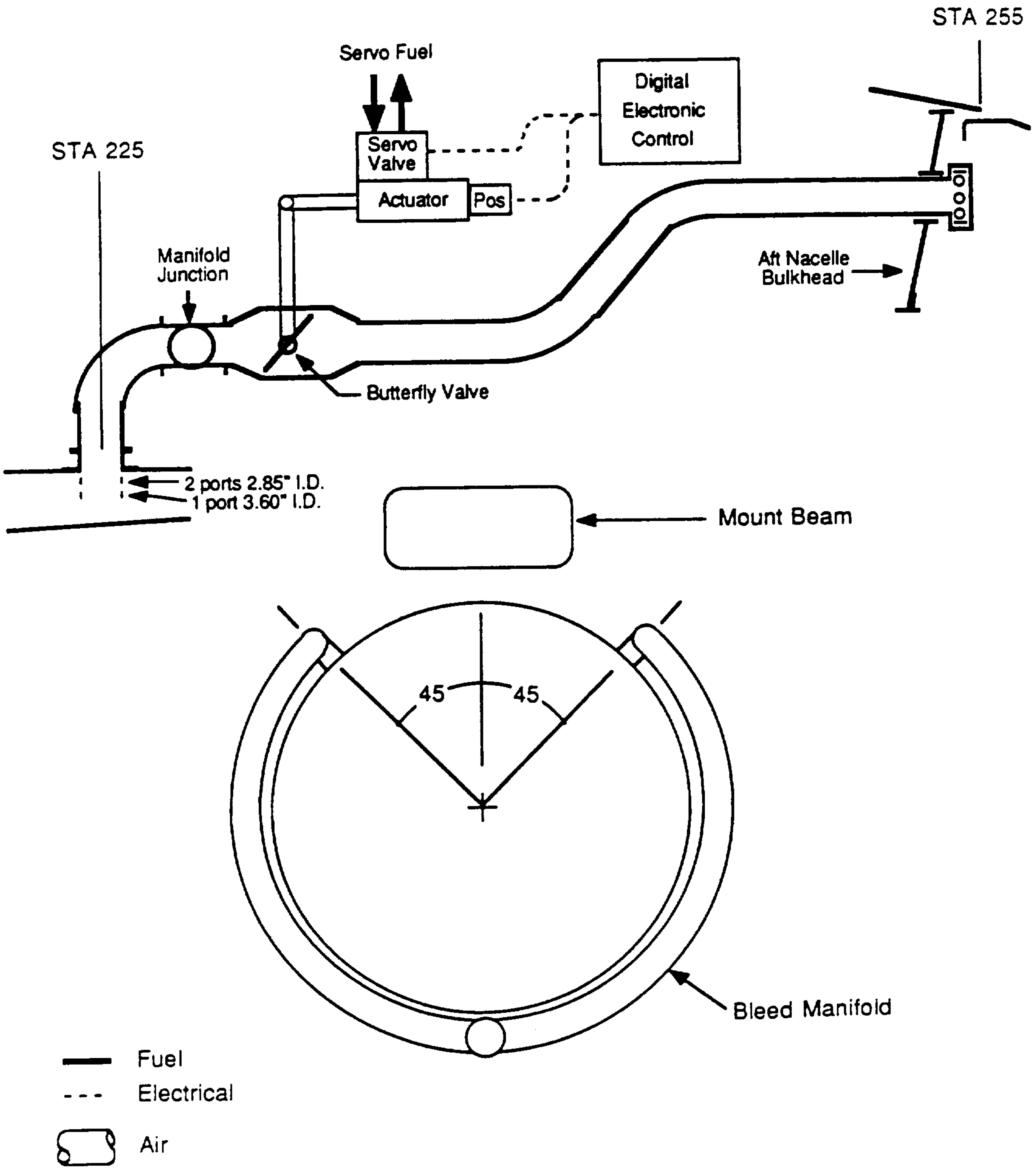


Figure 9-3. Duct Bleed System.

- $24{,}000\ F_N/\partial$ to Idle
- Blade Out Incident

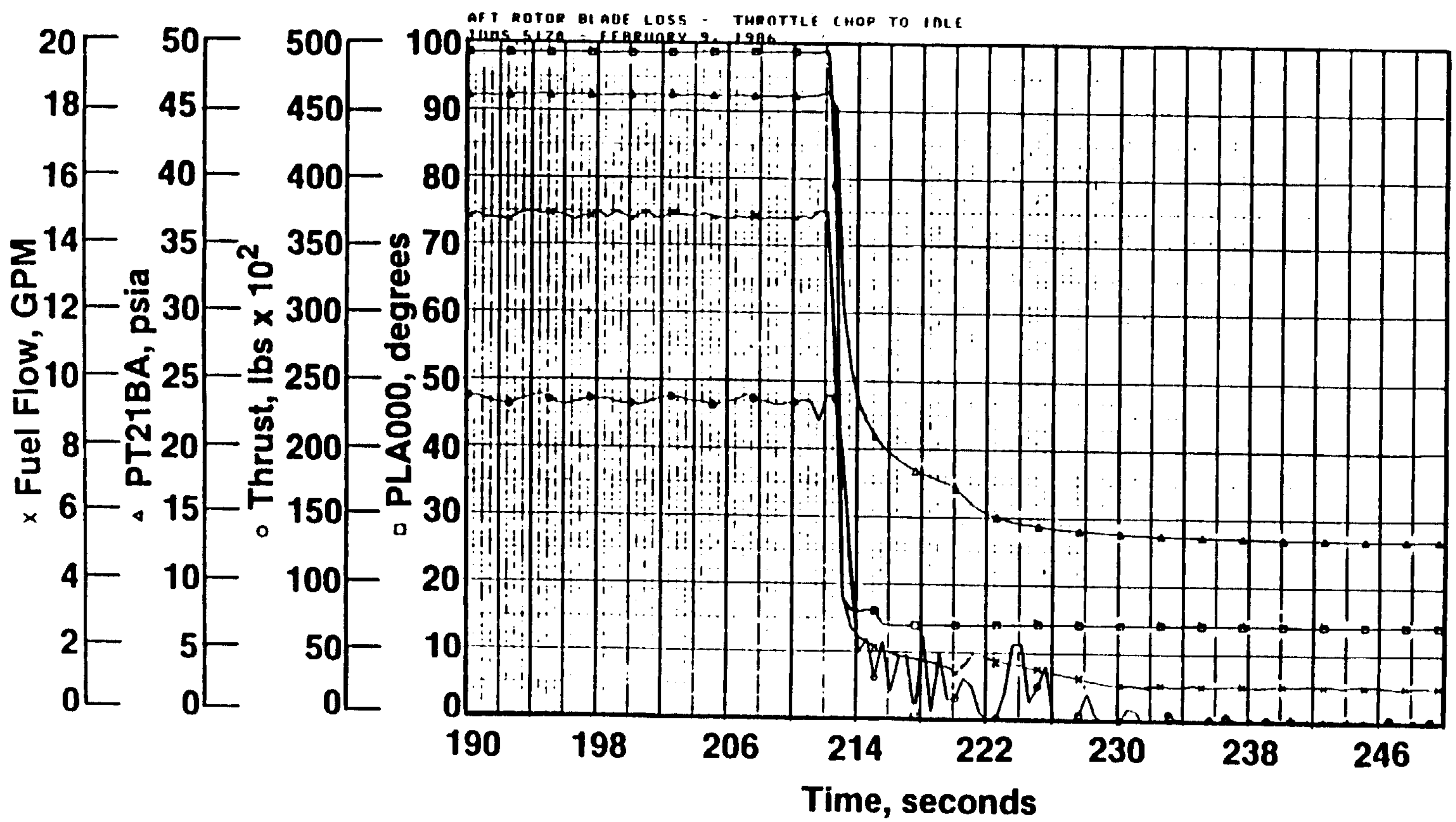


Figure 9-4. Throttle Chop Decels.

- 24,000 $F_N/\partial$ to Idle
- P46Q2 Control Prior to Chop
- Blade Out Incident

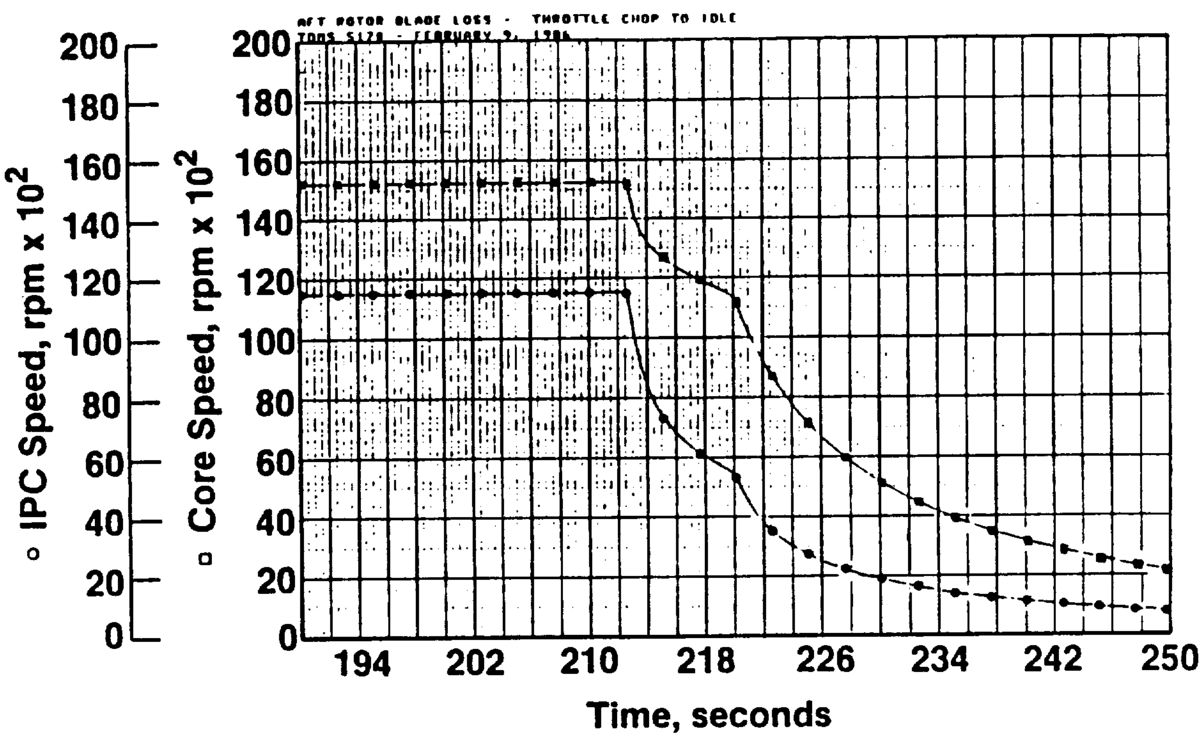


Figure 9-5. Throttle Chop.

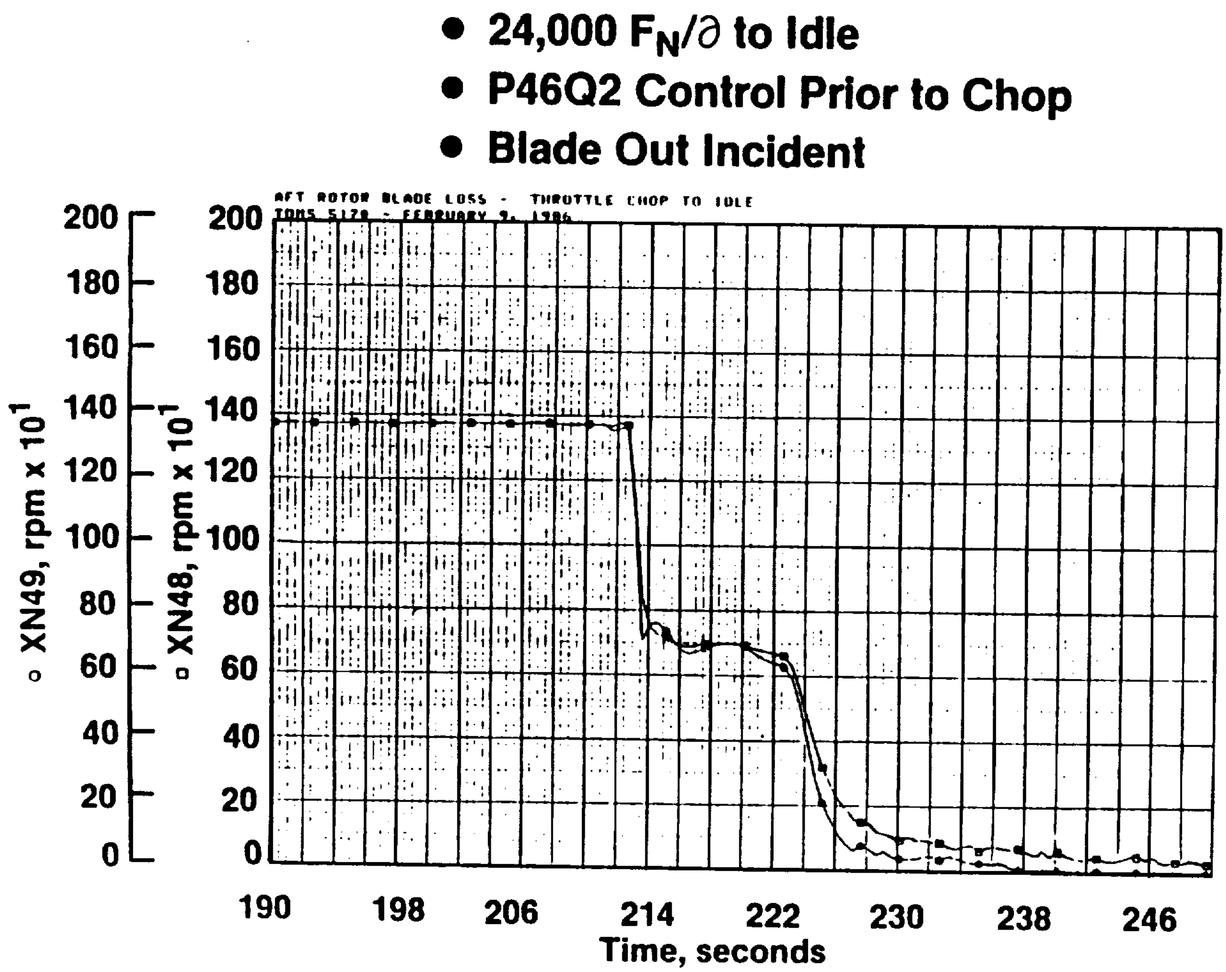


Figure 9-6. Throttle Chop.

ORIGINAL PAGE IS
OF POOR QUALITY

- 24,000 $F_N/\partial$ to Idle
- P46Q2 Control Prior to Chop
- Blade Out Incident

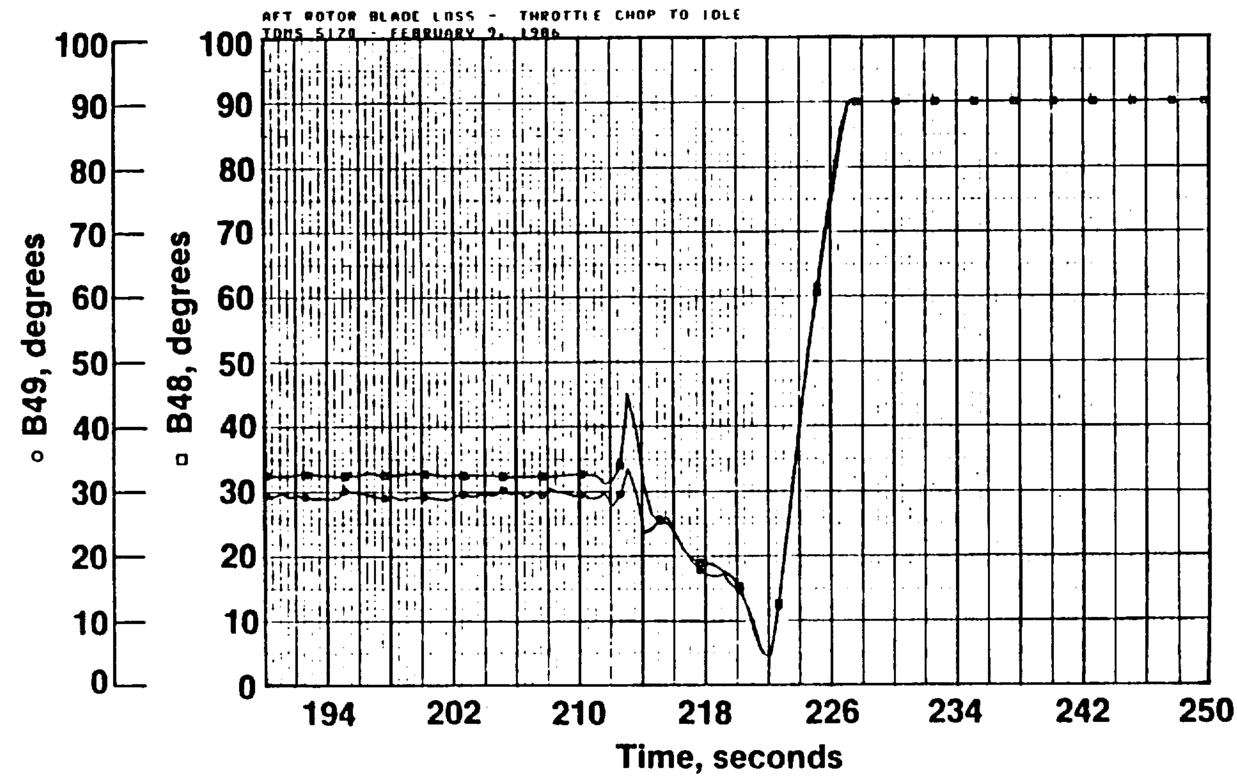


Figure 9-7. Throttle Chop.

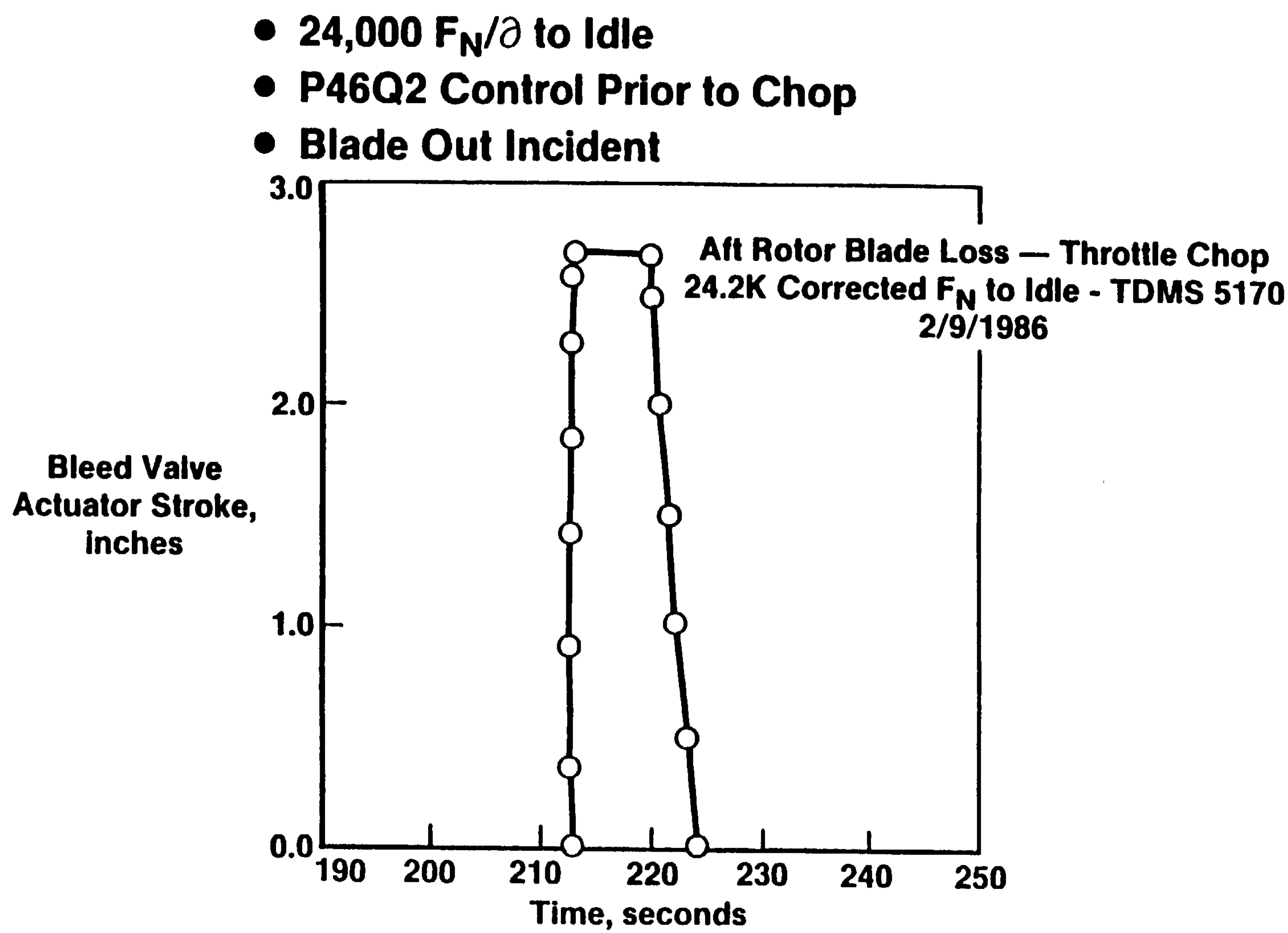


Figure 9-8. Throttle Chop.

### 9.2.4 Control Parameters

All control parameters were stable.

### 9.2.5 Vibration System

The vibration monitoring system proved to be functional; however, it was discovered that there was not enough gain in the amplifier for small vibration signals. As a result of the blade-out incident, readings were gathered that allowed for the scaling of the vibration signal. To increase its gain by a factor of four, the amplifier was reworked; this change was implemented during Build 3 testing.

### 9.2.6 Overspeed System

The capability of the overspeed system was demonstrated during an overspeed incident. During a throttle burst from 550 to 1150 rpm, the fan pitch actuator became force-limited and was unable to modulate fan pitch to control rear rotor speed. An overspeed condition resulted, which was quickly sensed by the overspeed system which immediately shut down the engine in a controlled manner.

### 9.2.7 Reverse Testing

Limited by the telemetry system, this due to high temperatures, reverse testing for Build 2 consisted of a throttle push from idle to 1000 rpm (3000 lb reverse thrust at static conditions). Figures 9-9 through 9-12 illustrate a transient from forward idle, to reverse idle; then throttle is pushed until a maximum propulsor speed of 1000 rpm is obtained, followed by a decel and return to forward idle. The fan speed is controlled by modulating pitch in forward thrust, and PLA is used to schedule pitch directly in reverse thrust, hence, the difference in propulsor speeds in reverse thrust.

### 9.2.8 Control System Modifications

Two areas of the control system hardware were modified during this build to improve performance. The hardware modified was the pitch actuation system transfer valves and the watchdog monitor circuit of the control computer.

- **Forward Idle to Reverse Idle**
- **Throttle Push to 1000 rpm Maximum Fan Speed**
- **Return to Forward Idle**

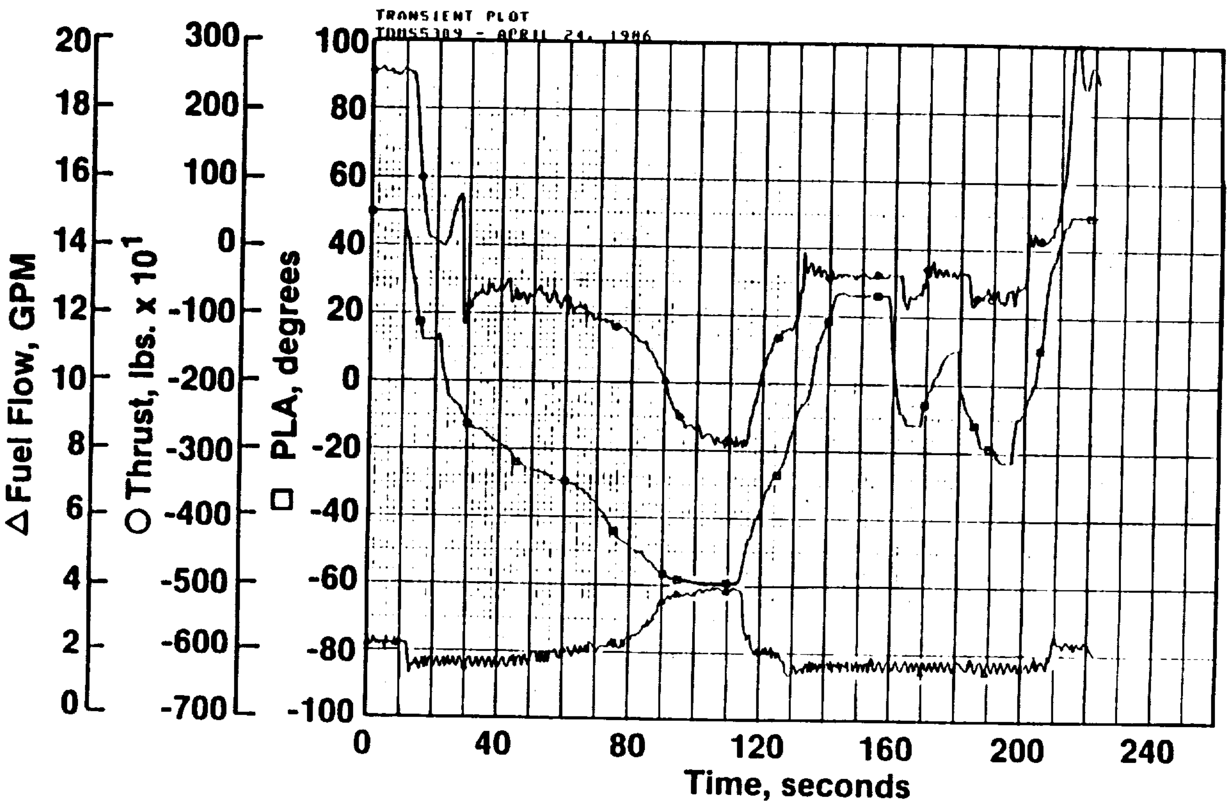


Figure 9-9. Reverse Thrust.

- **Forward Idle to Reverse Idle**
- **Throttle Push to 1000 rpm Maximum Fan Speed**
- **Return to Forward Idle**

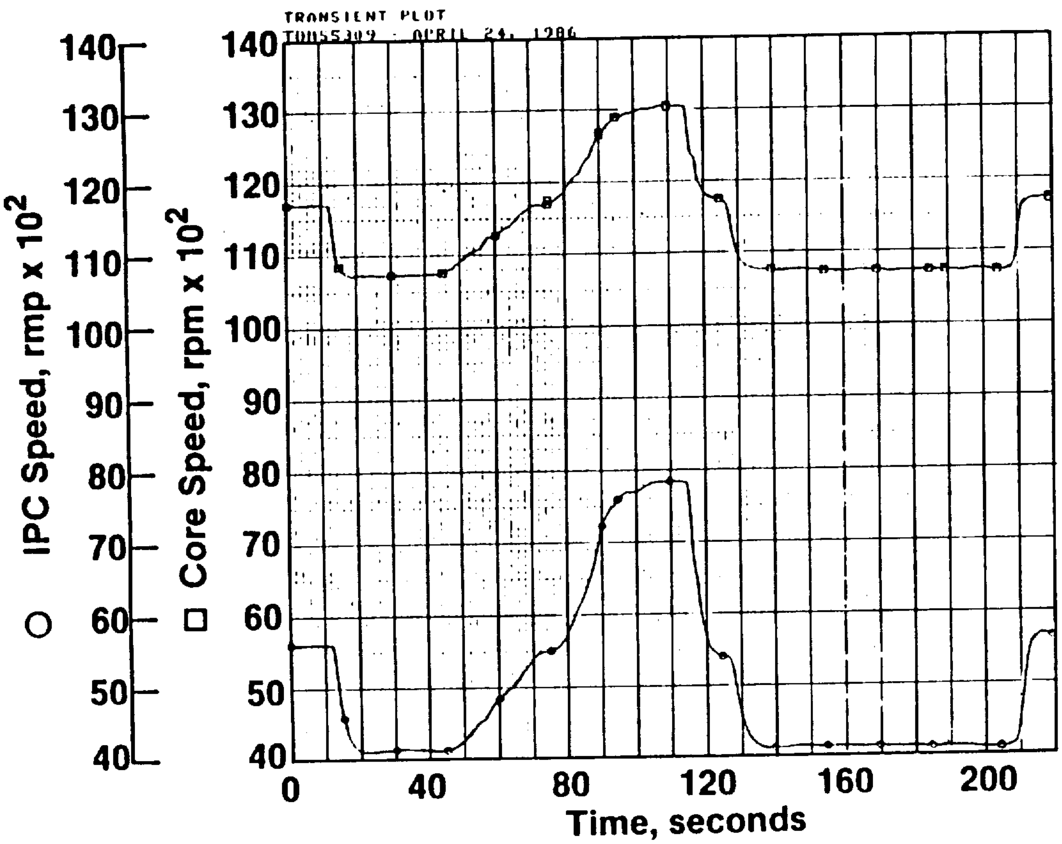


Figure 9-10. Reverse Thrust.

- **Forward Idle to Reverse Idle**
- **Throttle Push to 1000 rpm Maximum Fan Speed**
- **Return to Forward Idle**

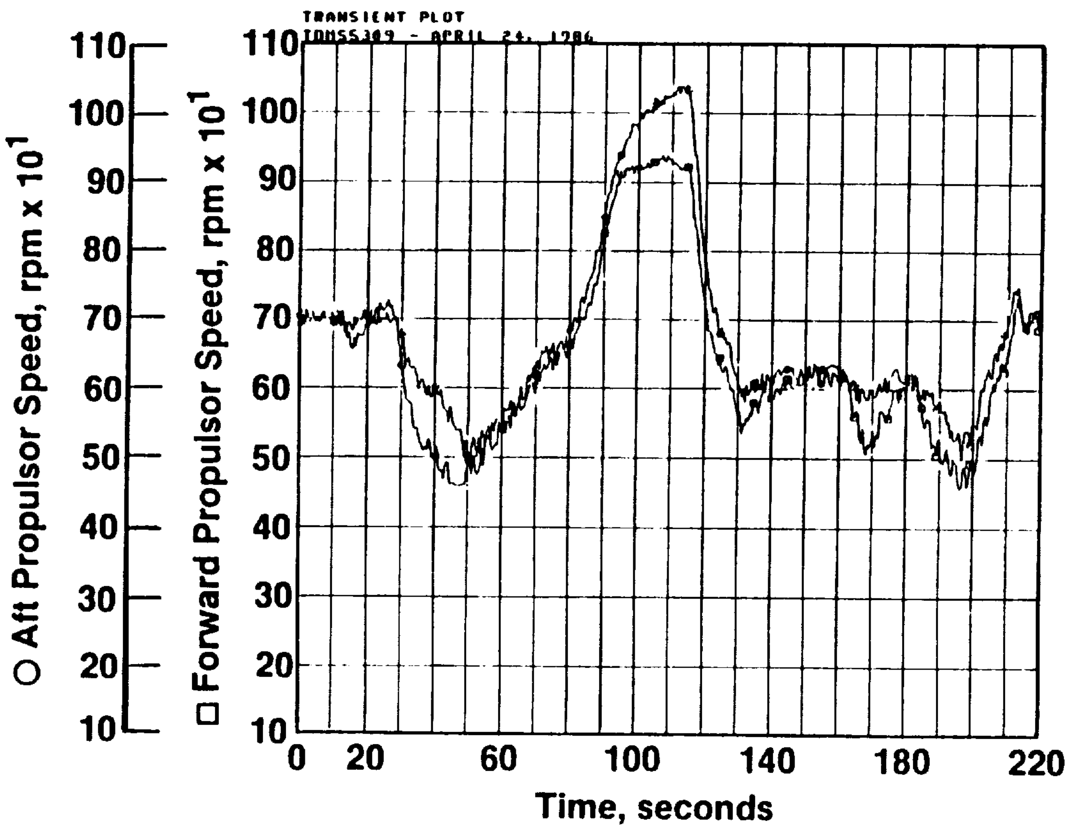


Figure 9-11. Reverse Thrust.

ORIGINAL PAGE IS
OF POOR QUALITY

- Forward Idle to Reverse Idle
- Throttle Push to 1000 rpm Maximum Fan Speed
- Return to Forward Idle

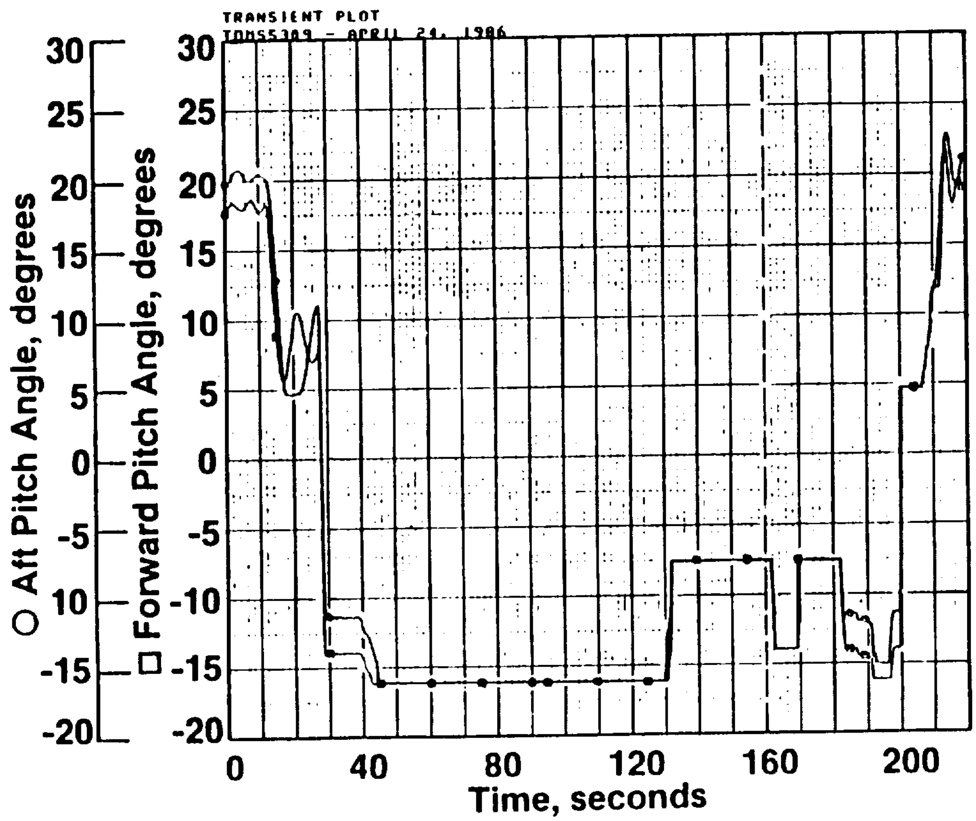


Figure 9-12. Reverse Thrust.

The transfer valves exhibited erratic performance during the beginning of this build. It was determined that the filtering of the hydraulic oil was inadequate. To correct this problem, the filters for the hydraulic system were changed from 5 micron to 3 micron.

The watchdog monitor circuit on the control initiated several inadvertent automatic shutdowns, later discovered to be caused by noise on the backplane of the control propagating into the watchdog circuit and inducing erroneous pulses. This condition was corrected by adding filters to all high speed lines on the watchdog circuit card.

## 9.3 BUILD 3 - ENGINE CONTROL TESTING

Build 3 testing was the most successful portion of the ground test, both in terms of time on test and control system testing.

### 9.3.1 Endurance Testing

Pitch and EPR controller gains were optimized during the 100 LCF cycles which were performed (Reference Figure 3-54).

### 9.3.2 Core Response Modifications

The gas generator response time was reduced with an orifice/accumulator system (Figure 9-13) in the CDP (compressor discharge pressure) line to the HMU (hydromechanical unit) and a control rate control. This modification was due to an overspeed incident caused by a force-limited actuator. The orifice/accumulator was sized to give an 8-second idle-to-rated-thrust response.

### 9.3.3 Reverse Thrust Testing

Reverse testing during Build 3 achieved maximum speeds of 850 rpm limited by high telemetry temperatures.

### 9.3.4 UPS (Uninterruptable Power Supply) Systems

The UPS systems for the control were successfully demonstrated during this build. The UPS powered the control computer, the overspeed unit, and the peripheral computer. The UPS systems were tested, by removing/reconnecting

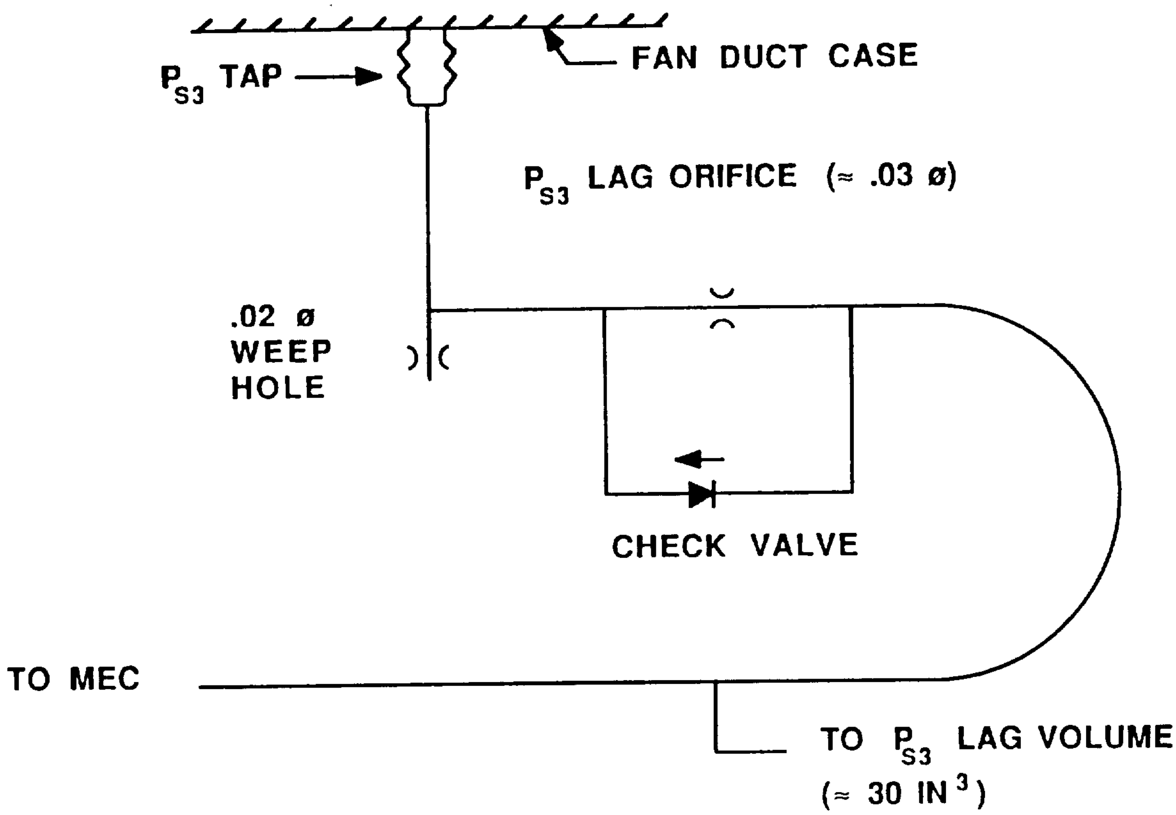


Figure 9-13. $P_{S3}$ Accumulator Configuration.

input power, both statically and with the engine running without affecting control performance in any way.

### 9.3.5 Transient Testing

Transient testing consisted of accelerations, decelerations, and throttle bodes. The controller was found to exhibit an underdamped response above 2.85 engine pressure ratio.

Figures 9-14 through 9-17 depict a throttle burst from idle to approximately 18,500 lbf. Satisfactory control response was demonstrated.

## 9.4 SUMMARY

Testing of the UDF™ provided valuable data and demonstrated the viability of the unducted fan concept and its control system.

Further, test results verified that the control system concepts of using EPR as the thrust parameter and utilizing EPR to schedule propulsor speed are sound. The modulation of pitch to maintain scheduled propulsor speed has been demonstrated statically and for Mach numbers up to 0.1.

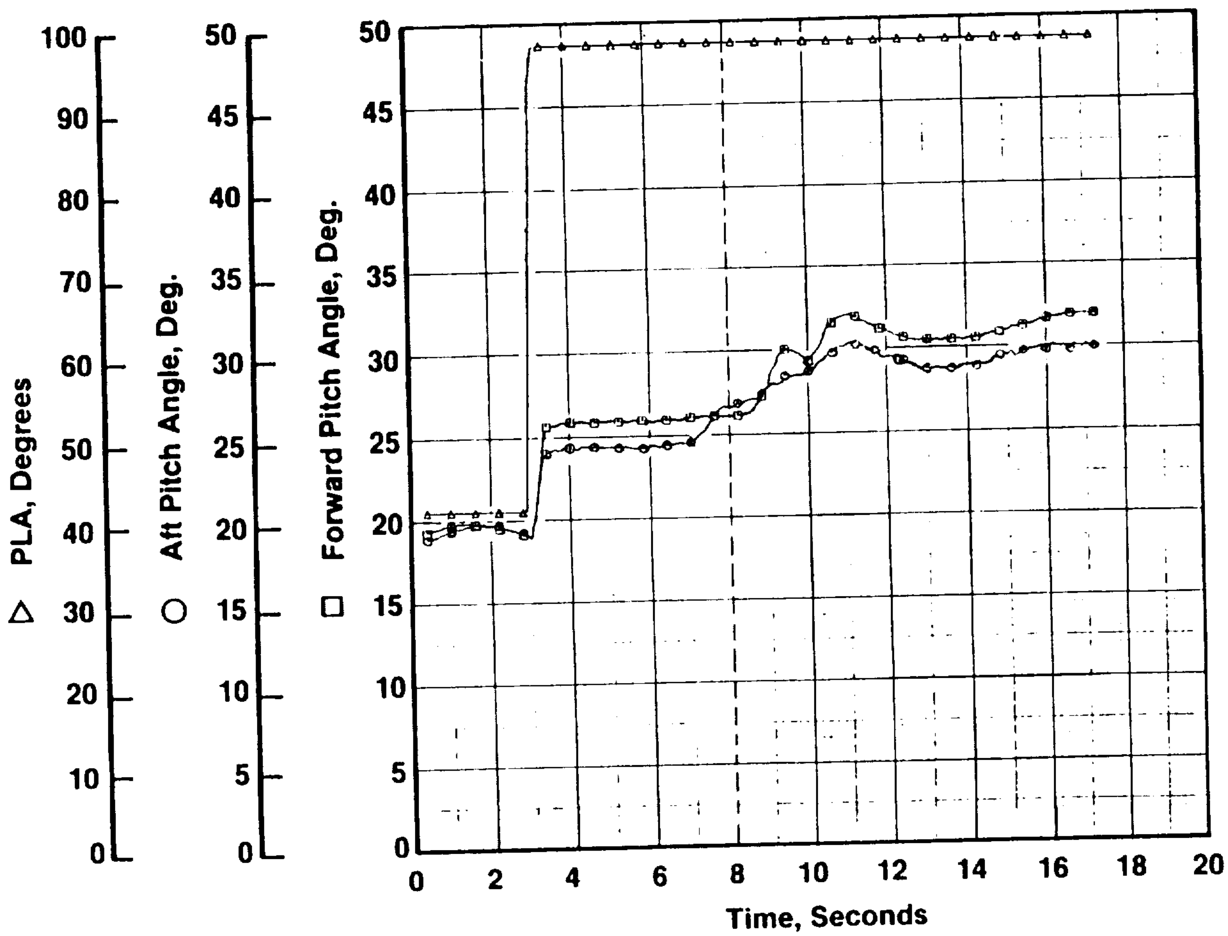


Figure 9-14. Throttle Burst.

ORIGINAL PAGE IS
OF POOR QUALITY

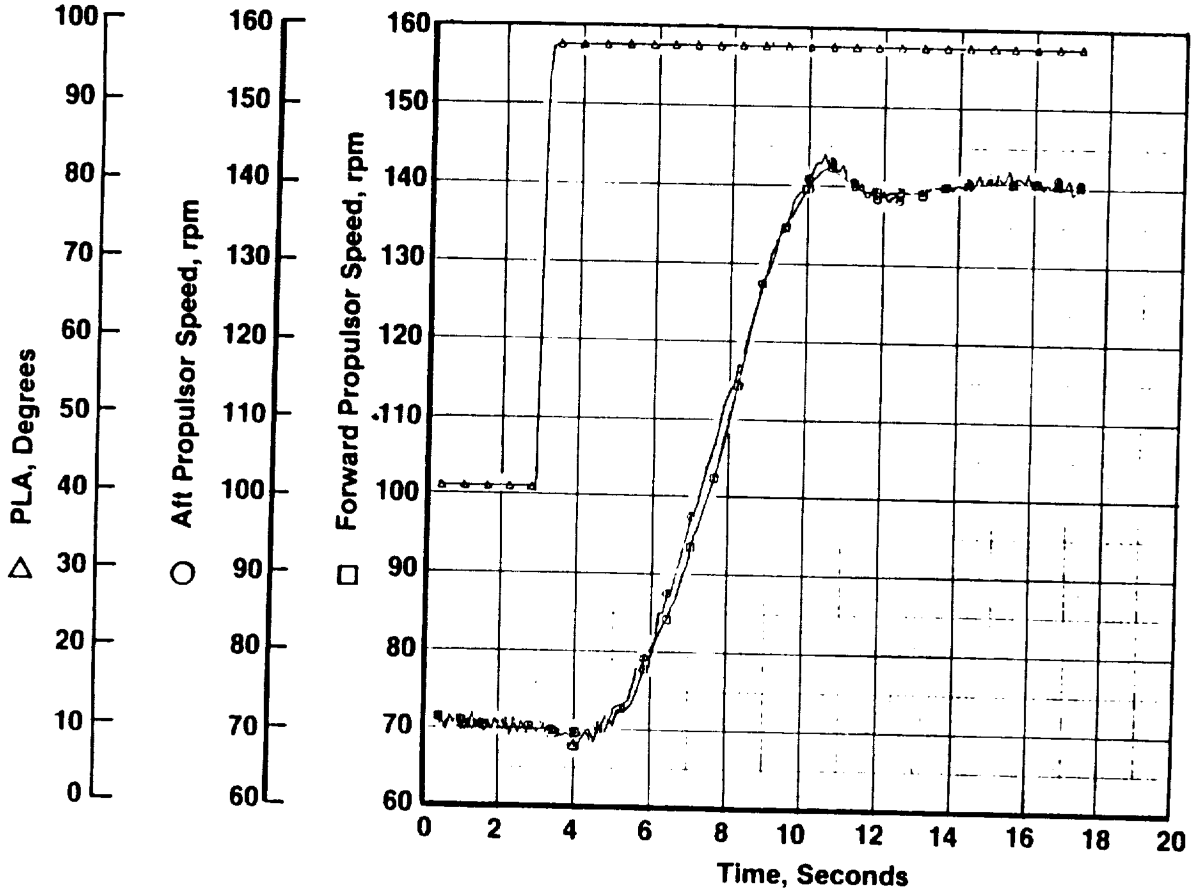


Figure 9-15. Throttle Burst.

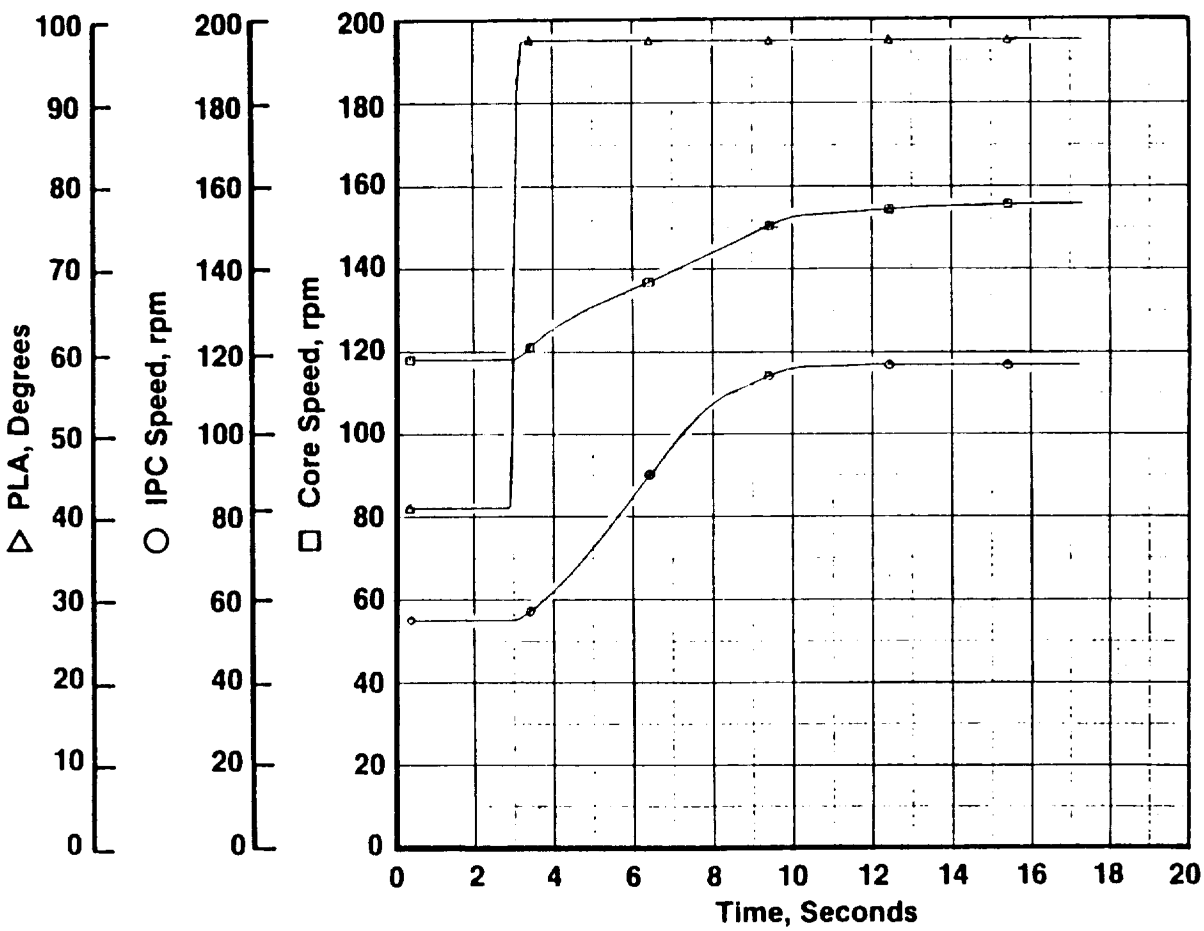


Figure 9-16. Throttle Burst.

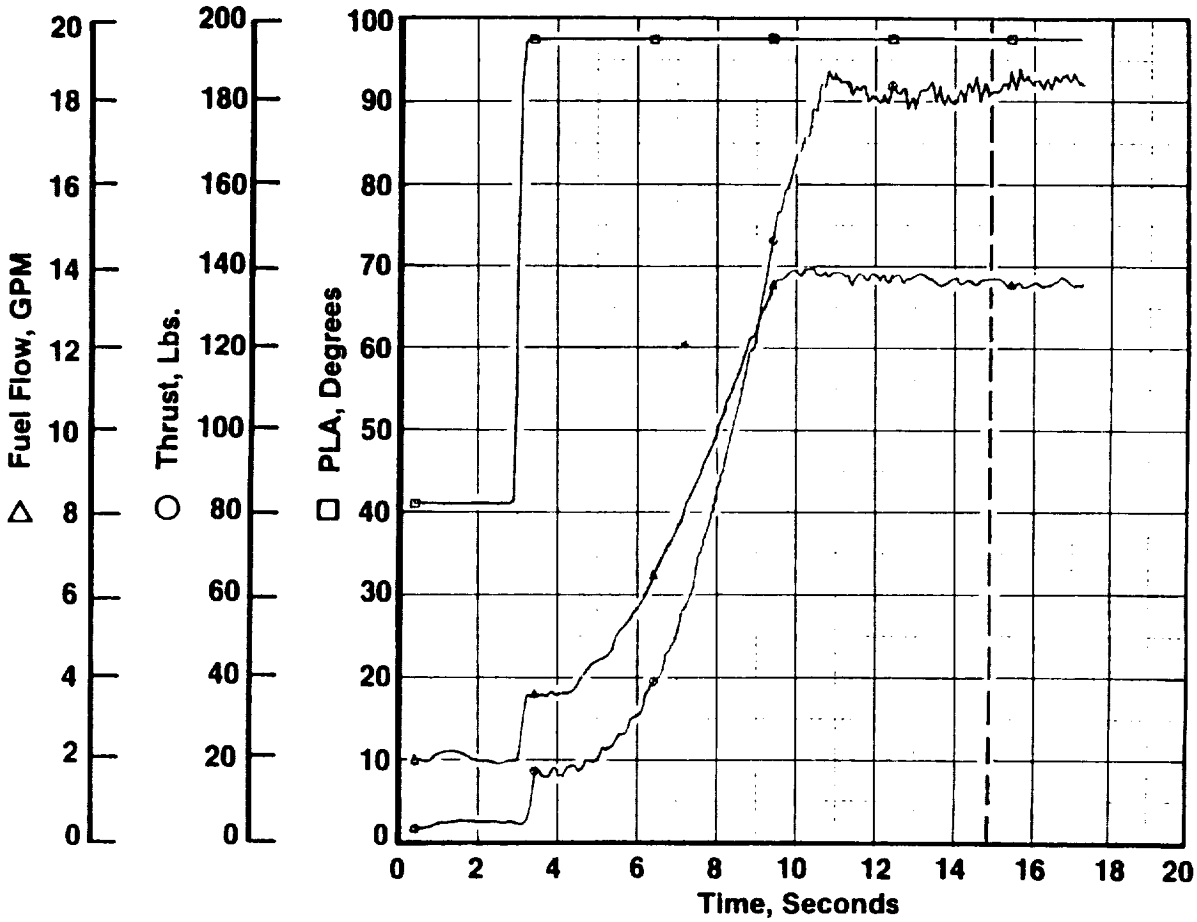


Figure 9-17. Throttle Burst.

# 10.0 NACELLE STRUCTURES

No problems occurred for any of the nacelle structures components during ground testing conducted at Peebles, Ohio.

The fan blade airfoil loss provided valuable data pertaining to the nacelle structural and dynamic integrity. No structural damage occurred, and the isolators absorbed the unbalance as expected. Based on data taken during the airfoil loss, the isolator/mount structure provided a minimum margin of safety of 0.47 and an average margin of safety of 2.54 for all components.

Strain measurements taken on the strut during ground testing revealed extremely low stress levels. The maximum stress level recorded, 1.4 kpsi peak to peak, corresponds to a margin of safety of 80.4 based on shear strengths of the strut material. The minimum margin of safety was found in the composite mid-fairing. Based on the interlaminar shear strength, this margin was 2.7, which is an acceptable figure. Based on the strain measurements, the acoustic fatigue of the strut and fairings was deemed to be of little concern.

## 10.1 FAN BLADE AIRFOIL LOSS

The fan blade airfoil loss incurred on February 9, 1986 caused a 262,000 gm-inch (577 lb-inch) unbalance load. This failure occurred at a fan speed of 1371 rpm and a thrust level of 24,000 pounds. Engine, isolator, mount beam, and strut accelerometers were located as shown in Figure 10-1.

At blade-out, the rear-mount horizontal vibration level reached 200 mils double amplitude, while its normal level is 10 mils. The front mount along the horizontal axis reached 95 mils, while its normal level is 15 mils. The engine was then chopped to idle (680 rpm) in 1.23 seconds, where it remained for 9.0 seconds before being shut down. Vibration levels of the vertical axes of the front and rear mounts reached 200 mils DA (double amplitude) from their normal levels of 2 mils each. As attested in Table 10-1, the maximum vibration levels occurred in the rigid body modes during coast down.

Mount loads were estimated based on relative motion across the isolators and on the isolator dynamic spring rates (from the Barry Qualification Test

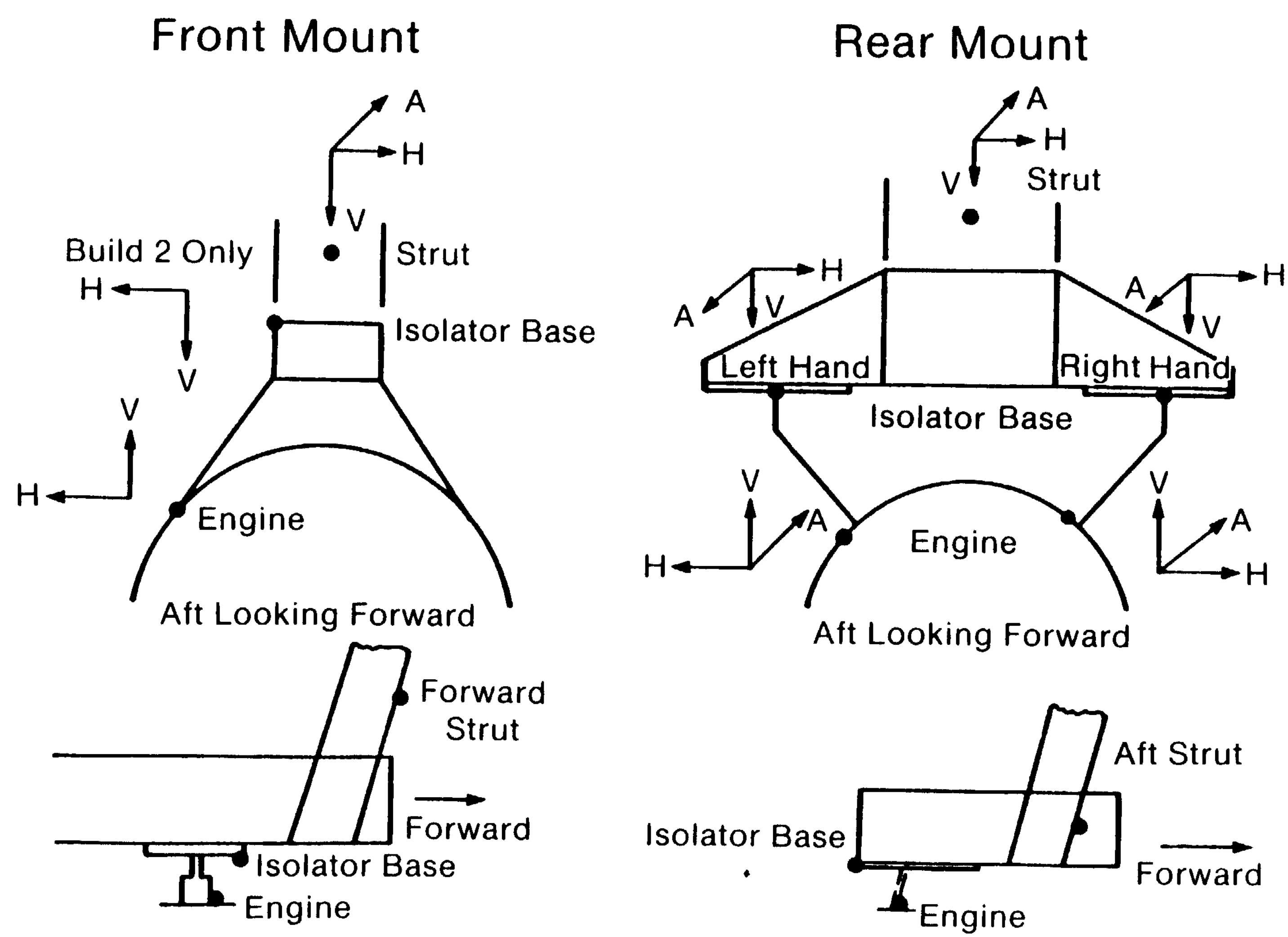


Figure 10-1. UDF™ Engine 082-001 Accelerometer Definition.

Report). Table 10-2 shows that these loads were well below the design loads. The minimum margin of safety turned out to be 0.47, which was for the rear mount along the axial axis at 460 rpm; the load it carried (40.9 kips) was the maximum load for the system. The average margin of safety for the isolators was 2.54.

Table 10-1. Vibration Response.

| Sensor | Displacement, mils DA | | |
|---|---|---|---|
| | 1370 rpm | Idle (680 rpm) | Coast Down (rpm) |
| Front Mount Vertical | 80 | 200 | 560 (460) |
| Front Mount Horizontal | 95 | 50 | 385 (280) |
| Right Rear Vertical | 170 | 200 | 450 (200) |
| Right Rear Horizontal | 200 | 105 | 165 (200) |
| Right Rear Axial | 95 | 330 | 980 (460) |
| Left Rear Vertical* | --- | --- | --- |
| Left Rear Horizontal | 120 | 130 | 430 (200) |
| Left Rear Axial* | --- | --- | --- |

* Sensor Inoperable Before Event

The overall response of the isolators indicated that they functioned as designed, significantly reducing the motion at the pylon/mount interface and softening with increased loading. The resonant speeds of the system decreased for the airfoil loss event. Further, the isolators reduced mount loads on the engine and pylon. These loads were well within design limits.

Physically, the isolators performed as designed during the airfoil loss. No wear or deformation of the isolator structure was incurred (or in any other structure). The Met-L-Flex wire mesh showed some minor deformation in the aft isolators. The mesh in the front isolator was undamaged. All isolators were sent to the manufacturer, Barry Controls, for inspection and testing. Despite the fact that all the load-deflection data for the isolators indicated little

Table 10-2. UDF™ Engine Mount Loads Due to Airfoil Loss.

| Mount | Direction | rpm | Relative Motion* | Dynamic Spring Rate, K | Resulting Load**, lb | Design Loads, lb | Margin of Safety |
|---|---|---|---|---|---|---|---|
| Front | Horizontal | 280 | 0.100 | 133 | 13,330 | 60,000 | 3.50 |
| Front | Vertical | 460 | 0.145 | 165 | 24,000 | 80,000 | 2.33 |
| Rear | Radial | 200 | 0.202 | 81.3 | 16,400 | 50,000 | 2.05 |
| Rear | Radial | 460 | 0.108 | 107 | 11,600 | 50,000 | 3.31 |
| Rear | Axial | 200 | 0.075 | 175 | 13,100 | 60,000 | 3.58 |
| Rear | Axial | 460 | 0.292 | 140 | 40,900 | 60,000 | 0.47 |

* Relative Motion Assumes Vibration in Phase Across Isolator
** Stiffness Data from Barry Qualification Test Report for Applied Loads and Deflections

change and were still within limits, the wire mesh in the aft isolators was replaced. The front isolators were used "as is."

Predictions that maximum loads would occur in subidle modes were verified. However, modes were not matched for the front mount (Tables 10-3 and 10-4). Also, as predicted, the highest load occurs on the aft mount in the axial direction. Both magnitude and speed were in good agreement with prediction; however, the front mount loads measured were higher than predicted.

## 10.2 STRAIN EVALUATION OF THE STRUT

Extensive strain tests were performed on various strut components during ground testing. Corresponding stress levels were calculated and recorded. As illustrated in Table 10-5, the greatest stress level recorded was in the upper middle portion of the mount beam at a high pressure compressor speed of 7800 rpm. This stress level, 1.4 kpsi peak-to-peak, is well within the acceptable levels and corresponds to a margin of safety of 80.4 (compared with the ultimate shear strength of the material of which it is made - AMS 5528 stainless steel). The minimum margin of safety occurs in the mid-fairing in the axial direction at an intermediate pressure compressor. The recorded stress level is 0.96 kpsi, peak-to-peak. This corresponds to a margin of safety of 2.7 with respect to the interlaminar shear strength.

Appendix B shows the range of data tested in terms of calculated stress versus frequencies and speeds; figures contained therein (Figures B-1 through and B-40) illustrate the positioning of the strain gages used. Note that some are arranged in rosettes; while others are uniaxial.

## 10.3 ACOUSTIC FATIGUE

A preliminary acoustic fatigue analysis of the strut fairing calculated a response frequency of 174 Hz (the fundamental blade passing frequency range for the engine operating range, 600 to 1400 rpm, is 80 to 187 Hz); however, this figure is questionable due to the numerous assumptions and uncertainties involved in the calculation. The operating conditions assumed were those of cruise. Further, the panel was assumed flat; whereas, a slight panel curvature or irregularity would increase the response frequency; finally, the damping ratio was estimated rather than known.

Table 10-3. UDF™ Engine Comparison of Mount Loads for Airfoil-Out Event.

| | Maximum Load | | | |
|---|---|---|---|---|
| | Modified Nastran Model | | Test Results* | |
| Location | Load, lb | rpm | Load, lb | rpm |
| FMV | 8,800 | 228 | 24,000 | 460 |
| FMH | 7,500 | 528 | 13,300 | 280 |
| RRMR | 10,500 | 228 | 16,400 | 260 |
| RRMA | 44,000 | 444 | 40,900 | 460 |
| LRMR | 12,000 | 228 | --- | --- |
| LRMA | 31,000 | 420 | --- | --- |

* Using Barry Mount Data and Relative Deflection, Unbalance = 262,000 gm-inch

Table 10-4. UDF™ Engine Airfoil-Out Event Comparison of Deflections (Absolute).

| | Maximum Displacement, mils DA | | | |
|---|---|---|---|---|
| | Modified Nastran Model | | Measured Test Results | |
| Location | Deflection, mils | rpm | Deflection, mils | rpm |
| FMV | 440 | 228 | 560 | 460 |
| FMH | 1120 | 540 | 385 | 280 |
| RRMR | 600 | 450 | 350 | 200 |
| RRMA | 1100 | 420 | 988 | 460 |
| LRMR | 750 | 228 | --- | --- |
| LRMA | 1100 | 420 | --- | --- |

Note: Unbalance = 262,000 gm-inch

Table 10-5. Stress Data - Strut.

| GAUGE | XN2 | XN25 | XN48 |
|---|---|---|---|
| FAIRING, VERT | 2 (0.37) | 3 (0.15) | 1 (0.15) |
| FAIRING, DIAG | 3 (0.056) | 3 (0.091) | 1 (0.54) |
| FAIRING, AXIAL | 2 (0.96) | 2 (0.20) | 2 (0.19) |
| FWD ISO | 3 (0.72) | 3 (0.74) | 1 (0.91) |
| RR OF SPAR, VERT | 0 | 0 | 4 (0.059)* |
| RR OF SPAR, DIAG | 0 | 0 | 4 (0.015)* |
| RR OF SPAR, HORIZ | 0 | 0 | 4 (0)* |
| SIDE OF SPAR, VERT | 0 | 0 | 4 (0.29)* |
| SIDE OF SPAR, HORZ | 0 | 0 | 4 (0.22)* |
| SIDE OF SPAR, DIAG | 0 | 0 | 4 (0.12)* |
| LT AFT ISO CLEVIS | 2 (0.53) | 2 (0.5)* | 4 (0.59) |
| MT BM,TOP AFT,VERT | 3 (0.12) | 3 (0.10) | 3 (0.65) |
| MT BM,TOP AFT,DIAG | 0 | 0 | 4 (0.12) |
| MT BM,TOP AFT,HORZ | 3 (0.20) | 3 (0.18) | 3 (0.20) |
| MT BM,BTM AFT,HORZ | 3 (0.22) | 2 (0.17) | 3 (0.23) |
| MT BM,TOP MID,HORZ | 3 (0.01) | 2 (1.4) | 2 (0.20) |
| MT BM,TOP MID, VERT | 3 (0.44) | 3 (0.42) | 2 (0.21) |
| MT BM,BTM FWD,VERT | 3 (0.14) | 3 (0.02) | 2 or 4 (0) |
| AFT MT BM SUPT FTG,HOR | 2 (1.08) | 2 (0.21) | 2 (0.10) |
| RT AFT ISO CLEVIS | 2 (0.08) | 3 (0.94) | 3 (0.92) |
| RT RR MT, TANG | 0 | 0 | 4 (0.66)* |
| RR OF SPAR,LWR AFT,VER | 3 (0.36) | 3 (0.41) | 3 (0.36) |
| SAME, HORIZ | 3 (0.18) | 3 (0.15) | 2 (0.17) |
| RR OF SPAR,UPR AFT,VER | 0 | 0 | 4 (0)* |
| SAME, DIAG | 0 | 0 | 4 (0.50)* |
| SAME, HORIZ | 0 | 0 | 4 (0.12)* |

CODES:

0: NO DATA AVAILABLE
1: START/ACCELERATE
2: START/ACCELERATE TO 700
3: ACCELERATE TO 24,400 LBS.
4: ACCELERATE TO 24K FG
*: ONLY ONE DATA POINT AVAILABLE

FORMAT IS: CODE # (MAXIMUM STRESS IN KPSI PP)

For instance, if the curvature of the panel was as slight as 99 inches, this frequency would then become 383 Hz. What is known is that strain gage data discussed in Section 10.2 and displayed in Appendix B, show that stresses are relatively low. Thus, there appears to be no resonant vibration within the operating range of the engine and that acoustic fatigue is not a problem.

# 11.0 RESULTS

The 100+ hour ground test program of the UDF™ engine demonstrated the following:

- 25,000 lbf installed corrected thrust
- High fuel efficiency: 0.232 lb/hr/lbf installed corrected sfc (specific fuel consumption)
- 15,000+ physical total shaft horsepower
- Full propulsor speed (1393+ rpm)
- Advanced UDF™ aerodynamics that incorporates custom-tailored composite fan blades over an inner titanium spar that serves as the attachment mechanism to the engine for the fan blades
- Individually replaceable propulsor fan blades with the engine installed on the aircraft or test stand
- DEC (digital electronic control) provides overall engine control by monitoring gas generator power and speed and propulsor speeds and pitch angles; the engine utilizes the existing gas generator control and a separate propulsor control to minimize development costs without sacrificing control flexibility; this control system drives a hydraulic/mechanical actuation system that permits setting the fan blade pitch angle of the two fan blade rotors either together or differentially
- Flawless operation of the F404 gas generator
- Counterrotation of structures, turbines, and fan blades
- Reverse thrust capability
- Capability to withstand a fan blade airfoil loss with no structural or secondary damage
- Failure of Stage 1 turbine blades and the subsequent damage to following turbine blade rows; turbine structures withstood the failures with little or no damage.

Also demonstrated were the following capabilities:

- Running at full power statically
- Data was repeatable statically

- Prediction of low speed, low pressure, counterrotating turbine performance with accuracy comparable to that of the high speed, conventional, low pressure turbines

- Comparing data recorded early and late in the LCF testing, performance deterioration was confined to a dirty IPC; there was no evidence of mechanical deterioration

- F404 gas generator provided repeatable and predictable performance and was better than predicted at lower powers (below 70% takeoff power)

- UDF™ blade performance sensitivity to rotational speed was much greater than predicted

- At power coefficient = 1.32, thrust coefficient was 4% better than predicted (approximately 60% takeoff power)

- At power coefficient = 1.95, thrust coefficient was 4% worse than predicted (approximately 100% takeoff power)

- Power turbine efficiency was approximately as predicted, being within +1.5 points over the major portion of the operating range; the flow function was within +0.5% of prediction at high powers (above 80% takeoff thrust)

- Overall performance was better than predicted up to 92% takeoff power (23,000 lbf corrected installed thrust), and was poorer than predicted beyond 92% takeoff power (23,000 lbf corrected installed thrust) due to UDF™ speed sensitivity as noted above

- At 60% takeoff thrust (15,000 lbf), sfc was approximately 5.50% better than predicted

- At 92% takeoff thrust (23,000 lbf), sfc was approximately as predicted

- At 100% takeoff thrust (25,000 lbf), sfc was nearly 4.00% worse than predicted.

## 12.0 CONCLUSIONS

As a result of the 100+ hour UDF™ test program, it can be concluded that all of the major objectives of this engine can be and have been met. Some of these objectives are as follows:

- The demonstrated feasibility of an unducted, ungeared, counter-rotating ultra-high-bypass turbofan
- Capability to produce at least 25,000 lbf and at least 15,000 shaft horsepower with an engine of this configuration
- Exceptional fuel efficiency as compared to other turbofan or turbojet engines
- The capability to produce thrust with a new fan blade design of composite materials over a titanium spar
- The capability to control the engine and actuate the fan blades with a digital electronic control
- Capability to produce reverse thrust with the fan blades without the use of a thrust reverser
- UDF™ propulsor capable of producing thrust as predicted
- Current computer model cycle deck techniques can adequately model a counterrotating turbofan
- Propulsor deterioration (large seals, turbine, etc.) was not encountered over the duration of testing, which exceeded 100 hours
- Operation of the engine, and its performance, is stable at takeoff power statically.

As expected in an engine program utilizing such new technologies and concepts as the UDF™, numerous problems have been discovered. However, it is believed that none of these problems will present a major stumbling block to future flight test of this engine or to the development of this concept into an important new entry into the arena of subsonic commercial and military transport aircraft. Every problem that has occurred during ground testing has been addressed and adequately solved. Fine tuning may be necessary, and more problems may be discovered of course, as the testing of this engine continues. No significant fundamental aerodynamic or control problems were uncovered, and only two mechanical problems created significant setbacks to the test program. Both of these problems were solved by rather simple, but successful means:

1. Fan Blade Airfoil Loss - Although static component tests verified the integrity of the airfoil bonding to the titanium spar, actual engine testing brought into effect additional factors leading to the loss of one airfoil. At that time, only the adhesive qualities of the composite to titanium bonding agent held the airfoil to the spar. By adding positive retention features to the design (by adding fasteners), airfoil retention proved to be of no problem for the duration of testing and is not expected to present a problem in the future.

2. Turbine Blade Failure - Stage 1 turbine blade dynamic response was excessive due to insufficient damping, which eventually led to their failure. Damping, in the form of friction, was introduced to all blade rows by placing simple damper pins between each blade; this satisfactorily reduced the dynamic response.

## 13.0 SYMBOLS/ABBREVIATIONS

| | |
|---|---|
| ALF | Aft, Looking Forward |
| Beta Angle | Fan Blade Pitch Angle, degrees |
| BFM | Backflow Margin, % |
| BTAN91 | Front Rotor Pitch, degrees |
| BTAN92 | Rear Rotor Pitch, degrees |
| BTWT | Boeing Transonic Wind Tunnel |
| CV | Convex |
| DA | Double Amplitude |
| DEC | Digital Electronic Control |
| dia. | Diameter |
| DMS | Data Management System |
| DOD | Domestic Object Damage |
| DTAMB | ΔT from Standard Day/ISA Conditions |
| EB | Electron Beam |
| EDM | Electrical Discharge Machining |
| EPR | Engine Pressure Ratio |
| F404 Fan | Bypass Pressure Ratio |
| F404-GE-400 | Low Bypass Turbofan Gas Generator |
| FHV | Fuel Heating Valve |
| FMH | Front Mount, Horizontal |
| FMV | Front Mount, Vertical |
| FNI1QA | Installed Thrust, lb |
| FPI | Fluorescent Particle Inspection |
| $F_{sep}$ | Flow Separation Parameter |
| h | Coefficient of Heat Transfer (Btu/hr ft$^2$, ° F) |
| HCF | High Cycle Fatigue |
| Hz | Hertz, cycles/second |
| ID | Inner Diameter |
| 1F | First-Flexural Frequency, cycles/second |
| IGV | Inlet Guide Vanes |
| IPC | Intermediate Pressure Compressor |
| 1T | First-Torsional Frequency, cycles/second |
| LCF | Low Cycle Fatigue |

| | |
|---|---|
| LE | Leading Edge |
| LPT | Low Pressure Turbine |
| LRMA | Left Rear Mount, Axial |
| LRMR | Left Rear Mount, Radial |
| LRMV | Left Rear Mount, Vertical |
| LVDT | Linear Variable Differential Transducer |
| Max | Maximum |
| Min | Minimum |
| Mn | Mach Number |
| MPI | Magnetic Particle Inspection |
| OGV | Outlet Guide-Vanes |
| ON | 0-Nodal |
| P15/Pz | F404 Fan Bypass Pressure Ratio |
| P46Q2 | Gas Generator Pressure Ratio |
| P48Q2 | Engine Pressure Ratio |
| PLA | Power Lever Angle, degrees |
| $P_o$ | Ambient Pressure, psi |
| PRS | Stall Pressure Ratio |
| $P_s$ | Static Pressure, psi |
| PS3 | Gas Generator Compressor Discharge Pressure, psi |
| PT | Total Pressure, psi ... (also Power Turbine) |
| $PT_8$ | Power Turbine Exhaust Pressure, psi |
| PTO | Peebles Test Operation |
| $P_z$ | Compressor Inlet Pressure, psi |
| RDGS | Readings |
| RRMA | Right Rear Mount, Axial |
| RRMR | Right Rear Mount, Radial |
| S/D | Shutdown |
| sfc | Specific Fuel Consumption, lb/hr/lb |
| SFCI1R | Installed Specific Fuel Consumption, lb/lb |
| SG | Strain Gage |
| S/N | Serial Number |
| T46 | Propulsor Exhaust Gas Temperature, ° F |
| T46Q2 | Gas Generator Temperature Ratio |
| $T_{Amb}$ | Ambient Temperature, ° F |

| | |
|---|---|
| TAAP01 | Stage 1 Fan Telemetry Ring Cavity Thermocouple, ° F |
| TAAP02 | Stage 2 Fan Telemetry Ring Cavity Thermocouple, ° F |
| TAFC01 | Stage 1 Fan Telemetry Ring Cavity Thermocouple, ° F |
| TE | Trailing Edge |
| TT | Total Temperature, ° F |
| 2R | No. 2 Roller |
| UDF™ | GE36 Unducted Fan Engine |
| $W_{25}$ | HPC Inlet Flow, lb/second |
| W48R | Power Turbine Flow Function, Corrected |
| $X_h$ | Horizontal Displacement, inch |
| $X_v$ | Vertical Displacement, inch |
| XN48 | Stage 1 Propulsor Fan Speed, rpm |
| XN49 | Stage 2 Propulsor Fan Speed, rpm |
| ZN | Z-Nodal |

## 14.0 References


1. Carlson, S.L., "Engine Damage Report," No. GE36-003, March 18, 1986.

2. Carlson, S.L., "Engine Damage Report," No. GE36-004, August 14, 1986.

3. Cote, M.J., "GE36 Nacelle Fairing Sonic Fatigue Analysis," Memo of July 24, 1986.

4. Gaffney, E., Review of Airfoil Loss, "In The Unducted Fan Engine; GE Quarterly Review No. 8," May 13, 1986.

5. General Electric, "Full-Scale Technology Demonstration of a Modern Counterrotating Unducted Fan Engine Concept - Component Test," NASA Contract No. NAS3-24210, CR-180868, December 1987.

6. General Electric, "Full-Scale Technology Demonstration of a Modern Counterrotating Unducted Fan Engine Concept - Design," NASA Contract No. NAS3-24210, CR-180867, December 1987.

7. General Electric, "The Unducted Fan Engine - Quarterly Review No. 6, "NASA Contract No. NAS3-24210, August 16, 1985.

8. General Electric, "The Unducted Fan Engine - Quarterly Review No. 7," NASA Contract No. NAS3-24210, November 18, 1986.

9. General Electric, "The Unducted Fan Engine - Quarterly Review No. 8," NASA Contract No. NAS3-24210, May 13, 1987.

10. General Electric, "UDF™ Airworthiness Executive Review," NASA Contract No. NAS3-24210, July 1986.

11. Kirkpatrick, R.A., "Failure Report: Engine S/N 082-001/A: High Power Stall of October 2, 1985," December 13, 1985.

12. Kroger, J.P., "GE36 Second Ground Test," Test Project Sheet No. MA-004, January 13, 1986.

13. Nelson, E. (Barry Controls), "Qualification Test Report for 94624 Engine Isolators: GE-36 Demonstrator Engine Program," Document No. WD04624-1-005, Revision A, May 14, 1986.

14. Smith, R.E., "Engine Damage Report," No. GE36-002, Revision A, January 6, 1986.

# APPENDIX A

## STEADY-STATE TEST DATA - BUILD 3

## DATA LEGEND

| | |
|---|---|
| XN2 | IPC Physical Speed (rpm) |
| XN2R | IPC Corrected Speed (rpm) |
| PCN2R | Percent IPC Corrected Speed (%) |
| XN25 | HPC Physical Speed (rpm) |
| XN25R | HPC Corrected Speed (rpm) |
| PCN25R | Percent HPC Corrected Speed (%) |
| XN48 | Stage 1 Physical Speed (rpm) |
| XN49 | Stage 2 Physical Speed (rpm) |
| UT91R2 | Corrected Stage 1 Tip Speed (feet/second) |
| UT92R2 | Corrected Stage 2 Tip Speed (feet/second) |
| BTAN91 | Stage 1 Pitch Angle (degree) |
| BTAN92 | Stage 2 Pitch Angle (degree) |
| W13 | Bypass Duct Inlet Flow (lb/second) |
| W15 | Bypass Duct Exit Flow (lb/second) |
| WF36 | Fuel Flow (lb/hr) |
| WF36R2 | Corrected Fuel Flow (lb/hr) |
| FNI1QA | Corrected Installed Net Thrust (lb) |
| SFC184 | Corrected Installed Net Specific Fuel Consumption, FHV = 18,400 ($lb_{fuel}/lb_{thrust}$ hr) |
| TAMB | Ambient Temperature (° R) |
| T10 | Inlet Total Temperature (° R) |
| PAMB | Ambient Pressure (psia) |
| P10M | Inlet Total Pressure (psia) |
| HUMSER | Specific Humidity (grains/lb dry air) |
| RELHUM | Relative Humidity (%) |
| WINVAV | Average Wind Velocity (knots) |
| WINAAV | Average Wind Angle (degree) |
| XM0 | Mach Number |
| P46Q2 | Engine Pressure Ratio |
| CT46 | Calculated T46 (° R) |
| T46X | Measured T46 (° R) |

GE36/UDF-1 ENGINE 082001-03 TEST READINGS - SITE IIID
RDGS. 1 - 5 ON 06.20.86 RDGS. 6 - 15 ON 06.23.86
RDGS. 16 - 31 ON 06.24.86 RDGS. 32 - 47 ON 06.25.86
RDGS. 48 - 57 ON 06.26.86

| RDG. | 1 | 2 | 3 | 4 | 5 | 6 | 7 | 8 | 9 | 10 | 11 | 12 | 13 |
|---|---|---|---|---|---|---|---|---|---|---|---|---|---|
| XN2 | 0. | 724.28 | 538.03 | 4106.5 | 463.39 | 0. | 5592.4 | 5437.6 | 419.28 | 0. | 5470.1 | 678.21 | 678.21 |
| XN2R | 0. | 715.61 | 531.53 | 4072.5 | 457.43 | 0. | 5494.1 | 5337.1 | 410.45 | 0. | 5352.8 | 660.62 | 659.56 |
| PCN2R | 0. | 5.3927 | 4.0055 | 30.689 | 3.4471 | 0. | 41.402 | 40.219 | 3.0931 | 0. | 40.338 | 4.9783 | 4.9703 |
| XN25 | 0. | 85.38 | 118.9 | 10619. | 136.19 | 0. | 11776. | 11682. | 164.48 | 0. | 11717. | 143.52 | 143.52 |
| XN25R | 0. | 83.918 | 116.82 | 10258. | 129.41 | 0. | 11060. | 10988. | 158.22 | 0. | 10986. | 136.45 | 137.85 |
| PCN25R | 0. | .62532 | .8705 | 76.439 | .96428 | 0. | 82.416 | 81.881 | 1.179 | 0. | 81.863 | 1.0168 | 1.0272 |
| XN48 | 0. | 467.89 | 96.579 | 699.9 | 415.38 | 0. | 700.16 | 700.03 | 558.84 | 0. | 700.16 | 164.09 | 164.09 |
| XN49 | 0. | 0. | 10.314 | 687.04 | 699.49 | 0. | 700.43 | 700.3 | 700.43 | 0. | 700.43 | 699.49 | 699.49 |
| UT91R2 | 0. | 283.89 | 58.591 | 426.24 | 251.8 | 0. | 422.41 | 421.93 | 335.95 | 0. | 420.75 | 98.153 | 97.995 |
| UT92R2 | 0. | 0. | 6.0822 | 406.7 | 412.16 | 0. | 410.74 | 410.28 | 409.28 | 0. | 409.12 | 406.7 | 406.04 |
| BTAN91 | 80.59 | 86.6 | 86.734 | 9.8483 | 86.65 | 80.343 | 18.191 | 17.743 | 86.664 | 86.96 | 17.788 | 86.939 | 86.959 |
| BTAN92 | 80.306 | 86.093 | 86.22 | 10.089 | 86.082 | 80.266 | 19.719 | 19.041 | 86.52 | 86.764 | 19.118 | 86.701 | 86.731 |
| W13 | -.5 | -4.7497 | -5.4954 | 3.7509 | -5.497 | -.5 | 5.7381 | 5.4167 | -6.1277 | -.5 | 5.823 | -5.0419 | -5.1496 |
| W15 | 0. | -4.7497 | -5.4954 | 3.7509 | -5.497 | 0. | 5.7381 | 5.4167 | -6.1277 | 0. | 5.5897 | -5.0419 | -5.1496 |
| WF36 | 168.08 | 169.44 | 177.48 | 663.98 | 179.74 | 140.34 | 880.3 | 830.57 | 149.38 | 130.13 | 845.05 | 139.24 | 141.05 |
| WF36R2 | 169.66 | 172.06 | 180.04 | 677.01 | 182.03 | 140.96 | 889.74 | 838.42 | 150.21 | 129.07 | 850.25 | 139.21 | 140.8 |
| FN11QA | 0. | 0. | 0. | 690.66 | 0. | 10.518 | 2568.2 | 2289.3 | 0. | -2.7313 | 2321.9 | 0. | -.79557 |
| SFC184 | .5 | .5 | .5 | .9909 | .5 | 13.547 | .35022 | .37021 | .5 | -47.77 | .37016 | .5 | -178.9 |
| TAMB | 533.63 | 531.26 | 528.48 | 528.52 | 527.4 | 540.77 | 540.58 | 541.32 | 541.48 | 544.74 | 544.7 | 542.62 | 542.5 |
| T10 | 536.3 | 531.32 | 531.44 | 527.37 | 532.27 | 541.85 | 537.4 | 538.4 | 541.24 | 552.43 | 541.65 | 546.66 | 548.43 |
| PAMB | 14.24 | 14.247 | 14.258 | 14.263 | 14.266 | 14.204 | 14.204 | 14.203 | 14.203 | 14.198 | 14.19 | 14.188 | 14.179 |
| P10M | 14.24 | 14.247 | 14.258 | 14.263 | 14.267 | 14.209 | 14.204 | 14.204 | 14.205 | 14.199 | 14.192 | 14.189 | 14.18 |
| HUMSER | 67.567 | 64.473 | 59.714 | 57.572 | 58.289 | 113.7 | 107.7 | 112.01 | 110.48 | 93.645 | 96.205 | 91.979 | 94.29 |
| RELHUM | 52.566 | 54.392 | 55.479 | 53.464 | 56.263 | 68.958 | 65.825 | 66.756 | 65.532 | 50.176 | 51.546 | 52.73 | 54.202 |
| WINVAV | 7.3229 | 1.049 | 3.2623 | 2.6296 | 7.8227 | 2.4738 | 1.3076 | 5.6358 | 7.6706 | 4.0519 | 6.0543 | 4.6921 | 3.7711 |
| WINAAV | 161.53 | 117.66 | 149.43 | -139.57 | -165.66 | -128.1 | -152.9 | -12.692 | -9.4649 | -20.213 | 16.952 | -9.6835 | -17.435 |
| XMO | 0. | 0. | 0. | 0. | 0. | 0. | 0. | 0. | 0. | 0. | 0. | 0. | 0. |
| P46Q2 | 9.99+10 | 1.0011 | 1.0009 | 1.1009 | 1.0015 | 9.99+10 | 1.1953 | 1.1829 | 1.0013 | 9.99+10 | 1.1846 | 1.0012 | 1.0012 |
| CT46 | 9.99+10 | 846.28 | 870.65 | 1380.1 | 946.53 | 9.99+10 | 1347.7 | 1316.4 | 844.7 | 9.99+10 | 1341.4 | 830.16 | 814.5 |
| T46X | 537.98 | 685.03 | 568.15 | 1399.2 | 735.01 | 538.85 | 1326. | 1280.8 | 720.45 | 630.92 | 1311.6 | 703.99 | 629.3 |
| Comments | Zero | Zero | Zero | GI Speeds Mis-matched | Zero | Zero | F.I. | F.I. | Zero | Zero | F.I. | Zero | Zero |

GE36/UDF1 Peebles Tests
082001-03
Test Log - Site IIID
Sheet 001 of 029

GE36/UDF-1 ENGINE 082001-03 ...ST READINGS - SITE IIID
RDGS. 1 - 5 ON 06.20.86 RDGS. 6 - 15 ON 06.23.86
RDGS. 16 - 31 ON 06.24.86 RDGS. 32 - 47 ON 06.25.86
RDGS. 48 - 57 ON 06.26.86

| RDG. | 14 | 15 | 16 | 17 | 18 | 19 | 20 | 21 | 22 | 23 | 24 | 25 | 26 |
|---|---|---|---|---|---|---|---|---|---|---|---|---|---|
| XN2 | 5464.4 | 9157.2 | 10594. | 11096. | 0. | 5640.4 | 11030. | 102.86 | 0. | 5565.5 | 7339.5 | 8563.4 | 9888.7 |
| XN2R | 5355.1 | 8982.9 | 10391. | 10887. | 0. | 5573.1 | 10889. | 100.61 | 0. | 5481.9 | 7231.8 | 8436.6 | 9741.6 |
| PCN2R | 40.355 | 67.693 | 78.305 | 82.039 | 0. | 41.998 | 82.061 | .75816 | 0. | 41.31 | 54.497 | 63.577 | 73.411 |
| XN25 | 11705. | 13776. | 14647. | 15125. | 0. | 11770. | 15027. | 130.95 | 0. | 11757. | 12778. | 13462. | 14145. |
| XN25R | 10990. | 12134. | 12466. | 12615. | 0. | 11104. | 12582. | 123.74 | 0. | 11073. | 11697. | 12038. | 12307. |
| PCN25R | 81.891 | 90.42 | 92.889 | 94.001 | 0. | 82.739 | 93.757 | .92206 | 0. | 82.512 | 87.159 | 89.703 | 91.707 |
| XN48 | 700.16 | 906.58 | 1124.3 | 1269.2 | 0. | 699.9 | 1260.9 | 156.59 | 0. | 653.68 | 752. | 850.99 | 1006.5 |
| XN49 | 700.3 | 906.98 | 1124.8 | 1269.6 | 0. | 101.27 | 1261.3 | 126.58 | 0. | 784.82 | 852.33 | 951.46 | 1106.7 |
| UT91R2 | 421.37 | 546.13 | 677.17 | 764.69 | 0. | 424.68 | 764.46 | 94.058 | 0. | 395.39 | 455.02 | 514.85 | 608.9 |
| UT92R2 | 409.65 | 531.08 | 658.53 | 743.52 | 0. | 59.726 | 743.29 | 73.907 | 0. | 461.42 | 501.29 | 559.52 | 650.77 |
| BTAN91 | 17.724 | 28.578 | 29.471 | 29.782 | 86.903 | 18.901 | 30.295 | 86.876 | 87.148 | 19.486 | 24.846 | 27.131 | 28.71 |
| BTAN92 | 18.905 | 27.823 | 29.082 | 29.48 | 86.343 | 19.646 | 29.328 | 86.675 | 86.833 | 17.808 | 22.558 | 24.972 | 26.231 |
| W13 | 5.4412 | 10.14 | 12.192 | 12.982 | -.5 | 5.6613 | 13.867 | -7.1572 | -.5 | 5.1598 | 7.6467 | 9.3194 | 10.825 |
| W15 | 5.4412 | 10.14 | 12.192 | 12.982 | 0. | 5.6613 | 13.867 | -7.1572 | 0. | 5.1598 | 7.6467 | 9.3194 | 10.825 |
| WF36 | 837.38 | 2055.5 | 3174. | 4082.5 | 151.5 | 885.12 | 4239.2 | 168.65 | 155.66 | 851.31 | 1304.5 | 1767.7 | 2531.2 |
| WF36R2 | 845.25 | 2079.1 | 3210.5 | 4131.7 | 154.48 | 902.04 | 4318.3 | 169.43 | 152.97 | 862.89 | 1322.7 | 1792.4 | 2566.6 |
| FN11QA | 2356.6 | 8283. | 13222. | 16953. | 24.588 | 2657.8 | 17329. | 28.652 | 0. | 2541.3 | 4972.7 | 7220.3 | 10661. |
| SFC184 | .36258 | .25373 | .24545 | .24636 | 6.3511 | .34309 | .25191 | 5.9776 | .5 | .34324 | .26888 | .25094 | .24337 |
| TAMB | 542.03 | 540.8 | 540.39 | 540.05 | 531.95 | 534.21 | 534.67 | 534.29 | 537.82 | 538.13 | 537.39 | 537.62 | 537.94 |
| T10 | 540.04 | 538.99 | 539.12 | 538.81 | 531.03 | 531.27 | 532.11 | 542.11 | 558.92 | 534.62 | 534.24 | 534.38 | 534.45 |
| PAMB | 14.174 | 14.168 | 14.168 | 14.168 | 14.192 | 14.199 | 14.199 | 14.2 | 14.215 | 14.216 | 14.217 | 14.217 | 14.218 |
| P10M | 14.175 | 14.169 | 14.169 | 14.169 | 14.192 | 14.199 | 14.199 | 14.201 | 14.215 | 14.215 | 14.218 | 14.218 | 14.217 |
| HUMSER | 100.3 | 93.586 | 92.396 | 93.213 | 78.5 | 72.215 | 74.879 | 73.064 | 69.305 | 63.729 | 61.38 | 60.926 | 59.919 |
| RELHUM | 58.446 | 56.828 | 56.857 | 57.994 | 64.243 | 54.882 | 56.003 | 55.365 | 46.801 | 42.659 | 42.117 | 41.503 | 40.402 |
| WINVAV | 2.4232 | 4.4413 | 2.3847 | 4.2043 | 1.5986 | 1.5115 | 2.5894 | 7.6595 | 3.5378 | 2.942 | 2.4333 | 3.019 | 2.2477 |
| WINAAV | 11.632 | -35.053 | 26.309 | 7.1803 | -26.477 | 55.17 | -83.301 | 163.33 | 134.12 | 127.02 | -125.73 | 107.3 | 146.92 |
| XMO | 0. | 0. | 0. | 0. | 0. | 0. | 0. | 0. | 0. | 0. | 0. | 0. | 0. |
| P46Q2 | 1.1847 | 1.7205 | 2.1604 | 2.4895 | 9.99+10 | 1.2022 | 2.4854 | 1.0023 | 9.99+10 | 1.1955 | 1.3712 | 1.5572 | 1.9082 |
| CT46 | 1327.5 | 1476.2 | 1624. | 1722.5 | 9.99+10 | 1329.4 | 1771.3 | 942.82 | 9.99+10 | 1306.5 | 1352.9 | 1416.4 | 1538.4 |
| T46X | 1285.9 | 1472.8 | 1620.9 | 1707.5 | 544.7 | 1303.5 | 1738.4 | 740.19 | 619.62 | 1266.3 | 1333.6 | 1411. | 1536.6 |
| Comments | F.I. | Part Power | Part Power | Part Power | Zero | F.I. Bad XN49 | Part Power Unstable Data Acq. Incomplete | Zero | Zero | F.I. | Part | Part | Part |

Field Balance Run--------------→
Mismatched Speeds: (XN48-XN49)→
-130 -100 -100 -100

GE36/UDF1 Peebles Tests
082001-03
Test Log - Site IIID
Sheet 002 of 029

GE36/UDF-1 ENGINE 082001-03 .ST READINGS - SITE IIID
RDGS. 1 - 5 ON 06.20.86 RDGS. 6 - 15 ON 06.23.86
RDGS. 16 - 31 ON 06.24.86 RDGS. 32 - 47 ON 06.25.86
RDGS. 48 - 57 ON 06.26.86



| RDG. | 27 | 28 | 29 | 30 | 31 | 32 | 33 | 34 | 35 | 36 | 37 | 38 | 39 |
|---|---|---|---|---|---|---|---|---|---|---|---|---|---|
| XN2 | 10459. | 10799. | 86.428 | 86.428 | 0. | 1428.9 | 10355. | 9021.2 | 9050.5 | 9039.1 | 9038.7 | 9987. | 9991.3 |
| XN2R | 10301. | 10636. | 84.374 | 82.518 | 0. | 1421.2 | 10379. | 9020.6 | 9052.9 | 9029.8 | 9033. | 9975. | 9983.3 |
| PCN2R | 77.626 | 80.147 | .63583 | .62184 | 0. | 10.71 | 78.216 | 67.978 | 68.221 | 68.047 | 68.07 | 75.169 | 75.232 |
| XN25 | 14513. | 14844. | 87.999 | 87.999 | 0. | 4192. | 14370. | 13571. | 13576. | 13561. | 13557. | 14070. | 14074. |
| XN25R | 12437. | 12553. | 83.484 | 79.618 | 0. | 4061.2 | 12488. | 12172. | 12174. | 12168. | 12171. | 12356. | 12366. |
| PCN25R | 92.674 | 93.541 | .62209 | .59328 | 0. | 30.262 | 93.058 | 90.704 | 90.718 | 90.669 | 90.694 | 92.072 | 92.143 |
| XN48 | 1103.1 | 1199. | 642.3 | 642.3 | 0. | 7503.2 | 1105.1 | 899.22 | 903.37 | 900.15 | 900.69 | 1020.3 | 1020.2 |
| XN49 | 1203.6 | 1299.9 | 880.46 | 880.46 | 0. | 7503.2 | 1205.4 | 899.62 | 903.64 | 900.15 | 900.69 | 1020.2 | 1020.7 |
| UT91R2 | 667.17 | 725.18 | 385.06 | 376.59 | 0. | 4582.8 | 680.23 | 552.17 | 554.9 | 552.21 | 552.76 | 625.81 | 625.98 |
| UT92R2 | 707.55 | 764.17 | 513.06 | 501.77 | 0. | 4454.5 | 721.21 | 536.95 | 539.52 | 536.75 | 537.28 | 608.21 | 608.78 |
| BTAN91 | 29.606 | 29.612 | 87.178 | 87.148 | 87.293 | 87.041 | 28.448 | 27.449 | 27.41 | 27.83 | 27.327 | 28.63 | 28.163 |
| BTAN92 | 26.429 | 27.133 | 86.911 | 86.862 | 86.81 | 86.664 | 27.61 | 28.784 | 28.681 | 28.276 | 28.796 | 28.907 | 29.346 |
| W13 | 11.639 | 12.499 | -7.3808 | -7.3892 | -.5 | -1.029 | 12.349 | 10.64 | 10.607 | 11.284 | 11.549 | 11.734 | 11.687 |
| W15 | 11.639 | 12.499 | -7.3808 | -7.3892 | 0. | -1.029 | 12.349 | 10.64 | 10.607 | 11.078 | 11.014 | 11.734 | 11.687 |
| WF36 | 3039.1 | 3587.3 | 157.31 | 157.21 | 183.17 | 198.39 | 3131.1 | 2033.4 | 2045.6 | 2029.2 | 2028.2 | 2629.1 | 2623.5 |
| WF36R2 | 3080.8 | 3636.7 | 157.44 | 152.6 | 185.99 | 202.51 | 3232.2 | 2091.4 | 2104.8 | 2084.2 | 2084.3 | 2699.8 | 2695.5 |
| FNI1QA | 12914. | 15388. | -18.641 | 0. | 0. | 0. | 13639. | 8553.6 | 8673.7 | 8490.5 | 8518.6 | 0. | 11201. |
| SFC184 | .24115 | .2389 | -8.5379 | .5 | .5 | .5 | .23956 | .24717 | .2453 | .24814 | .24733 | .5 | ,24327 |
| TAMB | 538.65 | 538. | 538.63 | 535.62 | 526.33 | 516.58 | 518.34 | 521. | 521.69 | 522.59 | 522.05 | 522.47 | 522.06 |
| T10 | 534.71 | 534.7 | 544.23 | 568.99 | 531.55 | 524.32 | 516.24 | 518.74 | 518.4 | 519.74 | 519.33 | 519.92 | 519.5 |
| PAMB | 14.218 | 14.218 | 14.217 | 14.216 | 14.243 | 14.303 | 14.305 | 14.306 | 14.307 | 14.308 | 14.308 | 14.307 | 14.308 |
| P10M | 14.218 | 14.219 | 14.217 | 14.217 | 14.243 | 14.303 | 14.305 | 14.307 | 14.308 | 14.308 | 14.308 | 14.308 | 14.309 |
| HUMSER | 63.709 | 58.369 | 58.647 | 62.419 | 54.582 | 54.975 | 55.327 | 53.95 | 55.151 | 57.086 | 54.901 | 54.97 | 54.782 |
| RELHUM | 41.92 | 39.282 | 38.662 | 45.404 | 54.616 | 77.959 | 73.638 | 65.351 | 65.172 | 65.345 | 64.063 | 63.215 | 63.905 |
| WINVAV | 2.6083 | 4.0917 | 2.8129 | 4.172 | 1.3197 | 3.3211 | 7.5184 | 8.0547 | 8.1916 | 2.9925 | 7.4772 | 2.0767 | 6.5725 |
| WINAAV | 152.35 | 126. | 115.17 | 170.07 | 117.78 | -112.9 | 158.21 | 161.3 | 166.22 | -121.28 | 167.49 | -105.78 | -155.82 |
| XMO | 0. | 0. | 0. | 0. | 0. | 0. | 0. | 0. | 0. | 0. | 0. | 0. | 0. |
| P46Q2 | 2.1108 | 2.333 | 1.0018 | 1.0009 | 9.99+10 | 1.0016 | 2.156 | 1.723 | 1.7323 | 1.7243 | 1.7179 | 1.947 | 1.9494 |
| CT46 | 1598.1 | 1654.7 | 910.17 | 902.39 | 9.99+10 | 917.27 | 1563.1 | 1414.9 | 1412.8 | 1411.4 | 1409.5 | 1506.6 | 1500.7 |
| T46X | 1596.4 | 1649.9 | 738.79 | 629.72 | 573.68 | 549.73 | 1562.7 | 1414.2 | 1414.3 | 1412.2 | 1409.9 | 1508.5 | 1504.4 |
| Comments | Part Power Field Balance Run (cont'd) Mismatched Speeds -100 | Part Power -100 | Zero | Zero | Zero | Zero | Part Power Field Bal. Mismatched Speed -100 | Part Power Bleed Evaluation Stroke = 0% | Part Power 0% | Part Power 35% | Part Power 80% | Part Power 0% No FN | Part Power 0% |

GE36/UDF1 Peebles Tests
082001-03
Test Log - Site IIID
Sheet 003 of 029

GE36/UDF-1 ENGINE 082001-03 .ST READINGS - SITE IIID
RDGS. 1 - 5 ON 06.20.86 RDGS. 6 - 15 ON 06.23.86
RDGS. 16 - 31 ON 06.24.86 RDGS. 32 - 47 ON 06.25.86
RDGS. 48 - 57 ON 06.26.86

ORIGINAL PAGE IS OF POOR QUALITY

| RDG. | 40 | 41 | 42 | 43 | 44 | 45 | 46 | 47 | 48 | 49 | 50 | 51 | 52 |
|---|---|---|---|---|---|---|---|---|---|---|---|---|---|
| XN2 | 10012. | 10016. | 9991.5 | 10705. | 10690. | 10700. | 10705. | 587.5 | 0. | 6032.6 | 11321. | 11315. | 11325. |
| XN2R | 9999.2 | 9995.8 | 9963.3 | 10668. | 10658. | 10670. | 10657. | 583.94 | 0. | 6016.1 | 11251. | 11246. | 11246. |
| PCN2R | 75.352 | 75.327 | 75.081 | 80.388 | 80.318 | 80.404 | 80.307 | 4.4004 | 0. | 45.336 | 84.783 | 84.747 | 84.747 |
| XN25 | 14056. | 14080. | 14049. | 14703. | 14641. | 14655. | 14651. | 126.24 | 0. | 11888. | 15291. | 15283. | 15284. |
| XN25R | 12370. | 12369. | 12372. | 12560. | 12555. | 12575. | 12573. | 122.95 | 0. | 11246. | 12714. | 12754. | 12783. |
| PCN25R | 92.178 | 92.169 | 92.188 | 93.593 | 93.558 | 93.702 | 93.687 | .9162 | 0. | 83.798 | 94.736 | 95.039 | 95.256 |
| XN48 | 1017.2 | 1019.8 | 1009.9 | 1190.8 | 1180.8 | 1180.6 | 1174.2 | 106.89 | 0. | 699.76 | 1370.5 | 1360.5 | 1354.2 |
| XN49 | 1017.8 | 1020. | 1010.1 | 1191. | 1181.3 | 1181.5 | 1175.3 | 1128. | 0. | 0. | 1371.5 | 1362.2 | 1355.5 |
| UT91R2 | 623.86 | 624.97 | 618.4 | 728.71 | 722.94 | 722.97 | 717.83 | 65.244 | 0. | 428.54 | 836.35 | 830.37 | 825.86 |
| UT92R2 | 606.72 | 607.63 | 601.25 | 708.39 | 703.02 | 703.21 | 698.37 | 669.23 | 0. | 0. | 813.57 | 808.07 | 803.46 |
| BTAN91 | 28.142 | 28.461 | 28.727 | 29.785 | 28.954 | 28.744 | 28.98 | 87.206 | 82.055 | 20.581 | 30.604 | 30.178 | 29.942 |
| BTAN92 | 29.239 | 29.05 | 28.634 | 29.303 | 29.92 | 29.543 | 29.279 | 86.946 | 81.855 | 21.878 | 29.611 | 29.694 | 29.412 |
| W13 | 12.811 | 12.367 | 13.19 | 13.065 | 14.133 | 14.606 | 15.284 | -5.1923 | -.5 | 6.4506 | 14.011 | 14.624 | 15.68 |
| W15 | 12.206 | 12.367 | 12.052 | 13.065 | 13.843 | 13.863 | 14.003 | -5.1923 | 0. | 6.4506 | 14.011 | 14.161 | 13.781 |
| WF36 | 2605. | 2616.3 | 2564.5 | 3618.1 | 3537.5 | 3539.3 | 3501.9 | 166.64 | 164.08 | 977.7 | 4877.9 | 4717.1 | 4621.4 |
| WF36R2 | 2674.4 | 2683.4 | 2627.3 | 3704. | 3624.5 | 3626.9 | 3579.6 | 169.84 | 168.25 | 1002.2 | 4979.4 | 4815.7 | 4712.4 |
| FN11QA | 11101. | 11111. | 10808. | 15329. | 15094. | 15101. | 14816. | 0. | 0. | 3226.4 | 20240. | 19824. | 19449. |
| SFC184 | .24354 | .24414 | .24574 | .24426 | .24274 | .24279 | .24422 | .5 | .5 | .31401 | .24869 | .24557 | .24493 |
| TAMB | 523.06 | 523.59 | 524.94 | 524.9 | 524.77 | 524.92 | 525.34 | 526.04 | 523.73 | 524.08 | 527.92 | 528.25 | 529.24 |
| T10 | 520.02 | 520.78 | 521.61 | 522.33 | 521.79 | 521.62 | 523.38 | 525.02 | 521.13 | 521.52 | 525.19 | 525.11 | 525.95 |
| PAMB | 14.309 | 14.309 | 14.309 | 14.308 | 14.308 | 14.308 | 14.31 | 14.31 | 14.297 | 14.298 | 14.299 | 14.299 | 14.299 |
| P10M | 14.31 | 14.309 | 14.31 | 14.31 | 14.308 | 14.309 | 14.312 | 14.311 | 14.298 | 14.299 | 14.299 | 14.3 | 14.301 |
| HUMSER | 52.958 | 55.032 | 55.72 | 56.095 | 55.553 | 53.906 | 54.961 | 56.379 | 57.334 | 60.477 | 63.666 | 65.996 | 62.201 |
| RELHUM | 59.674 | 60.855 | 58.763 | 59.234 | 58.926 | 56.904 | 57.168 | 57.232 | 63.001 | 65.599 | 60.421 | 61.895 | 56.436 |
| WINVAV | 3.2132 | 2.5168 | 3.7491 | 8.1252 | 4.2212 | 2.3243 | 2.262 | 4.9036 | 1.1172 | 1.3106 | 2.624 | 3.5259 | 1.7794 |
| WINAAV | 119. | 151.17 | -61.304 | -43.078 | 146.41 | 111.06 | 33.033 | -36.545 | -90.63 | -147.83 | -51.425 | -63.637 | -36.56 |
| XMO | 0. | 0. | 0. | 0. | 0. | 0. | 0. | 0. | 0. | 0. | 0. | 0. | 0. |
| P46Q2 | 1.9388 | 1.944 | 1.9163 | 2.3244 | 2.3014 | 2.3001 | 2.2798 | 1.0018 | 9.99+10 | 1.2714 | 2.7705 | 2.7445 | 2.7072 |
| CT46 | 1494. | 1499.1 | 1486.8 | 1625.6 | 1605.5 | 1604. | 1601.5 | 874.1 | 9.99+10 | 1308.1 | 1774.7 | 1730. | 1716.9 |
| T46X | 1500.4 | 1504.6 | 1498.3 | 1619.4 | 1601.2 | 1598.1 | 1596.9 | 710.96 | 528.63 | 1277.4 | 1736.1 | 1708.6 | 1695. |
| Comments | Part Power | Part Power | Part Power | Part Power | Part Power | Part Power | Part Power | Zero | Zero | F.I. Bad XN49 | Part Power | Part Power | Part Power |
| | Bleed Evaluation | | | | | | | | | | Bleed Evaluation | | |
| | Stroke = 35% | 0% | 100% | 0% | 35% | 80% | 100% | | | | Stroke = 0% | 35% | 80% |

GE36/UDF1 Peebles Tests
082001-03
Test Log - Site IIID
Sheet 004 of 029

GE36/UDF-1 ENGINE 082001-0_ TEST READINGS - SITE II_
RDGS. 1 - 5 ON 06.20.86 RDGS. 6 - 15 ON 06.23.86
RDGS. 16 - 31 ON 06.24.86 RDGS. 32 - 47 ON 06.25.86
RDGS. 48 - 57 ON 06.26.86

| RDG. | 53 | 54 | 55 | 56 | 57 |
|---|---|---|---|---|---|
| XN2 | 11329. | 10751. | 10072. | 326.61 | 0. |
| XN2R | 11246. | 10668. | 9984.4 | 321.67 | 0. |
| PCN2R | 84.75 | 80.394 | 75.24 | 2.424 | 0. |
| XN25 | 15254. | 14699. | 14151. | 113.14 | 0. |
| XN25R | 12795. | 12611. | 12421. | 108.58 | 0. |
| PCN25R | 95.344 | 93.975 | 92.559 | .80912 | 0. |
| XN48 | 1341.8 | 1172.6 | 1016.8 | 446.33 | 0. |
| XN49 | 1342.7 | 1173.9 | 1018.6 | 481.02 | 0. |
| UT91R2 | 817.98 | 714.53 | 619.02 | 269.94 | 0. |
| UT92R2 | 795.64 | 695.32 | 602.72 | 282.78 | 0. |
| BTAN91 | 30.452 | 29.135 | 27.94 | 87.284 | 86.683 |
| BTAN92 | 29.261 | 29.379 | 28.564 | 86.959 | 86.384 |
| W13 | 16.6 | 15.637 | 13.911 | -6.4314 | -.5 |
| W15 | 13.206 | 12.097 | 10.646 | -6.4314 | 0. |
| WF36 | 4543.4 | 3432.1 | 2531.5 | 155.06 | 157.07 |
| WF36R2 | 4630.8 | 3495. | 2574.1 | 156.2 | 159.22 |
| FN11QA | 19009. | 14559. | 10726. | 0. | 0. |
| SFC184 | .24626 | .24266 | .2426 | .5 | .5 |
| TAMB | 529.64 | 530.39 | 530.98 | 534.99 | 536.16 |
| T10 | 526.31 | 526.78 | 527.77 | 534.71 | 536.23 |
| PAMB | 14.3 | 14.3 | 14.301 | 14.297 | 14.18 |
| P10M | 14.301 | 14.302 | 14.302 | 14.298 | 14.181 |
| HUMSER | 64.567 | 61.929 | 67.066 | 61.219 | 100.29 |
| RELHUM | 57.754 | 54.042 | 57.285 | 45.745 | 70.88 |
| WINVAV | 1.3753 | .35346 | .60236 | 4.4641 | 4.7464 |
| WINAAV | -81.896 | -67.648 | 4.581 | -6.8343 | -159.02 |
| XMO | 0. | 0. | 0. | 0. | 0. |
| P46Q2 | 2.6699 | 2.2727 | 1.9257 | 1.0014 | 9.99+10 |
| CT46 | 1707.5 | 1592.6 | 1483. | 876.21 | 9.99+10 |
| T46X | 1690.1 | 1585.9 | 1491.1 | 714.71 | 536.24 |

Comments: Part Power / Part Power / Part Power / Zero / Zero
Bleed Evaluation--------→
Stroke =
100% 100% 100%

GE36/UDF1 Peebles Tests
082001-03
Test Log - Site IIID
Sheet 005 of 029

ORI... IS
OF POOR QUALITY

GE36/UDF-1 ENGINE 082001-03 TEST READINGS - SITE IIID

RDGS. 57 - 70 ON 06.29.86 RDGS. 71 - 77 ON 06.30.86
RDGS. 78 - 149 ON 07.01.86 RDGS. 150 - 197 ON 07.03.86
RDGS. 198 - 209 ON 07.04.86 RDGS. 210 - 251 ON 07.05.86

| RDG. | 57 | 58 | 59 | 60 | 61 | 62 | 63 | 64 | 65 | 66 | 67 | 68 | 69 |
|---|---|---|---|---|---|---|---|---|---|---|---|---|---|
| XN2 | 0. | 11448. | 11415. | 11450. | 11444. | 761.61 | 0. | 5283.8 | 11442. | 5664.4 | 5739.7 | 11350. | 11409. |
| XN2R | 0. | 11276. | 11243. | 11260. | 11265. | 745.05 | 0. | 5210.5 | 11272. | 5593. | 5670.7 | 11208. | 11243. |
| PCN2R | 0. | 84.971 | 84.723 | 84.855 | 84.891 | 5.6146 | 0. | 39.266 | 84.943 | 42.147 | 42.733 | 84.465 | 84.726 |
| XN25 | 0. | 15489. | 15423. | 15502. | 15423. | 127.81 | 0. | 11519. | 15502. | 11839. | 11811. | 15131. | 15295. |
| XN25R | 0. | 12778. | 12778. | 12790. | 12792. | 122.63 | 0. | 10903. | 12777. | 11206. | 11180. | 12719. | 12750. |
| PCN25R | 0. | 95.214 | 95.216 | 95.306 | 95.324 | .91379 | 0. | 81.243 | 95.211 | 83.502 | 83.308 | 94.774 | 95.009 |
| XN48 | 0. | 1391.4 | 1370.3 | 1389.1 | 1368.8 | 513.84 | 0. | 699.9 | 1387.7 | 700.03 | 700.03 | 1290.5 | 1338.7 |
| XN49 | 0. | 1392. | 1371.5 | 1390.4 | 1370.2 | 137.84 | 0. | 700.83 | 1388.9 | 701.1 | 701.37 | 1291.4 | 1340.3 |
| UT91R2 | 0. | 841.57 | 828.78 | 838.91 | 827.49 | 308.69 | 0. | 423.84 | 839.51 | 424.46 | 424.72 | 782.62 | 810.16 |
| UT92R2 | 0. | 818.4 | 806.29 | 816.21 | 805.11 | 80.486 | 0. | 412.53 | 816.72 | 413.21 | 413.62 | 761.26 | 788.42 |
| BTAN91 | 86.683 | 30.425 | 30.527 | 30.205 | 29.74 | 87.257 | 86.736 | 17.007 | 30.314 | 18.95 | 19.024 | 30.458 | 29.975 |
| BTAN92 | 86.384 | 28.877 | 28.801 | 28.808 | 29.084 | 87.278 | 86.902 | 17.753 | 29.099 | 18.788 | 19.076 | 29.005 | 29.043 |
| W13 | -.5 | 13.514 | 14.649 | 13.695 | 15.249 | -4.4668 | -.5 | 5.6675 | 13.511 | 7.4598 | 7.9167 | 19.504 | 16.873 |
| W15 | 0. | 13.514 | 14.1 | 13.695 | 13.866 | -4.4668 | 0. | 5.4647 | 13.511 | 5.1858 | 5.3447 | 12.531 | 12.873 |
| WF36 | 157.07 | 4862.6 | 4687.3 | 4774.6 | 4670.8 | 156.92 | 161.47 | 813.71 | 4861.6 | 816.25 | 853.28 | 4420.9 | 4533.5 |
| WF36R2 | 159.22 | 4945.7 | 4766.6 | 4845.9 | 4746.4 | 157.94 | 163.79 | 829.33 | 4950.5 | 832.89 | 871.41 | 4514.3 | 4616.7 |
| FN11QA | 0. | 20234. | 19561. | 19956. | 19528. | 0. | 0. | 2180.2 | 20391. | 0. | 2573. | 17783. | 18765. |
| SFC184 | .5 | .24708 | .24633 | .24546 | .2457 | .5 | .5 | .38453 | .24542 | .5 | .34236 | .25662 | .2487 |
| TAMB | 536.16 | 537.6 | 537.12 | 538.7 | 538.78 | 540.18 | 534.77 | 534.26 | 533.58 | 532.9 | 532.65 | 532.64 | 532.39 |
| T10 | 536.23 | 534.64 | 534.72 | 536.27 | 535.24 | 541.97 | 536.81 | 533.35 | 534.47 | 532.01 | 531.36 | 531.83 | 534.07 |
| PAMB | 14.18 | 14.175 | 14.175 | 14.175 | 14.176 | 14.177 | 14.16 | 14.158 | 14.161 | 14.165 | 14.166 | 14.167 | 14.168 |
| P10M | 14.181 | 14.176 | 14.177 | 14.177 | 14.178 | 14.178 | 14.161 | 14.16 | 14.163 | 14.168 | 14.168 | 14.172 | 14.17 |
| HUMSER | 100.29 | 100.09 | 98.079 | 96.328 | 97.522 | 96.421 | 93.172 | 95.111 | 95.478 | 95.907 | 95.61 | 97.146 | 96.181 |
| RELHUM | 70.88 | 67.429 | 67.16 | 62.625 | 63.223 | 59.739 | 68.964 | 71.581 | 73.521 | 75.579 | 75.973 | 77.194 | 77.11 |
| WINVAV | 4.7464 | 4.4568 | 5.2019 | 4.5996 | 3.7526 | 2.7214 | .14307 | .25299 | 2.076 | 1.1041 | 1.1273 | 1.3079 | 1.9541 |
| WINAAV | -159.02 | 16.301 | -29.165 | 37.359 | -22.668 | -128.2 | -18.701 | 61.84 | -32.613 | -4.4225 | 1.8491 | 4.972 | -5.0498 |
| XMO | 0. | 0. | 0. | 0. | 0. | 0. | 0. | 0. | 0. | 0. | 0. | 0. | 0. |
| P46Q2 | 9.99+10 | 2.7869 | 2.7313 | 2.7694 | 2.7209 | 1.0013 | 9.99+10 | 1.1989 | 2.7926 | 1.2397 | 1.2279 | 2.5523 | 2.6504 |
| CT46 | 9.99+10 | 1779.1 | 1748.1 | 1763. | 1743.5 | 868.85 | 9.99+10 | 1320.5 | 1772.4 | 1210.4 | 1251.9 | 1741.2 | 1734.8 |
| T46X | 536.24 | 1743.4 | 1725. | 1732.7 | 1719. | 736.83 | 562.39 | 1299.1 | 1740.1 | 1228. | 1241.6 | 1707. | 1710.7 |
| Comments: | Zero | Part Power | Part Power | Part Power | Part Power | Zero | Zero | F.I. | Part Power | F.I. | Part Power | Part Power | Part Power |
| Bleed Evaluation Stroke = | | 0% | 35% | 80% | 100% | | | | 0% | 0% No FN | 100% | 100% | 80% |

GE36/UDF1 Peebles Tests
082001-03
Test Log - Site IIID
Sheet 006 of 029

NOTE:
Manual Control T2 →

GE36/UDF-1 ENGINE 082001-03 ST READINGS - SITE IIID
RDGS. 57 - 70 ON 06.29.86 RDGS. 71 - 77 ON 06.30.86
RDGS. 78 - 149 ON 07.01.86 RDGS. 150 - 197 ON 07.03.86
RDGS. 198 - 209 ON 07.04.86 RDGS. 210 - 251 ON 07.05.86

| RDG. | 70 | 71 | 72 | 73 | 74 | 75 | 76 | 77 | 78 | 79 | 80 | 81 | 82 |
|---|---|---|---|---|---|---|---|---|---|---|---|---|---|
| XN2 | 11393. | 81.428 | 11318. | 0. | 5622.2 | 5612.2 | 5615.8 | 5620.3 | 116.79 | 11364. | 11354. | 11391. | 11389. |
| XN2R | 11263. | 79.943 | 11186. | 0. | 5571.4 | 5561.2 | 5565. | 5570. | 114.54 | 11284. | 11278. | 11316. | 11314. |
| PCN2R | 84.877 | .60244 | 84.297 | 0. | 41.985 | 41.908 | 41.937 | 41.974 | .86315 | 85.034 | 84.99 | 85.274 | 85.26 |
| XN25 | 15383. | 130.95 | 15313. | 0. | 11725. | 11736. | 11740. | 11742. | 137.76 | 15350. | 15353. | 15403. | 15404. |
| XN25R | 12754. | 122.98 | 12716. | 0. | 11097. | 11109. | 11116. | 11117. | 129.5 | 12740. | 12755. | 12786. | 12789. |
| PCN25R | 95.034 | .91641 | 94.753 | 0. | 82.69 | 82.777 | 82.828 | 82.836 | .96496 | 94.932 | 95.042 | 95.277 | 95.296 |
| XN48 | 1379.6 | 109.71 | 1361.3 | 0. | 700.16 | 700.03 | 700.3 | 700.03 | 309.43 | 1378.5 | 1378. | 1395.2 | 1395.4 |
| XN49 | 1380.9 | 129.4 | 1361.6 | 0. | 701.37 | 701.1 | 701.1 | 701.1 | 101.27 | 1379.7 | 1378.6 | 1395.8 | 1396.6 |
| UT91R2 | 837.5 | 66.141 | 826.29 | 0. | 426.08 | 425.98 | 426.16 | 426.03 | 186.36 | 840.54 | 840.53 | 851.19 | 851.25 |
| UT92R2 | 814.85 | 75.829 | 803.32 | 0. | 414.87 | 414.69 | 414.7 | 414.74 | 59.284 | 817.73 | 817.39 | 827.68 | 828.13 |
| BTAN91 | 30.335 | 87.146 | 30.725 | 76.706 | 18.937 | 19.064 | 18.962 | 18.803 | 86.764 | 29.95 | 29.889 | 29.638 | 29.618 |
| BTAN92 | 28.761 | 87.257 | 28.717 | 81.62 | 18.988 | 18.969 | 19.366 | 19.357 | 86.729 | 29.608 | 29.467 | 29.364 | 29.44 |
| W13 | 13.749 | -7.4455 | 14.318 | -.5 | 5.9546 | 5.6503 | 5.8283 | 5.7034 | -7.1141 | 13.594 | 13.584 | 13.214 | 13.325 |
| W15 | 13.749 | -7.4455 | 14.318 | 0. | 5.9546 | 5.6503 | 5.8283 | 5.7034 | -7.1141 | 13.594 | 13.584 | 13.214 | 13.325 |
| WF36 | 4711. | 171.33 | 4769.5 | 176.23 | 887.71 | 880.28 | 877.46 | 875.26 | 179.79 | 4895.9 | 4843.6 | 4855.1 | 4848.3 |
| WF36R2 | 4818.1 | 173.36 | 4874.2 | 179.78 | 908.92 | 901.36 | 898.55 | 896.49 | 181.64 | 5037.3 | 4985.9 | 4998.2 | 4991.2 |
| FN11QA | 19848. | 0. | 19378. | 0. | 2685.2 | 2638.3 | 2632.6 | 2653.5 | 0. | 20427. | 20346. | 20630. | 20611. |
| SFC184 | .24539 | .5 | .25427 | .5 | .34217 | .34536 | .34503 | .34152 | .5 | .24928 | .24772 | .24491 | .24479 |
| TAMB | 531.63 | 531.39 | 529.67 | 529.46 | 529.26 | 529.36 | 529.33 | 529.31 | 527.98 | 527.3 | 526.9 | 526.84 | 526.8 |
| T10 | 530.73 | 538.12 | 530.93 | 531.13 | 528.17 | 528.22 | 528.18 | 528.09 | 539.21 | 526.08 | 525.69 | 525.54 | 525.57 |
| PAMB | 14.168 | 14.172 | 14.173 | 14.183 | 14.188 | 14.187 | 14.186 | 14.185 | 14.173 | 14.17 | 14.17 | 14.172 | 14.171 |
| P10M | 14.169 | 14.173 | 14.177 | 14.184 | 14.19 | 14.189 | 14.188 | 14.187 | 14.175 | 14.171 | 14.171 | 14.173 | 14.172 |
| HUMSER | 95.405 | 93.624 | 92.822 | 101.94 | 101.48 | 101.92 | 101.41 | 102.3 | 100.09 | 98.114 | 95.181 | 96.457 | 95.504 |
| RELHUM | 78.481 | 77.694 | 81.689 | 90.247 | 90.488 | 90.568 | 90.215 | 91.022 | 93.192 | 93.511 | 92.064 | 93.452 | 92.684 |
| WINVAV | 2.7495 | .0001 | 1.7592 | 2.5319 | 1.1485 | 2.148 | 1.8073 | 1.9152 | 2.4646 | 3.3228 | 2.5153 | 4.5126 | 4.9621 |
| WINAAV | -10.889 | -71.231 | -45.818 | -172.01 | 159.77 | -108.03 | -158.7 | -143.18 | 169.71 | -149.76 | -165.61 | -122.38 | -161.17 |
| XM0 | 0. | 0. | 0. | 0. | 0. | 0. | 0. | 0. | 0. | 0. | 0. | 0. | 0. |
| P46Q2 | 2.7472 | 1.0009 | 2.7166 | 9.99+10 | 1.2304 | 1.2295 | 1.2291 | 1.2293 | 1.0009 | 2.7773 | 2.7744 | 2.8081 | 2.8074 |
| CT46 | 1744.7 | 888.33 | 1795.7 | 9.99+10 | 1324.7 | 1317.9 | 1310.7 | 1306.8 | 930.87 | 1785.7 | 1770.2 | 1750.7 | 1749.2 |
| T46X | 1717.7 | 641.58 | 1729. | 541.42 | 1288.7 | 1284.3 | 1279.7 | 1268.7 | 661.24 | 1742.5 | 1729.6 | 1718.6 | 1717.5 |

| Comments: | 70 | 71 | 72 | 73 | 74 | 75 | 76 | 77 | 78 | 79 | 80 | 81 | 82 |
|---|---|---|---|---|---|---|---|---|---|---|---|---|---|
| | Part Power Bleed Eval. Stroke = 35% | Zero | Part Power | Zero | F.I. | F.I. | F.I. | F.I. | Zero | Part Power | Part Power | Down Pt. 1a | Power Cal. Pt. 1b |

High Rel. Humidity (Rain?)

Manual Control T2 ⟶

GE36/UDF1 Peebles Tests
082001-03
Test Log - Site IIID
Sheet 007 of 029

GE36/UDF-1 ENGINE 082001-03 TEST READINGS - SITE IIID

RDGS. 57 - 70 ON 06.29.86 RDGS. 71 - 77 ON 06.30.86
RDGS. 78 - 149 ON 07.01.86 RDGS. 150 - 197 ON 07.03.86
RDGS. 198 - 209 ON 07.04.86 RDGS. 210 - 251 ON 07.05.86

| RDG. | 83 | 84 | 85 | 86 | 87 | 88 | 89 | 90 | 91 | 92 | 93 | 94 | 95 |
|---|---|---|---|---|---|---|---|---|---|---|---|---|---|
| XN2 | 11308. | 11310. | 10983. | 10978. | 10685. | 10686. | 10327. | 10328. | 10329. | 9781.8 | 9776.3 | 8885.5 | 8885.8 |
| XN2R | 11235. | 11237. | 10913. | 10908. | 10619. | 10620. | 10265. | 10266. | 10267. | 9724.5 | 9717.8 | 8832.6 | 8832.6 |
| PCN2R | 84.665 | 84.683 | 82.24 | 82.203 | 80.025 | 80.031 | 77.355 | 77.36 | 77.371 | 73.282 | 73.231 | 66.561 | 66.561 |
| XN25 | 15327. | 15328. | 15015. | 15010. | 14721. | 14721. | 14386. | 14384. | 14383. | 14044. | 14037. | 13580. | 13578. |
| XN25R | 12767. | 12767. | 12671. | 12667. | 12580. | 12580. | 12468. | 12466. | 12466. | 12350. | 12342. | 12164. | 12162. |
| PCN25R | 95.135 | 95.137 | 94.42 | 94.388 | 93.74 | 93.741 | 92.908 | 92.893 | 92.89 | 92.028 | 91.971 | 90.643 | 90.624 |
| XN48 | 1369.3 | 1369.7 | 1265.8 | 1265.4 | 1179.4 | 1179.3 | 1083.3 | 1083.5 | 1084.2 | 996.46 | 994.99 | 886.09 | 885.42 |
| XN49 | 1370.3 | 1371. | 1266.9 | 1266.1 | 1180.4 | 1180.8 | 1084.5 | 1085. | 1085.1 | 997.67 | 996.73 | 887.03 | 887.03 |
| UT91R2 | 835.41 | 835.67 | 772.42 | 772.17 | 719.81 | 719.77 | 661.22 | 661.37 | 661.83 | 608.34 | 607.36 | 540.9 | 540.48 |
| UT92R2 | 812.66 | 813.07 | 751.43 | 750.95 | 700.21 | 700.5 | 643.42 | 643.73 | 643.86 | 592.03 | 591.39 | 526.31 | 526.3 |
| BTAN91 | 29.885 | 29.653 | 29.537 | 29.648 | 29.31 | 29.219 | 29.07 | 28.875 | 29.071 | 27.998 | 27.809 | 26.985 | 26.698 |
| BTAN92 | 29.375 | 29.476 | 29.353 | 29.23 | 29.125 | 29.186 | 28.69 | 28.941 | 28.767 | 28.362 | 28.243 | 27.472 | 27.65 |
| W13 | 13.238 | 13.251 | 12.975 | 13.005 | 12.618 | 12.609 | 11.931 | 11.842 | 12.011 | 11.067 | 10.963 | 9.7849 | 9.9043 |
| W15 | 13.238 | 13.251 | 12.975 | 13.005 | 12.618 | 12.609 | 11.931 | 11.842 | 12.011 | 11.067 | 10.963 | 9.7849 | 9.9043 |
| WF36 | 4671. | 4675. | 4009.3 | 4007.5 | 3465.6 | 3461.1 | 2909.2 | 2912.3 | 2916.9 | 2428.9 | 2433.9 | 1913.4 | 1915.6 |
| WF36R2 | 4809. | 4813.6 | 4128.4 | 4126.4 | 3568.8 | 3564.8 | 2995.9 | 2999.2 | 3004.1 | 2501.6 | 2506.3 | 1970.8 | 1972.9 |
| FN11QA | 19884. | 19922. | 0. | 17176. | 14909. | 14928. | 0. | 12505. | 12489. | 10374. | 10358. | 8012.3 | 8010.1 |
| SFC184 | .24449 | .24425 | .5 | .24285 | .24196 | .2414 | .5 | .24244 | .24316 | .24376 | .24459 | .24865 | .24898 |
| TAMB | 526.69 | 526.71 | 526.63 | 526.56 | 526.45 | 526.44 | 526.43 | 526.38 | 526.29 | 526.2 | 526.25 | 526.17 | 526.22 |
| T10 | 525.45 | 525.43 | 525.31 | 525.31 | 525.14 | 525.07 | 524.97 | 524.99 | 524.92 | 524.79 | 524.94 | 524.91 | 524.93 |
| PAMB | 14.171 | 14.171 | 14.17 | 14.171 | 14.171 | 14.171 | 14.172 | 14.172 | 14.172 | 14.172 | 14.173 | 14.169 | 14.169 |
| P10M | 14.173 | 14.172 | 14.172 | 14.173 | 14.173 | 14.172 | 14.174 | 14.173 | 14.174 | 14.174 | 14.174 | 14.17 | 14.17 |
| HUMSER | 96.437 | 96.526 | 96.481 | 95.93 | 94.879 | 95.395 | 95.793 | 94.947 | 95.705 | 95.273 | 95.73 | 94.864 | 95.253 |
| RELHUM | 93.94 | 93.962 | 94.151 | 93.861 | 93.21 | 93.731 | 94.154 | 93.522 | 94.523 | 94.402 | 94.688 | 94.101 | 94.324 |
| WINVAV | 5.1581 | 3.3497 | 3.1338 | 2.4933 | 4.3682 | 1.7148 | 4.0479 | 1.4784 | 2.3773 | 1.1536 | 4.3176 | 2.2481 | 4.8718 |
| WINAAV | -155.83 | -162.4 | -142.09 | 131.71 | 166.44 | -143.54 | -139.88 | 133.66 | 155.19 | -132.07 | 144.19 | -110.49 | 168. |
| XMO | 0. | 0. | 0. | 0. | 0. | 0. | 0. | 0. | 0. | 0. | 0. | 0. | 0. |
| P46Q2 | 2.7479 | 2.7487 | 2.5124 | 2.5104 | 2.3078 | 2.3095 | 2.0895 | 2.0906 | 2.0917 | 1.9025 | 1.901 | 1.6924 | 1.6922 |
| CT46 | 1730.7 | 1730.9 | 1663.3 | 1664.9 | 1608.5 | 1607.4 | 1546.4 | 1547.9 | 1548.9 | 1480.4 | 1485.8 | 1405.9 | 1407.4 |
| T46X | 1705.3 | 1700.4 | 1642. | 1642.8 | 1597.3 | 1598.6 | 1541.1 | 1542.7 | 1543.4 | 1480.9 | 1483.9 | 1403.1 | 1404.3 |

Comments: Down Power Calibration
Manual Control T2
High Relative Humidity (Rain?)

| Pt.2a | Pt.2b | Pt.3a | Pt.3b | Pt.4a | Pt.4b | Pt.5a | Pt.5b | Pt.5c | Pt.6a | Pt.6b | Pt.7a | Pt.7b |
|---|---|---|---|---|---|---|---|---|---|---|---|---|
| | | No FN | | | | No FN | | | | | | |

GE36/UDF1 Peebles Tests
082001-03
Test Log - Site IIID
Sheet 008 of 029

GE36/UDF-1 ENGINE 082001-0 TEST READINGS - SITE IIID
RDGS. 57 - 70 ON 06.29.86 RDGS. 71 - 77 ON 06.30.86
RDGS. 78 - 149 ON 07.01.86 RDGS. 150 - 197 ON 07.03.86
RDGS. 198 - 209 ON 07.04.86 RDGS. 210 - 251 ON 07.05.86

| RDG. | 96 | 97 | 98 | 99 | 100 | 101 | 102 | 103 | 104 | 105 | 106 | 107 | 108 |
|---|---|---|---|---|---|---|---|---|---|---|---|---|---|
| XN2 | 7870.1 | 7871.6 | 6314.7 | 6313.3 | 5429.7 | 5431.2 | 4169.2 | 8756.5 | 8755.4 | 8008.8 | 8008.6 | 7130.3 | 7131.3 |
| XN2R | 7824.7 | 7826.3 | 6278.1 | 6277.5 | 5397.9 | 5400.2 | 4144.2 | 8709.9 | 8708.8 | 7967.4 | 7966.3 | 7093.3 | 7094.6 |
| PCN2R | 58.965 | 58.978 | 47.311 | 47.306 | 40.678 | 40.695 | 31.23 | 65.636 | 65.627 | 60.041 | 60.033 | 53.454 | 53.463 |
| XN25 | 13035. | 13034. | 12153. | 12151. | 11616. | 11614. | 10728. | 13463. | 13463. | 13074. | 13074. | 12605. | 12605. |
| XN25R | 11912. | 11910. | 11414. | 11414. | 11055. | 11054. | 10366. | 12099. | 12101. | 11922. | 11920. | 11679. | 11679. |
| PCN25R | 88.762 | 88.75 | 85.053 | 85.051 | 82.38 | 82.372 | 77.246 | 90.159 | 90.169 | 88.836 | 88.825 | 87.028 | 87.03 |
| XN48 | 791.38 | 790.85 | 699.49 | 700.43 | 700.16 | 700.16 | 700.16 | 789.91 | 789.91 | 789.78 | 789.38 | 789.91 | 789.64 |
| XN49 | 792.59 | 792.32 | 700.83 | 701.37 | 701.24 | 701.24 | 701.1 | 790.85 | 790.98 | 790.98 | 790.98 | 791.12 | 791.12 |
| | | | | | | | | | | | | | |
| UT91R2 | 483.18 | 482.86 | 427.06 | 427.69 | 427.45 | 427.51 | 427.38 | 482.5 | 482.49 | 482.49 | 482.2 | 482.56 | 482.42 |
| UT92R2 | 470.37 | 470.22 | 415.9 | 416.27 | 416.12 | 416.18 | 415.98 | 469.55 | 469.62 | 469.7 | 469.65 | 469.77 | 469.79 |
| BTAN91 | 25.271 | 25.015 | 21.321 | 21.639 | 17.658 | 17.594 | 10.516 | 29.949 | 29.962 | 26.973 | 26.243 | 23.235 | 22.582 |
| BTAN92 | 26. | 25.922 | 22.799 | 22.674 | 18.687 | 18.795 | 11.076 | 29.361 | 29.508 | 26.773 | 26.536 | 23.267 | 23.822 |
| | | | | | | | | | | | | | |
| W13 | 8.6834 | 8.5114 | 6.261 | 6.3375 | 5.7189 | 5.7571 | 3.838 | 10.103 | 10.287 | 8.6711 | 8.7659 | 7.332 | 7.4253 |
| W15 | 8.6834 | 8.5114 | 6.261 | 6.3375 | 5.6233 | 5.5881 | 3.838 | 10.103 | 10.287 | 8.6711 | 8.7659 | 7.332 | 7.4253 |
| | | | | | | | | | | | | | |
| WF36 | 1470.2 | 1472.2 | 1002.5 | 1004.8 | 827.29 | 828.84 | 653.57 | 1842.8 | 1839.1 | 1523. | 1524.1 | 1227.7 | 1229.5 |
| WF36R2 | 1514.5 | 1516.7 | 1032.4 | 1034.9 | 851.86 | 853.7 | 672.9 | 1899.6 | 1895.7 | 1569.6 | 1570.5 | 1265.1 | 1267.1 |
| FN11QA | 5900.6 | 5898.2 | 3575.6 | 3531.6 | 2462.2 | 2464. | 919.47 | 7267.8 | 7275.2 | 6077.2 | 6105.9 | 4743.9 | 4776.9 |
| SFC184 | .25945 | .25994 | .29187 | .29623 | .34974 | .35024 | .73979 | .26421 | .26341 | .26108 | .26001 | .26958 | .26814 |
| | | | | | | | | | | | | | |
| TAMB | 526.14 | 526.06 | 525.91 | 526.08 | 525.89 | 525.78 | 525.85 | 525.5 | 525.58 | 525.42 | 525.42 | 525.37 | 525.3 |
| T10 | 524.71 | 524.69 | 524.74 | 524.61 | 524.8 | 524.64 | 524.95 | 524.24 | 524.24 | 524.07 | 524.18 | 524.09 | 524.05 |
| PAMB | 14.169 | 14.169 | 14.171 | 14.171 | 14.171 | 14.17 | 14.169 | 14.17 | 14.17 | 14.175 | 14.175 | 14.175 | 14.175 |
| P10M | 14.171 | 14.17 | 14.173 | 14.172 | 14.173 | 14.172 | 14.171 | 14.171 | 14.172 | 14.176 | 14.176 | 14.177 | 14.176 |
| HUMSER | 94.687 | 94.807 | 94.235 | 94.371 | 94.321 | 92.696 | 93.671 | 92.817 | 92.352 | 92.374 | 92.44 | 91.673 | 93.67 |
| RELHUM | 94.027 | 94.379 | 94.346 | 93.906 | 94.484 | 93.254 | 93.96 | 94.271 | 93.546 | 94.119 | 94.206 | 93.581 | 95.809 |
| WINVAV | 1.3367 | 2.2079 | 4.6007 | 2.2312 | 1.1312 | 3.1201 | 1.5844 | 1.647 | 1.2155 | 2.6504 | 1.6465 | 2.4408 | 2.3434 |
| WINAAV | -65.167 | -101.96 | 153.11 | -105.64 | -151.98 | -161.49 | -157.23 | 148.19 | 99.952 | -116.19 | 99.564 | 82.246 | -153.69 |
| XMO | 0. | 0. | 0. | 0. | 0. | 0. | 0. | 0. | 0. | 0. | 0. | 0. | 0. |
| | | | | | | | | | | | | | |
| P46Q2 | 1.5053 | 1.5055 | 1.301 | 1.3006 | 1.2156 | 1.2158 | 1.1204 | 1.6476 | 1.6467 | 1.5244 | 1.5244 | 1.4027 | 1.4027 |
| CT46 | 1337.4 | 1339.7 | 1274.5 | 1276.5 | 1269.1 | 1270.8 | 1328.8 | 1400.1 | 1397.1 | 1348.1 | 1348.4 | 1306.4 | 1306.8 |
| T46X | 1331.4 | 1332.8 | 1246. | 1247. | 1220.9 | 1246.1 | 1343. | 1390.1 | 1388.7 | 1340.2 | 1341.1 | 1290.7 | 1291.5 |

Comments: Down Power Calibration → "EPR POWER HOOK" 1 →
Manual Control T2 →
High Relative Humidity (Rain) →

| Pt.8a | Pt.8b | Pt.9a | Pt.9b | Pt.10a F.I. | Pt.10b F.I. | Pt.11 G.I. | Pt.1a | Pt.1b | Pt.2a | Pt.2b | Pt.3a | Pt.3b |
|---|---|---|---|---|---|---|---|---|---|---|---|---|

GE36/UDF1 Peebles Tests
082001-03
Test Log - Site IIID
Sheet 009 of 029

GE36/UDF-1 ENGINE 082001-03 TEST READINGS - SITE IIID
RDGS. 57 - 70 ON 06.29.86 RDGS. 71 - 77 ON 06.30.86
RDGS. 78 - 149 ON 07.01.86 RDGS. 150 - 197 ON 07.03.86
RDGS. 198 - 209 ON 07.04.86 RDGS. 210 - 251 ON 07.05.86

| RDG. | 109 | 110 | 111 | 112 | 113 | 114 | 115 | 116 | 117 | 118 | 119 | 120 | 121 |
|---|---|---|---|---|---|---|---|---|---|---|---|---|---|
| XN2 | 7741.8 | 9558.9 | 9559.8 | 9306. | 9308.5 | 8468.1 | 8455.1 | 7055.5 | 7056.7 | 10372. | 10379. | 10179. | 10181. |
| XN2R | 7702. | 9510.3 | 9511.5 | 9257.9 | 9261.8 | 8425.9 | 8411.8 | 7019.1 | 7019.5 | 10321. | 10327. | 10130. | 10132. |
| PCN2R | 58.041 | 71.668 | 71.677 | 69.766 | 69.795 | 63.495 | 63.39 | 52.895 | 52.898 | 77.774 | 77.825 | 76.336 | 76.355 |
| XN25 | 12914. | 13885. | 13888. | 13751. | 13751. | 13336. | 13335. | 12577. | 12573. | 14383. | 14388. | 14212. | 14213. |
| XN25R | 11810. | 12276. | 12279. | 12220. | 12221. | 12054. | 12053. | 11669. | 11664. | 12464. | 12465. | 12401. | 12402. |
| PCN25R | 88.004 | 91.475 | 91.5 | 91.061 | 91.068 | 89.818 | 89.81 | 86.95 | 86.915 | 92.873 | 92.883 | 92.41 | 92.414 |
| XN48 | 790.45 | 883.68 | 884.08 | 883.68 | 883.54 | 884.08 | 883.14 | 883.41 | 883.41 | 988.02 | 988.43 | 987.89 | 987.36 |
| XN49 | 791.38 | 885.02 | 884.88 | 885.02 | 884.88 | 885.15 | 884.88 | 884.88 | 885.02 | 988.69 | 988.96 | 989.1 | 989.23 |
| UT91R2 | 482.91 | 539.9 | 540.17 | 539.86 | 539.86 | 540.2 | 539.56 | 539.7 | 539.64 | 603.75 | 603.99 | 603.73 | 603.44 |
| UT92R2 | 469.95 | 525.58 | 525.52 | 525.54 | 525.54 | 525.71 | 525.49 | 525.46 | 525.49 | 587.25 | 587.4 | 587.54 | 587.66 |
| BTAN91 | 25.796 | 30.514 | 31.19 | 29.567 | 29.681 | 25.592 | 25.425 | 20.22 | 20.28 | 31.2 | 31.212 | 29.799 | 29.379 |
| BTAN92 | 26.274 | 29.19 | 29.101 | 28.516 | 28.427 | 26.035 | 25.797 | 21.091 | 21.014 | 29.85 | 30.124 | 29.854 | 29.963 |
| W13 | 5.9692 | 11.496 | 11.275 | 10.843 | 10.853 | 9.4526 | 9.5407 | 7.0128 | 6.8518 | 12.684 | 12.811 | 11.856 | 11.776 |
| W15 | 5.9692 | 11.496 | 11.275 | 10.843 | 10.853 | 9.4526 | 9.5407 | 7.0128 | 6.8518 | 12.684 | 12.811 | 11.856 | 11.776 |
| WF36 | 1474.6 | 2287.3 | 2283.8 | 2134.1 | 2137. | 1721.9 | 1718.2 | 1209.2 | 1212.3 | 2950.1 | 2953.3 | 2697.4 | 2698.6 |
| WF36R2 | 1519.3 | 2356.4 | 2352.9 | 2198.1 | 2201.5 | 1774. | 1770. | 1245.7 | 1248.9 | 3042.9 | 3046. | 2782.9 | 2784.6 |
| FN11QA | 0. | 9114.7 | 9110.6 | 8688.2 | 8668.7 | 7156.3 | 7151.1 | 4602.2 | 4617.7 | 11792. | 11811. | 11194. | 11200. |
| SFC184 | .5 | .26133 | .26106 | .25575 | .25672 | .25059 | .25021 | .27363 | .27341 | .26085 | .2607 | .2513 | .25134 |
| TAMB | 525.28 | 525.32 | 525.28 | 525.34 | 525.54 | 525.22 | 525.3 | 525.36 | 525.34 | 524.99 | 525.02 | 524.91 | 524.97 |
| T10 | 524.04 | 523.98 | 523.95 | 524.06 | 523.91 | 523.89 | 524.02 | 524.06 | 524.18 | 523.82 | 523.83 | 523.72 | 523.64 |
| PAMB | 14.18 | 14.183 | 14.184 | 14.185 | 14.185 | 14.183 | 14.181 | 14.179 | 14.177 | 14.171 | 14.17 | 14.168 | 14.169 |
| P10M | 14.18 | 14.185 | 14.185 | 14.187 | 14.187 | 14.186 | 14.184 | 14.181 | 14.178 | 14.173 | 14.174 | 14.171 | 14.17 |
| HUMSER | 90.893 | 91.576 | 91.308 | 92.01 | 92.452 | 91.348 | 89.662 | 93.168 | 92.011 | 91.553 | 91.959 | 90.732 | 91.011 |
| RELHUM | 93.147 | 93.716 | 93.591 | 94.108 | 93.865 | 93.8 | 91.854 | 95.146 | 94.048 | 94.676 | 94.985 | 94.085 | 94.187 |
| WINVAV | 3.8504 | 2.1101 | .97881 | 1.2416 | 3.2066 | 1.59 | 2.6592 | 2.3706 | 2.6219 | 2.5572 | 2.3114 | 3.4157 | 2.0326 |
| WINAAV | 152.85 | -155.02 | -151.76 | -59.463 | -29.707 | -58.405 | -27.854 | -62.716 | -56.198 | 121.92 | 157.02 | 167.08 | -123.53 |
| XM0 | 0. | 0. | 0. | 0. | 0. | 0. | 0. | 0. | 0. | 0. | 0. | 0. | 0. |
| P46Q2 | 1.4234 | 1.8253 | 1.8253 | 1.7731 | 1.773 | 1.6118 | 1.6098 | 1.4007 | 1.4007 | 2.0872 | 2.0895 | 1.994 | 1.9949 |
| CT46 | 1355.4 | 1466.2 | 1464.1 | 1439. | 1439.3 | 1376.7 | 1377.5 | 1303.1 | 1306.2 | 1553.3 | 1551. | 1519.9 | 1520. |
| T46X | 1334.1 | 1462.9 | 1461.3 | 1436.7 | 1436.1 | 1372.9 | 1373.5 | 1293.5 | 1295.1 | 1545.6 | 1544.3 | 1517.9 | 1517.9 |
| Comments: | Aborted Point No FN | Pt.1a | Pt.1b | Pt.2a | Pt.2b | Pt.3a | Pt.3b | Pt.4a | Pt.4b | Pt.1a | Pt.1b | Pt.2a | Pt.2b |

Readings 110–117: "EPR Power Hook" 2; Manual Control T2; High Relative Humidity (Rain?)

Readings 118–121: "EPR Power Hook" 3

GE36/UDF1 Peebles Tests
082001-03
Test Log - Site IIID
Sheet 010 of 029

GE36/UDF-1 ENGINE 082001-03 ST READINGS - SITE IIID
RDGS. 57 - 70 ON 06.29.86 RDGS. 71 - 77 ON 06.30.86
RDGS. 78 - 149 ON 07.01.86 RDGS. 150 - 197 ON 07.03.86
RDGS. 198 - 209 ON 07.04.86 RDGS. 210 - 251 ON 07.05.86

| RDG. | 122 | 123 | 124 | 125 | 126 | 127 | 128 | 129 | 130 | 131 | 132 | 133 | 134 |
|---|---|---|---|---|---|---|---|---|---|---|---|---|---|
| XN2 | 8822.2 | 8806.7 | 7744.7 | 7739.3 | 300.54 | 0. | 0. | 409.46 | 0. | 10833. | 10831. | 11163. | 11167. |
| XN2R | 8780.6 | 8763.1 | 7707.4 | 7700.9 | 298.17 | 0. | 0. | 403.95 | 0. | 10709. | 10701. | 11030. | 11036. |
| PCN2R | 66.169 | 66.037 | 58.082 | 58.032 | 2.2469 | 0. | 0. | 3.0441 | 0. | 80.698 | 80.643 | 83.12 | 83.164 |
| XN25 | 13537. | 13532. | 12973. | 12969. | 90.095 | 0. | 0. | 115.76 | 0. | 14893. | 14907. | 15191. | 15198. |
| XN25R | 12143. | 12141. | 11882. | 11878. | 87.378 | 0. | 0. | 110.29 | 0. | 12625. | 12634. | 12710. | 12717. |
| PCN25R | 90.487 | 90.466 | 88.537 | 88.51 | .65111 | 0. | 0. | .82182 | 0. | 94.073 | 94.146 | 94.71 | 94.765 |
| XN48 | 987.76 | 987.49 | 976.1 | 977.17 | 460.39 | 0. | 0. | 514.77 | 0. | 1206.5 | 1207.4 | 1197.9 | 1197.8 |
| XN49 | 989.1 | 989.5 | 989.23 | 989.5 | 479.14 | 0. | 0. | 539.15 | 0. | 1307.2 | 1308.4 | 1298.9 | 1299.5 |
| UT91R2 | 603.71 | 603.41 | 596.54 | 597.1 | 280.5 | 0. | 0. | 311.86 | 0. | 732.39 | 732.63 | 726.87 | 726.94 |
| UT92R2 | 587.61 | 587.71 | 587.64 | 587.7 | 283.75 | 0. | 0. | 317.49 | 0. | 771.32 | 771.69 | 766.09 | 766.56 |
| BTAN91 | 24.114 | 23.891 | 20.682 | 20.688 | 87.118 | 86.948 | 86.89 | 86.834 | 87.004 | 29.723 | 29.8 | 31.441 | 31.383 |
| BTAN92 | 24.94 | 24.912 | 21.545 | 21.503 | 87.087 | 86.976 | 86.867 | 86.92 | 86.999 | 27.102 | 26.916 | 28.026 | 28.327 |
| W13 | 9.6551 | 9.3895 | 7.9772 | 7.7816 | -6.1845 | -.5 | -.5 | -5.7185 | -.5 | 12.273 | 11.978 | 13.169 | 13.192 |
| W15 | 9.6551 | 9.3895 | 7.9772 | 7.7816 | -6.1845 | 0. | 0. | -5.7185 | 0. | 12.273 | 11.978 | 13.169 | 13.192 |
| WF36 | 1907.5 | 1900.5 | 1448.2 | 1448.3 | 183.28 | 171.87 | 170.83 | 171.46 | 170.88 | 3631.5 | 3604.7 | 4199.8 | 4200.4 |
| WF36R2 | 1967.8 | 1960.2 | 1493.5 | 1493.2 | 188.13 | 175.2 | 173.98 | 174.83 | 174.06 | 3723. | 3693.1 | 4304.1 | 4306.4 |
| FN11QA | 8110.4 | 8109.8 | 5870.5 | 5852.2 | 0. | 0. | 0. | 0. | 0. | 15538. | 15442. | 17130. | 17212. |
| SFC184 | .24526 | .24434 | .25717 | .25792 | .5 | .5 | .5 | .5 | .5 | .24222 | .24177 | .25399 | .25291 |
| TAMB | 524.89 | 524.95 | 524.91 | 524.95 | 525.04 | 531.99 | 532.14 | 532.6 | 532.18 | 532.31 | 532.32 | 532.25 | 532.33 |
| T10 | 523.6 | 523.85 | 523.69 | 523.86 | 526.94 | 532.18 | 533.6 | 532.93 | 534.8 | 530.8 | 531.28 | 531.25 | 531.04 |
| PAMB | 14.169 | 14.169 | 14.172 | 14.173 | 14.173 | 14.176 | 14.162 | 14.157 | 14.137 | 14.129 | 14.128 | 14.127 | 14.125 |
| P10M | 14.172 | 14.17 | 14.174 | 14.175 | 14.175 | 14.176 | 14.163 | 14.158 | 14.139 | 14.131 | 14.132 | 14.13 | 14.128 |
| HUMSER | 91.779 | 91.473 | 91.117 | 92.322 | 91.687 | 108.31 | 113.42 | 115.87 | 115.91 | 115.97 | 113.59 | 113.48 | 114.58 |
| RELHUM | 95.222 | 94.739 | 94.515 | 95.616 | 94.666 | 87.814 | 91.313 | 91.741 | 92.955 | 92.545 | 90.67 | 90.799 | 91.398 |
| WINVAV | 5.566 | 4.0384 | 2.9572 | 1.7913 | 2.4753 | 1.804 | 2.6792 | 2.5888 | 6.7578 | 5.4003 | 6.6822 | 7.4165 | 7.0775 |
| WINAAV | -45.912 | -38.488 | -41.98 | -54.588 | -176.18 | 165.89 | 162.14 | -36.515 | -47.08 | -32.524 | -14.119 | -33.064 | -21.301 |
| XMO | 0. | 0. | 0. | 0. | 0. | 0. | 0. | 0. | 0. | 0. | 0. | 0. | 0. |
| P46Q2 | 1.6938 | 1.6911 | 1.5058 | 1.505 | 1.0012 | 9.99+10 | 9.99+10 | 1.0014 | 9.99+10 | 2.3602 | 2.3583 | 2.5633 | 2.566 |
| CT46 | 1408. | 1409. | 1339.1 | 1340.3 | 942.25 | 9.99+10 | 9.99+10 | 937.39 | 9.99+10 | 1646. | 1638.8 | 1699.5 | 1695.6 |
| T46X | 1406.9 | 1406.6 | 1335. | 1336.1 | 717.32 | 553.66 | 551.26 | 729.56 | 608.03 | 1639.9 | 1633.6 | 1679.1 | 1677.6 |

Comments: "EPR Power Hook" 3 → Zero Zero Zero Zero Zero Trim Balance Run →
Manual Control T2 → Mismatched speeds, (XN48-XN49 = -100)
High Relative Humidity (Rain?) →
Pt.3a Pt.3b Pt.4a Pt.4b →

GE36/UDF1 Peebles Tests
082001-03
Test Log - Site IIID
Sheet 011 of 029

GE36/UDF-1 ENGINE 082001-03 TEST READINGS - SITE IIID
RDGS. 57 - 70 ON 06.29.86 RDGS. 71 - 77 ON 06.30.86
RDGS. 78 - 149 ON 07.01.86 RDGS. 150 - 197 ON 07.03.86
RDGS. 198 - 209 ON 07.04.86 RDGS. 210 - 251 ON 07.05.86

| RDG. | 135 | 136 | 137 | 138 | 139 | 140 | 141 | 142 | 143 | 144 | 145 | 146 | 147 |
|---|---|---|---|---|---|---|---|---|---|---|---|---|---|
| XN2 | 11271. | 11277. | 11440. | 11440. | 11583. | 11585. | 11132. | 11132. | 11378. | 11380. | 11512. | 11512. | 11684. |
| XN2R | 11139. | 11144. | 11308. | 11309. | 11451. | 11454. | 11007. | 11007. | 11252. | 11253. | 11386. | 11384. | 11553. |
| PCN2R | 83.938 | 83.977 | 85.218 | 85.219 | 86.295 | 86.313 | 82.948 | 82.95 | 84.791 | 84.797 | 85.799 | 85.785 | 87.058 |
| XN25 | 15288. | 15295. | 15428. | 15430. | 15543. | 15545. | 15186. | 15186. | 15405. | 15408. | 15515. | 15517. | 15652. |
| XN25R | 12745. | 12748. | 12785. | 12787. | 12817. | 12819. | 12715. | 12716. | 12785. | 12786. | 12814. | 12815. | 12849. |
| PCN25R | 94.968 | 94.991 | 95.27 | 95.28 | 95.503 | 95.52 | 94.749 | 94.753 | 95.266 | 95.276 | 95.484 | 95.489 | 95.746 |
| XN48 | 1197.5 | 1198.1 | 1197.5 | 1198.1 | 1197.9 | 1198.2 | 1297.7 | 1297.6 | 1298. | 1297.9 | 1297.7 | 1298.1 | 1297.9 |
| XN49 | 1299.2 | 1299.2 | 1299.5 | 1298.9 | 1298.9 | 1298.7 | 1398.7 | 1399.3 | 1399. | 1398.7 | 1398.7 | 1398.6 | 1399. |
| UT91R2 | 726.73 | 727.06 | 726.95 | 727.23 | 727.25 | 727.49 | 788. | 787.9 | 788.21 | 788.05 | 788.17 | 788.27 | 788.04 |
| UT92R2 | 766.36 | 766.36 | 766.74 | 766.39 | 766.5 | 766.42 | 825.56 | 825.85 | 825.76 | 825.51 | 825.73 | 825.51 | 825.67 |
| BTAN91 | 31.75 | 31.687 | 32.851 | 33.085 | 34.403 | 34.396 | 29.967 | 29.89 | 30.64 | 30.717 | 31.341 | 31.376 | 31.909 |
| BTAN92 | 28.639 | 28.706 | 29.182 | 29.078 | 29.438 | 29.435 | 27.486 | 27.65 | 28.304 | 28.407 | 28.506 | 28.315 | 29.114 |
| W13 | 13.456 | 13.519 | 13.635 | 13.896 | 14.061 | 14.02 | 12.485 | 12.548 | 13.177 | 13.145 | 13.593 | 13.47 | 13.716 |
| W15 | 13.456 | 13.519 | 13.635 | 13.896 | 14.061 | 14.02 | 12.485 | 12.548 | 13.177 | 13.145 | 13.593 | 13.47 | 13.716 |
| WF36 | 4397.3 | 4402. | 4715.8 | 4712.3 | 5002.7 | 5002.4 | 4188.6 | 4188.4 | 4652.5 | 4652.5 | 4920.3 | 4915.4 | 5270.7 |
| WF36R2 | 4508.5 | 4512.9 | 4837.7 | 4833.8 | 5133.3 | 5134. | 4299.6 | 4298.9 | 4776. | 4775.6 | 5052.1 | 5046.1 | 5410.6 |
| FN11QA | 17747. | 17753. | 18493. | 18474. | 19092. | 19099. | 17928. | 17952. | 19377. | 19390. | 20067. | 20053. | 21015. |
| SFC184 | .2568 | .25697 | .26444 | .2645 | .2718 | .27173 | .24244 | .24207 | .24916 | .24897 | .2545 | .25437 | .26026 |
| TAMB | 532.21 | 532.36 | 532.14 | 532.09 | 531.91 | 531.83 | 531.52 | 531.46 | 531.32 | 531.28 | 531.23 | 531.19 | 531.12 |
| T10 | 531.1 | 531.1 | 530.79 | 530.85 | 530.7 | 530.59 | 530.48 | 530.5 | 530.42 | 530.53 | 530.25 | 530.44 | 530.54 |
| PAMB | 14.125 | 14.125 | 14.123 | 14.123 | 14.122 | 14.121 | 14.119 | 14.119 | 14.12 | 14.119 | 14.119 | 14.12 | 14.12 |
| P10M | 14.127 | 14.128 | 14.125 | 14.126 | 14.125 | 14.124 | 14.121 | 14.122 | 14.123 | 14.122 | 14.123 | 14.122 | 14.122 |
| HUMSER | 113.34 | 113.02 | 112.16 | 111.86 | 111.82 | 111.87 | 110.68 | 111.41 | 109.98 | 110.28 | 111.23 | 109.04 | 109.67 |
| RELHUM | 90.783 | 90.092 | 90.075 | 89.991 | 90.506 | 90.778 | 90.777 | 91.531 | 90.821 | 91.193 | 92.108 | 90.475 | 91.204 |
| WINVAV | 5.6517 | 5.4682 | 6.2839 | 7.3706 | 7.5661 | 6.5787 | 5.8379 | 7.2179 | 6.2727 | 8.2222 | 7.4408 | 6.7403 | 10.205 |
| WINAAV | -8.0927 | -14.537 | -15.674 | -20.098 | -28.514 | -23.497 | -17.647 | -21.818 | -15.04 | -17.285 | -21.006 | -17.588 | -33.897 |
| XMO | 0. | 0. | 0. | 0. | 0. | 0. | 0. | 0. | 0. | 0. | 0. | 0. | 0. |
| P46Q2 | 2.633 | 2.6349 | 2.7431 | 2.7427 | 2.8388 | 2.8401 | 2.5768 | 2.5763 | 2.7356 | 2.7366 | 2.8258 | 2.8247 | 2.943 |
| CT46 | 1715.5 | 1715.3 | 1743. | 1741.6 | 1766.3 | 1764.9 | 1698.4 | 1698.4 | 1740.7 | 1740. | 1762.2 | 1762.4 | 1792.9 |
| T46X | 1694.5 | 1694.5 | 1713.5 | 1712.8 | 1737.3 | 1736.9 | 1680.2 | 1680.2 | 1720.5 | 1720.6 | 1735.4 | 1735.4 | 1764.9 |

Comments: Trim Balance Run
Mismatched Speeds (XN48 - XN49 = -100)
High Relative Humidity (Rain?)

GE36/UDF1 Peebles Tests
082001-03
Test Log - Site IIID
Sheet 012 of 029

GE36/UDF-1 ENGINE 082001-03 TEST READINGS - SITE IIID
RDGS. 57 - 70 ON 06.29.86 RDGS. 71 - 77 ON 06.30.86
RDGS. 78 - 149 ON 07.01.86 RDGS. 150 - 197 ON 07.03.86
RDGS. 198 - 209 ON 07.04.86 RDGS. 210 - 251 ON 07.05.86

| RDG. | 148 | 149 | 150 | 151 | 152 | 153 | 154 | 155 | 156 | 157 | 158 | 159 | 160 |
|---|---|---|---|---|---|---|---|---|---|---|---|---|---|
| XN2 | 11688. | 602.68 | 0. | 10737. | 183.93 | 10766. | 10770. | 10526. | 10528. | 9660.6 | 9654. | 8767.4 | 8764.2 |
| XN2R | 11565. | 595.32 | 0. | 10717. | 183.39 | 10749. | 10754. | 10510. | 10513. | 9647.2 | 9640.4 | 8755. | 8751.5 |
| PCN2R | 87.149 | 4.4862 | 0. | 80.759 | 1.382 | 81.005 | 81.036 | 79.203 | 79.224 | 72.699 | 72.648 | 65.976 | 65.949 |
| XN25 | 15655. | 129.9 | 0. | 14713. | 92.19 | 14717. | 14727. | 14521. | 14522. | 13952. | 13949. | 13500. | 13495. |
| XN25R | 12856. | 126.03 | 0. | 12583. | 90.101 | 12572. | 12581. | 12527. | 12528. | 12337. | 12336. | 12157. | 12152. |
| PCN25R | 95.8 | .93911 | 0. | 93.762 | .6714 | 93.679 | 93.745 | 93.343 | 93.352 | 91.933 | 91.926 | 90.586 | 90.551 |
| XN48 | 1297.9 | 672.3 | 0. | 1084.7 | 377.88 | 1084.9 | 1084.6 | 1084.6 | 1084.9 | 1085. | 1084.9 | 1084.9 | 1084.9 |
| XN49 | 1398.7 | 661.05 | 0. | 1085.5 | 413.51 | 1085.7 | 1085.9 | 1085.9 | 1086.2 | 1085.8 | 1086.1 | 1086.1 | 1086.2 |
| UT91R2 | 788.56 | 407.81 | 0. | 664.84 | 231.37 | 665.2 | 665.02 | 665.06 | 665.29 | 665.37 | 665.28 | 665.27 | 665.25 |
| UT92R2 | 826.05 | 389.76 | 0. | 646.71 | 246.1 | 647.06 | 647.2 | 647.24 | 647.46 | 647.22 | 647.37 | 647.36 | 647.42 |
| BTAN91 | 31.979 | 87.203 | 86.602 | 31.923 | 86.712 | 32.185 | 32.023 | 30.694 | 30.359 | 26.584 | 26.222 | 23.076 | 22.88 |
| BTAN92 | 29.203 | 87.217 | 84.768 | 29.426 | 86.732 | 29.477 | 29.66 | 28.651 | 28.749 | 25.39 | 25.567 | 22.75 | 23.074 |
| W13 | 13.782 | -4.9219 | -.5 | 13.653 | -6.7314 | 13.901 | 13.732 | 13.052 | 12.725 | 10.541 | 11.039 | 8.8799 | 9.1387 |
| W15 | 13.782 | -4.9219 | 0. | 13.653 | -6.7314 | 13.901 | 13.732 | 13.052 | 12.725 | 10.541 | 11.039 | 8.8799 | 9.1387 |
| WF36 | 5282.3 | 175.39 | 190.91 | 3594.6 | 187.92 | 3668.4 | 3655.8 | 3239.6 | 3241. | 2387.7 | 2387.7 | 1896. | 1896.2 |
| WF36R2 | 5427.5 | 179.62 | 197.12 | 3719.1 | 194.01 | 3796.3 | 3783.3 | 3351.5 | 3354.3 | 2470.7 | 2470. | 1961.7 | 1961.6 |
| FN11QA | 21062. | 0. | -.22841 | 14389. | 0. | 14531. | 14558. | 13495. | 13512. | 10490. | 10507. | 8200.2 | 8227.9 |
| SFC184 | .26049 | .5 | -872.36 | .26127 | .5 | .26409 | .26271 | .25106 | .25095 | .23809 | .23764 | .24183 | .241 |
| TAMB | 531.24 | 531.05 | 522.41 | 521.82 | 521.59 | 521.26 | 521.2 | 521.25 | 521.18 | 521. | 520.94 | 520.83 | 520.87 |
| T10 | 529.84 | 531.58 | 521.84 | 520.68 | 521.72 | 520.25 | 520.27 | 520.21 | 520.11 | 520.12 | 520.13 | 520.14 | 520.18 |
| PAMB | 14.12 | 14.12 | 14.185 | 14.188 | 14.189 | 14.193 | 14.193 | 14.194 | 14.194 | 14.194 | 14.195 | 14.195 | 14.196 |
| P10M | 14.122 | 14.121 | 14.186 | 14.19 | 14.19 | 14.195 | 14.194 | 14.199 | 14.195 | 14.195 | 14.199 | 14.195 | 14.197 |
| HUMSER | 110.94 | 108.34 | 75.88 | 74.874 | 74.336 | 73.235 | 73.235 | 72.812 | 72.764 | 72.961 | 72.543 | 72.194 | 71.84 |
| RELHUM | 91.861 | 90.337 | 86.279 | 86.953 | 87.055 | 86.826 | 87.004 | 86.377 | 86.536 | 87.306 | 87.013 | 86.922 | 86.383 |
| WINVAV | 7.3455 | 6.8006 | 2.652 | 2.3281 | 1.0232 | 3.0268 | 3.2939 | 2.4016 | 2.9972 | 1.3622 | .83494 | 1.3939 | 1.846 |
| WINAAV | -22.608 | -24.642 | -22.79 | 17.23 | -16.239 | -53.574 | -44.912 | 15.338 | 12.472 | 25.349 | 28.983 | -5.7549 | 11.328 |
| XM0 | 0. | 0. | 0. | 0. | 0. | 0. | 0. | 0. | 0. | 0. | 0. | 0. | 0. |
| P46Q2 | 2.9475 | 1.0031 | 9.99+10 | 2.3279 | 1.0017 | 2.3517 | 2.3544 | 2.2161 | 2.217 | 1.894 | 1.8929 | 1.6976 | 1.6969 |
| CT46 | 1790.3 | 907.71 | 9.99+10 | 1623.2 | 947.76 | 1635.1 | 1627.7 | 1574.9 | 1574.7 | 1471. | 1470. | 1403. | 1404.5 |
| T46X | 1763.5 | 725.26 | 531.92 | 1607.6 | 715.26 | 1615.1 | 1601.6 | 1568. | 1567.7 | 1474.5 | 1475.8 | 1404.7 | 1405.7 |

| Comments: | 148 | 149 | 150 | 151 | 152 | 153 | 154 | 155 | 156 | 157 | 158 | 159 | 160 |
|---|---|---|---|---|---|---|---|---|---|---|---|---|---|
| | Trim. Bal. Run. Mis-matched Speeds High Humidity | Zero | Zero | Part Power | Zero | "EPR POWER HOOK" 4 → | | | | | | | |
| | | | | | | Pt.1a | Pt.1b | Pt.2a | Pt.2b | Pt.3a | Pt.3b | Pt.4a | Pt.4b |

GE36/UDF1 Peebles Tests
082001-03
Test Log - Site IIID
Sheet 013 of 029

GE36/UDF-1 ENGINE 082001-03 TEST READINGS - SITE IIID
RDGS. 57 - 70 ON 06.29.86 RDGS. 71 - 77 ON 06.30.86
RDGS. 78 - 149 ON 07.01.86 RDGS. 150 - 197 ON 07.03.86
RDGS. 198 - 209 ON 07.04.86 RDGS. 210 - 251 ON 07.05.86

| RDG. | 161 | 162 | 163 | 164 | 165 | 166 | 167 | 168 | 169 | 170 | 171 | 172 | 173 |
|---|---|---|---|---|---|---|---|---|---|---|---|---|---|
| XN2 | 11055. | 11054. | 10848. | 10848. | 10270. | 10275. | 9154.3 | 9155.8 | 11444. | 11449. | 11156. | 11158. | 10592. |
| XN2R | 11034. | 11036. | 10833. | 10835. | 10257. | 10265. | 9146.4 | 9147.8 | 11438. | 11445. | 11147. | 11151. | 10584. |
| PCN2R | 83.146 | 83.166 | 81.634 | 81.647 | 77.295 | 77.356 | 68.925 | 68.936 | 86.196 | 86.25 | 84. | 84.032 | 79.761 |
| XN25 | 15031. | 15033. | 14844. | 14844. | 14335. | 14333. | 13716. | 13713. | 15372. | 15376. | 15139. | 15137. | 14634. |
| XN25R | 12688. | 12692. | 12635. | 12636. | 12482. | 12481. | 12257. | 12252. | 12799. | 12802. | 12735. | 12735. | 12585. |
| PCN25R | 94.543 | 94.577 | 94.154 | 94.16 | 93.01 | 93.003 | 91.335 | 91.297 | 95.372 | 95.398 | 94.896 | 94.896 | 93.776 |
| XN48 | 1174.6 | 1174.8 | 1174.5 | 1175.2 | 1174.8 | 1174.6 | 1174.8 | 1175.2 | 1254.9 | 1254.9 | 1255.3 | 1254.6 | 1254.5 |
| XN49 | 1176.1 | 1176.2 | 1175.7 | 1176. | 1176. | 1176.2 | 1176.1 | 1176.2 | 1255.9 | 1256.2 | 1255.9 | 1256.3 | 1255.9 |
| UT91R2 | 719.9 | 720.22 | 720.22 | 720.79 | 720.5 | 720.61 | 720.79 | 721.02 | 770.24 | 770.36 | 770.2 | 769.99 | 769.76 |
| UT92R2 | 700.63 | 700.94 | 700.78 | 701.09 | 701.04 | 701.39 | 701.41 | 701.48 | 749.32 | 749.59 | 749.04 | 749.47 | 749.09 |
| BTAN91 | 32.017 | 31.486 | 30.864 | 30.792 | 27.375 | 27.173 | 22.929 | 23.061 | 33.04 | 32.532 | 30.793 | 31.366 | 28.026 |
| BTAN92 | 29.284 | 29.749 | 29.104 | 28.909 | 26.2 | 26.503 | 22.974 | 22.889 | 29.565 | 29.878 | 29.37 | 29.046 | 26.834 |
| W13 | 13.655 | 13.456 | 12.241 | 12.752 | 10.981 | 10.999 | 9.1915 | 8.7562 | 13.908 | 13.947 | 16.107 | 13.489 | 11.806 |
| W15 | 13.655 | 13.456 | 12.241 | 12.752 | 10.981 | 10.999 | 9.1915 | 8.7562 | 13.908 | 13.947 | 15.808 | 13.489 | 11.806 |
| WF36 | 4185.1 | 4181.1 | 3807.4 | 3811.3 | 2899.4 | 2911.5 | 2112.2 | 2112.7 | 4996.4 | 4999. | 4418.9 | 4421.6 | 3405.1 |
| WF36R2 | 4327.7 | 4326.4 | 3940.7 | 3945.8 | 3000.2 | 3013.9 | 2186.4 | 2186.8 | 5178. | 5181.5 | 4575.7 | 4579.9 | 3524.4 |
| FNI1QA | 16737. | 16867. | 15895. | 15881. | 12791. | 12857. | 9312.6 | 9303. | 19472. | 19590. | 18334. | 18297. | 15021. |
| SFC184 | .26138 | .25929 | .25061 | .25116 | .2371 | .23696 | .23733 | .23762 | .2688 | .26737 | .25229 | .25302 | .23719 |
| TAMB | 521.28 | 521.34 | 521.24 | 521.11 | 520.78 | 520.64 | 520.48 | 520.44 | 520.18 | 520.13 | 520.07 | 520.1 | 520.06 |
| T10 | 520.72 | 520.38 | 520.14 | 519.92 | 519.98 | 519.71 | 519.57 | 519.58 | 519.15 | 518.99 | 519.54 | 519.27 | 519.47 |
| PAMB | 14.198 | 14.199 | 14.2 | 14.2 | 14.202 | 14.202 | 14.202 | 14.202 | 14.204 | 14.205 | 14.207 | 14.207 | 14.208 |
| P10M | 14.198 | 14.196 | 14.195 | 14.195 | 14.199 | 14.199 | 14.2 | 14.2 | 14.199 | 14.2 | 14.202 | 14.203 | 14.206 |
| HUMSER | 70.186 | 70.156 | 69.791 | 70.175 | 69.769 | 70.012 | 69.805 | 69.959 | 69.657 | 70.187 | 69.073 | 69.451 | 69.151 |
| RELHUM | 83.245 | 83.026 | 82.899 | 83.725 | 84.237 | 84.971 | 85.178 | 85.506 | 85.935 | 86.727 | 85.565 | 85.962 | 85.723 |
| WINVAV | 3.3679 | 2.4447 | 2.964 | 3.209 | 2.1319 | 1.6139 | 2.1175 | 1.174 | 2.2912 | 2.0476 | 4.0252 | 3.2148 | 2.3576 |
| WINAAV | -7.4529 | 26.522 | 18.307 | 17.188 | -22.659 | -4.2657 | 71.84 | 129.42 | -33.508 | 28.718 | -45.19 | 13.269 | -13.38 |
| XMO | 0. | 0. | 0. | 0. | 0. | 0. | 0. | 0. | 0. | 0. | 0. | 0. | 0. |
| P46Q2 | 2.5551 | 2.556 | 2.4329 | 2.4343 | 2.1003 | 2.1028 | 1.7921 | 1.793 | 2.8434 | 2.8475 | 2.6588 | 2.6603 | 2.2981 |
| CT46 | 1678.2 | 1674.6 | 1636.3 | 1634.2 | 1539.9 | 1542.2 | 1435.5 | 1437.8 | 1748.9 | 1746.2 | 1684.6 | 1692.1 | 1594.4 |
| T46X | 1647.3 | 1645.5 | 1612. | 1611.7 | 1538.6 | 1540.3 | 1438.4 | 1439.8 | 1715.4 | 1713.2 | 1663.6 | 1664.2 | 1587.6 |
| Comments: | "EPR POWER HOOK" 5 → | | | | | | | | "EPR POWER HOOK" 6 → | | | | |
| | Pt.1a | Pt.1b | Pt.2a | Pt.2b | Pt.3a | Pt.3b | Pt.4a | Pt.4b | Pt.1a | Pt.1b | Pt.2a | Pt.2b | Pt.3a |

GE36/UDF1 Peebles Tests
082001-03
Test Log - Site IIID
Sheet 014 of 029

GE36/UDF-1 ENGINE 082001-0: :ST READINGS - SITE IIID
RDGS. 57 - 70 ON 06.29.86 RDGS. 71 - 77 ON 06.30.86
RDGS. 78 - 149 ON 07.01.86 RDGS. 150 - 197 ON 07.03.86
RDGS. 198 - 209 ON 07.04.86 RDGS. 210 - 251 ON 07.05.86

| RDG. | 174 | 175 | 176 | 177 | 178 | 179 | 180 | 181 | 182 | 183 | 184 | 185 | 186 |
|---|---|---|---|---|---|---|---|---|---|---|---|---|---|
| XN2 | 10592. | 10244. | 10239. | 10241. | 5784.1 | 422.86 | 0. | 10979. | 10986. | 11121. | 11712. | 10936. | 135.71 |
| XN2R | 10588. | 10242. | 10237. | 10239. | 5781. | 420.37 | 0. | 10874. | 10884. | 10999. | 11578. | 10815. | 133.36 |
| PCN2R | 79.79 | 77.181 | 77.142 | 77.158 | 43.565 | 3.1678 | 0. | 81.945 | 82.018 | 82.889 | 87.246 | 81.498 | 1.0049 |
| XN25 | 14631. | 14316. | 14312. | 14311. | 11887. | 167.62 | 0. | 14996. | 15005. | 15168. | 15671. | 14993. | 114.71 |
| XN25R | 12586. | 12480. | 12476. | 12475. | 11335. | 162.78 | 0. | 12620. | 12629. | 12679. | 12827. | 12636. | 110.31 |
| PCN25R | 93.786 | 92.995 | 92.969 | 92.956 | 84.465 | 1.2129 | 0. | 94.038 | 94.105 | 94.481 | 95.585 | 94.16 | .82202 |
| XN48 | 1254.7 | 1255. | 1254.7 | 1255.3 | 700.3 | 573.85 | 0. | 1254.2 | 1256.6 | 1301.5 | 1299.9 | 1230.7 | 227.85 |
| XN49 | 1256.2 | 1255.9 | 1256.1 | 1256.2 | 701.1 | 122.83 | 0. | 1255.7 | 1257.4 | 1399.3 | 1398.9 | 1357.5 | 268.17 |
| UT91R2 | 770.23 | 770.56 | 770.37 | 770.68 | 429.82 | 350.32 | 0. | 762.86 | 764.47 | 790.48 | 789.1 | 747.41 | 137.49 |
| UT92R2 | 749.55 | 749.54 | 749.6 | 749.66 | 418.27 | 72.888 | 0. | 742.38 | 743.55 | 826.08 | 825.42 | 801.28 | 157.29 |
| BTAN91 | 27.878 | 25.748 | 25.903 | 25.91 | 20.23 | 87.248 | 77.765 | 29.383 | 29.463 | 29.925 | 32.511 | 29.665 | 87.286 |
| BTAN92 | 27.055 | 25.458 | 25.412 | 25.348 | 20.319 | 87.188 | 77.559 | 29.666 | 29.505 | 27.249 | 28.605 | 26.647 | 87.238 |
| W13 | 11.604 | 10.664 | 10.629 | 10.676 | 6.3215 | -5.6218 | -.5 | 12.875 | 12.974 | 12.598 | 13.852 | 12.469 | -7.1869 |
| W15 | 11.604 | 10.664 | 10.629 | 10.676 | 5.593 | -5.6218 | 0. | 12.875 | 12.974 | 12.598 | 13.852 | 12.469 | -7.1869 |
| WF36 | 3407.5 | 2903.3 | 2898.2 | 2903.3 | 848.42 | 186.94 | 168.22 | 4019.3 | 4010.9 | 4271.1 | 5415.2 | 3868.6 | 161.11 |
| WF36R2 | 3529.1 | 3006.9 | 3001.6 | 3006.6 | 877.64 | 191.88 | 167.11 | 4101. | 4093.1 | 4348.9 | 5512.2 | 3938.8 | 162.46 |
| FN11QA | 15090. | 13009. | 12964. | 12981. | 2965.9 | 0. | 0. | 16889. | 16958. | 18199. | 21213. | 16638. | 0. |
| SFC184 | .23641 | .23366 | .23406 | .23413 | .29913 | .5 | .5 | .24547 | .244 | .24156 | .26267 | .2393 | .5 |
| TAMB | 520.02 | 519.85 | 519.82 | 519.85 | 520.3 | 520.53 | 531.47 | 532.16 | 531.85 | 533.04 | 533.56 | 534.07 | 533.94 |
| T10 | 519.06 | 518.84 | 518.87 | 518.89 | 519.22 | 524.83 | 548.52 | 528.68 | 528.48 | 530.22 | 530.75 | 530.38 | 537.18 |
| PAMB | 14.209 | 14.21 | 14.21 | 14.21 | 14.213 | 14.213 | 14.244 | 14.242 | 14.241 | 14.243 | 14.241 | 14.238 | 14.237 |
| P10M | 14.205 | 14.208 | 14.208 | 14.208 | 14.213 | 14.214 | 14.246 | 14.239 | 14.24 | 14.241 | 14.238 | 14.238 | 14.239 |
| HUMSER | 69.057 | 69.244 | 69.007 | 68.857 | 64.324 | 67.137 | 62.86 | 53.117 | 59.604 | 58.552 | 57.614 | 60.032 | 52.517 |
| RELHUM | 85.736 | 86.48 | 86.296 | 85.998 | 79.155 | 81.916 | 52.649 | 43.567 | 49.32 | 46.566 | 45.027 | 46.089 | 40.558 |
| WINVAV | 1.3263 | 1.4311 | 1.5607 | 1.8261 | 2.5259 | 1.702 | 2.0863 | 8.7989 | 7.4522 | .87259 | 3.3704 | 2.9745 | 7.3289 |
| WINAAV | 72.559 | 56.546 | -14.545 | 11.273 | 60.439 | -164.73 | 111.96 | -158.36 | 162.5 | 82.663 | -111.01 | 149.86 | 171.44 |
| XMO | 0. | 0. | 0. | 0. | 0. | 0. | 0. | 0. | 0. | 0. | 0. | 0. | 0. |
| P46Q2 | 2.3004 | 2.1048 | 2.1038 | 2.1045 | 1.3657 | 1.0022 | 9.99+10 | 2.4772 | 2.4817 | 2.583 | 2.9754 | 2.4477 | 1.0026 |
| CT46 | 1594.5 | 1542.7 | 1542.5 | 1544.2 | 1164.4 | 947.22 | 9.99+10 | 1699.9 | 1689.8 | 1721.7 | 1811.2 | 1669.8 | 899.81 |
| T46X | 1588.5 | 1541.2 | 1542.1 | 1543. | 1220.4 | 721.84 | 559.36 | 1666.6 | 1660.7 | 1689.9 | 1775.3 | 1644.4 | 735.05 |

| Comments: | "EPR POWER HOOK" 6 → | | | | F.I. | Zero | Zero | Part Power | Part Power | Part Power | Part Power | Part Power | Zero |
|---|---|---|---|---|---|---|---|---|---|---|---|---|---|
| | Pt.3b | Pt.4a | Pt.4b | Pt.4c | Bad Reading | | | Pt.1a | Pt.1b | | | | |

GE36/UDF1 Feebles Tests
082001-03
Test Log - Site IIID
Sheet 015 of 029

GE36/UDF-1 ENGINE 082001-03 TEST READINGS - SITE IIID

RDGS. 57 - 70 ON 06.29.86 RDGS. 71 - 77 ON 06.30.86
RDGS. 78 - 149 ON 07.01.86 RDGS. 150 - 197 ON 07.03.86
RDGS. 198 - 209 ON 07.04.86 RDGS. 210 - 251 ON 07.05.86

| RDG. | 187 | 188 | 189 | 190 | 191 | 192 | 193 | 194 | 195 | 196 | 197 | 198 | 199 |
|---|---|---|---|---|---|---|---|---|---|---|---|---|---|
| XN2 | 0. | 12115. | 12121. | 12144. | 8151.3 | 11842. | 11530. | 11540. | 11534. | 201.25 | 0. | 504.82 | 0. |
| XN2R | 0. | 11992. | 11997. | 12040. | 8072. | 11734. | 11434. | 11451. | 11426. | 199.88 | 0. | 505.2 | 0. |
| PCN2R | 0. | 90.369 | 90.407 | 90.731 | 60.829 | 88.422 | 86.167 | 86.294 | 86.104 | 1.5063 | 0. | 3.8071 | 0. |
| XN25 | 0. | 15953. | 15989. | 15997. | 13472. | 15763. | 15519. | 15526. | 15535. | 104.24 | 0. | 129.38 | 0. |
| XN25R | 0. | 12858. | 12893. | 12908. | 12439. | 12849. | 12791. | 12802. | 12801. | 101.2 | 0. | 126.78 | 0. |
| PCN25R | 0. | 95.816 | 96.073 | 96.184 | 92.688 | 95.743 | 95.31 | 95.396 | 95.388 | .75413 | 0. | .94468 | 0. |
| XN48 | 0. | 1398.1 | 1398.1 | 1398.1 | 964.99 | 1398.2 | 1398.1 | 1398.1 | 1398.5 | 374.13 | 0. | 103.14 | 0. |
| XN49 | 0. | 1398.5 | 1399.1 | 1399.3 | 969.81 | 1398.9 | 1399.1 | 1399.1 | 1399.4 | 431.32 | 0. | 116.27 | 0. |
| UT91R2 | 0. | 849.79 | 849.73 | 851.19 | 586.83 | 850.77 | 851.38 | 851.91 | 850.76 | 228.19 | 0. | 63.387 | 0. |
| UT92R2 | 0. | 826.23 | 826.58 | 828.07 | 573.25 | 827.35 | 828.18 | 828.7 | 827.5 | 255.71 | 0. | 69.454 | 0. |
| BTAN91 | 87.336 | 33.139 | 33.124 | 32.935 | 20.224 | 30.825 | 30.085 | 30.748 | 31.182 | 87.255 | 87.278 | 87.253 | 86.866 |
| BTAN92 | 85.574 | 30.054 | 30.276 | 30.481 | 20.377 | 30.138 | 29.35 | 29.839 | 29.148 | 87.14 | 85.442 | 87.131 | 86.917 |
| W13 | -.5 | 14.817 | 14.697 | 14.646 | 51.451 | 14.115 | 13.783 | 13.517 | 13.244 | -6.7529 | -.5 | -5.3 | -.5 |
| W15 | 0. | 14.817 | 14.697 | 14.646 | 51.451 | 14.115 | 13.783 | 13.517 | 13.244 | -6.7529 | 0. | -5.3 | 0. |
| WF36 | 162.3 | 6592.5 | 6523.7 | 6590.2 | 2429. | 5853.4 | 5208.1 | 5176.7 | 5115.9 | 181.52 | 190.3 | 190.45 | 189.34 |
| WF36R2 | 158.72 | 6723.6 | 6652.5 | 6735.8 | 2476.5 | 5977. | 5323. | 5295.5 | 5221.6 | 185.68 | 193.6 | 196.77 | 192.92 |
| FN11QA | 1.5865 | 24344. | 24309. | 24524. | 2993.1 | 23094. | 21355. | 21404. | 21208. | -15.366 | 0. | 0. | 0. |
| SFC184 | 101.13 | .2792 | .27663 | .27764 | .8364 | .26163 | .25197 | .25009 | .24888 | -12.215 | .5 | .5 | .5 |
| TAMB | 533.89 | 528.93 | 529.47 | 528.67 | 528.82 | 528.56 | 527.69 | 527.57 | 527.47 | 525.5 | 522.01 | 518.15 | 529.97 |
| T10 | 561.68 | 529.4 | 529.47 | 527.66 | 528.91 | 528.28 | 527.42 | 526.77 | 528.5 | 525.79 | 529.68 | 517.88 | 527.27 |
| PAMB | 14.235 | 14.24 | 14.241 | 14.242 | 14.242 | 14.242 | 14.242 | 14.242 | 14.242 | 14.244 | 14.249 | 14.25 | 14.271 |
| P10M | 14.237 | 14.238 | 14.242 | 14.24 | 14.243 | 14.24 | 14.241 | 14.244 | 14.241 | 14.245 | 14.25 | 14.252 | 14.273 |
| HUMSER | 49.69 | 59.717 | 54.082 | 60.142 | 56.723 | 62.711 | 62.285 | 60.208 | 61.896 | 60.495 | 63.104 | 56.639 | 65.236 |
| RELHUM | 38.462 | 54.559 | 48.57 | 55.454 | 52.07 | 58.003 | 59.348 | 57.635 | 59.436 | 62.225 | 73.304 | 75.581 | 57.574 |
| WINVAV | 3.4719 | 2.4118 | 2.2317 | 1.0139 | 3.0652 | 1.6798 | 2.0436 | 1.7738 | 2.4212 | 1.3143 | 1.2973 | 1.0878 | 6.5432 |
| WINAAV | -163.45 | -6.0663 | 14.235 | -18.007 | -109.41 | -7.3376 | 1.7137 | 7.9257 | 25.487 | .37115 | -28.527 | -24.851 | -37.498 |
| XMO | 0. | 0. | 0. | 0. | 0. | 0. | 0. | 0. | 0. | 0. | 0. | 0. | 0. |
| P46Q2 | 9.99+10 | 3.32 | 3.3236 | 3.3546 | 0. | 3.1072 | 2.8926 | 2.9014 | 2.8868 | 1.0013 | 9.99+10 | 1.0027 | 9.99+10 |
| CT46 | 9.99+10 | 1925.9 | 1904.9 | 1897.1 | 2526.5 | 1852. | 1804.8 | 1787.8 | 1780.9 | 930.45 | 9.99+10 | 929.7 | 9.99+10 |
| T46X | 601.82 | 1879.7 | 1863.5 | 1858. | 1291.5 | 1805.1 | 1752.9 | 1745.5 | 1743.1 | 714.45 | 630.28 | 710.77 | 549.18 |
| Comments: | Zero | DOWN POWER CAL., HIGH POWER → | | | | | | | | Zero | Zero | Zero | Zero |
| | | Pt.1a Max PLA | Pt.1b Max PLA | Max PLA+ | BAD POINT Incomplete Reading | Pt.2a Possibly Incomplete | Pt.3a | Pt.3b | Pt.3c | | | | |

GE36/UDF1 Peebles Tests
082001-03
Test Log - Site IIID
Sheet 016 of 029

GE36/UDF-1 ENGINE 082001-( EST READINGS - SITE IIID
RDGS. 57 - 70 ON 06.29.86 RDGS. 71 - 77 ON 06.30.86
RDGS. 78 - 149 ON 07.01.86 RDGS. 150 - 197 ON 07.03.86
RDGS. 198 - 209 ON 07.04.86 RDGS. 210 - 251 ON 07.05.86

| RDG. | 200 | 201 | 202 | 203 | 204 | 205 | 206 | 207 | 208 | 209 | 210 | 211 | 212 |
|---|---|---|---|---|---|---|---|---|---|---|---|---|---|
| XN2 | 471.61 | 0. | 11594. | 11645. | 11626. | 11683. | 11700. | 11546. | 11575. | 11056. | 11514. | 11484. | 104.11 |
| XN2R | 465.86 | 0. | 11457. | 11517. | 11500. | 11564. | 11568. | 11417. | 11458. | 10942. | 11405. | 11407. | 103.05 |
| PCN2R | 3.5106 | 0. | 86.337 | 86.792 | 86.664 | 87.141 | 87.171 | 86.038 | 86.348 | 82.455 | 85.943 | 85.963 | .77653 |
| XN25 | 136.19 | 0. | 15564. | 15615. | 15599. | 15639. | 15647. | 15537. | 15544. | 15100. | 15500. | 15444. | 152.95 |
| XN25R | 132.74 | 0. | 12772. | 12800. | 12801. | 12813. | 12792. | 12782. | 12788. | 12675. | 12775. | 12758. | 147.06 |
| PCN25R | .98915 | 0. | 95.168 | 95.381 | 95.387 | 95.478 | 95.322 | 95.246 | 95.288 | 94.45 | 95.193 | 95.069 | 1.0958 |
| XN48 | 616.04 | 0. | 1397.6 | 1398.1 | 1397.9 | 1397.6 | 1397.6 | 1397.8 | 1397.6 | 1279.6 | 1397.6 | 1397.8 | 236.29 |
| XN49 | 619.79 | 0. | 1398.6 | 1399. | 1398.3 | 1398.9 | 1398.7 | 1398.7 | 1398.9 | 1280.8 | 1398.5 | 1399. | 281.3 |
| | | | | | | | | | | | | | |
| UT91R2 | 373.7 | 0. | 848.11 | 849.13 | 849.19 | 849.55 | 848.59 | 848.81 | 849.62 | 777.7 | 850.1 | 852.66 | 143.62 |
| UT92R2 | 365.45 | 0. | 824.93 | 825.91 | 825.66 | 826.48 | 825.47 | 825.61 | 826.55 | 756.64 | 826.77 | 829.51 | 166.19 |
| BTAN91 | 86.895 | 79.922 | 30.898 | 31.368 | 31.116 | 31.046 | 31.62 | 31.212 | 30.567 | 30.088 | 30.209 | 30.874 | 87.113 |
| BTAN92 | 86.857 | 79.841 | 28.992 | 29.731 | 29.847 | 30.212 | 30.359 | 29.296 | 29.536 | 28.865 | 29.371 | 29.471 | 87.129 |
| | | | | | | | | | | | | | |
| W13 | -5.7943 | -.5 | 14.132 | 13.86 | 13.909 | 14.05 | 14.183 | 13.54 | 13.949 | 13.086 | 13.582 | 13.74 | -7.1265 |
| W15 | -5.7943 | 0. | 14.132 | 13.86 | 13.909 | 14.05 | 14.183 | 13.54 | 13.949 | 13.086 | 13.582 | 13.74 | -7.1265 |
| | | | | | | | | | | | | | |
| WF36 | 167.83 | 166.81 | 5303.9 | 5375. | 5341.1 | 5473.8 | 5562. | 5156.1 | 5228.1 | 4095.7 | 5124. | 5165.6 | 179.37 |
| WF36R2 | 170.14 | 168.46 | 5390.5 | 5468.6 | 5434.5 | 5574.5 | 5656.6 | 5244. | 5323.6 | 4168.6 | 5221.6 | 5284.3 | 182.43 |
| FN11QA | 0. | 0. | 21402. | 21739. | 21718. | 22071. | 22216. | 21132. | 21374. | 17328. | 21096. | 21170. | 0. |
| SFC184 | .5 | .5 | .2546 | .25429 | .25295 | .25532 | .25739 | .25086 | .25178 | .24319 | .25021 | .25233 | .5 |
| | | | | | | | | | | | | | |
| TAMB | 532.73 | 533.57 | 531.67 | 530.45 | 529.82 | 530.1 | 530.95 | 530.17 | 529.72 | 529.28 | 528.81 | 526.64 | 528.13 |
| T10 | 531.55 | 535.45 | 531.19 | 530.22 | 530.04 | 529.39 | 530.59 | 530.41 | 529.3 | 529.56 | 528.71 | 525.64 | 529.41 |
| PAMB | 14.264 | 14.247 | 14.25 | 14.253 | 14.253 | 14.254 | 14.251 | 14.254 | 14.256 | 14.257 | 14.256 | 14.259 | 14.258 |
| P10M | 14.266 | 14.249 | 14.251 | 14.254 | 14.257 | 14.256 | 14.253 | 14.255 | 14.259 | 14.258 | 14.259 | 14.261 | 14.26 |
| HUMSER | 64.593 | 75.625 | 74.366 | 79.608 | 74.766 | 75.027 | 74.892 | 73.585 | 74.568 | 73.056 | 73.966 | 77.018 | 74.583 |
| RELHUM | 51.911 | 58.862 | 61.74 | 68.822 | 66.112 | 65.71 | 63.701 | 64.318 | 66.171 | 65.839 | 67.718 | 75.933 | 69.894 |
| WINVAV | 6.028 | 1.2663 | 1.7037 | 2.8463 | 1.6761 | 2.3268 | 1.6221 | 2.2019 | 2.7516 | 2.2083 | 2.4046 | 3.0244 | 1.7111 |
| WINAAV | 8.1875 | 144.89 | -22.761 | -28.388 | 12.106 | 13.664 | 46.51 | -42.139 | 29.641 | 23.411 | 12.249 | -14.782 | 2.1186 |
| XMO | 0. | 0. | 0. | 0. | 0. | 0. | 0. | 0. | 0. | 0. | 0. | 0. | 0. |
| | | | | | | | | | | | | | |
| P46Q2 | 1.002 | 9.99+10 | 2.9092 | 2.9471 | 2.9344 | 2.9806 | 2.9827 | 2.8769 | 2.9077 | 2.5348 | 2.8722 | 2.8734 | 1.001 |
| CT46 | 872.66 | 9.99+10 | 1829.2 | 1819. | 1817.2 | 1825.5 | 1850.3 | 1802.8 | 1803.2 | 1682.6 | 1793.6 | 1802.5 | 948.35 |
| T46X | 724.75 | 547.95 | 1779.5 | 1776.2 | 1772.4 | 1780.1 | 1800.4 | 1758.1 | 1759.3 | 1653.8 | 1749.4 | 1754.9 | 719.65 |

| Comments: | Zero | Zero | LCF CYCLES → | | | | | | | | | | |
|---|---|---|---|---|---|---|---|---|---|---|---|---|---|
| | | | Pt.1 | Pt.2 | Pt.3 | Pt.4 | Pt.5 | Pt.6 | Pt.7 | Pull Back Pt. For Vibs. | Pt.8 | Pt.9 | Zero |

GE36/UDF1 Peebles Tests
082001-03
Test Log - Site IIID
Sheet 017 of 029

GE36/UDF-1 ENGINE 082001-[illegible] TEST READINGS - SITE IIID
RDGS. 57 - 70 ON 06.29.86 RDGS. 71 - 77 ON 06.30.86
RDGS. 78 - 149 ON 07.01.86 RDGS. 150 - 197 ON 07.03.86
RDGS. 198 - 209 ON 07.04.86 RDGS. 210 - 251 ON 07.05.86

| RDG. | 213 | 214 | 215 | 216 | 217 | 218 | 219 | 220 | 221 | 222 | 223 | 224 | 225 |
|---|---|---|---|---|---|---|---|---|---|---|---|---|---|
| XN2 | 0. | 11481. | 11516. | 11489. | 11475. | 11471. | 11471. | 11456. | 282.14 | 0. | 11439. | 11473. | 11476. |
| XN2R | 0. | 11357. | 11396. | 11396. | 11395. | 11401. | 11408. | 11392. | 280.32 | 0. | 11394. | 11410. | 11407. |
| PCN2R | 0. | 85.587 | 85.88 | 85.876 | 85.867 | 85.915 | 85.967 | 85.849 | 2.1124 | 0. | 85.864 | 85.985 | 85.958 |
| XN25 | 0. | 15453. | 15503. | 15462. | 15447. | 15440. | 15429. | 15422. | 122.57 | 0. | 15369. | 15434. | 15432. |
| XN25R | 0. | 12732. | 12771. | 12767. | 12770. | 12770. | 12763. | 12764. | 119.16 | 0. | 12734. | 12770. | 12758. |
| PCN25R | 0. | 94.874 | 95.165 | 95.131 | 95.156 | 95.159 | 95.105 | 95.113 | .88793 | 0. | 94.887 | 95.159 | 95.064 |
| XN48 | 0. | 1397.8 | 1397.8 | 1397.8 | 1397.4 | 1397.8 | 1397.5 | 1397.5 | 431.32 | 0. | 1397.4 | 1397.6 | 1397.6 |
| XN49 | 0. | 1398.7 | 1398.7 | 1399. | 1399. | 1398.6 | 1398.7 | 1398.6 | 470.7 | 0. | 1398.6 | 1398.7 | 1398.6 |
| UT91R2 | 0. | 849.13 | 849.46 | 851.44 | 852.11 | 853.13 | 853.45 | 853.41 | 263.16 | 0. | 854.72 | 853.59 | 853.07 |
| UT92R2 | 0. | 825.91 | 826.23 | 828.32 | 829.2 | 829.73 | 830.27 | 830.15 | 279.15 | 0. | 831.51 | 830.33 | 829.74 |
| BTAN91 | 87.033 | 30.729 | 30.546 | 30.756 | 30.694 | 31.07 | 31.161 | 31.107 | 87.138 | 87.08 | 30.49 | 30.855 | 30.85 |
| BTAN92 | 87.127 | 29.552 | 29.813 | 29.318 | 29.546 | 29.568 | 29.407 | 29.253 | 87.179 | 87.125 | 29.403 | 29.533 | 29.564 |
| W13 | -.5 | 13.839 | 13.728 | 13.622 | 13.897 | 13.669 | 13.95 | 13.843 | -6.3554 | -.5 | 14.219 | 13.862 | 14.05 |
| W15 | 0. | 13.839 | 13.728 | 13.622 | 13.897 | 13.669 | 13.95 | 13.843 | -6.3554 | 0. | 14.219 | 13.862 | 14.05 |
| WF36 | 178.62 | 5102.3 | 5114.5 | 5090.6 | 5093.7 | 5093.4 | 5128.8 | 5076.5 | 181.8 | 186.77 | 5157.4 | 5119.8 | 5155.4 |
| WF36R2 | 180.98 | 5191.9 | 5206.8 | 5198.9 | 5209.3 | 5215.9 | 5256.2 | 5202. | 185.89 | 189.71 | 5294.6 | 5243.4 | 5273.5 |
| FN11QA | 0. | 20963. | 21143. | 21031. | 21107. | 21111. | 21139. | 21028. | 0. | .11087 | 21205. | 21204. | 21203. |
| SFC184 | .5 | .25036 | .24895 | .24989 | .24949 | .24976 | .25136 | .25007 | .5 | 1729.7 | .2524 | .24997 | .25142 |
| TAMB | 528.38 | 530.99 | 527.69 | 527.7 | 526.33 | 525.72 | 525.5 | 525.45 | 525.39 | 523.49 | 523.17 | 525.04 | 525.83 |
| T10 | 532.54 | 530.02 | 529.61 | 527.15 | 526.02 | 525.06 | 524.47 | 524.52 | 525.44 | 530.11 | 522.81 | 524.39 | 525.03 |
| PAMB | 14.254 | 14.253 | 14.254 | 14.255 | 14.255 | 14.256 | 14.255 | 14.256 | 14.256 | 14.264 | 14.263 | 14.266 | 14.272 |
| P10M | 14.255 | 14.255 | 14.256 | 14.257 | 14.258 | 14.257 | 14.258 | 14.258 | 14.258 | 14.265 | 14.264 | 14.268 | 14.274 |
| HUMSER | 75.293 | 73.494 | 75.927 | 74.906 | 76.225 | 75.769 | 76.541 | 76.658 | 75.077 | 77.036 | 76.729 | 78.684 | 78.832 |
| RELHUM | 69.917 | 62.476 | 72.21 | 71.234 | 75.955 | 77.134 | 78.508 | 78.764 | 77.331 | 84.786 | 85.407 | 82.021 | 79.964 |
| WINVAV | 1.6997 | 1.0864 | 2.3884 | 2.2434 | 1.4316 | 2.6265 | 2.52 | 2.5319 | .67314 | 1.3366 | 2.9263 | 2.5411 | 1.5504 |
| WINAAV | 5.7865 | 29.185 | 74.409 | -5.8209 | 6.9428 | 7.921 | -8.0449 | .32143 | -4.4376 | -52.011 | -6.1593 | 50.804 | -8.784 |
| XMO | 0. | 0. | 0. | - 0. | 0. | 0. | 0. | 0. | 0. | 0. | 0. | 0. | 0. |
| P46Q2 | 9.99+10 | 2.8373 | 2.8668 | 2.8621 | 2.8643 | 2.8635 | 2.8727 | 2.8611 | 1.0021 | 9.99+10 | 2.8639 | 2.8715 | 2.8714 |
| CT46 | -9.99+10 | 1811.8 | 1795.9 | 1787.2 | 1785.8 | 1783.2 | 1790.8 | 1780.9 | 933.11 | 9.99+10 | 1801.9 | 1784. | 1797.3 |
| T46X | 635.32 | 1767.7 | 1755.1 | 1747.2 | 1744.7 | 1743.3 | 1747.7 | 1740.5 | 718.53 | 612.55 | 1756.8 | 1743.5 | 1754.3 |
| Comments: | Zero | LCF CYCLES → Pt.10 | Pt.11 | Pt.12 | Pt.13 | Pt.14 | Pt.15 | Pt.16 Incomplete | Zero | Zero | LCF CYCLES → Pt.16 Redone | Pt.17 | Pt.18 |

GE36/UDF1 Peebles Tests
082001-03
Test Log - Site IIID
Sheet 018 of 029

GE36/UDF-1 ENGINE 082001-03 TEST READINGS - SITE IIID
RDGS. 57 - 70 ON 06.29.86 RDGS. 71 - 77 ON 06.30.86
RDGS. 78 - 149 ON 07.01.86 RDGS. 150 - 197 ON 07.03.86
RDGS. 198 - 209 ON 07.04.86 RDGS. 210 - 251 ON 07.05.86

| RDG. | 226 | 227 | 228 | 229 | 230 | 231 | 232 | 233 | 234 | 235 | 236 | 237 | 238 |
|---|---|---|---|---|---|---|---|---|---|---|---|---|---|
| XN2 | 11468. | -999. | 0. | 11670. | 11737. | 11674. | 11691. | 11674. | 11644. | 11682. | 11691. | 11670. | 11654. |
| XN2R | 11395. | -999. | 0. | 11399. | 11462. | 11400. | 11423. | 11409. | 11380. | 11416. | 11428. | 11413. | 11400. |
| PCN2R | 85.874 | -999. | 0. | 85.902 | 86.379 | 85.911 | 86.081 | 85.977 | 85.756 | 86.028 | 86.121 | 86.004 | 85.912 |
| XN25 | 15431. | -999. | 0. | 15691. | 15750. | 15703. | 15715. | 15700. | 15686. | 15709. | 15711. | 15692. | 15680. |
| XN25R | 12761. | -999. | 0. | 12761. | 12784. | 12778. | 12783. | 12781. | 12779. | 12785. | 12783. | 12783. | 12779. |
| PCN25R | 95.087 | -999. | 0. | 95.091 | 95.261 | 95.215 | 95.254 | 95.236 | 95.222 | 95.265 | 95.251 | 95.25 | 95.227 |
| XN48 | 1397.6 | -999. | 0. | 1397.6 | 1397.8 | 1397.6 | 1397.1 | 1398.1 | 1397.8 | 1397.5 | 1397.5 | 1397.8 | 1397.8 |
| XN49 | 1402.1 | -999. | 0. | 1399. | 1398.3 | 1399. | 1399. | 1398.3 | 1398.9 | 1398.7 | 1398.9 | 1399. | 1399.4 |
| UT91R2 | 852.89 | -999. | 0. | 838.38 | 838.29 | 838.17 | 838.25 | 839.05 | 838.86 | 838.63 | 838.91 | 839.46 | 839.67 |
| UT92R2 | 831.63 | -999. | 0. | 815.69 | 815.13 | 815.48 | 815.88 | 815.72 | 816. | 815.86 | 816.2 | 816.66 | 817.1 |
| BTAN91 | 30.72 | -999. | 77.575 | 31.012 | 31.215 | 30.895 | 30.942 | 31.132 | 30.741 | 31.121 | 30.475 | 30.599 | 30.474 |
| BTAN92 | 29.471 | -999. | 82.452 | 29.332 | 29.504 | 29.535 | 29.738 | 29.312 | 29.595 | 29.654 | 29.593 | 29.83 | 29.594 |
| W13 | 13.825 | -999. | -.5 | 13.667 | 13.688 | 13.515 | 13.489 | 13.324 | 13.281 | 13.482 | 13.548 | 13.435 | 13.578 |
| W15 | 13.825 | -999. | 0. | 13.667 | 13.688 | 13.515 | 13.489 | 13.324 | 13.281 | 13.482 | 13.548 | 13.435 | 13.578 |
| WF36 | 5124.7 | -999. | 130.74 | 5239.7 | 5329.7 | 5188. | 5225.4 | 5194.7 | 5132.1 | 5208.1 | 5238.8 | 5197.5 | 5167.9 |
| WF36R2 | 5240. | -999. | 129.71 | 5230.1 | 5318.5 | 5176.7 | 5217.3 | 5188. | 5125.8 | 5201.4 | 5234.4 | 5196.4 | 5169.2 |
| FN11QA | 21166. | -999. | 0. | 20795. | 21166. | 20771. | 20922. | 20820. | 20696. | 20886. | 20967. | 20879. | 20800. |
| SFC184 | .25025 | -999. | .5 | .25424 | .254 | .25193 | .25208 | .2519 | .25037 | .25174 | .25236 | .25158 | .25122 |
| TAMB | 526.46 | -999. | 546.35 | 546.13 | 546.18 | 546.12 | 546.02 | 545.74 | 545.63 | 545.01 | 544.96 | 544.52 | 543.9 |
| T10 | 525.26 | -999. | 547.19 | 543.6 | 543.82 | 543.87 | 543.35 | 543.04 | 543.08 | 543.16 | 542.81 | 542.3 | 542.03 |
| PAMB | 14.273 | -999. | 14.286 | 14.278 | 14.278 | 14.277 | 14.278 | 14.28 | 14.279 | 14.279 | 14.279 | 14.278 | 14.277 |
| P10M | 14.275 | -999. | 14.289 | 14.281 | 14.281 | 14.281 | 14.282 | 14.283 | 14.282 | 14.281 | 14.281 | 14.281 | 14.28 |
| HUMSER | 81.393 | -999. | 93.613 | 94.977 | 95.805 | 101.54 | 102.61 | 98.377 | 98.113 | 102.39 | 103.81 | 105.65 | 107.01 |
| RELHUM | 80.756 | -999. | 47.943 | 48.937 | 49.278 | 52.255 | 52.959 | 51.297 | 51.327 | 54.593 | 55.411 | 57.172 | 59.043 |
| WINVAV | 2.8332 | -999. | 4.6554 | 8.7407 | 6.9053 | 5.871 | 5.6385 | 5.2867 | 5.2784 | 5.5226 | 5.6124 | 4.6918 | 5.1901 |
| WINAAV | -14.051 | -999. | -42.05 | -37.212 | -19.554 | -19.544 | 12.032 | -31.585 | -31.149 | -24.903 | -19.851 | -12.571 | -23.706 |
| XMO | 0. | -999. | 0. | 0. | 0. | 0. | 0. | 0. | 0. | 0. | 0. | 0. | 0. |
| P46Q2 | 2.8674 | -999. | 9.99+10 | 2.8595 | 2.901 | 2.8596 | 2.8722 | 2.8676 | 2.8458 | 2.8676 | 2.8804 | 2.8648 | 2.8628 |
| CT46 | 1789.9 | -999. | 9.99+10 | 1850.9 | 1847.4 | 1834.3 | 1834.3 | 1830.8 | 1823.6 | 1832. | 1833.5 | 1828. | 1822.9 |
| T46X | 1749.3 | -999. | 557.49 | 1806.1 | 1806.8 | 1791.8 | 1794.5 | 1790.7 | 1786.3 | 1791.8 | 1794.1 | 1789.2 | 1785.1 |
| Comments: | LCF Cycle Pt.19 | Zero | Zero | LCF CYCLES → Pt.20 | Pt.21 | Pt.22 | Pt.23 | Pt.24 | Pt.25 | Pt.26 | Pt.27 | Pt.28 | Pt.29 |

GE36/UDF1 Feebles Tests
082001-03
Test Log - Site IIID
Sheet 019 of 029

GE36/UDF-1 ENGINE 0B2001-03 TEST READINGS - SITE IIID
RDGS. 252 - 304 ON 07.06.86 RDGS. 305 - 330 ON 07.07.86
RDGS. 331 - 358 ON 07.08.86

| RDG. | 252 | 253 | 254 | 255 | 256 | 257 | 258 | 259 | 260 | 261 | 262 | 263 | 264 |
|---|---|---|---|---|---|---|---|---|---|---|---|---|---|
| XN2 | 0. | 11532. | 11551. | 11536. | 11512. | 11520. | 11547. | 11465. | -999. | 0. | 11522. | 11547. | 11561. |
| XN2R | 0. | 11378. | 11409. | 11400. | 11367. | 11392. | 11409. | 11333. | -999. | 0. | 11397. | 11418. | 11428. |
| PCN2R | 0. | 85.743 | 85.977 | 85.906 | 85.659 | 85.851 | 85.974 | 85.402 | -999. | 0. | 85.882 | 86.044 | 86.118 |
| XN25 | 0. | 15502. | 15529. | 15518. | 15497. | 15503. | 15525. | 15459. | -999. | 0. | 15486. | 15524. | 15534. |
| XN25R | 0. | 12740. | 12770. | 12767. | 12755. | 12770. | 12768. | 12752. | -999. | 0. | 12749. | 12773. | 12776. |
| PCN25R | 0. | 94.935 | 95.154 | 95.134 | 95.042 | 95.157 | 95.14 | 95.026 | -999. | 0. | 94.998 | 95.18 | 95.2 |
| XN48 | 0. | 1397.8 | 1397.8 | 1397.6 | 1397.6 | 1397.6 | 1397.8 | 1397.6 | -999. | 0. | 1397.6 | 1397.6 | 1397.6 |
| XN49 | 0. | 1398.7 | 1398.9 | 1399. | 1398.7 | 1399. | 1398.7 | 1398.7 | -999. | 0. | 1398.7 | 1398.7 | 1398.7 |
| UT91R2 | 0. | 846.93 | 847.83 | 848.13 | 847.44 | 848.81 | 848.11 | 848.42 | -999. | 0. | 848.94 | 848.71 | 848.42 |
| UT92R2 | 0. | 823.77 | 824.72 | 825.18 | 824.35 | 825.84 | 824.92 | 825.31 | -999. | 0. | 825.81 | 825.58 | 825.3 |
| BTAN91 | 87.022 | 31.032 | 30.946 | 30.336 | 30.915 | 30.995 | 31.151 | 30.607 | -999. | 87.004 | 30.85 | 31.008 | 31.148 |
| BTAN92 | 87.068 | 28.943 | 29.245 | 29.42 | 28.912 | 29.441 | 29.782 | 29.144 | -999. | 87.129 | 29.169 | 29.553 | 29.202 |
| W13 | -.5 | 13.955 | 13.74 | 13.683 | 13.47 | 13.442 | 13.579 | 13.73 | -999. | -.5 | 13.985 | 13.726 | 13.621 |
| W15 | 0. | 13.955 | 13.74 | 13.683 | 13.47 | 13.442 | 13.579 | 13.73 | -999. | 0. | 13.985 | 13.726 | 13.621 |
| WF36 | 166.76 | 5177.9 | 5151.8 | 5127.2 | 5044.1 | 5095.7 | 5138.6 | 4981.1 | -999. | 173.42 | 5156.6 | 5156.4 | 5175.8 |
| WF36R2 | 167.17 | 5237.4 | 5217.5 | 5195.3 | 5104.7 | 5168.3 | 5205.5 | 5048.6 | -999. | 173.73 | 5229.1 | 5227.9 | 5243.9 |
| FN11QA | 0. | 20860. | 20955. | 20925. | 20638. | 20846. | 20974. | 20505. | -999. | -1.3553 | 20944. | 21056. | 21047. |
| SFC184 | .5 | .2538 | .2517 | .25098 | .25004 | .25062 | .25089 | .24888 | -999. | -129.58 | .25239 | .25098 | .25186 |
| TAMB | 532.94 | 532.31 | 532.02 | 531.87 | 531.61 | 531.29 | 532.13 | 531.87 | -999. | 531.42 | 531.2 | 531.08 | 530.72 |
| T10 | 538.89 | 532.78 | 531.65 | 531.17 | 532.04 | 530.32 | 531.3 | 530.8 | -999. | 538.78 | 530.15 | 530.44 | 530.8 |
| PAMB | 14.289 | 14.288 | 14.29 | 14.292 | 14.294 | 14.294 | 14.293 | 14.295 | -999. | 14.3 | 14.3 | 14.298 | 14.3 |
| P10M | 14.291 | 14.289 | 14.293 | 14.294 | 14.296 | 14.296 | 14.295 | 14.297 | -999. | 14.302 | 14.302 | 14.3 | 14.303 |
| HUMSER | 104.52 | 105.44 | 102.73 | 102.35 | 103.65 | 104.26 | 102.34 | 102.78 | -999. | 101.62 | 100.53 | 100.51 | 102.51 |
| RELHUM | 82.803 | 85.289 | 83.986 | 84.109 | 85.916 | 87.362 | 83.367 | 84.493 | -999. | 84.845 | 84.608 | 84.913 | 87.647 |
| WINVAV | 2.7125 | 3.5787 | 3.0577 | 3.8805 | 2.9405 | 3.4935 | 3.4693 | 2.9146 | -999. | .84414 | 2.4213 | 2.6902 | 2.5535 |
| WINAAV | -20.378 | -32.196 | -12.888 | 7.2764 | -23.078 | 2.8457 | 3.1051 | -5.08 | -999. | -32.74 | 3.5376 | 22.477 | -30.946 |
| XMO | 0. | 0. | 0. | 0. | 0. | 0. | 0. | 0. | -999. | 0. | 0. | 0. | 0. |
| P46Q2 | 9.99+10 | 2.8475 | 2.8633 | 2.86 | 2.8339 | 2.8499 | 2.8583 | 2.8168 | -999. | 9.99+10 | 2.8541 | 2.8653 | 2.8726 |
| CT46 | -9.99+10 | 1825.9 | 1801.5 | 1796.9 | 1789.4 | 1792.4 | 1800.2 | 1782.6 | -999. | 9.99+10 | 1807.6 | 1800. | 1800.9 |
| T46X | 625.94 | 1785. | 1765.6 | 1761.1 | 1754.2 | 1756.7 | 1763.8 | 1748. | -999. | 713.69 | 1771.3 | 1763.4 | 1764. |
| Comments: | Zero | LCF CYCLES Pt.37 Redone | Pt.38 | Pt.39 | Pt.40 | Pt.41 | Pt.42 | Pt.43 | Zero | Zero | Pt.44 | Pt.45 | Pt.46 |

GE36/UDF1 Peebles Tests
0B2001-03
Test Log - Site IIID
Sheet 021 of 029

GE36/UDF-1 ENGINE 082001-03 TEST READINGS - SITE IIID
RDGS. 252 - 304 ON 07.06.86 RDGS. 305 - 330 ON 07.07.86
RDGS. 331 - 358 ON 07.08.86

| RDG. | 265 | 266 | 267 | 268 | 269 | 270 | 271 | 272 | 273 | 274 | 275 | 276 | 277 |
|---|---|---|---|---|---|---|---|---|---|---|---|---|---|
| XN2 | 11520. | 11561. | 11572. | 11566. | 11534. | 11535. | 11530. | 360. | 0. | 11554. | 11559. | 11550. | 11582. |
| XN2R | 11393. | 11439. | 11455. | 11452. | 11414. | 11425. | 11423. | 355.84 | 0. | 11409. | 11405. | 11394. | 11408. |
| PCN2R | 85.858 | 86.201 | 86.326 | 86.303 | 86.011 | 86.096 | 86.083 | 2.6815 | 0. | 85.977 | 85.948 | 85.862 | 85.971 |
| XN25 | 15500. | 15535. | 15534. | 15530. | 15507. | 15502. | 15496. | 139.33 | 0. | 15531. | 15563. | 15559. | 15613. |
| XN25R | 12768. | 12782. | 12780. | 12780. | 12770. | 12773. | 12771. | 134.74 | 0. | 12753. | 12779. | 12778. | 12791. |
| PCN25R | 95.139 | 95.246 | 95.228 | 95.229 | 95.16 | 95.181 | 95.163 | 1.0041 | 0. | 95.033 | 95.222 | 95.215 | 95.311 |
| XN48 | 1397.6 | 1397.8 | 1398.1 | 1397.6 | 1397.8 | 1397.8 | 1397.6 | 498.84 | 0. | 1397.5 | 1397.5 | 1397.2 | 1397.5 |
| XN49 | 1398.9 | 1398.9 | 1398.7 | 1398.7 | 1398.7 | 1398.9 | 1398.9 | 539.15 | 0. | 1398.9 | 1399.1 | 1399. | 1399. |
| UT91R2 | 848.87 | 849.28 | 849.9 | 849.84 | 849.42 | 850.2 | 850.34 | 302.79 | 0. | 847.41 | 846.79 | 846.43 | 845.36 |
| UT92R2 | 825.82 | 826.14 | 826.51 | 826.68 | 826.2 | 827.03 | 827.25 | 318.1 | 0. | 824.48 | 824.03 | 823.76 | 822.56 |
| BTAN91 | 30.625 | 30.987 | 31.457 | 31.34 | 31.095 | 30.763 | 31.113 | 87.029 | 86.984 | 30.979 | 31.039 | 30.71 | 31.098 |
| BTAN92 | 29.06 | 29.901 | 29.615 | 29.689 | 29.414 | 29.575 | 29.465 | 87.149 | 87.093 | 29.047 | 29.068 | 29.155 | 29.383 |
| W13 | 13.773 | 13.676 | 13.655 | 13.715 | 13.659 | 13.705 | 13.735 | -6.0613 | -.5 | 14.043 | 13.752 | 13.691 | 13.387 |
| W15 | 13.773 | 13.676 | 13.655 | 13.715 | 13.659 | 13.705 | 13.735 | -6.0613 | 0. | 14.043 | 13.752 | 13.691 | 13.387 |
| WF36 | 5097.3 | 5191.7 | 5227.9 | 5218.7 | 5137.4 | 5153.4 | 5146.1 | 177.66 | 170.34 | 5247.4 | 5170.7 | 5140.8 | 5206.3 |
| WF36R2 | 5167.3 | 5266. | 5306.8 | 5298.7 | 5210.2 | 5232.3 | 5226.2 | 179.66 | 169.95 | 5299.3 | 5216.6 | 5184.9 | 5240.1 |
| FN11QA | 20863. | 21211. | 21246. | 21223. | 20991. | 21069. | 21038. | 0. | 0. | 21056. | 20915. | 20850. | 21004. |
| SFC184 | .25037 | .25096 | .25249 | .25238 | .25091 | .25104 | .25111 | .5 | .5 | .25441 | .25213 | .25137 | .25219 |
| TAMB | 530.38 | 530.17 | 529.89 | 529.54 | 529.86 | 529.43 | 529.53 | 529.79 | 531.23 | 533.46 | 534.61 | 535.02 | 536.57 |
| T10 | 530.24 | 529.83 | 529.26 | 529.03 | 529.65 | 528.69 | 528.41 | 530.87 | 540.78 | 531.97 | 532.75 | 532.99 | 534.55 |
| PAMB | 14.302 | 14.303 | 14.303 | 14.304 | 14.308 | 14.309 | 14.309 | 14.313 | 14.322 | 14.324 | 14.324 | 14.324 | 14.324 |
| P10M | 14.305 | 14.305 | 14.305 | 14.305 | 14.31 | 14.312 | 14.313 | 14.314 | 14.324 | 14.327 | 14.327 | 14.327 | 14.328 |
| HUMSER | 101.77 | 100.81 | 100.7 | 101.74 | 100.39 | 100.41 | 101.01 | 99.057 | 101.67 | 102.01 | 105.85 | 108.25 | 106.68 |
| RELHUM | 88.04 | 87.877 | 88.612 | 90.605 | 88.456 | 89.803 | 90.003 | 87.544 | 85.576 | 79.665 | 79.453 | 80.122 | 75.028 |
| WINVAV | 3.0664 | 2.1615 | 2.2359 | 2.3509 | 1.4518 | 2.4786 | 2.6833 | .67881 | 1.0259 | 3.2599 | 3.2093 | 4.8278 | 5.1766 |
| WINAAV | -48.952 | 22.963 | 16.972 | -1.5047 | -20.351 | 3.7005 | -17.04 | 128.09 | -46.081 | -26.939 | -12.201 | -11.938 | -12.834 |
| XMO | 0. | 0. | 0. | 0. | 0. | 0. | 0. | 0. | 0. | 0. | 0. | 0. | 0. |
| P46Q2 | 2.8518 | 2.8788 | 2.8892 | 2.8884 | 2.8643 | 2.8707 | 2.8665 | 1.0032 | 9.99+10 | 2.8697 | 2.8654 | 2.8605 | 2.8701 |
| CT46 | 1791.1 | 1799.7 | 1803. | 1801.6 | 1795.8 | 1793.5 | 1791.4 | 930.98 | 9.99+10 | 1824.3 | 1802.9 | 1799.1 | 1811.6 |
| T46X | 1756.2 | 1764.1 | 1766.1 | 1764.6 | 1759.3 | 1757.5 | 1757.3 | 729.08 | 681.74 | 1784.7 | 1767.7 | 1765.7 | 1776.1 |
| Comments: | LCF CYCLES → | | | | | | | | | | | | |
| | Pt.47 | Pt.48 | Pt.49 | Pt.50 | Pt.51 | Pt.52 | Pt.53 | Zero | Zero | Pt.54 | Pt.55 | Pt.56 | Pt.57 |

GE36/UDF1 Peebles Tests
082001-03
Test Log - Site IIID
Sheet 022 of 029

GE36/UDF-1 ENGINE 082001-0_ TEST READINGS - SITE IIID
RDGS. 252 - 304 ON 07.06.86 RDGS. 305 - 330 ON 07.07.86
RDGS. 331 - 358 ON 07.08.86

| RDG. | 278 | 279 | 280 | 281 | 282 | 283 | 284 | 285 | 286 | 287 | 288 | 289 | 290 |
|---|---|---|---|---|---|---|---|---|---|---|---|---|---|
| XN2 | 11621. | 11636. | 11613. | 11635. | 11630. | 11632. | 90.893 | 0. | 11666. | 11640. | 11669. | 121.79 | 11663. |
| XN2R | 11433. | 11439. | 11407. | 11424. | 11409. | 11407. | 88.947 | 0. | 11406. | 11379. | 11399. | 118.67 | 11393. |
| PCN2R | 86.158 | 86.204 | 85.964 | 86.087 | 85.978 | 85.963 | .67029 | 0. | 85.953 | 85.753 | 85.898 | .89424 | 85.858 |
| XN25 | 15651. | 15651. | 15645. | 15671. | 15660. | 15666. | 97.952 | 0. | 15705. | 15689. | 15720. | 111.57 | 15670. |
| XN25R | 12798. | 12793. | 12788. | 12794. | 12788. | 12790. | 94.35 | 0. | 12775. | 12782. | 12785. | 107.04 | 12750. |
| PCN25R | 95.363 | 95.327 | 95.292 | 95.338 | 95.292 | 95.308 | .70306 | 0. | 95.197 | 95.246 | 95.271 | .79762 | 95.005 |
| XN48 | 1397.1 | 1397.6 | 1397.8 | 1397.8 | 1396.7 | 1396. | 684.49 | 0. | 1396.2 | 1394. | 1396.8 | 104.08 | 1397.8 |
| XN49 | 1398.6 | 1399.1 | 1398.5 | 1398.7 | 1399. | 1398.9 | 688.24 | 0. | 1398.7 | 1399. | 1398.7 | 177.22 | 1399. |
| UT91R2 | 844.1 | 843.79 | 843.14 | 842.75 | 841.43 | 840.77 | 411.35 | 0. | 838.28 | 836.92 | 837.91 | 62.277 | 838.56 |
| UT92R2 | 821.34 | 821.03 | 819.93 | 819.71 | 819.21 | 818.88 | 402.02 | 0. | 816.3 | 816.39 | 815.55 | 103.07 | 815.79 |
| BTAN91 | 31.236 | 30.87 | 31.185 | 31.116 | 30.992 | 31.627 | 87.057 | 86.972 | 31.506 | 30.702 | 31.828 | 87.062 | 30.898 |
| BTAN92 | 29.555 | 29.545 | 29.204 | 29.614 | 29.497 | 29.528 | 87.26 | 87.175 | 29.359 | 29.263 | 28.923 | 87.24 | 29.433 |
| W13 | 13.567 | 13.655 | 13.473 | 13.446 | 13.539 | 13.199 | -7.4642 | -.5 | 13.721 | 13.357 | 13.31 | -7.4284 | 13.631 |
| W15 | 13.567 | 13.655 | 13.473 | 13.446 | 13.539 | 13.199 | -7.4642 | 0. | 13.721 | 13.357 | 13.31 | -7.4284 | 13.631 |
| WF36 | 5268.5 | 5259.5 | 5198.3 | 5243.7 | 5197.1 | 5183.6 | 160.98 | 137.39 | 5282.3 | 5152.9 | 5197.8 | 150.7 | 5217.6 |
| WF36R2 | 5293.3 | 5278.9 | 5211.5 | 5253.5 | 5201.4 | 5185.7 | 160.38 | 135.59 | 5260.5 | 5131.4 | 5170.8 | 149.25 | 5191.3 |
| FN11QA | 21102. | 21076. | 20870. | 21057. | 20857. | 20833. | 0. | 0. | 20860. | 20667. | 20726. | 0. | 20758. |
| SFC184 | .25357 | .25319 | .25243 | .2522 | .25209 | .25163 | .5 | .5 | .25492 | .25099 | .25219 | .5 | .25281 |
| TAMB | 538.03 | 538.62 | 539.67 | 540.52 | 541.18 | 541.62 | 542.42 | 544.66 | 545.75 | 545.85 | 546.58 | 546.93 | 547.13 |
| T10 | 535.84 | 536.65 | 537.57 | 538.07 | 538.94 | 539.26 | 541.6 | 549.03 | 542.58 | 542.67 | 543.58 | 546.31 | 543.46 |
| PAMB | 14.326 | 14.327 | 14.326 | 14.325 | 14.325 | 14.325 | 14.327 | 14.329 | 14.329 | 14.329 | 14.327 | 14.327 | 14.326 |
| P10M | 14.329 | 14.329 | 14.328 | 14.329 | 14.328 | 14.328 | 14.33 | 14.332 | 14.332 | 14.331 | 14.33 | 14.33 | 14.329 |
| HUMSER | 104.96 | 108.85 | 110.29 | 100.13 | 100.99 | 108.23 | 112.58 | 108.25 | 108.72 | 103.61 | 104.19 | 101.94 | 104.07 |
| RELHUM | 70.365 | 71.504 | 69.981 | 61.936 | 61.123 | 64.483 | 65.298 | 58.485 | 56.732 | 53.953 | 52.989 | 51.298 | 52.025 |
| WINVAV | 5.2456 | 5.3941 | 3.7938 | 6.6219 | 4.1834 | 5.5384 | 6.3687 | 9.0881 | 6.4686 | 3.2953 | 2.7595 | 7.0233 | 3.5479 |
| WINAAV | -24.319 | 11.592 | -26.696 | 8.3128 | 41.399 | -8.0851 | -20.815 | 7.1789 | -25.184 | -20.565 | 21.69 | 40.733 | 36.176 |
| XMO | 0. | 0. | 0. | 0. | 0. | 0. | 0. | 0. | 0. | 0. | 0. | 0. | 0. |
| P46Q2 | 2.8838 | 2.8842 | 2.8641 | 2.8774 | 2.8615 | 2.8566 | 1.0011 | 9.99+10 | 2.8561 | 2.8413 | 2.8543 | 1.0024 | 2.8394 |
| CT46 | 1821.4 | 1822.7 | 1817.8 | 1823.8 | 1822.8 | 1819.5 | 893.33 | 9.99+10 | 1853.7 | 1827. | 1830.1 | 871.38 | 1849.1 |
| T46X | 1783.8 | 1784.6 | 1780.7 | 1786.7 | 1783.8 | 1783.3 | 738.09 | 650.84 | 1815. | 1787.9 | 1794.6 | 741.01 | 1807.5 |

Comments: LCF CYCLES →

| | | | | | | | | | | | | |
|---|---|---|---|---|---|---|---|---|---|---|---|---|
| Pt.58 | Pt.59 | Pt.60 | Pt.61 | Pt.62 | Pt.63 | Zero | Zero | Pt.64 | Pt.65 | Pt.66 Incomplete | Zero | Pt.66 Redone |



GE36/UDF1 Peebles Tests
082001-03
Test Log - Site IIID
Sheet 023 of 029

GE36/UDF-1 ENGINE 082001-03 ..ST READINGS - SITE IIID
RDGS. 252 - 304 ON 07.06.86 RDGS. 305 - 330 ON 07.07.86
RDGS. 331 - 358 ON 07.08.86

| RDG. | 291 | 292 | 293 | 294 | 295 | 296 | 297 | 298 | 299 | 300 | 301 | 302 | 303 |
|---|---|---|---|---|---|---|---|---|---|---|---|---|---|
| XN2 | 11702. | 11706. | 11636. | 586.96 | 0. | 11688. | 11715. | 11673. | 11642. | 11631. | 11683. | 11646. | 155. |
| XN2R | 11428. | 11431. | 11348. | 571.01 | 0. | 11456. | 11491. | 11460. | 11427. | 11404. | 11460. | 11434. | 151.51 |
| PCN2R | 86.118 | 86.141 | 85.517 | 4.303 | 0. | 86.33 | 86.591 | 86.357 | 86.112 | 85.942 | 86.359 | 86.162 | 1.1417 |
| XN25 | 15721. | 15725. | 15684. | 89.571 | 0. | 15709. | 15730. | 15688. | 15664. | 15659. | 15702. | 15664. | 133.05 |
| XN25R | 12779. | 12779. | 12767. | 85.633 | 0. | 12803. | 12816. | 12803. | 12799. | 12788. | 12804. | 12796. | 123.68 |
| PCN25R | 95.225 | 95.227 | 95.132 | .6381 | 0. | 95.404 | 95.502 | 95.4 | 95.369 | 95.288 | 95.41 | 95.348 | .92158 |
| XN48 | 1397.5 | 1397.6 | 1397.8 | 599.16 | 0. | 1397.9 | 1397.8 | 1397.5 | 1397.8 | 1397.5 | 1397.5 | 1397.2 | 211.91 |
| XN49 | 1398.7 | 1398.1 | 1398.9 | 624.48 | 0. | 1398.9 | 1399.3 | 1399. | 1399. | 1399. | 1399. | 1399.1 | 299.11 |
| UT91R2 | 838.12 | 838.13 | 837.12 | 357.95 | 0. | 841.42 | 841.96 | 842.49 | 842.54 | 841.51 | 841.81 | 842.37 | 127.2 |
| UT92R2 | 815.36 | 814.9 | 814.31 | 362.63 | 0. | 818.42 | 819.25 | 819.76 | 819.66 | 818.82 | 819.1 | 819.88 | 174.52 |
| BTAN91 | 30.764 | 31.096 | 30.084 | 87.033 | 77.596 | 31.305 | 31.687 | 31.664 | 31.227 | 31.093 | 31.425 | 31.096 | 86.971 |
| BTAN92 | 29.687 | 29.149 | 29.416 | 87.316 | 77.313 | 30.055 | 29.977 | 29.75 | 30.005 | 29.916 | 29.976 | 29.791 | 87.18 |
| W13 | 13.317 | 13.274 | 13.154 | -5.3592 | -.5 | 13.183 | 13.206 | 13.151 | 13.114 | 13.066 | 13.053 | 13.2 | -6.9885 |
| W15 | 13.317 | 13.274 | 13.154 | -5.3592 | 0. | 13.183 | 13.206 | 13.151 | 13.114 | 13.066 | 13.053 | 13.2 | -6.9885 |
| WF36 | 5228.2 | 5240.7 | 5065.5 | 148.49 | 147.58 | 5275.7 | 5319.2 | 5267.2 | 5194.4 | 5163.7 | 5265.5 | 5213.9 | 164.47 |
| WF36R2 | 5199.8 | 5214.2 | 5032.3 | 146.84 | 146.79 | 5283.2 | 5332. | 5285. | 5209.9 | 5170.7 | 5274.9 | 5228.8 | 163.71 |
| FN11QA | 20936. | 20825. | 20374. | 0. | 0. | 21151. | 21259. | 21104. | 20984. | 20844. | 21105. | 20931. | 0. |
| SFC184 | .25107 | .25311 | .24968 | .5 | .5 | .2525 | .25353 | .25315 | .25098 | .25076 | .25265 | .25252 | .5 |
| TAMB | 547.4 | 546.75 | 547.98 | 547.95 | 540.88 | 540.73 | 539.73 | 539.23 | 539.1 | 539.79 | 539.9 | 539.04 | 538.5 |
| T10 | 543.83 | 543.92 | 545.34 | 548.05 | 544.08 | 539.87 | 539.08 | 538.21 | 538.34 | 539.45 | 539.07 | 538.15 | 542.86 |
| PAMB | 14.325 | 14.323 | 14.318 | 14.317 | 14.306 | 14.305 | 14.306 | 14.308 | 14.31 | 14.313 | 14.314 | 14.316 | 14.318 |
| P10M | 14.329 | 14.321 | 14.317 | 14.32 | 14.308 | 14.302 | 14.303 | 14.305 | 14.308 | 14.311 | 14.312 | 14.313 | 14.32 |
| HUMSER | 104.37 | 96.827 | 97.939 | 96.974 | 121.33 | 113.21 | 111.28 | 114.87 | 112.65 | 110.78 | 105.18 | 105.72 | 105.79 |
| RELHUM | 51.709 | 49.057 | 47.691 | 47.268 | 73.727 | 69.251 | 70.371 | 73.766 | 72.711 | 69.954 | 66.27 | 68.5 | 69.784 |
| WINVAV | 2.9323 | 6.138 | 4.9741 | 4.45 | 2.834 | 1.7139 | 2.6758 | 2.2137 | 2.4386 | 2.5759 | 3.4535 | 2.4244 | .94296 |
| WINAAV | -12.17 | 28.313 | 26.877 | -17.783 | 2.6201 | 52.371 | 20.459 | -37.067 | 41.334 | 43.684 | 26.024 | 15.795 | -10.726 |
| XMO | 0. | 0. | 0. | 0. | 0. | 0. | 0. | 0. | 0. | 0. | 0. | 0. | 0. |
| P46Q2 | 2.8627 | 2.8656 | 2.8183 | 1.0037 | 9.99+10 | 2.8816 | 2.9034 | 2.8831 | 2.8589 | 2.8441 | 2.8825 | 2.8646 | 1.0018 |
| CT46 | 1836.1 | 1841. | 1825.6 | 860.18 | 9.99+10 | 1832.7 | 1830.1 | 1827.1 | 1820.1 | 1823.1 | 1829.1 | 1825.3 | 932.94 |
| T46X | 1798.9 | 1800.4 | 1788.3 | 738.52 | 580.67 | 1795.4 | 1795.2 | 1789.6 | 1783.6 | 1785.4 | 1791.4 | 1785. | 722.39 |

Comments: LCF CYCLES →

| | | | | | | | | | | | | |
|---|---|---|---|---|---|---|---|---|---|---|---|---|
| Pt.67 | Pt.68 | Pt.69 | Zero | Zero | Pt.71 | Pt.72 | Pt.73 | Pt.74 | Pt.75 | Pt.76 | Pt.77 | Zero |

(NOTE: No DMS reading for point 701)

GE36/UDF1 Peebles Tests
082001-03
Test Log - Site IIID
Sheet 024 of 029

GE36/UDF-1 ENGINE 082001- TEST READINGS - SITE IIID
RDGS. 252 - 304 ON 07.06.86 RDGS. 305 - 330 ON 07.07.86
RDGS. 331 - 358 ON 07.08.86

| RDG. | 304 | 305 | 306 | 307 | 308 | 309 | 310 | 311 | 312 | 313 | 314 | 315 | 316 |
|---|---|---|---|---|---|---|---|---|---|---|---|---|---|
| XN2 | 155. | 11566. | 11597. | 11598. | 11583. | 11545. | 11692. | 11586. | 11582. | 11586. | 11561. | 441.61 | 11558. |
| XN2R | 151.24 | 11369. | 11395. | 11421. | 11402. | 11368. | 11517. | 11407. | 11412. | 11399. | 11388. | 434.42 | 11384. |
| PCN2R | 1.1397 | 85.678 | 85.872 | 86.066 | 85.924 | 85.667 | 86.789 | 85.962 | 85.997 | 85.897 | 85.817 | 3.2737 | 85.786 |
| XN25 | 133.05 | 15557. | 15602. | 15587. | 15578. | 15546. | 15659. | 15579. | 15573. | 15590. | 15554. | 166.05 | 15529. |
| XN25R | 124.53 | 12750. | 12770. | 12774. | 12773. | 12764. | 12793. | 12773. | 12775. | 12775. | 12765. | 159.28 | 12737. |
| PCN25R | .92791 | 95.007 | 95.159 | 95.189 | 95.177 | 95.115 | 95.329 | 95.18 | 95.195 | 95.194 | 95.118 | 1.1869 | 94.911 |
| XN48 | 211.91 | 1397.4 | 1397.6 | 1397.6 | 1397.2 | 1397.2 | 1397.8 | 1397.6 | 1397.8 | 1397.6 | 1397.5 | 534.47 | 1397.4 |
| XN49 | 299.11 | 1399. | 1398.9 | 1399. | 1399.4 | 1399.3 | 1399.3 | 1399. | 1399.1 | 1399. | 1399. | 556.03 | 1398.9 |
| | | | | | | | | | | | | | |
| UT91R2 | 126.97 | 843.56 | 843.34 | 845.2 | 844.65 | 844.9 | 845.55 | 845.05 | 845.73 | 844.37 | 845.38 | 322.87 | 845.19 |
| UT92R2 | 174.21 | 820.89 | 820.44 | 822.33 | 822.27 | 822.43 | 822.74 | 822.18 | 822.84 | 821.52 | 822.58 | 326.49 | 822.39 |
| BTAN91 | 86.945 | 30.419 | 31.245 | 31.138 | 30.505 | 30.644 | 32.014 | 30.727 | 31.184 | 31.021 | 30.919 | 87.03 | 31.144 |
| BTAN92 | 87.153 | 29.149 | 29.485 | 29.34 | 29.671 | 29.288 | 29.806 | 29.567 | 29.376 | 29.157 | 29.393 | 87.204 | 28.852 |
| | | | | | | | | | | | | | |
| W13 | -7.1299 | 13.663 | 13.132 | 13.235 | 13.38 | 13.02 | 13.188 | 13.193 | 13.446 | 13.47 | 13.43 | -5.7376 | 13.769 |
| W15 | -7.1299 | 13.663 | 13.132 | 13.235 | 13.38 | 13.02 | 13.188 | 13.193 | 13.446 | 13.47 | 13.43 | -5.7376 | 13.769 |
| | | | | | | | | | | | | | |
| WF36 | 161.11 | 5132.8 | 5136. | 5161.9 | 5127.1 | 5056.2 | 5368.9 | 5134.9 | 5130.1 | 5114.4 | 5086.3 | 171.91 | 5162.7 |
| WF36R2 | 159.95 | 5156. | 5156.2 | 5198. | 5160.4 | 5091.2 | 5410.9 | 5172.6 | 5171.1 | 5144. | 5124.8 | 172.7 | 5200.2 |
| FN11QA | 0. | 20620. | 20777. | 20872. | 20799. | 20567. | 21424. | 20801. | 20818. | 20712. | 20666. | 0. | 20726. |
| SFC184 | .5 | .25277 | .25086 | .25175 | .2508 | .25024 | .2553 | .25138 | .2511 | .25106 | .25069 | .5 | .25363 |
| | | | | | | | | | | | | | |
| TAMB | 537.57 | 536.73 | 537.86 | 535.27 | 535.26 | 535.54 | 535.64 | 535.38 | 535.51 | 536.18 | 534.5 | 535.2 | 531.96 |
| T10 | 544.8 | 536.73 | 537.22 | 534.85 | 535.24 | 534.93 | 534.52 | 535.04 | 534.29 | 535.91 | 534.53 | 535.98 | 534.67 |
| PAMB | 14.32 | 14.318 | 14.317 | 14.317 | 14.316 | 14.316 | 14.312 | 14.309 | 14.309 | 14.31 | 14.311 | 14.312 | 14.313 |
| P10M | 14.321 | 14.315 | 14.315 | 14.315 | 14.315 | 14.314 | 14.31 | 14.306 | 14.311 | 14.313 | 14.312 | 14.314 | 14.314 |
| HUMSER | 107.75 | 109.21 | 107.35 | 110.85 | 108.13 | 107.42 | 109.3 | 106.29 | 108.17 | 107.31 | 106.58 | 106.85 | 106.48 |
| RELHUM | 73.277 | 76.303 | 72.278 | 81.262 | 79.348 | 78.098 | 79.138 | 77.68 | 78.683 | 76.348 | 80.205 | 78.566 | 87.284 |
| WINVAV | 1.4407 | 2.1952 | 2.8558 | 3.3787 | 3.0981 | 3.5961 | 3.4321 | 2.2606 | 3.0785 | 2.2291 | 3.0035 | 1.1511 | 3.3196 |
| WINAAV | 7.6801 | 46.372 | 25.076 | -37.059 | 21.133 | 11.003 | 71.7642 | 46.753 | 3.142 | -15.26 | 13.773 | -26.234 | -27.476 |
| XMO | 0. | 0. | 0. | 0. | 0. | 0. | 0. | 0. | 0. | 0. | 0. | 0. | 0. |
| | | | | | | | | | | | | | |
| P46Q2 | 1.001 | 2.8292 | 2.839 | 2.8572 | 2.846 | 2.8217 | 2.9184 | 2.8465 | 2.8474 | 2.8399 | 2.8314 | 1.002 | 2.8314 |
| CT46 | 903.42 | 1827.7 | 1816.8 | 1809.8 | 1808.7 | 1802.8 | 1827.8 | 1811.2 | 1804.6 | 1807.9 | 1804. | 914.91 | 1829.5 |
| T46X | 696.74 | 1784. | 1780.6 | 1774.5 | 1772.4 | 1765.3 | 1791.1 | 1772.9 | 1770.5 | 1772.8 | 1767.7 | 730.21 | 1788.5 |

Comments: LCF CYCLES →

| Zero | Pt.78 | Pt.79 | Pt.80 | Pt.81 | Pt.82 | Pt.84 | Pt.85 | Pt.86 | Pt.87 | Pt.88 | Zero | Pt.89 |
|---|---|---|---|---|---|---|---|---|---|---|---|---|

(NOTE: No DMS reading for point 831)

GE36/UDF-1 ENGINE 082001-0. EST READINGS - SITE IIID
RDGS. 252 - 304 ON 07.06.86 RDGS. 305 - 330 ON 07.07.86
RDGS. 331 - 358 ON 07.08.86

| RDG. | 317 | 318 | 319 | 320 | 321 | 322 | 323 | 324 | 325 | 326 | 327 | 328 | 329 |
|---|---|---|---|---|---|---|---|---|---|---|---|---|---|
| XN2 | 11592. | 11588. | 11595. | 11604. | 11585. | 11604. | 11558. | 11522. | 166.07 | 0. | 11574. | 11564. | 11590. |
| XN2R | 11429. | 11424. | 11425. | 11443. | 11416. | 11434. | 11413. | 11371. | 164.05 | 0. | 11424. | 11411. | 11425. |
| PCN2R | 86.129 | 86.092 | 86.1 | 86.228 | 86.029 | 86.165 | 86.006 | 85.691 | 1.2363 | 0. | 86.087 | 85.992 | 86.096 |
| XN25 | 15574. | 15574. | 15580. | 15583. | 15578. | 15591. | 15541. | 15518. | 99.523 | 0. | 15541. | 15557. | 15590. |
| XN25R | 12776. | 12772. | 12771. | 12778. | 12776. | 12777. | 12773. | 12765. | 96.313 | 0. | 12756. | 12778. | 12787. |
| PCN25R | 95.198 | 95.175 | 95.165 | 95.213 | 95.198 | 95.212 | 95.178 | 95.117 | .71768 | 0. | 95.049 | 95.219 | 95.285 |
| XN48 | 1397.6 | 1397.1 | 1397.1 | 1397.8 | 1397.6 | 1397.5 | 1397.8 | 1397.6 | 262.54 | 0. | 1397.4 | 1397.6 | 1397.5 |
| XN49 | 1398.9 | 1398.9 | 1398.9 | 1399.1 | 1398.9 | 1398.7 | 1399. | 1399. | 309.43 | 0. | 1398.9 | 1398.9 | 1398.9 |
| UT91R2 | 846.21 | 845.84 | 845.38 | 846.43 | 845.74 | 845.66 | 847.57 | 847.07 | 159.27 | 0. | 847. | 846.94 | 845.97 |
| UT92R2 | 823.23 | 823.18 | 822.74 | 823.52 | 822.77 | 822.7 | 824.55 | 824.15 | 182.45 | 0. | 824.16 | 823.94 | 823.07 |
| BTAN91 | 31.535 | 31.285 | 30.975 | 31.61 | 31.465 | 30.849 | 30.902 | 30.687 | 87.056 | 86.96 | 30.841 | 30.805 | 30.947 |
| BTAN92 | 29.223 | 29.19 | 29.065 | 29.239 | 29.16 | 29.355 | 29.1 | 29.435 | 87.198 | 87.092 | 29.524 | 29.282 | 29.495 |
| W13 | 13.556 | 13.528 | 13.312 | 13.309 | 13.375 | 13.513 | 13.452 | 13.303 | -6.9756 | -.5 | 14.027 | 13.594 | 13.584 |
| W15 | 13.556 | 13.528 | 13.312 | 13.309 | 13.375 | 13.513 | 13.452 | 13.303 | -6.9756 | 0. | 14.027 | 13.594 | 13.584 |
| WF36 | 5172.3 | 5163.1 | 5162. | 5192.3 | 5142.9 | 5182.2 | 5127.5 | 5041.3 | 174.48 | 166.82 | 5243.9 | 5140.9 | 5167.7 |
| WF36R2 | 5216.8 | 5207. | 5202.7 | 5239.5 | 5184.7 | 5223.6 | 5182.3 | 5091. | 176.23 | 166.55 | 5290.8 | 5184.2 | 5203.5 |
| FN11QA | 20917. | 20862. | 20817. | 20924. | 20818. | 20951. | 20835. | 20622. | 0. | 0. | 20993. | 20820. | 20900. |
| SFC184 | .25211 | .2523 | .25264 | .25313 | .25176 | .25203 | .25144 | .24956 | .5 | .5 | .25476 | .25171 | .25168 |
| TAMB | 532.29 | 533.33 | 533.79 | 533.2 | 533.58 | 533.81 | 531.73 | 531.65 | 531.19 | 532.68 | 533.75 | 534.2 | 535.28 |
| T10 | 533.58 | 533.64 | 534.22 | 533.41 | 534.18 | 534.17 | 531.98 | 532.5 | 531.52 | 539.84 | 532.38 | 532.66 | 533.79 |
| PAMB | 14.313 | 14.313 | 14.312 | 14.31 | 14.309 | 14.312 | 14.314 | 14.315 | 14.318 | 14.33 | 14.331 | 14.333 | 14.333 |
| P10M | 14.316 | 14.316 | 14.314 | 14.312 | 14.311 | 14.314 | 14.316 | 14.317 | 14.32 | 14.332 | 14.333 | 14.335 | 14.336 |
| HUMSER | 109.65 | 106.39 | 106.28 | 107.42 | 103.51 | 102.28 | 102.67 | 104.98 | 106.66 | 105.99 | 107.64 | 109.5 | 110.05 |
| RELHUM | 88.821 | 83.298 | 81.939 | 84.436 | 80.398 | 78.856 | 84.91 | 87.024 | 89.783 | 84.913 | 83.163 | 83.308 | 80.754 |
| WINVAV | 3.3948 | 2.6571 | 3.3841 | 4.5399 | 2.44 | 3.1757 | 1.8904 | 3.4553 | 1.5749 | 1.2339 | 3.2275 | 4.022 | 4.3768 |
| WINAAV | -28.241 | -13.556 | -28.821 | -39.569 | -36.011 | -51.621 | -47.031 | -43.399 | -1.5978 | -22.52 | 4.3432 | -5.7813 | -6.3353 |
| XMO | 0. | 0. | 0. | 0. | 0. | 0. | 0. | 0. | 0. | 0. | 0. | 0. | 0. |
| P46Q2 | 2.8586 | 2.857 | 2.8562 | 2.8618 | 2.8481 | 2.8623 | 2.8492 | 2.8179 | 1.0016 | 9.99+10 | 2.852 | 2.847 | 2.8565 |
| CT46 | 1808.2 | 1808.2 | 1809.7 | 1811.2 | 1808. | 1811.9 | 1801.6 | 1793.7 | 924.54 | 9.99+10 | 1833.3 | 1804.8 | 1808.4 |
| T46X | 1773.4 | 1773. | 1773.8 | 1775.3 | 1773.7 | 1776. | 1766.1 | 1761.9 | 727.31 | 632.74 | 1791.2 | 1770.3 | 1773.1 |

Comments: LCF CYCLES →

| | | | | | | | | | | | | |
|---|---|---|---|---|---|---|---|---|---|---|---|---|
| Pt.90 | Pt.91 | Pt.92 | Pt.93 | Pt.94 | Pt.95 | Pt.96 | Pt.97 | Zero | Zero | Pt.98 | Pt.99 | Pt.100 |

GE36/UDF1 Peebles Tests
082001-03
Test Log - Site IIID
Sheet 026 of 029

GE36/UDF-1 ENGINE 082001-03 TEST READINGS - SITE IIID
RDGS. 252 - 304 ON 07.06.86 RDGS. 305 - 330 ON 07.07.86
RDGS. 331 - 358 ON 07.08.86

| RDG. | 330 | 331 | 332 | 333 | 334 | 335 | 336 | 337 | 338 | 339 | 340 | 341 | 342 |
|---|---|---|---|---|---|---|---|---|---|---|---|---|---|
| XN2 | 316.61 | 0. | 11590. | 96.428 | 11435. | 11905. | 691.25 | 10902. | 11199. | 10709. | 10891. | 11051. | 11278. |
| XN2R | 311.45 | 0. | 11414. | 95.004 | 11302. | 11768. | 682.42 | 10758. | 11060. | 10576. | 10756. | 10918. | 11143. |
| PCN2R | 2.347 | 0. | 86.013 | .71593 | 85.169 | 88.682 | 5.1426 | 81.068 | 83.347 | 79.697 | 81.058 | 82.277 | 83.968 |
| XN25 | 113.67 | 0. | 15571. | 120.48 | 15428. | 15815. | 134.62 | 14904. | 15177. | 14743. | 14947. | 15085. | 15280. |
| XN25R | 109.79 | 0. | 12757. | 116.3 | 12747. | 12859. | 129.64 | 12569. | 12671. | 12543. | 12617. | 12655. | 12712. |
| PCN25R | .81808 | 0. | 95.063 | .86664 | 94.985 | 95.819 | .96603 | 93.659 | 94.42 | 93.467 | 94.017 | 94.301 | 94.725 |
| XN48 | 402.26 | 0. | 0. | 0. | 1300. | 1300. | 0. | 1199. | 1200. | 1200.2 | 1299.6 | 1299.7 | 1299.2 |
| XN49 | 442.57 | 0. | 1399. | 236.29 | 1399.3 | 1398.7 | 332.87 | 1100.9 | 1100.9 | 1100.8 | 1201.1 | 1200.3 | 1200.9 |
| UT91R2 | 243. | 0. | 0. | 0. | 789.01 | 789.12 | 0. | 726.56 | 727.81 | 727.88 | 788.23 | 788.56 | 788.28 |
| UT92R2 | 259.87 | 0. | 822.37 | 138.96 | 825.47 | 825.27 | 196.15 | 648.46 | 649.04 | 648.9 | 708.12 | 707.87 | 708.23 |
| BTAN91 | 87.041 | 77.459 | 30.693 | 87.011 | 31.722 | 33.354 | 87.003 | 30.799 | 32.04 | 29.324 | 28.663 | 30.035 | 30.87 |
| BTAN92 | 87.209 | 77.273 | 29.452 | 87.156 | 28.829 | 29.863 | 87.097 | 30.892 | 31.25 | 29.768 | 29.278 | 30.016 | 30.829 |
| W13 | -6.4015 | -.5 | 13.655 | -7.3441 | 13.464 | 14.194 | -4.5868 | 13.247 | 14.031 | 12.356 | 12.406 | 12.932 | 13.639 |
| W15 | -6.4015 | 0. | 13.655 | -7.3441 | 13.464 | 14.194 | -4.5868 | 13.247 | 14.031 | 12.356 | 12.406 | 12.932 | 13.639 |
| WF36 | 167.02 | 286.99 | 5166.2 | 170.53 | 4836.2 | 5821.9 | 174.1 | 3776.1 | 4264.3 | 3389.8 | 3741.8 | 4029.9 | 4449.3 |
| WF36R2 | 167.52 | 288.05 | 5212.1 | 171.99 | 4905.3 | 5907.1 | 176.16 | 3820.5 | 4319.9 | 3432.8 | 3790. | 4083.6 | 4508.9 |
| FN11QA | 0. | 0. | 20899. | 0. | 19651. | 21953. | 16.518 | 15205. | 16411. | 14183. | 15858. | 16771. | 17991. |
| SFC184 | .5 | .5 | .2521 | .5 | .25233 | .272 | 10.781 | .254 | .26609 | .24466 | .2416 | .24613 | .25334 |
| TAMB | 536.55 | 536.19 | 535.32 | 534.12 | 531.42 | 531.69 | 532.16 | 533.41 | 532.77 | 532.85 | 532.77 | 532.45 | 532.26 |
| T10 | 536. | 537.49 | 534.8 | 534.34 | 530.99 | 530.84 | 532.17 | 532.67 | 531.72 | 531.83 | 531.7 | 531.37 | 531.31 |
| PAMB | 14.334 | 14.299 | 14.287 | 14.287 | 14.282 | 14.281 | 14.281 | 14.283 | 14.284 | 14.284 | 14.285 | 14.285 | 14.286 |
| P10M | 14.336 | 14.299 | 14.289 | 14.288 | 14.283 | 14.283 | 14.282 | 14.284 | 14.285 | 14.286 | 14.287 | 14.287 | 14.288 |
| HUMSER | 110.12 | 111.52 | 110.33 | 108.58 | 108.66 | 108.91 | 109.22 | 106.31 | 106.89 | 106.81 | 107.09 | 107.28 | 107.26 |
| RELHUM | 77.484 | 79.196 | 80.593 | 82.577 | 90.477 | 89.869 | 88.702 | 82.835 | 85.081 | 84.8 | 85.262 | 86.318 | 86.872 |
| WINVAV | 2.7594 | .01362 | 2.2952 | 2.7118 | 1.8074 | 1.8358 | .48994 | 2.3319 | 1.618 | 3.1844 | 2.8655 | 3.9975 | 4.0501 |
| WINAAV | -23.511 | -3.6021 | 14.356 | 15.772 | -17.945 | 11.204 | 2.2016 | 12.715 | -1.6365 | 11.214 | 1.3371 | -11.102 | 8.5497 |
| XMO | 0. | 0. | 0. | 0. | 0. | 0. | 0. | 0. | 0. | 0. | 0. | 0. | 0. |
| P46Q2 | 1.0026 | 9.99+10 | 2.8472 | 1.0018 | 2.7558 | 3.0845 | 1.0014 | 2.361 | 2.5422 | 2.2506 | 2.3807 | 2.4813 | 2.6226 |
| CT46 | 899.04 | 9.99+10 | 1820.1 | 909.63 | 1769.6 | 1843. | 904.43 | 1681.6 | 1709.4 | 1615.7 | 1658.3 | 1685.3 | 1724.9 |
| T46X | 727.15 | 555.93 | 1783.7 | 722.17 | 1737.7 | 1810.4 | 720.94 | 1658.6 | 1676. | 1608. | 1638.5 | 1661.7 | 1695. |

Comments: Zero | Zero | Part Power Bad XN48 | Zero | Trim Balance → Mis-matched speeds | Zero | Trim Balance → Mis-matched speeds →

GE36/UDF1 Peebles Tests
082001-03
Test Log - Site IIID
Sheet 027 of 029

GE36/UDF-1 ENGINE 082001-03 TEST READINGS - SITE IIID
RDGS. 252 - 304 ON 07.06.86 RDGS. 305 - 330 ON 07.07.86
RDGS. 331 - 358 ON 07.08.86

| RDG. | 343 | 344 | 345 | 346 | 347 | 348 | 349 | 350 | 351 | 352 | 353 | 354 | 355 |
|---|---|---|---|---|---|---|---|---|---|---|---|---|---|
| XN2 | 11537. | 343.04 | 0. | 12061. | 192.14 | 192.14 | 192.14 | 192.14 | 192.14 | 192.14 | 192.14 | 192.14 | 192.14 |
| XN2R | 11391. | 338.42 | 0. | 11814. | 187.27 | 187.06 | 186.87 | 186.82 | 186.73 | 186.62 | 186.63 | 186.39 | 186.35 |
| PCN2R | 85.842 | 2.5503 | 0. | 89.025 | 1.4113 | 1.4097 | 1.4082 | 1.4078 | 1.4072 | 1.4063 | 1.4064 | 1.4046 | 1.4043 |
| XN25 | 15500. | 114.71 | 0. | 16010. | 108.95 | 108.95 | 108.95 | 108.95 | 108.95 | 108.95 | 108.95 | 108.95 | 108.95 |
| XN25R | 12771. | 110.99 | 0. | 12867. | 103.8 | 103.58 | 103.48 | 103.65 | 103.84 | 103.94 | 104.2 | 104.21 | 104.55 |
| PCN25R | 95.167 | .82703 | 0. | 95.879 | .7735 | .77181 | .77108 | .77237 | .77377 | .77449 | .77648 | .77653 | .77904 |
| XN48 | 1299.6 | 103.14 | 0. | 1397.4 | 97.517 | 96.579 | 96.579 | 98.454 | 97.517 | 97.517 | 97.517 | 97.517 | 97.517 |
| XN49 | 1200.6 | 458.52 | 0. | 1398.5 | 429.45 | 429.45 | 429.45 | 429.45 | 429.45 | 429.45 | 429.45 | 429.45 | 429.45 |
| UT91R2 | 787.99 | 62.487 | 0. | 840.49 | 58.367 | 57.74 | 57.68 | 58.784 | 58.198 | 58.164 | 58.167 | 58.093 | 58.078 |
| UT92R2 | 707.58 | 270.01 | 0. | 817.59 | 249.84 | 249.56 | 249.3 | 249.23 | 249.12 | 248.97 | 248.99 | 248.67 | 248.61 |
| BTAN91 | 31.821 | 87.059 | 86.96 | 32.17 | 86.922 | 86.919 | 86.921 | 86.919 | 86.921 | 86.92 | 86.922 | 87.08 | 87.088 |
| BTAN92 | 31.237 | 87.202 | 87.174 | 29.918 | 87.093 | 87.068 | 87.072 | 87.075 | 87.07 | 87.065 | 87.065 | 85.486 | 85.49 |
| W13 | 14.002 | -6.2052 | -.5 | 14.273 | -7.1532 | -7.199 | -7.2296 | -7.284 | -7.3102 | -7.3098 | -7.3433 | -7.4088 | -7.4429 |
| W15 | 14.002 | -6.2052 | 0. | 14.273 | -7.1532 | -7.199 | -7.2296 | -7.284 | -7.3102 | -7.3098 | -7.3433 | -7.4088 | -7.4429 |
| WF36 | 4934.9 | 173.33 | 145.59 | 6103.8 | 145.8 | 141.92 | 138.87 | 137.15 | 136.53 | 136.11 | 136.38 | 129.89 | 129.81 |
| WF36R2 | 4996.7 | 175.13 | 145.29 | 6110.4 | 144.81 | 140.73 | 137.5 | 135.76 | 135.05 | 134.53 | 134.83 | 128.22 | 128.12 |
| FN11QA | 19135. | 0. | 0. | 22947. | 0. | 0. | 0. | 0. | 0. | 0. | 0. | 0. | 0. |
| SFC184 | .26396 | .5 | .5 | .26918 | .5 | .5 | .5 | .5 | .5 | .5 | .5 | .5 | .5 |
| TAMB | 532.91 | 532.57 | 540.15 | 543.69 | 544.31 | 544.76 | 545.28 | 545.14 | 544.99 | 545.22 | 545.56 | 546.24 | 546.06 |
| T10 | 532.04 | 532.92 | 542.15 | 540.66 | 545.98 | 547.23 | 548.38 | 548.67 | 549.15 | 549.81 | 549.75 | 551.15 | 551.43 |
| PAMB | 14.287 | 14.288 | 14.295 | 14.291 | 14.293 | 14.293 | 14.293 | 14.293 | 14.293 | 14.292 | 14.291 | 14.288 | 14.286 |
| P10M | 14.289 | 14.289 | 14.296 | 14.295 | 14.295 | 14.295 | 14.296 | 14.295 | 14.296 | 14.295 | 14.292 | 14.29 | 14.287 |
| HUMSER | 106.98 | 107.05 | 117.4 | 114.12 | 113.57 | 114.57 | 116.92 | 115.1 | 114.22 | 115.38 | 116.87 | 114.85 | 113.54 |
| RELHUM | 84.784 | 85.798 | 73.056 | 63.358 | 61.832 | 61.472 | 61.662 | 61. | 60.843 | 60.979 | 61.069 | 58.752 | 58.411 |
| WINVAV | 1.6926 | 2.6073 | 3.5739 | 7.9273 | 6.4991 | 6.3887 | 3.2672 | 3.5945 | 6.0797 | 6.0945 | 6.3706 | 6.9769 | 2.866 |
| WINAAV | 18.137 | -1.1191 | -52.506 | -17.017 | 9.4036 | -14.742 | 36.853 | 35.472 | -18.244 | 10.382 | 27.22 | 23.613 | -16.095 |
| XMO | 0. | 0. | 0. | 0. | 0. | 0. | 0. | 0. | 0. | 0. | 0. | 0. | 0. |
| P46Q2 | 2.7834 | 1.0021 | 9.99+10 | 3.134 | 1.0014 | 1.0013 | 1.0009 | 1.0008 | 1.0009 | 1.0008 | 1.001 | 1.001 | 1.0009 |
| CT46 | 1769.5 | 907.86 | 9.99+10 | 1904.3 | 857.45 | 847.95 | 841.03 | 830.13 | 825.22 | 824.94 | 818.78 | 804. | 797.89 |
| T46X | 1737.7 | 722.6 | 599.27 | 1870.3 | 653.85 | 661.43 | 663.39 | 666.83 | 667.7 | 659.1 | 661.06 | 646.5 | 637.11 |

| Comments: | 343 | 344 | 345 | 346 | 347 | 348 | 349 | 350 | 351 | 352 | 353 | 354 | 355 |
|---|---|---|---|---|---|---|---|---|---|---|---|---|---|
| | Trim Bal. Mis-matched Speeds | Zero | Zero | Part Power (Max Thrust?) | Zeros → Cool Down Period - time in minutes: +0 | +5 | +10 | +15 | +20 | +25 | +30 | +35 | +40 |

GE36/UDF1 Feebles Tests
082001-03
Test Log - Site IIID
Sheet 028 of 029

GE36/UDF-1 ENGINE 082001-03 TEST READINGS - SITE IIID
RDGS. 252 - 304 ON 07.06.86 RDGS. 305 - 330 ON 07.07.86
RDGS. 331 - 358 ON 07.08.86

| RDG. | 356 | 357 | 358 |
|---|---|---|---|
| XN2 | 0. | 5348.6 | 94.464 |
| XN2R | 0. | 5239.1 | 92.57 |
| PCN2R | 0. | 39.481 | .69759 |
| XN25 | 0. | 11678. | 141.43 |
| XN25R | 0. | 10976. | 136.77 |
| PCN25R | 0. | 81.786 | 1.0192 |
| XN48 | 0. | 700.03 | 124.71 |
| XN49 | 0. | 701.37 | 701.37 |
| UT91R2 | 0. | 421.08 | 75.048 |
| UT92R2 | 0. | 410.08 | 410.26 |
| BTAN91 | 87.165 | 17.624 | 86.832 |
| BTAN92 | 85.544 | 18.01 | 86.878 |
| W13 | -.5 | 5.3388 | -7.5599 |
| W15 | 0. | 5.3388 | -7.5599 |
| WF36 | 125.42 | 826.12 | 152.07 |
| WF36R2 | 123.88 | 830.97 | 153.06 |
| FN11QA | 3.8527 | 2175.7 | 0. |
| SFC184 | 32.503 | .38609 | .5 |
| TAMB | 549.31 | 541.55 | 540.52 |
| T10 | 552.38 | 540.58 | 540.11 |
| PAMB | 14.257 | 14.213 | 14.21 |
| P10M | 14.259 | 14.215 | 14.211 |
| HUMSER | 108.41 | 114.37 | 114.33 |
| RELHUM | 50.297 | 67.668 | 69.933 |
| WINVAV | 4.9213 | 4.6068 | 5.2789 |
| WINAAV | 10.421 | -12.914 | -16.406 |
| XMO | 0. | 0. | 0. |
| P46Q2 | 9.99+10 | 1.1993 | 1.0017 |
| CT46 | -9.99+10 | 1340.2 | 853.09 |
| T46X | 590.38 | 1302.3 | 737.58 |

| Comments: | Zero | F.I. | Zero |
|---|---|---|---|

GE36/UDF1 Peebles Tests
082001-03
Test Log - Site IIID
Sheet 029 of 029

## APPENDIX B

## STRAIN DATA FOR THE STRUT

Figures B-1 and B-2 illustrate the locations of all the gages read except KD FAR1, KD FAR2, and KD FAR3. These three make up the vertical, diagonal, and axial axes, respectively, of a gage rosette located centrally on the inner surface of the mid-fairing.

The following graphs (Figures B-3 through B-40) contain maximum stress locations calculated from strains read on gages located as shown in Figures B-1 and B-2. These are shown versus engine frequencies and speeds as read from test diagrams. Each graph (with the exceptions of those combined because only one situation for each was recorded) displays the maximum stress versus speed or frequency for one gage only. Different situations are labeled for each point. Note that almost all are labeled with either an XN2, an XN25, or an XN48. These correspond to engine speeds as follows:

- XN2 refers to the intermediate pressure compressor
- XN25 refers to the high pressure compressor
- XN48 refers to the Stage 1 propulsor.

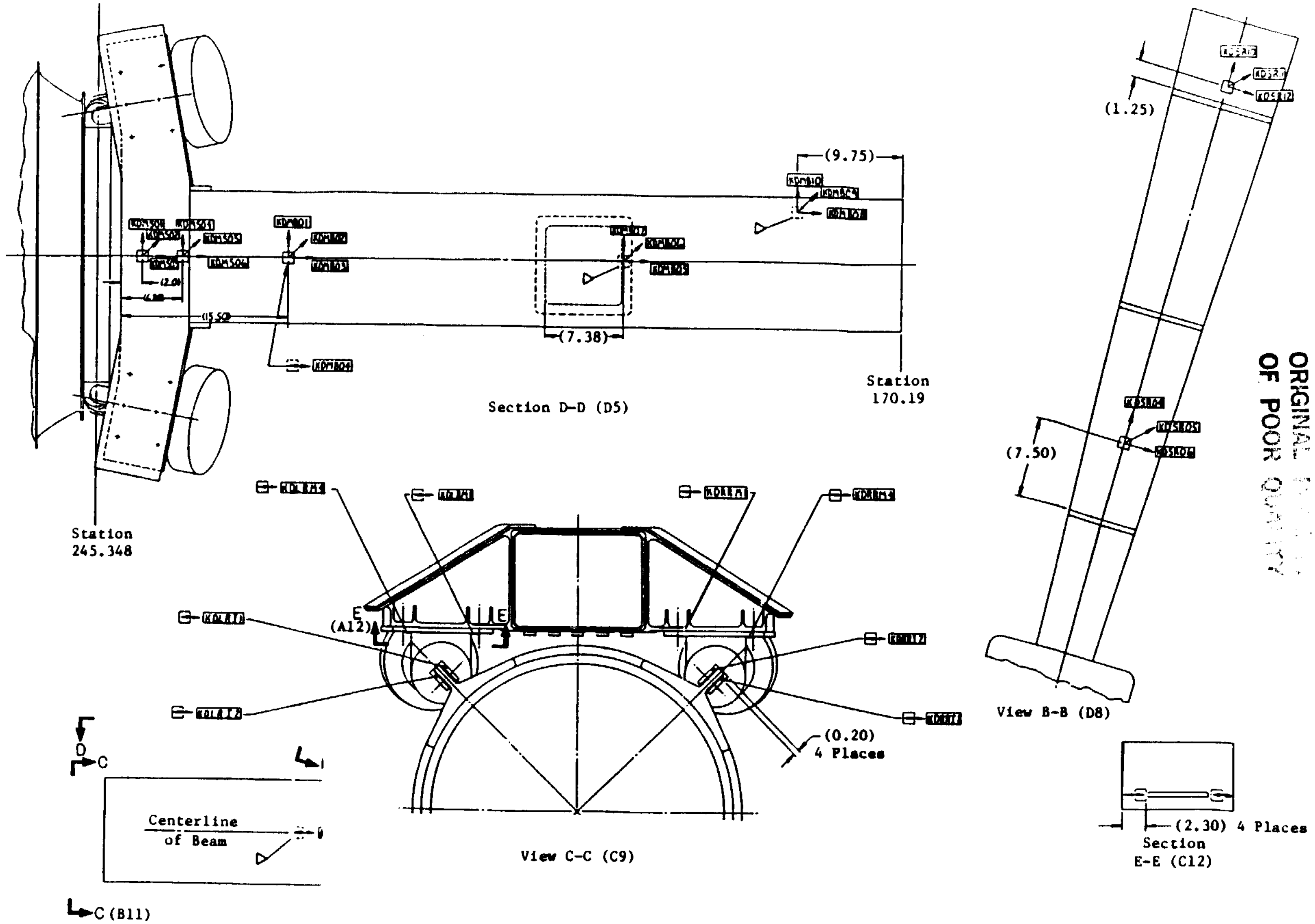


Figure B-1. Strain Gage Locations on Strut.

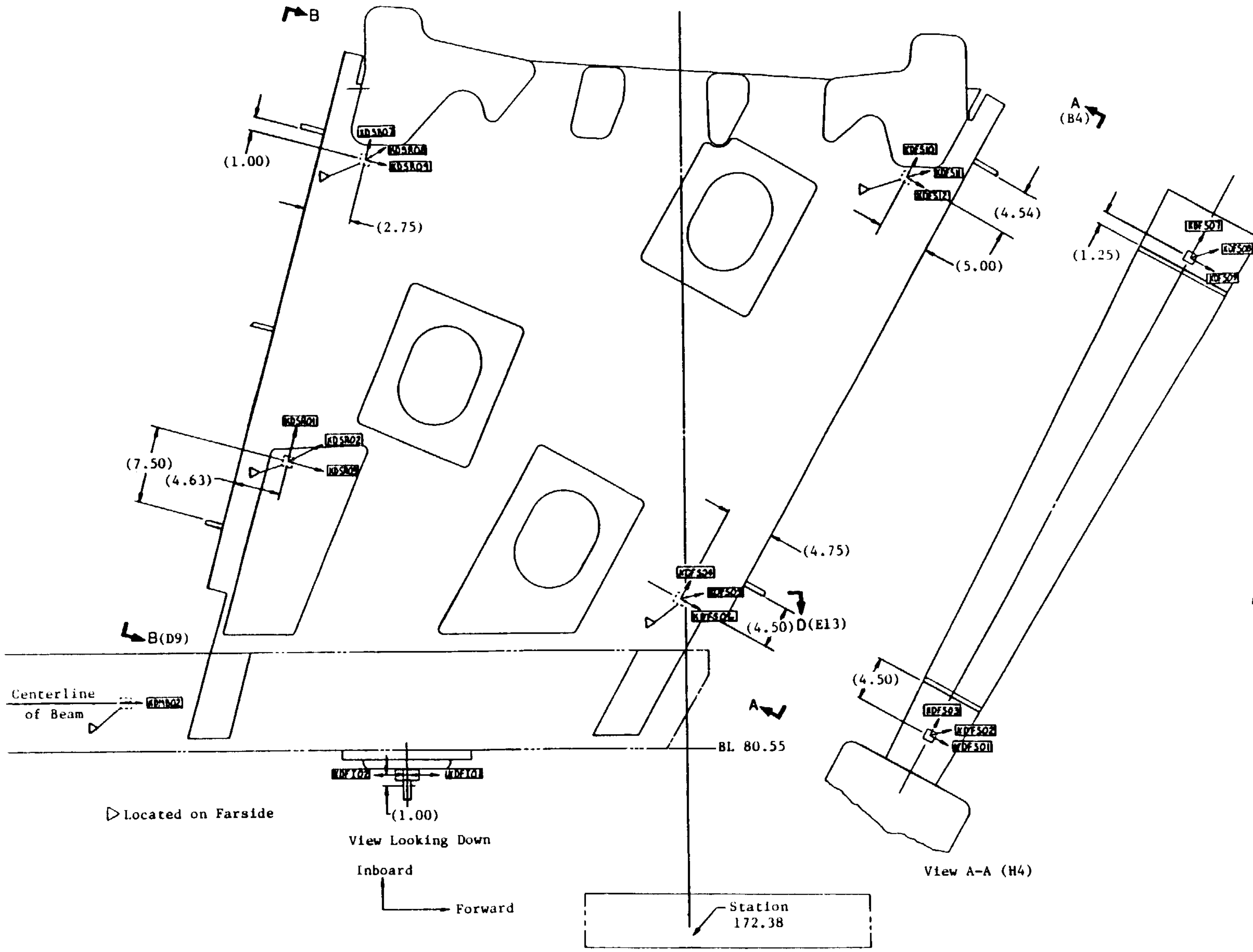


Figure B-2. Nacelle Instrumentation.

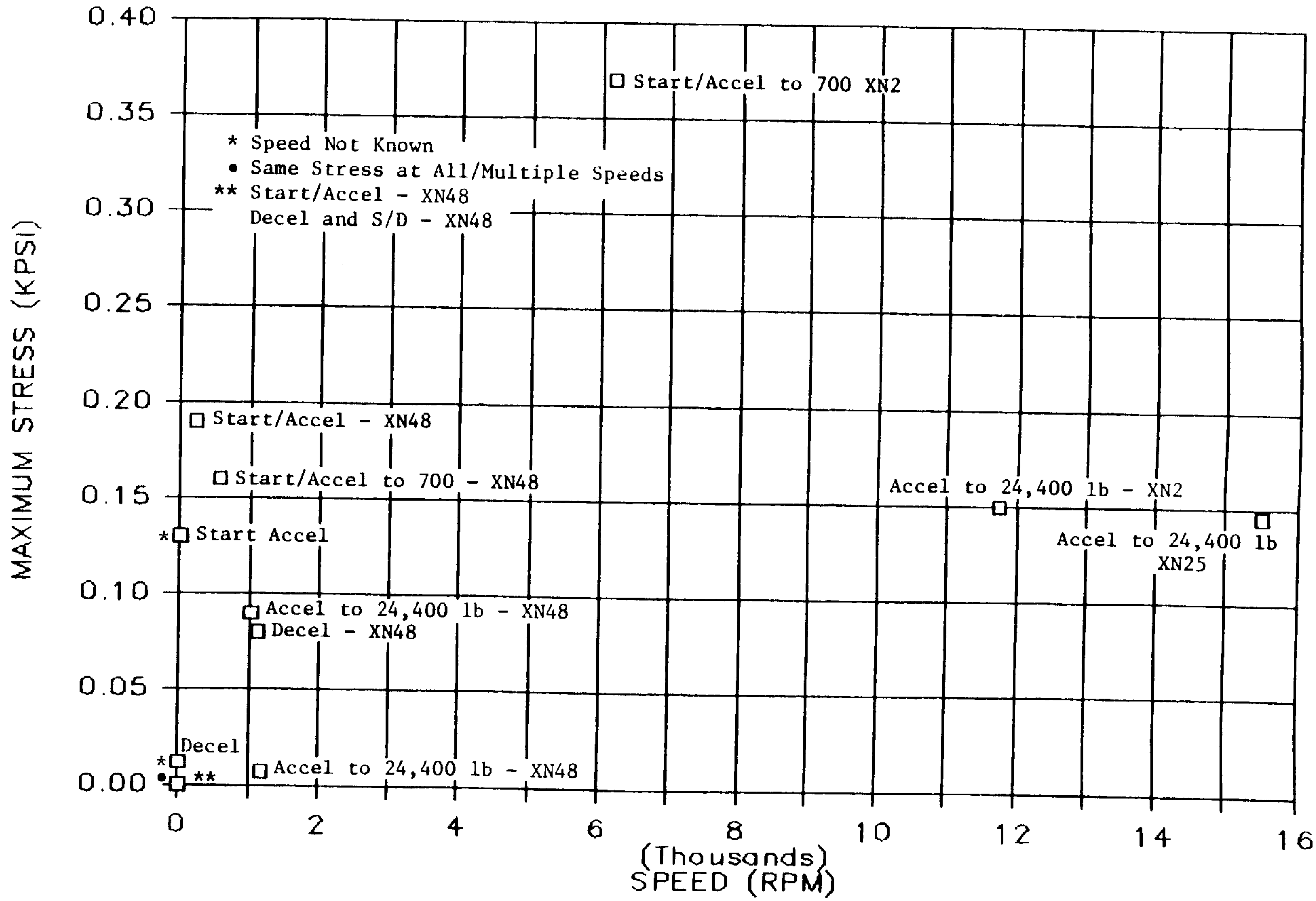


Figure B-3. Fairing Rosette No. 1 Vertical Axis (KD FAR1) Stress Versus Speed.

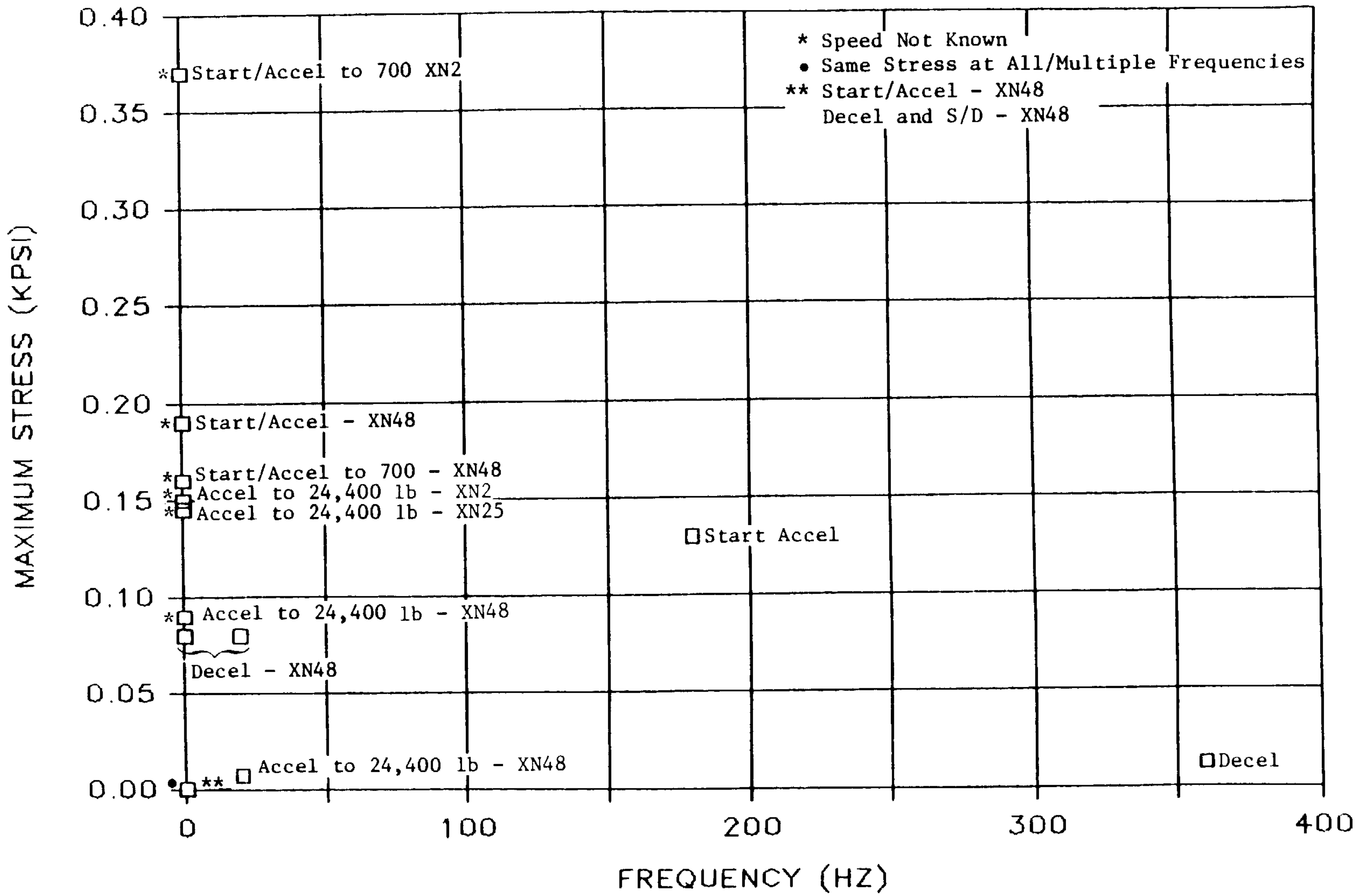


Figure B-4. Fairing Rosette No. 1 Vertical Axis (KD FAR1) Stress Versus Frequency.

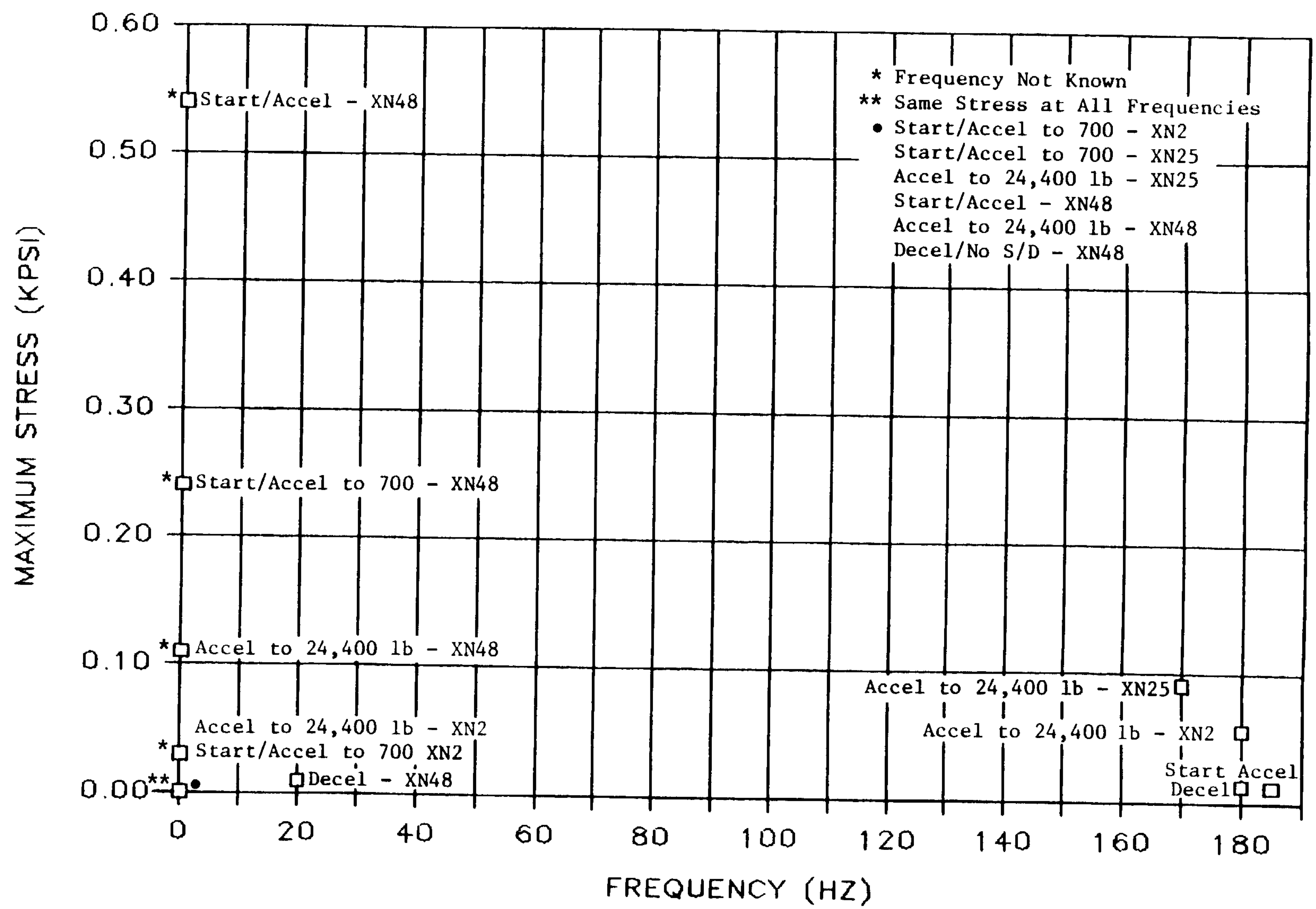


Figure B-5. Fairing Rosette No. 1 Diagonal Axis (KD FAR2) Stress Versus Frequency.

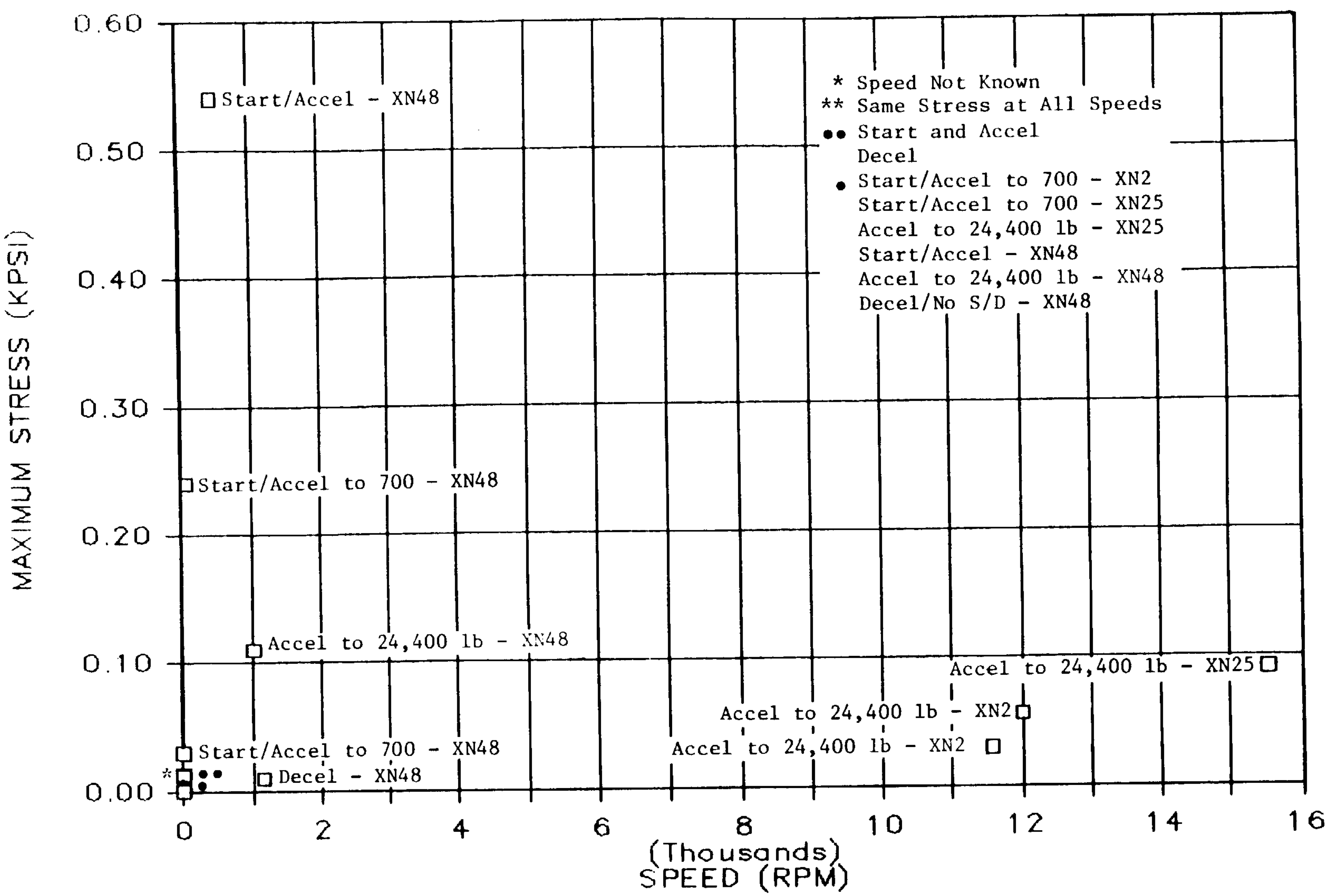


Figure B-6. Fairing Rosette No. 1 Diagonal Axis (KD FAR2), Stress Versus Speed.

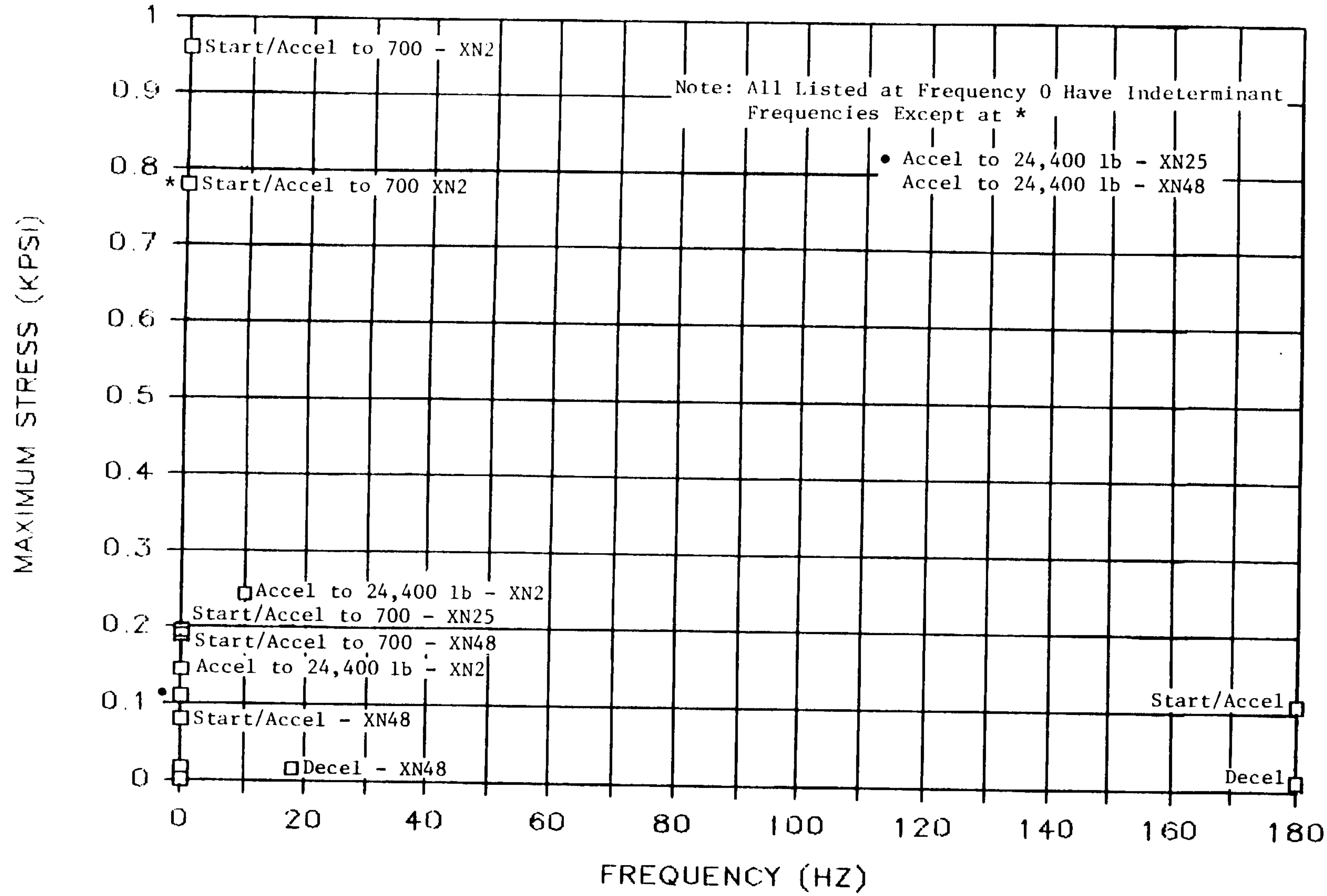


Figure B-7. Fairing Rosete No. 1 Axial Axis (KD FAR3), Stress Versus Frequency.

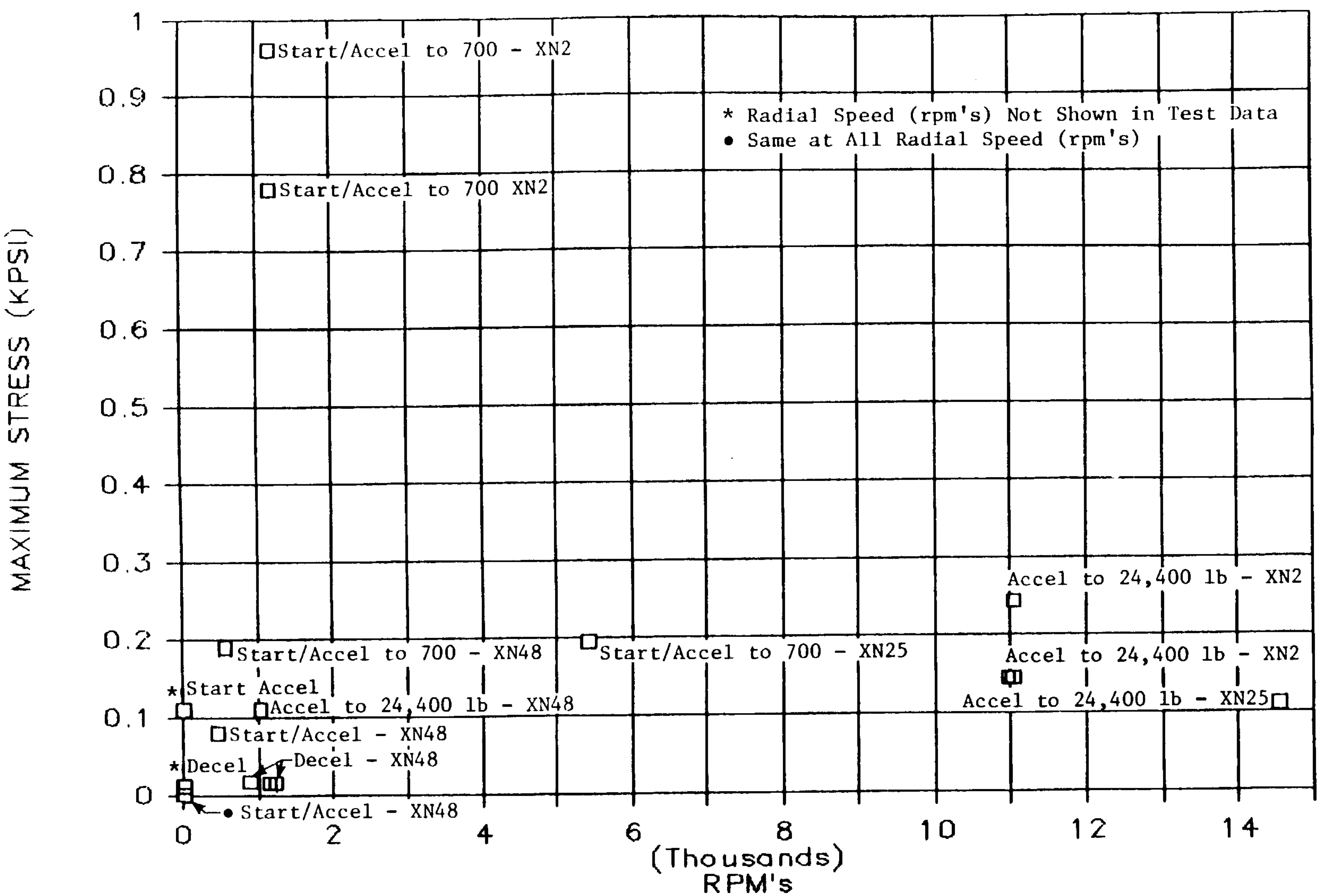


Figure B-8. Fairing Rosette No. 1 Axial Axis (KD FAR3), Stress Versus Speed.

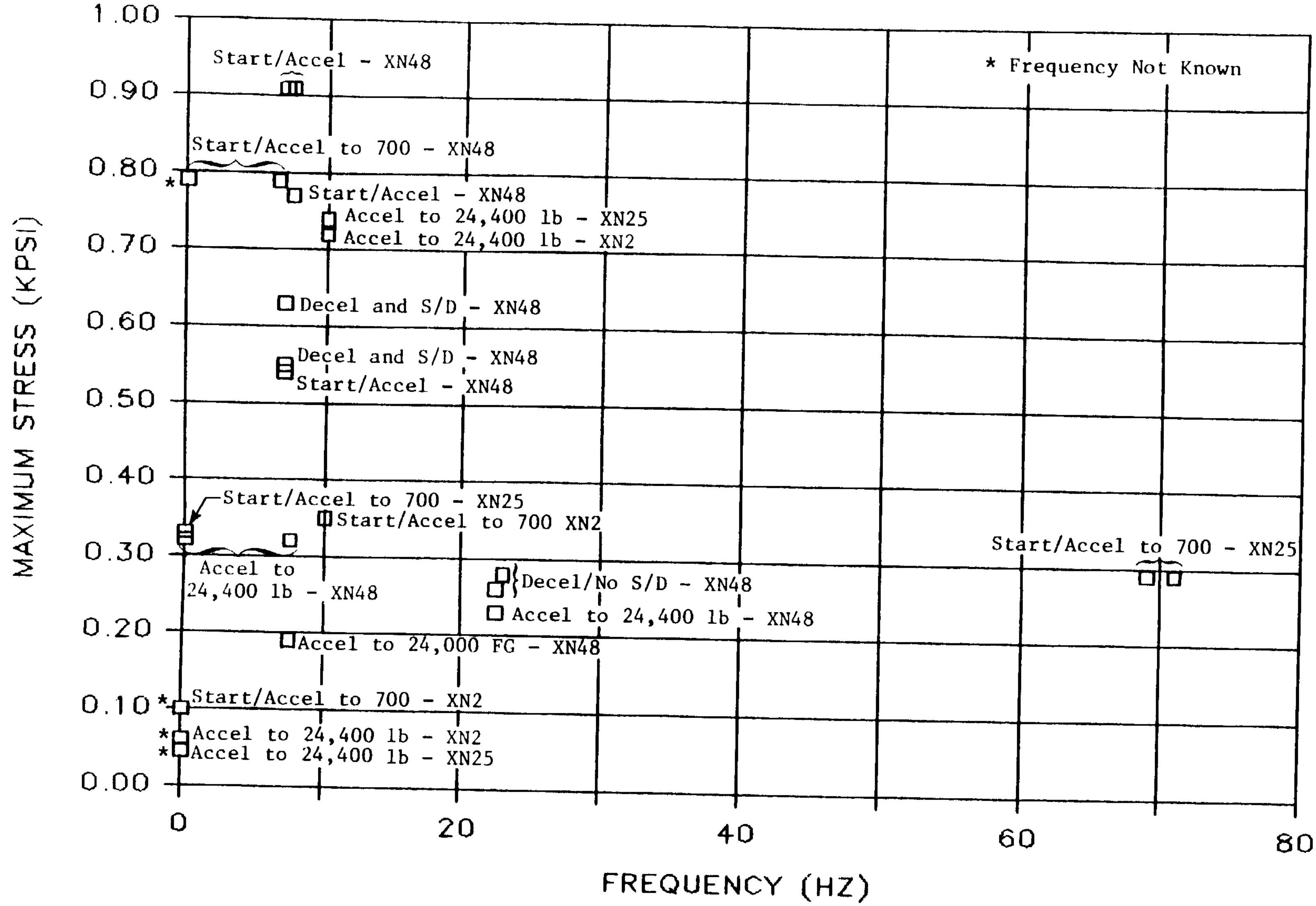


Figure B-9. Forward Isolator (KD F101), Stress Versus Frequency.

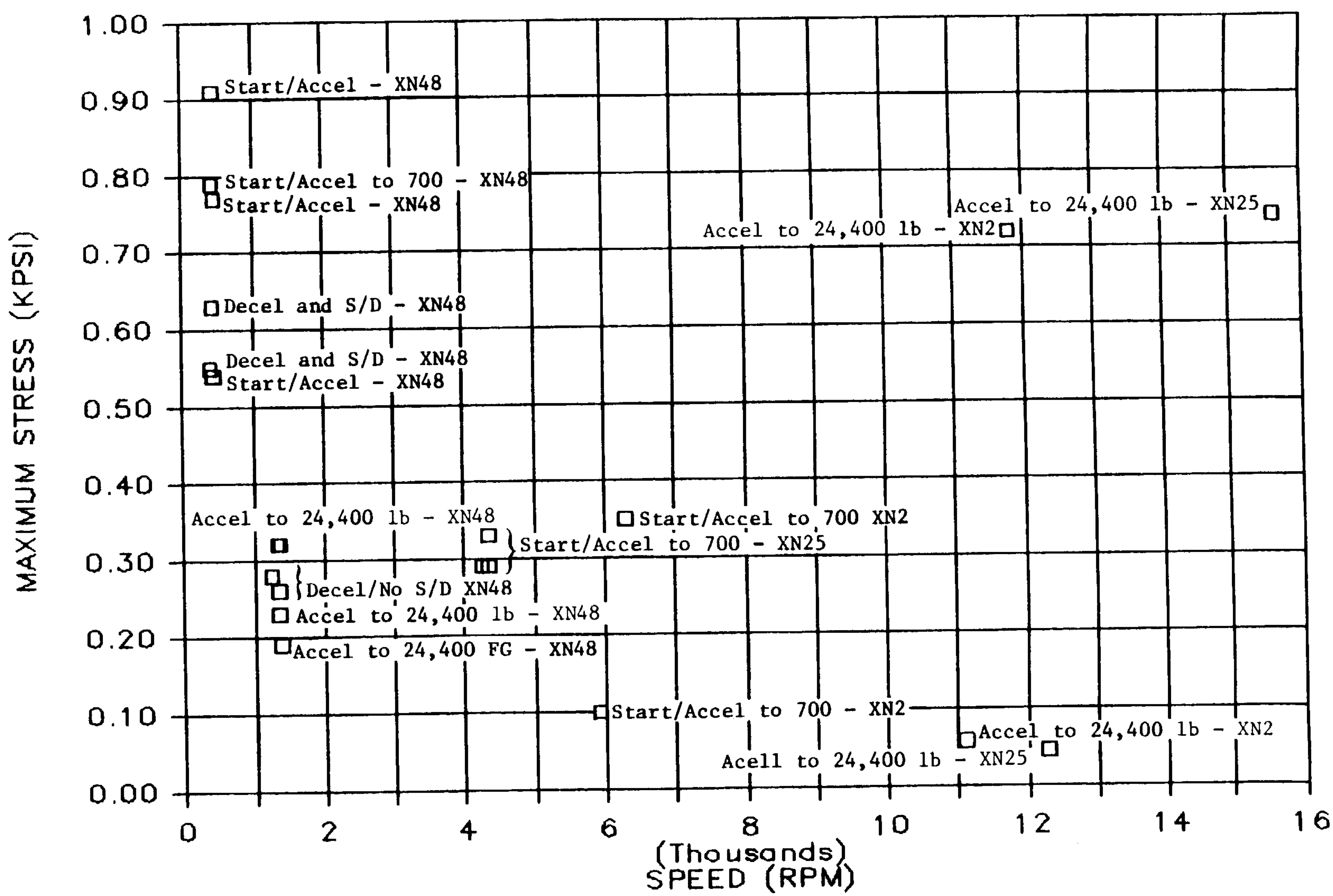


Figure B-10. Forward Isolator (KD F101), Stress Versus Speed.

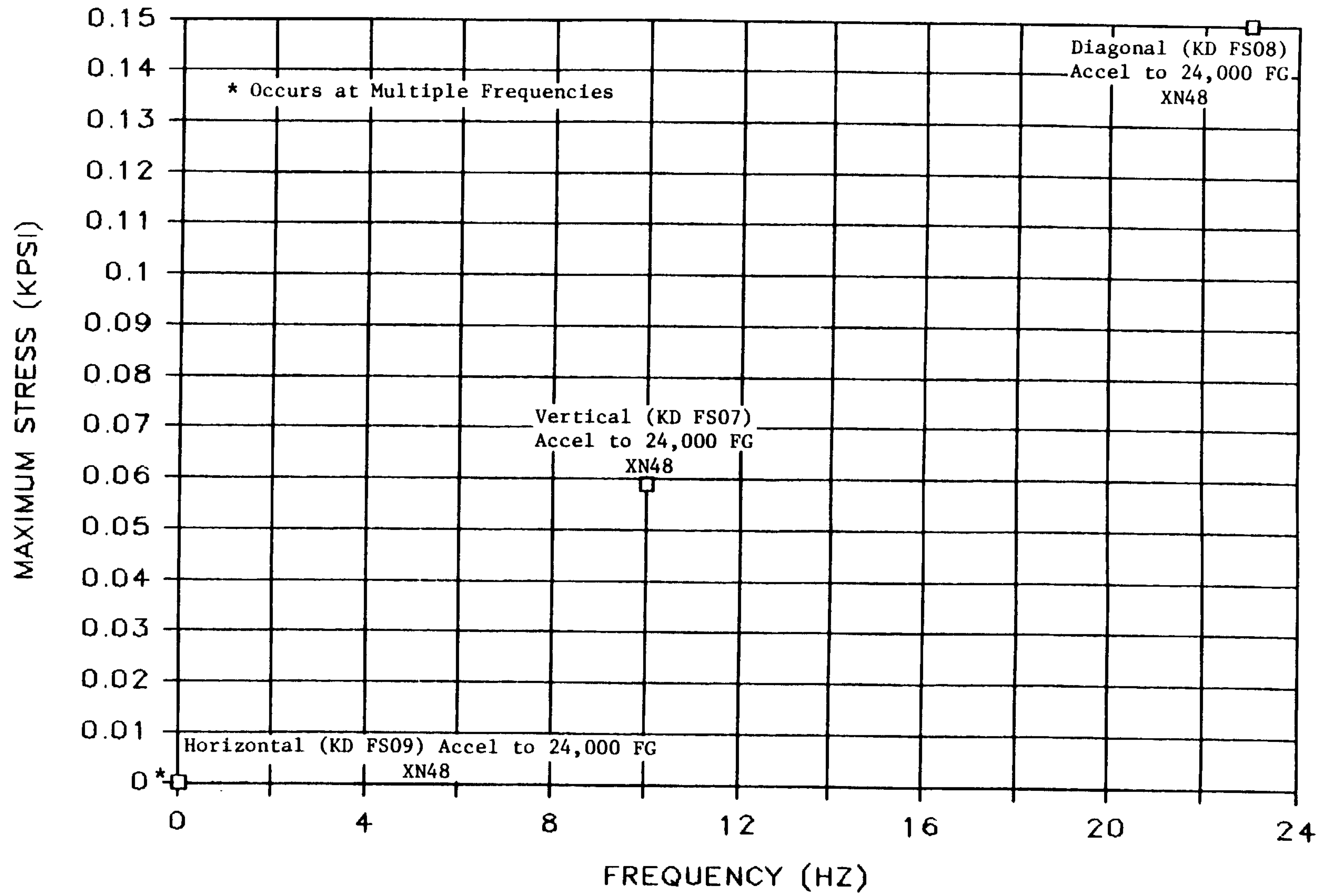


Figure B-11. Back of Spar - Upper Forward (KD FS07, KD FS08, and KD FS09), Stress Versus Frequency.

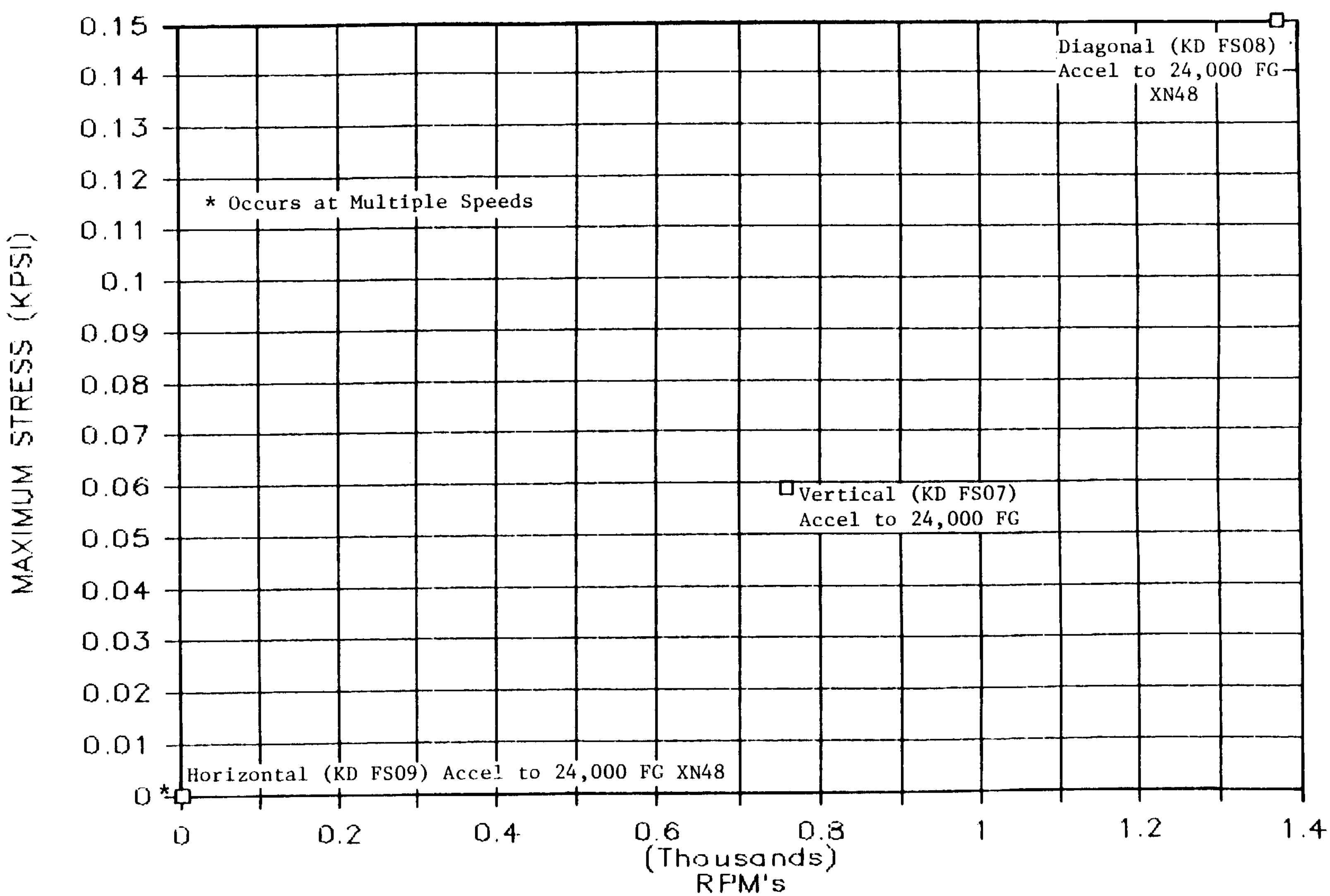


Figure B-12. Back of Spar - Upper Forward (KD FS07, KD FS08, and KD FS09), Stress Versus Speed.

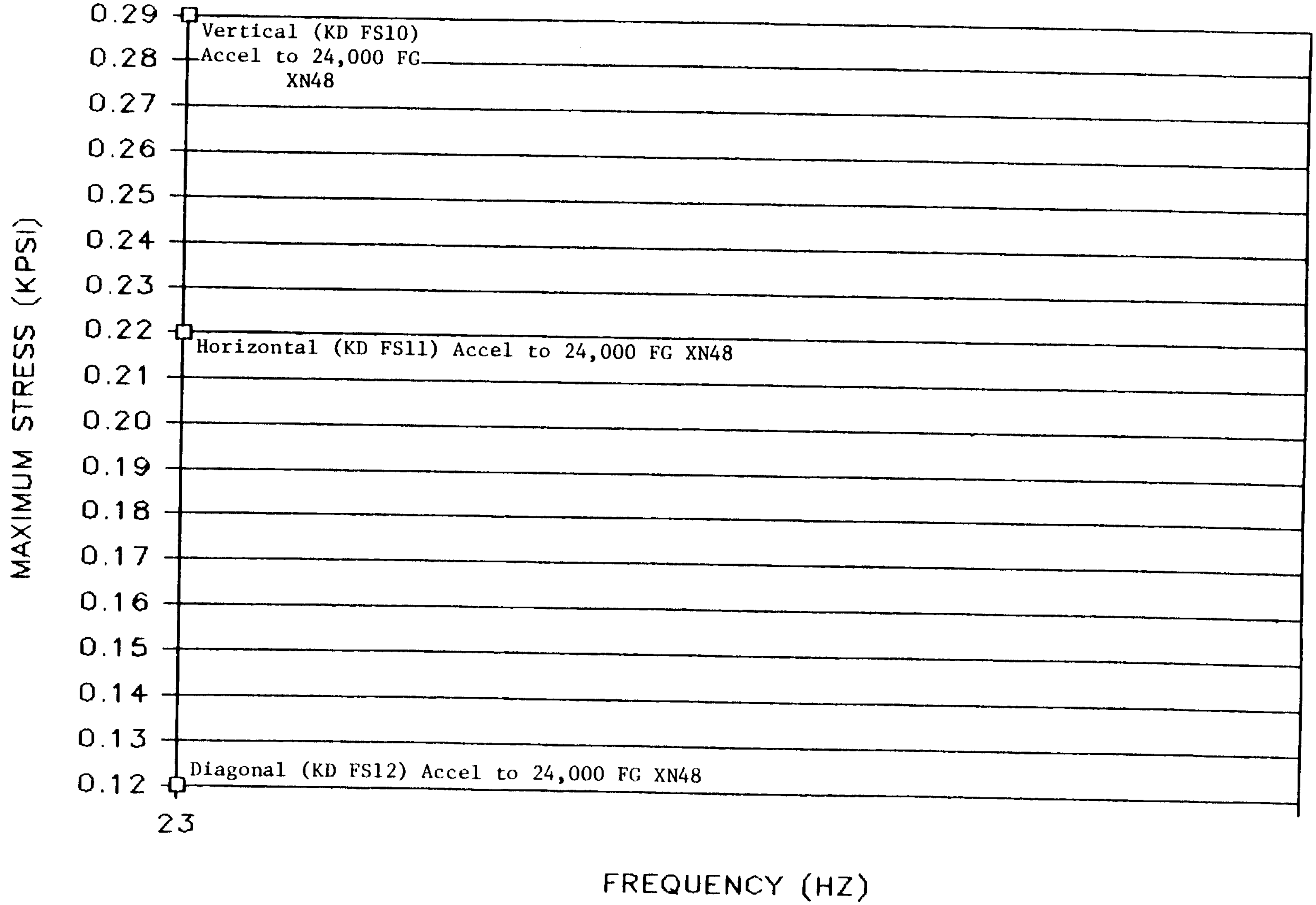


Figure B-13. Side of Spar - Upper Forward Vertical, Horizontal, and Axial (KD FS10, 11, and 12) Stress Versus Frequency.

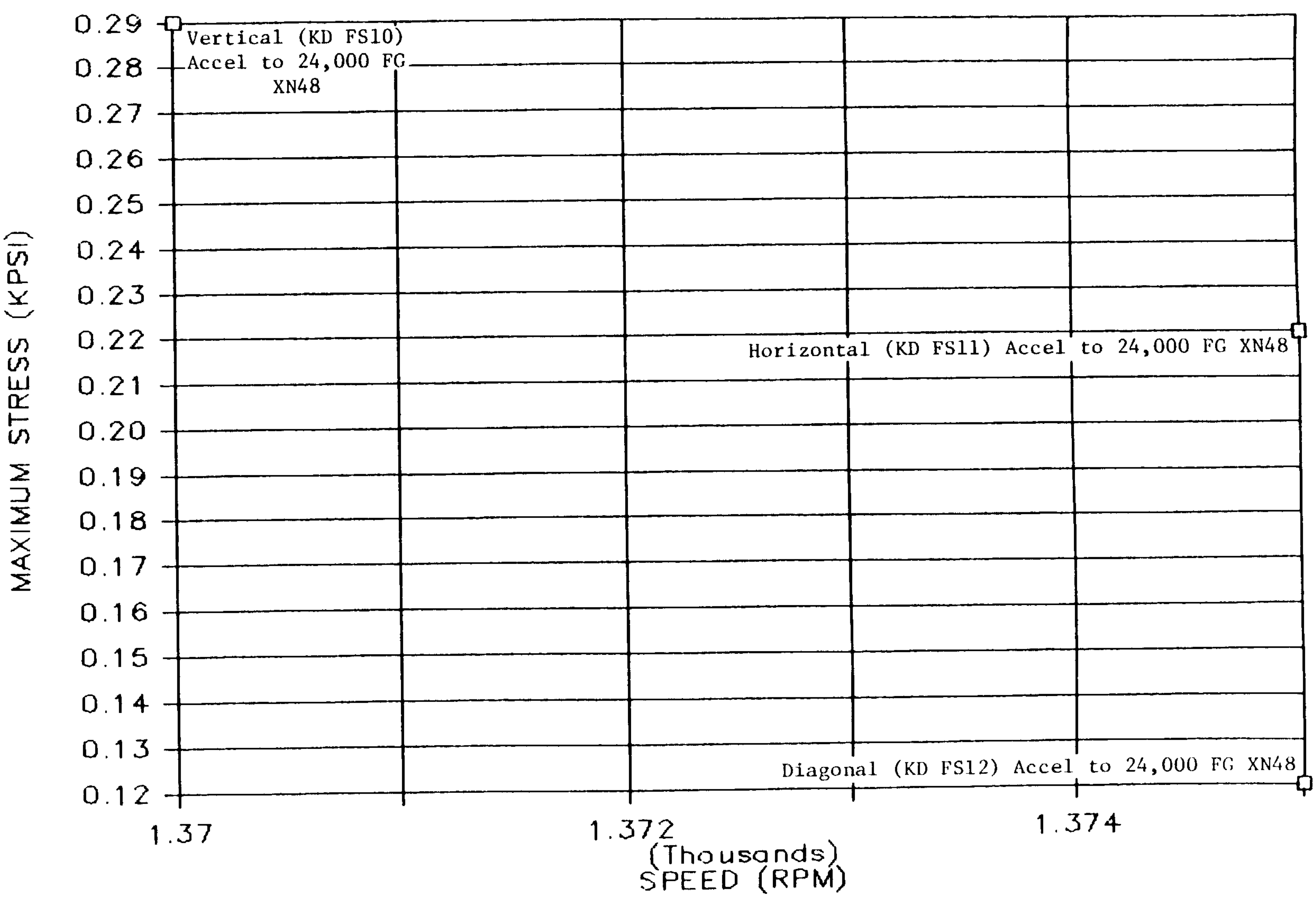


Figure B-14. Side of Spar - Upper Forward Vertical, Horizontal, and Axial (KD FS10, 11, and 12) Stress Versus Speed.

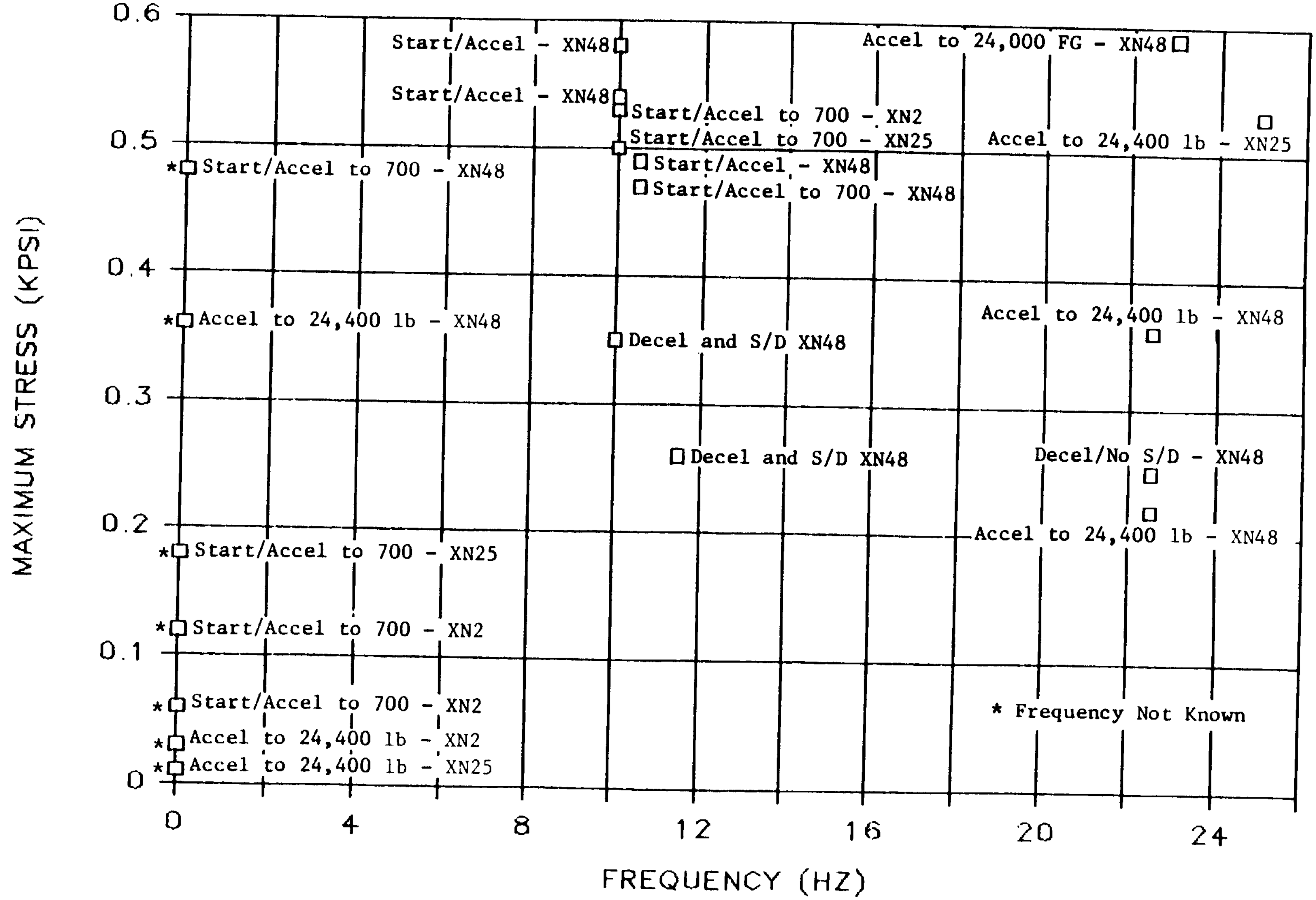


Figure B-15. Left Aft Isolator Clevis Axial (KD LRI1), Stress Versus Frequency.

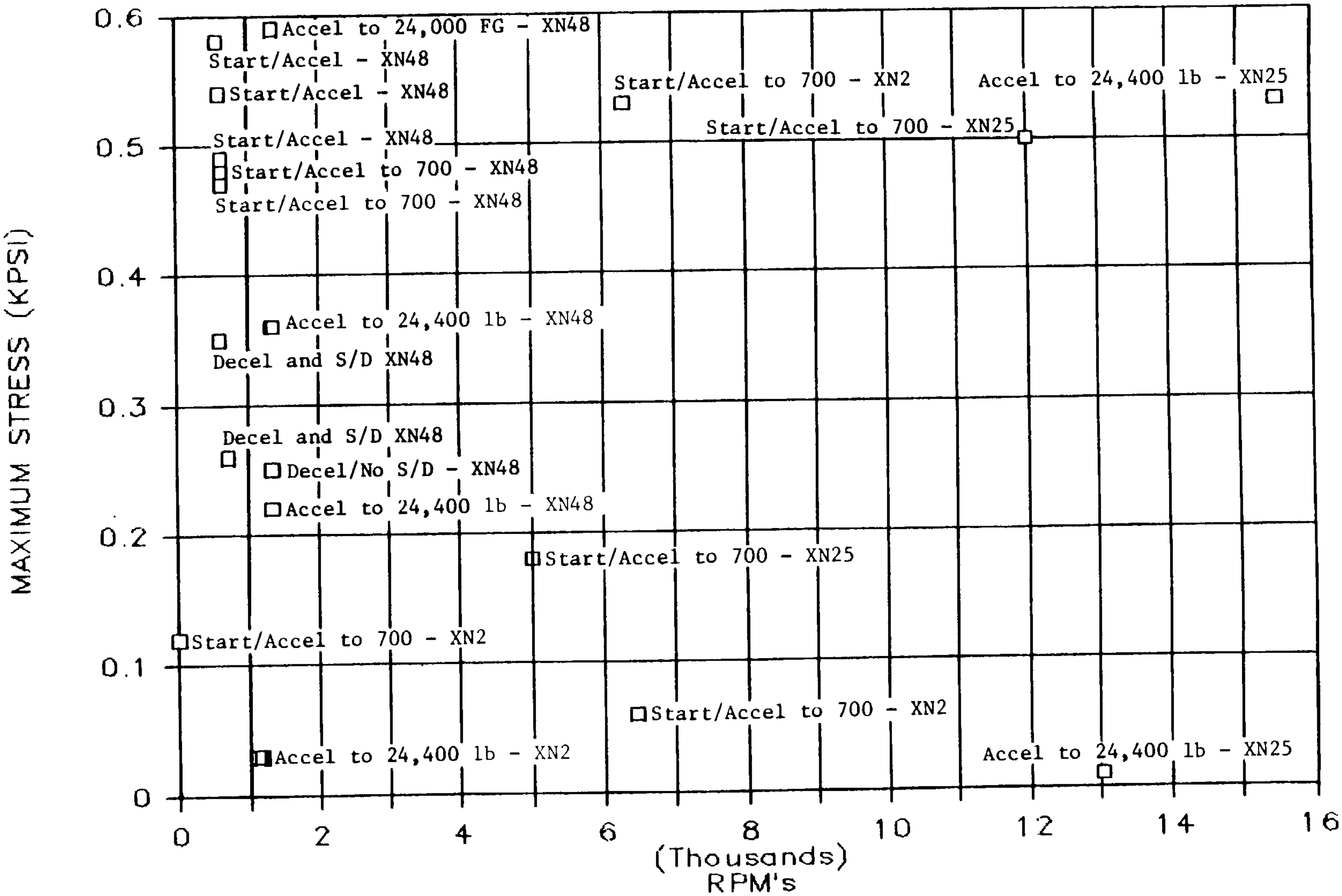


Figure B-16. Left Aft Isolator Clevis Axial (KD LRI1), Stress Versus Speed.

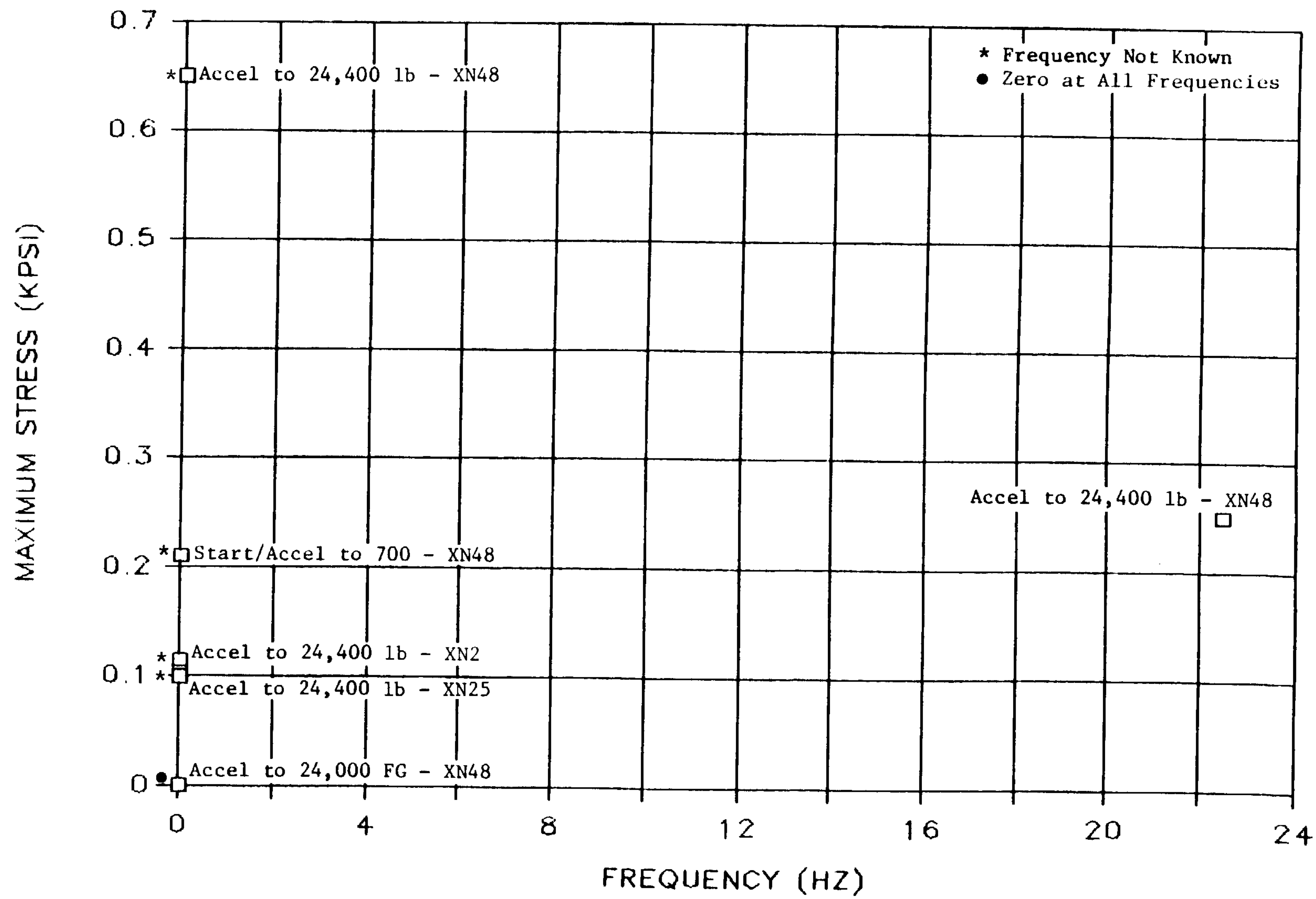


Figure B-17. Top of Mount Beam - Aft Vertical (KD MB01), Stress Versus Frequency.

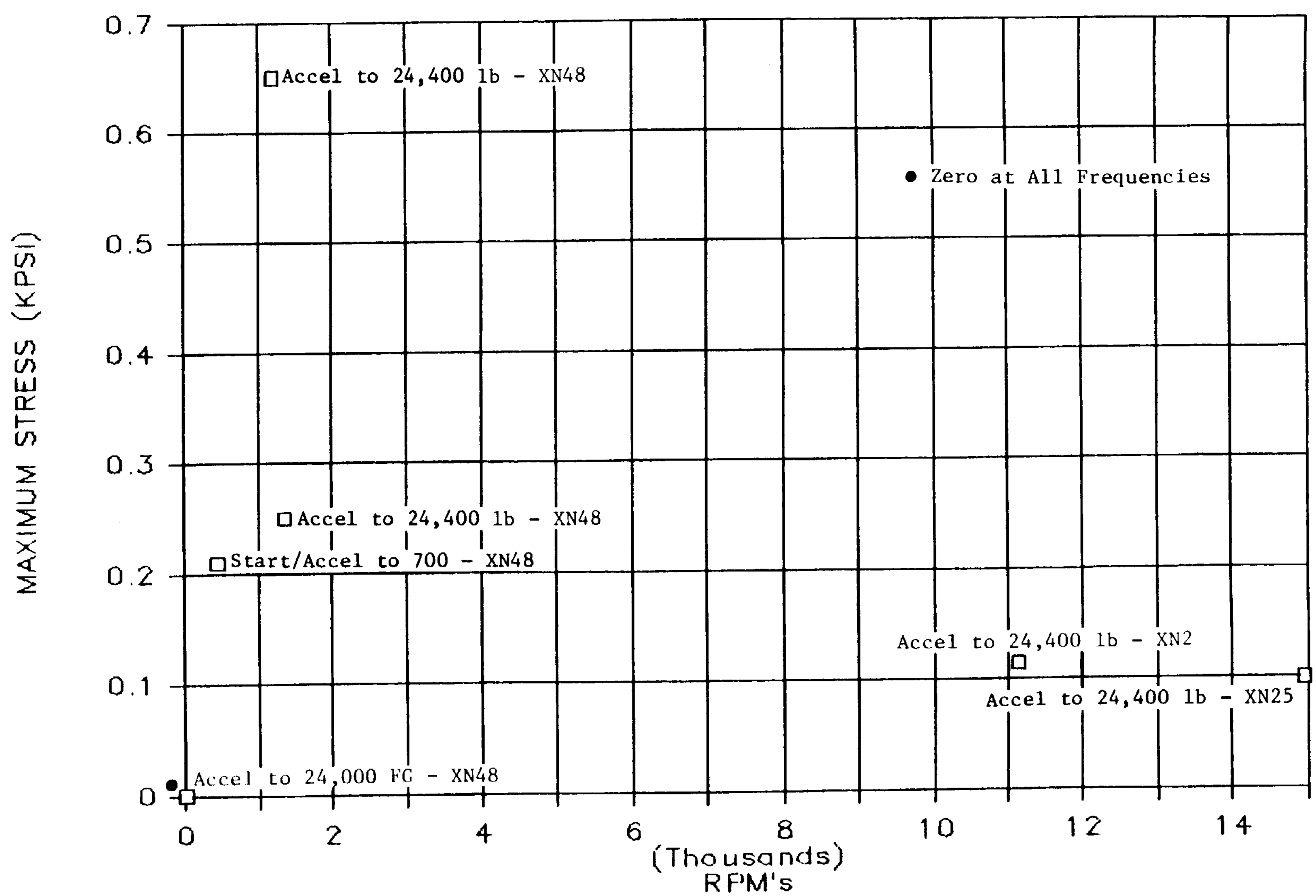


Figure B-18. Top of Mount Beam - Aft Vertical (KD MB01), Stress Versus Speed.

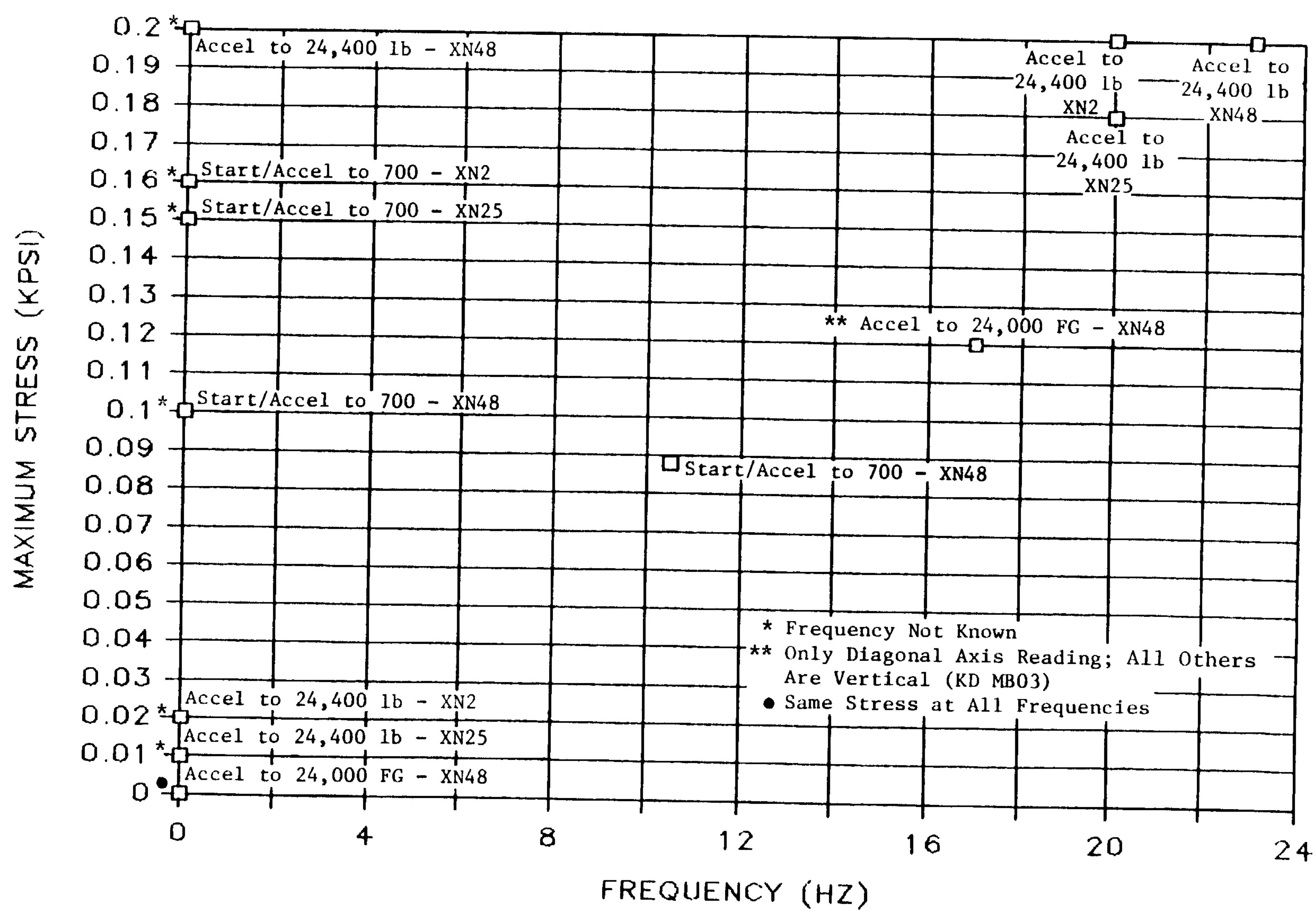


Figure B-19. Top of Mount Beam - Aft Diagonal and Horizontal (KD MB02 and KD MB03), Stress Versus Frequency.

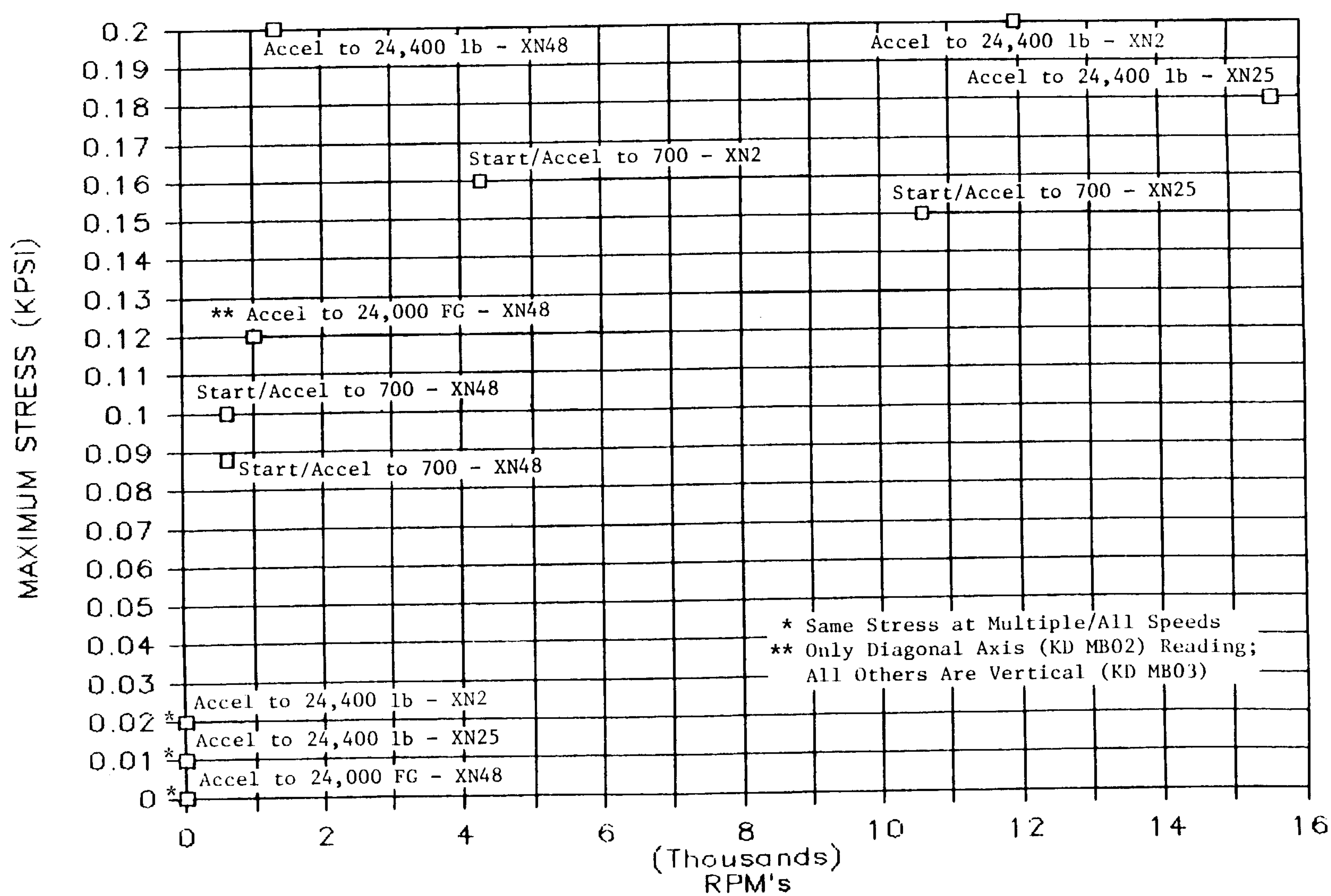


Figure B-20. Top of Mount Beam - Aft Diagonal and Horizontal (KD MB02 and KD MB03), Stress Versus Speed.

ORIGINAL PAGE IS
OF POOR QUALITY

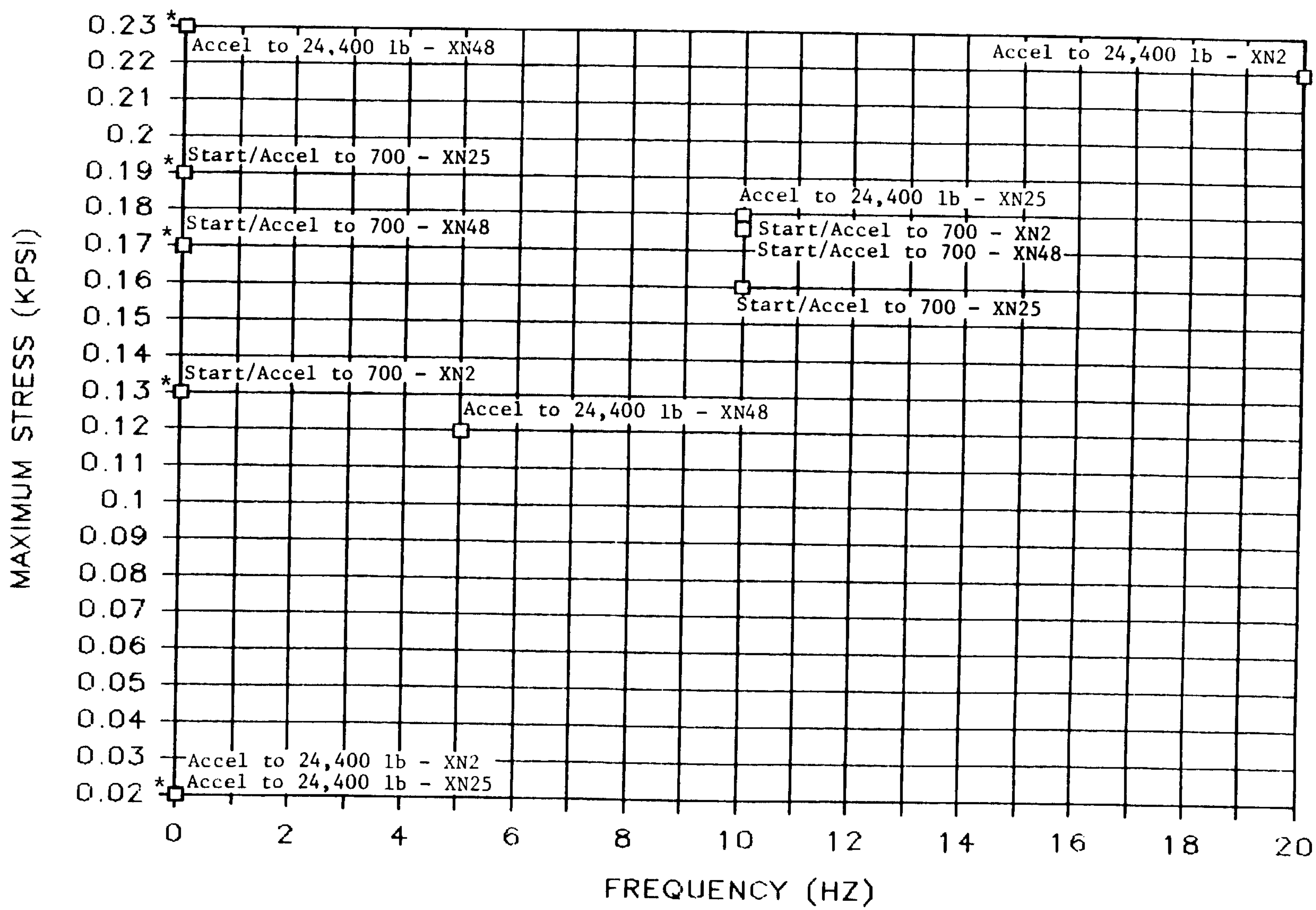


Figure B-21. Bottom of Mount Beam - Aft Horizontal (KD MB04), Stress Versus Frequency.

ORIGINAL PAGE IS
OF POOR QUALITY

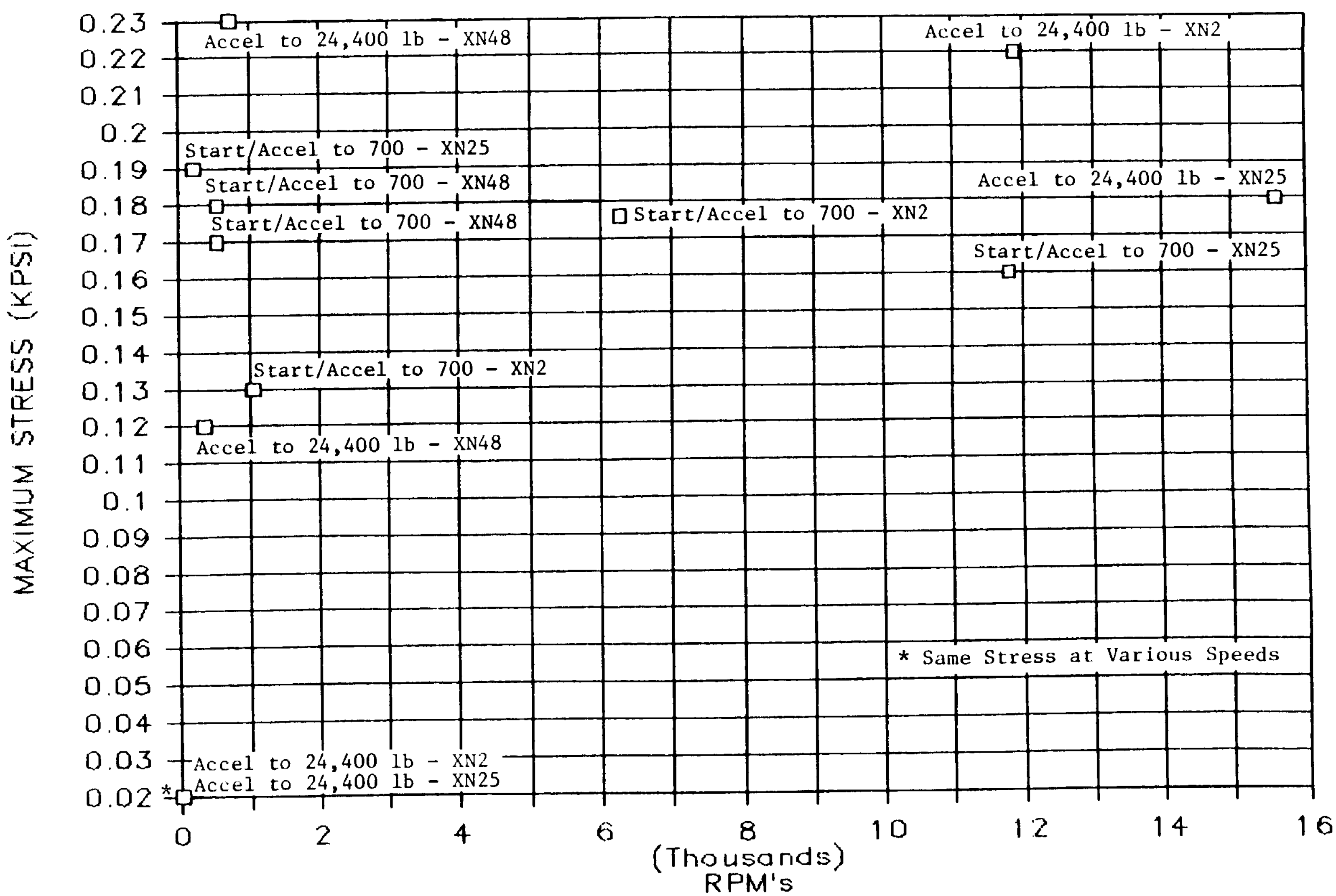


Figure B-22. Bottom of Mount Beam - Aft Horizontal (KD MB04), Stress Versus Speed.

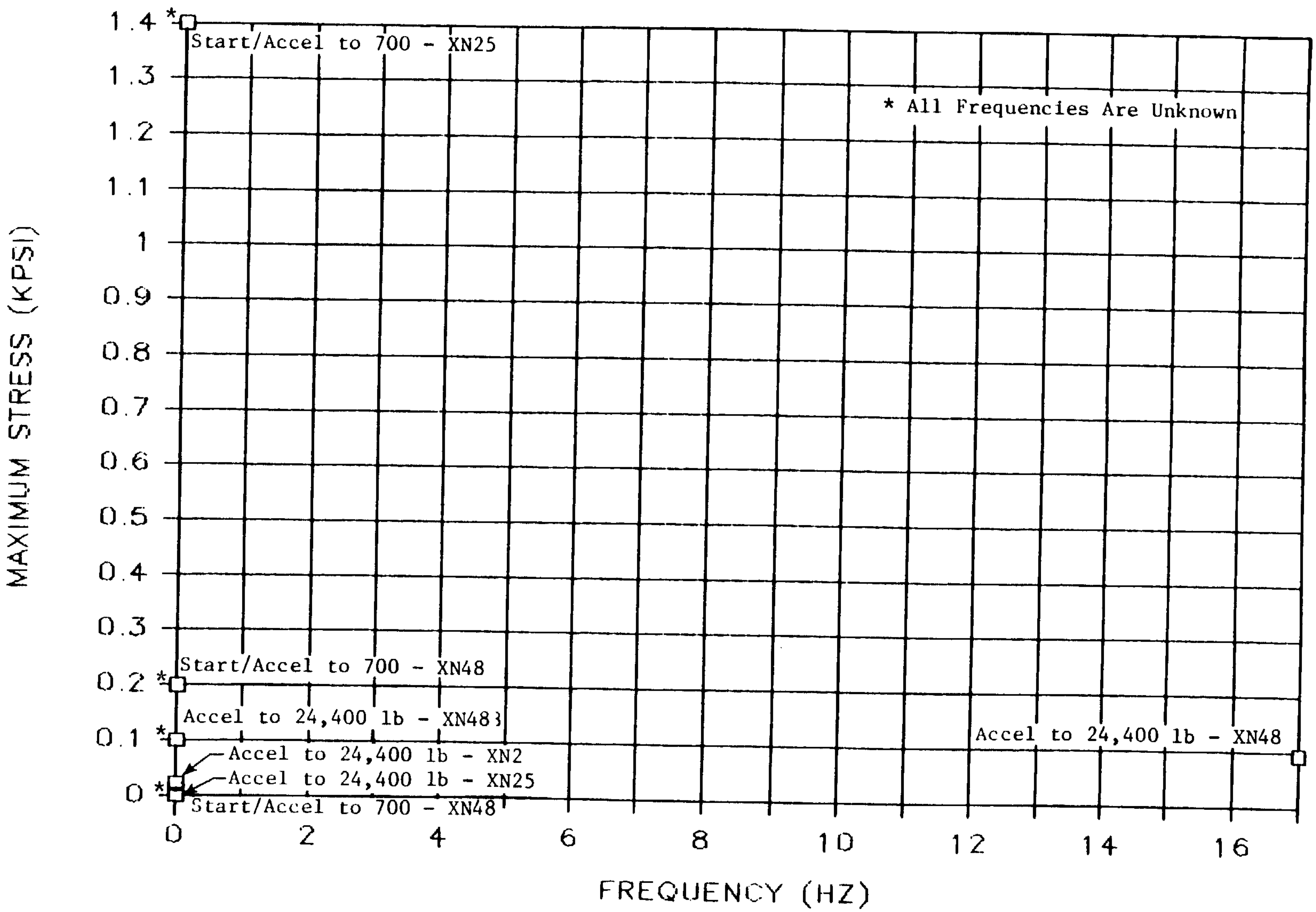


Figure B-23. Top of Mount Beam - Mid Horizontal (KD MB05), Stress Versus Frequency.

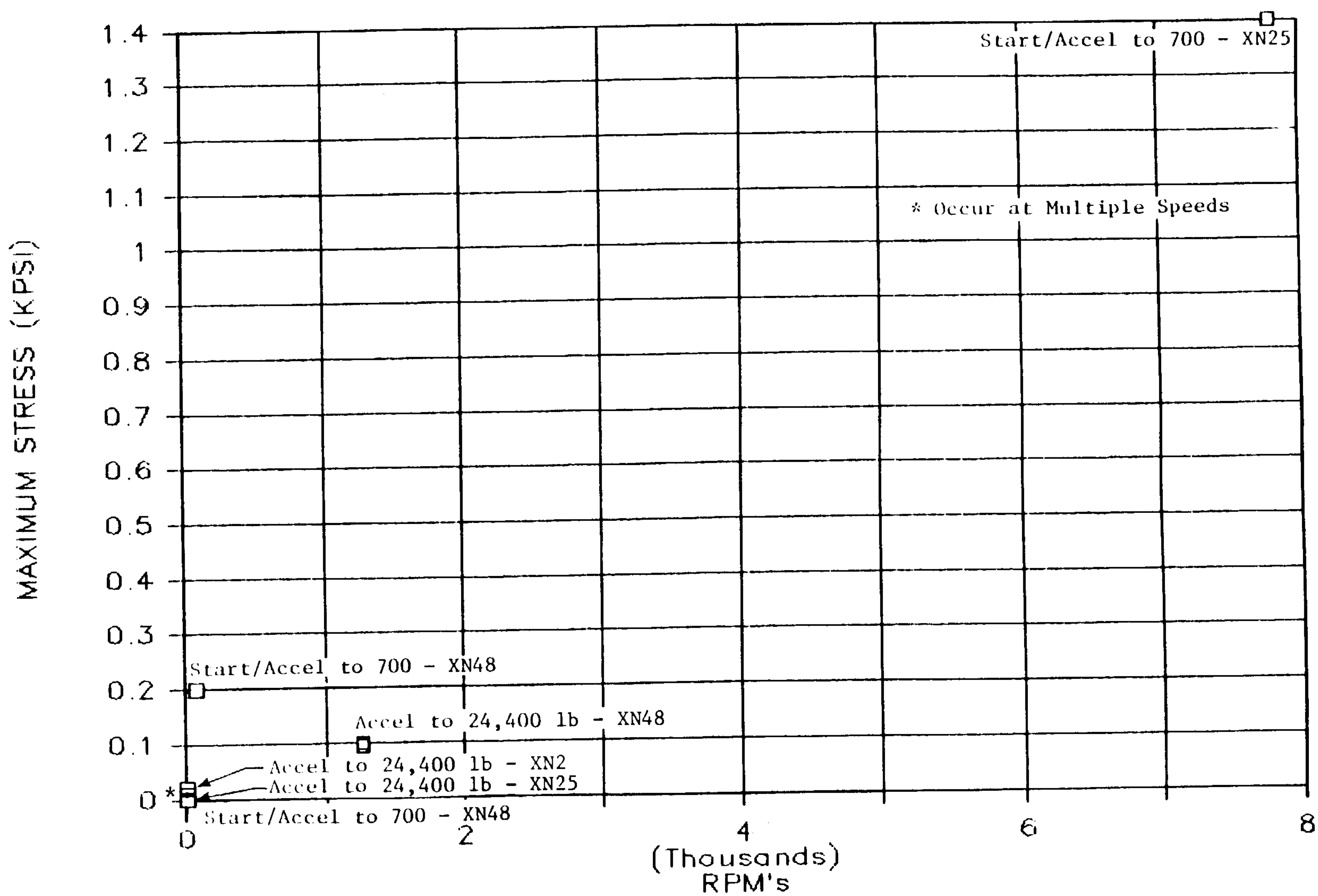


Figure B-24. Top of Mount Beam - Mid Horizontal (KD MB05), Stress Versus Speed.

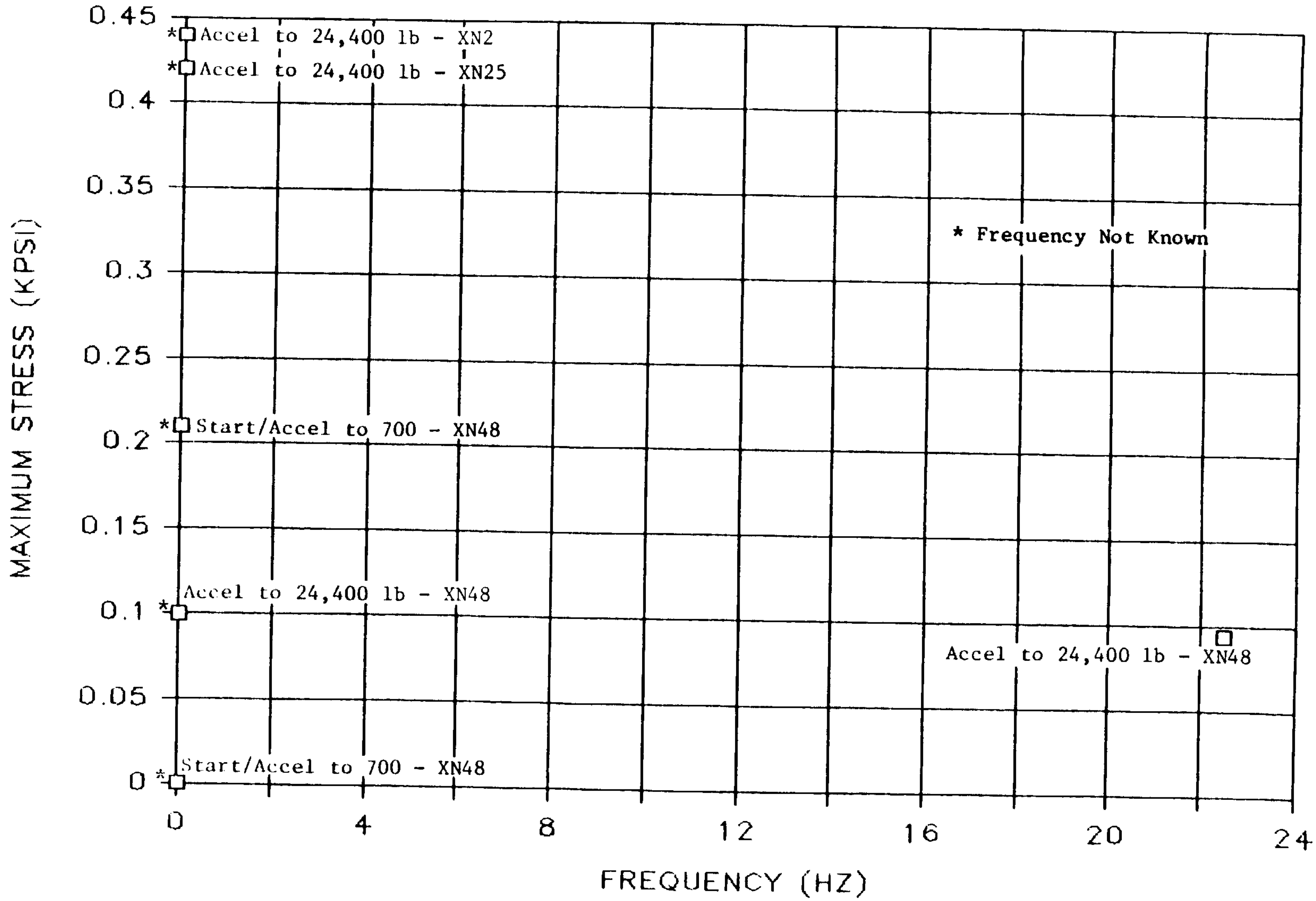


Figure B-25. Top of Mount Beam - Mid Vertical (KD MB07), Stress Versus Frequency.

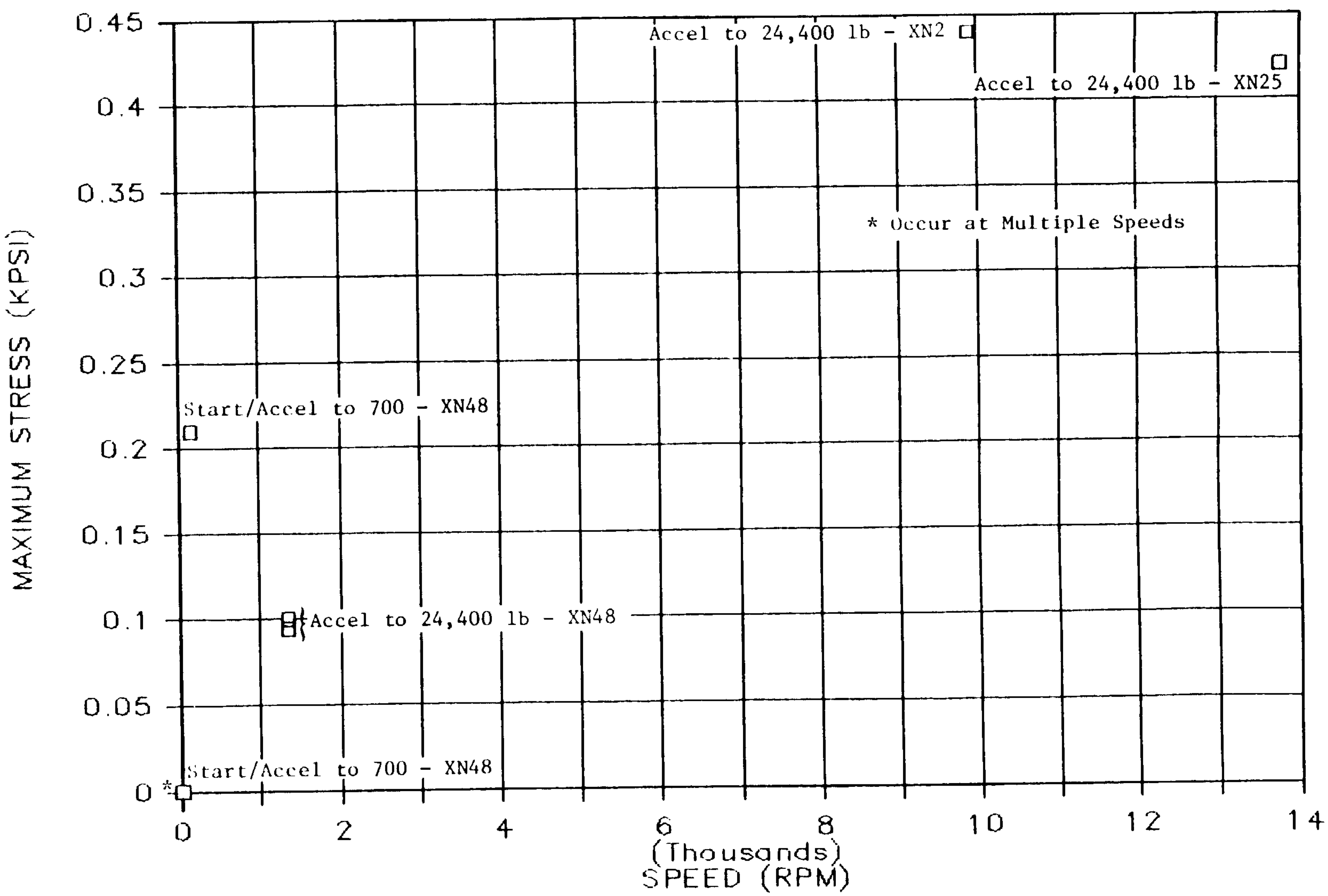


Figure B-26. Top of Mount Beam - Mid Vertical (KD MB07), Stress Versus Speed.

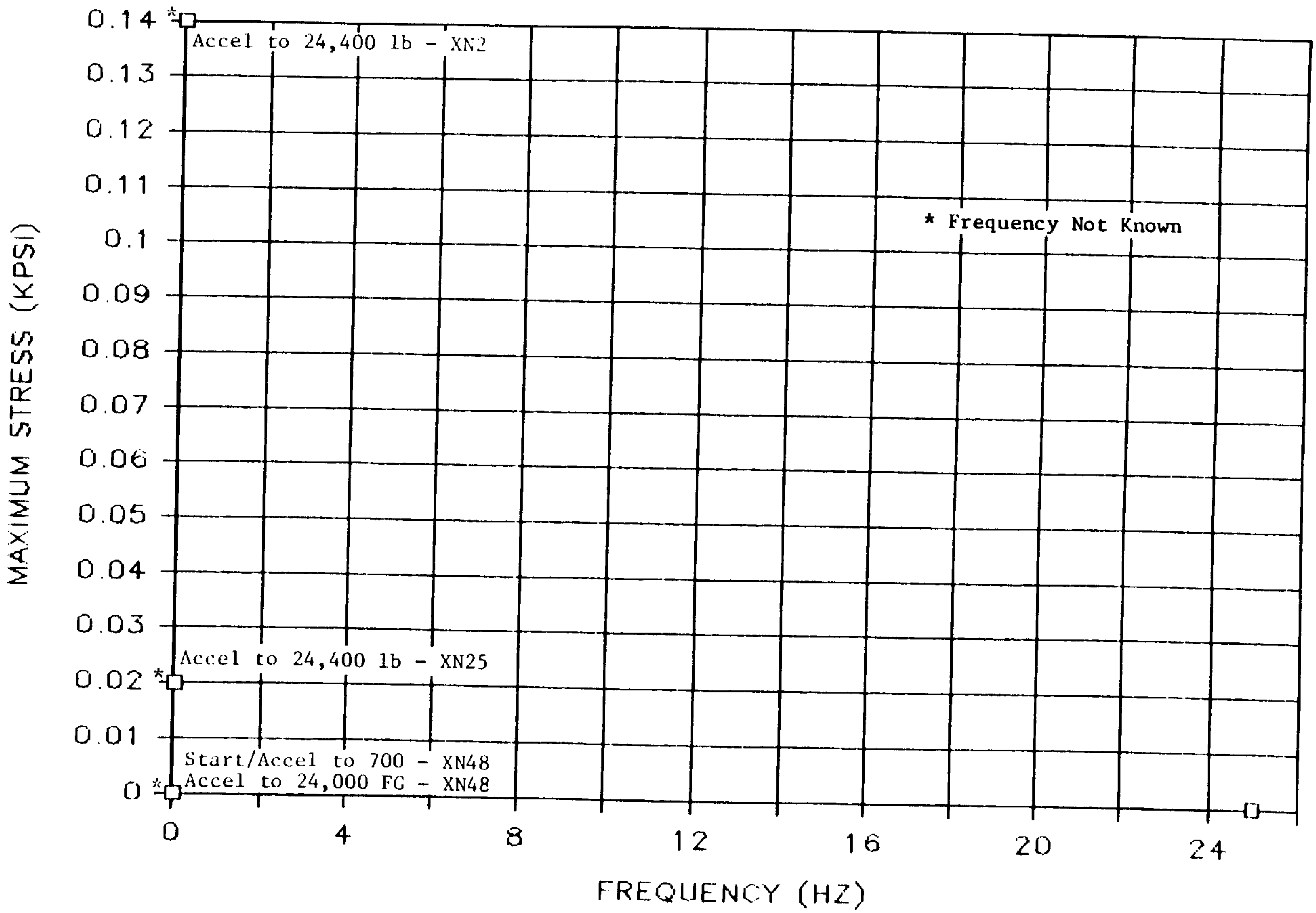


Figure B-27. Bottom of Mount Beam - Forward Vertical (KD MB10), Stress Versus Frequency.

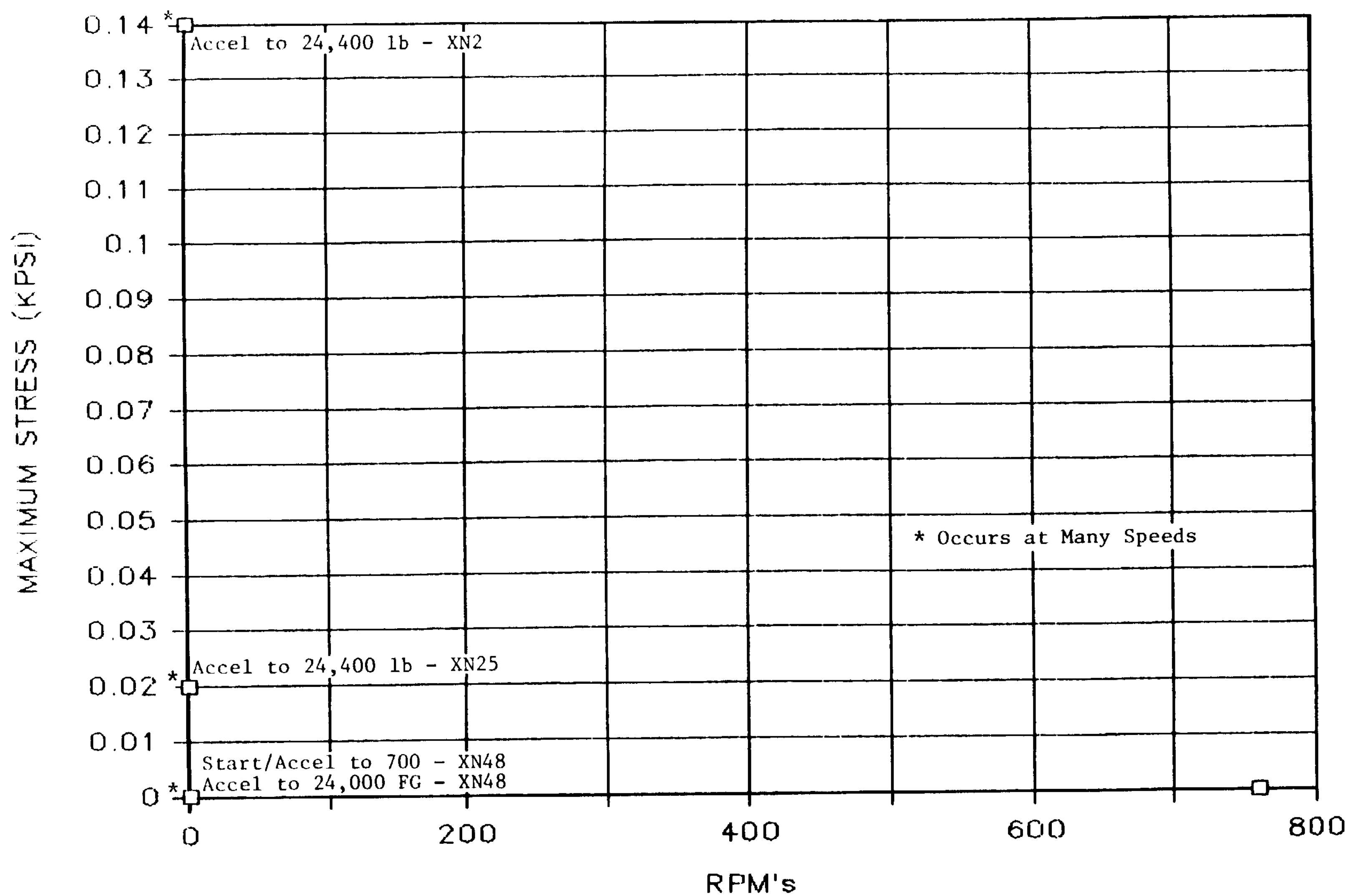


Figure B-28. Bottom of Mount Beam - Forward Vertical (KD MB10), Stress Versus Speed.

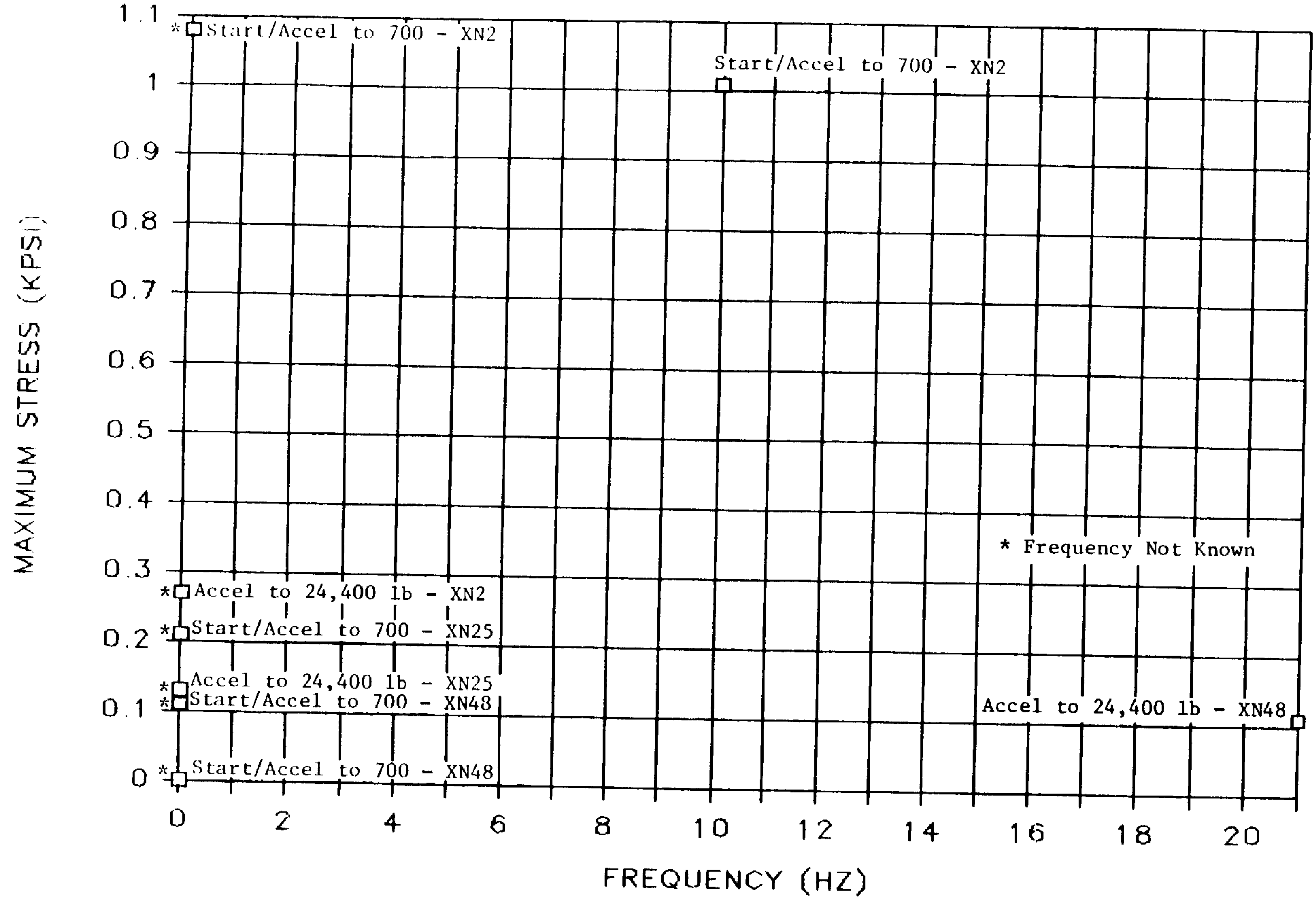


Figure B-29. Aft Mount Beam Support Fitting Horizontal (KD MS03), Stress Versus Frequency.

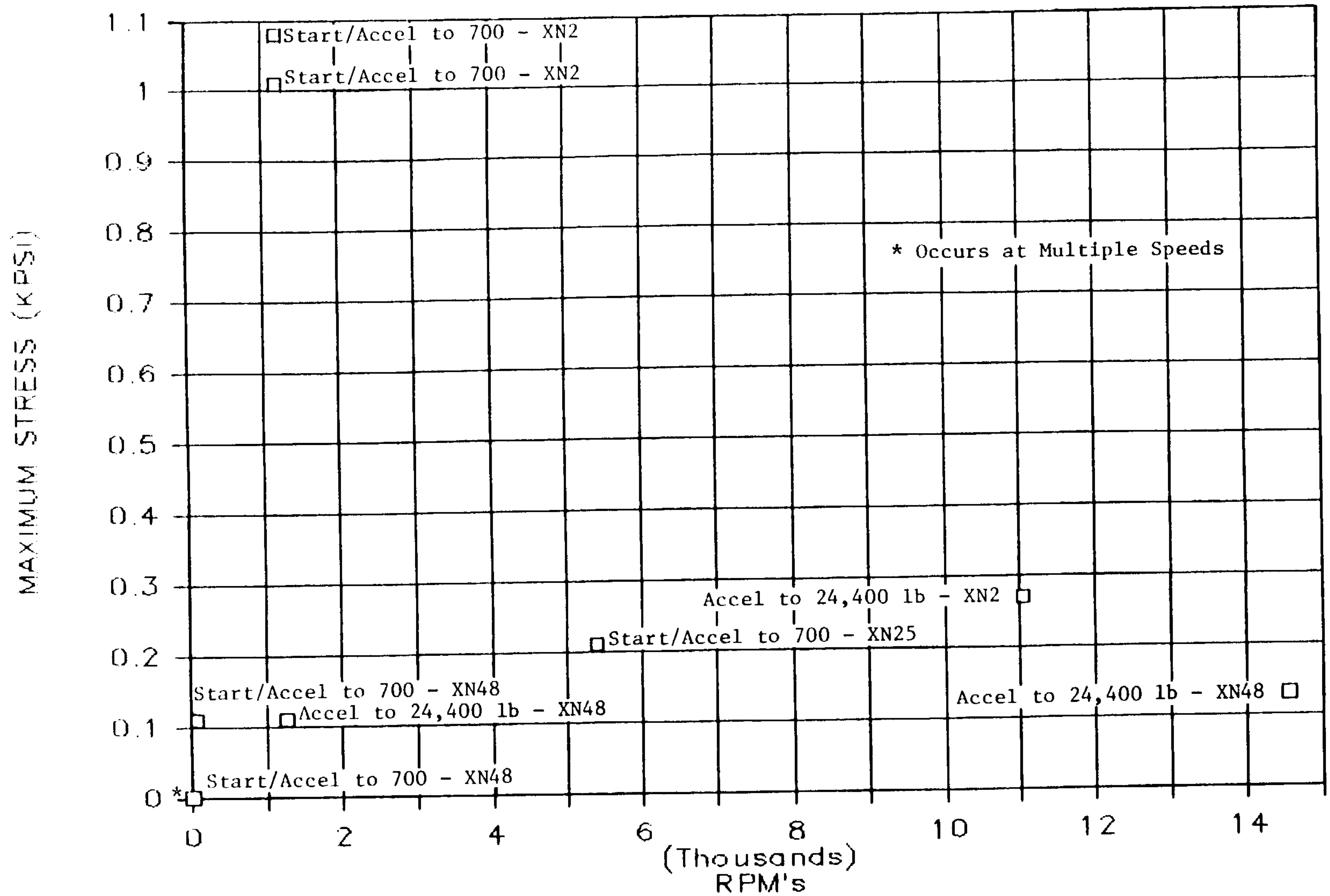


Figure B-30. Aft Mount Beam Support Fitting Horizontal (KD MS03), Stress Versus Speed.

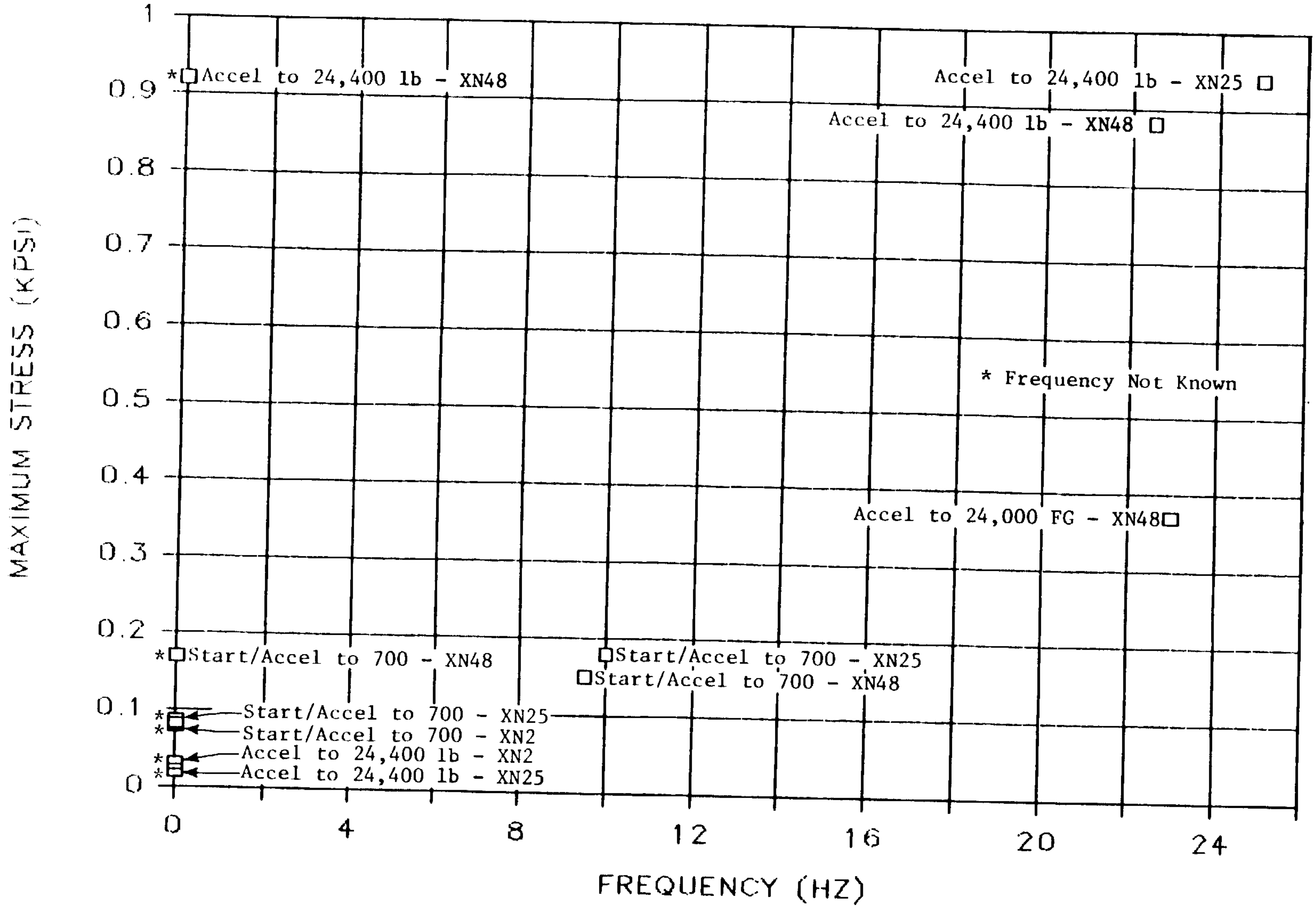


Figure B-31. Right Aft Isolator Clevis Axial (KD RRI1), Stress Versus Frequency.

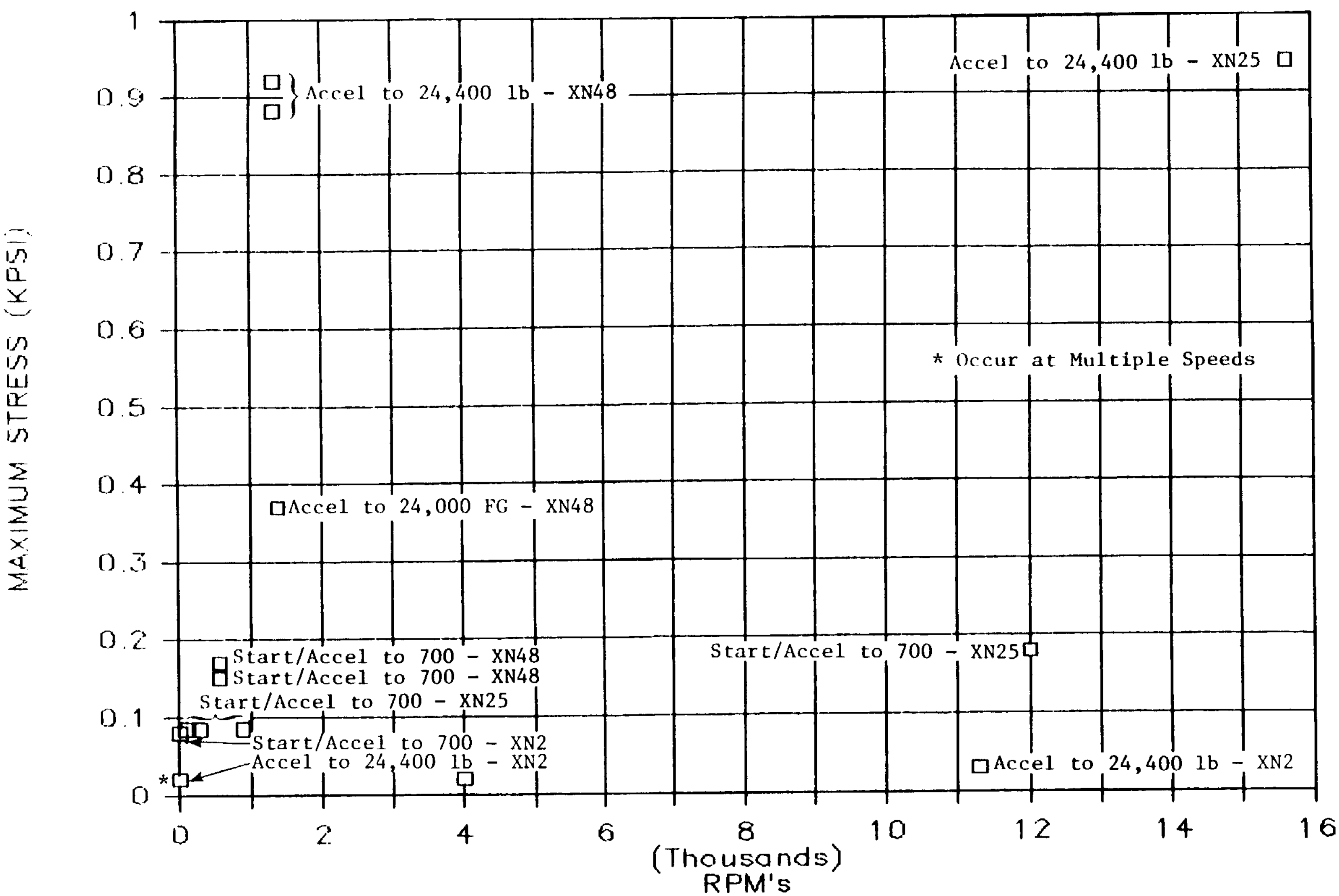


Figure B-32. Right Aft Isolator Clevis Axial (KD RRI1), Stress Versus Speed.

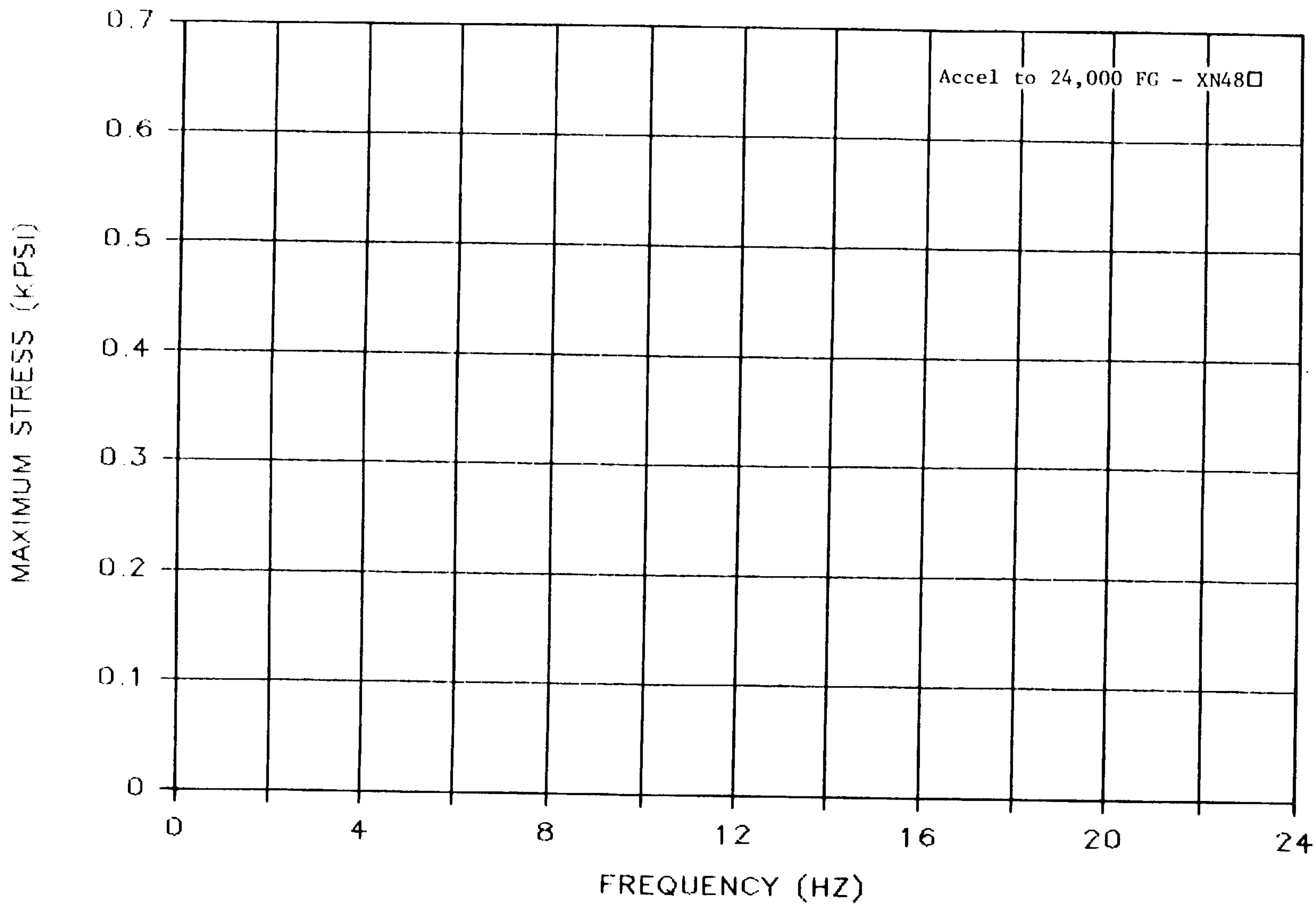


Figure B-33. Right Rear Mount Rosette No. 1 Tangential (KD RRM1), Stress Versus Frequency.

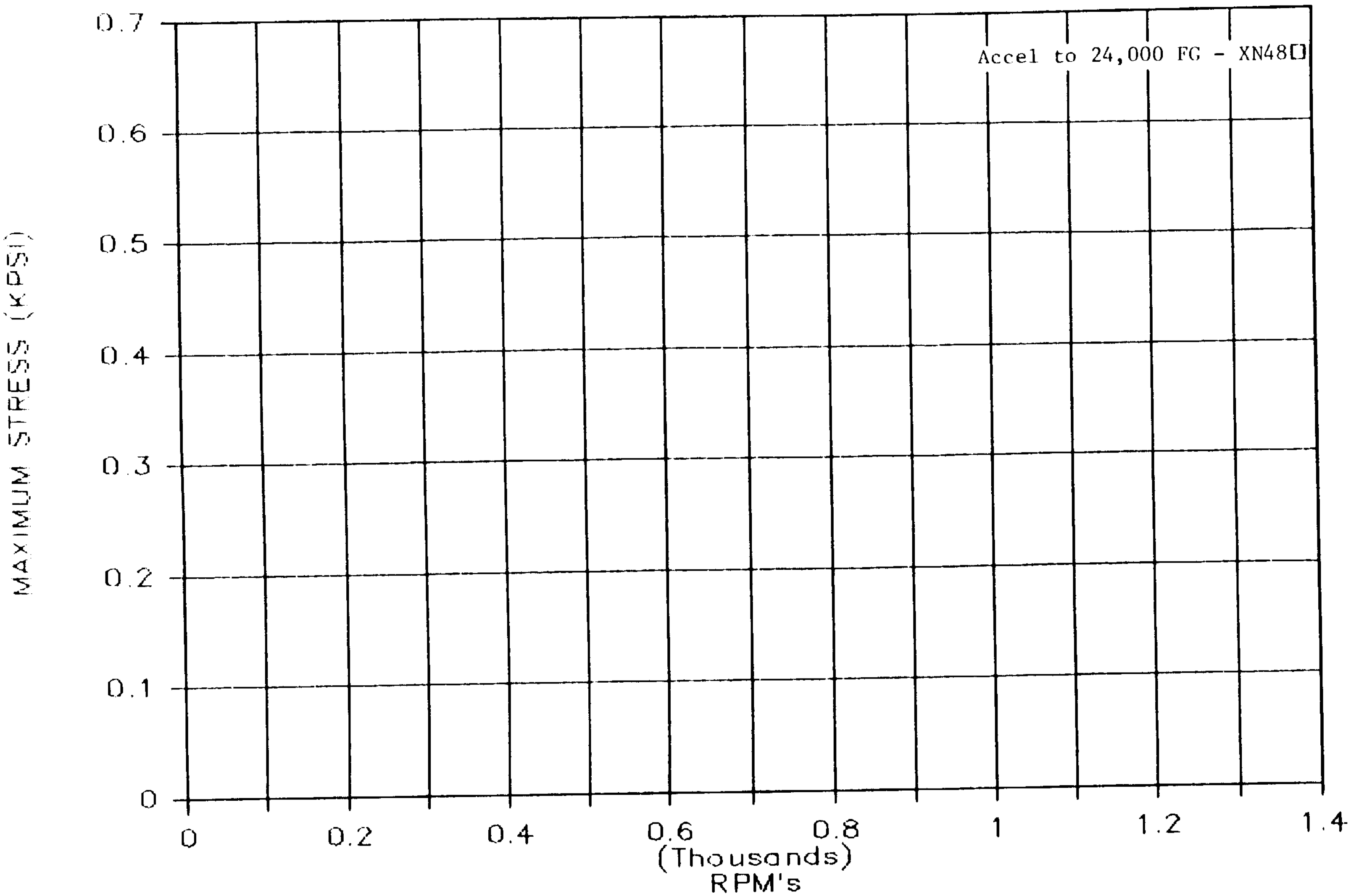


Figure B-34. Right Rear Mount Rosette No. 1 Tangential (KD RRM1), Stress Versus Speed.

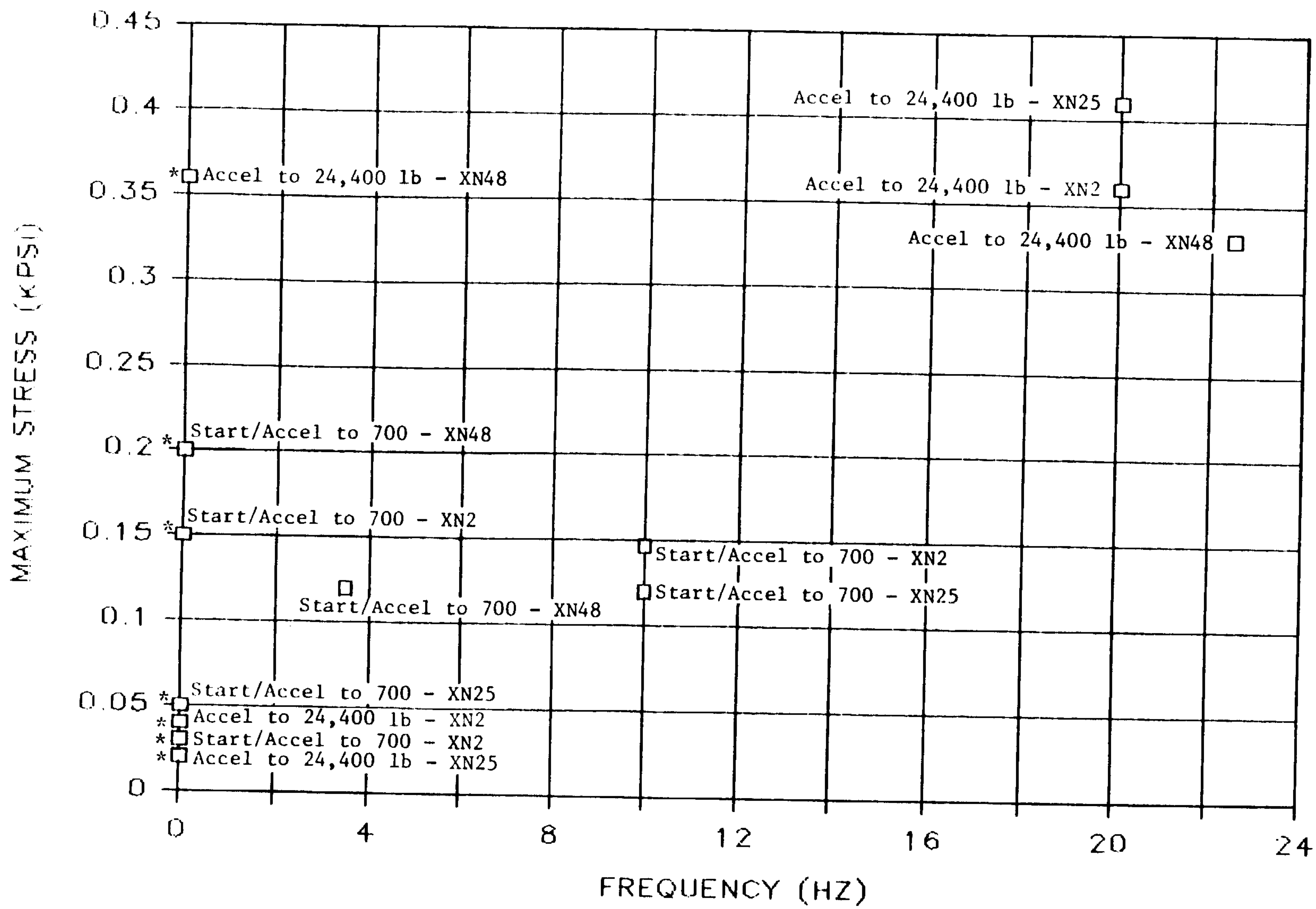


Figure B-35. Back of Spar - Lower Aft Vertical (KD SR04), Stress Versus Frequency.

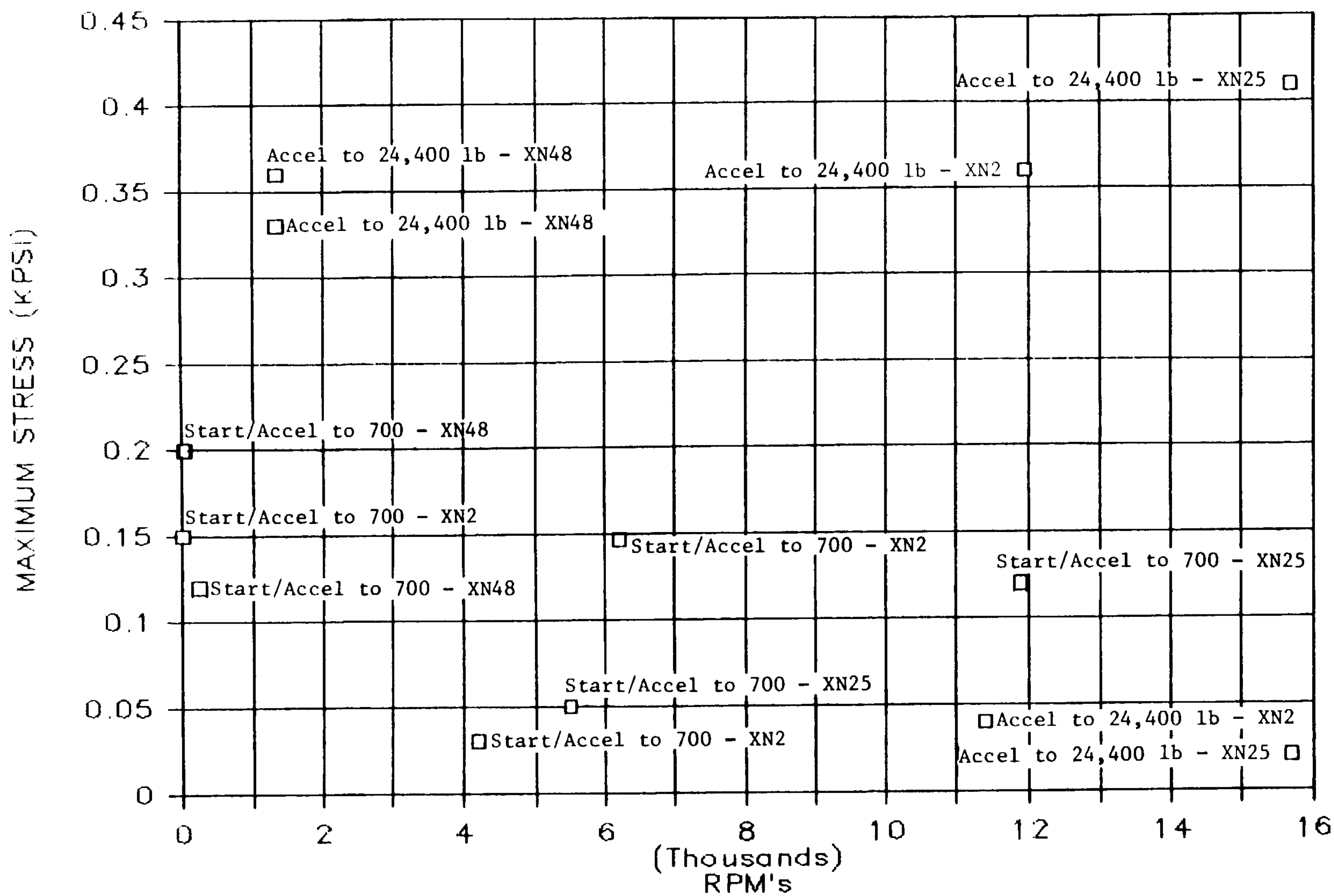


Figure B-36. Back of Spar - Lower Aft Vertical (KD SR04), Stress Versus Speed.

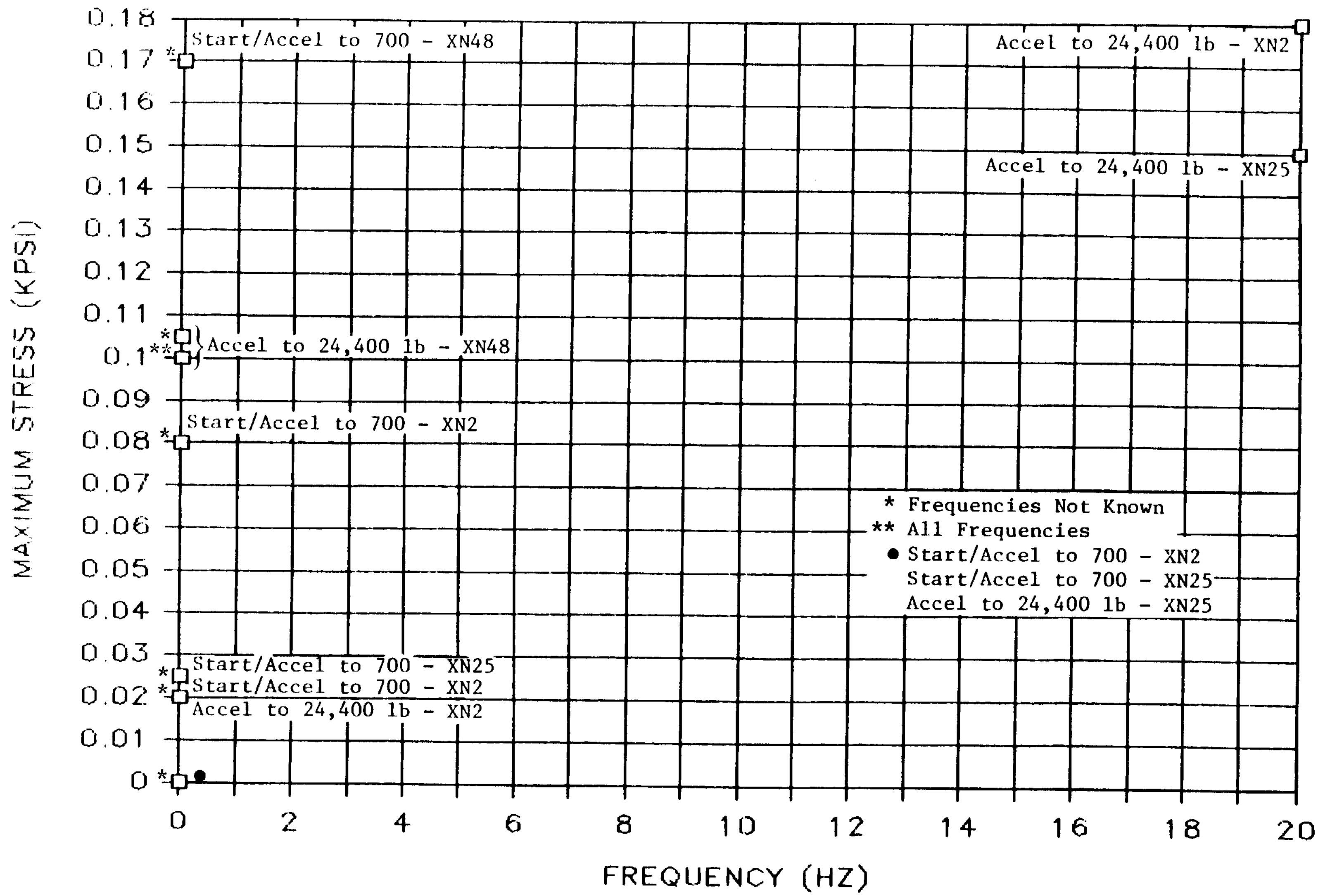


Figure B-37. Back of Spar - Lower Aft Horizontal (KD SR06), Stress Versus Frequency.

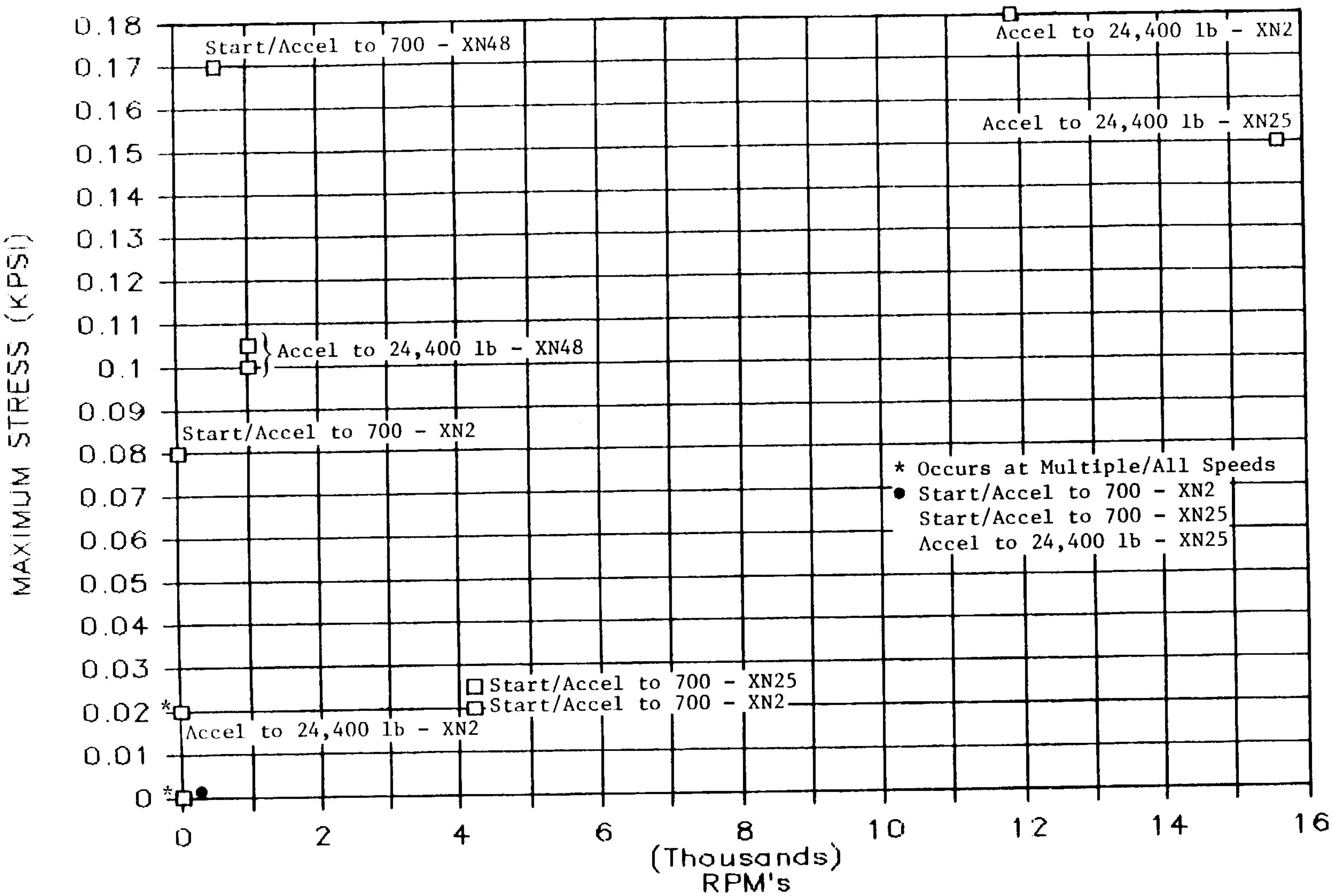


Figure B-38. Back of Spar - Lower Aft Horizontal (KD SR06), Stress Versus Speed.

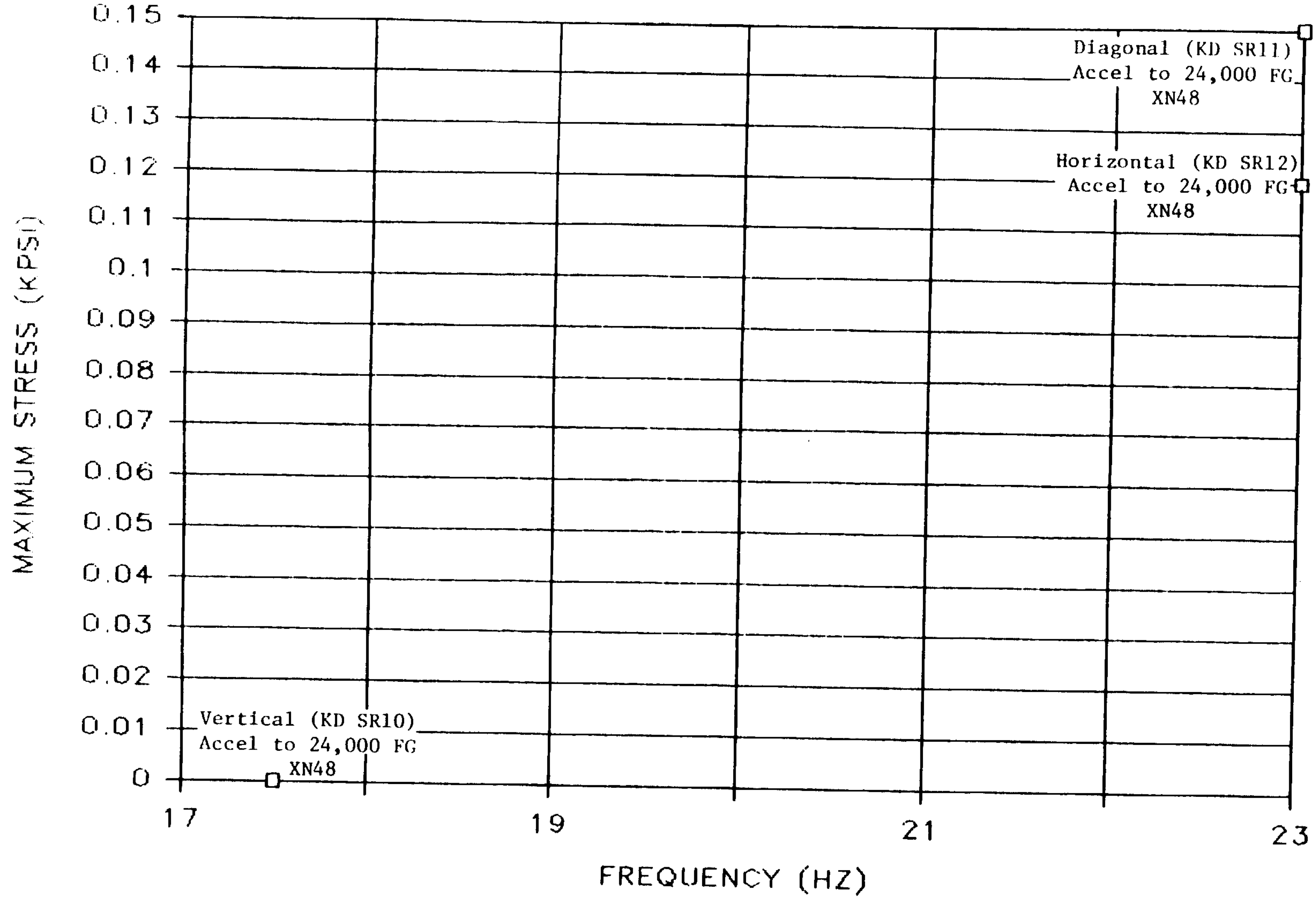


Figure B-39. Back of Spar - Upper Aft Vertical, Diagonal, and Horizontal (KD SR10), Stress Versus Frequency.

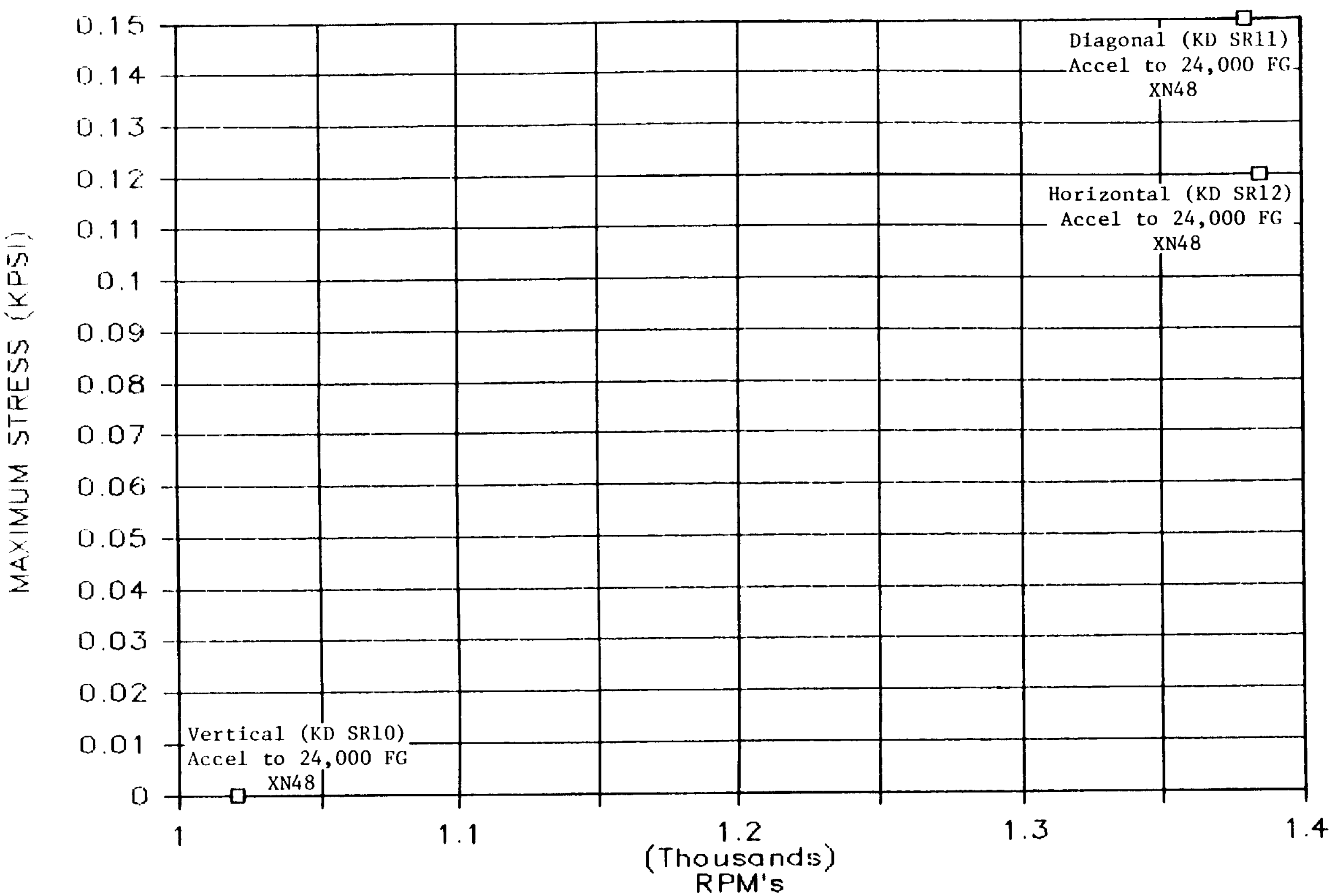


Figure B-40. Back of Spar - Upper Aft Vertical, Diagonal, and Horizontal (KD SR10, 11, and 12), Stress Versus Speed.

# DISTRIBUTION

## Government Agencies

NASA Headquarters
600 Independence Avenue, SW
Washington, DC 20546
Attn: R/R.S. Colladay
RJ/C.C. Rosen
RP/G.M. Reck
RP/J.R. Facey

NASA Lewis Research Center
21000 Brookpark Road
Cleveland, Ohio 44135

| | |
|---|---|
| Attn: J.A. Ziemianski | MS 86-1 |
| R.J. Shaw | MS 86-1 |
| P.G. Batterton | MS 86-1 |
| G.K. Sievers | MS 100-5 |
| M.J. Hartmann | MS 3-7 |
| R.E. Kielb | MS 23-3 |
| L.J. Kiraly | MS 23-3 |
| J.F. Groeneweg | MS 86-7 |
| J.C. Williams | MS 500-211 |
| R.W. Niedzwiecki | MS 77-6 (2 copies) |
| D.W. Drier | MS 86-2 |
| B.A. Miller | MS 5-3 |
| J.J. Reinmann | MS 77-10 |
| L.J. Bober | MS 86-7 |
| A.G. Powers | MS 86-4 |
| J.J. Coy | MS 86-4 |
| R.E. Coltrin | MS 77-10 |
| C.L. Ball | MS 77-6 |
| E.A. Willis | MS 86-1 |
| L. Reid | MS 77-10 |
| E.T. Meleason | MS 77-10 |
| R.D. Hager | MS 86-7 (3 copies) |
| Library | MS 60-3 (2 copies) |
| Report Control Office | MS 60-1 |
| Tech. Utilization Office | MS 7-3 |
| D.C. Mikkelson | MS 6-12 (2 copies) |
| AFSC Liaison Office | MS 501-3 |
| Army R & T Propulsion Lab | MS 77-12 |

NASA Ames Research Center
Moffett Field, CA 94035

| | |
|---|---|
| Attn: R.P. Bencze | MS 227-6 |
| R.C. Smith | MS 227-6 |

NASA Langley Research Center
Hampton, VA 23665
Attn: D.G. Stephens MS 462
Research Information Center MS 151A

NASA Scientific and Technical Information Facility
P.O. Box 8757
B.W.I. Airport, MDE 21240
Attn: Accession Dept. (20 copies)

NASA Dryden Flight Research Center
P.O. Box 273
Edwards, CA 93523
Attn: D-OP/R.S. Baron (2 copies)

Department of Defense
Washington, DC 20301
Attn: R. Standahar, 3D1089 Pentagon

Wright-Patterson Air Force Base
Dayton, OH 45433
Attn: AFWAL/PO/Col. J. Radloff
AFWAL/POTA/M.F. Schmidt
AFWAL/POT/H.I. Bush
ASD/EN/Col. L.G. vanPelt
ADS/SR/K.I. Collier

Eustis Directorate
U.S. Army Air Mobility
R & D Laboratory
Fort Eustis, VA 23604
Attn: J. White
J. Gomez, Jr.

Navy Department
Naval Air Systems Command
Arlington, VA 20360
Attn: G. Derderian, AIR-310-E

Naval Air Propulsion Test Center
Trenton, NJ 08628
Attn: P.J. Mangione, MSPE-32
R. Valeri, MSPE-34

U.S. Naval Air Test Center
Code SY-53
Patuxent River, MD 20670
Attn: E.A. Lynch

USAVRAD Command
P.O. Box 209
St. Louis, MO 63166
Attn: R.M. Titus

Department of Transportation
NASA/DOT Joint Office of Noise Abatement
Washington, DC 20590
Attn: C. Foster

Federal Aviation Administration
New England Region
12 New England Executive Park
Burlington, MA 01803
Attn: D.P. Salvano

Engine Manufacturers

AVCO Lycoming
550 S. Main Street
Stratford, CT 06497
Attn: H. Moellmann

Detroit Diesel/Allison Division
P.O. Box 894
Indianapolis, IN 46206
Attn: B. Wallace

Garrett Turbine Engine Company
111 South 34th Street
P.O. Box 5217
Phoenix, AZ 85010
Attn: R. Heldenbrand

Garrett Turbine Engine Company
Torrance, CA 90509
Attn: F.E. Faulkner

General Electric Company/AEG
1 Neumann Way
Evendale, Ohio 45215
Attn: T.F. Donohue

General Electric Company/AEG
1000 Western Avenue
Lynn, MA 01910
Attn: B. Weinstein

General Electric Company
P.O. Box 88186
Cleveland, OH 44181
Attn: M.H. Rudasill

Pratt & Whitney Aircraft Group
United Technologies Corporation
Engineering Division
400 Main Street
East Hartford, CT 06108
Attn: R.W. Hines 161-04
G.L. Brines 162-25
G.L. Bywaters 162-23

Pratt & Whitney Aircraft Group
United Technologies Corporation
Military Products Division
P.O. Box 2691
West Palm Beach, FL 33402
Attn: R.E. Davis 713-11
T.R. Hampton 713-07

Pratt & Whitney Aircraft Group
United Technologies Corporation
24500 Center Ridge Road
Suite 280
Westlake, OH 44145
Attn: A. Leiser

Teledyne CAE, Turbine Engines
1330 Laskey Road
Toledo, OH 43612
Attn: R.H. Gaylord

Williams International
2280 West Maple Road
Walled Lake, MI 48088
Attn: R. vanNimwegen
R. Horn

Airframe Manufacturers

Boeing Commercial Airplane Company
P.O. Box 3707
Seattle, WA 98124
Attn: Dr. C.G. Hodge
F. Davenport
J. Farrell

Boeing Company
Wichita Division
P.O. Box 7730
Wichita, KS 67277
Attn: D. Tarkelson
C.T. Havey

Cessna Aircraft Company
P.O. Box 154
Wichita, KS 67201
Attn: D. Ellis Dept 178

Douglas Aircraft Company
McDonnell Douglas Corporation
3855 Lakewood Boulevard
Long Beach, CA 90846
Attn: M. Klotzsche
W. Orlowski

Gates Learjet Corporation
P.O. Box 7707
Wichita, KS 67277
Attn: E. Schiller

General Dynamics Convair
P.O. Box 80844
San Diego, CA 92138
Attn: S. Campbell

Grumman Aerospace Corporation
South Oyster Bay Road
Bethpage, NY 11714
Attn: N.F. Dannenhoffer

Gulfstream Aerospace Corporation
P.O. Box 2206
Savannah, GA 31402-2206
Attn: R. Wodkowski

Lockheed-California Company
Burbank, CA 91502
Attn: J.F. Stroud D/75-42
R. Tullis D/75-21

Lockheed-Georgia Company
86 S. Cobb Drive
Marietta, GA 30063
Attn: W.E. Arndt D/71-01, Zone 13

McDonnell Aircraft Company
McDonnell Douglas Corporation
P.O. Box 516
St. Louis, MO 63166
Attn: G. Phariss

Rockwell International
International Airport
Los Angeles Division
Los Angeles, CA 90009
Attn: A.W. Martin

<u>Airlines</u>

American Airlines
Maintenance and Engineering Center
Tulsa, OK 74151
Attn: C. Wellmershauser

Continental Airlines, Inc.
2929 Allen Parkway
Houston, TX 77019
Attn: J. Arpey

Delta Airlines, Inc.
Hartsfield-Atlanta International Airport
Atlanta, GA 30320
Attn: J.T. Davis

Eastern Airlines
International Airport
Miami, FL 33148
Attn: E. Upton

Federal Express Corporation
Box 727
Memphis, TN 38194
Attn: J. Riedmeyer

Pan American World Airways, Inc.
JFK International Airport
Jamaica, NY 11430
Attn: R. Valeika

Trans World Airlines
605 Third Avenue
New York, NY 10016
Attn: K. Johnson

United Airlines
Maintenance Operations Center
San Francisco International Airport
San Francisco, CA 94128
Attn: J. Goodwine

## Others

Hamilton Standard
United Aircraft Corporation
Windsor Locks, CT 06096
Attn: B. Gatzen MS 1-2-11
S. Ludemann MS 1-2-11

Massachusetts Institute of Technology
Department of Astronautics and Aeronautics
Cambridge, MA 02139
Attn: Library

Penn State University
Department of Aerospace Engineering
233 Hammond Building
University Park, PA 16802
Attn: Dr. B. Lakshminarayana

Rohr Corporation
P.O. Box 878
Foot and H Street
Chula Vista, CA 92012
Attn: Library

TRW, Inc.
TRW Equipment Group
23555 Euclid Avenue
Cleveland, OH 44117
Attn: I. Toth

University of Michigan
Gas Dynamics Laboratories
Aerospace Engineering Building
Ann Arbor, MI 48109
Attn: Dr. C.W. Kaufmann

University of Tennessee Space Institute
Tullahoma, TN 37388
Attn: Dr. V. Smith

Cessna Aircraft Company
McCauley Accessory Division
3535 McCauley Drive
Vandalia, OH 45377
Attn: H.G. Starnes

Hartzell Propeller Products
P.O. Box 1458
1800 Covington Avenue
Piqua, OH 45356
Attn: D. Edinger

University of Washington
Seattle, WA 98195
Attn: Dr. R. Decher

[redacted]

| | | |
|---|---|---|
| 1. Report No. CR-180869 | 2. Government Accession No. | 3. Recipient's Catalog No. |
| 4. Title and Subtitle<br>Full-Scale Technology Demonstration of a Modern Counterrotating Unducted Fan Engine Concept - Engine Test | | 5. Report Date<br>December 1987 |
| | | 6. Performing Organization Code<br>535-03-01 |
| 7. Author(s)<br>GE36 Design and Systems Engineering | | 8. Performing Organization Report No. |
| | | 10. Work Unit No. |
| 9. Performing Organization Name and Address<br>GE Aircraft Engines<br>One Neumann Way<br>Cincinnati, Ohio 45215 | | 11. Contract or Grant No.<br>NAS3-24210 |
| | | 13. Type of Report and Period Covered<br>Topical |
| 12. Sponsoring Agency Name and Address<br>NASA Lewis Research Center<br>21000 Brookpark Road<br>Cleveland, Ohio 44135 | | 14. Sponsoring Agency Code |
| 15. Supplementary Notes | | |

16. Abstract

The UDF™ (unducted fan) engine is an innovative aircraft engine concept that is based on an ungeared, counterrotating, unducted, ultra-high-bypass turbofan configuration. This engine is being developed by GE Aircraft Engines to provide a high thrust-to-weight ratio power plant with exceptional fuel efficiency for subsonic aircraft application.

This report covers the successful ground testing of this engine. A test program exceeding 100-hours duration was completed, in which all of the major goals were achieved. The following accomplishments were successfully demonstrated: full thrust (25,000 lb); full counterrotating rotor speeds (1393+ rpm); low specific fuel consumption (< 0.24/lb/hr/lb); new composite fan blade design; counterrotation of structures, turbines, and fan blades; control system; actuation system; and reverse thrust.

| | |
|---|---|
| 17. Key Words (Suggested by Author(s))<br>Undducted Fan (UDF™); Counterrotation; Ultra-High-Bypass Fan; Propfan | 18. Distribution Statement<br>[redacted] |

| | | | |
|---|---|---|---|
| 19. Security Classif. (of this report) | 20. Security Classif. (of this page) | 21. No. of Pages | 22. Price |
| Unclassified | Unclassified | 326 | |